

Appendix H: Dispersion Modelling

Titahi Bay Outfall Modelling



Wellington Water Ltd

Report 44801085

June 2018

Titahi Bay Outfall Modelling

Prepared for Wellington Water Ltd
Represented by Edward Yong



Titahi Bay Wastewater discharge location. 29th November 2017, X-Craft drone imagery.

Project manager	John Oldman
Project number	44801085
Approval date	15.08.2018
Revision	Final V02

CONTENTS

1	Executive Summary	3
2	Introduction	4
3	Field Data Collection	7
3.1	Current and Water Level Data	7
3.2	Dye Test.....	8
4	Monitoring Data Review.....	10
5	Model Setup.....	13
5.1	Models Used	13
5.2	Grid	13
5.3	Bathymetry	15
5.4	Boundary Condition	16
6	Model Calibration	18
6.1	Broad Scale Currents.....	18
6.2	Water Levels	26
6.3	Currents	29
6.4	Contaminant Concentrations at Monitoring Sites	35
6.5	Near field processes (New Section).....	37
7	Scenario Results	43
7.1	Average Discharge Scenario	44
7.2	Peak Discharge Scenario	50
7.3	Design Discharge Scenario	56
8	Summary.....	62
9	References.....	63
A	Representative Drone photos.....	67
B	Mana Marina Tidal Analysis.....	78
C	Monitoring Data Regression Plots	82
D	Review discussion document	89



1 Executive Summary

A calibrated depth-averaged hydrodynamic and advection-dispersion model has been used to quantify the dynamics of the treated wastewater plume discharged from the Wastewater Treatment Plant just to the south of Titahi Bay at Kaumanga Point.

The report provides details of field data carried out for the study, a review of monitoring data used to calibrate the model, an overview of the hydrodynamics of the area offshore of the discharge and results from long-term model simulations. Appended to this report are the outcomes of the peer review process carried out by Greater Wellington Regional Council which focussed on the appropriateness of using a depth-averaged model for simulating the dynamics of the treated wastewater plume.

Offshore of the discharge point, relatively strong, complex currents occur especially the area between Mana Island and Kaumanga Point. Closer to the discharge site itself there are a number of exposed rocky reefs and the water depth in the immediate vicinity of the discharge site is relatively shallow.

Near-field modelling of the discharge indicates that rapid vertical mixing will occur due to a combination of entrainment of ambient seawater into the discharge area and downward vertical mixing due to the outfall configuration. Within 25-50 m of the discharge point the near-field modelling indicates that the treated wastewater plume would occupy the top 70-90% of the water column and that significant increases in salinity would occur.

Such increases in salinity result in reduced buoyancy of the treated wastewater plume which is likely to be broken down by vertical diffusion and turbulent mixing (due to currents and waves).

Sensitivity testing of the calibrated depth-averaged model and a three-dimensional model show that the use of a three-dimensional model would only be justified if more accurate predictions of treated wastewater concentrations were required inside the near-field (i.e. inside the statutory 200 m mixing zone) or if better estimates of treated wastewater concentrations were required at sites well offshore of the discharge during periods of sustained offshore winds.

The depth-averaged model has been calibrated against currents and water levels collected specifically for this study and against water level data from the Mana Marina. The model performance is very good in terms of predicting water levels and provides a good level of prediction with respect to currents immediately offshore of the outfall.

In addition, a qualitative analysis of broader scale currents has been carried out which confirms the model's ability to simulate current offshore of Porirua Harbour and in and around Mana Island.

Data from long term monitoring at key beach sites along the coast and a dye test carried out in December 2017 has been used to confirm the model's ability to simulate the dynamics of the treated wastewater plume in the near shore zone.

A series of long-term model runs have been carried out which provide quantification of the levels of dilution achieved and the dynamics of the plume under a broad range of tide and wind conditions for three different discharge regimes – Average (300 L/s), Peak (1100 L/s) and Design (1500 L/s) discharge rates.

Model results can be used to quantify the dynamics of the treated wastewater plume and to assess the relative risk associated with each of the discharge rates considered.

All results are presented in terms of percentage treated wastewater so that further improvements in wastewater quality associated with any future scenarios being considered scenarios can also be assessed.

2 Introduction

Wellington Water commissioned DHI Water and Environment to carry out a plume dilution modelling study for the Porirua City wastewater treatment plant (WWTP) outfall which discharges treated wastewater just to the south of Titahi Bay (Figure 2-1).



Figure 2-1. Location of the Porirua City Wastewater Treatment Plant.

The outfall currently discharges treated wastewater from the Wastewater Treatment Plant and consists of an outfall structure (Figure 2-2) discharging into the near shore zone immediately offshore of the Plant (Figure 2-3). This part of the coast consists of exposed rocky reefs with pockets of coarse sand and cobbles and the water depth in the immediate vicinity of the discharge site is relatively shallow.

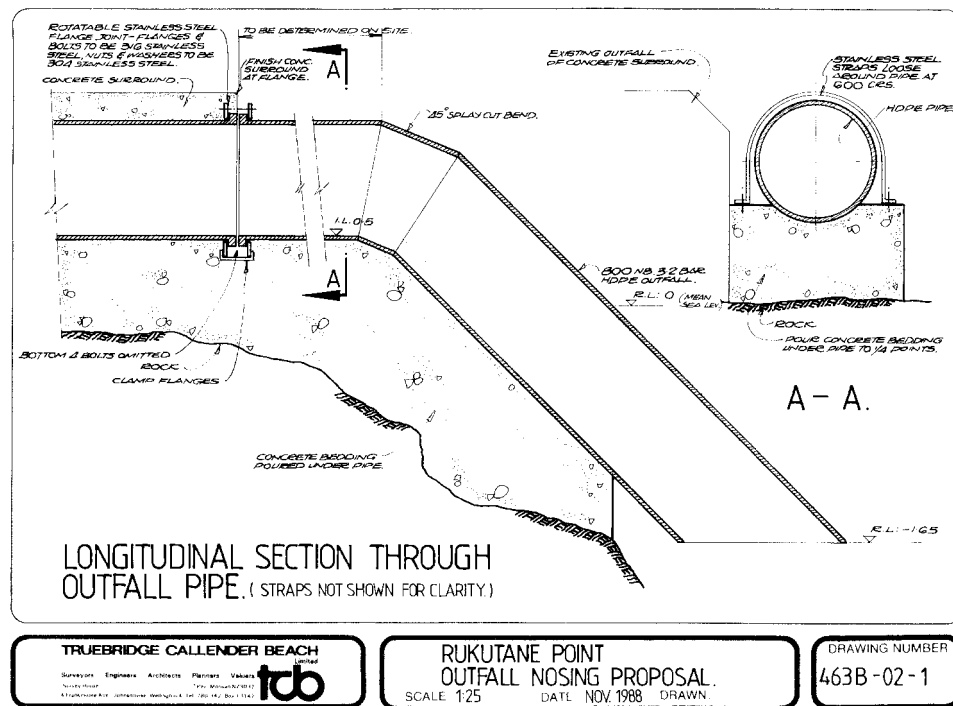


Figure 2-2. Design diagram for the Titahi Bay outfall. Note that the last section of outfall is no longer present so that the discharge occurs at a height of approximately 0.8 m above mean sea level (just above the high-water level).

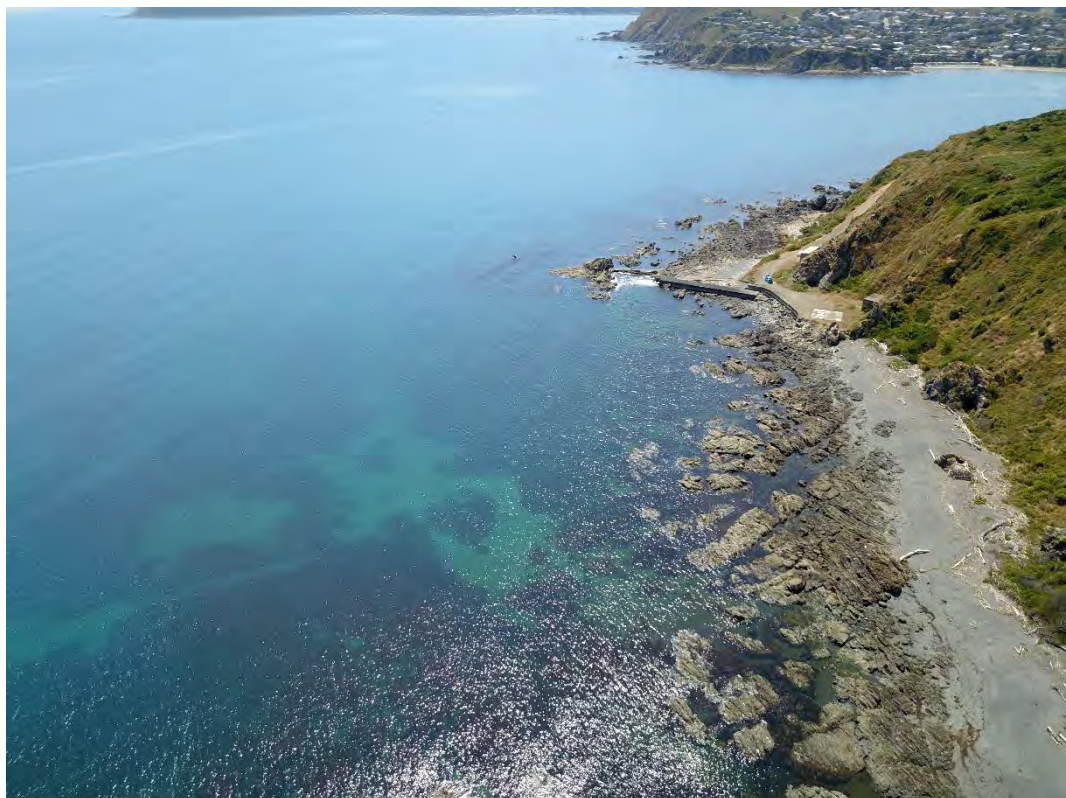


Figure 2-3. Aerial photo of the area just to the south of the discharge point showing the areas of rocky reef (X-Craft drone imagery, 29.11.17).

The current consent to discharge treated effluent will expire July 2020.

On average, the discharge of treated wastewater through the outfall occurs at a rate of 300 L/s, in line with the average consented discharge rate of 24,000 m³ per day. Peak discharge rates of 1100 L/s can occur in line with the peak consented discharge rate of 92,800 m³ per day. Planned plant upgrades will increase the fully treated flow through the plant to a maximum of 1500 L/s by June 2020.

Future population growth in Porirua City and Wellington City's northern suburbs of around 110,000 is predicted to occur in the area serviced by the WWTP.

The work detailed in this report will assist Wellington Water with the renewal process for the existing consent and provide information in relation to the consultation that will happen around that renewal process.

The report provides details of field data carried out for the study (Section 3), a review of monitoring data (Section 4), an overview of the model setup (Section 5) plus an overview of the hydrodynamics of the area offshore of the discharge based on previous studies and a quantitative calibration of a hydrodynamic model against water levels and current meter data (Section 6). The report also provides details of results from long-term model simulations for current average, peak and maximum design WWTP flow rates (Section 7).

3 Field Data Collection

3.1 Current and Water Level Data

A current meter deployment was undertaken in November/December 2017 in conjunction with a qualitative dye test during that deployment to provide an understanding of the plume dynamics. Unfortunately, the current meter that was deployed malfunctioned resulting in the memory being corrupted and no data being collected. Efforts were made to try and recover data but they were not successful.

A second deployment was carried out during January/February 2018. On the retrieval date (14th March) it was discovered that the current meter had sustained some minor damage after having been dragged out of position. The battery pack compartment had a breach and the unit had flooded, resulting in total loss of data.

The third deployment used both a moored acoustic doppler current meter (ADCP¹) and downward facing ADCP. Currents, water levels and waves were successfully recorded for the period from the 26th April 2018 through to the 2nd June 2018. The instrument site was located ~500 m offshore of the WWTP at Longitude 174.8198°, latitude -41.1033° at a mean water depth of 13.8 m (Figure 3-1).



Figure 3-1. Location of the current meter deployed offshore of the WWTP between the 26th of April 2018 and the 2nd of June 2018

Figure 3-2 shows the winds for the deployment period from the Mana Island automated weather station and the waves recorded during the deployment.

¹ This instrument records currents through the water column rather than just at a single point in the water column.

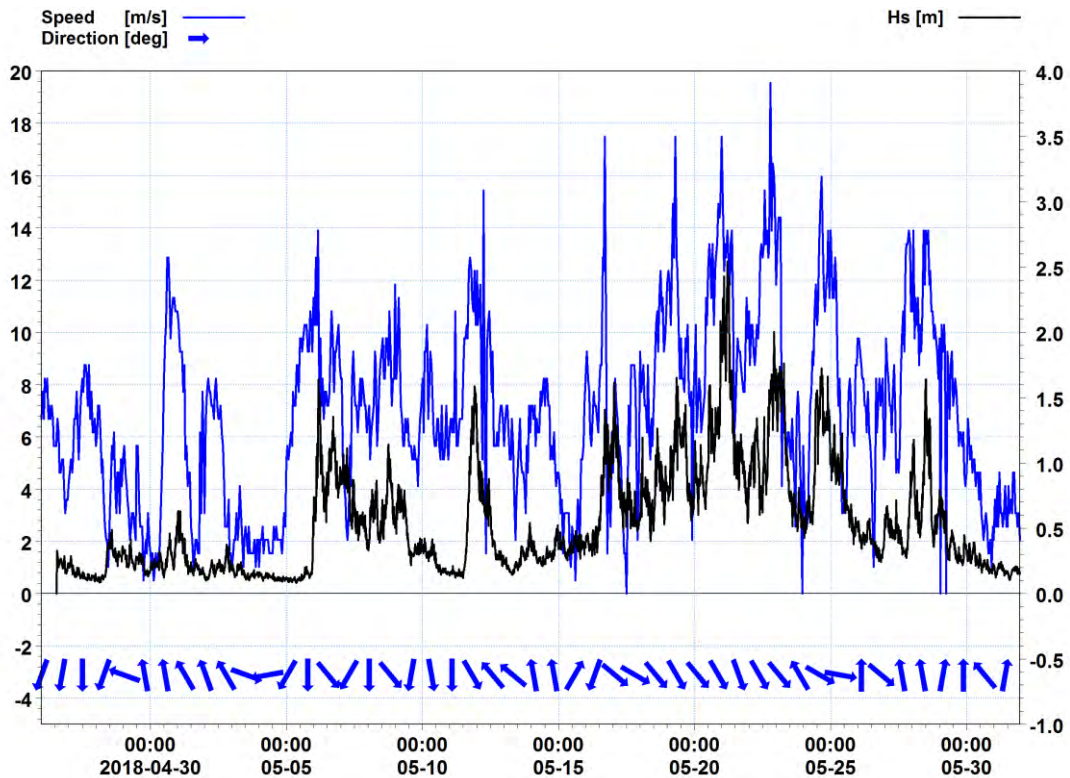


Figure 3-2. Wind and wave data for the period of the current meter deployment.

3.2 Dye Test

A qualitative dye test was carried out on the 29th November 2017. This involved the injection of Rhodamine dye at the WWTP and subsequent tracking of the dye patch using drone imagery. Selected images from the dye test are provided in Appendix A and a full copy of the images and the movie taken during the dye test have been provided to Wellington Water.

This data is used to provide estimates of the dispersion coefficient, to use for the advection-dispersion model and secondly to give a qualitative comparison of the predicted plume behaviour. French-Mackay et al. (2007) indicate that the observed spread of a dye plume over time is linear then a dispersion coefficient can be estimated from the change in plume dimensions with time as follows;

$$L^2 = 32 D t$$

Where L is the estimated plume dimension from the digitised drone images, t is time and D is the horizontal dispersion coefficient.

From the slope of that relationship (Figure 3-3), the dispersion coefficient for the dye plume is estimated to be 0.037 m²/s. This is consistent with data from the earlier work carried out in relation to dye tests carried out in 1975 (MWD, 1975) and within the range recommended literature values of 0.10 to 0.06 m²/s (DHI, 2017).

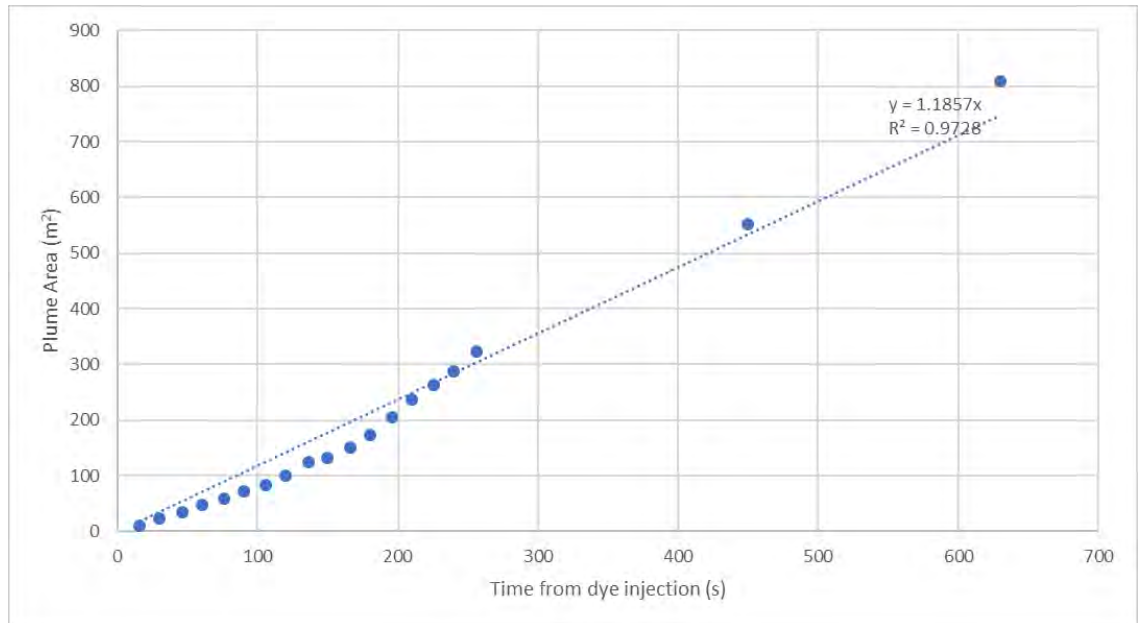


Figure 3-3. Relationship between dye plume area and time from injection based on drone images.

4 Monitoring Data Review

Wellington Water has been monitoring water quality at key beach sites to the north and south of the WWTP (Figure 4-1) since 2014, along with effluent water quality.



Figure 4-1. Beach monitoring sites.

Treated wastewater quality data from 2010 shows a reduction in the frequency of high count events (i.e. > 10000 cfu/100 mL, highlighted in Figure 4-2) and an overall increase in treated wastewater quality leading to a steady reduction in the average treated wastewater concentration.

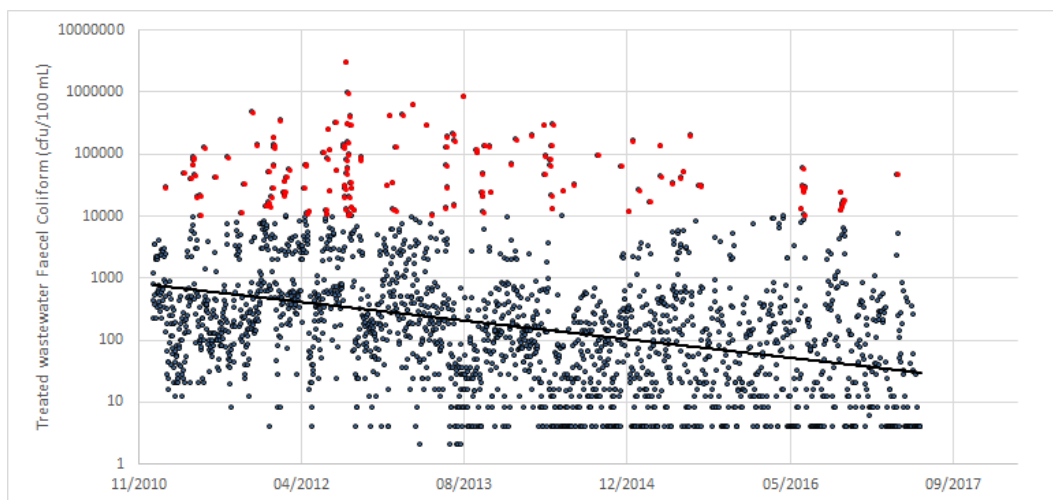


Figure 4-2. Observed treated wastewater faecal coliform concentrations at the WWTP (2011-2017).

At the beach monitoring sites (Figure 4-1) both faecal coliform and enterococci data shows a high degree of variability which reflects both the variability of the treated wastewater (Figure 4-2) and the role that tides and winds play in transporting the treated wastewater plume to the different monitoring sites.

While the time-series of monitoring data (e.g. Figure 4-3 for the monitoring site 200 m south-west of the outfall) could have been used to carry out the model calibration there are many gaps in the treated wastewater quality data which would have to be interpolated and the observed (and interpolated data) would have to be assumed to be a representative concentration for each days discharge.

Similarly, the beach monitoring data is only labelled as mid-tide, high-tide etc. so that an accurate temporal comparison could not be done.

Recent work carried out for Auckland Council Safeswim project has shown significant variability between replicate samples for enterococci in the Waitemata Harbour and laboratory analysis of sample has a relatively low accuracy (+/- 50% Ben Tuckey pers comm).

Appendix C contains regression plots of the observed faecal coliform concentrations at each of the beach monitoring sites versus the treated wastewater faecal coliform concentration for all paired data between April 2014-April 2017 (n=85). The data shows an obvious presence of other contaminant sources with high observations at a beach monitoring sites when low effluent concentrations are observed. Such outliers do not significantly affect the slope of the regression line at each of the monitoring sites.

The slope of the regression line gives a measure of the average level of dilution that is achieved at each of the beach monitoring sites. This same metric (the average long-term dilution) is used for calibrating the contaminant model (Section 6.4).

Data in Table 1 shows percentile values from the monitoring data at each of the beach sites and for the treated wastewater, along with the slope of the linear regression between the observed data at the beach monitoring site and treated wastewater concentration.

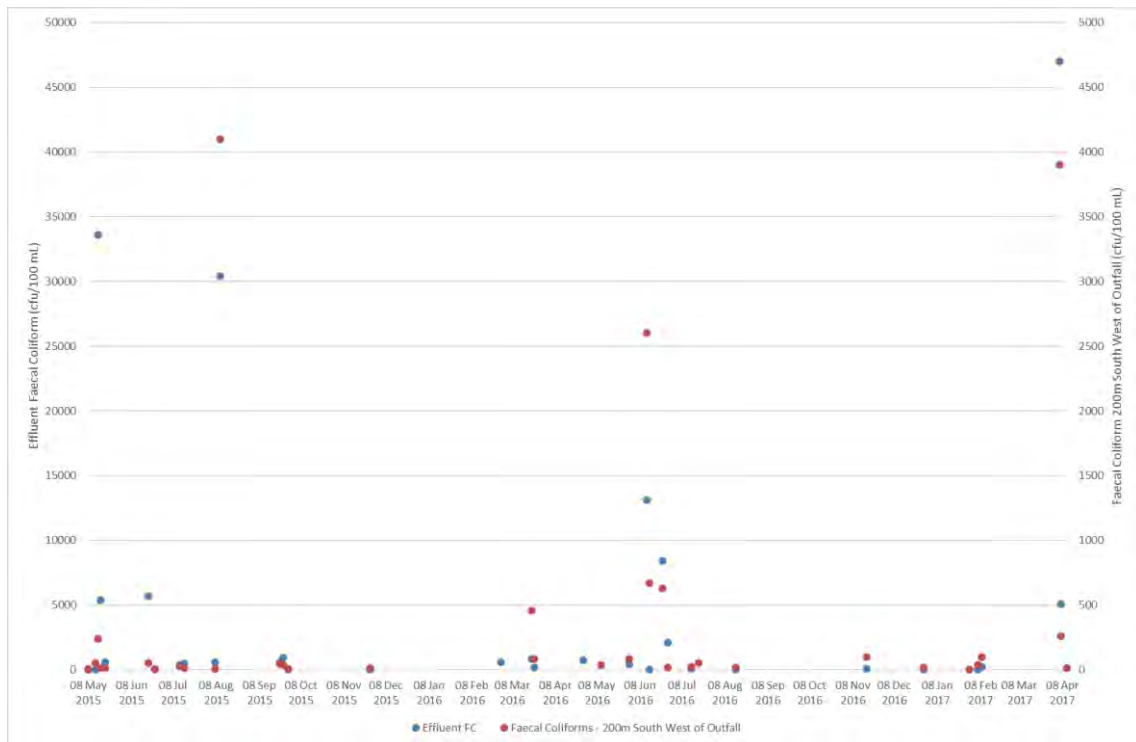


Figure 4-3. Time-series of observed faecal coliform in the effluent and at the monitoring site 200m south-west of the outfall. Note the different scales for the effluent (left) and monitoring site (right).

Table 1 Summary of Faecal Coliform beach monitoring data 2014-2017.

Site	50 th percentile value (cfu/100 mL)	95 th percentile value (cfu/100 mL)	Slope of the linear regression (treated wastewater concentration vs observed concentration)
Treated Wastewater	64	33280	-
200m south west of the outfall	24	3770	0.071
200m east of the outfall	8	913	0.028
Titahi Beach (South)	49	460	0.006
Titahi Beach	20	367	0.003
Ti Korohiwa Rocks	8	264	0.005
Mount Cooper	8	458	0.002

5 Model Setup

5.1 Models Used

The model used for this study are the MIKE21 hydrodynamic model (HD) coupled to the advection dispersion model (AD).

The MIKE21 HD model simulates the variations in water levels and currents in an estuary or open coastal area and takes into account variations in density, bathymetry and external forcings such as winds, large scale pressure variations and offshore tidal variations. It uses a cell-centred finite volume methodology allowing variable resolution grid cell sizes within the same computational grid.

The MIKE 21 AD module simulates the spreading of dissolved substances such as salt and includes linear processing so that contaminants such as faecal coliform, enterococci and viruses can be simulated.

The approach used in this study have been widely used international to assess the impacts of discharges to the marine receiving environment (Ao & Goblick, 2016, Danish et al., 2015, GHD, 2013, Menendez et al. 2013 and Ozcan and Gokce, 2002) and have used for the following recent resource consent projects.

Watercare, 2017. Coastal Marine Area within the Waiuku Estuary adjacent to the Clarks Beach Golf Course, Clarks Beach, Manukau

Watercare 2017. Warkworth and Snells Wastewater Treatment Plant resource consent hearing under the Auckland Unitary Plan. Mahurangi River

Environment Bay of Plenty 2013-2018. Kaituna River Rediversion and Ongatoro / Maketū Estuary Enhancement Project

5.2 Grid

The grid that was developed for this work is an extension of the grid initially developed for Greater Wellington Regional Council in relation to water quality issues in Porirua Harbour and the work carried out for the Transmission Gully work (SKM, 2011). That model has been extensively calibrated against observed water levels and currents within Porirua Harbour and is being used on an ongoing basis to provide forecasts of microbial contaminant levels. In addition, the same model has been used as the basis for the Whaitua work being carried out for Greater Wellington Regional Council to look at long term simulations of nutrients, sediments, metal and microbial contaminants in relation to future land use within the catchment.

For this project the model grid was extended 15 kilometres north and south of the Porirua Harbour entrance (Figure 5-1) and refined in and around the area of the outfall (Figure 5-2 and Figure 5-3).

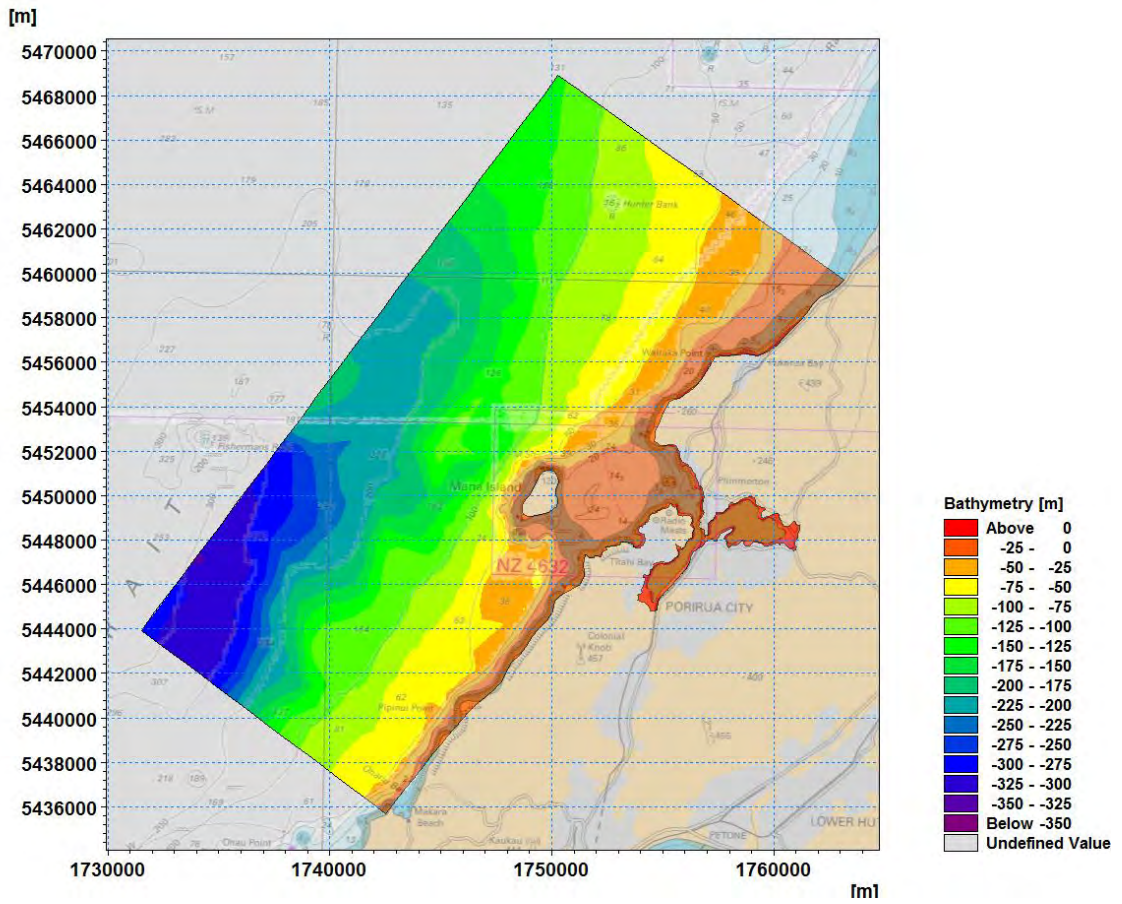


Figure 5-1. Extent of the Titahi Bay outfall model grid.

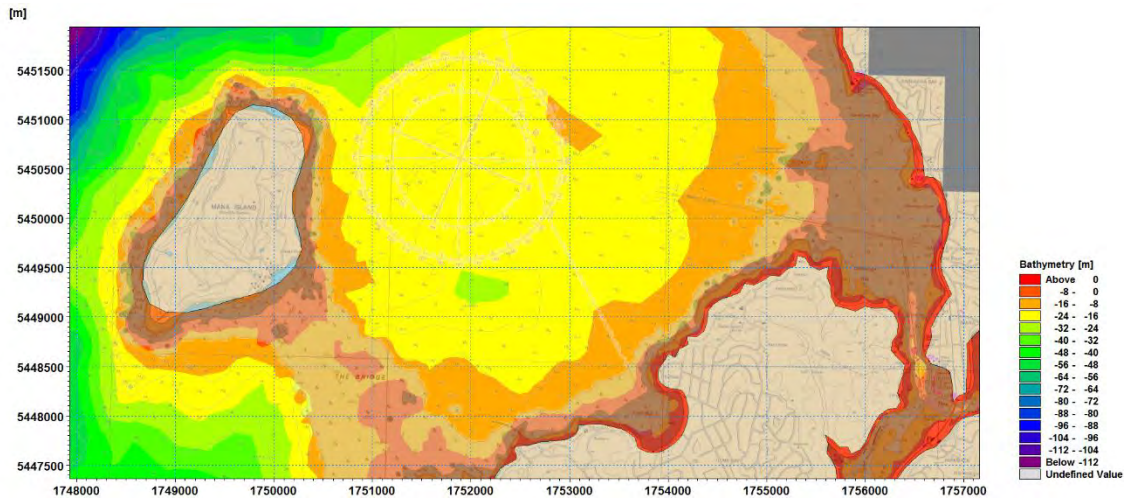


Figure 5-2. Detail of the model grid around Mana Island.

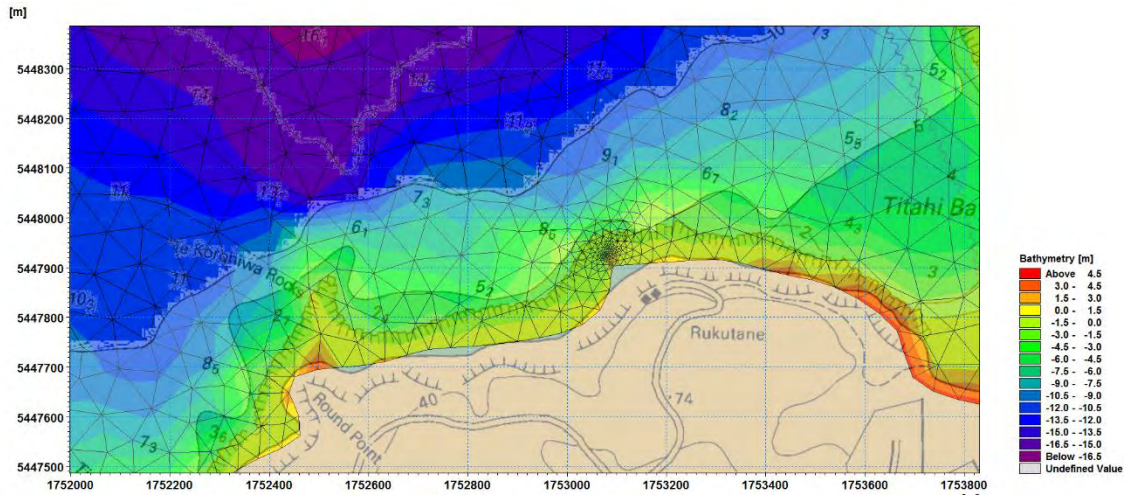


Figure 5-3. Detail of high resolution grid in the vicinity of the outfall.

5.3 Bathymetry

Bathymetry data (Figure 5-4) was sourced from relevant LINZ Chart information and extensive bathymetric surveys within the harbour (DML, 2015). All data was reduced to a common mean sea level vertical datum (assumed to be 1.0 m above Chart Datum).

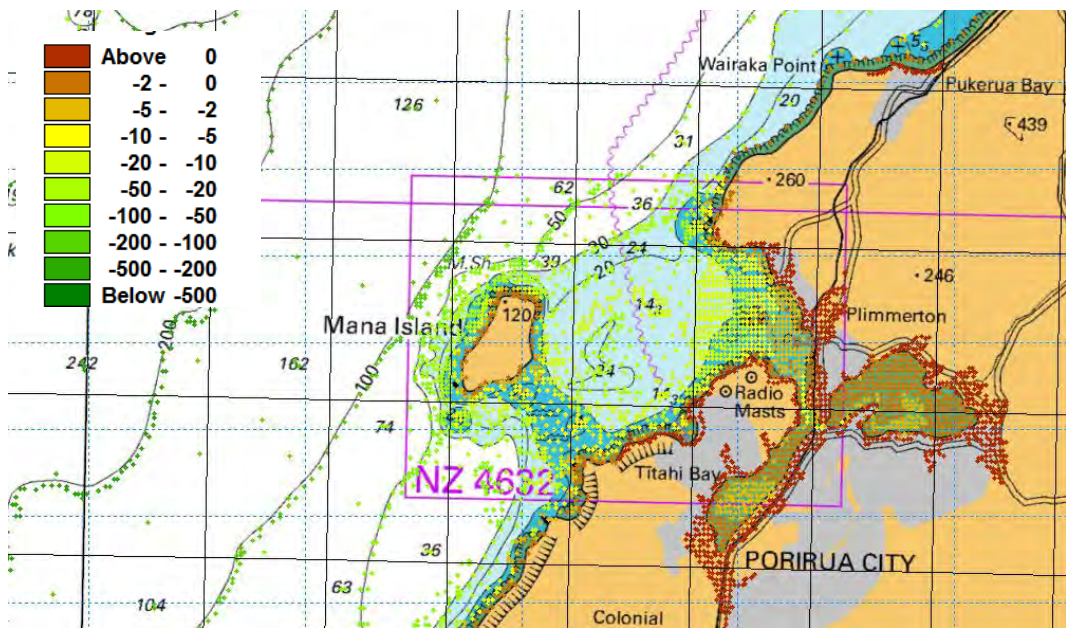


Figure 5-4. Bathymetric data used to create the model mesh.

5.4 Boundary Condition

Winds were obtained from the Mana Island automated weather station from MetService from 1st January 2013 to 31st May 2018. The wind rose for that period is shown in Figure 5-5.

From the long term wind record, a 4 month period was chosen which had a similar distribution of wind speeds and directions as the long term record. This period ran from the 29th January 2017 through to the 13th May 2017 and contains a number of larger wind events (Figure 5-6) including periods of moderate onshore and offshore winds. The wind rose for the chosen period (Figure 5-7) is very similar to the one for the long term record (Figure 5-5).

The tidal boundary conditions for the model were derived from tidal constituent data from a tidal analysis of 9 years of water levels from the Mana Marina tide gauge (Appendix B). The predicted tide level was applied to both the northern and southern boundary of the model with an adjustment for slope along both boundaries determined by the wind data.

Part of the calibration process was to determine the phase difference between the northern and southern boundary of the model (Section 6).

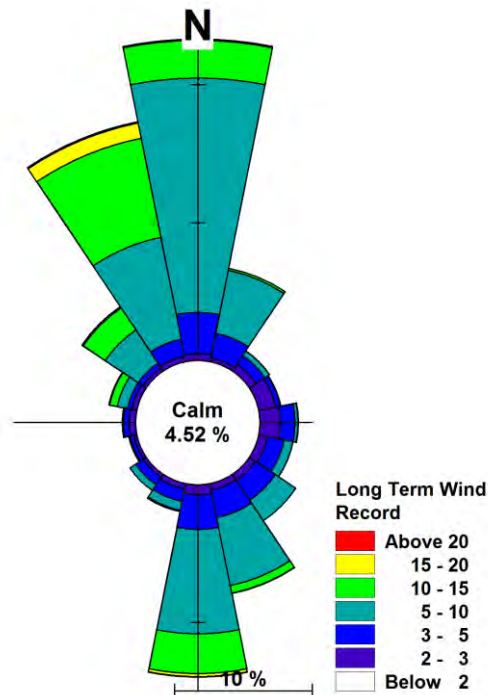


Figure 5-5. Wind rose for the period January 1st 2013 through to May 31st 2018.

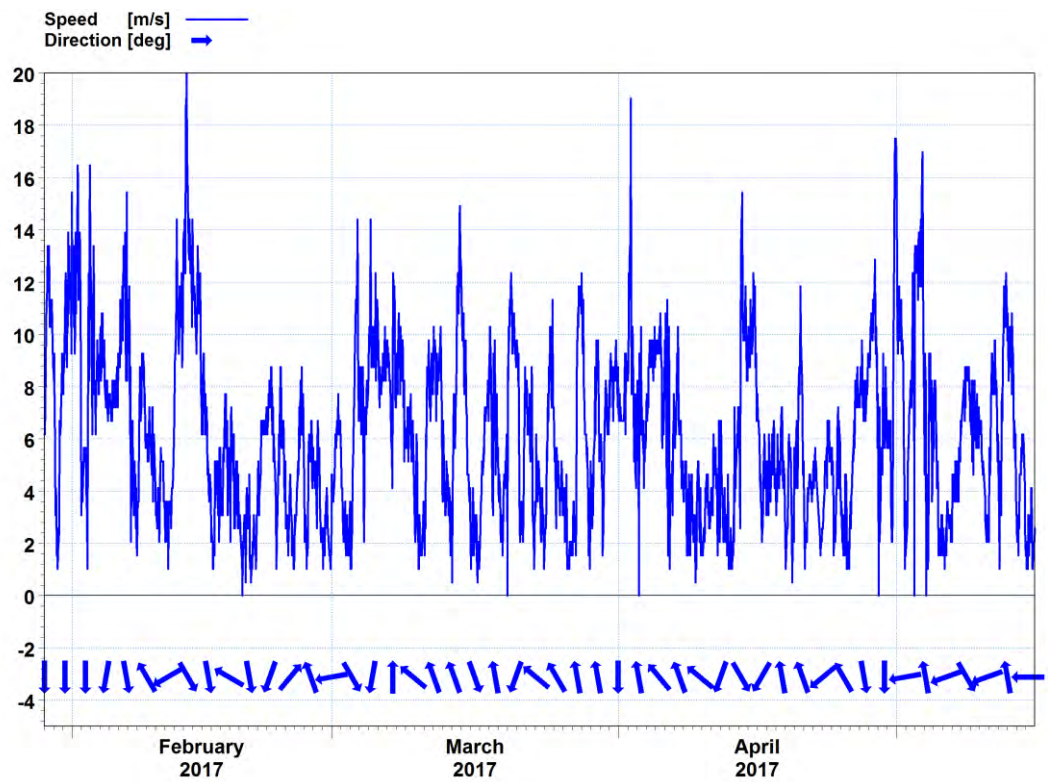


Figure 5-6. Wind speeds and direction for the representative period.

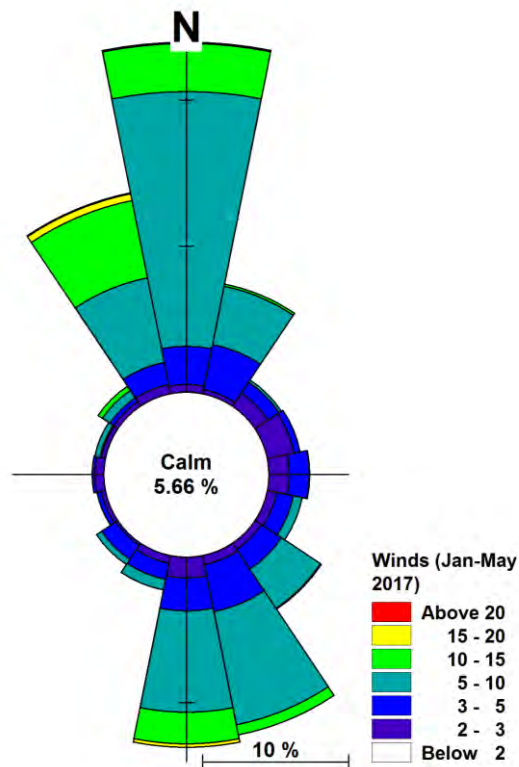


Figure 5-7. Wind rose for the period January 29th 2017 through to May 13th 2017.

6 Model Calibration

It was found that the best match to observed water levels and currents was obtained with a phase difference of 23 minutes between the northern and southern tidal boundaries of the model. This is consistent with the LINZ published phase difference between Mana Marina and Paraparaumu Beach of 20 minutes.

The bed roughness set to a value of $60 \text{ m}^{1/3}/\text{s}$ inside Porirua Harbour and in the area immediate offshore of the harbour. Elsewhere the roughness was set to a value of $20 \text{ m}^{1/3}/\text{s}$ to obtain a good calibration against observed water levels and current across the “Bridge” (the area between Mana Island and Kaumanga Point).

Model results were very sensitive to the eddy viscosity term which was adjusted to give the best fit to the observed current speeds and direction at the current meter site.

Table 2 Model parameters adjusted for the calibration process.

Model parameter	Description
Phase between the northern and southern boundary	23 minutes
Bed roughness	Offshore set to a Manning’s roughness of $20 \text{ m}^{1/3}/\text{s}$ inshore set to $60 \text{ m}^{1/3}/\text{s}$.
Eddy Viscosity	Smargorinsky value of 1 with a maximum eddy viscosity of $100 \text{ m}^2/\text{s}$.
Maximum speed	1.03
Wind friction	Varying linearly with wind speed (0.001255 for 7 m/s winds and 0.002425 for 25 m/s winds)
Density	Function of salinity

6.1 Broad Scale Currents

An extensive field data campaign was carried out in the mid-seventies in relation to investigating potential outfall sites along the coast between Porirua Harbour and Pipinui Point (10 km south of the Porirua Harbour entrance). This included a number of quantitative dye tests, drogue measurements and current meter deployments at nine sites (as detailed in MWD, 1975).

Unfortunately, the 1975 report contains limited quantitative information on observed currents but does contain a good description of the broad scale current offshore of the WWTP.

As noted in the report large eddies are formed near the Bridge during both the flooding and ebbing tide. This is confirmed by modelling carried out in the mid-seventies (Bradford and Wooding, 1975) who conclude that flows in the lee of Mana Island can be “complicated, and not well understood”.

During the early part of the flood tide a counter-clockwise eddy forms to the south of Mana Island (Figure 6-1) when winds are from the north. During the latter part of the flood tide (Figure 6-2) the predominant flows are to the north but it can be seen that flows are deflected offshore of Mana Island. During the early part of the ebb tide a counter-clockwise eddy forms to the south of Mana Island (Figure 6-3). During the latter part of the flood tide (Figure 6-4) the predominant flows are to the south with no evidence of an eddy.

Similar patterns of current occur when winds are from the south (Figures 6-5 to 6-8).

Model results (Figures 6-9 to 6-12) show similar patterns of strength of currents - although as noted in the MWD report general current direction shown in Figures 6-1 to 6-8 may often vary by $\pm 20^\circ$ and the velocity by ± 0.10 m/s.

Predicted currents across the Bridge (Table 3) are in broad agreement with the typical observed currents shown in Figures 6-1 through to 6-8 .

Table 3 Predicted percentile current speeds across the Bridge.

	Current Speed (m/s)
50 th percentile speed	0.42
75 th percentile speed	0.62
90 th percentile speed	0.77
Maximum speed	1.03

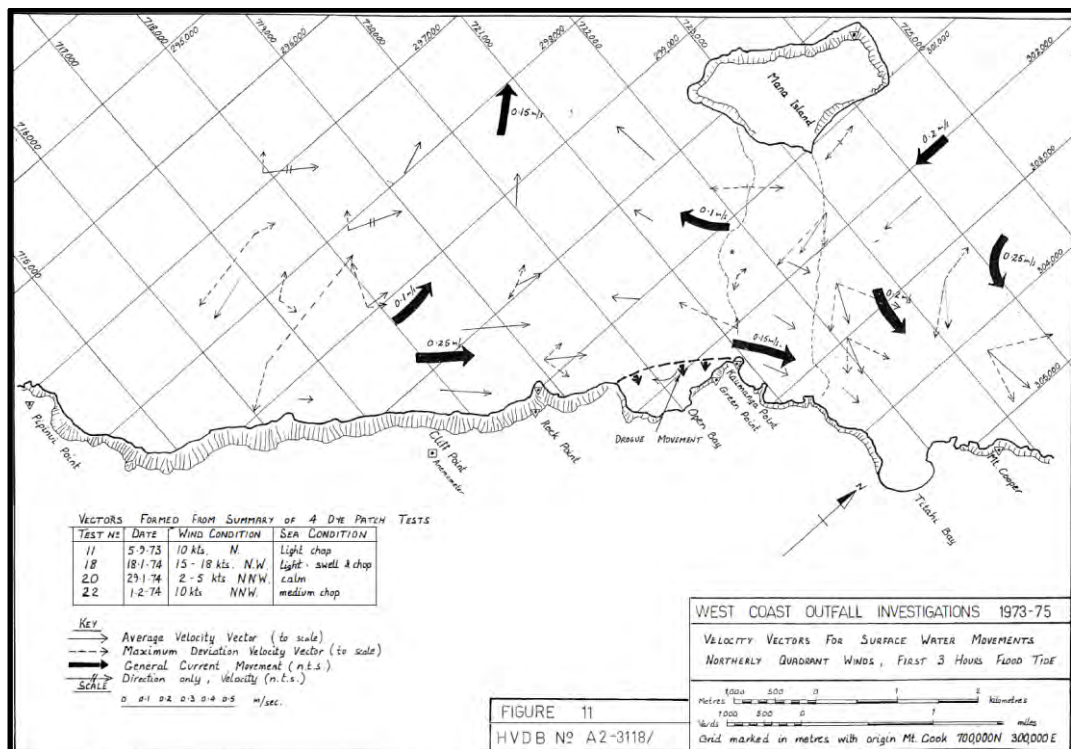


Figure 6-1. Broad scale current patterns to the south of Porirua Harbour during the first three hours of a flood tide for winds from the north. Data is derived from a combination of dye test data and drogue tracks (MWD, 1975).

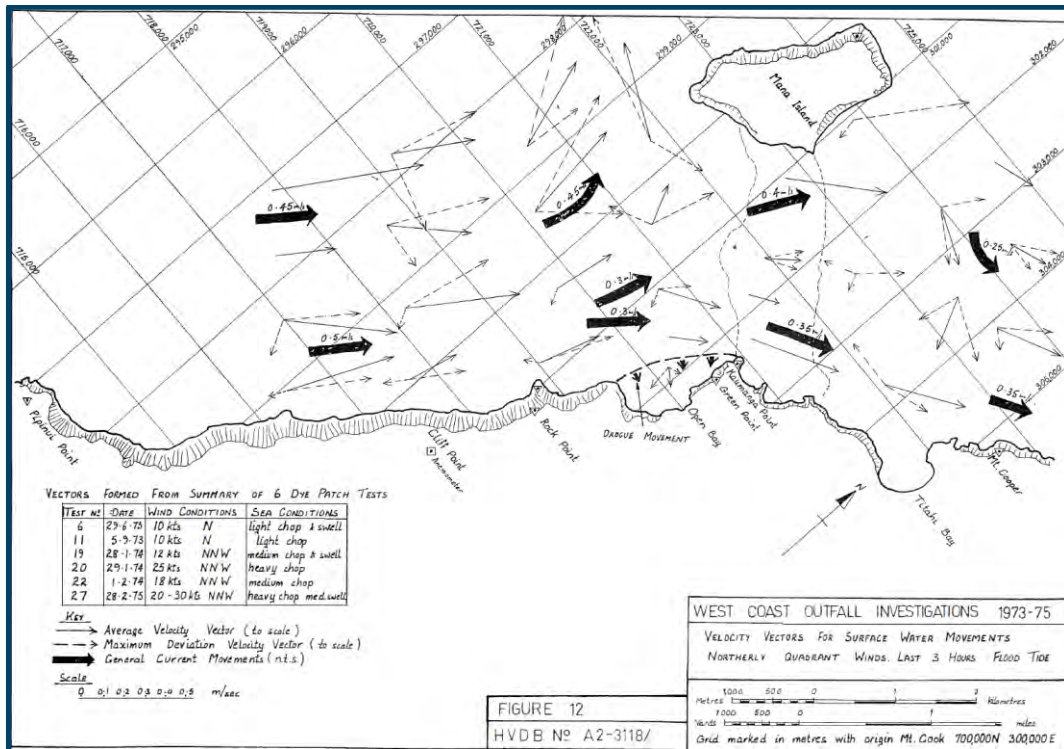


Figure 6-2. Broad scale current patterns to the south of Porirua Harbour during the last three hours of a flood tide for winds from the north. Data is derived from a combination of dye test data and drogue tracks (MWD, 1975).

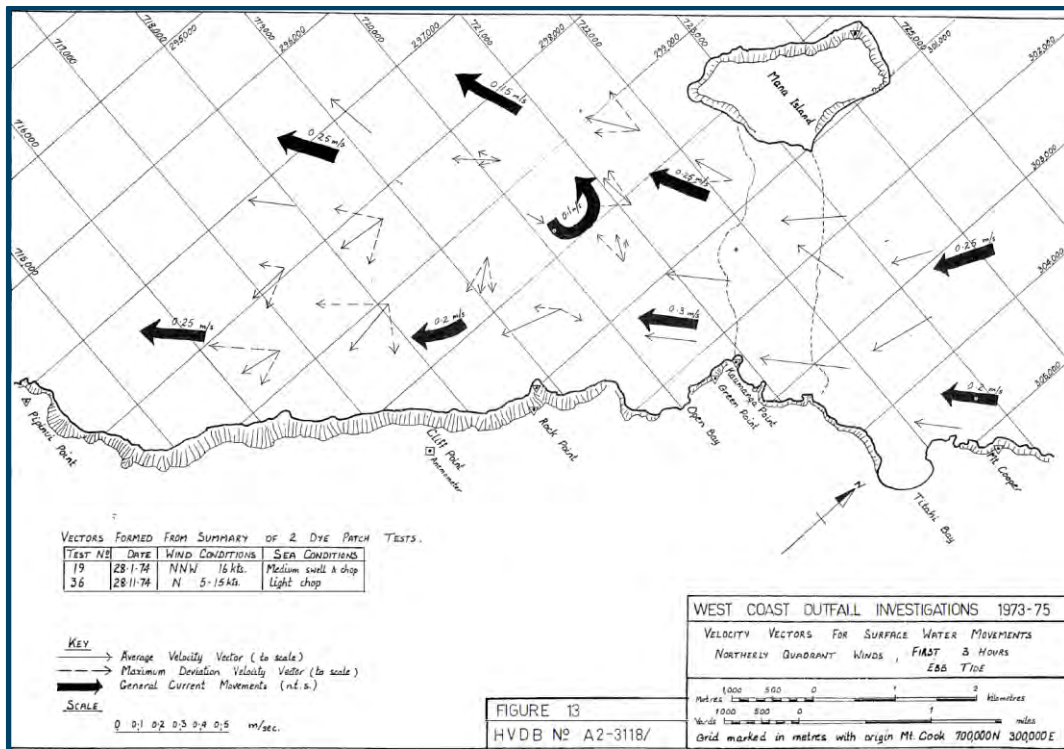


Figure 6-3. Broad scale current patterns to the south of Porirua Harbour during the first three hours of an ebb tide for winds from the north. Data is derived from a combination of dye test data and drogue tracks (MWD, 1975).

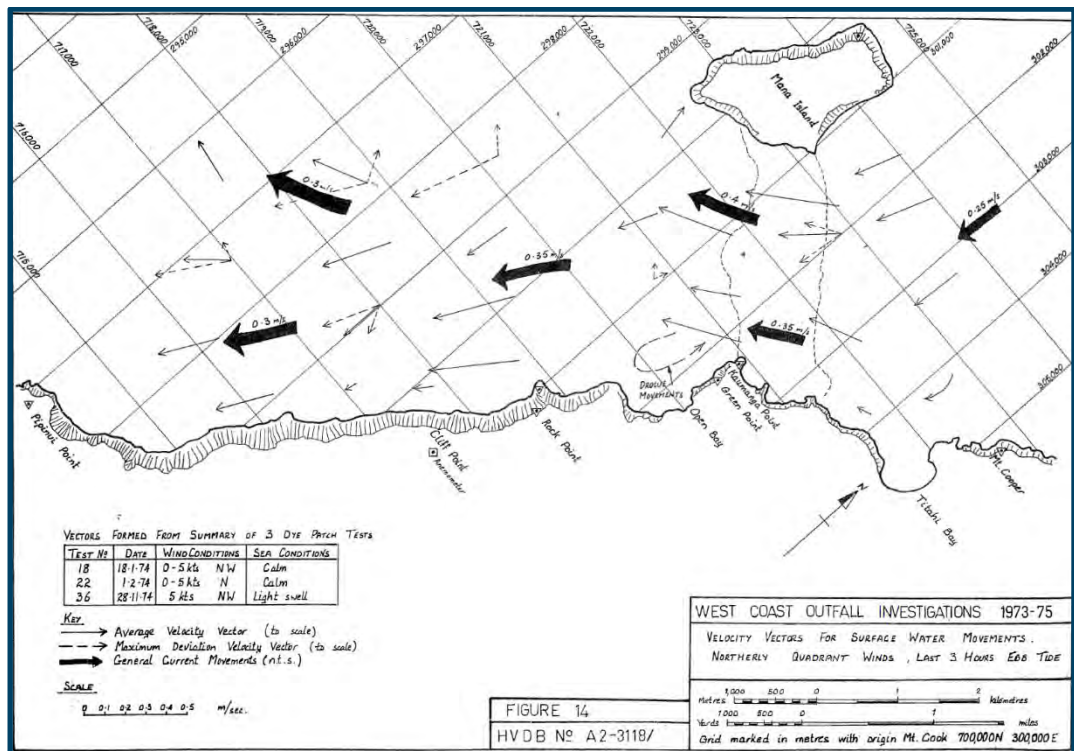


Figure 6-4. Broad scale current patterns to the south of Porirua Harbour during the last three hours of an ebb tide for winds from the north. Data is derived from a combination of dye test data and drogue tracks (MWD, 1975).

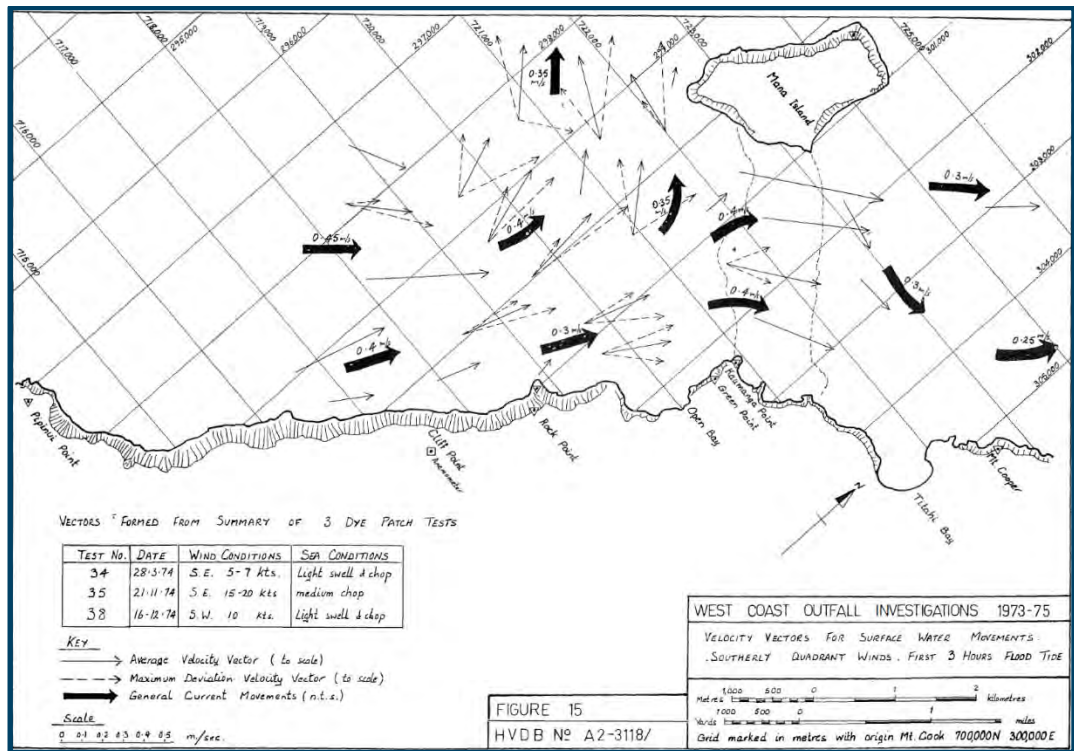


Figure 6-5. Broad scale current patterns to the south of Porirua Harbour during the first three hours of a flood tide for winds from the south. Data is derived from a combination of dye test data and drogue tracks (MWD, 1975).

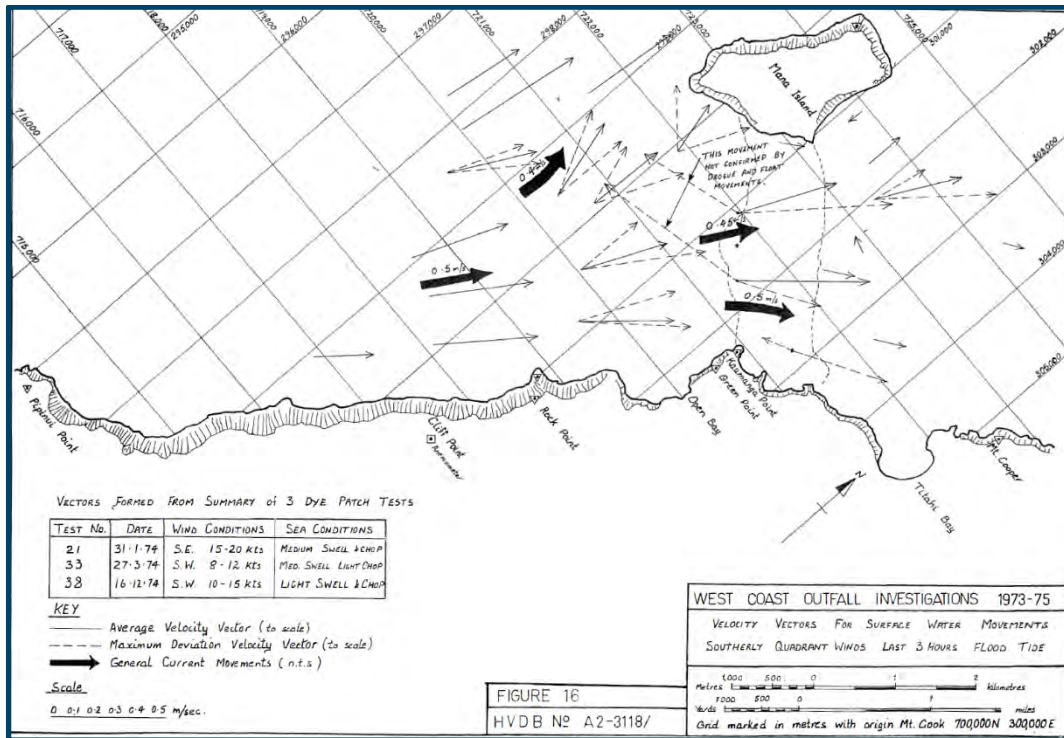


Figure 6-6 Broad scale current patterns to the south of Porirua Harbour during the last three hours of a flood tide for winds from the south. Data is derived from a combination of dye test data and drogue tracks (MWD, 1975).

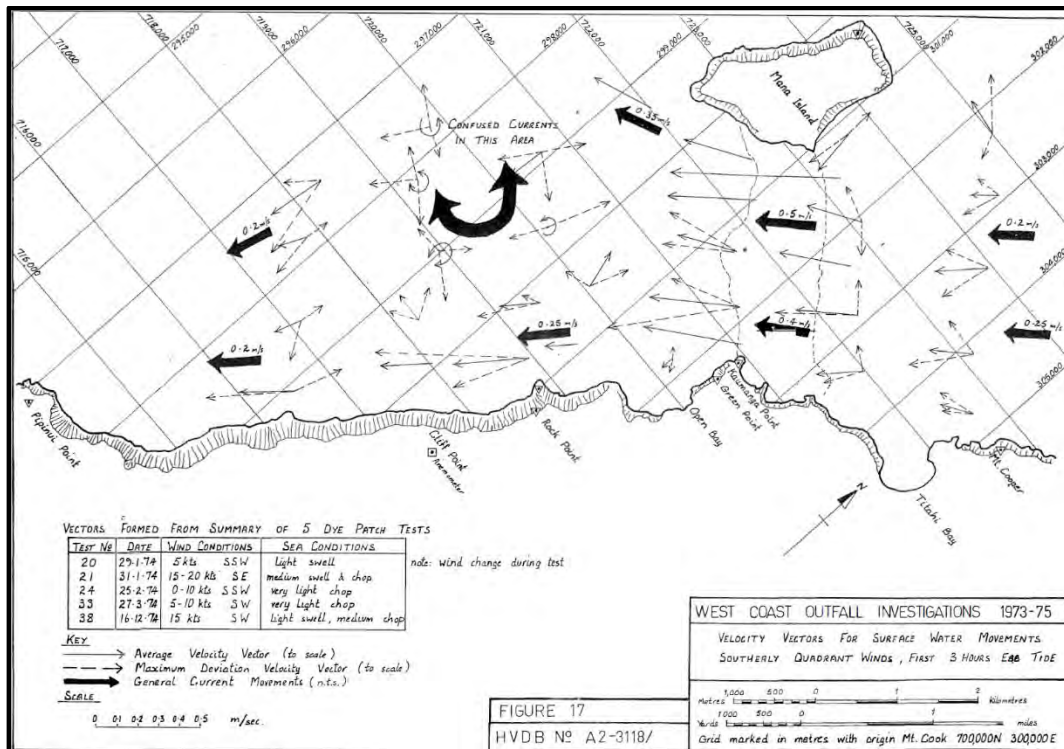


Figure 6-7. Broad scale current patterns to the south of Porirua Harbour during the first three hours of an ebb tide for winds from the south. Data is derived from a combination of dye test data and drogue tracks (MWD, 1975).

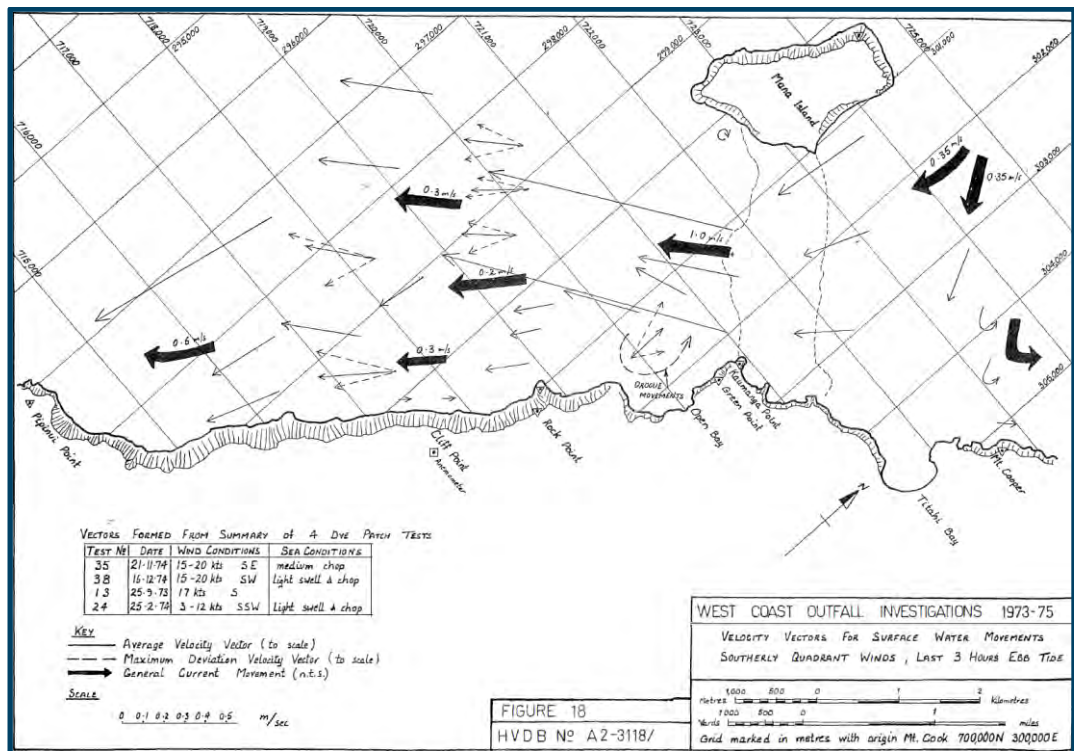


Figure 6-8. Broad scale current patterns to the south of Porirua Harbour during the last three hours of an ebb tide for winds from the south. Data is derived from a combination of dye test data and drogue tracks (MWD, 1975).

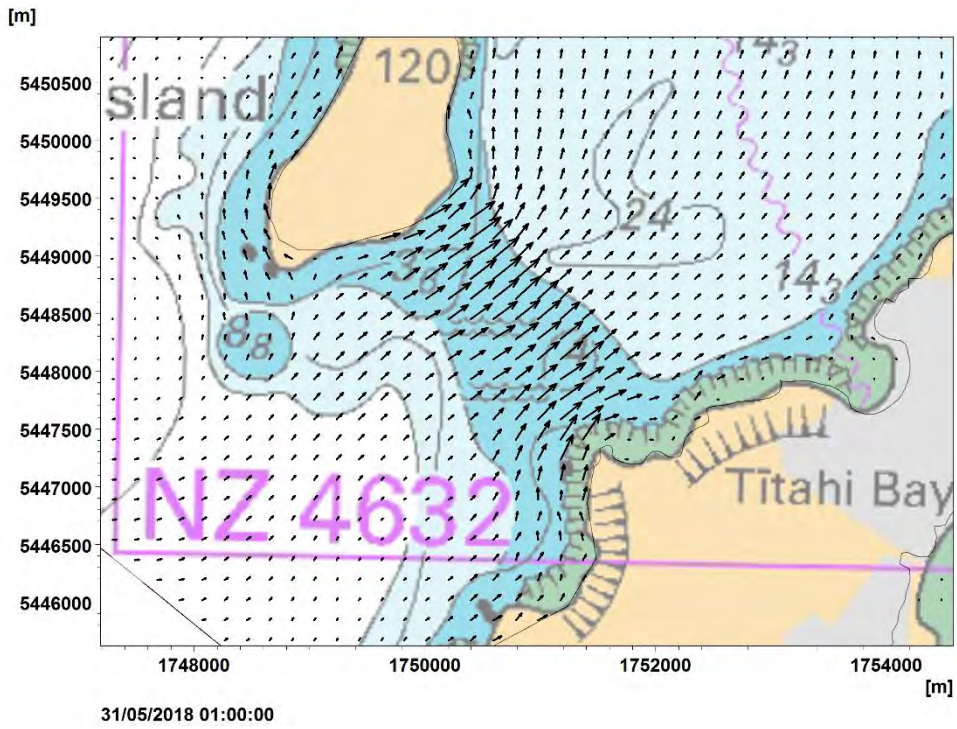


Figure 6-9. Typical broad scale currents during the early part of the flood tide.

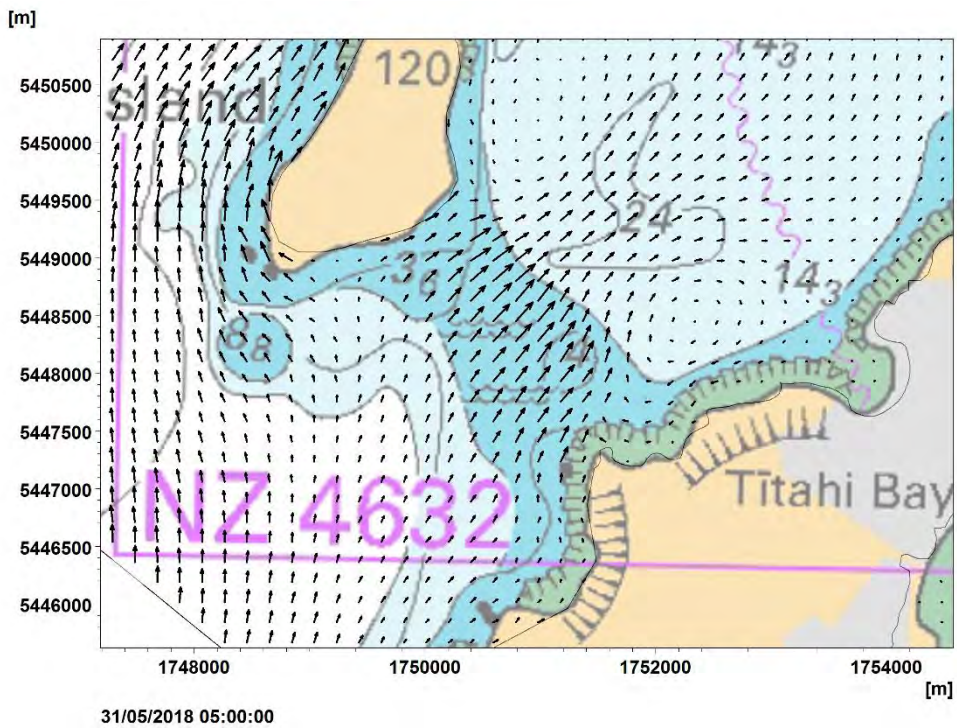


Figure 6-10. Typical broad scale currents during the latter part of the flood tide.

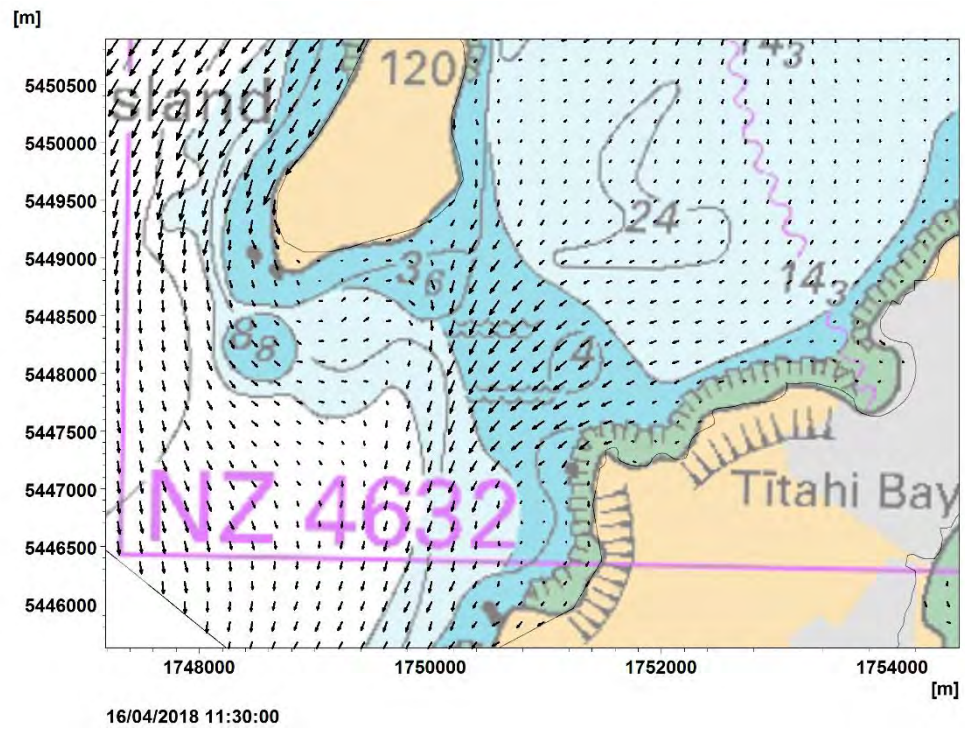


Figure 6-11. Typical broad scale currents during the early part of the ebb tide.

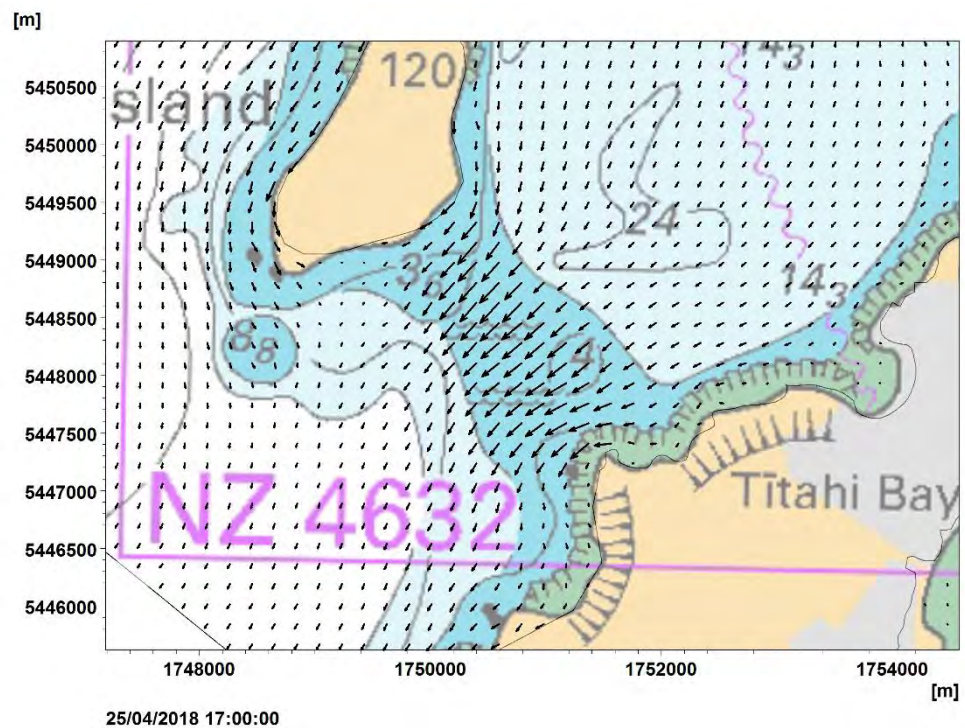


Figure 6-12. Typical broad scale currents during the latter part of the ebb tide.

6.2 Water Levels

Water levels at both the Mana Marina and from the ADCP have been used to calibrate the model.

Figure 6-13 shows the observed and predicted water levels from the model for the period of the first (unsuccessful) current meter deployment.

As shown in Table 4, the quantitative measures of the calibration show that the model performs very well with respect to predicted tides at the Mana Marina.

Note that the goodness-of-fit measures provide an indication of how well the modelled data fits the observation and are based on r^2 (the coefficient of determination), the coefficient of efficiency or Nash-Sutcliffe coefficient (Nash and Sutcliffe, 1970), and the index of agreement (Willmott et al., 1985).

Predicted water levels at the current meter site (Figure 6-14) show a similar level of agreement (Table 5) although for the later part of the deployment there is a shift in observed water levels which increases error estimates and reduces the goodness-of-fit measures.

This vertical shift in the observed values indicates some movement of the ADCP following the large wave event of the 22nd of May (Figure 3-2). Diver observations indicate active bedforms in the deployment indicating active sediment movement (particularly during wave events) and so a vertical movement of the order of those observed (0.1 m) is very probable (Marc Jary, Cawthron pers comm).

Overall, using typical qualitative descriptions (e.g. Moriasi et al. 2007), the model performance is “very good” in terms of predicting water levels.

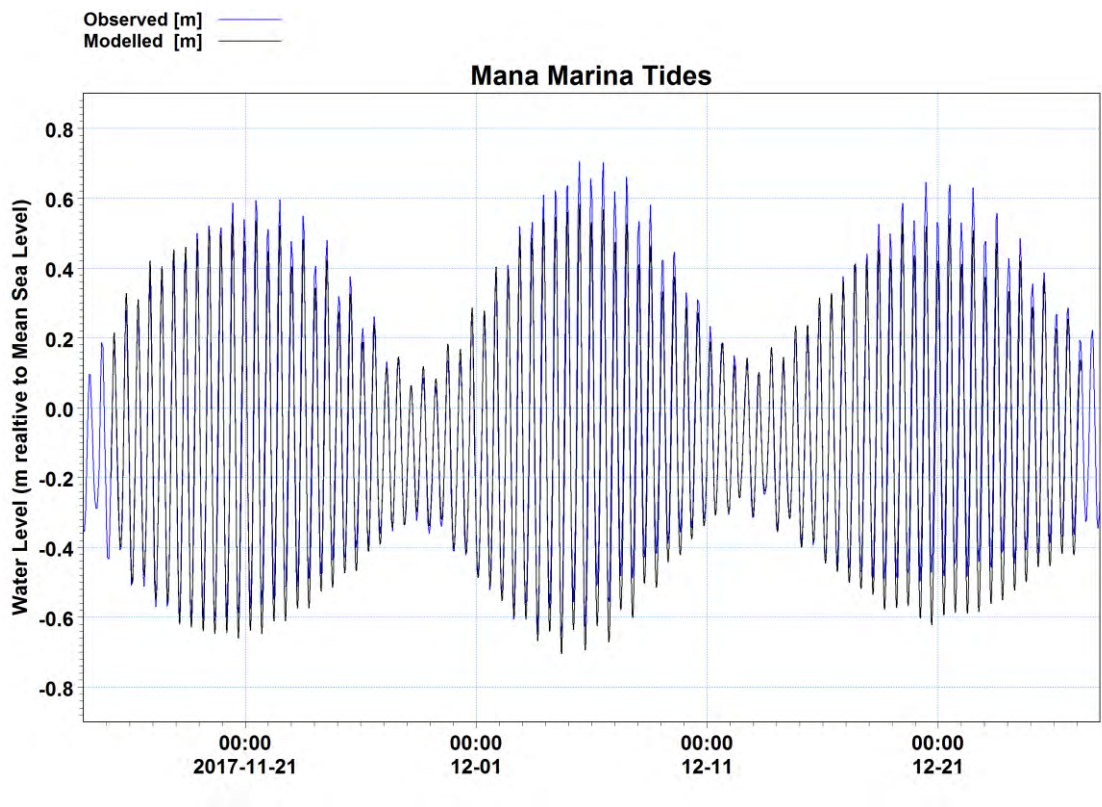


Figure 6-13. Observed and modelled water levels at the Mana Marina for the period of the first (failed instrument deployment). Observed data shown in blue and model predictions shown in black.

Table 4 Quantitative calibration values for water levels at Mana Marina.

Beach Monitoring Site	
Mean Error	0.0465
Mean Absolute Error	0.0718
Root Mean Square Error	0.0948
Standard deviation of residuals	0.0826
Coefficient of determination	0.9325
Coefficient of efficiency	0.9030
Index of agreement	0.9766

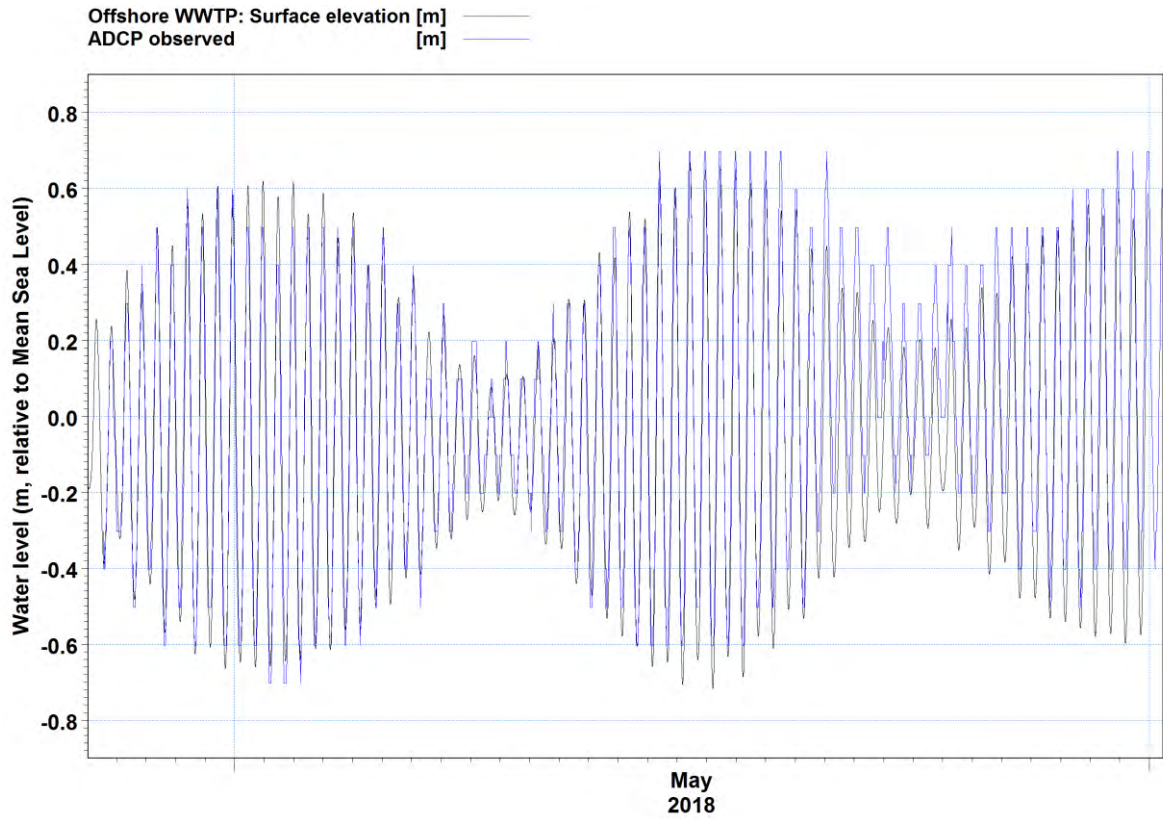


Figure 6-14. Observed and modelled water levels at current meter site. Observed data shown in blue and model predictions shown in black.

Table 5 Quantitative calibration values for water levels at the current meter site.

Beach Monitoring Site	Full record
Mean Error	0.0553
Mean Absolute Error	0.0927
Root Mean Square Error	0.1162
Standard deviation of residuals	0.1022
Coefficient of determination	0.9088
Coefficient of efficiency	0.8763
Index of agreement	0.9693

6.3 Currents

Depth-averaged currents from the current meter have been used to calibrate the model.

Overall the model under predicts the peak observed currents and does not predict the high degree of variability observed in the currents.

For example, between the 26th April and the 5th May (Figure 6-15) the peak currents during the spring tides are not well reproduced by the model although the phasing of the timing of the flood and ebb tide are reasonably well reproduced (Figure 6-16).

During the period of stronger northerly winds and associated waves (Figure 3-2) the predicted current strengths are reasonably well calibrated although the observed peak ebb tide current (every alternative peak in the figure) is not well represented in the model (Figure 6-17 and Figure 6-18) and although the phasing of the ebb and flood tides are again well reproduced (Figures 6-19 and 6-20).

During the latter part of the deployment the peak currents are underpredicted by the model (Figure 6-21) and the phasing of timing of the flood and ebb tide are reasonably well reproduced (Figure 6-22).

Table 6 shows the quantitative measures of the calibration and indicate that although the model does not reproduce the observed variability (i.e. Root Mean Square Error and Standard deviation of residuals) it still provides a “good” level of prediction of the currents at the current meter site using the typical qualitative descriptions of Moriasi et al. 2007.

This calibration, along with the qualitative calibration of broader scale currents, provide confidence in the model’s ability to reproduce both the broad scale currents offshore of Porirua Harbour and the currents in the near shore zone which transport the treated wastewater plume.

Further work could be carried out to improve the calibration of the hydrodynamic model including increasing the resolution of the model across the Bridge and the area immediately offshore of the WWTP, the inclusion of a wave model and investigating the use of spatially varying winds fields. However, as discussed in the next section the model performs very well in terms of predicting the treated wastewater concentrations at the beach monitoring sites so while extra work could improve the predictive capability of the model offshore of the WWTP (i.e. 10 m plus water depth and 500-1000 m offshore) such effort may not improve the predictive capability of the model with respect to the movement of the treated wastewater plume in the near shore/intertidal area.

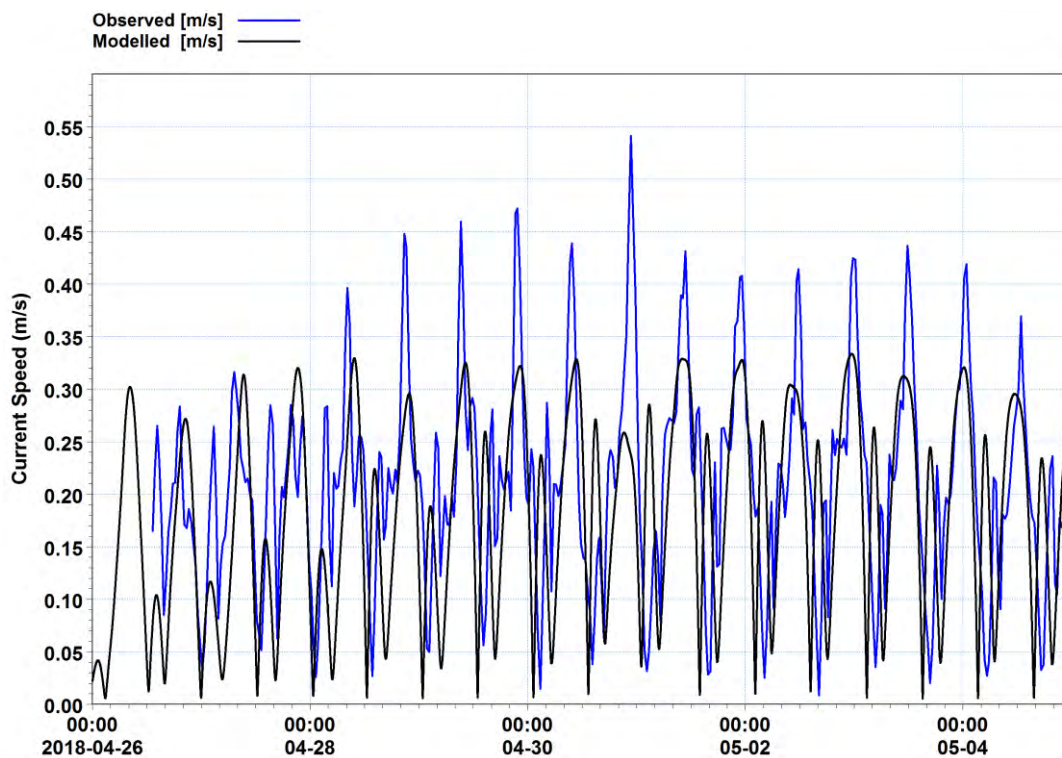


Figure 6-15. Observed and modelled depth-average current speed 26th April through to 5th of May 2018. Observed data shown in blue and model predictions shown in black.

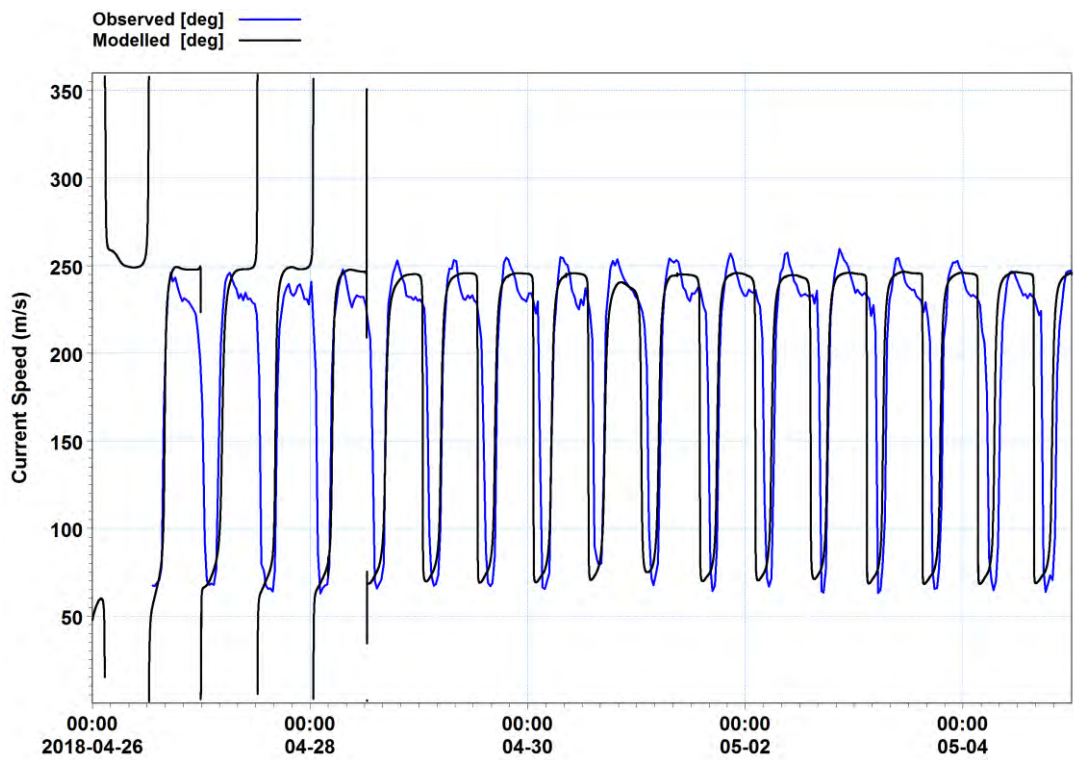


Figure 6-16. Observed and modelled current direction for the period 26th April through to 3rd May 2018. Observed data shown in blue and model predictions shown in black.

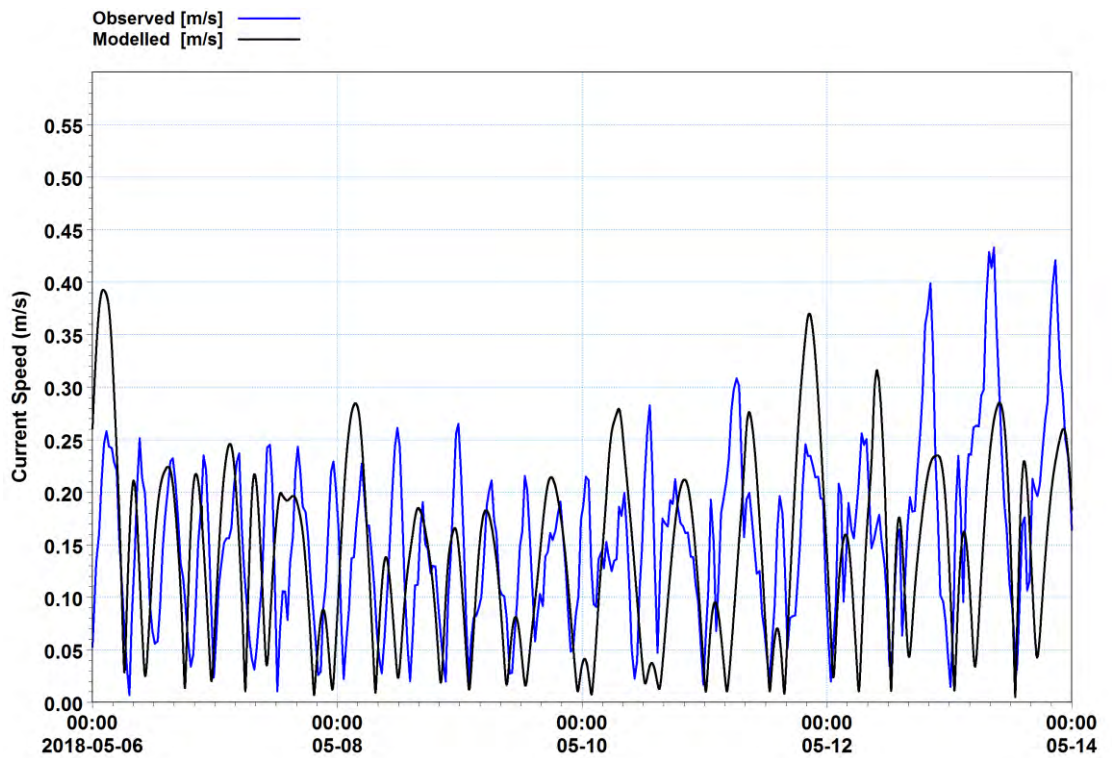


Figure 6-17. Observed and modelled depth-average current speed 6th May through to 14th of May 2018. Observed data shown in blue and model predictions shown in black.

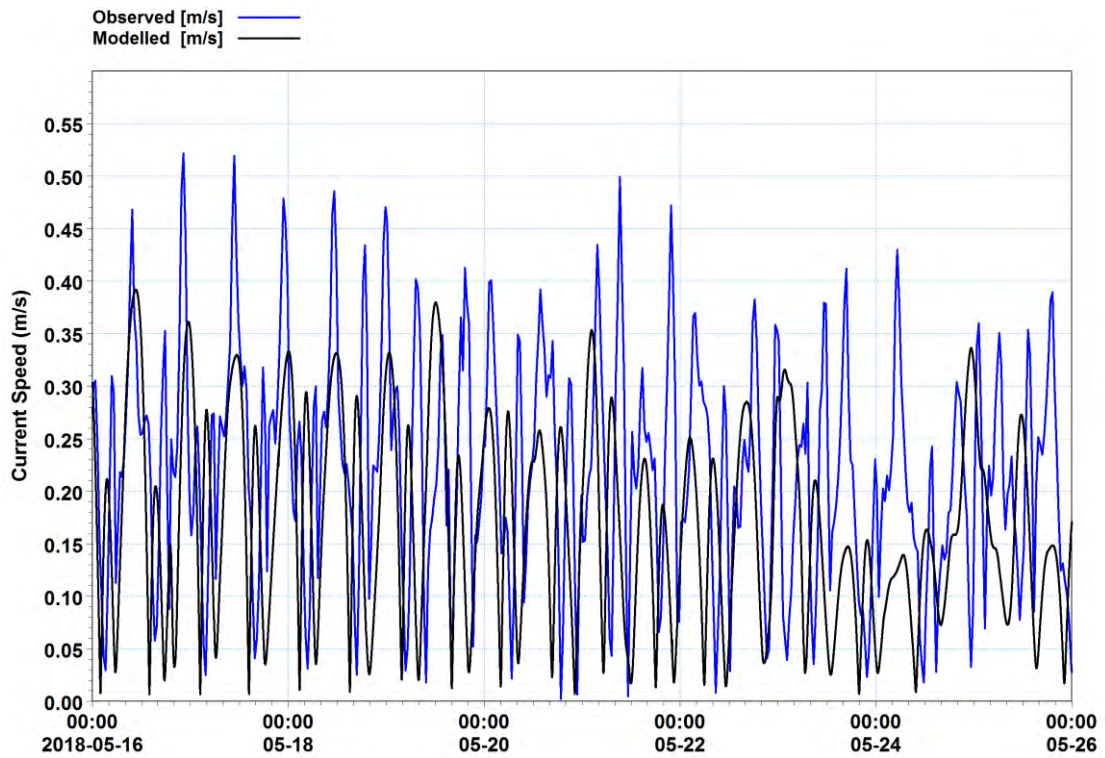


Figure 6-18. Observed and modelled depth-average current speed 16th May through to 25th of May 2018. Observed data shown in blue and model predictions shown in black.

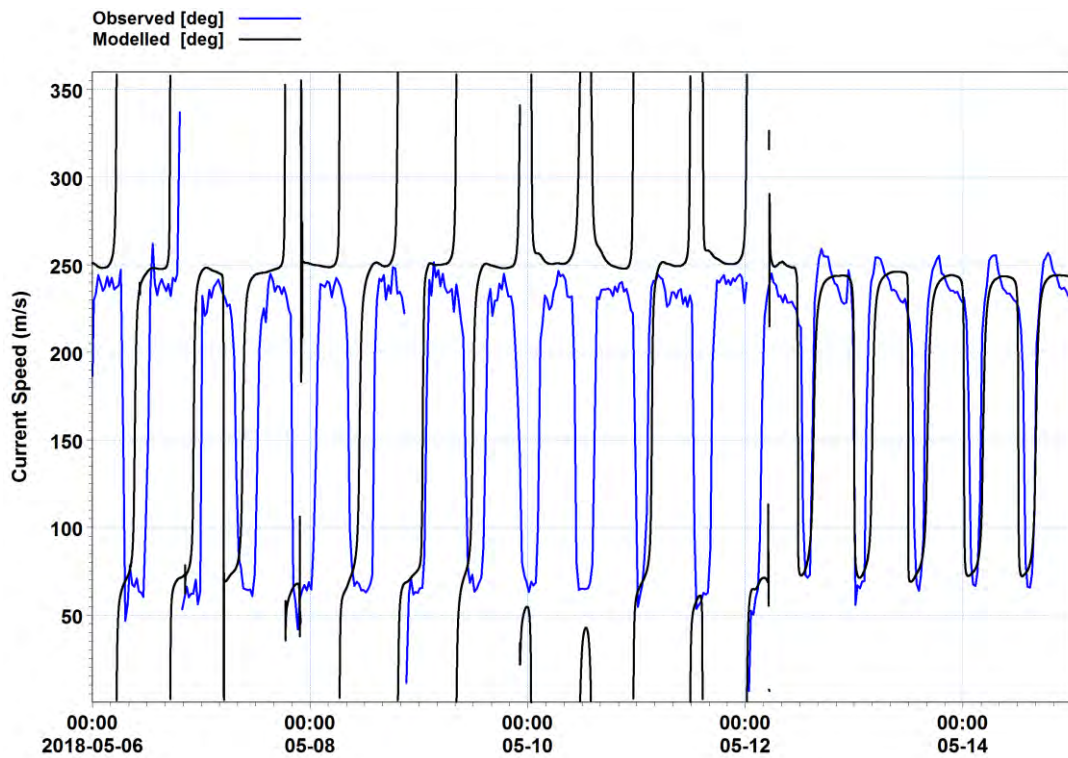


Figure 6-19. Observed and modelled depth-average current direction 6th May through to 14th of May 2018. Observed data shown in blue and model predictions shown in black.

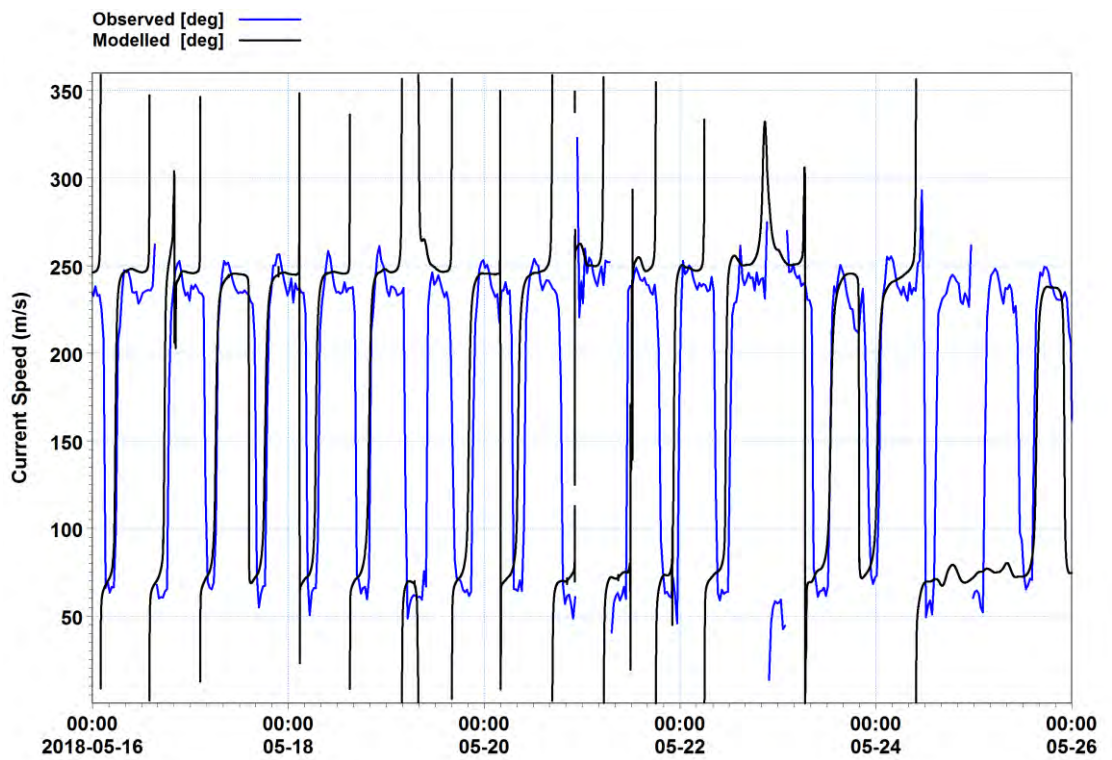


Figure 6-20. Observed and modelled depth-average direction 16th May through to 25th of May 2018. Observed data shown in blue and model predictions shown in black.

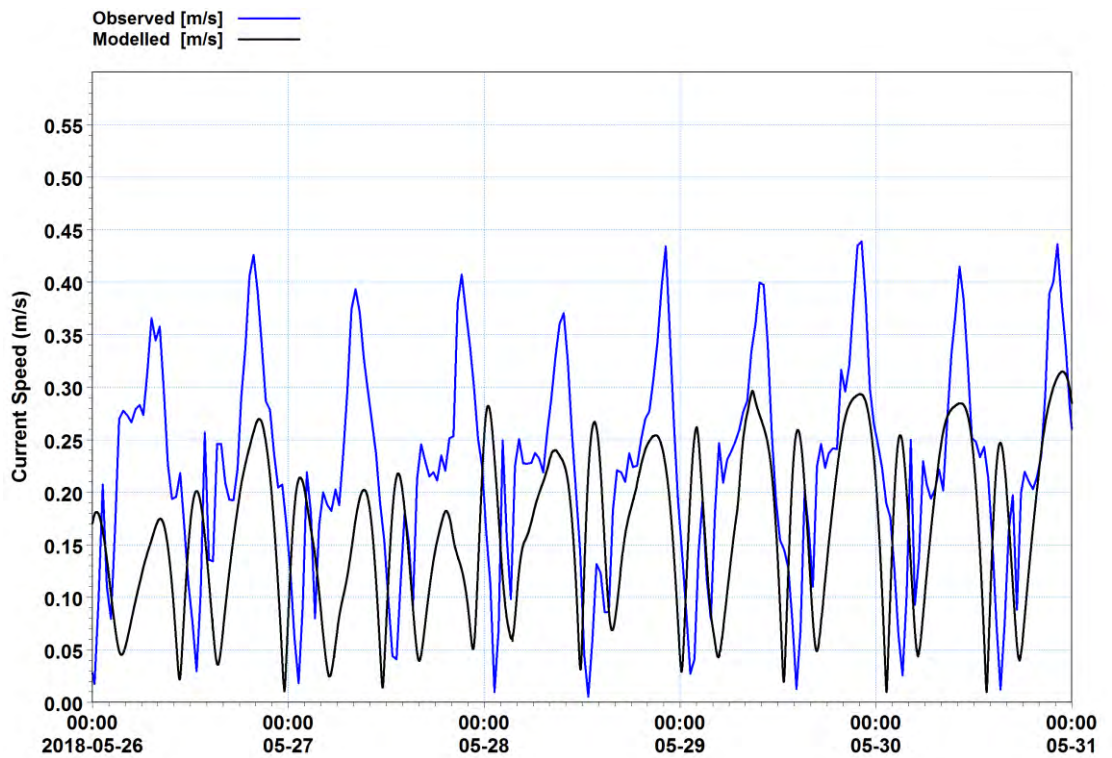


Figure 6-21. Observed and modelled depth-average current speed 26th May through to 31st of May 2018. Observed data shown in blue and model predictions shown in black.

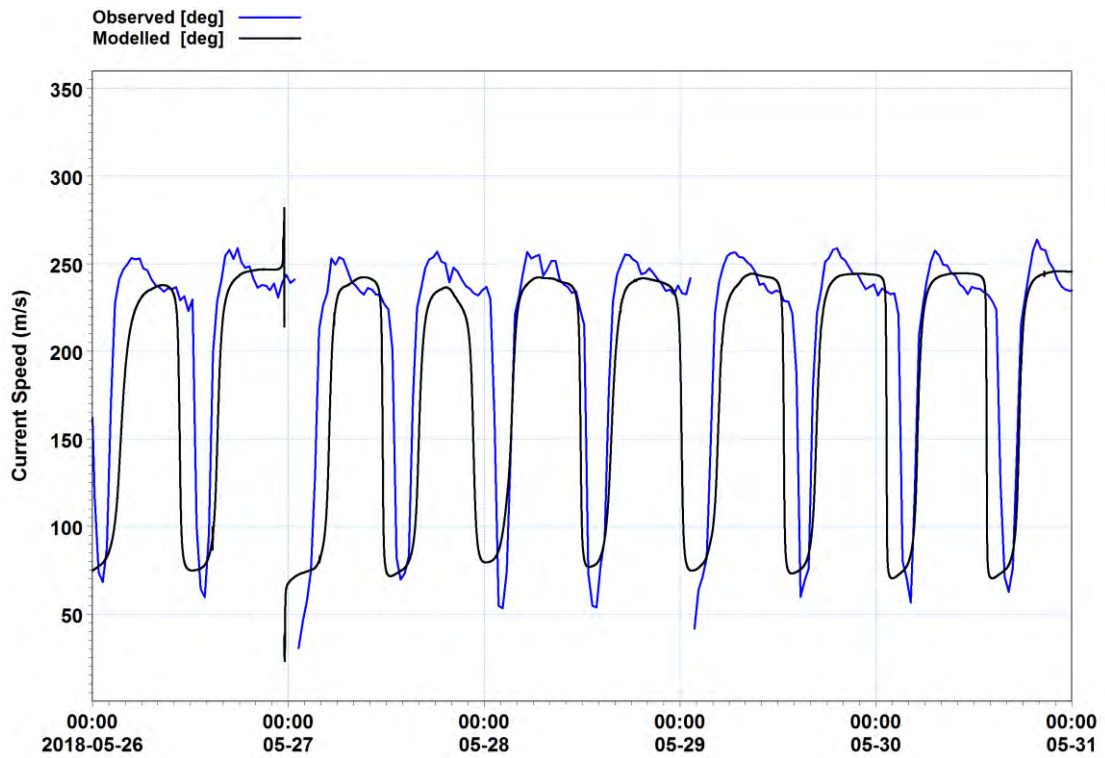


Figure 6-22. Observed and modelled depth-average direction 26th May through to 31st of May 2018. Observed data shown in blue and model predictions shown in black.

Table 6 Quantitative calibration values for current speed at the current meter site.

Beach Monitoring Site	Full record
Mean Error	0.0326
Mean Absolute Error	0.0958
Root Mean Square Error	0.1173
Standard deviation of residuals	0.1127
Coefficient of determination	0.1039
Coefficient of efficiency	0.6701
Index of agreement	0.5803

6.4 Contaminant Concentrations at Monitoring Sites

Having calibrated the hydrodynamic model, the next step in the calibration process was to ensure that the predicted dispersion of contaminants from the discharge are adequately modelled.

The calibration involved using the predicted dispersion coefficient ($0.037 \text{ m}^2/\text{s}$) and running a series of long-term model simulations (for the period chosen as being representative, Section 5) with different decay rates to match the observed ratio of treated wastewater Faecal Coliform concentrations at each of the beach monitoring sites.

If the decay rate is set too high there will be more inactivation of faecal coliform and predicted concentrations at the beach monitoring sites would be too low. Conversely, a lower decay rate would result in less inactivation and higher predicted concentrations at the beach sites.

It was found that a decay rate of 0.083 h^{-1} provided the best overall fit and lowest sum of squares error against the observed data (Table 7). This value is close the typical observed decay rates that occur at depth in saline waters of 0.104 h^{-1} (Maraccini et. al, 2016) and slightly lower than the typical summer daylight decay rates for enterococci of 0.140 h^{-1} (e.g. Noble et. al 1999)

With this decay rate, the model provides good estimates of the mean concentration (averaged over the 85 paired observations) at all of the beach monitoring sites except for Mount Cooper. As discussed in the results section of the report, it is only during sustained south-westerly winds that the model predicts the typical observed levels of contamination along the shoreline at Mount Cooper. At other times, it is likely that sources of contamination other than the WWTP discharge are influencing the observed contaminant levels at the Mount Cooper site.

Could be done but very sporadic data and data include obvious overflows (which the mean comparison approach. Have full daily flow but no effluent quality data, would need to interpolate between data. How representative is the daily effluent quality data The monitoring data has no time just a state of tide so large errors. Plus replicates from Safeswim so huge variations.

There are very few events in the time-series data where there is a period of high discharge concentration and matching elevated observations at the monitoring sites. There are periods where high observations occur when discharge concentrations are very low (indicating other overflows). The model could be run for a full two years but this would provide maybe 6 –8 points on a calibration plot. Using the regression approach ignores some of the outliers (associated with overflows)

Table 7 Calibration of Faecal Coliform decay parameter against beach monitoring data.

Beach Monitoring Site	Observed Mean Concentration (as percent of Treated Wastewater)	Decay Rate 0.139 h ⁻¹	Decay Rate 0.083 h ⁻¹	Decay Rate 0.060 h ⁻¹	Decay Rate 0.046 h ⁻¹
200m south west of the outfall	7.10	5.66	8.75	10.17	11.42
200m east of the outfall	2.80	2.31	2.94	3.55	3.88
Titahi Beach (South)	0.60	0.34	0.78	1.15	1.46
Titahi Beach	0.30	0.07	0.19	0.36	0.51
Ti Korohiwa Rocks	0.50	0.28	0.56	0.84	1.03
Mount Cooper	0.20	0.00	0.01	0.03	0.05
Overall ratio of predicted to observed		0.70	1.15	1.26	1.42
Sum of errors		-2.84	1.73	4.60	6.85

6.5 Near field processes (New Section)

The use of a two-dimensional model to accurately simulate the dynamics of a buoyant treated wastewater plume into the marine receiving environment is reliant on accurately schematising the near-field mixing processes into the two-dimensional model. This can only be achieved if the plume becomes fully-mixed in the vertical.

Jirka et al. (1981) define the near field as the region where momentum dominates over buoyancy. In this region the plume dynamics are driven by the enhanced velocities of the discharge as it initially enters the coastal region. In this region the momentum of the jet generates significant turbulence, which can result in rapid horizontal and vertical mixing of the plume with ambient waters and entrainment of ambient waters into the near-field region.

Beyond the near-field, the plume becomes passive (i.e. its momentum does not affect local hydrodynamics) and the combined effects of its buoyancy and the ambient receiving environment dominant its dynamics.

The area immediately offshore of the Titahi outfall is complex (Figure 6-23) and the outfall structure sits above the water surface (Figure 2-2).

Near-field models (such as VISJET (Cheung et al. 2000) or CORMIX (Doneker and Jirka, 2007)) generally assume uniform bathymetry and ambient currents in the immediate vicinity of a discharge and have physical restrictions on how discharge structures can be represented within them. For example, the height of a discharge above the water surface in CORMIX is limited to a certain ratio of discharge height to water depth.

However, to provide some quantification of the near-field mixing of the Titahi discharge a number of CORMIX simulations (for combinations of water level and ambient currents) have been carried out which indicate that that rapid vertical mixing will occur within the near-field due to a combination of entrainment of ambient seawater into the discharge area and downward vertical mixing due to the outfall configuration.



Figure 6-23. Area immediately offshore of the Titahi Bay outfall.

CORMIX model results indicate that the treated wastewater plume would occupy the top 70-90% of the water column and that within 25-50 metres the salinity within the plume itself would increase from 0 PSU to between 10 and 30 PSU. These salinity results from the CORMIX runs are in reasonable agreement with the MIKE21 results (Figure 6-24 – discussed in detail in Section 7).

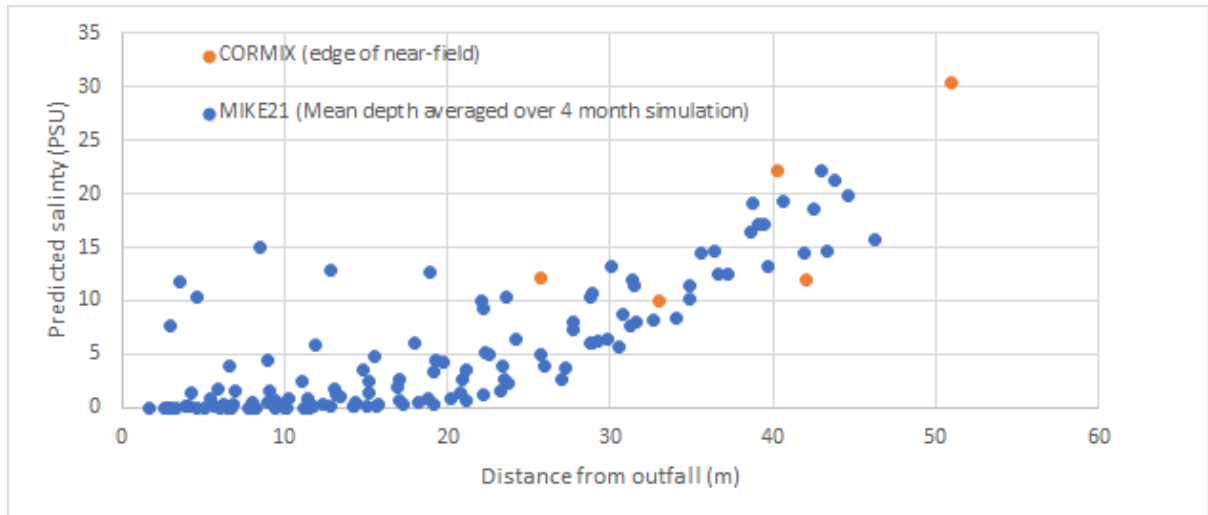


Figure 6-24. Model results from schematic CORMIX model simulations and the results from the MIKE21 average discharge scenario in the immediate vicinity of the discharge point.

Such increases in salinity in the near-field will significantly reduce the buoyancy of the treated wastewater plume. Strong stratification (i.e. a layer of freshwater overlying ambient seawater) can only be maintained occur if there is a large volume of freshwater being discharged relative to the tidal velocity in the receiving environment. For example, Geyer and Farmer (1989) indicate that strong stratification can only be maintained in an estuarine setting when freshwater plume discharges result in a current in excess of 10-30% the typical tidal current.

The current due to the Titahi outfall discharge will be very small beyond the nearfield region and so any stratification that does occur beyond the near-field will be quickly broken down by diffusion and turbulent mixing (due to currents and waves).

An analysis of monitoring data shows 0.5 m waves occur 23% of the time, 1.0 m waves 16 % of the time and 2.0 m waves 8% of the time. Data from the ADCP deployment period show similar statistics (i.e. waves of greater than 0.5 m occur for 40% of the time and waves greater than 1.0 m occur for 14% of the time).

Based on these results, the difference between a 2D model (which assumes full-vertical mixing within the near-field) and a 3D model (where the near-field stratification is schematised into the layers of the model within the near-field) would be relatively small even in the immediate vicinity of the discharge. Beyond this, the differences between a 2D model and 3D model will minimal.

One other important process that a 2D model does not include is the additional movement of the surface layer of water due to winds. The depth to which the wind stress may affect the currents is dependent on wind speed (Weber, 1983, Chang et al. 2012). Wind stress is included in the MIKE21 model and will have the most influence in shallow water. That is, currents are enhanced by the presence of winds in the 2D model.

In terms of model results this will mean that the 2D model may under predict the offshore movement of the surface layer of the treated wastewater plume during periods of offshore winds (model results will be higher in the near shore zone) but at other times the 2D model will perform reasonably well with respect to the movement of the treated wastewater plume.

Based on the Mana Island wind record winds from the south-east (i.e. offshore) occur for 27% of the time and, for sustained events², mean speeds of between 5 and 7 m/s can occur. Approximately three-quarters of the sustained events are less than 20-hour duration.

However, even within such events there are significant variations in wind speed and direction that do occur and the net effect of wind driven surface currents on the movement of the treated wastewater plume will be minimal - the surface plume excursion distance will be underestimated by the 2D model when winds are blowing in the direction of the tidal current but equally if the wind opposes the tidal currents the surface plume excursion distance predicted by the 2D model maybe more than would be observed.

The potential magnitude of the differences in model predictions can be illustrated by examining results from a 2D and 3D model with a schematic wind condition.

The calibrated 2D model was setup as a 5-layer 3D model³. At the discharge site, the surface layer would represent a layer 20 cm thick at low water. All of the treated wastewater is released into this layer which represents a worst-case condition compared to the schematic CORMIX runs which indicated the treated wastewater could be present in the top 4 layers (80%) of the model (i.e. greater initial vertical mixing than assumed by the 3D model).

Both the 2D and 3D models were run for a schematic tide and wind scenario – a spring tidal range for 4 days with an 8 m/s wind from the south for two days (transporting the treated wastewater plume offshore) followed by an onshore 8 m/s wind for 2 days which then transports the plume towards the coast and the monitoring sites. In the absence of any calibration data, the vertical dispersion in the 3D model was setup using a scaled eddy viscosity formulation⁴.

Model results for the 2D model are shown in Figure 6-25 while those from the 3D model are shown in Figure 6-26.

Apart from the area in the immediate vicinity of the discharge the results show very subtle differences.

The predicted plume footprint from the 2D model extends slightly further north than the 3D model (because the plume tends to be transported closer to the coast and is therefore advected by stronger near-shore wind driven currents compared to the 3D plume).

The plume is transported further offshore in the 3D model which is most apparent offshore of Titahi Beach.

At a site in 5 m water depth (~300 m offshore of Titahi Beach) the average salinity in the surface layer of the 3D model is predicted to be 31.6 PSU (equivalent to a dilution of 80) compared to the 2D model prediction of 31.8 PSU (equivalent to a dilution of 160).

At a site closer to the beach itself the difference between the two models is much less - 31.34 PSU in the surface layer of 3D model (an equivalent dilution 48) compared to 31.39 PSU in the 2D model (an equivalent dilution of 52).

At a site 50 m north-east of the outfall the average salinity in the surface layer of the 3D model is predicted to be 29.3 PSU (equivalent to a dilution of 11.8) compared to the 2D model prediction of 29.4 PSU (equivalent to a dilution of 12.4).

² Offshore winds that occur for more than 3-hour duration.

³ The water column in the 5-layer model is represented by 5 equally spaced layers in the water column.

⁴ Adjusting this factor would from the basis of any calibration and/or sensitivity testing of the 3D model.

At a site 100 m north-east of the outfall the average salinity is predicted to be 31.30 PSU in the surface layer of the 3D model (an equivalent dilution 46) compared to a predicted salinity of 31.52 PSU in the 2D model (an equivalent dilution of 67).

These predicted differences would be much less if 1) it was assumed some degree of vertical mixing in the near-field (i.e. not the worst-case assumption of the full discharge in the surface layer of the 3D model) and 2) any enhanced mixing due to waves were to be included in the model.

Figure 6-27 shows the difference in predicted salinity within the surface layer of the 3D model and the 2D model results. It can be seen that it is only within the first 50-100 m of the discharge that there is any significant difference between the two modelling approaches with regard to predicted salinity.

These results indicate that the used of 3D model would be justified if;

- 1) Accurate predictions of treated wastewater concentrations were required inside the near-field (i.e. inside the statutory 200 m mixing zone),
- 2) More accurate model results were required at deep water sites for periods of sustained offshore winds.

Figure 6-27 also illustrates the zone where vertical stratification of the water column could be expected to be observed (i.e. where significant differences in observed salinities and contaminants in the vertical could be expected). Within this zone any observations would have to include salinity meters at the both the surface and at depth.

Based on typical plume dynamics from the calibrated 2D model, three sites may be required, one in the pool in the immediate vicinity of the discharge another to the south-west (towards the 200m south-west monitoring site) and a third just offshore of the discharge site.

Beyond this zone a single point observation in the water column could be used. Based on the typical plume dynamics from the calibrated 2D model two sites maybe required some 50-100 m away from the discharge site.

Salinity data would need to be collected that covered a range of winds, tidal ranges and wave conditions so a deployment period of at least 2 weeks would be required to capture the spring-neap tidal variation. A longer period would probably be necessary to capture a range of winds.

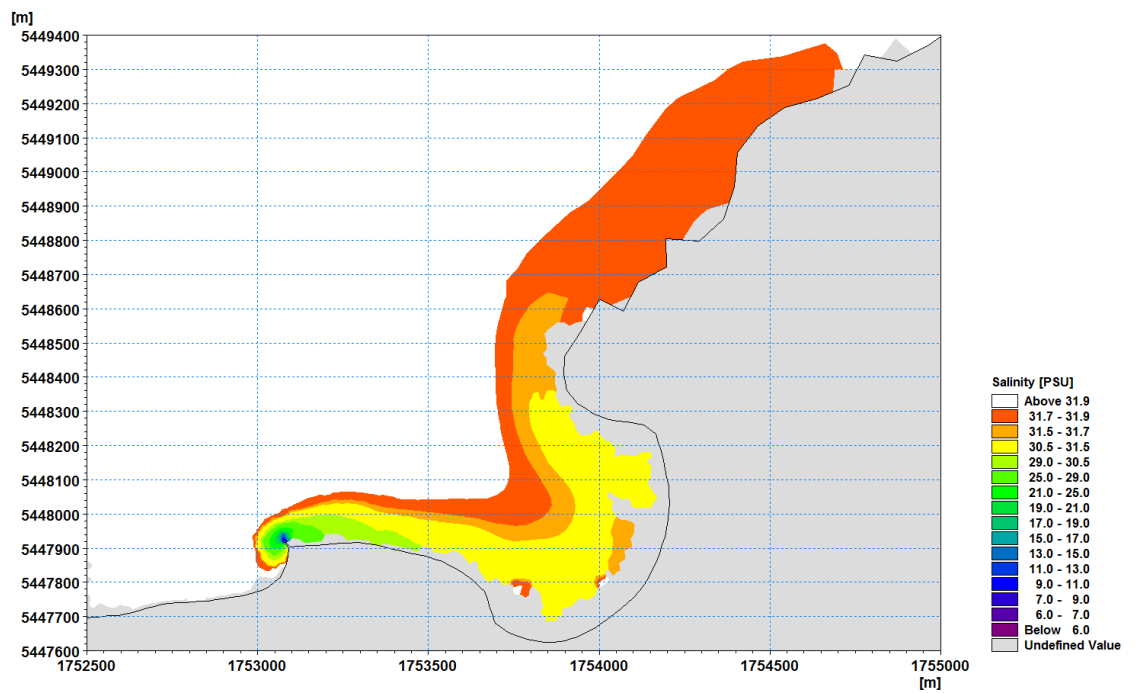


Figure 6-25. Predicted average salinity over the 4-day period of the schematic scenario from the 2D model.

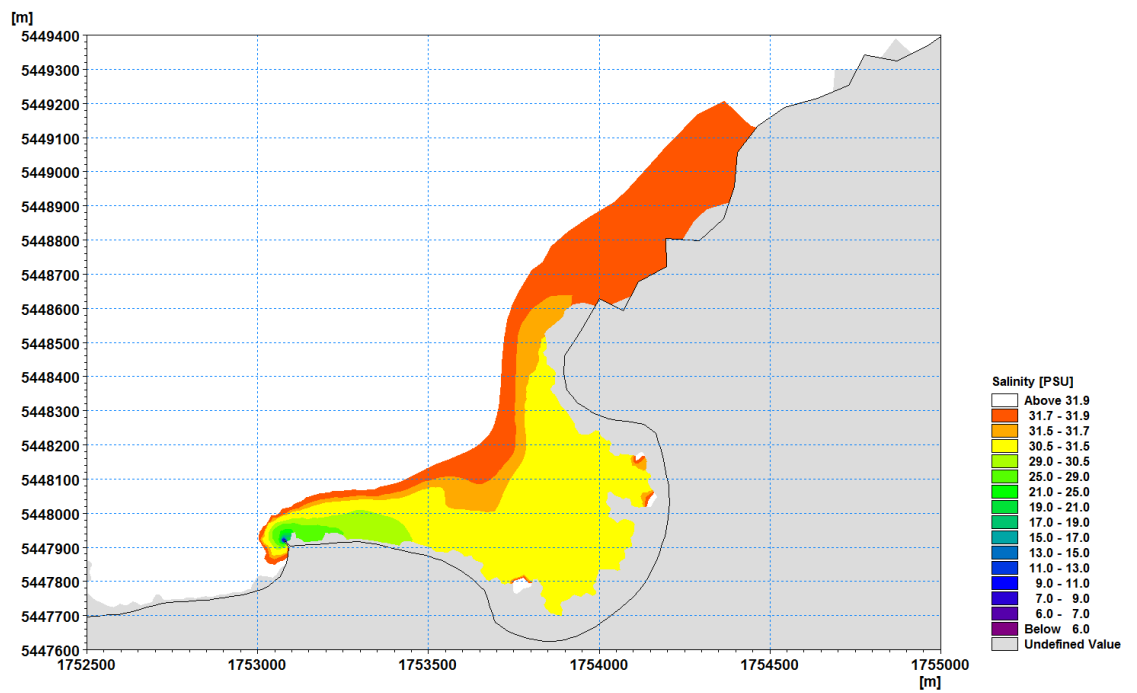


Figure 6-26. Predicted average salinity over the 4-day period of the schematic scenario from the top layer of the 3D model.

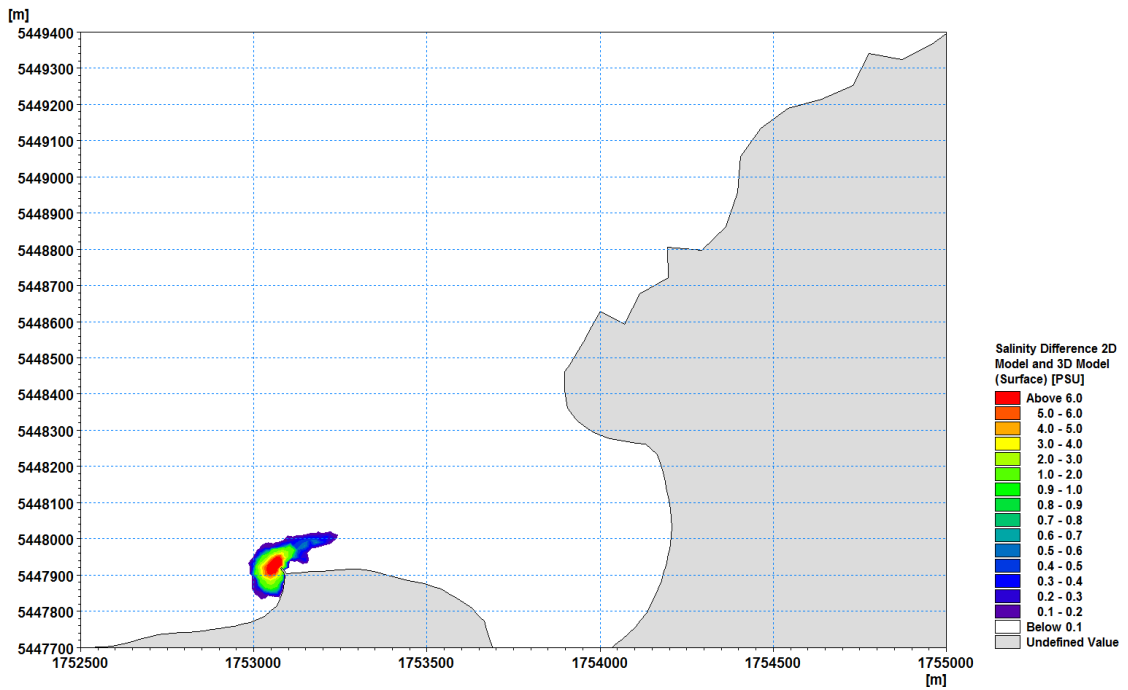


Figure 6-27. Difference in average salinity from the 2D model and the surface layer of the 3D model over the duration of the 4-day schematic scenario. Higher values occur in the 3D model because it has been assumed all the treated wastewater is discharged into the surface layer of the model.

7 Scenario Results

The calibrated model was run for the selected time period for the three discharge rates being considered average (300 L/s), peak (1100 L/s) and the design discharge (1500 L/s).

For each of these scenario runs the time-series of predicted concentrations at the beach monitoring sites is provided along with percentile estimates and spatial plots of the predicted 50th and 95th percentile concentrations.

Table 8 shows a summary of the predicted concentrations at the beach monitoring sites for the average discharge scenario. Figure 7-1 and Figure 7-2 show the time series plots of the predicted concentrations at the beach monitoring sites for the average discharge scenario while. Figure 7-3 shows the predicted mean salinity, while Figures 7-4 and 7-5 show the 50th and 95th percentile concentrations.

Table 9 shows a summary of the predicted concentrations at the beach monitoring sites for the peak discharge scenario. Figure 7-6 and Figure 7-7 show the time series plots of the predicted concentrations at the beach monitoring sites for the peak discharge scenario while. Figure 7-8 shows the predicted mean salinity, while Figures 7-9 and 7-10 show the 50th and 95th percentile concentrations.

Table 10 shows a summary of the predicted concentrations at the beach monitoring sites for the design discharge scenario. Figure 7-11 and Figure 7-12 show the time series plots of the predicted concentrations at the beach monitoring sites for the design discharge scenario while. Figure 7-13 shows the predicted mean salinity, while Figures 7-14 and 7-15 show the 50th and 95th percentile concentrations.

These results can be used to assess how the dynamics of the treated wastewater plume changes with the different discharge rates and to assess the relative risk associated with the average, peak and design discharge rates.

All results are presented in terms of percentage treated wastewater so that further improvements in wastewater quality associated with any future scenarios being considered scenarios can also be assessed.

7.1 Average Discharge Scenario

Table 8. Average and percentile concentrations (% treated wastewater) at beach monitoring data for the average WWTP discharge rate of 300 L/s.

Site	Average concentration (% treated wastewater)	75 th percentile concentration (% treated wastewater)	90 th percentile concentration (% treated wastewater)	95 th percentile concentration (% treated wastewater)
200m south west of the outfall	8.750	10.811	13.151	14.588
200m east of the outfall	2.935	4.572	5.443	5.832
Titahi Beach (South)	0.776	1.159	1.694	2.028
Titahi Beach	0.193	0.288	0.461	0.612
Ti Korohiwa Rocks	0.561	0.707	1.025	1.249
Mount Cooper	0.015	0.017	0.041	0.061

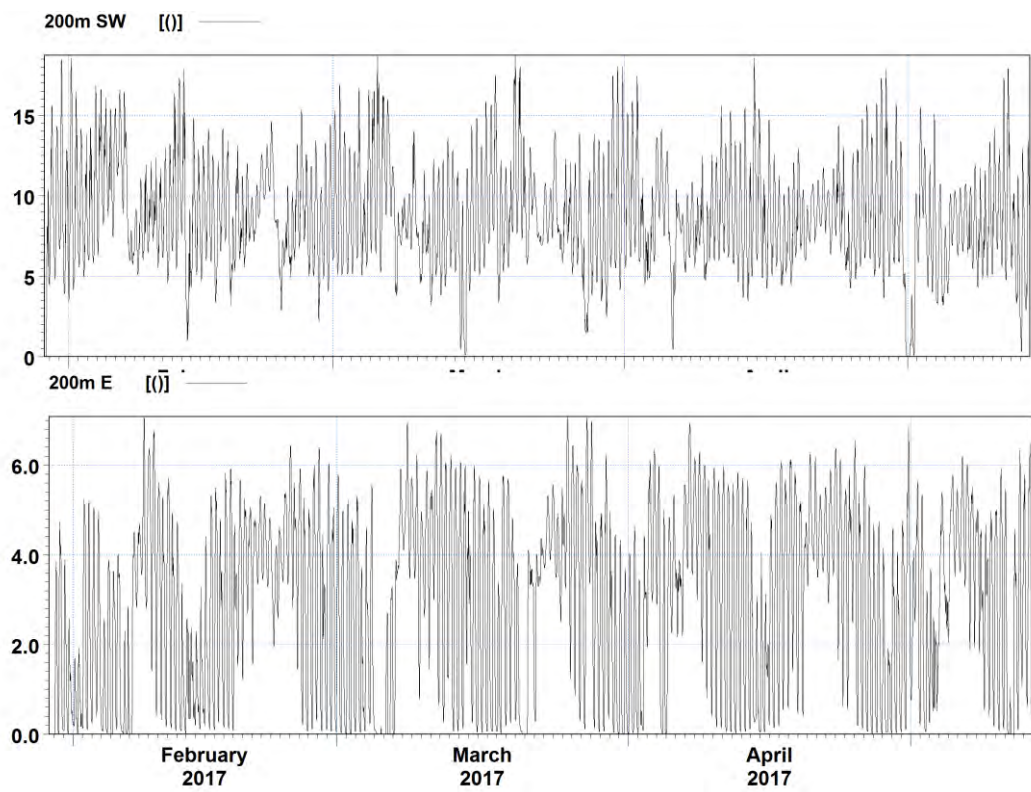


Figure 7-1. Time-series plots of the predicted concentrations at the monitoring sites near the outfall for the average WWTP discharge rate of 300 L/s.

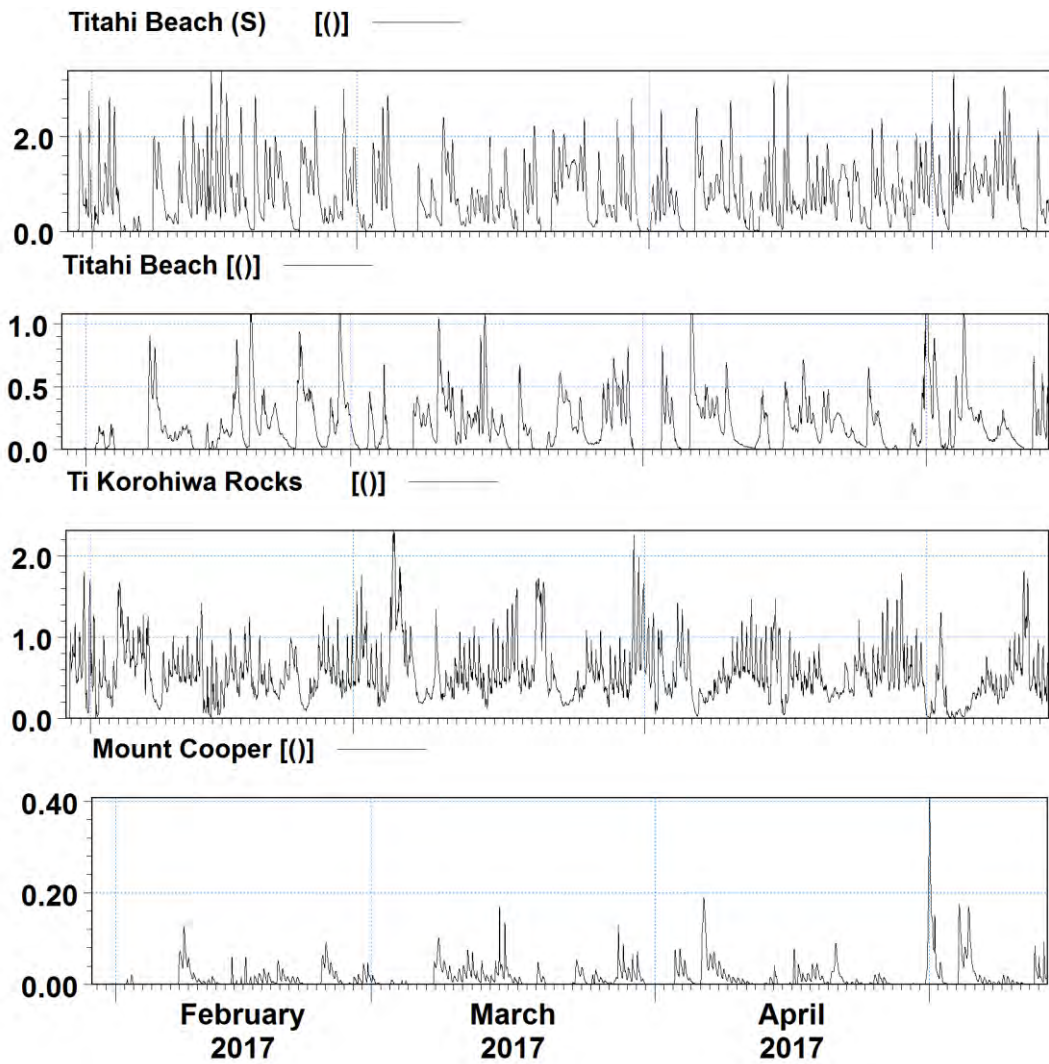


Figure 7-2. Time-series plots of the predicted concentrations at the beach monitoring sites for the average WWTP discharge rate of 300 L/s.

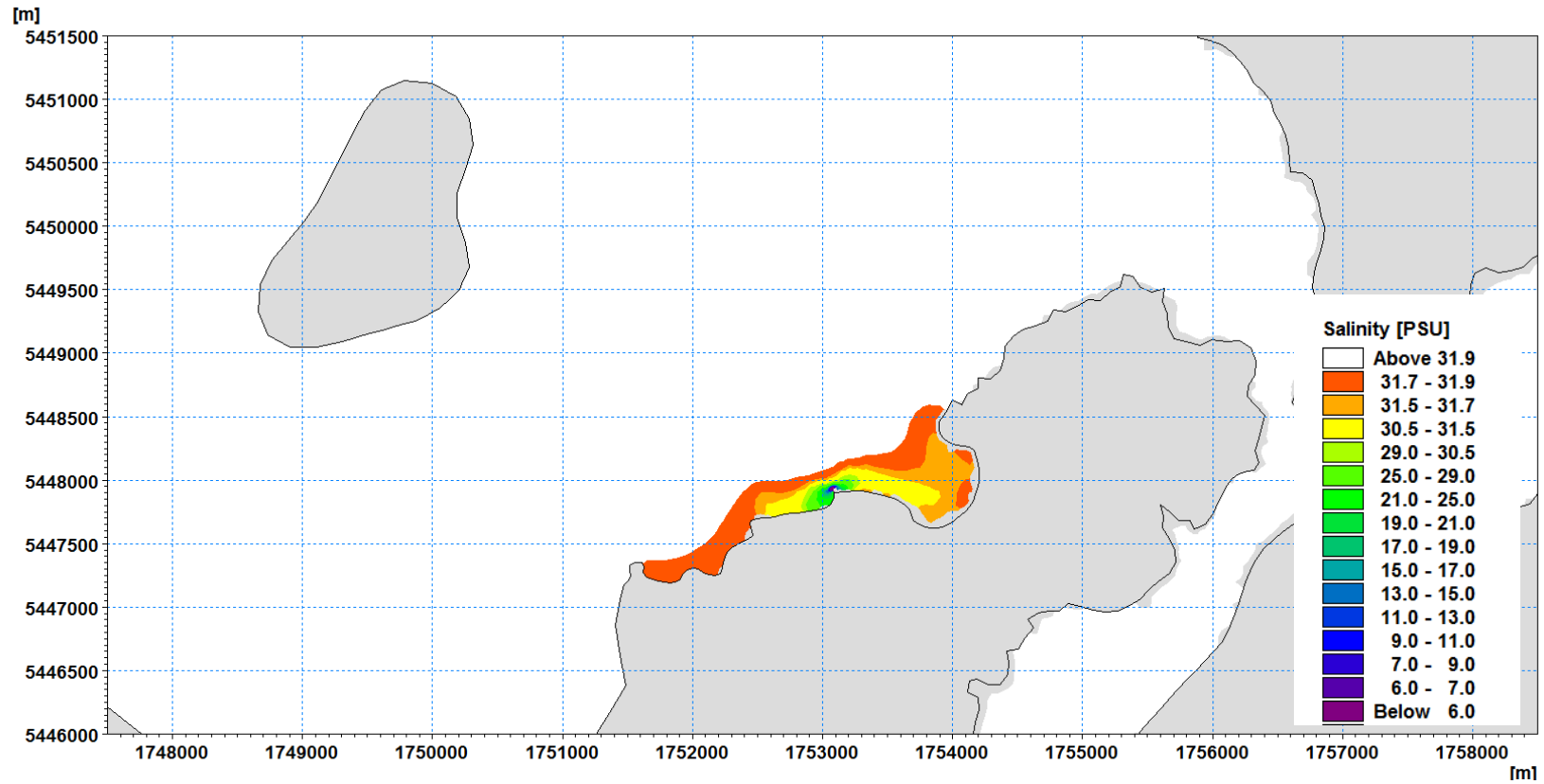


Figure 7-3. Predicted mean salinity for the average WWTP discharge rate.

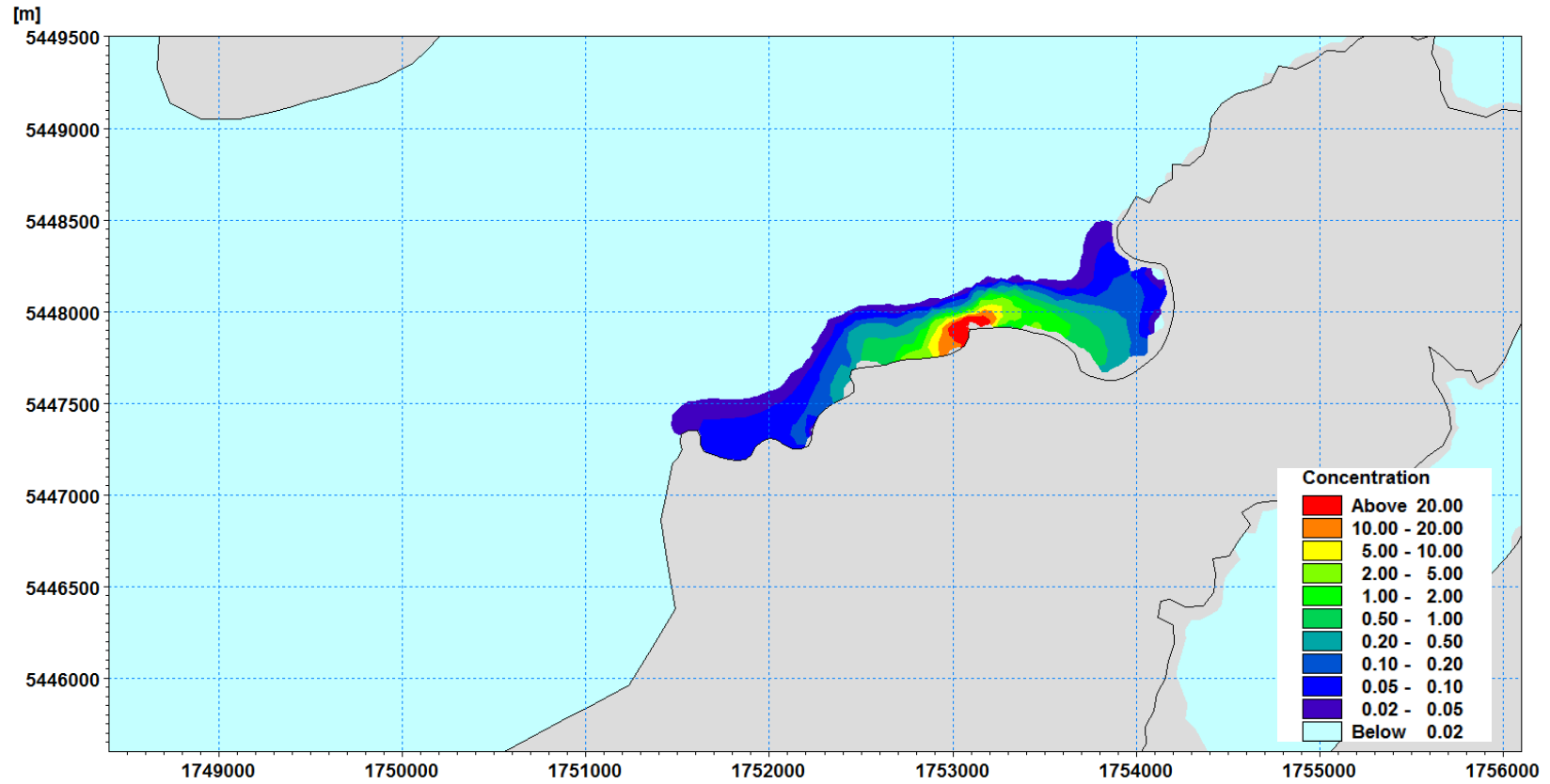


Figure 7-4. 50th percentile concentration (% treated wastewater) for the average WWTP discharge rate.

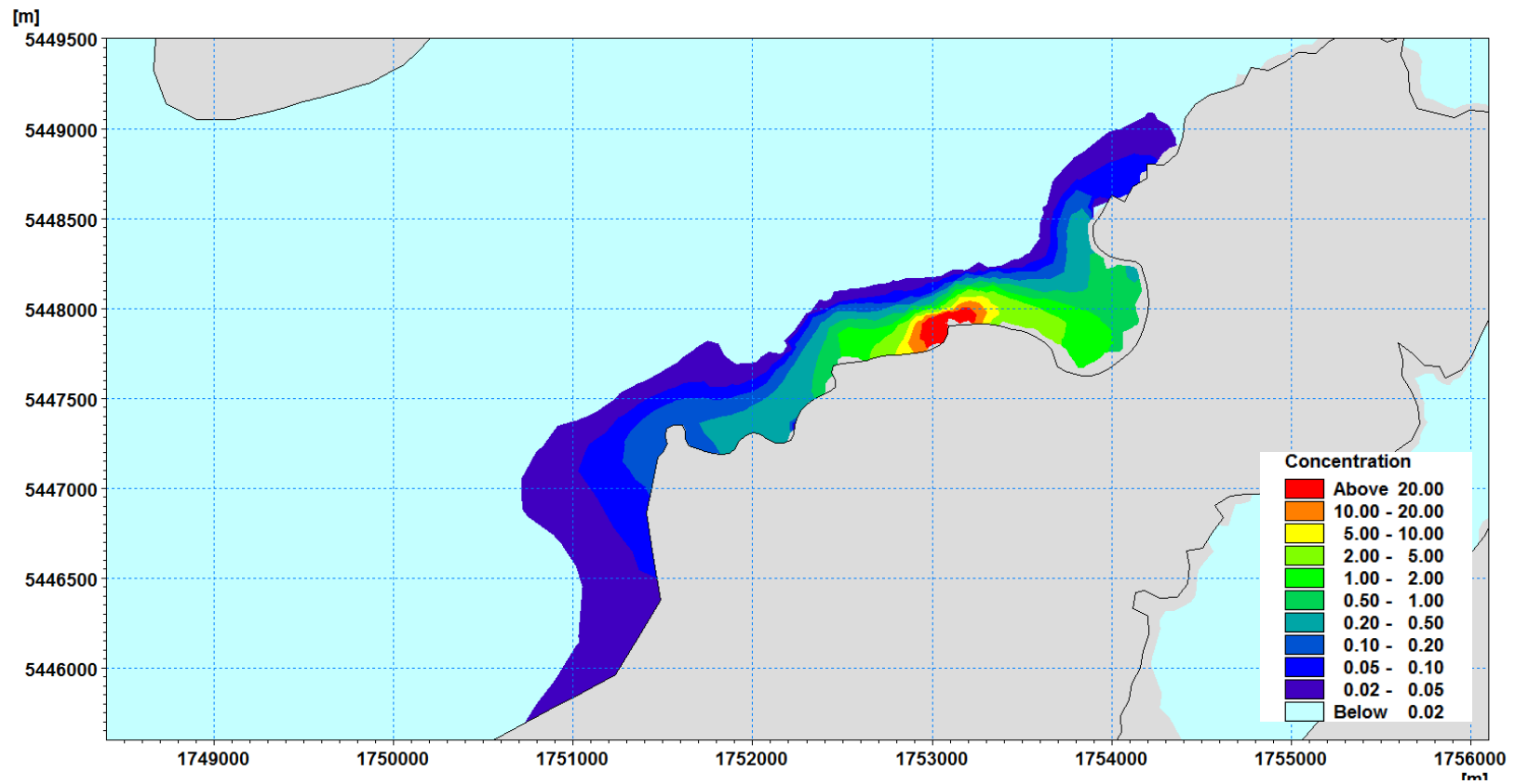


Figure 7-5. 95th percentile concentration (% treated wastewater) for the average WWTP discharge rate.

7.2 Peak Discharge Scenario

Table 9 Average and percentile concentrations (% treated wastewater) at beach monitoring data for the peak WWTP discharge rate of 1100 L/s.

Site	Average concentration (% treated wastewater)	75 th percentile concentration (% treated wastewater)	90th percentile concentration (% treated wastewater)	95th percentile concentration (% treated wastewater)
200m south west of the outfall	27.753	33.452	37.135	39.128
200m east of the outfall	12.703	15.275	17.617	18.871
Titahi Beach (South)	4.380	5.703	6.671	7.273
Titahi Beach	1.245	1.782	2.217	2.494
Ti Korohiwa Rocks	2.322	2.807	3.271	3.633
Mount Cooper	0.067	0.091	0.163	0.224

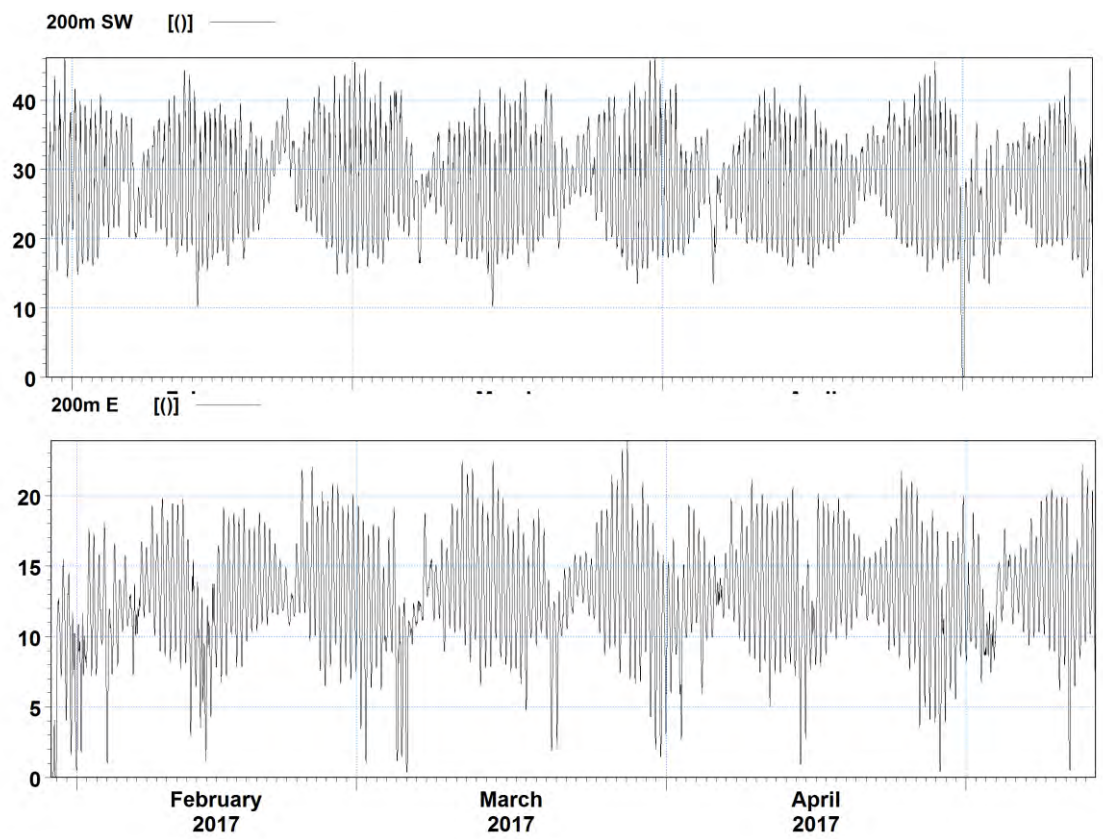


Figure 7-6. Time-series plots of the predicted concentrations at the monitoring sites near the outfall for the peak WWTP discharge rate of 1100 L/s.

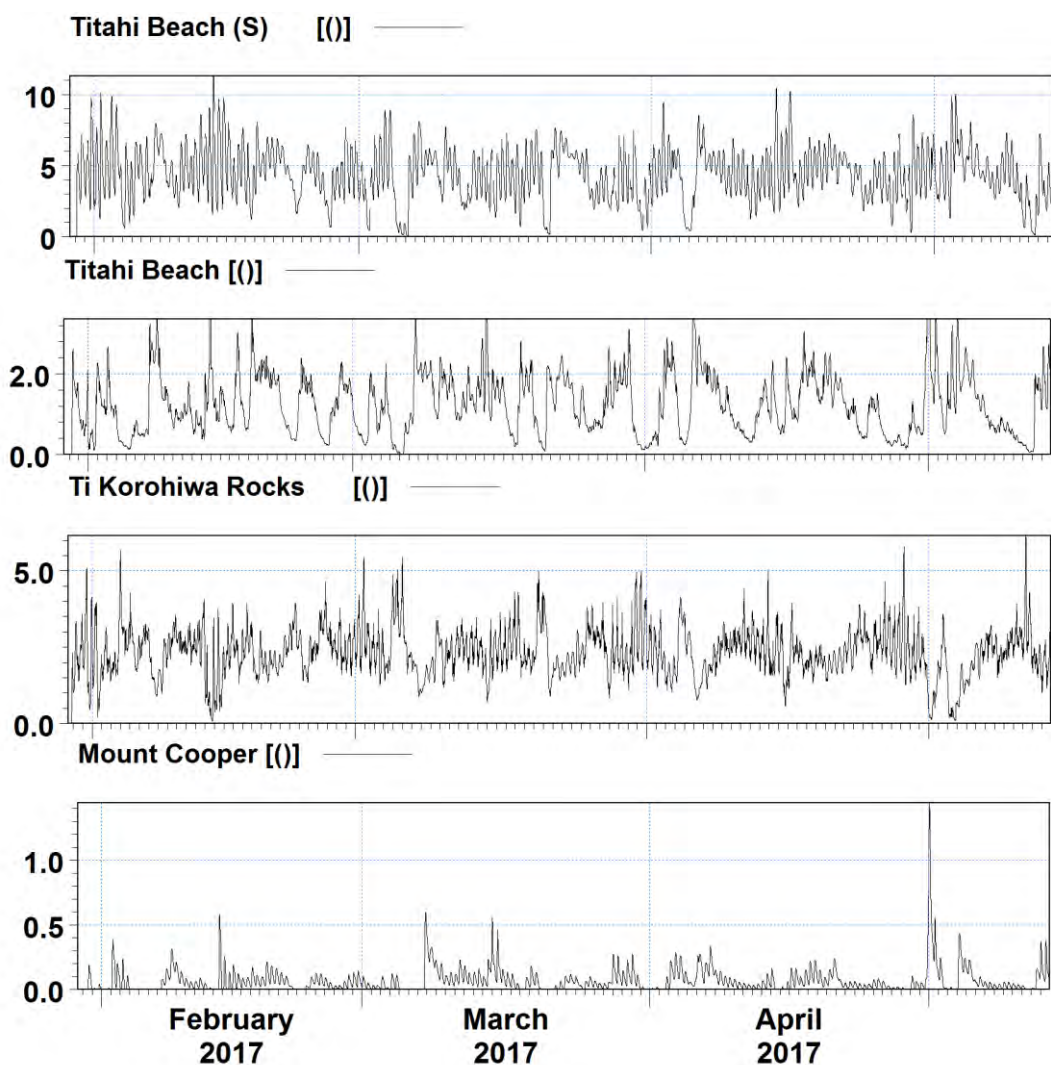


Figure 7-7. Time-series plots of the predicted concentrations at the beach monitoring sites for the peak WWTP discharge rate of 1100 L/s.

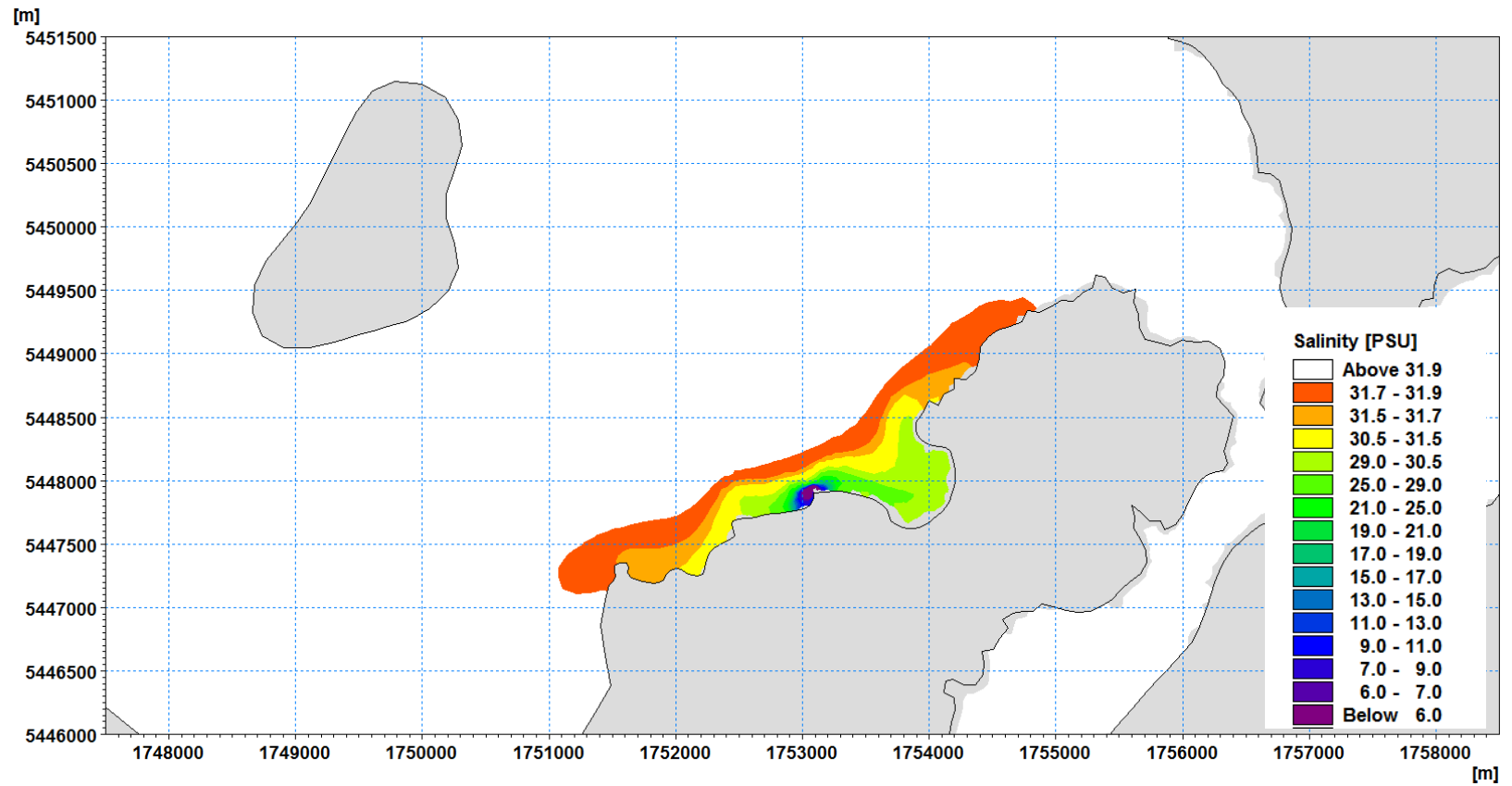


Figure 7-8. Predicted mean salinity for the peak WWTP discharge rate of 1100 L/s.

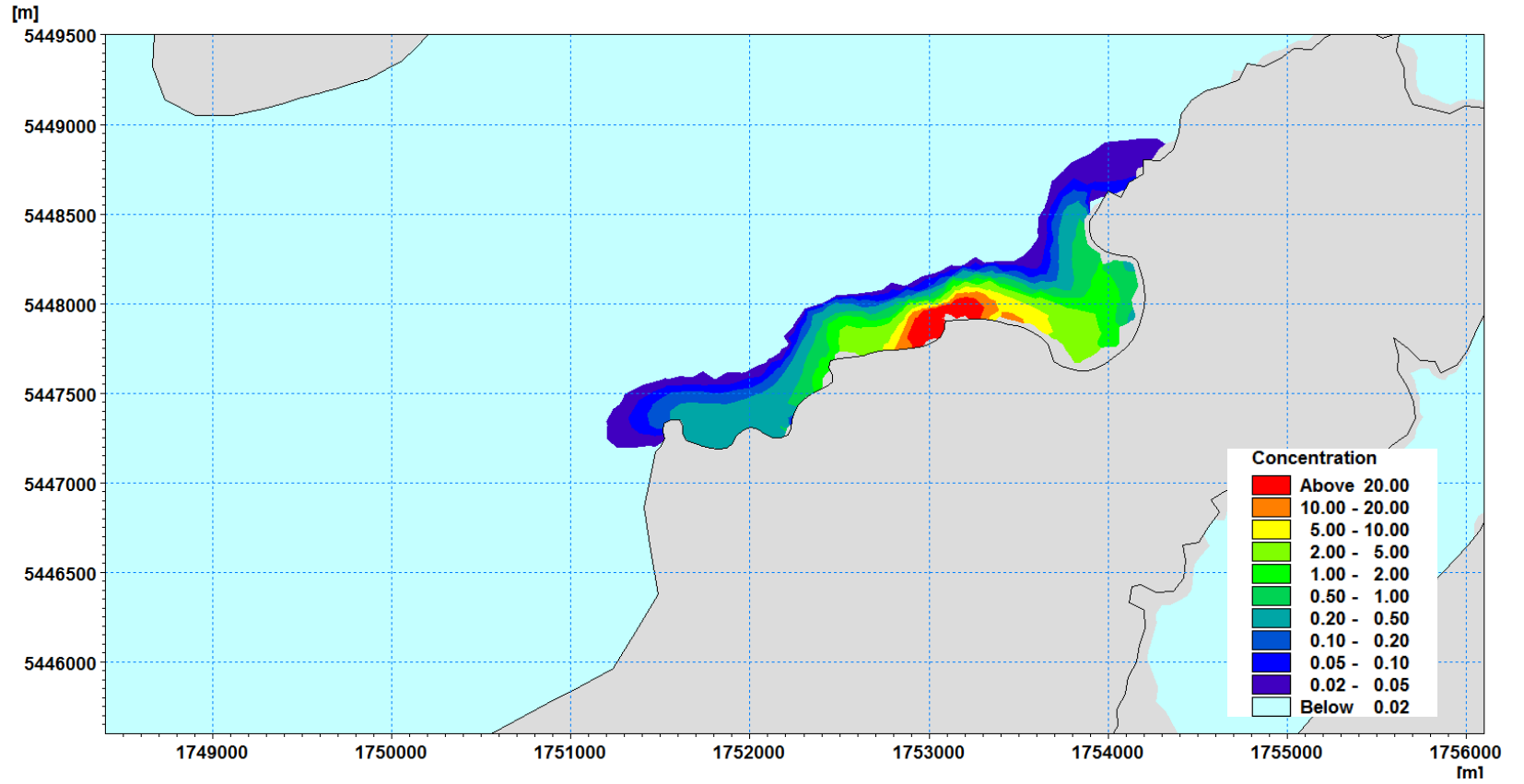


Figure 7-9. 50th percentile concentration for the peak WWTP discharge rate of 1100 L/s.

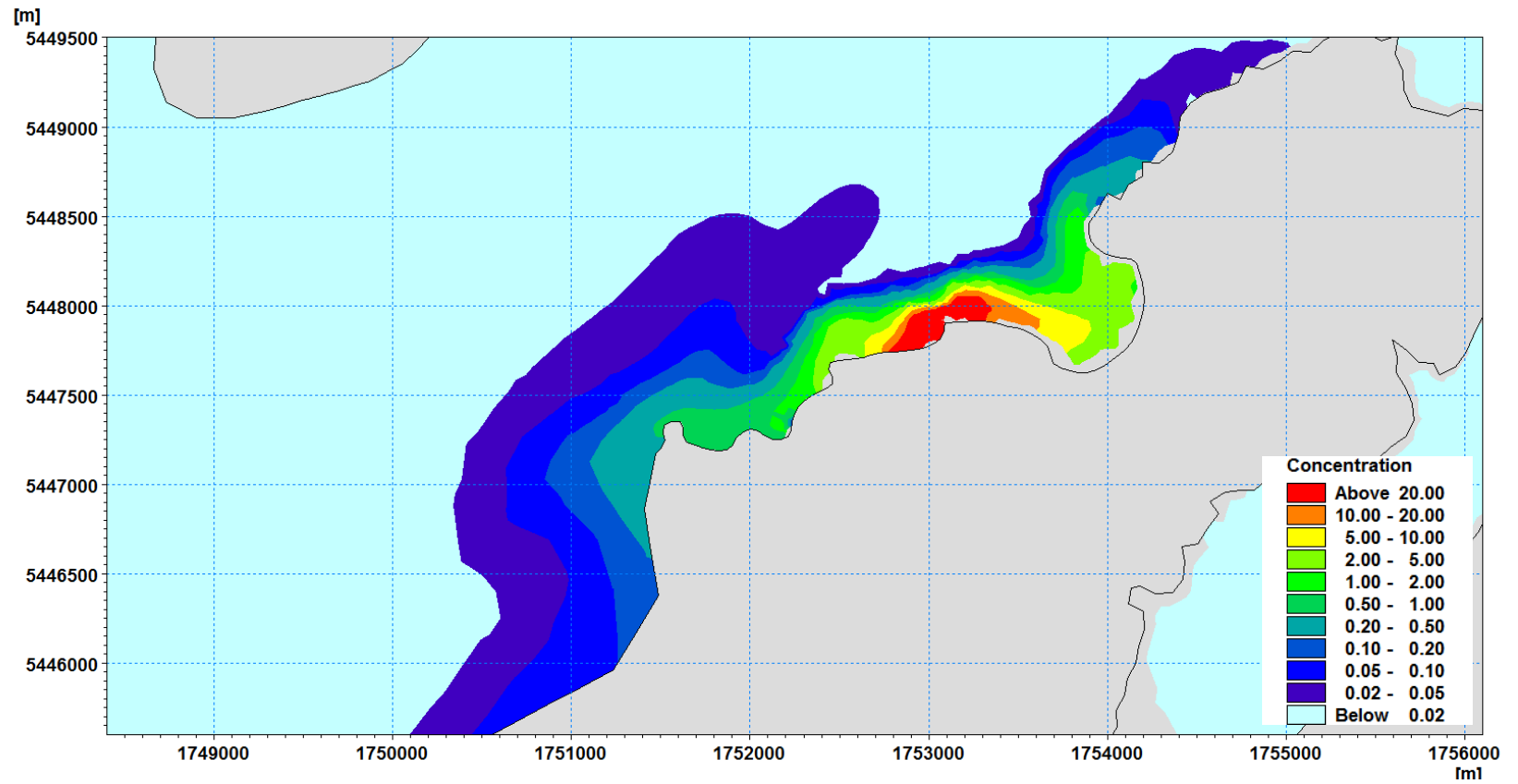


Figure 7-10. 95th percentile concentration for the peak WWTP discharge rate of 1100 L/s.

7.3 Design Discharge Scenario

Table 10 Average and percentile concentrations (% treated wastewater) at beach monitoring data for the design WWTP discharge rate of 1500 L/s.

Site	Average concentration (% treated wastewater)	75 th percentile concentration (% treated wastewater)	90 th percentile concentration (% treated wastewater)	95 th percentile concentration (% treated wastewater)
200m south west of the outfall	36.015	42.501	46.477	48.999
200m east of the outfall	16.256	18.771	21.515	22.946
Titahi Beach (South)	6.108	7.653	8.867	9.657
Titahi Beach	1.799	2.493	3.035	3.354
Ti Korohiwa Rocks	3.707	4.429	5.137	5.508
Mount Cooper	0.092	0.126	0.213	0.274

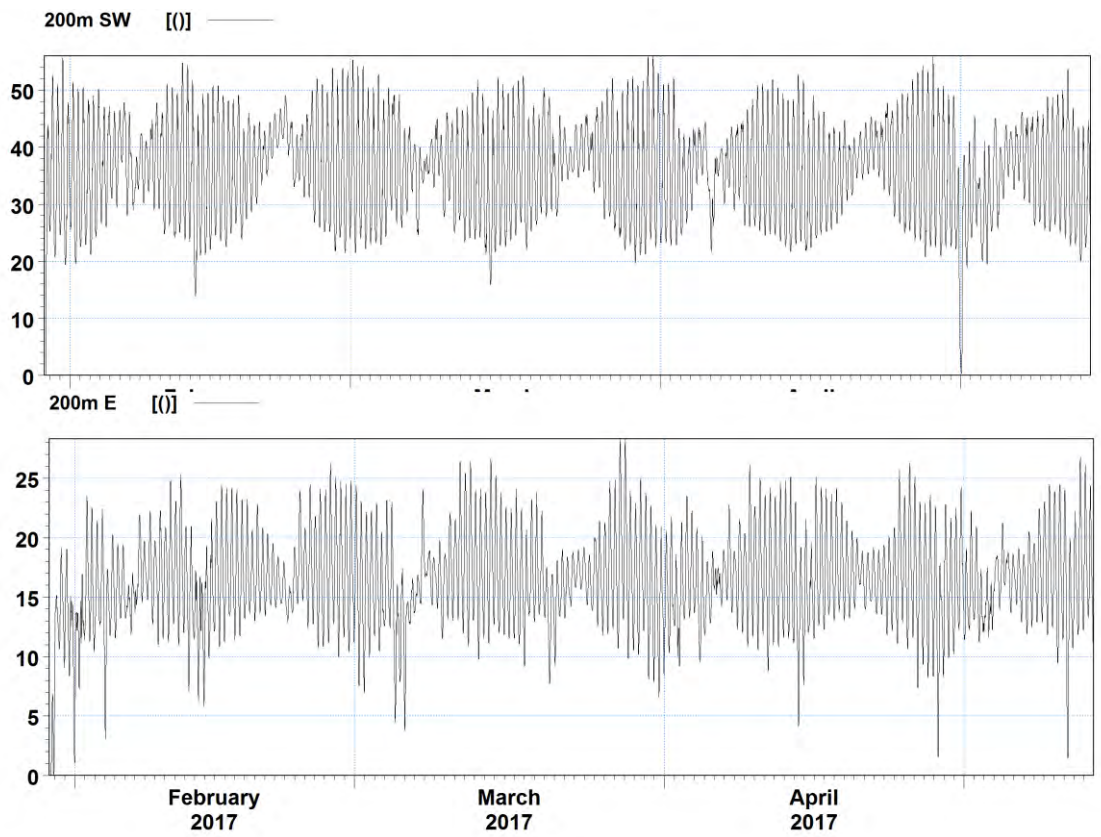


Figure 7-11. Time-series plots of the predicted concentrations at the monitoring sites near the outfall for the design WWTP discharge rate of 1500 L/s.

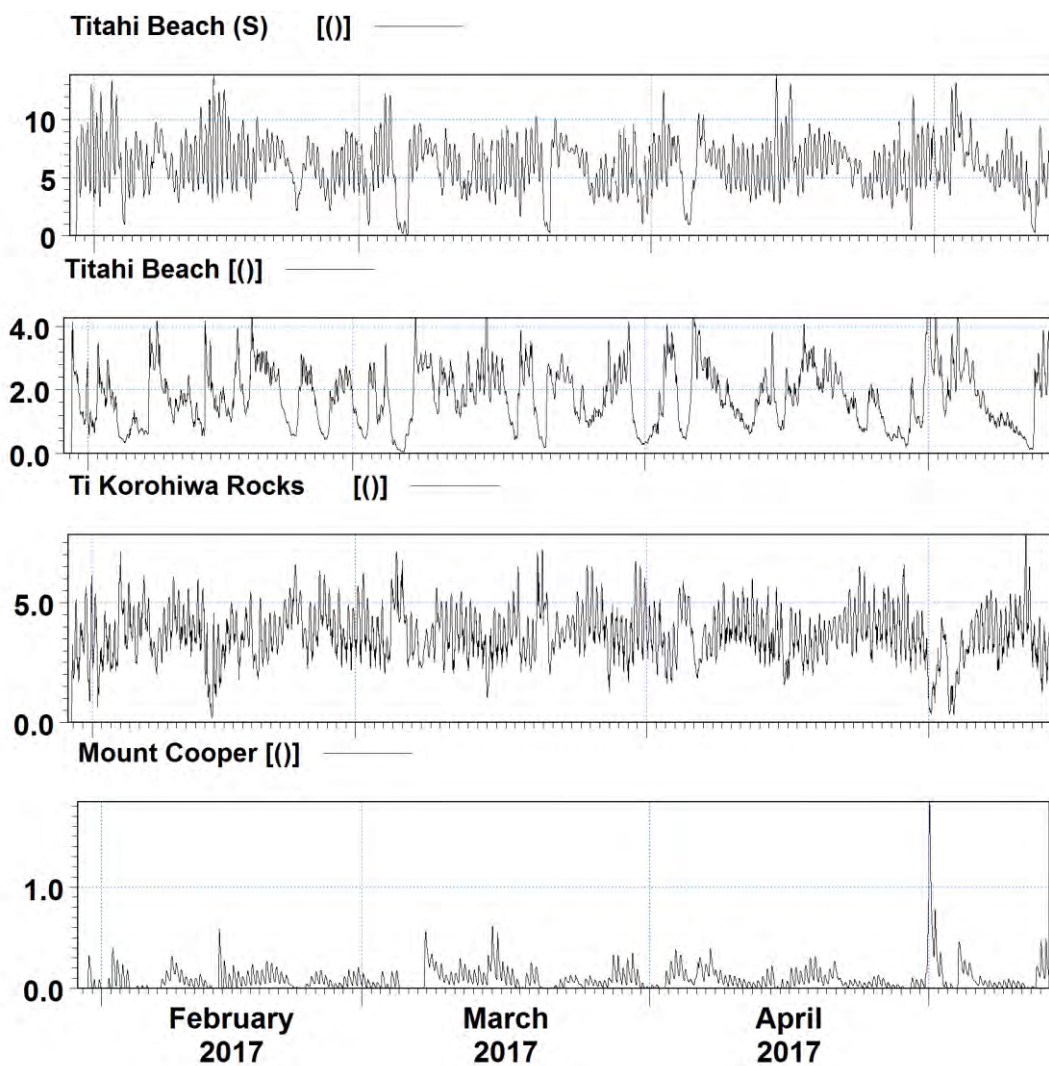


Figure 7-12. Time-series plots of the predicted concentrations at the beach monitoring sites for the design WWTP discharge rate of 1500 L/s.

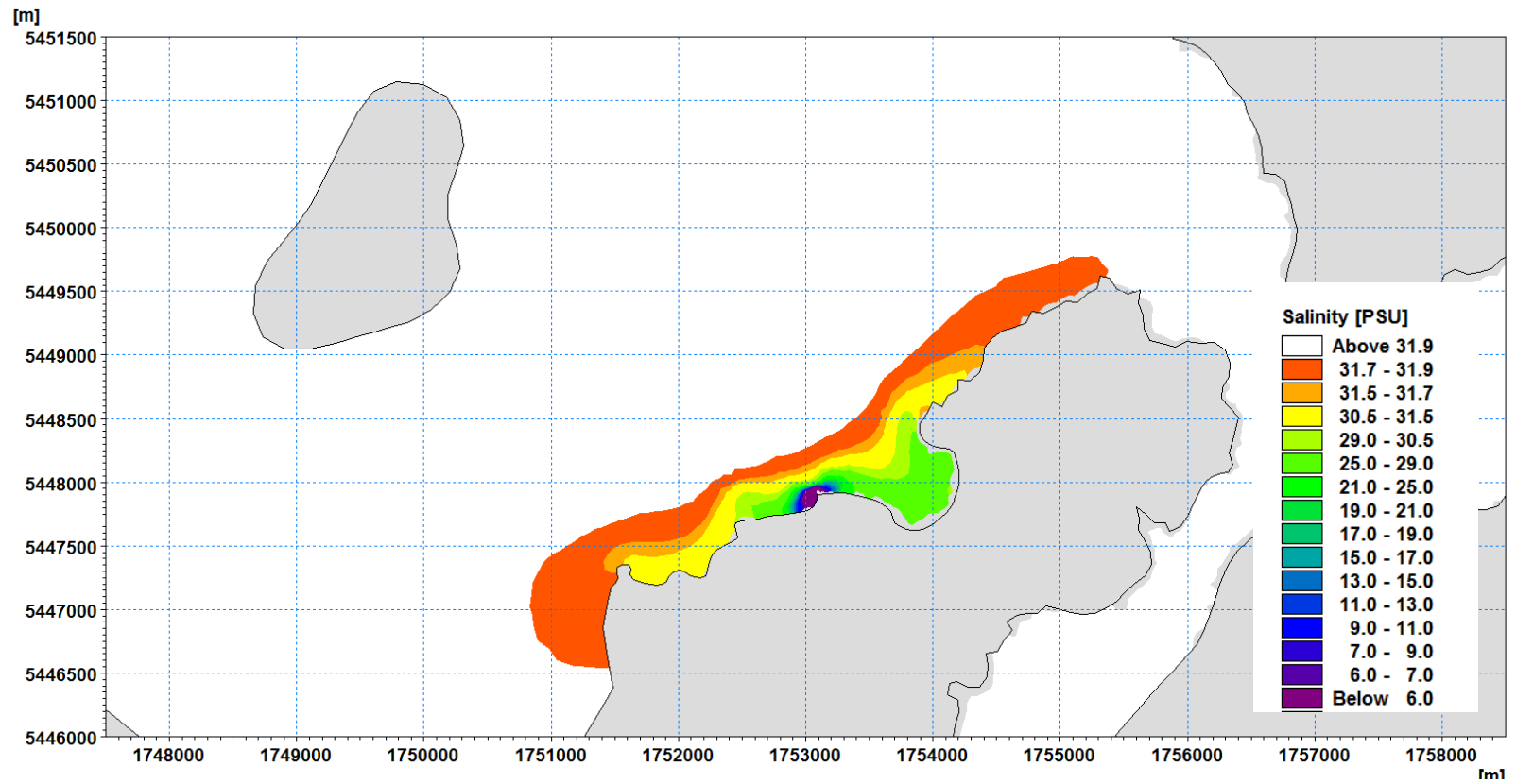


Figure 7-13. Predicted mean salinity for the design WWTP discharge rate of 1500 L/s.

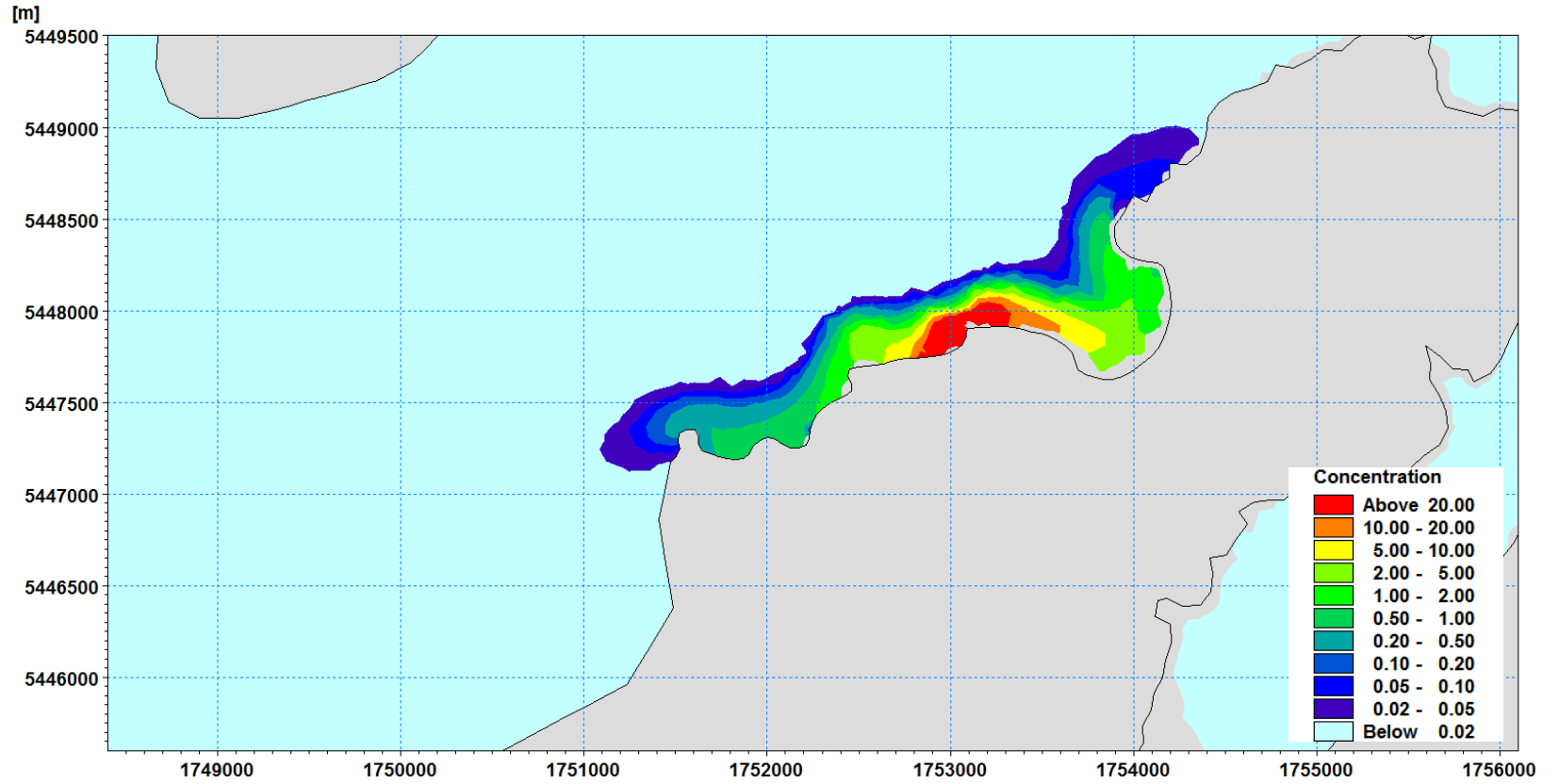


Figure 7-14. 50th percentile concentration for the design WWTP discharge rate of 1500 L/s.

Scenario Results

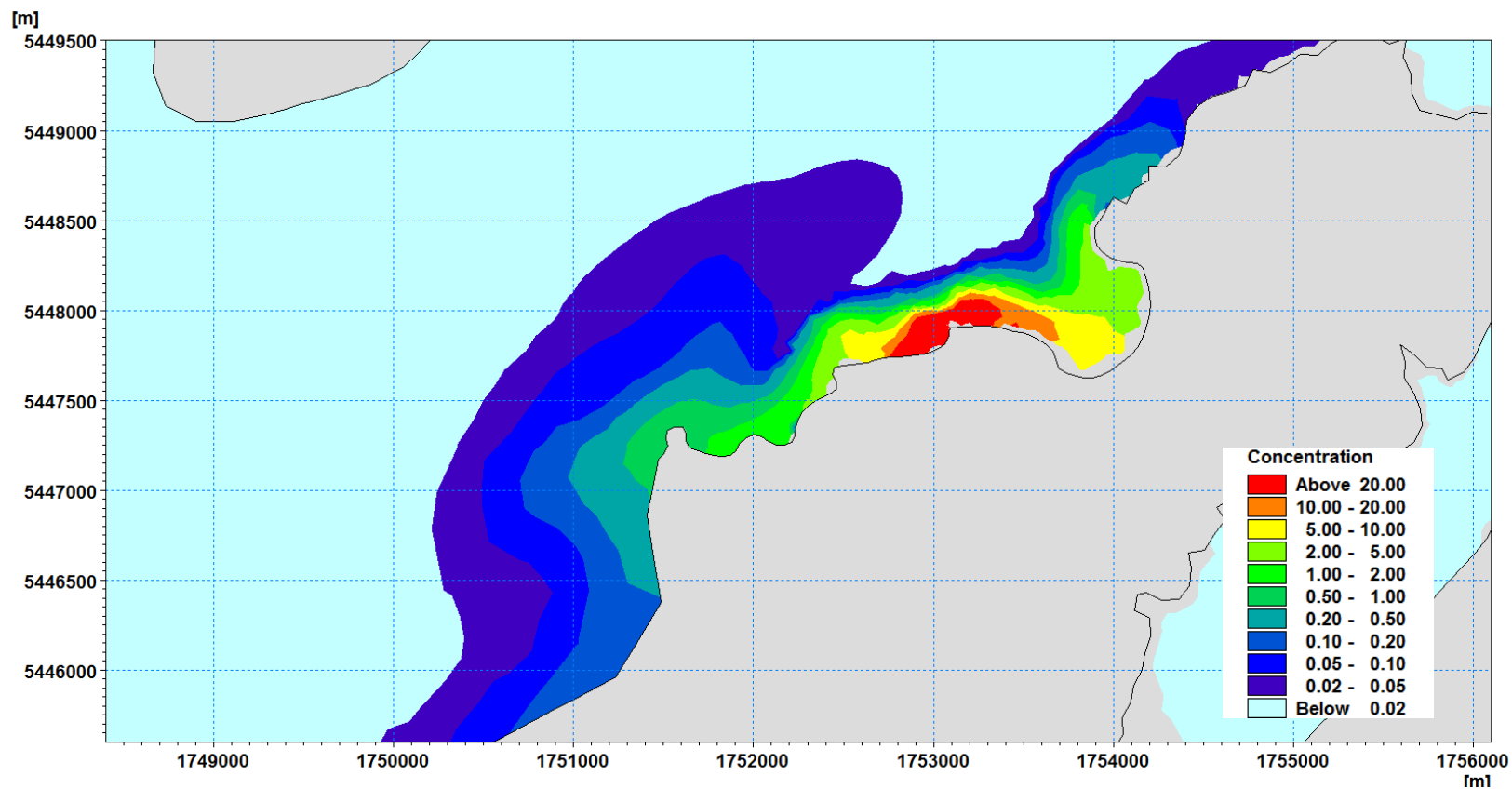


Figure 7-15. 95th percentile concentration for the design WWTP discharge rate of 1500 L/s.

8 Summary

A calibrated hydrodynamic and advection-dispersion model has been used to quantify the dynamics of the treated wastewater plume discharged from the Bells Island Wastewater Treatment Plant just to the south of Titahi Bay at Kaumanga Point.

This part of the coast consists of exposed rocky reefs with pockets of coarse sand and cobbles.

The water depth in the immediate vicinity of the discharge site is relatively shallow.

Offshore of the discharge point, relatively strong complex currents occur especially the area between Mana Island and Kaumanga Point.

The model has been calibrated against currents and water levels collected specifically for this study and against water level data from the Mana Marina. The model performance is very good in terms of predicting water levels and provides a good level of prediction with respect to currents immediately offshore of the outfall.

In addition, a qualitative analysis of broader scale currents has been carried out which confirms the models ability to simulate current offshore of Porirua Harbour and in and around Mana Island.

Data from long term monitoring at key beach sites along the coast and a dye test carried out in December 2017 has been used to confirm the model's ability to simulate the dynamics of the treated wastewater plume in the near shore zone.

A series of long-term model runs have been carried out which provide quantification of the levels of dilution achieved and the dynamics of the plume under a broad range of tide and wind conditions for three different discharge regimes – Average (300 L/s), Peak (1100 L/s) and Design (1500 L/s) discharge rates.

Model results can be used to quantify the dynamics of the treated wastewater plume and to assess the relative risk associated with each of the discharge rates considered.

All results are presented in terms of percentage treated wastewater so that further improvements in wastewater quality associated with any future scenarios being considered scenarios can also be assessed.

9 References

- Ao, Y & Goblick GN 2016. Application of Hydrodynamic Modelling to Predict Viral Impacts from Wastewater Treatment Plant Discharges Adjacent to Shellfish Growing Areas. Recreational Waters Conference.
- Bradford E., and Wooding R.A. 1976. Tidal flow near Mana Island, Cook Strait, New Zealand, *New Zealand Journal of Marine and Freshwater Research*, 10:1, 31-42.
- Chang, YC, Chen, GY, Tseng, RS, Centurioni, LR and Chu PC 2012. Observed near-surface currents under high wind speeds, *J. Geophys. Res.*, 117, C11026
- Cheung, S.K.B. & Leung, Dexter & Wang, W & Lee, J.H.W. & Cheung, V. 2000. VISJET-a computer ocean outfall modelling system. *Computer Graphics International Proceedings*.
- Danish, DR, Mudgal, BV, Dhinesh, G., Ramanamurthy MV 2015. Mathematical Model Study of the Effluent Disposal from a Desalination Plant in the Marine Environment at Tuticorin, India. In: Baawain M., Choudri B., Ahmed M., Purnama A. (eds) *Recent Progress in Desalination, Environmental and Marine Outfall Systems*.
- DHI 2017. MIKE21 and MINK3 Flow Model. Advection-Dispersion Module. Scientific Documentation.
- DML 2015. Te Awarua-O-Porirua Harbour. Report of Survey & Verification Of Sedimentation Rates Project No. Sp00041. Report Prepared for Porirua City Council
- Doneker, R.L. and G.H. Jirka, 2007. CORMIX User Manual: A Hydrodynamic Mixing Zone Model and Decision Support System for Pollutant Discharges into Surface Waters", EPA-823-K-07-001.
- French-McCay, D., Mueller, C., Jayko, K., Longval, B., Schroeder, M., Nordhausen, Wa., Lampinen, M., Ohlmann, C., Terrill, E., Carter, M., Otero, M., Kim, SY, and Payne, J. 2007. Evaluation of Field-Collected Data Measuring Fluorescein Dye Movements and Dispersion for Dispersed Oil Transport Modeling. *Proceedings of the 30th Arctic and Marine Oilspill Program, AMOP Technical Seminar*. 2.
- Geyer, WR, Farmer, DM 1989. Tide induced variation of the dynamics of a salt wedge estuary. *Journal of Physical Oceanography* 28, 1060–1072.
- GHD 2013. City of Rehoboth Beach Wastewater Treatment Plant Ocean Outfall Project. Environmental Impact Statement. Report prepared for City of Delaware.
- Jirka, G.H., E.E. Adams, and K.D. Stolzenbach, *Buoyant Surface Jets* *Journ. Hyd. Div., ASCE*, Vol. 107, No. HY11, pp. 1467-1487.
- Jitendra P. & Tripathy. JK 2011. Numerical Simulation of Advection-Dispersion for monitoring thermal plume re-circulation in a shallow coastal environment. *Applied Ecology and Environmental Research*. 9. 341 10 [4.6 m³/s discharge]
- Maraccini P.A., Catharine, M., Mattioli, M., Sassoubre, L.M., Cao, Y., Griffith, J.F., Ervin, J.S., Van De Werfhorst, L.C and Boehm, A.B. 2016. Solar Inactivation of Enterococci and Escherichia coli in Natural Waters: Effects of Water Absorbance and Depth *Environ. Sci. Technol.* 2016, 50, 5068–5076.
- Menendez, AN, Badano, ND, Lopolito MF & Re M. 2013. Water quality assessment for a coastal zone through numerical modelling, *Journal of Applied Water Engineering and Research*, 1:1, 8-16

Ministry of Works 1975. Wellington Region West Coast Sewer Outfall Oceanographic Investigations. Report prepared for Hutt Valley Drainage Board.

Moriasi, D. N., J. G. Arnold, M. W. Van Liew, R. L. Bingner, R. D. Harmel and T. L. Veith 2007. Model Evaluation Guidelines for Systematic Quantification of Accuracy in Watershed Simulations. Transactions of the ASABE 50(3): 885–900. Nash, J.E., Sutcliffe, J. 1970. River flow forecasting through conceptual models, Part I A discussions of principles, J. Hydrol., 10, 282-290.

Noble, R.T., Lee, I.M. and Schiff, K.C. 1994. Inactivation of indicator micro-organisms from various sources of faecal contamination in seawater and freshwater. Journal of Applied Microbiology 2004, 96, 464–472

Ozcan M. & Gokce KT 2002. Numerical Model Applications in Outfall Design: Case Studies From Turkey. 2nd International Conference on Marine Waste Water Discharges

SKM 2011. Transmission Gully Project. Assessment of Hydrology and Stormwater Effects. Technical Report 14 prepared for New Zealand Transport Authority.

Weber, JE 1983. Steady Wind and Wave Induced Currents in the Open Ocean. Journal of Physical Oceanography 13, 524–530

Willmott, C.J., Ackleson, S.G., Davis, R.E., Feddema, J.J, Klink, K.M., Leg-ates, D.R., O'Donnell, J., Rowe, C.M., 1985. Statistics for the evaluation and comparison of models, J. Geophys. Res., 90, 8995-9005.



APPENDIX A – Drone Photos



Figure A.1 Drone image of the dye test as the dye emerges from the outfall at 10:30 on the 29th November 2017.



Figure A.2 Drone image of the dye test at 10:31 on the 29th November 2017.



Figure A.3 Drone image of the dye test at 10:32 on the 29th November 2017.



Figure A.4 Drone image of the dye test at 10:33 on the 29th November 2017.



Figure A.5 Drone image of the dye test at 10:34 on the 29th November 2017.



Figure A.6 Drone image of the dye test at 10:35 on the 29th November 2017.



Figure A.7 Drone image of the dye test at 10:36 on the 29th November 2017.



Figure A.8 Drone image of the dye test at 10:37 on the 29th November 2017.



Figure A.9 Drone image of the dye test at 10:38 on the 29th November 2017.



Figure A.10 Drone image of the dye test at 10:39 on the 29th November 2017.



Figure A.11 Drone image of the dye test at 10:40 on the 29th November 2017.



Figure A.12 Drone image of the dye test at 10:41 on the 29th November 2017.



Figure A.13 Drone image of the dye test at 10:42 on the 29th November 2017.



Figure A.14 Drone image of the dye test at 10:45 on the 29th November 2017.



Figure A.15 Drone image of the dye test at 10:49 on the 29th November 2017.



Figure A. 16 Drone image of the dye test at 10:53 on the 29th November 2017.



Figure A.17 Drone image of the dye test at 10:56 on the 29th November 2017.



Figure A.18 Drone image of the dye test at 11:06 on the 29th November 2017.

APPENDIX B – Mana Marina Tidal Analysis

Table B.1 Mana Marina tidal constituent data based on tidal analysis of observations 2009-2018.

Constituent	Amplitude (m)	Phase (°)	Constituent	Amplitude (m)	Phase (°)	Constituent	Amplitude (m)	Phase (°)
M2	0.3752	278.58	H1	0.0075	171.85	S4	0.0019	251.1
S2	0.2166	342.44	MF	0.0072	204.88	NO1	0.0018	99.08
K2	0.0639	342.54	MN4	0.0068	178.78	SIG1	0.0017	20.02
N2	0.0459	281.01	2MS6	0.0068	175.62	RHO1	0.0016	350.68
SA	0.0303	134.83	LDA2	0.0065	287.02	PI1	0.0016	191.25
M4	0.024	220.6	H2	0.0062	92.97	GAM2	0.0016	251.33
O1	0.0218	26.64	M6	0.0059	137.32	MSN2	0.0016	144.36
SK3	0.0185	156.47	MK4	0.0045	278.62	SN4	0.0016	236.57
T2	0.0171	349.76	EPS2	0.0042	288.26	CHI1	0.0011	204.14
M3	0.0168	189.13	MKS2	0.0042	41.9	SO1	0.0011	249.72
K1	0.0162	181.12	S1	0.0041	304.46	2SK5	0.0011	188.48
MU2	0.0152	310.08	P1	0.004	167.48	ALP1	0.001	9.63
L2	0.015	297.25	2MN6	0.0033	116.69	UPS1	0.001	304.34
SSA	0.0146	146.72	MM	0.0029	96.1	OQ2	0.001	262.22
MS4	0.0146	272.84	R2	0.0027	300.74	MSK6	0.001	244.47
MSM	0.0106	187.63	SK4	0.0027	152.26	2MK5	0.0009	113.64
SO3	0.0103	88.98	ETA2	0.0026	12.95	M8	0.0009	73.66
MK3	0.0095	144	MO3	0.0026	66.75	PSI1	0.0007	289.48
NU2	0.0088	271.02	J1	0.0025	221.43	3MK7	0.0006	63.04
Q1	0.0086	357.02	2SM6	0.0023	235.8	THE1	0.0005	232.19
2N2	0.0085	279.94	2Q1	0.0022	345.9	TAU1	0.0004	228.8
MSF	0.0083	179.26	2MK6	0.002	175.38	BET1	0.0004	112.33
			OO1	0.0019	273.28	PHI1	0.0004	212.91



Observed Mana Marina Tides [m]

Detrended for sea level rise

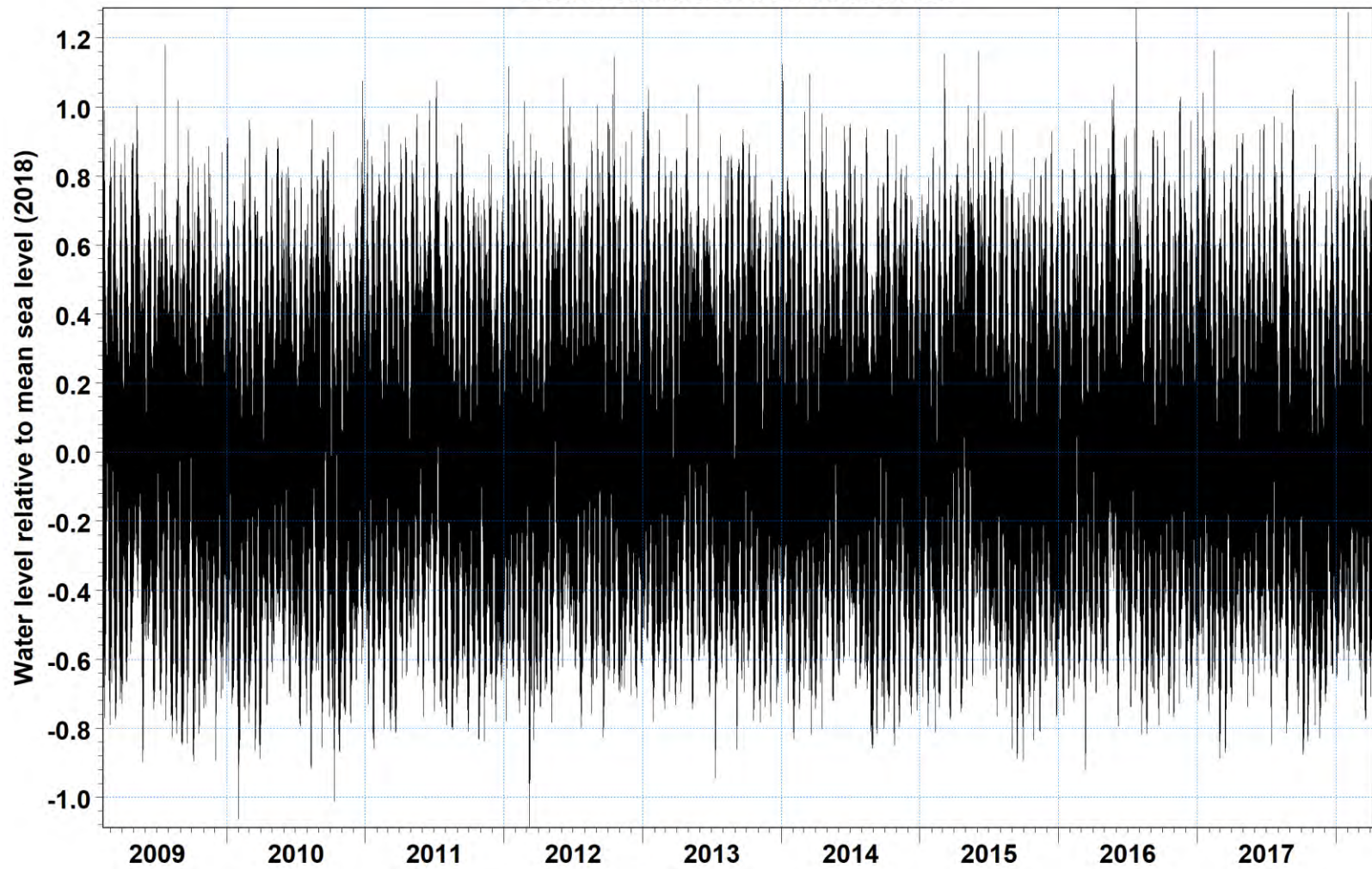


Figure B.1. Observed Mana Marina tides detrended for sea level rise of 10.1 mm per annum.

APPENDIX C – Monitoring Data Regression Plots

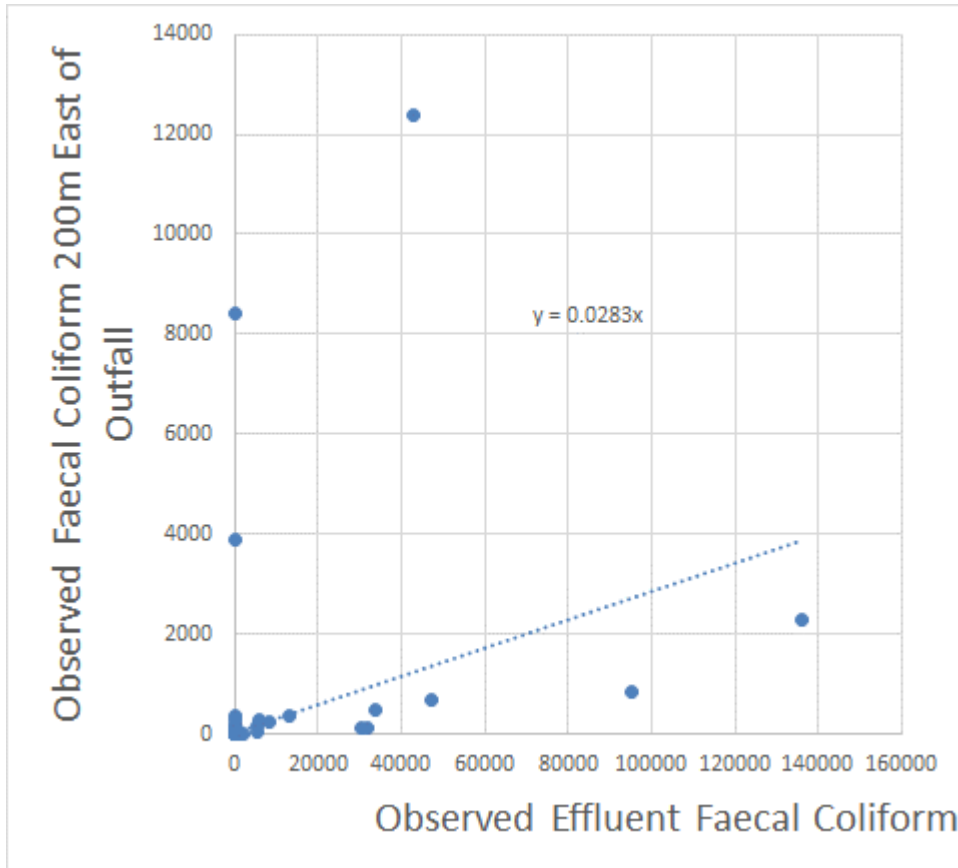


Figure C-1. Regression plot of the observed faecal coliform data 200 m east of the outfall and the treated wastewater concentration for all paired data (n=85).

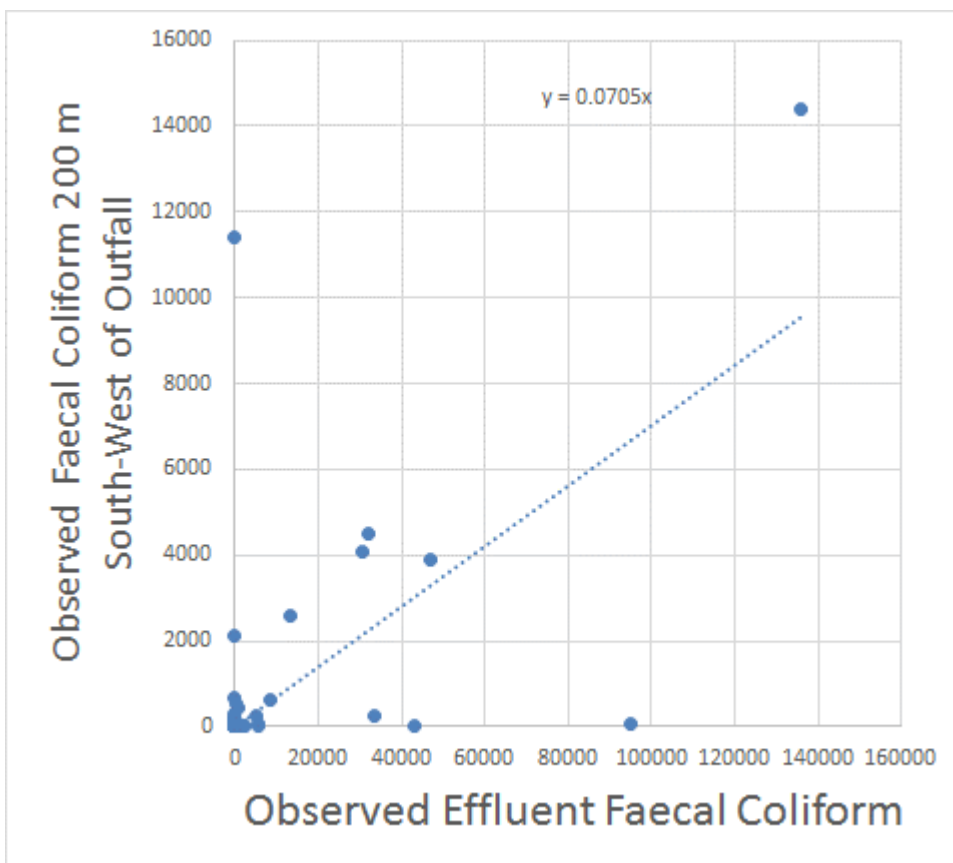


Figure C-2. Regression plot of the observed faecal coliform data 200 m south-west of the outfall and the treated wastewater concentration for all paired data (n=85).

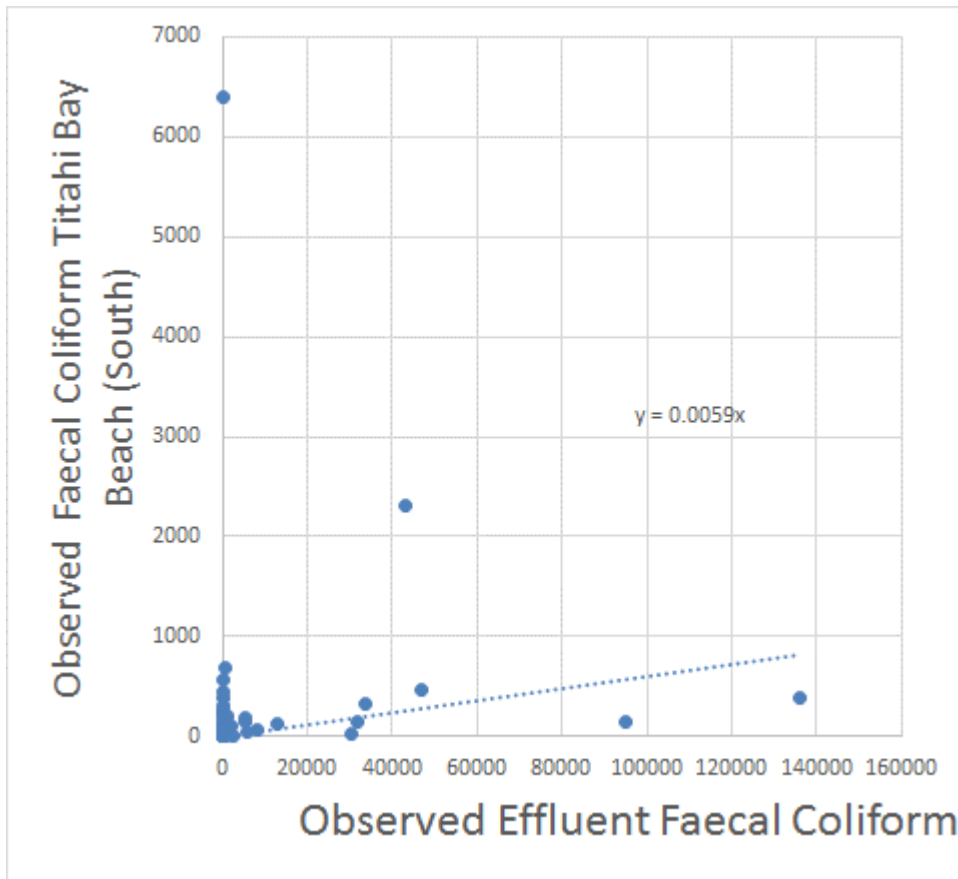


Figure C-3. Regression plot of the observed faecal coliform data at Titahi Bay South and the treated wastewater concentration for all paired data (n=85).

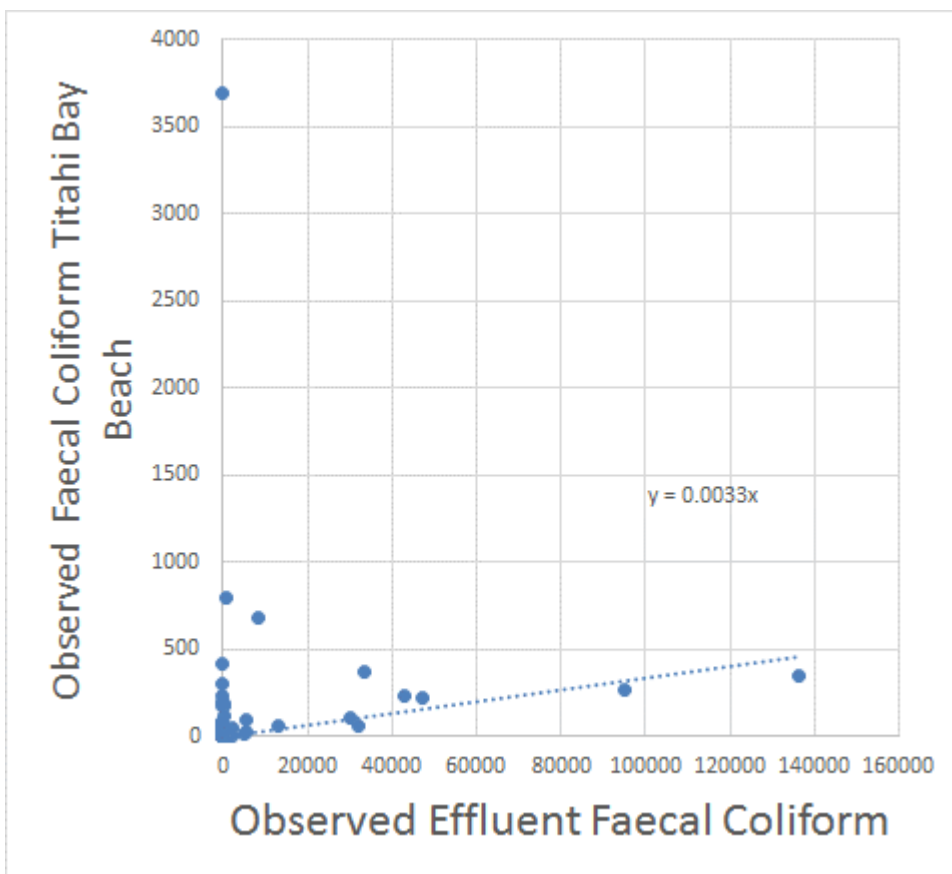


Figure C-4. Regression plot of the observed faecal coliform data at Titahi Bay and the treated wastewater concentration for all paired data (n=85).

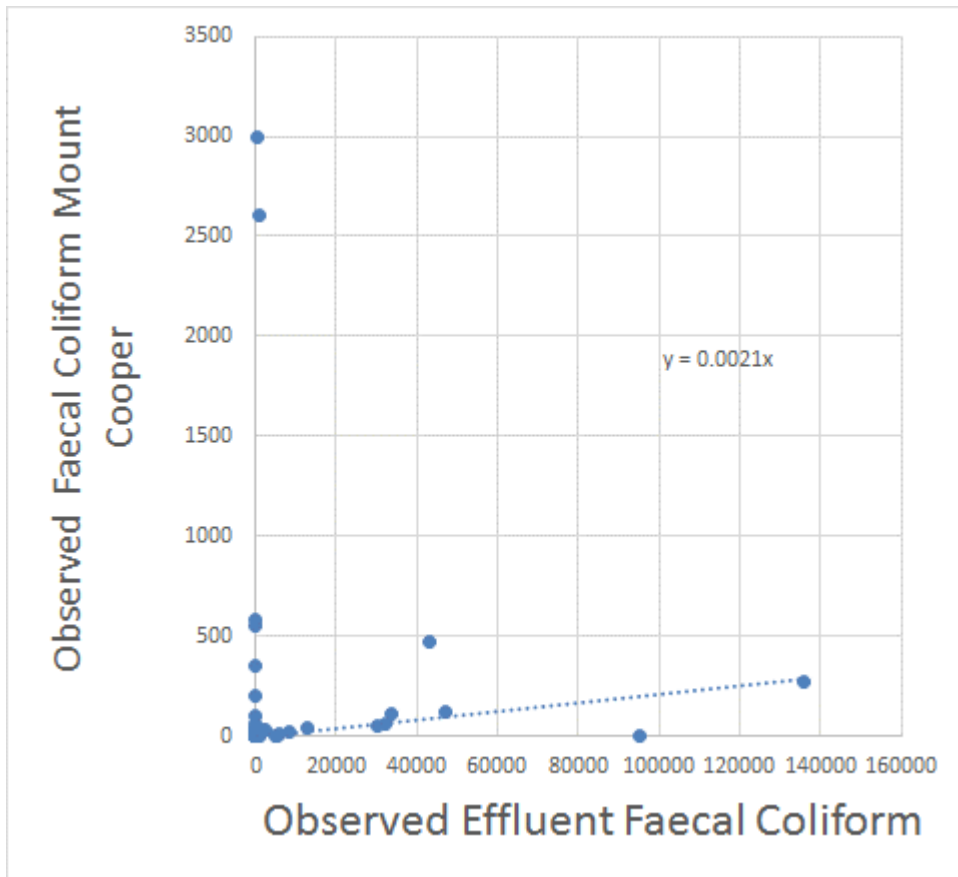


Figure C-5. Regression plot of the observed faecal coliform data at Mount Cooper and the treated wastewater concentration for all paired data (n=85).

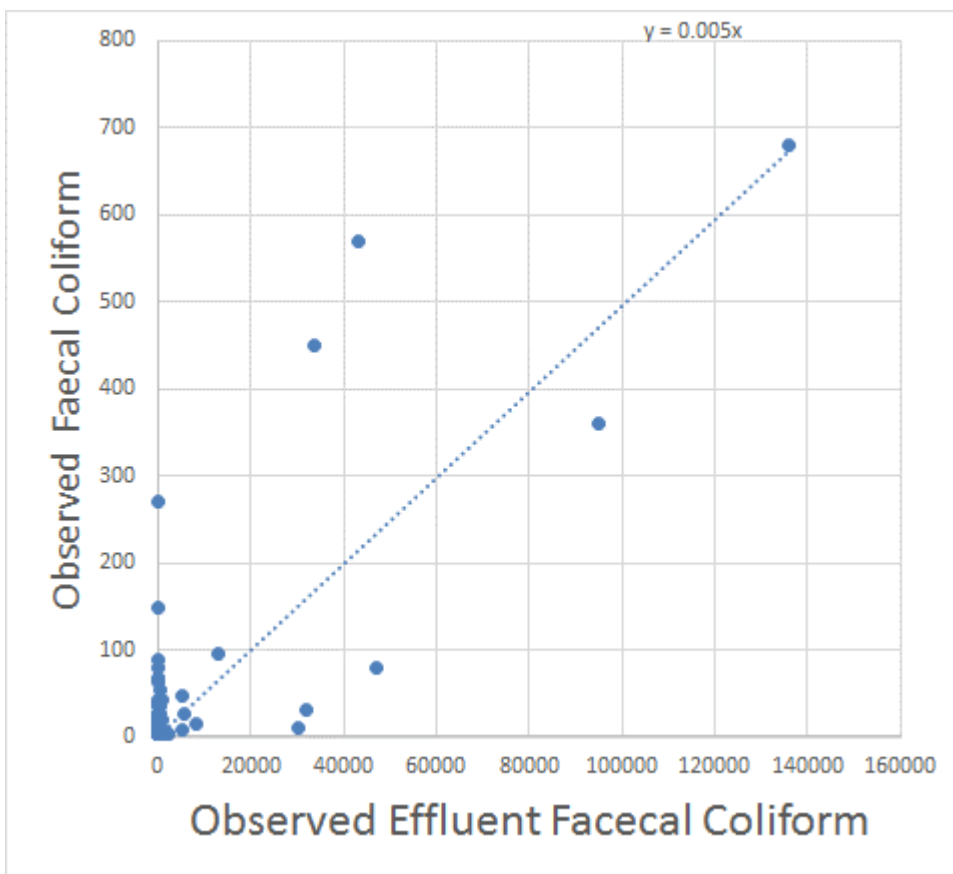


Figure C-6. Regression plot of the observed faecal coliform data at Te Korohiwa Rocks and the treated wastewater concentration for all paired data (n=85).

APPENDIX D – Review discussion document, Dougal Greer and John Oldman

Wellington Water
Private Bag 39804,
Wellington Mail Centre
5045

Att: Stewart McKenzie

**DHI Water and Environment
Ltd**

B:HIVE, Smales Farm
74 Taharoto Road
Takapuna 0622 Auckland

Private Bag 93504
Takapuna 0622 Auckland
New Zealand

+64 9 912 9638 Telephone

info.nz@dhigroup.com
www.dhigroup.com

44801085/04

JWO

25/07/2018

Concerning – eCoast Review of Titahi Bay Modelling Report

Dear Stewart

The following are the key concerns that have been raised by the peer review by eCoast of the DHI report "Titahi Bay Outfall Modelling" Draft V02 Dated 18/6/18.

1. Modelled concentration of wastewater will be lower than observed concentration at the surface and higher than the observed concentration at depth because the treated wastewater plume will float at the surface (para. 6 pg 2). Surface concentrations are likely to be considerably higher than predicted by the AD model (para 8, pg 3).
2. Wind driven surface layer currents are not represented in the HD y which will lead to an underestimation of plume excursion (para. 6 pg 2).
3. Calibration against time-series observations would provide a more thorough calibration of the AD model (para 7 pg 2).
4. The AD model will be less accurate offshore and model results should be treated with caution further offshore (para 6 pg 3).
5. The HD model should not be used for providing estimates of dilution (para 1 pg 4). The HD model will only provide a limited description of the freshwater plume (para5, pg 7).

Each of these concerns have been discussed in detail between John Oldman (DHI) and Dougal Greer (eCoast).

The following provides details of those discussions, areas of agreement and disagreement and an outline of the any major implications in terms of modelling of the existing Titahi Bay outfall.

There was a general discussion about the design of the field work and why Cawthron opted for carrying out a qualitative dye test as opposed to the deployment of salinity gauges.

Firstly, discussions with Cawthron indicated that detecting a salinity signal that could be attributed to the outfall will become increasingly difficult with distance from the outfall due to natural background variability in salinity, the level of potential dilution achieved and the presence of other freshwater sources along this part of the coast.

Because of the potential dynamic nature of the plume movement Cawthron and DHI agreed that a number of salinity sites would be required.

Cawthron were also concerned about the relatively high risk of damage to instruments due to wave climate at the site and the subsequent potential for data loss.

Based on previous experience with similar projects, Cawthron advised that a qualitative dyetest would provide valuable data on plume dynamics (albeit for only one set of conditions). The dye test was planned to be carried out during spring low tide with no winds/waves when plume mixing would be minimal.

1. *Modelled concentration of wastewater will be lower than observed concentration at the surface and higher than the observed concentration at depth because the treated wastewater plume will float at the surface (para. 6 pg 2 of eCoast review). Surface concentrations are likely to be considerably higher than predicted by the AD model (para 8, pg 3 of eCoast review).*

In the absence of field data and because of the complexities of the near-field processes it is agreed that it is difficult to accurately quantify what difference in vertical concentrations might be expected within the near-field region (i.e. within the first 10-50 m of the discharge). It is agreed that mixing in the near-field (i.e. close to the discharge within the pool immediately next to the discharge site) will be relatively high because of the configuration of the outfall structure itself, the water depth at the discharge location and complexities in the bathymetry in the immediate vicinity of the discharge.

Modelling such processes is very difficult and a certain degree of schematisation of the near-field processes is required for any far-field model. A 2D model assumes complete vertical mixing at the discharge location (i.e. all the discharge is released into a single model cell at the discharge location). Within a 3D model a certain portion of the discharge is assigned to each layer within the model cell at the discharge location. Further vertical mixing in the 3D model then occurs due to the presence of waves, wind and tidal currents and is influenced by the buoyancy of the plume (determined by its salinity).

It is agreed that, once the plume leaves the near-field, there will be certain situations (during sustained offshore winds) where there will be limited vertical mixing of the treated wastewater plume. Under such conditions, winds will influence the movement of the surface layer which will result in higher concentrations in the surface layer than those predicted by the depth-averaged model.

Onshore winds will tend to move the treated wastewater plume into shallower water where waves (which have not been modelled) will enhance vertical mixing of the water column so the depth-averaged model results will provide relatively accurate prediction of treated wastewater concentrations in the near-shore.

It is agreed that the largest differences between predicted plume dynamics using a 2D and 3D model will occur under periods of sustained offshore winds and in the absence of waves.

Based on the Mana Island wind record winds from the south-east (i.e. offshore) occur for 27% of the time and for sustained events (i.e. events greater than 3-hours of offshore) mean speeds of between 5 and 7 m/s occur. Approximately three-quarters of these events are less than 20-hour duration.

An analysis of monitoring data shows that 0.5 m waves occur 23% of the time, 1.0 m waves 16 % of the time and 2.0 m waves 8% of the time. Data from the ADCP deployment period show similar statistics (i.e. waves of greater than 0.5 m occur for 40% of the time and waves greater than 1.0 m occur for 14% of the time).

2. *Wind driven surface layer currents are not represented in the HD model which will lead to an underestimation of plume excursion (para. 6 pg 2 of eCoast review).*

It is agreed that, if a wind is blowing in a reasonably constant direction for a number of tidal cycles the surface layer, as well as being influenced by the tidal currents, will be transported in the general direction of the wind.

Under such conditions, the “downwind” plume concentrations in the surface layer will be higher than is estimated by the depth-averaged model.

It is agreed that there will also be times when the wind will hinder the excursion of the surface plume.

It is agreed that during periods of higher onshore winds vertical mixing will be enhanced by waves so any discrepancies between a depth-averaged and 3D model will be minimal.

3. *Calibration against time-series observations would provide a more thorough calibration of the AD model (para 7 pg 2 of eCoast review).*

There is agreement that, because of the sporadic nature of the monitoring data, there would be little benefit in carrying out a model simulation that spans the three years of data where there is overlapping beach monitoring and effluent quality data.

There are gaps in data for both the daily effluent flow data and effluent quality data. Such gaps would have to be interpolated which would introduce an unknown level of uncertainty to the model results.

It is unknown how representative the daily effluent quality data

The beach monitoring data has no time stamp associated with it (just a state of tide flag) so there would be large errors associated with estimating exactly when samples were collected.

Recent work carried out for the Auckland Council Safeswim has shown significant variations in replicates collected during rainfall events and it has been determined that laboratory result may have an accuracy of less than 20%.

At times the measured bacteria concentrations are higher at monitoring locations than at the outfall. Such elevated bacteria counts cannot therefore be attributed to the outfall and such events would have to be removed from the dataset.

4. *The AD model will be less accurate offshore and model results should be treated with caution further offshore (para 6 pg 3 of eCoast review).*

It is agreed that the largest differences between a 2D and 3D model would occur when the plume is transported in deeper waters during periods of sustained offshore winds and in the absence of waves.

Plume dilution will increase with distance offshore and vertical mixing of the treated wastewater plume under such conditions will be minimised.

It is agreed that, under these conditions, the predicted depth averaged concentrations will be approximately representative of the average salinity through the water column. If the potential for higher concentrations in the surface layer is not of concern at offshore sites then the 2D results can be used to assess the effects of the existing discharge at offshore sites.

John Oldman is of the opinion that because of degree of near-field mixing that occurs, salinity will be significantly increased (above 0 PSU) in the near field. As such, even under conditions identified above, vertical mixing will occur which that will lead to relatively small differences in predicted salinities between the surface layer and at depth. This could only be confirmed through calibrating a 3D model and/or carrying sensitivity testing of a 3D model.

Dougal Greer is of the opinion that a floating layer of treated wastewater could persist over some distance. In the absence of measured data it is hard to say how far in this instance.

5. *The HD model should not be used for providing estimates of dilution (para 1 pg 4). The HD model will only provide a limited description of the freshwater plume (para5, pg 7).*

It is agreed that the salinity results from the depth-averaged model can be used to provide estimates of the potential plume footprint in the near shore. If the stratification is not of concern, then it could also be used to estimate the plume footprint in deeper water. This would be achieved by identifying areas where the lowest levels of dilutions will be achieved (i.e. where plume impacts may be expected to be of concern) and where very large dilutions will be achieved (and the plume will have little influence on contaminant levels). Typically, such data is used to guide the site selection process for any QMRA work.

Dilution estimates for other non-conservative contaminants should only be derived when appropriate decay factors have been applied to the contaminant of concern.

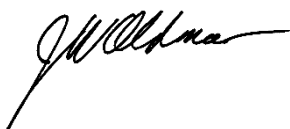
John Oldman is of the opinion that the 4-month simulations provide a very good description of the potential transport pathways of the plume because it models a very wide range of winds. Because of the limited time when vertical mixing is minimised, the variability in such transport pathways due to the potential differences between a 2D and 3D model will be relatively small compared to the variability predicted during the 4-month simulation.

Further information required:

1. **Can time series comparisons of measured and modelled Faecal Coliform be provided?**
Discussed above
2. **Are the axis labels the wrong way around in Fig 3-3 or is the dispersion coefficient incorrect?**
Yes this section of the report has been rewritten. Derived dispersion coefficient is correct (0.037 m³/s) and falls within the range of literature value 0.01 – 0.06 (reference to be supplied).
3. **Can axis labels be added to the plots in Appendix C?**
Done.
4. **Where in the water column were Faecal Coliform samples taken?**
Something to be check with Wellington Water.
5. **How was wastewater represented in the HD model?**
The discharge schematised as a zero-salinity discharge into channelised quadrilateral element. This provide realistic discharge velocities in line with what could be expected from the 800 mm diameter outfall.
6. **Can you confirm that plots of concentration in Section 7 are from the AD model and not the HD model?**
Concentration plots in the report are from AD model.

Best regards

DHI

A handwritten signature in black ink, appearing to read 'John Oldman', written in a cursive style.

John Oldman
Principal Coastal Scientist

Titahi Bay Outfall Options



Titahi Bay Outfall Options

Prepared for Wellington Water Ltd
Represented by Steve Hutchison



Titahi Bay Wastewater discharge location. 29th November 2017, X-Craft drone imagery.

Project manager	John Oldman
Project number	44801313
Approval date	3 rd April 2020
Revision	Final - Including overflow events and cross referencing to Population and Flows Memo

CONTENTS

1	Executive Summary	iii
2	Introduction	1
2.1	Discharge Scenarios	2
2.2	Details of Offshore Outfalls.....	3
3	Model Assumptions	4
3.1	Mesh	4
3.2	Winds.....	5
3.3	Source Concentration	7
3.4	Inactivation Rates	7
4	Near Field Modelling	9
5	Far Field Modelling	13
5.1	Average Dry Weather flows	13
5.1.1	Current Average Dry Weather Simulations	14
5.1.2	Future Average Dry Weather Simulations	16
	Results for 390 L/s future average dry weather flow	16
	Results for 455 L/s future average dry weather flow	25
5.2	Future PWWF Scenarios	31
5.2.1	Typical Winds and Spring Tide - 1500 L/s PWWF	31
5.2.2	Onshore Winds and Spring Tide - 1500 L/s PWWF	38
5.2.3	Typical Winds and Neap Tide - 1500 L/s PWWF	44
5.2.4	Onshore Winds and Neap Tide - 1500 L/s PWWF.....	51
5.3	Future Overflow Scenarios	57
5.3.1	Typical Winds and Spring Tide – Overflow Scenarios	59
5.3.2	Onshore Winds and Spring Tide - Overflow Scenarios.....	66
5.3.3	Typical Winds and Neap Tide - Overflow Scenarios	73
5.3.4	Onshore Winds and Neap Tide - Overflow Scenarios.....	80

References	87
Appendix A – CORMIX Near-field dilution vs Distance	88
Appendix B – Existing ADF time-series results at monitoring sites	100
Appendix C – Time-series results at monitoring sites for a 390 L/s Future ADF	106
Appendix D – Time-series at Monitoring site 200 m SW of existing discharge (PWWF discharge and overflow scenarios).....	112
Appendix E – Time-series at Monitoring site 200 m E of existing discharge (PWWF discharge and overflow scenarios).....	120
Appendix F – Time-series at Ti Korohiwa Rocks Monitoring site (PWWF discharge and overflow scenarios)	128
Appendix G – Time-series at Titahi Beach South Monitoring site (PWWF discharge and overflow scenarios)	136
Appendix H – Time-series at Titahi Beach Monitoring site (PWWF discharge and overflow scenarios)	144
Appendix I – Time-series at Mt Couper Monitoring site (PWWF discharge and overflow scenarios)	152

1 Executive Summary

This report provides details of the modelling carried out to assess alternative discharge options for the existing Titahi Bay wastewater treatment plant (WWTP).

Currently, the treated wastewater is discharged from the WWTP via a shoreline structure located at Rukutane Point.

The alternative discharge site considered include a new shoreline discharge at Round Point (to the east of the existing discharge point) and two offshore outfalls located 250 m and 525 m offshore of the existing discharge location in 10 m and 15 m respectively.

The assessment of these alternative discharge locations has been done using a calibrated hydrodynamic model of the area offshore of Titahi Bay. The model has been calibrated against observed water levels, currents and data from a dye test data as detailed in *Titahi Bay Outfall Modelling: DHI report 44801085*.

Near-field modelling of the existing shoreline discharge indicates that rapid vertical mixing will occur due to a combination of entrainment of ambient seawater into the discharge area and downward vertical mixing due to the discharge structure configuration. Water depth in the immediate vicinity of the existing discharge site is relatively shallow which results in relative low levels of dilution. Model results from the simulation of the existing shoreline discharge compare favourable to monitoring data collected both in the immediate vicinity of the existing discharge and at Titahi Beach.

Details of the location of the alternative discharge sites are discussed in Section 2. Model assumptions and setup details are presented in Section 3. Details of the near-field modelling of the offshore outfalls are presented in Section 4, while a complete description of the model results are presented in Section 5.

For this report, the alternative discharge locations are assessed in the context of the levels of dilution achieved by the existing discharge for current day flows (300 L/s) and potential future average dry weather flows of both 390 L/s and 455 L/s. Subsequent to the completion of the modelling a future average dry weather flow rate of 440 L/s has been derived¹. This future average dry weather rate (440 L/s) is modelled in detail in Oldman and Dada (2019) as part of the Quantitative Microbiological Risk Assessment.

This report also presents results for a future peak wet weather flow of 1500 L/s.

In addition, this report provides results for an overflow scenario where a peak discharge rate of 2600 L/s occurs. Subsequently Wellington Water has determined to manage the network so that inflow to the WWTP does not exceed 1500 L/s during the proposed consent period. As a consequence, the predicted concentrations associated with the 2,600 L/s scenario presented in this report will not occur.

For the dry weather and peak wet weather flows continuous fixed flows rates are assumed while for the future overflow scenarios time-varying discharge rates has been used based on outputs from network model simulations.

Both Enterococci and Viruses have been modelled with appropriate, time-varying inactivation rates.

For both pathogens a source concentration of 1000 count/100 mL has been assumed.

Current Day Dry Weather Flow

¹ Porirua WWTP Consent – Population and Flows and Climate Change Memo dated January 31st 2020.

Discharges via the existing structure at Rukutane Point under the current day dry weather flow rate of 300 L/s result in predicted 95th percentile concentrations at the monitoring sites near the existing discharge that range from 111 to 128 count/100 mL. At the Titahi Beach monitoring sites the 95th percentile concentrations range from 18 to 62 count/100 mL while at the more remote monitoring sites at Te Korohiwa Rocks and Mount Couper the 95th percentile concentrations range from 3 to 9 count/100 mL.

Future Dry Weather Flow

For a future dry weather flow rate of 455 L/s (the highest of the two future rates considered) there is a corresponding increase in percentile concentrations at the monitoring sites – ranging from 175 to 200 count/100 mL at the sites near the existing discharge, between 30 to 89 count/100 mL at the Titahi Beach sites and between 5 to 13 count/100 mL at the more remote monitoring sites.

For a new shoreline discharge at Round Point percentile concentrations at the Ti Korohiwa Rocks monitoring site (which is adjacent to the new shoreline discharge) increase by a factor of between 26 and 47 occur resulting in the predicted 95th percentile concentration of between 280 and 290 count/100 mL. At the monitoring site east of the existing discharge point (towards Round Point) the reductions in percentile concentration range between 38 and 53%. At all the other monitoring sites reductions of the predicted percentile concentrations range from 82-95%.

Estimates of dilution achieved immediately over the 10 m deep outfall range from around 150-340 and increase to between 230 and 500 for the 15 m deep outfall. In the area around the outfall sites, relatively strong, complex currents occur resulting in a high degree of subsequent dilution leading to significant levels of dilution at the shoreline.

The reduction of the predicted percentile concentrations at the monitoring sites near the existing discharge and the Titahi Beach sites for the 10 m outfall range between 87 and 96%. Reductions in percentile concentrations at the Ti Korohiwa Rocks range between 55 and 63% while at the Mount Couper site reductions in the percentile concentrations range between 38 and 66% occur.

Model results indicate that there are times when the 10 m outfall option result in higher concentrations at the Mount Couper monitoring site compared to the concentrations that occur with the existing shoreline discharge. This relates to the relative travel time of the treated wastewater plume and the level of inactivation that occurs as the plume either traverses Titahi Beach (in the case of the existing discharge) or travels more directly to the Mount Couper site from the 10 m outfall.

For the 15 m outfall the higher initial dilutions achieved and the increase distance from the shore results in reductions of the predicted percentile concentrations at the monitoring sites near the existing discharge and the Titahi Beach sites of around 99%. Reductions in percentile concentrations at the Ti Korohiwa Rocks range between 95 and 97% while at the Mount Couper site reductions in the percentile concentrations of between 84 and 93% occur. Concentrations at the Mount Couper site are nearly always less than those predicted to occur under the existing shoreline discharge.

Future Peak Wet Weather Flows

Depending on the prevailing wind at the time of the peak wet weather flow, a discharge from the existing shoreline structure at Rukutane Point results in predicted 99th percentile concentrations at the monitoring sites near the existing discharge that range from 291 to 630 count/100 mL. At the Titahi Beach monitoring sites the 99th percentile concentrations range from 55 to 204 count/100 mL while at the more remote monitoring sites at Te Korohiwa Rocks and Mount Couper the 99th percentile concentration ranges from 4 to 22 count/100 mL.

For a new shoreline discharge at Round Point percentile concentrations at the monitoring site to the east of the existing discharge are reduced by between 13 and 84%. At the monitoring site to the east of the existing discharge percentile concentrations are reduced between 75 and 93%. At the Ti Korohiwa Rocks monitoring site (which is adjacent to the new shoreline discharge) percentile concentrations are increased by a factor of between 11 and 54. At the Mount Couper monitoring site reductions in percentile concentrations range from 75 to 92%.

For the 10m outfall option, the percentile concentrations at the monitoring site to the west of the existing discharge site are reduced by at least 95%. For the monitoring site east of the existing discharge percentile concentrations are reduced by at least 89%. At the Ti Korohiwa Rocks site percentile concentrations are reduced between 6 and 75%. At the Mount Couper site percentile concentrations are reduced between 15 and 74%. Under neap tide and more typical wind conditions there are times when the predicted concentrations at the Ti Korohiwa Rocks site are higher compared to those predicted for the existing shoreline discharge. Similarly, there are times under neap tides and more typical wind conditions when concentrations at the Mount Couper site are higher than those predicted for the existing shoreline discharge.

For the 15m outfall option, the percentile concentrations at the monitoring sites to the west and east of the existing discharge site are reduced by at least 99%. Similar levels of reductions occur at the Titahi Beach monitoring sites. At the Ti Korohiwa Rocks site percentile concentrations are reduced between 82 and 97%. At the Mount Couper site percentile concentrations are reduced between 56 and 94%.

Future Overflow Scenario

Depending on the prevailing wind at the time, an overflow from the existing shoreline structure at Rukutane Point results in predicted 99th percentile concentrations at the monitoring sites near the existing discharge that range from 275 to 730 count/100 mL. At the Titahi Beach monitoring sites, the 99th percentile concentrations range from 74 to 247 count/100 mL while at the more remote monitoring sites at Te Korohiwa Rocks and Mount Couper the 99th percentile concentrations are around 25 count/100 mL.

For an overflow via the new shoreline discharge at Round Point percentile concentrations at the monitoring site immediately west of the existing discharges are reduced by between 4 and 39%. At the monitoring site immediately east of the existing discharge reductions in percentile concentrations generally range from 25 to 41% although under neap tides and onshore winds there is a small (< 5%) increase in the predicted 90th percentile concentration at this site. At the Titahi Beach sites reductions in the percentile concentrations range from 25 to 42%. At the Ti Korohiwa Rocks monitoring site (which is adjacent to the new shoreline discharge) increases in the percentile concentrations of between 23 and 42 % occur. At the Mount Couper site reductions in the percentile concentrations range from 7 to 38%.

For an overflow via the 10 m outfall, reductions in the predicted percentile concentrations of at least 86% occur at the monitoring site near the existing discharge and the Titahi Beach sites. At Ti Korohiwa Rocks site reductions in percentile concentrations of between 46 and 75% occur while at the Mount Couper site reductions in the predicted percentile concentrations of between 27 and 78% occur.

For an overflow via the 15 m outfall, reductions in the predicted percentile concentrations of at least 77% occur. At all other monitoring sites reductions in percentile concentrations of at least 95% are predicted to occur.

2 Introduction

This report provides details of the modelling carrying out which assessing discharge options for the existing Titahi Bay wastewater treatment plant (WWTP).

Currently, the treated wastewater is discharged from the WWTP via a shoreline structure located at Rukutane Point (Figure 2-1). This report considers offshore outfalls at water depths of 10m and 15m offshore of Rukutane Point and a new shoreline discharge towards Round Point.

The baseline conditions modelled are the current average dry weather discharge from the existing shoreline discharge point. Alternative discharge site considered include a new shoreline discharge at Round Point (to the east of the existing discharge point) and two offshore outfalls located 250 m and 525 m offshore of the existing discharge location in 10 m and 15 m respectively.

Discharge scenarios considered include future average dry weather flow, future peak wet weather flows and a future overflow scenario which includes a split of flows through the WWTP and an overflow component.

A hydrodynamic model of the area offshore of the existing discharge was developed and calibrated against water level, current and dye test data as detailed in DHI (2018). This model is used to assess the proposed discharges in the context of the existing discharge location.

Near field modelling of the offshore outfalls has been carried out to assess the applicability of a depth-averaged model for the assessment of the offshore outfalls.

The report provides an overview of the model assumptions, boundary data and input data used (Section 1), details of the near-field modelling (Section 4) and the assessment of each of the discharge options in the context of the existing discharge (Section 5).

Based on this report a preferred discharge option will be selected. For this preferred option, an annual simulation will be carried out to provide data for a full quantitative microbial risk assessment.



Figure 2-1. Location of existing shoreline discharge, offshore outfalls and new shoreline discharge at Round Point.

2.1 Discharge Scenarios

Data in Table 1 and Table 2 show the discharge scenarios considered. The current average dry weather flow is derived from the average from WWTP monitoring data for the period 30.09.2017 to 30.09.2018. The future average dry weather flow is derived from population increase from 84,000 in 2018 to 108,287 in 2051 (Mott MacDonald, 2016).

Table 1. Average dry weather and peak wet weather discharge scenarios.

	Current ADF Scenario	Future ADF Scenarios			Future PWWF Scenarios	
WWTP Flows	300 L/s (ADF)	390 L/s (ADF)	390 L/s (ADF)	390 L/s (ADF)	1500 L/s	1500 L/s
Year	2018	2054	2054	2054	2054	2054
Flow Duration	Continuous	Continuous	Continuous	Continuous	12 hours	12 hours
Discharge location	Existing Shoreline Rukutane Point	Existing Shoreline Rukutane Point	New Shoreline Round Point	New Ocean Outfall Round Point	New Shoreline Round Point	New Ocean Outfall Round Point

Table 2. Overflow discharge scenarios.

	Overflow Scenarios		
WWTP Flows	Time-varying hydrograph	Time-varying hydrograph	Time-varying hydrograph
Year	2054	2054	2054
Flow Duration	36 hours above future ADF rate	36 hours above future ADF rate	36 hours above future ADF rate
Discharge location	Existing Shoreline Rukutane Point	Existing Shoreline Rukutane Point	New Ocean Outfall Round Point
Outfall location	Existing Shoreline Rukutane Point	New Shoreline Round Point	New Ocean Outfall Round Point

2.2 Details of Offshore Outfalls

Both of the offshore outfall options being considered would consist of a 150 m long diffuser with an inner diameter of 1.0 m with 60 alternating ports spaced 2.5 m apart. The ports would be fitted with 150 mm duckbill valves that would maintain high jet velocities for the Average Dry Weather (ADF) discharges being considered (390-455 L/s) and the design discharge of 1500 L/s.

Manufacturer data indicates that for the future ADF discharge, an equivalent port diameter of 60 mm could be achieved with duck bill valves. For the future PWWF discharge, an equivalent port diameter of 100 mm could be achieved. This would result in jet velocities of around 2.5 m/s.

The centre of the diffusers would be located at the coordinates shown in Table 3.

This would mean that the 10 m outfall diffuser would sit between 175 and 325 m offshore of the existing discharge structure and the 15 m outfall diffuser would sit between 450 and 600 m offshore of the existing discharge structure.

Table 3. Location of the centre of the diffuser for the 10 m and 15m offshore outfall options.

Offshore outfall Option	Latitude	Longitude
10 m outfall	174° 49.28'	41° 06.23'
15 m outfall	174° 49.17'	41° 06.10'

3 Model Assumptions

For this work the previously calibrated depth-averaged model of the area immediately offshore of Titahi Bay and Porirua Harbour (Figure 3-1) was used to assess the potential impacts of the proposed discharges. Details of the calibration of the model against observed water level data, current metre data and dye test information are presented in DHI (2018).

3.1 Mesh

For the assessment of the future options, the resolution of the mesh was decreased to provide 50 m² elements (~10 m element faces) in the area between the existing and new shoreline discharge points (Figure 3-2). In addition, the resolution of the mesh offshore of Rukutane and Round Point was adjusted to provide good representation of the near-field region across both proposed diffusers. The mean element area in this area was 200 m² (~20 m element faces).

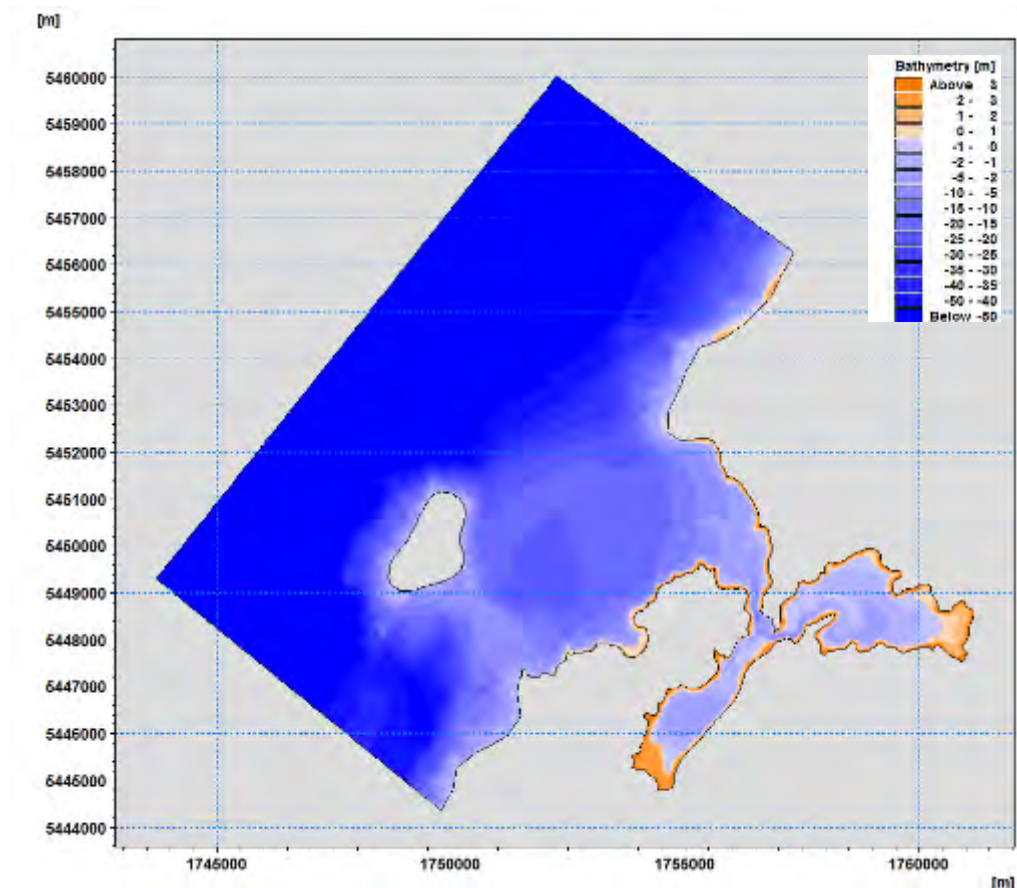


Figure 3-1. Extent of the Titahi Bay model grid.

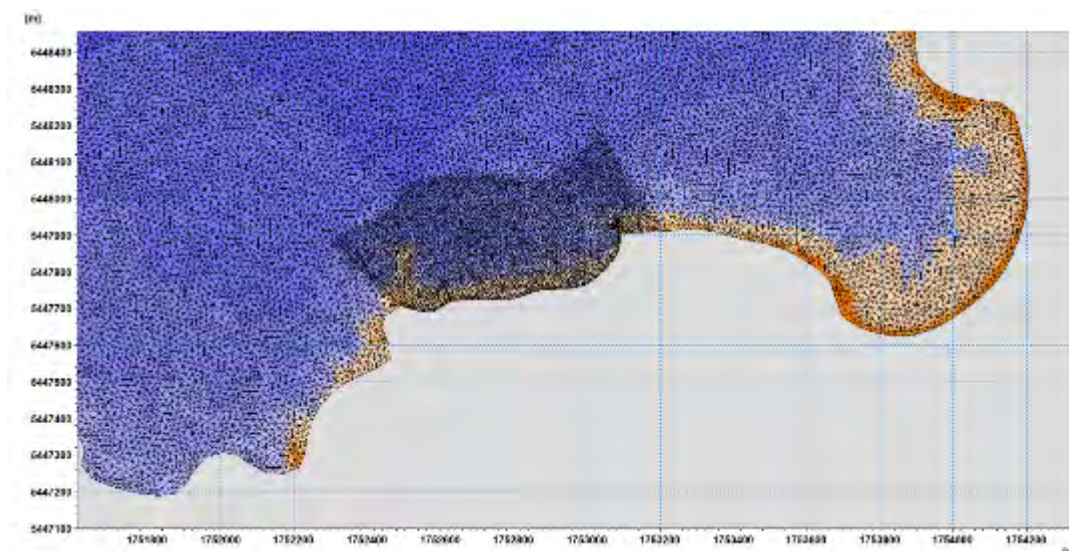


Figure 3-2. Mesh detail offshore of the WWTP.

The near-field modelling of the offshore outfalls (Section 4) indicates that, for the diffuser design being considered, the discharge from the offshore outfalls would be very close to fully mixed in the water column except when ambient currents are very low. Data from a current meter deployed midway between the two offshore outfalls indicate that such currents only occur for a very limited time each tidal cycle.

Detailed modelling of the existing discharge structure and data from the dye test indicate that full mixing of the treated wastewater plume from a shoreline structure would occur relatively rapidly

This means that the depth-averaged model is fit for purpose for the assessment of the proposed discharges.

3.2 Winds

The assessment of the existing discharge (DHI, 2017) used a 5-month period (Jan-May 2017) for the model simulations. Because of the time-constraints on this project and the number of discharge options being considered (Table 1 and Table 2) it was not feasible to run each of the scenarios being considered for the 5-month period. Instead, a 6-week period was chosen that had representative winds based on an analysis of the available long-term wind record from Mana Island.

Analysis of the long-term wind record indicated that the 6-week period from the 11.08.07 has a very similar distribution of wind speeds (Table 4) and directions (Figure 3-3) to the long-term record.

Figure 3-4 shows the wind speed and direction for the 6-week period. It includes a period of relatively strong north-easterly winds at the start of the period followed by more typical wind speeds and with highly variable direction. This 6-week period is used for simulating the ADF scenarios (Table 1).

For the PWWF scenarios (Table 1), the initial part of the wind record is used for simulating an onshore wind condition while the middle part of the 6-week wind record is used for simulating more typical wind conditions that occur during the 12-hour peak discharge.

Table 4. Percentile winds speed from the representative 6-week period (11.08.07-22.09.07) and the long-term wind record (2013-2018) from Mana Island automated weather station.

Offshore outfall Option	Latitude	Longitude
95 th Percentile wind speed	11.4 m/s	11.4 m/s
90 th Percentile wind speed	9.7 m/s	10.2 m/s
75 th Percentile wind speed	8.0 m/s	8.0 m/s
50 th Percentile wind speed	5.9 m/s	5.7 m/s

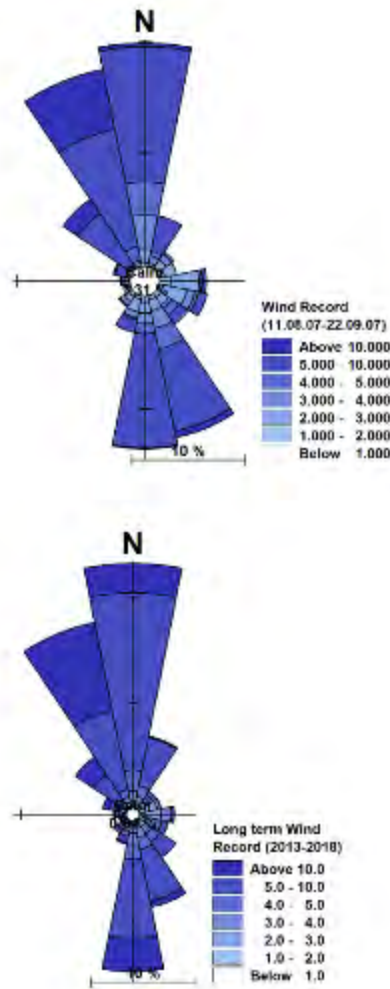


Figure 3-3. Wind rose for the representative 6-week period (11.08.07-22.09.07) and the long-term wind record (2013-2018) from Mana Island automated weather station.

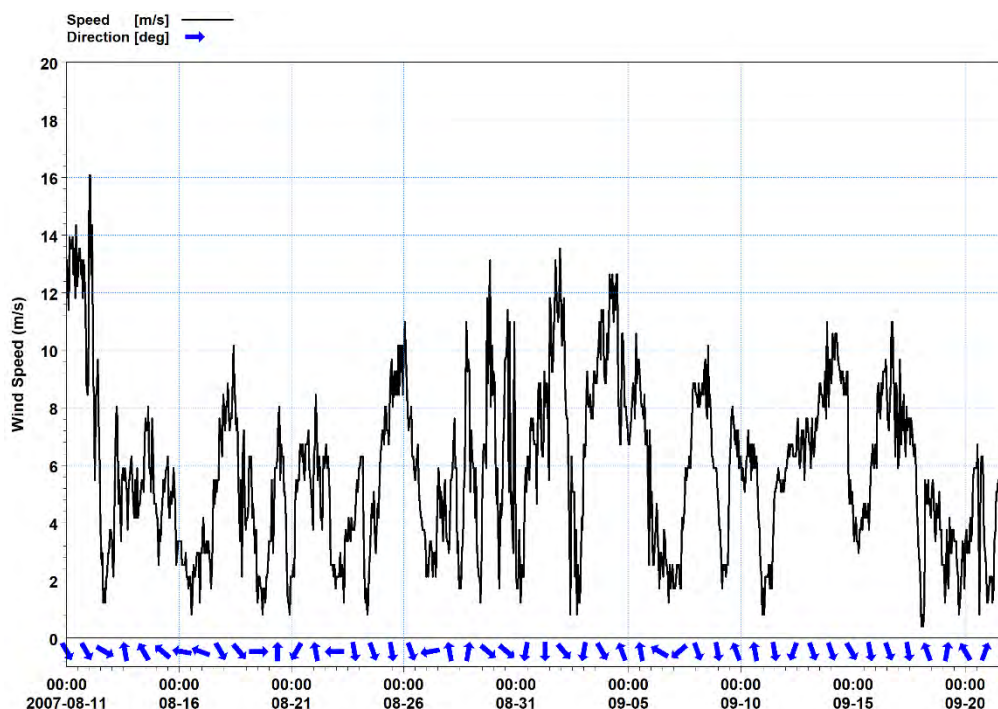


Figure 3-4. Time-series of wind speed and directions for the 6-week period (11.08.07-22.09.07) used for assessing the proposed discharges.

3.3 Source Concentration

It has been assumed that the source concentration for the scenarios is 1000 Ent/100 mL and 1000 Virus/100 mL.

3.4 Inactivation Rates

The previous modelling (DHI, 2018), assumed a constant decay rate of 0.083 h^{-1} . This inactivation is close to typical observed decay rates that occur at depth in saline waters of 0.104 h^{-1} (Maraccini et. al, 2016) and lower than the typical summer daylight decay rates for Enterococci reported by Noble et. al 1994 (0.140 h^{-1}). This probably reflects the turbid nature of the waters offshore of the treatment plant.

For this assessment of the proposed discharges time varying inactivation rates for both Viruses and Enterococci have been considered.

Viruses were modelled assuming worst case dark (nighttime) inactivation coefficient for of 0.015 h^{-1} and a daytime coefficient of 0.045 h^{-1} . These wintertime inactivation coefficients were derived from data presented in Sinton et. al (1999)

For Enterococci, the dark inactivation coefficient was assumed to be 0.013 h^{-1} while the daytime coefficient was assumed to be 0.19 h^{-1} . These winter inactivation coefficients were derived from data presented in Sinton et. al (1994) and Noble et. al (1994).

Inactivation rates for summer will be higher so the model results will provide conservative (i.e. higher) estimates of predicted concentrations of Viruses and Enterococci than could occur in summer.

The seasonal and daily variation for inactivation rates for both Viruses and Enterococci were derived based on the above dark and light inactivation rates. The seasonal variation

in the maximum dark and light rates were derived using a sigmoidal variation based on the number of days to and from winter solstice as follows;

$$k_{DayNumber} = k_{winter} + (k_{summer} + k_{winter}) / (1 + \exp(6 - 12 * DayNumber / 182))$$

Where k_{summer} or k_{winter} are the dark (or light) inactivation rates (as above) and $k_{DayNumber}$ is the daily maximum dark (or light) inactivation rate for the day of year being considered – where $DayNumber$ is defined as the time to or from the winter solstice;

$$DayNumber = \text{abs}(\text{Day of the Year} - 182)$$

Lastly, the light inactivation rate was modulated on an hourly basis based on the observed solar radiation from the Paraparaumu Aero Automated Weather Station for August 2007 (this being the nearest station to Titahi Bay with solar radiation dating back to 2007). The hourly inactivation rate (Figure 3-5) was assumed to be the predicted maximum daily inactivation rate (from above formula) multiplied by the ratio of the observed hourly solar radiation to the maximum clear sky solar radiation for the day being considered.

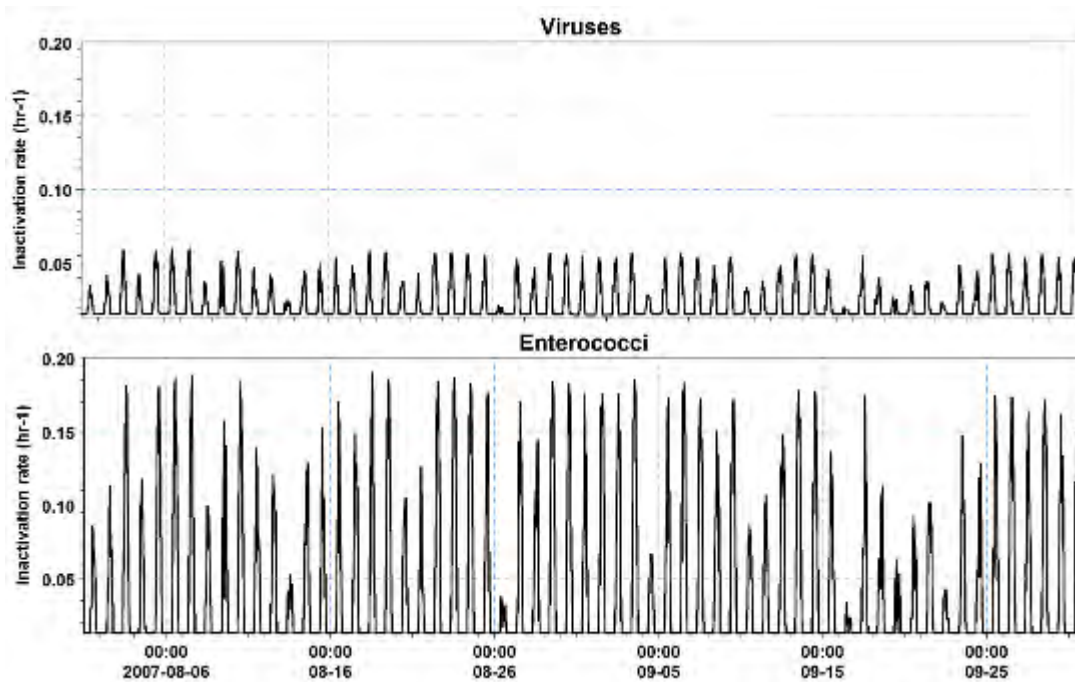


Figure 3-5. Time-series of inactivation rates for Viruses (top panel) and Enterococci (bottom panel) for the 6-week simulation period.

4 Near Field Modelling

The following gives an overview of the CORMIX modelling undertaken for the two offshore outfall options being considered (Table 3) for the future ADF rate of 390 L/s.

Near field modelling of the higher future ADF rate (455 L/s) has not been carried but results using the 390 L/s ADF rate can be scaled to provide approximate estimates of near field dilution that could be achieved.

The near-field region can be defined as the region where momentum dominates over buoyancy (Jirka et al. 1981). In this region the plume dynamics are driven by the enhanced velocities of the discharge as it initially enters the coastal region. In this region the momentum of the jet generates significant turbulence, which can result in rapid horizontal and vertical mixing of the plume with ambient waters and entrainment of ambient waters into the near-field region. Within this region it is necessary to use specialised near-field models (such as VISJET, Cheung et al. 2000 or CORMIX, Doneker and Jirka, 2007) to resolve to spatial and temporal physical processes that occur.

Beyond the near-field, the plume becomes passive (i.e. its momentum does not affect local hydrodynamics) and the combined effects of its buoyancy and the ambient receiving environment dominant its dynamics. Here it is appropriate to use the calibrated depth-average model to quantify the dynamics of the treated wastewater plume.

CORMIX assumes a uniform bathymetry and ambient current in the immediate vicinity of a discharge. As such, a number of schematised steady state ambient current and water depth conditions need to be modelled to quantify the near-field dynamics of an ocean outfall.

Current and water depth data at the centre of the diffusers were extracted from the long-term model simulations carried out for the assessment of the existing shoreline discharge (DHI, 2018). Data at the 10 m outfall site is shown in Figure 4-1. The figure also shows the combinations of schematic water depth and ambient current conditions used for the CORMIX modelling. Data from the 15 m outfall showed a very similar distribution of ambient currents and so the schematic conditions modelled included the same ambient currents but an addition 5.0 m of water depth.

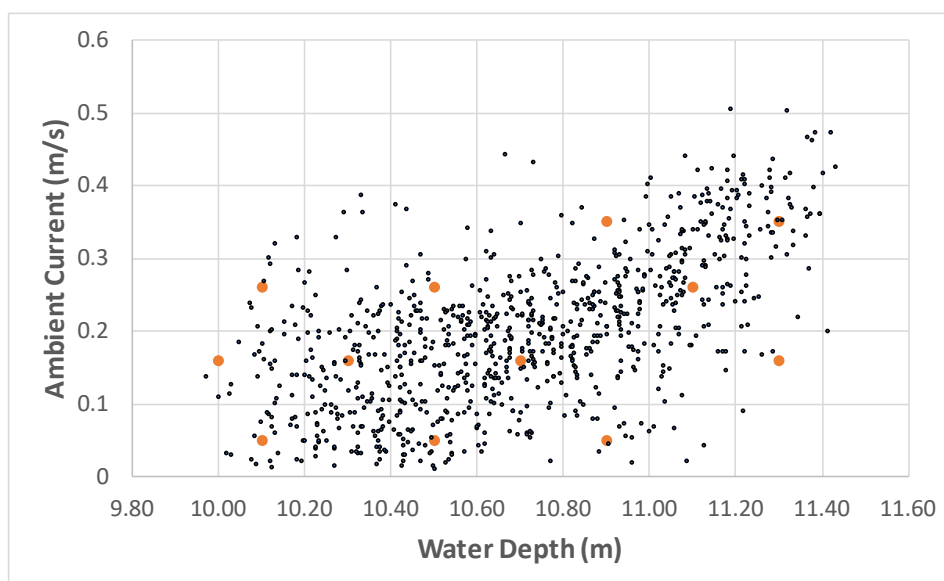


Figure 4-1. Predicted water depths and ambient current over the centre of the 10 m offshore outfall diffuser. Schematic water depth and ambient currents used in the CORMIX modelling shown as orange symbols.

Results from the CORMIX modelling are shown in Table 5 and Table 6 for the 10 m and 15 m outfalls respectively. The data shows that the treated wastewater plume is very close to being fully mixed in the vertical for the range of ambient current and water depths that could be expected.

It is only when ambient currents of less than 0.05 m/s (not presented here) that the treated wastewater plume is not fully mixed in the water column. The CORMIX results under these very low ambient currents also indicate such currents would have to occur for more than an hour for a non-vertically mixed plume to fully develop a stable structure. Current meter data shows low ambient currents only occur for around 20 minutes either side of high and low water. So

Appendix A provides figures of the predicted dilution versus distance for CORMIX simulations listed in Table 5 and Table 6.

Table 5. CORMIX results from the 10 m offshore outfall.

ID	Water depth (m)	Ambient current (m/s)	Vertical mixing (% of water column)	NFR (m)	Dilution at edge of NFR	100 m Dilution	200 m Dilution
A	10.1	0.08	100%	65	186	196	214
B	10.5	0.08	100%	69	195	204	225
C	10.9	0.16	92%	52	198	211	229
D	10.0	0.16	93%	52	181	194	210
E	10.3	0.16	92%	52	187	199	217
F	11.3	0.16	93%	52	205	219	238
G	10.7	0.16	92%	52	194	208	225
H	11.1	0.26	97%	47	303	318	337
I	10.5	0.26	97%	47	287	300	319
J	10.1	0.26	97%	47	276	289	307
K	10.9	0.35	98%	45	392	406	425
L	11.3	0.35	98%	45	407	421	441

Table 6. CORMIX results from the 15 m offshore outfall.

ID	Water depth (m)	Ambient current (m/s)	Vertical mixing (% of water column)	NFR (m)	Dilution at edge of NFR	100 m Dilution	200 m Dilution
A	15.1	0.08	100%	115	298	-	330
B	15.5	0.08	100%	119	307	-	336
C	15.9	0.16	92%	53	289	309	333
D	15.0	0.16	92%	53	272	291	316
E	15.3	0.16	92%	52	278	297	322
F	16.3	0.16	92%	52	295	316	342
G	15.7	0.16	93%	52	285	304	330
H	16.1	0.26	96%	48	442	461	489
I	15.5	0.26	96%	48	426	445	470
J	15.1	0.26	96%	47	414	433	459
K	15.9	0.35	100%	80	569	577	608
L	16.3	0.35	100%	82	583	592	622

5 Far Field Modelling

In this section of the report results from the calibrated far-field model are presented for each of the discharge scenarios considered.

Time-series results at the beach monitoring sites (Figure 5-1) are provided in Appendices B-I. Tabulated estimates of the percentile concentrations for each of the monitoring sites are provided in each of the following sections of the report along with spatial plots of the 95th percentile concentrations of the plume.



Figure 5-1. Beach monitoring sites.

5.1 Average Dry Weather flows

In this section of the report the current average dry weather flow of 300 L/s and a representative average dry weather flow for a future scenario are considered.

All scenarios are run for the constant discharge rates shown in Table 7.

Table 7. Average dry weather scenarios.

	Current ADF Scenario	Future ADF Scenarios		
WWTP Flows	300 L/s (ADF)	390 L/s (ADF)	390 L/s (ADF)	390 L/s (ADF)
Year	2018	2054	2054	2054
Flow Duration	Continuous	Continuous	Continuous	Continuous
Discharge location	Existing Shoreline Rukutane Point	Existing Shoreline Rukutane Point	New Shoreline Round Point	New Ocean Outfall Round Point

5.1.1 Current Average Dry Weather Simulations

Table 8 and Table 9 provide the percentile values for Enterococci and Viruses respectively for the existing shoreline discharge for the current ADF (300 L/s).

At the monitoring sites near the existing discharge the 95th percentile concentration ranges from 111 to 128 count/100 mL.

At the Titahi Beach monitoring sites the 95th percentile concentration ranges from 18 to 62 count/100 mL.

At the Te Korohiwa Rocks and Mount Couper monitoring sites the 95th percentile concentration ranges from 3 to 9 count/100 mL.

Viral concentrations are higher because of their lower inactivation rates (Figure 3-5).

Figure 5-2 and Figure 5-3 show the spatial plot of the predicted 95th percentile concentration for Enterococci and Viruses respectively. As previously reported, there is a band of higher concentration treated wastewater both to the west of the discharge point and moving into Titahi Bay. Because of the lower inactivation rates for Viruses, the footprint for the viral plume (Figure 5-3) is slightly larger than the Enterococci one.

Appendix B contains figures of the predicted time-series of data the monitoring sites.

This data provides the benchmark for assessing the discharge options being considered.

The percentile values are generally higher than those reported earlier (DHI, 2018) due to the lower (time-varying) inactivation rates used (Section 3.4). However, the time-series plots for the 6-week simulation show similar patterns of variations to the longer-term simulations carried out earlier (DHI, 2018) which relate to the wind speed and direction time and spring/neap tidal variations. This gives a good indication that the time period chosen is representative of the longer-term wind climate.

Table 8. Percentile estimates of Enterococci concentration (Ent/100 mL) at the monitoring sites, current ADF flow rate of 300 L/s.

Percentile	200 m SW	200 m E	Titahi Beach South	Titahi Beach	Ti Korohiwa	Mount Couper
50	43.3	54.6	21.9	5.5	3.1	0.5
90	96.1	106.5	48.5	15.1	6.9	2.0
95	111.1	121.4	56.4	17.7	7.9	3.0

Table 9. Percentile estimates of Virus concentration (Virus/100 mL) at the monitoring sites, current ADF flow rate of 300 L/s.

Percentile	200 m SW	200 m E	Titahi Beach South	Titahi Beach	Ti Korohiwa	Mount Couper
50	54.8	62.3	28.3	9.4	4.2	1.0
90	104.3	115.3	54.7	20.7	8.2	3.8
95	121.4	128.1	62.0	24.7	9.4	5.6

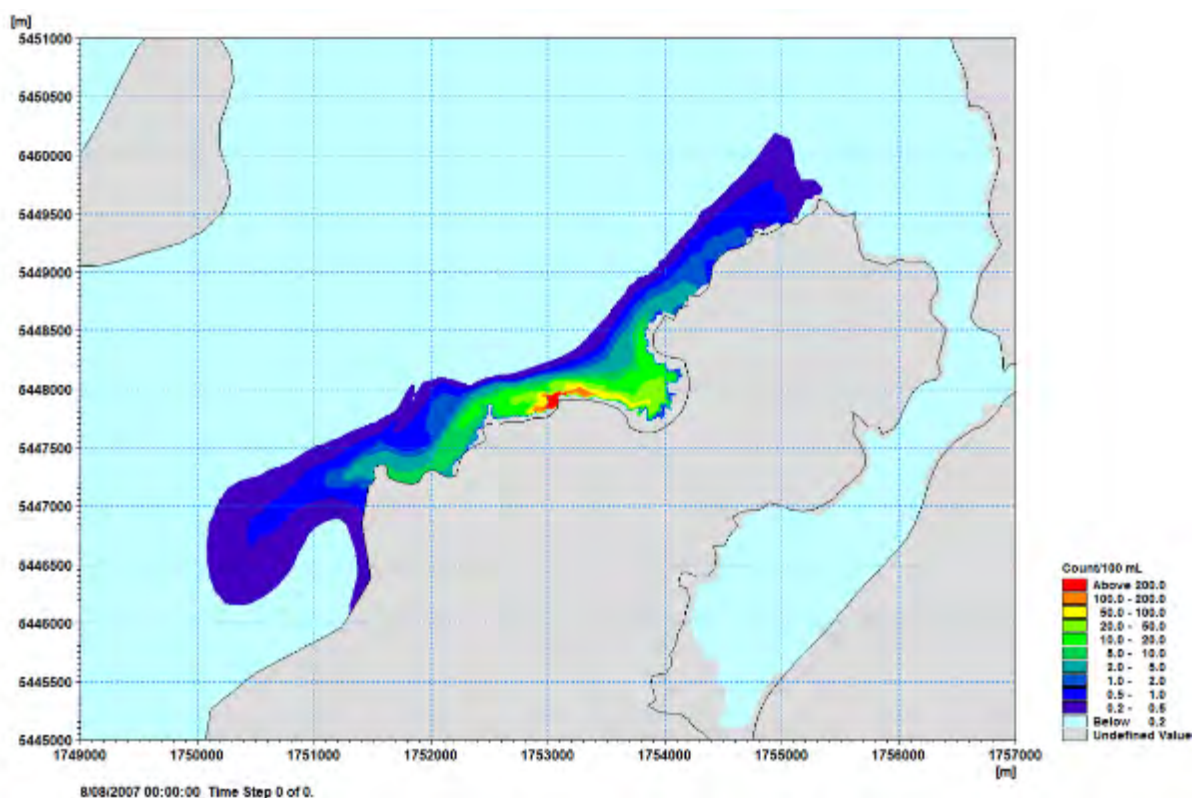


Figure 5-2. Predicted 95th percentile Enterococci concentration (Ent/100 mL), for the existing shoreline discharge for the current ADF flow rate of 300 L/s.

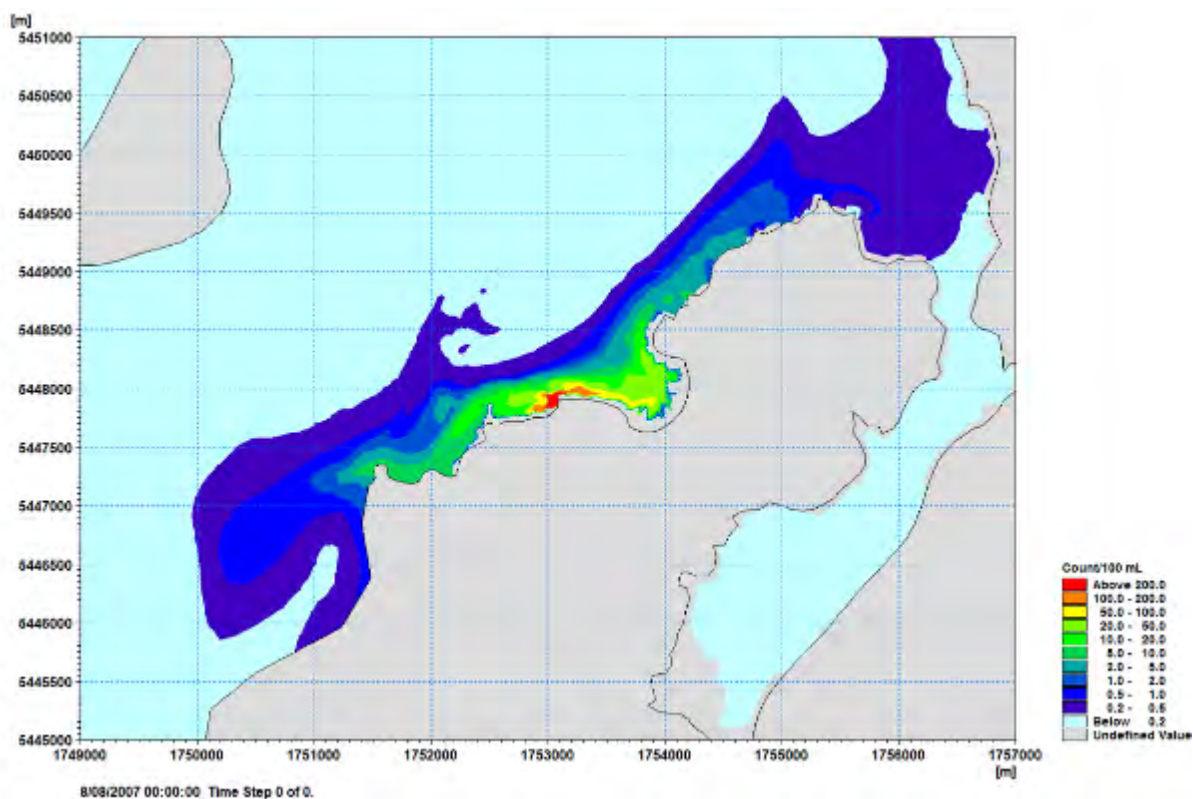


Figure 5-3. Predicted 95th percentile Virus concentration (Virus/100 mL), for the existing shoreline discharge for the current ADF flow rate of 300 L/s.

5.1.2 Future Average Dry Weather Simulations

This section of the report provides details of two future average dry weather flow conditions (390 and 455 L/s) which cover the range of the potential future dry weather discharge regimes being considered.

Results for 390 L/s future average dry weather flow

Table 10 and Table 11 provide percentile values for Enterococci and Virus respectively for the existing shoreline discharge and the discharge options for the future ADF (390 L/s).

Appendix C contains figures of the predicted time-series of data the monitoring sites.

The following provides an overview of the results of this scenario.

For the **existing shoreline** discharge the 95th percentile concentration ranges from 151 to 169 count/100 mL at the sites near the existing discharge

At the Titahi Beach sites the 95th percentile concentration ranges from 24 to 76 count/100 mL.

At the Te Korohiwa Rocks and Mount Couper monitoring sites the 95th percentile concentration ranges from 4 to 12 count/100 mL.

The **new shoreline** at Round Point discharge results in a reduction of the predicted percentile concentrations at the 200 m SW monitoring site of between 32 and 48%. At the 200 m E monitoring site the predicted percentile concentrations are reduced by between 85 and 95%. For the Titahi Beach monitoring sites the reductions in the predicted percentile concentrations ranges from 84-95%. At the Ti Korohiwa Rocks monitoring site (which is adjacent to the new shoreline discharge), increases of between 21 and 45 occur resulting in a predicted 95th percentile concentration of around 250 count/100 mL at this site. At the Mount Couper site reductions in the percentile concentrations of between 80 and 84% occur.

The **10 m outfall** option results in reduction in the predicted percentile concentrations at the 200 m SW monitoring site of around 98%. Similar reductions in the predicted percentile concentrations are predicted at the 200 m E monitoring site. At the Titahi Beach monitoring sites reductions in the predicted percentile concentrations of between 85 and 96% occur. Reductions in the predicted percentile concentrations at the Ti Korohiwa Rocks range between 58 and 65% while at the Mount Couper site reductions in the percentile concentrations of between 36 and 63% occur.

However, there are times when the 10 m outfall option result in similar (or higher) concentrations at the Mount Couper site compared to the existing shoreline discharge. During periods of onshore winds, the treated wastewater plume from the existing shoreline discharge is more constrained in the near shore zone. This results in highest concentrations at the monitoring sites with the existing shoreline discharge. During such periods the 10 m outfall option provides lower overall concentrations (Figure 5-4). During more typical winds (Figure 5-5), peak concentrations are higher with the 10 m outfall option compared to the existing shoreline discharge.

For the existing shoreline discharge, the treated wastewater plume must first traverse Titahi Beach to reach Mount Couper shoreline. This longer travel time (compared to the 10 m outfall plume which is transported directly to the Mount Couper shoreline by ambient tidal currents) results in more opportunity for inactivation and dilution.

This means that, at times, the increase in near-field dilution achieved by the 10 m outfall (~250-fold) compared to the dilution achieved by the existing shoreline (of the order of only 10-20-fold) is not sufficient to always produce lower concentrations at the Mount Couper site.

The **15 m outfall** option discharge results in a reduction of the predicted percentile concentrations at the 200 m SW monitoring site of greater than 99%. Similar reductions in the predicted percentile concentrations are seen at the 200 m E monitoring site. At the Titahi Beach monitoring sites reductions in the predicted percentile concentrations of more than 98.5% occur. Reductions in the percentile concentrations at the Ti Korohiwa Rocks range between 96 and 97% while at the Mount Couper site reductions in the percentile concentrations of between 84 and 93% occur. Unlike for the 10 m outfall option, concentrations are nearly always less than under the existing shoreline discharge (Figure 5-6 and Figure 5-7).

Figures 5-8 to 5-15 show the spatial plots of the predicted 95th percentile estimates for each of the discharge options. These plots indicate the area impacted by each of the discharges and in particular the significant reduction in concentrations achieved by the outfall options.

Table 10. Percentile estimates of Enterococci concentration (Ent/100 mL) at the monitoring sites, future ADF flow rate of 390 L/s. Highlighted cells indicate percentile values that are higher than for the existing shoreline discharge.

Discharge Point	Percentile	200 m SW	200 m E	Titahi Beach South	Titahi Beach	Ti Korohiwa	Mount Couper
Existing Shoreline	50	83.0	72.2	29.0	7.9	4.2	0.7
	90	139.6	133.9	60.7	19.9	8.8	2.6
	95	156.7	151.3	69.8	23.9	10.0	3.9
New Shoreline	50	43.0	3.8	1.6	0.8	186.1	0.1
	90	86.8	14.5	5.3	2.1	237.8	0.5
	95	106.2	19.6	8.3	2.5	248.9	0.7
10 m Outfall	50	1.4	1.7	1.4	1.2	1.7	0.4
	90	2.3	3.4	2.6	2.2	3.1	1.7
	95	2.6	3.9	3.0	2.6	3.7	2.0
15 m outfall	50	0.1	0.2	0.1	0.1	0.2	0.1
	90	0.2	0.3	0.3	0.2	0.3	0.3
	95	0.2	0.3	0.3	0.2	0.3	0.4

Table 11. Percentile estimates of Virus concentration (Virus/100 mL) at the monitoring sites, future ADF flow rate of 390 L/s. Highlighted cells indicate percentile values that are higher than for the existing shoreline discharge.

Discharge Point	Percentile	200 m SW	200 m E	Titahi Beach South	Titahi Beach	Ti Korohiwa	Mount Couper
Existing Shoreline	50	99.0	80.8	37.2	13.4	5.7	1.3
	90	150.7	145.0	67.7	27.6	10.6	5.1
	95	169.9	159.6	76.0	31.8	12.0	7.0
New Shoreline	50	51.1	5.8	3.0	1.7	194.0	0.3
	90	96.5	19.1	8.3	3.5	242.0	1.0
	95	114.8	23.4	12.0	4.5	251.3	1.3
10 m Outfall	50	1.9	2.3	2.1	2.0	2.0	0.7
	90	3.3	4.4	3.6	3.0	4.1	2.2
	95	3.6	5.0	4.0	3.3	4.5	2.6
15 m outfall	50	0.2	0.3	0.3	0.2	0.2	0.2
	90	0.3	0.4	0.4	0.3	0.4	0.4
	95	0.4	0.5	0.4	0.3	0.4	0.5

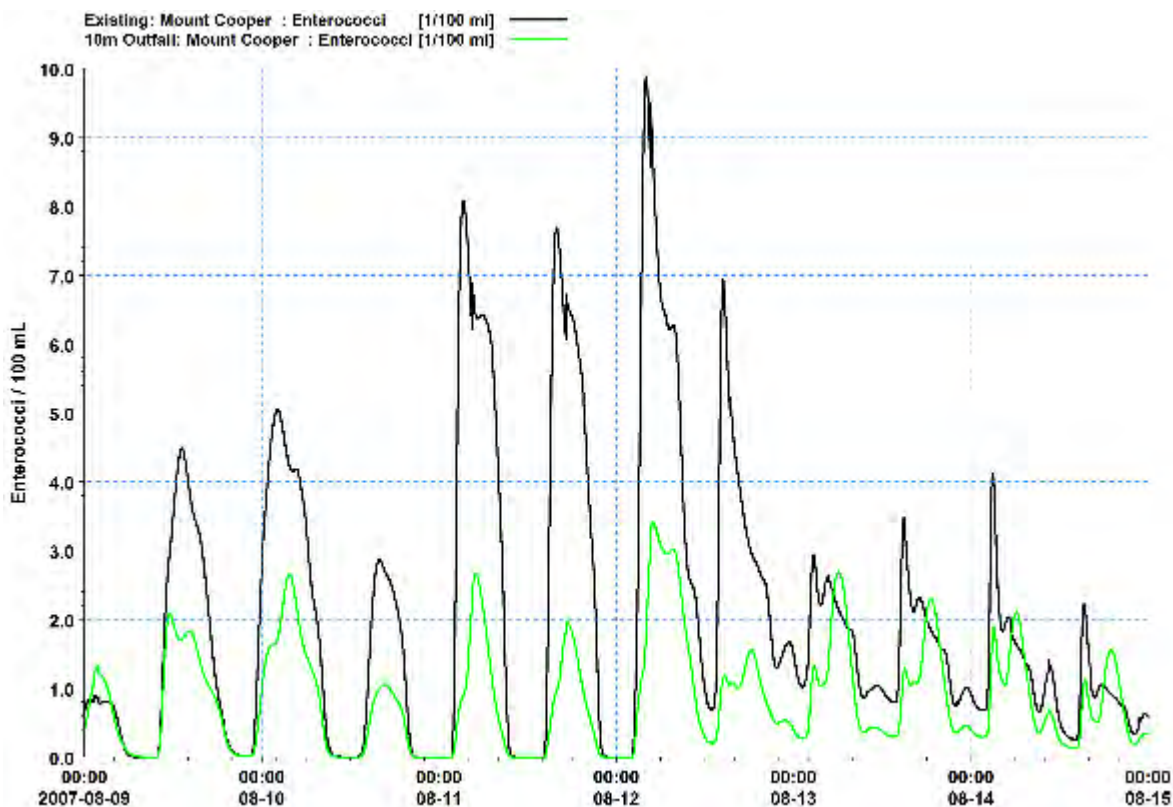


Figure 5-4. Predicted Enterococci concentration (Ent/100 mL) during period of stronger onshore wind for the existing shoreline discharge and the 10 m outfall option.

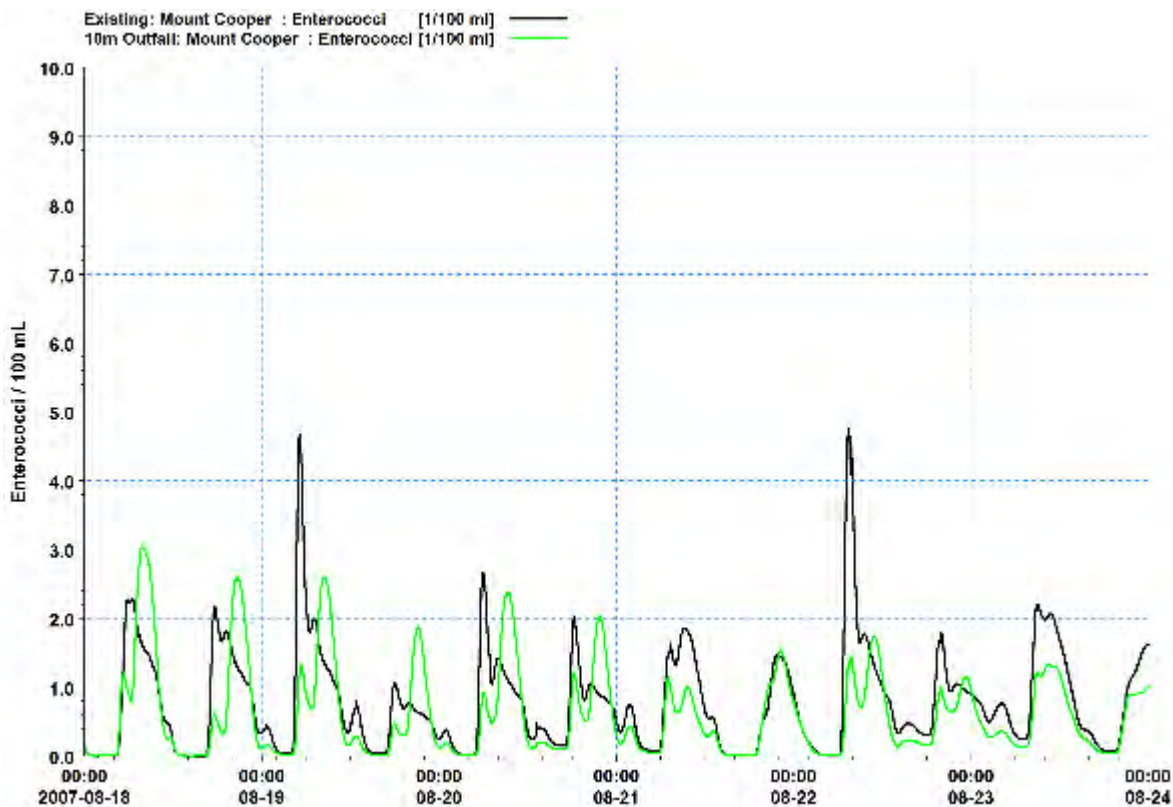


Figure 5-5. Predicted Enterococci concentration (Ent/100 mL) during period of moderate winds for the existing shoreline discharge and the 10 m outfall option.

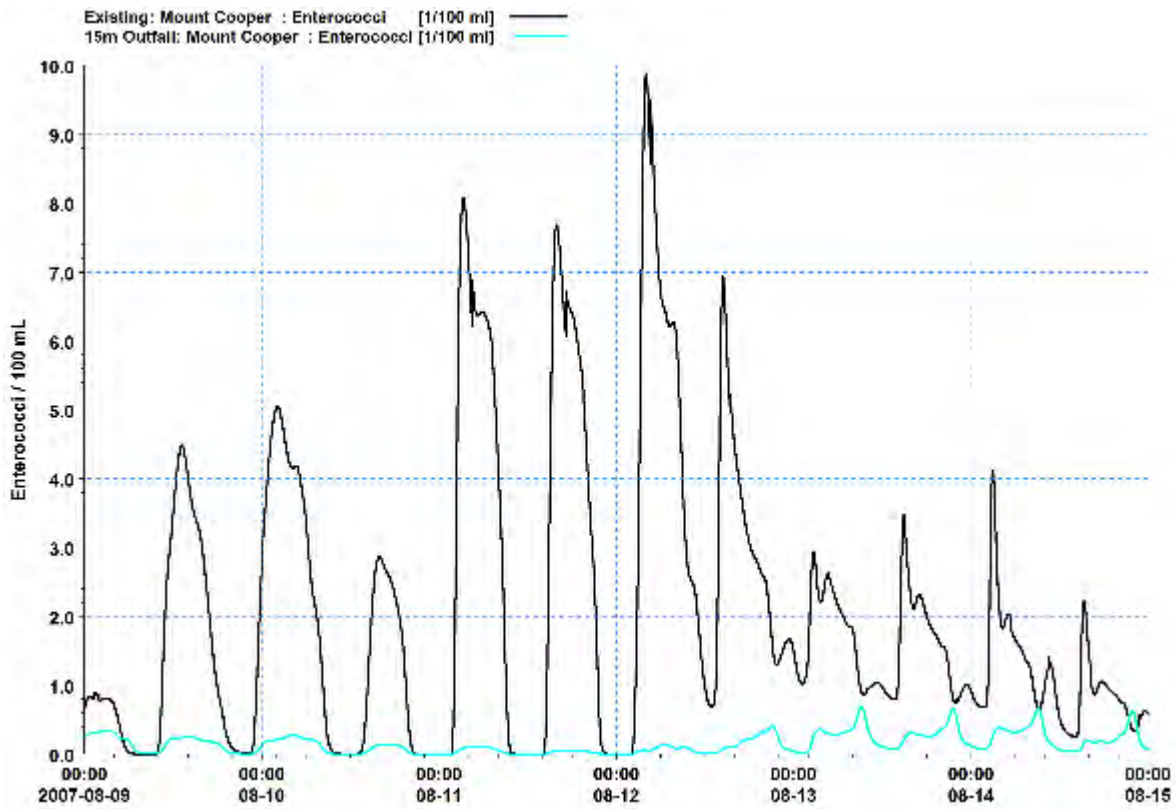


Figure 5-6. Predicted Enterococci concentration (Ent/100 mL) during period of stronger onshore wind for the existing shoreline discharge and the 15 m outfall option.

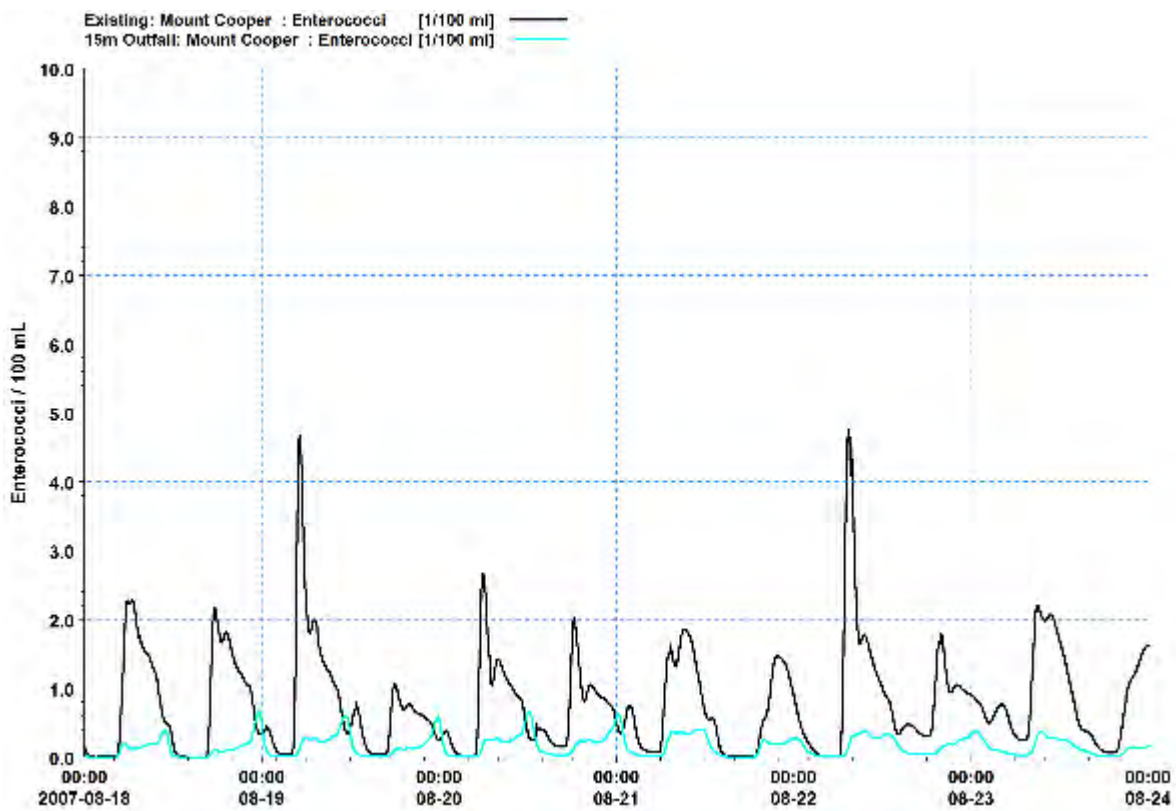


Figure 5-7. Predicted Enterococci concentration (Ent/100 mL) during period of moderate winds for the existing shoreline discharge and the 10 m outfall option.

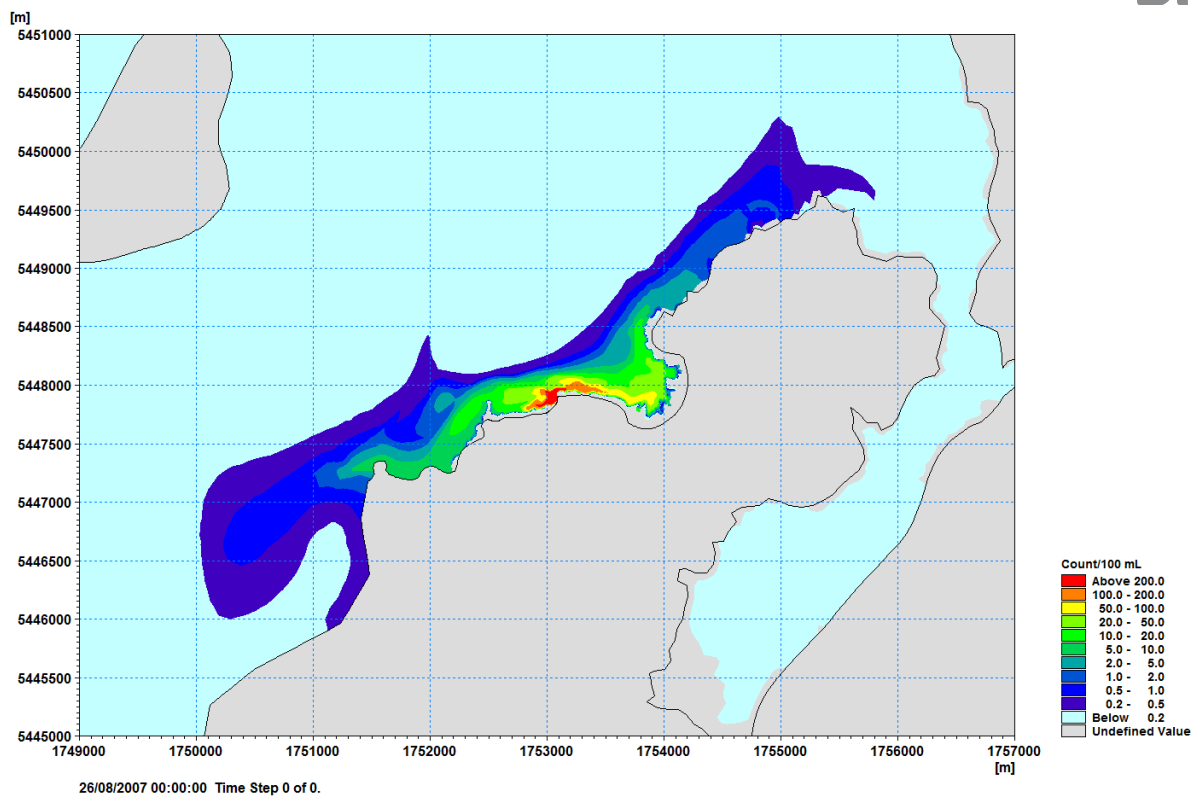


Figure 5-8. Predicted 95th percentile Enterococci concentration (Ent/100 mL), for the existing shoreline discharge for the future ADF flow rate of 390 L/s.

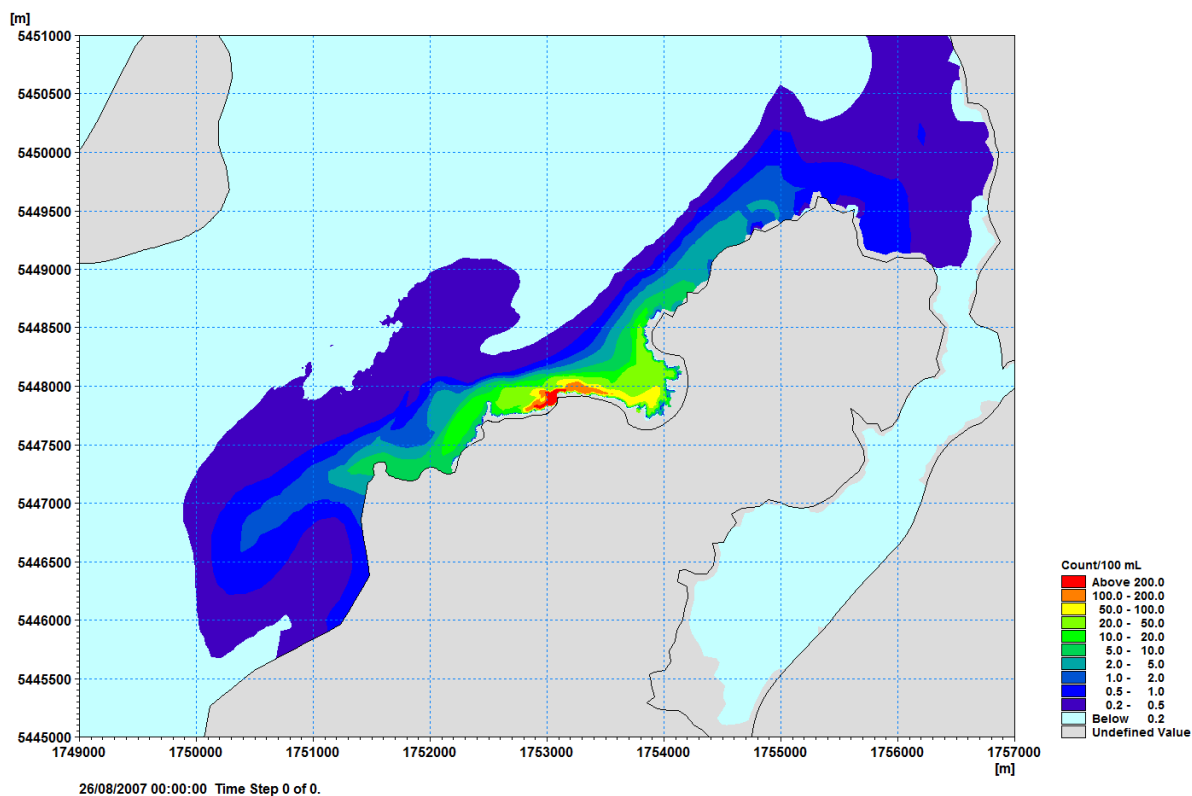


Figure 5-9. Predicted 95th percentile Virus concentration (Virus/100 mL), for the existing shoreline discharge for the future ADF flow rate of 390 L/s.

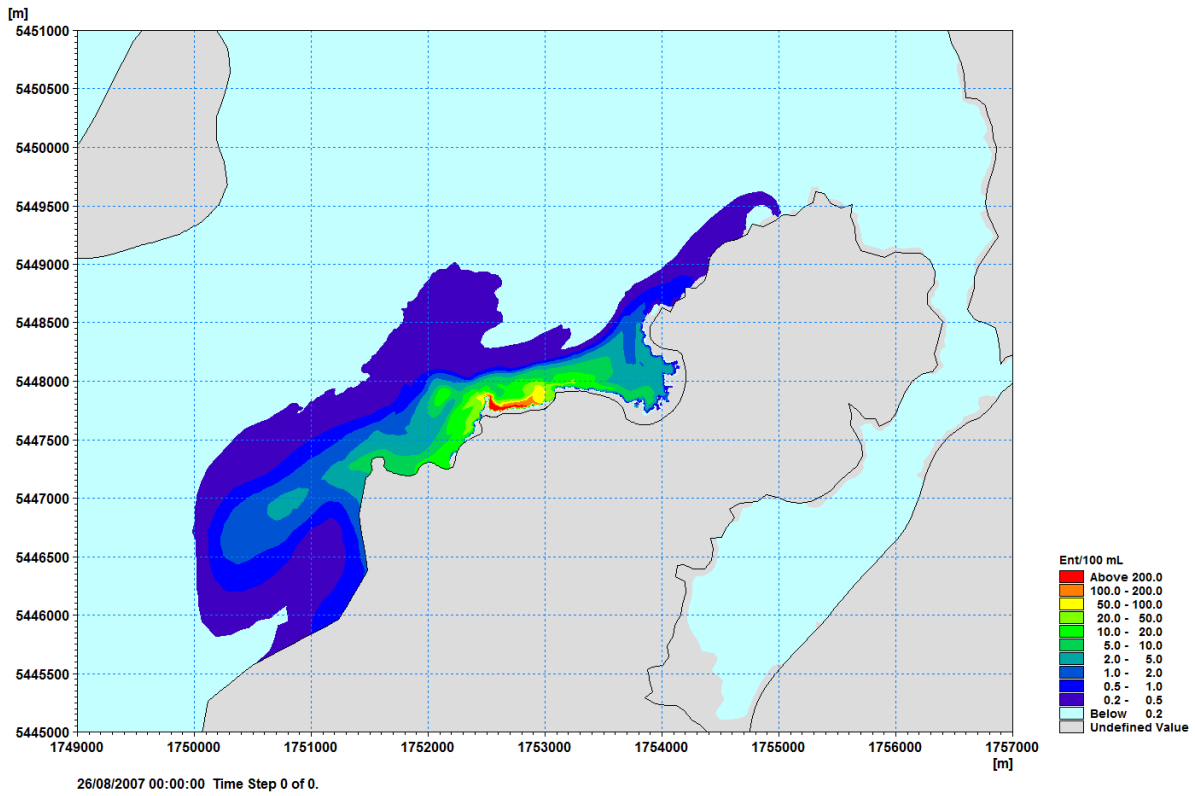


Figure 5-10. Predicted 95th percentile Enterococci concentration (Ent/100 mL), for the new shoreline discharge for the future ADF flow rate of 390 L/s.

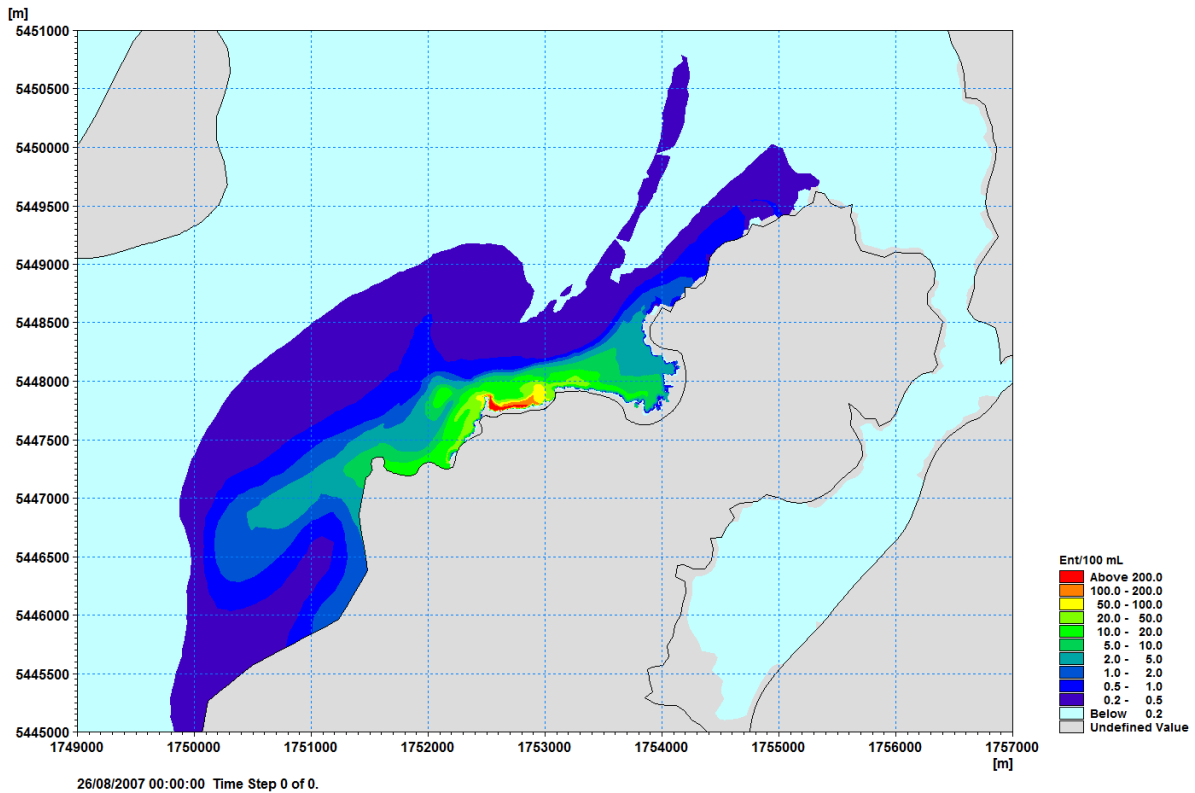


Figure 5-11. Predicted 95th percentile Virus concentration (Virus/100 mL), for the new shoreline discharge for the future ADF flow rate of 390 L/s.

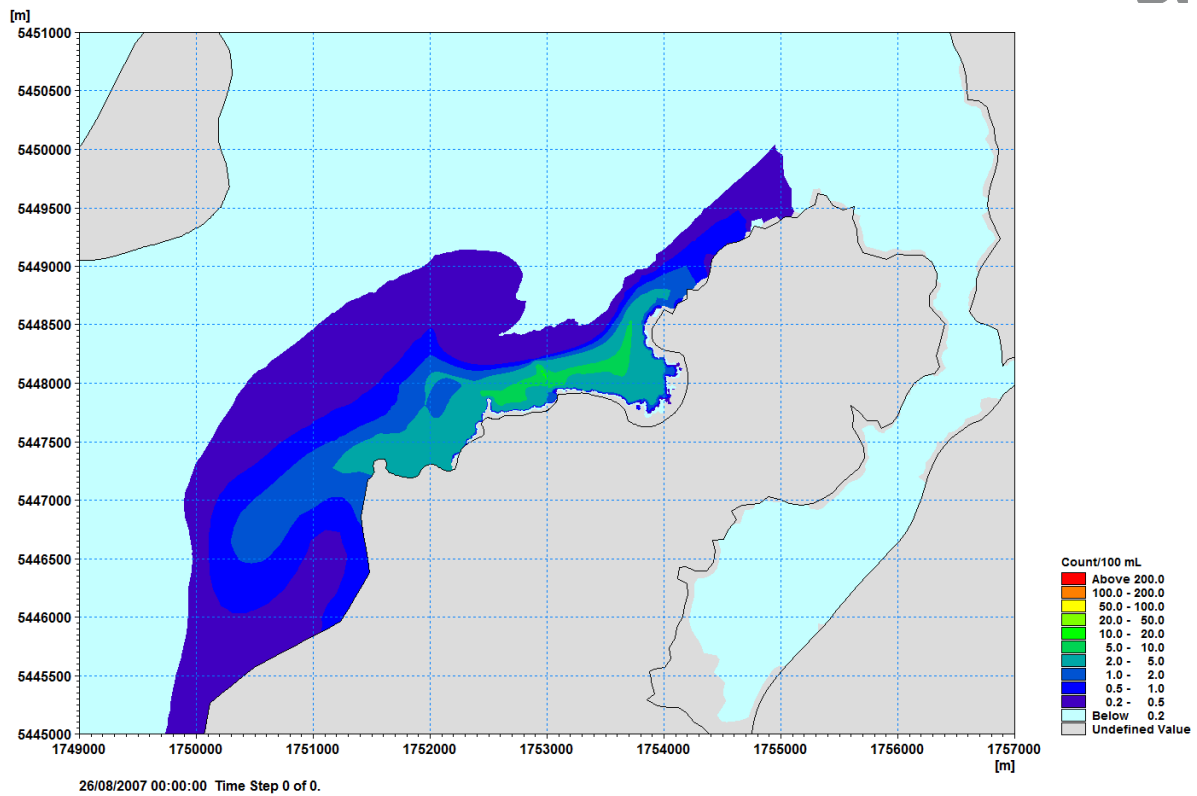


Figure 5-12. Predicted 95th percentile Enterococci concentration (Ent/100 mL), for the 10 m outfall option for the future ADF flow rate of 390 L/s.

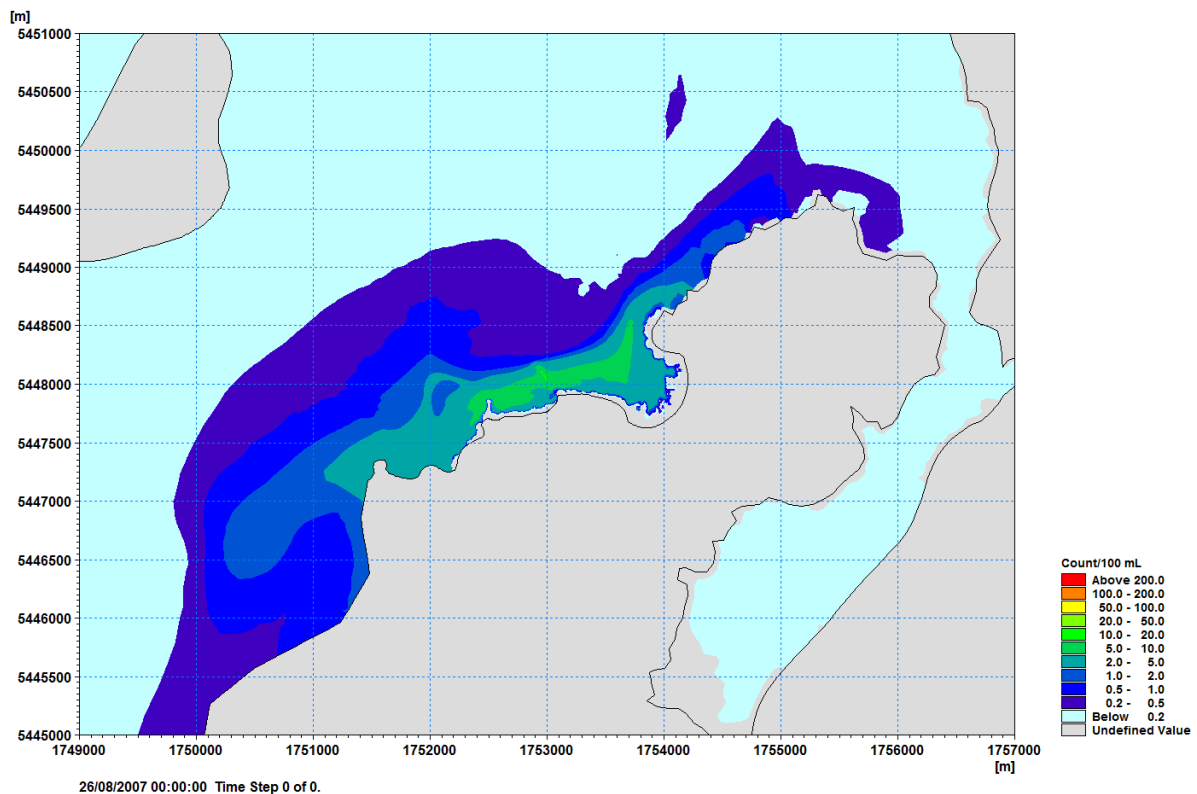


Figure 5-13. Predicted 95th percentile Virus concentration (Virus/100 mL), for the 10 m outfall option for the future ADF flow rate of 390 L/s.

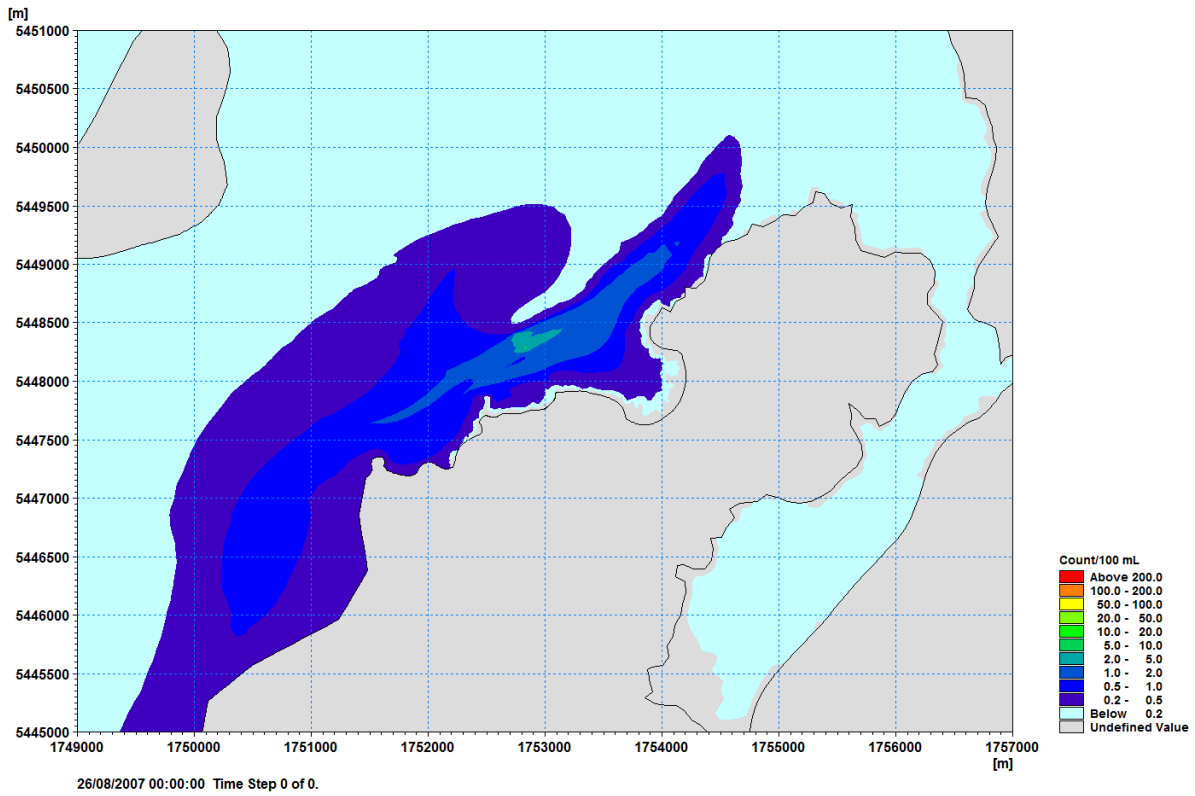


Figure 5-14. Predicted 95th percentile Enterococci concentration (Ent/100 mL), for the 15 m outfall option for the future ADF flow rate of 390 L/s.

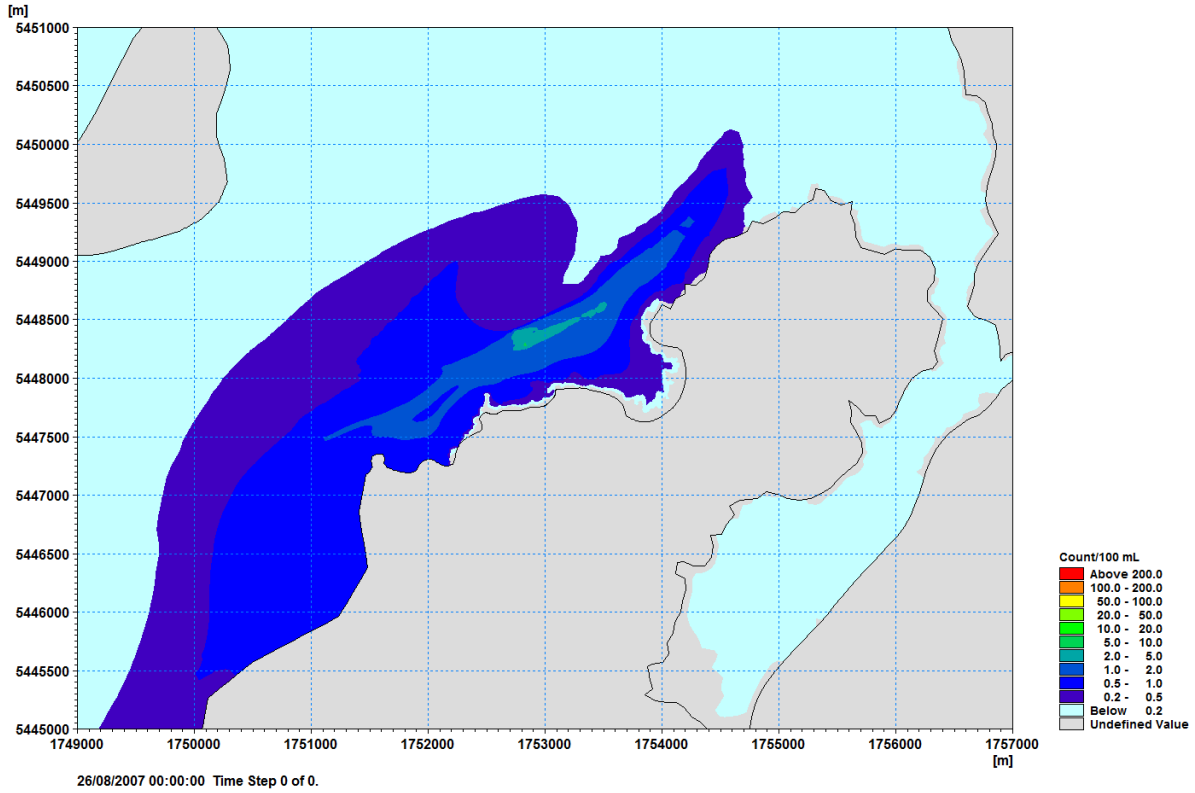


Figure 5-15. Predicted 95th percentile Virus concentration (Virus/100 mL), for the 15 m outfall option for the future ADF flow rate of 390 L/s.

Results for 455 L/s future average dry weather flow

The following provide results from a continuous discharge of 455 L/s for the discharge options being considered.

Time series plots for this scenario are not provided as results from the 390 L/s in the previous section and in Appendix C can be used to provide an understanding of the plume dynamics. The following provides an overview of this results of the scenario.

Table 12 and Table 13 provide percentile values for Enterococci and Virus respectively for the existing shoreline discharge and the discharge options for the future ADF (455 L/s).

For the **existing shoreline** discharge the 95th percentile concentration ranges from 175 to 200 count/100 mL at the sites near the existing discharge

At the Titahi Beach sites the 95th percentile concentration ranges from 30 to 89 count/100 mL.

At the Te Korohiwa Rocks and Mount Couper monitoring sites the 95th percentile concentration ranges from 5 to 13 count/100 mL.

The **new shoreline** at Round Point discharge results in a reduction of the predicted percentile concentrations at the 200 m SW monitoring site of between 38 and 53%. At the 200 m E monitoring site the predicted percentile concentrations are reduced by between 86 and 95%. For the Titahi Beach monitoring sites the reductions in the predicted percentile concentrations ranges from 84-95%. At the Ti Korohiwa Rocks monitoring site (which is adjacent to the new shoreline discharge), increases of between 26 and 47 occur resulting in a predicted 95th percentile concentration of around 280-290 count/100 mL at this site. At the Mount Couper site reductions in the percentile concentrations of between 82 and 85% occur.

The **10 m outfall** option results in reduction in the predicted percentile concentrations at the 200 m SW monitoring site of around 98%. Similar reductions in the predicted percentile concentrations are predicted at the 200 m E monitoring site. At the Titahi Beach monitoring sites reductions in the predicted percentile concentrations of between 87 and 96% occur. Reductions in the predicted percentile concentrations at the Ti Korohiwa Rocks range between 55 and 63% while at the Mount Couper site reductions in the percentile concentrations of between 38 and 65% occur.

The **15 m outfall** option discharge results in a reduction of the predicted percentile concentrations at the 200 m SW monitoring site of greater than 99%. Similar reductions in the predicted percentile concentrations are seen at the 200 m E monitoring site. At the Titahi Beach monitoring sites reductions in the predicted percentile concentrations of more than 98.7% occur. Reductions in the percentile concentrations at the Ti Korohiwa Rocks range between 95 and 97% while at the Mount Couper site reductions in the percentile concentrations of between 84 and 93% occur.

Figures 5-16 to 5-19 show the spatial plots of the predicted 95th percentile estimates for each of the discharge options. These plots indicate the area impacted by each of the discharges and in particular the significant reduction in concentrations achieved by the outfall options.

Table 12. Percentile estimates of Enterococci concentration (Ent/100 mL) at the monitoring sites, future ADF flow rate of 455 L/s. Highlighted cells indicate percentile values that are higher than for the existing shoreline discharge.

Discharge Point	Percentile	200 m SW	200 m E	Titahi Beach South	Titahi Beach	Ti Korohiwa	Mount Couper
Existing Shoreline	50	99.6	88.2	33.9	10.6	4.5	0.8
	90	165.3	155.7	70.8	25.2	9.6	3.2
	95	184.4	174.5	81.4	29.7	11.1	4.6
New Shoreline	50	46.9	4.5	1.8	0.9	213.2	0.1
	90	89.4	16.1	6.2	2.3	271.9	0.6
	95	112.5	21.6	9.7	2.8	283.4	0.8
10 m Outfall	50	1.7	2.1	1.6	1.4	2.0	0.5
	90	2.6	3.9	3.0	2.5	3.6	2.0
	95	2.9	4.6	3.5	2.9	4.2	2.4
15 m outfall	50	0.1	0.2	0.2	0.1	0.2	0.1
	90	0.2	0.3	0.3	0.2	0.3	0.4
	95	0.3	0.4	0.3	0.3	0.4	0.5

Table 13. Percentile estimates of Virus concentration (Virus/100 mL) at the monitoring sites, future ADF flow rate of 455 L/s. Highlighted cells indicate percentile values that are higher than for the existing shoreline discharge.

Discharge Point	Percentile	200 m SW	200 m E	Titahi Beach South	Titahi Beach	Ti Korohiwa	Mount Couper
Existing Shoreline	50	117.7	96.4	43.4	18.0	6.3	1.7
	90	177.9	167.7	78.9	34.5	11.6	6.4
	95	200.6	182.5	88.7	39.1	13.3	8.5
New Shoreline	50	55.9	6.9	3.5	2.0	221.1	0.3
	90	99.2	20.9	9.7	4.1	275.7	1.1
	95	123.7	25.6	14.0	5.3	285.7	1.4
10 m Outfall	50	2.3	2.7	2.4	2.4	2.4	0.8
	90	3.8	5.0	4.2	3.4	4.6	2.6
	95	4.1	5.7	4.7	3.7	5.2	3.0
15 m outfall	50	0.2	0.3	0.3	0.2	0.3	0.2
	90	0.4	0.5	0.4	0.4	0.5	0.5
	95	0.4	0.5	0.5	0.4	0.5	0.6

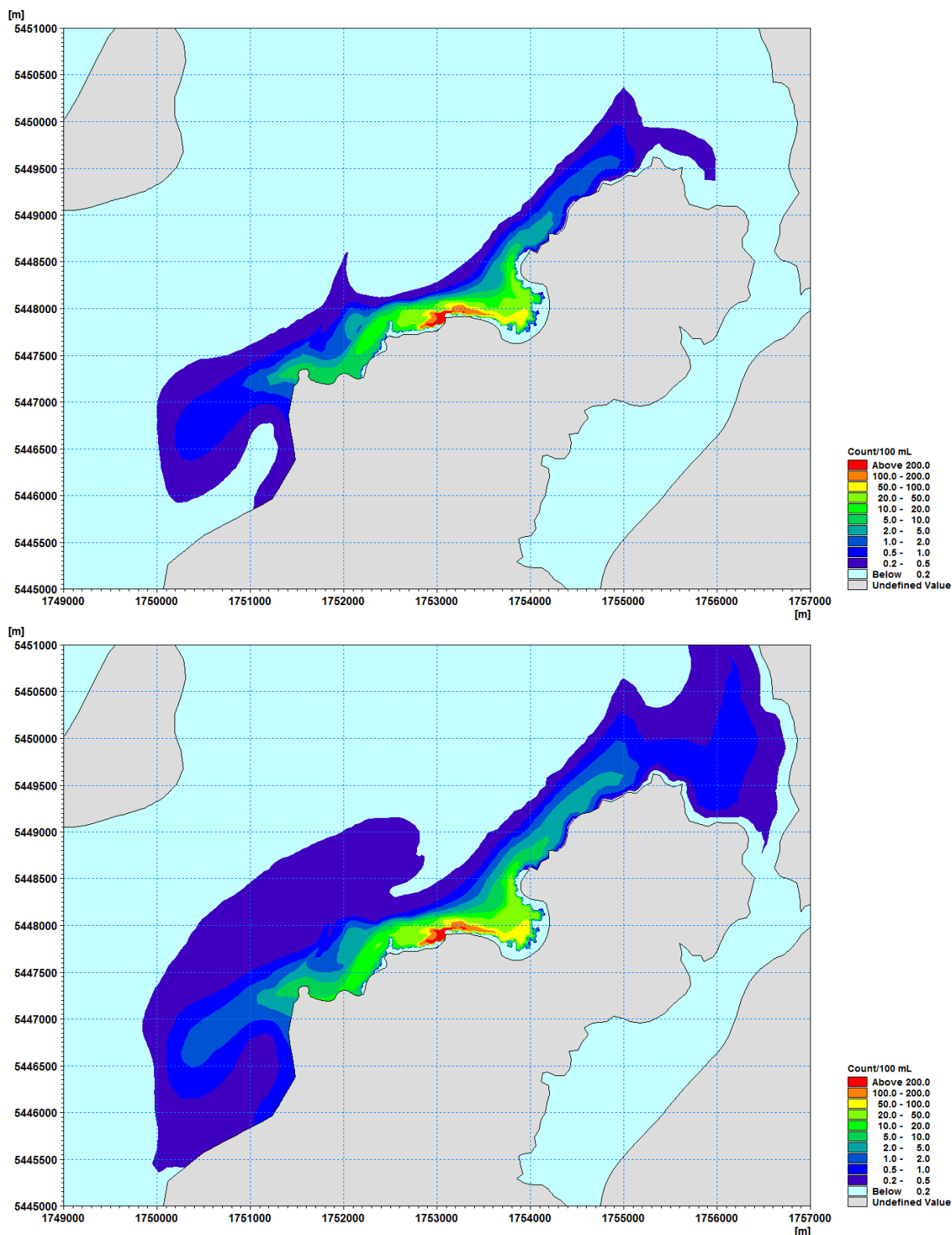


Figure 5-16. 95th percentile concentrations for *Enterococci* (top panel) and *Viruses* (bottom panel) a future average weather flow rate from the existing shoreline discharge point.

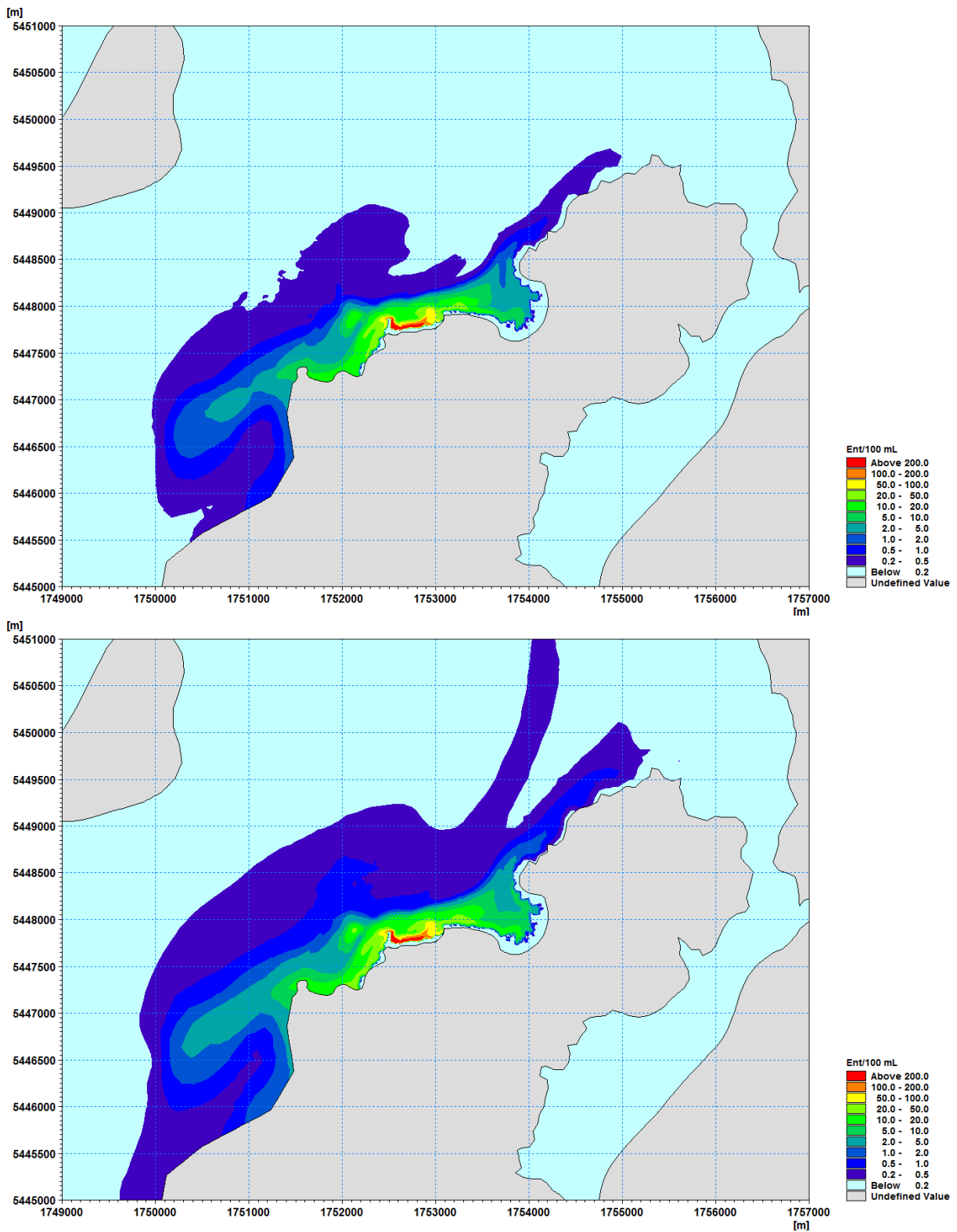


Figure 5-17. 95th percentile concentrations for *Enterococci* (top panel) and *Viruses* (bottom panel) a future average weather flow rate from the new shoreline discharge point.

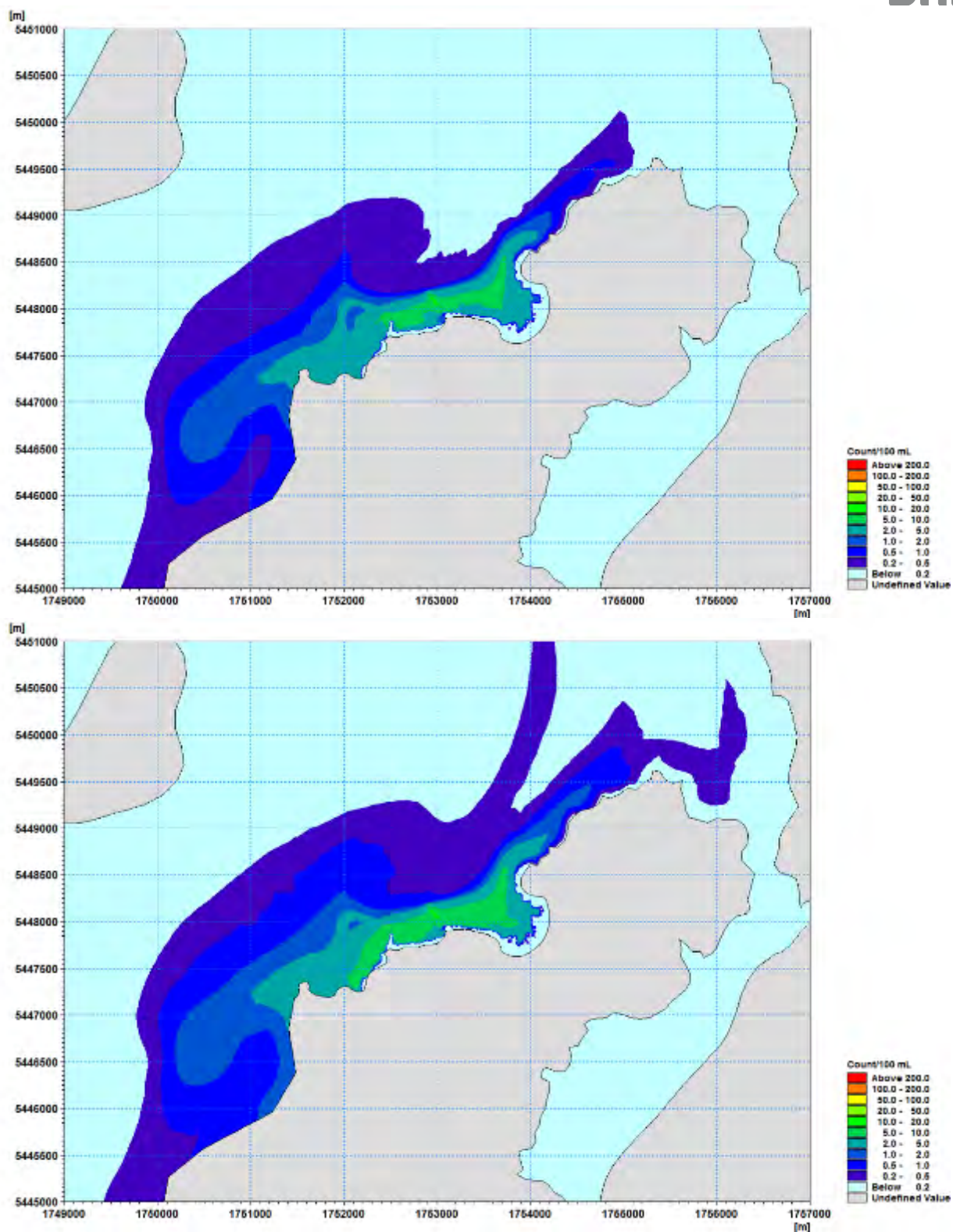


Figure 5-18. 95th percentile concentrations for *Enterococci* (top panel) and *Viruses* (bottom panel) a future average weather flow rate from a 10m deep outfall.

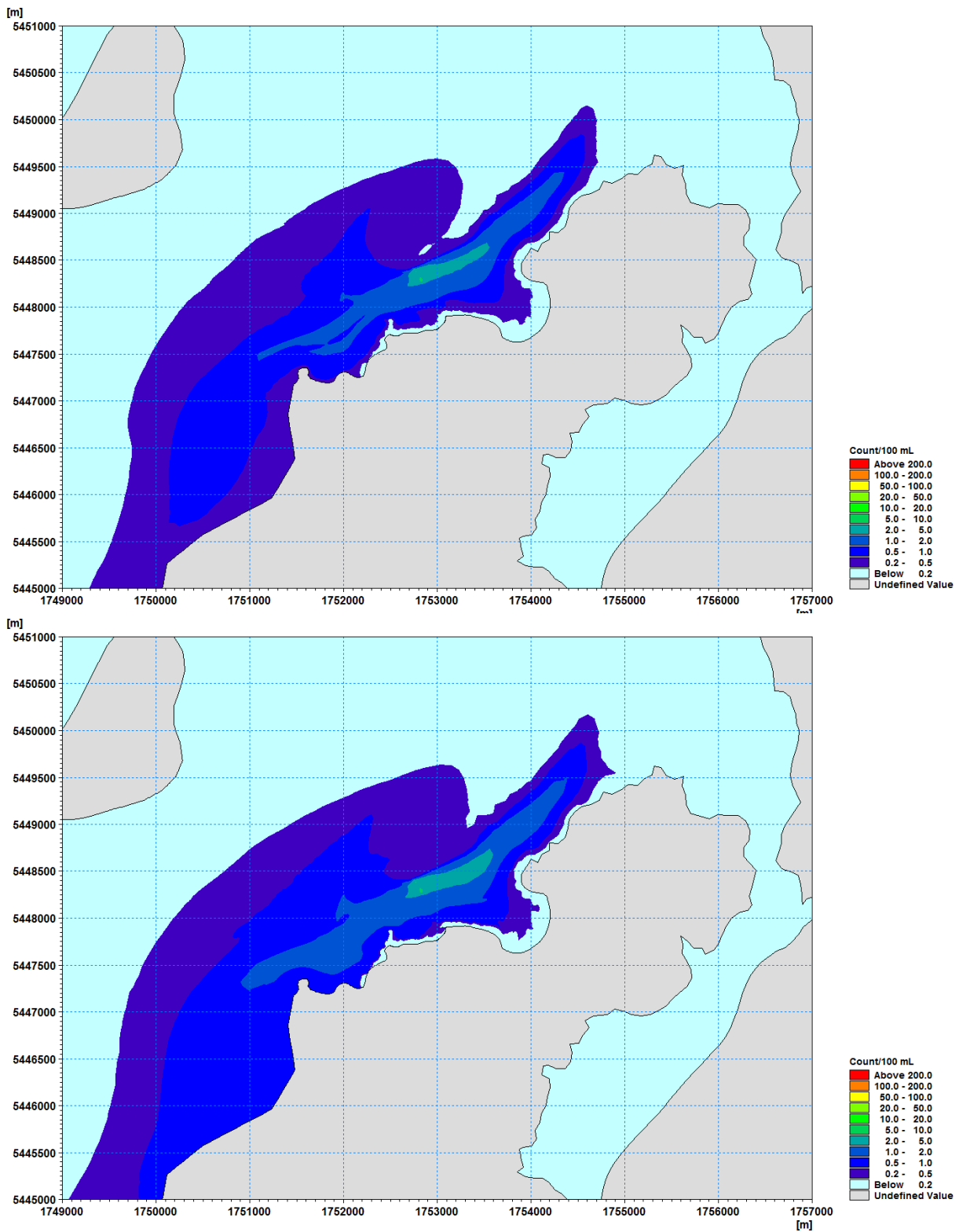


Figure 5-19. 95th percentile concentrations for *Enterococci* (top panel) and *Viruses* (bottom panel) a future average weather flow rate from a 15m deep outfall.

5.2 Future PWWF Scenarios

In this section of the report, future peak wet weather flows are considered as shown in Table 14.

Four different receiving environment conditions are considered – onshore winds, typical winds during both neap and spring tides.

Table 14. Future peak wet weather discharge scenarios.

	Future PWWF Scenarios	
WWTP Flows	1500 L/s	1500 L/s
Year	2054	2054
Flow Duration	12 hours	12 hours
Discharge location	New Shoreline Round Point	New Ocean Outfall Round Point

5.2.1 Typical Winds and Spring Tide - 1500 L/s PWWF

Table 15 and Table 16 provide percentile values for Enterococci and Virus for the existing shoreline discharge and the discharge options for the future PWWF (1500 L/s) for typical winds and spring tides. Appendices D-I contain figures of the predicted time-series of data the monitoring sites.

For the **existing shoreline** discharge the 99th percentile concentration ranges from 291 to 630 count/100 mL at the sites near the existing discharge

At the Titahi Beach sites the 99th percentile concentration ranges from 89 to 174 count/100 mL.

At the Te Korohiwa Rocks and Mount Couper monitoring sites the 99th percentile concentration ranges from 13 to 16 count/100 mL.

For the **new shoreline** discharge reduction in percentile concentrations at the 200 m SW monitoring site range between 47 and 78% are achieved. At the 200 m E monitoring site reductions in the percentile concentrations of between 81 and 91% occur. At the Te Titahi Beach monitoring sites percentile concentrations are reduced by between 91 and 95%. Percentile concentrations at the Ti Korohiwa Rocks increase by a factor of between 18 to 41 resulting in 99th percentile value of 540 count/100 mL.

For the **10m outfall** discharge reductions in the percentile concentration at the 200 m SW site are more than 98% while at the site 200 m E site percentile concentrations are reduced by at least 96%. At the Titahi Beach monitoring sites percentile concentrations are reduced by between 87 and 95 %. Percentile concentrations at the Ti Korohiwa Rocks site decrease by between 52 and 64%. Percentile concentrations at the Mount Couper decrease by between 42 and 73 %. Concentrations at the Mount Couper site are higher during the first tidal cycle compared to the existing discharge – this again relates to the travel time for the treated wastewater plume.

For the **15m outfall** discharge reductions in the percentile concentration at the 200 m SW, the 200 m E site and the Titahi Beach sites are more than 99%. Percentile concentrations at the Ti Korohiwa Rocks site decrease by between 95 and 97%. Percentile concentrations at the Mount Couper decrease by between 89 and 94%.

Concentrations at the Mount Couper site are higher during the first tidal cycle compared to the existing discharge – this again relates to the travel time for the treated wastewater plume (Figure I-1, Figure I-2, Appendix I).

Figures 5-20 to 5-27 show the spatial plots of the predicted 95th percentile estimates for each of the discharge options. These plots indicate the area impacted by each of the discharges and in particular the significant reduction in concentrations achieved by the outfall options.

Table 15. Percentile estimates of Enterococci concentration (Ent/100 mL) at the monitoring sites, future PWWF for typical winds and spring tide. Highlighted cells indicate percentile values that are higher than for the existing shoreline discharge.

Discharge Point	Percentile	200 m SW	200 m E	Titahi Beach South	Titahi Beach	Ti Korohiwa	Mount Couper
Existing Shoreline	90	98.2	69.2	68.9	21.1	3.5	1.1
	95	291.9	171.0	119.7	66.2	10.0	2.4
	99	604.6	291.1	159.7	89.3	14.2	13.4
New Shoreline	90	47.1	6.6	4.2	1.2	97.3	0.2
	95	73.6	16.6	5.8	3.6	407.9	0.5
	99	149.8	54.7	10.4	5.7	540.4	1.2
10 m Outfall	90	0.7	2.9	4.1	2.6	1.7	0.4
	95	4.5	4.9	7.7	5.4	4.2	1.4
	99	6.1	8.7	8.8	7.7	6.7	4.1
15 m outfall	90	0.1	0.1	0.1	0.1	0.1	0.1
	95	0.3	0.5	0.2	0.1	0.3	0.3
	99	0.5	0.9	0.3	0.1	0.8	1.1

Table 16. Percentile estimates of Virus concentration (Virus/100 mL) at the monitoring sites, future PWWF for typical winds and spring tide. Highlighted cells indicate percentile values that are higher than for the existing shoreline discharge.

Discharge Point	Percentile	200 m SW	200 m E	Titahi Beach South	Titahi Beach	Ti Korohiwa	Mount Couper
Existing Shoreline	90	108.6	74.5	72.9	41.0	5.6	2.3
	95	374.4	180.4	125.3	70.2	12.0	4.9
	99	630.3	295.6	174.0	96.8	16.3	15.1
New Shoreline	90	57.2	10.5	6.7	3.3	98.6	0.4
	95	81.1	20.1	7.9	5.7	433.6	1.1
	99	159.1	56.8	16.3	8.9	541.0	1.7
10 m Outfall	90	1.2	3.1	4.8	5.2	2.3	0.7
	95	4.7	5.0	7.9	6.7	4.3	1.7
	99	6.2	9.0	9.0	7.8	6.8	4.2
15 m outfall	90	0.2	0.3	0.2	0.1	0.2	0.1
	95	0.4	0.5	0.3	0.2	0.4	0.3
	99	0.5	0.9	0.5	0.2	0.8	1.1

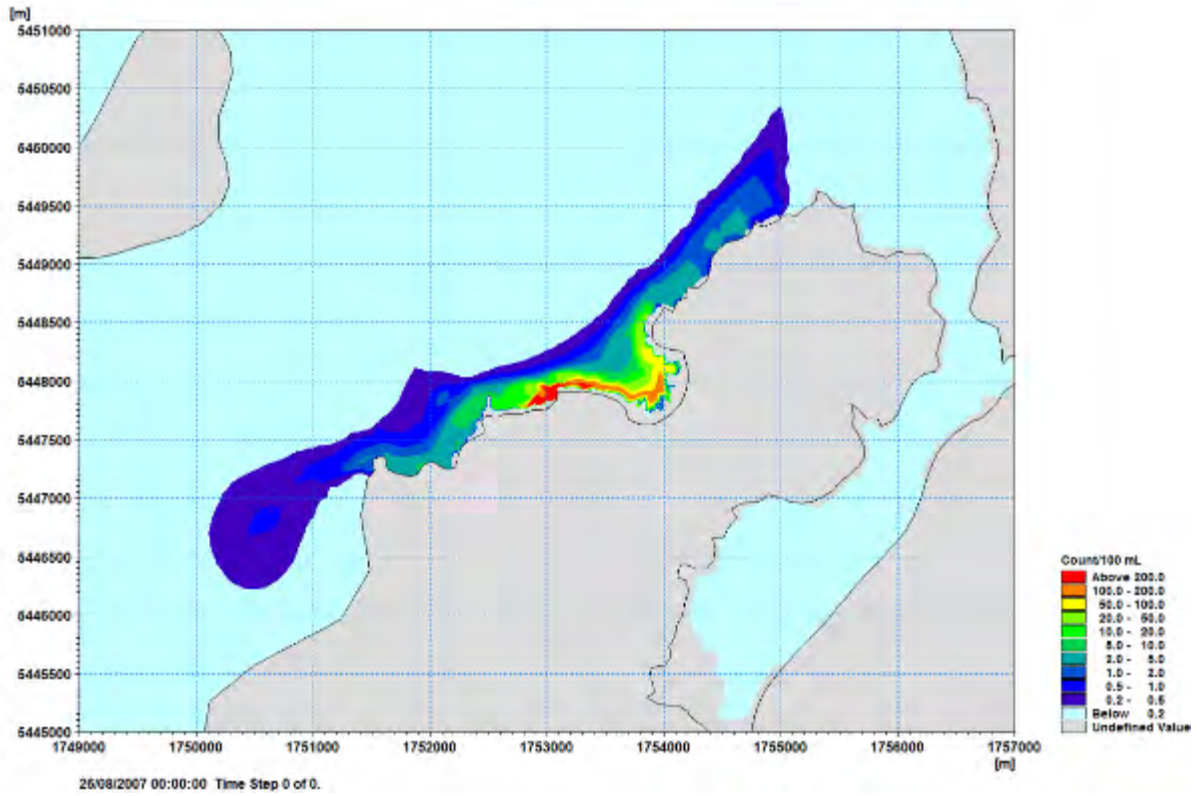


Figure 5-20. Predicted 95th percentile Enterococci concentration (Ent/100 mL), for the existing shoreline discharge for typical winds and spring tide for the future PWWF flow rate of 1500 L/s.

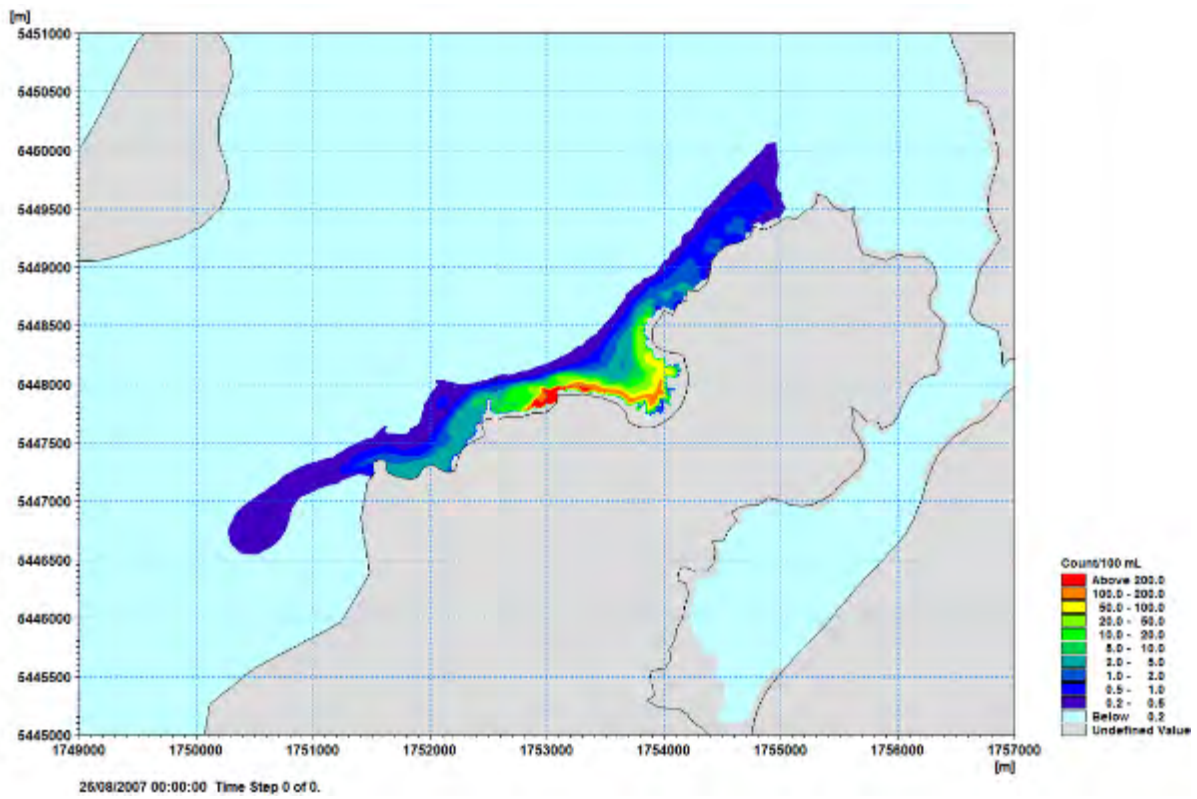


Figure 5-21. Predicted 95th percentile Virus concentration (Virus/100 mL), for the existing shoreline discharge for typical winds and spring tide for the future PWWF flow rate of 1500 L/s.

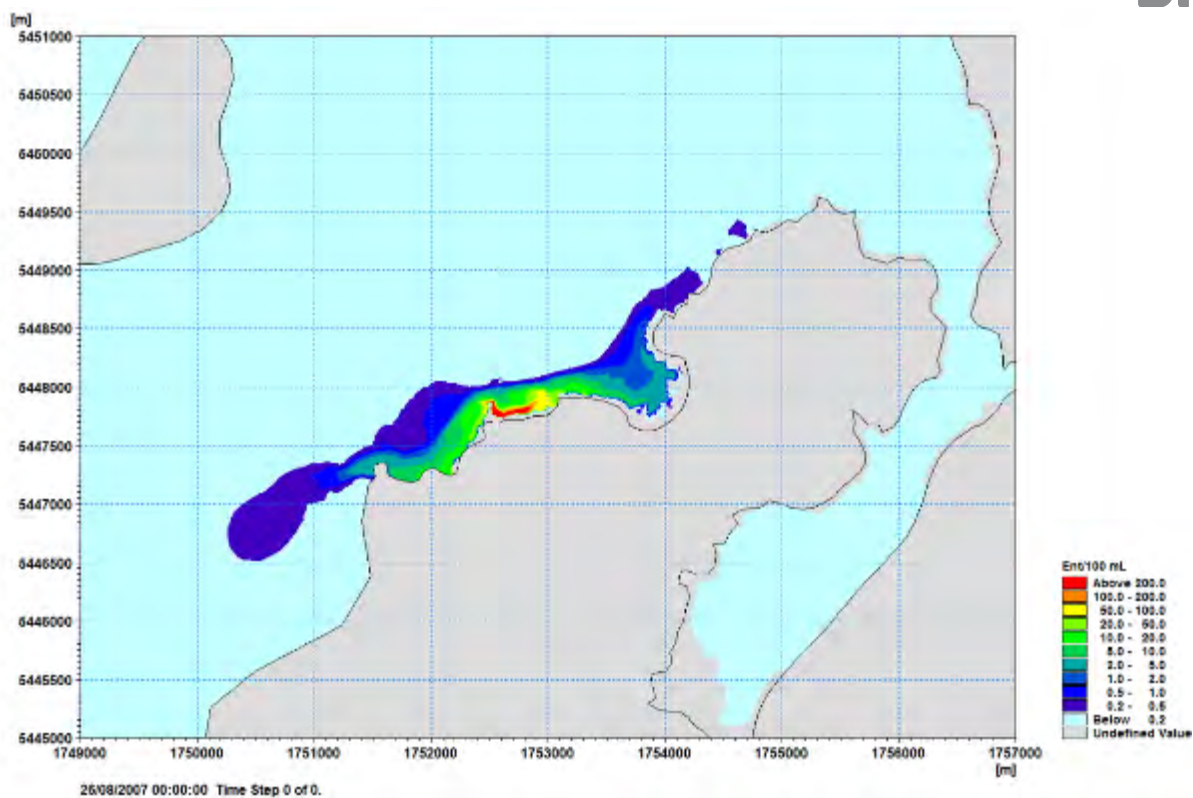


Figure 5-22. Predicted 95th percentile Enterococci concentration (Ent/100 mL), for the new shoreline discharge for typical winds and spring tide for the future PWWF flow rate of 1500 L/s.

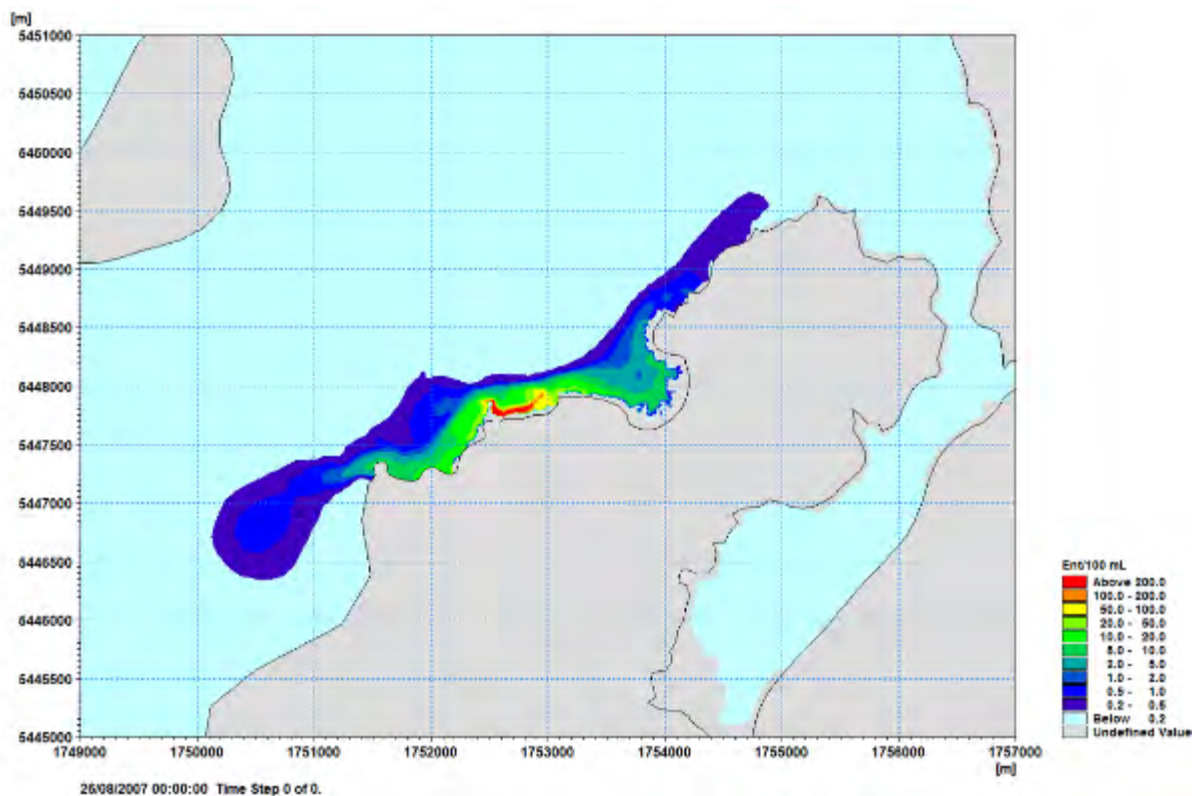


Figure 5-23. Predicted 95th percentile Virus concentration (Virus/100 mL), for the new shoreline discharge for typical winds and spring tide for the future PWWF flow rate of 1500 L/s.

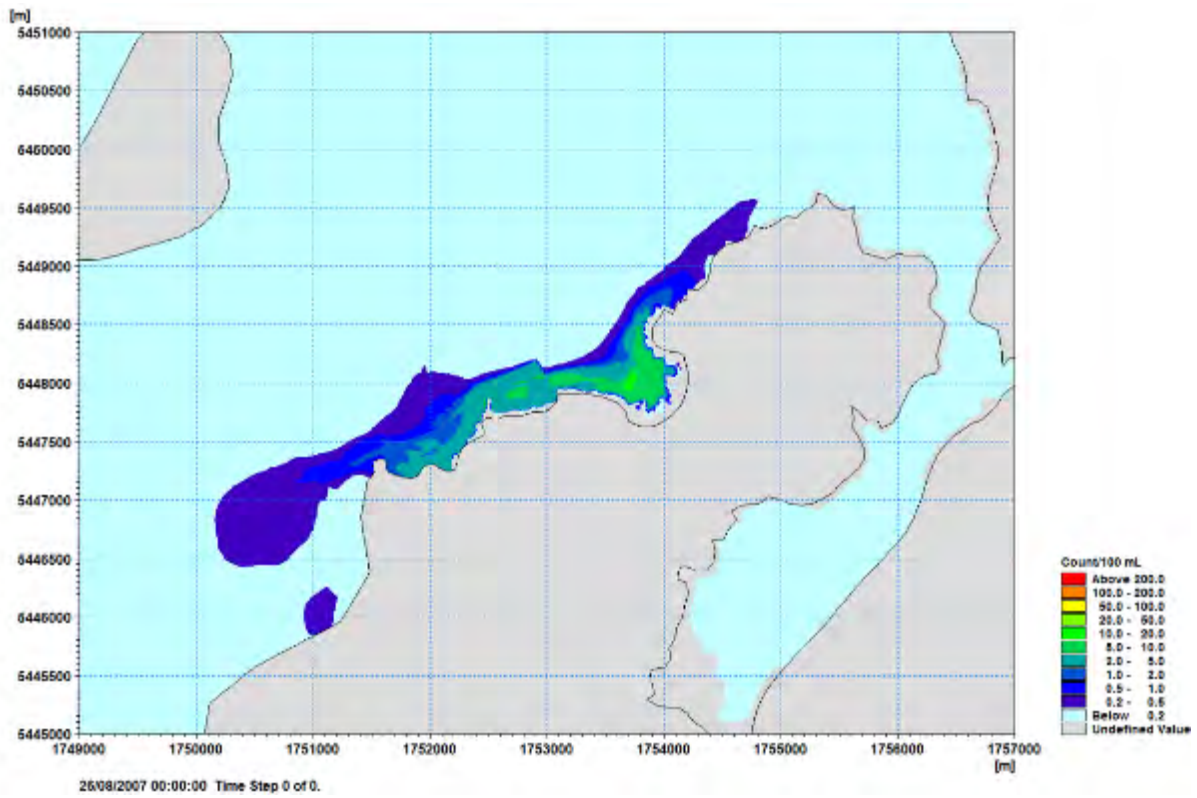


Figure 5-24. Predicted 95th percentile Enterococci concentration (Ent/100 mL), for the 10 m outfall option for typical winds and spring tide for the future PWWF flow rate of 1500 L/s.

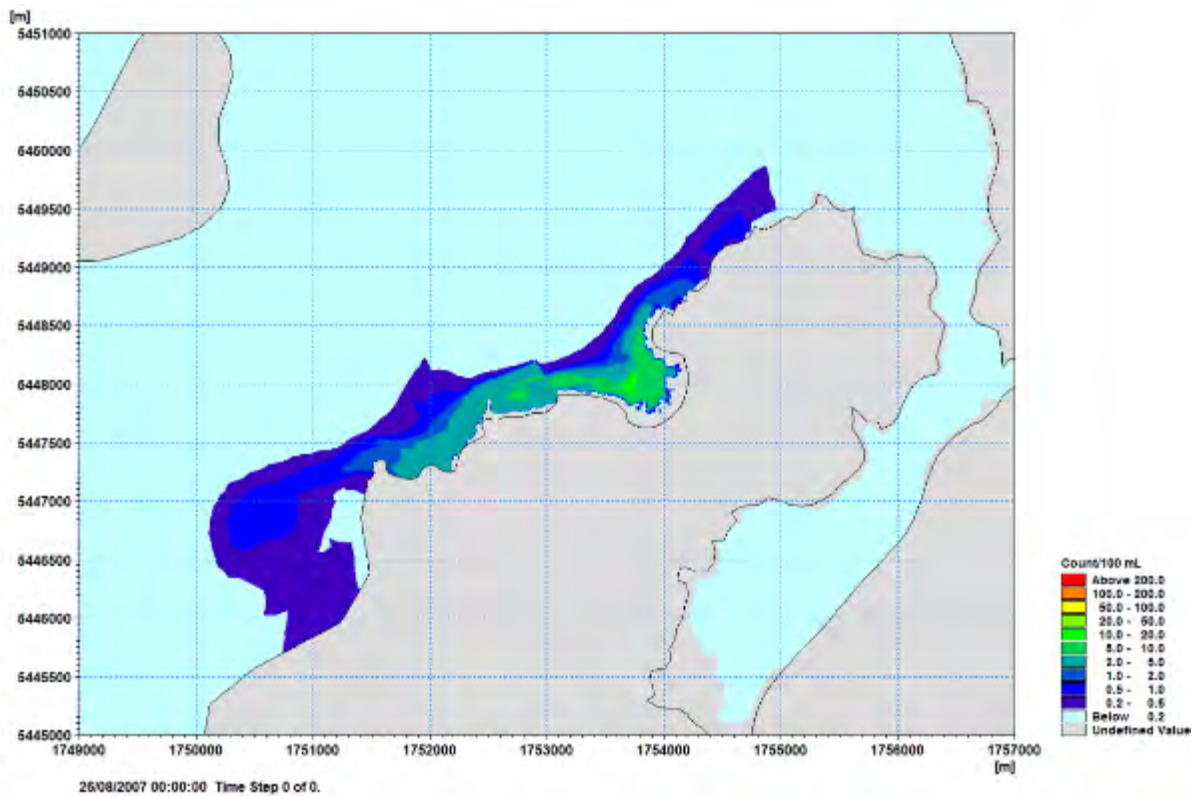


Figure 5-25. Predicted 95th percentile Virus concentration (Virus/100 mL), for the 10 m outfall option for typical winds and spring tide for the future PWWF flow rate of 1500 L/s.

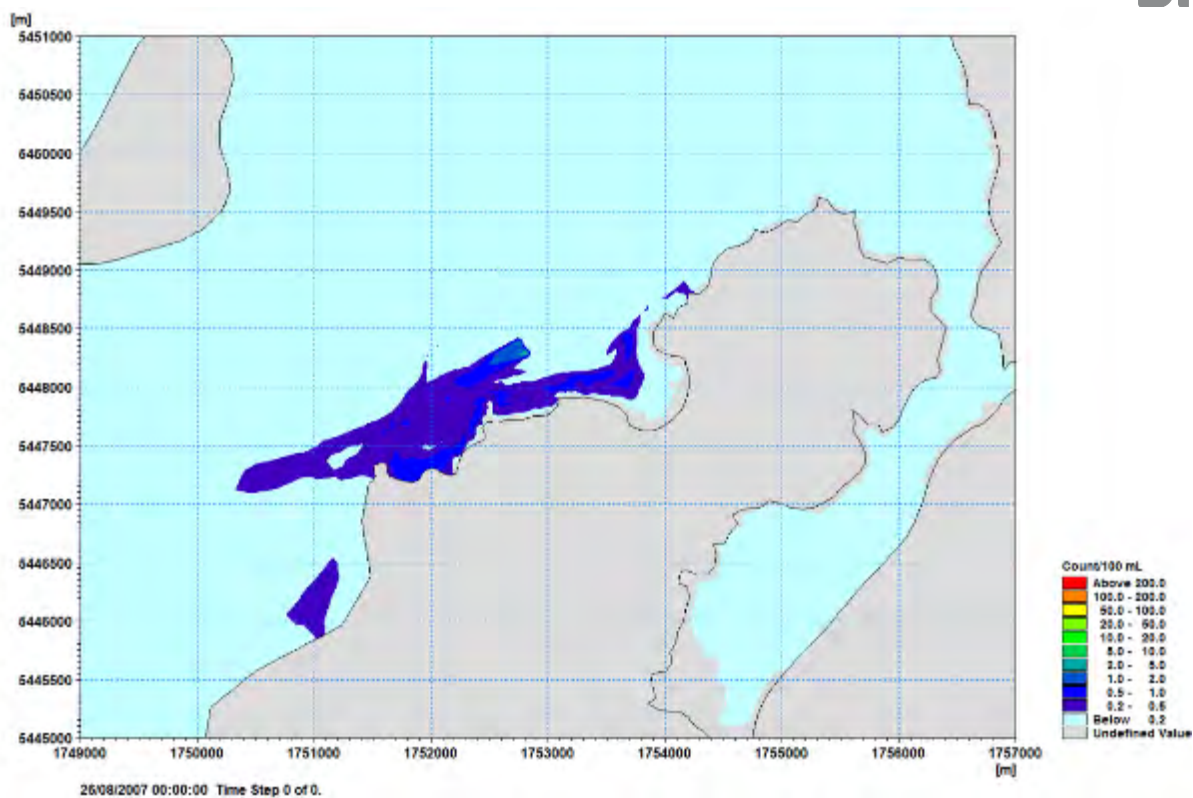


Figure 5-26. Predicted 95th percentile Enterococci concentration (Ent/100 mL), for the 15 m outfall option for typical winds and spring tide for the future PWWF flow rate of 1500 L/s.

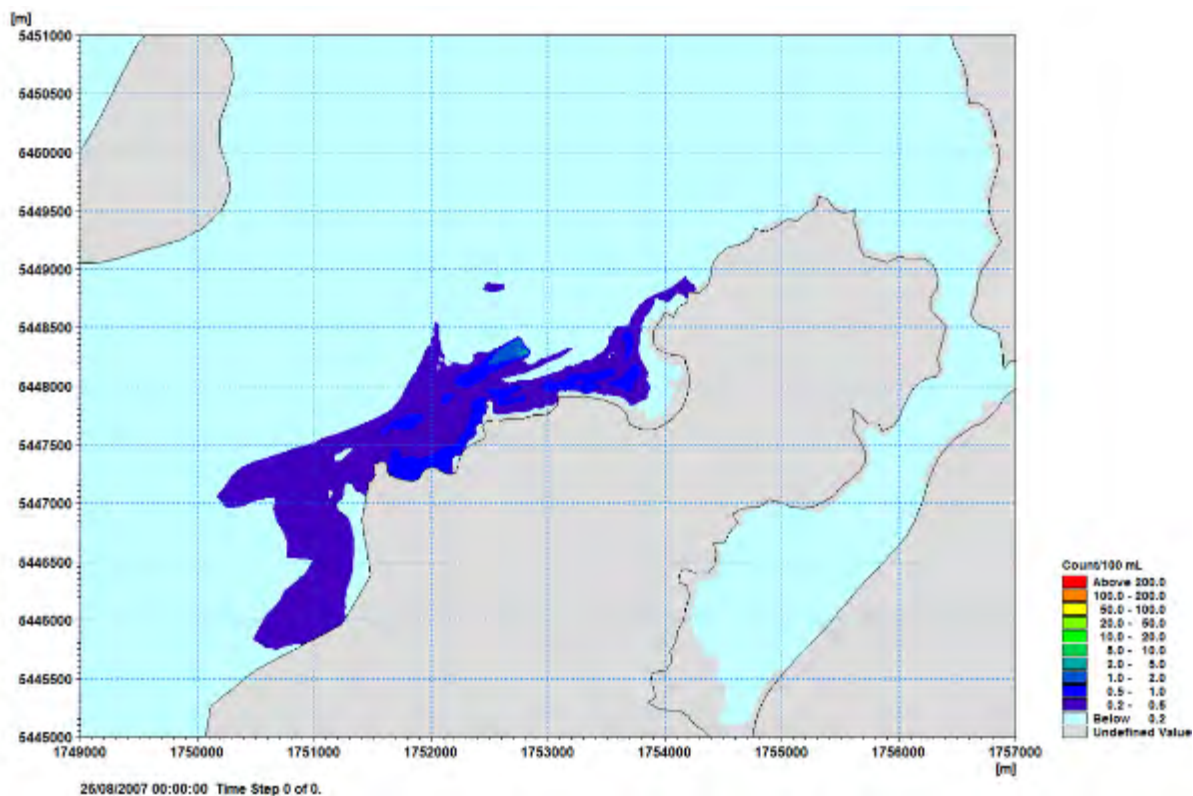


Figure 5-27. Predicted 95th percentile Virus concentration (Virus/100 mL), for the 15 m outfall option for typical winds and spring tide for the future PWWF flow rate of 1500 L/s.

5.2.2 Onshore Winds and Spring Tide - 1500 L/s PWWF

Table 17 and Table 18 provide percentile values for Enterococci and Virus for the existing shoreline discharge and the discharge options for the future PWWF (1500 L/s) for onshore winds and spring tides. Appendices D-I contain figures of the predicted time-series of data the monitoring sites.

For the **existing shoreline** discharge the 99th percentile concentration ranges from 291 to 630 count/100 mL at the sites near the existing discharge

At the Titahi Beach sites the 99th percentile concentration ranges from 55 to 151 count/100 mL.

At the Te Korohiwa Rocks and Mount Couper monitoring sites the 99th percentile concentration ranges from 4 to 22 count/100 mL.

For the **new shoreline** discharge reduction in percentile concentrations at the 200 m SW monitoring site of between 58 and 84% are achieved. At the 200 m E monitoring site percentile concentrations are reduced by between 85 and 91%. At the Titahi Beach sites reductions in the percentile concentrations range from 89 to 97%. Increased percentile concentrations at the Ti Korohiwa Rocks site range from a factor of 11 to 28 resulting in 99th percentile value of 560 count/100 mL. At the Mount Couper site percentile concentrations are reduced by between 15% and 57%.

For the **10m outfall** discharge reduction in percentile concentrations at the 200 m SW monitoring site are greater than 98%. At the 200 m E monitoring site percentile concentrations are reduced by at least 94%. At the Titahi Beach sites reductions in the percentile concentrations range from 88 to 94%. At the Ti Korohiwa monitoring site percentile concentrations are reduced by between 46% and 75%. At the Mount Couper site percentile concentrations are reduced by between 82% and 92%.

Concentrations at the Mount Couper site are higher during the first tidal cycle compared to the existing discharge – this again relates to the travel time for the treated wastewater plume.

For the **15m outfall** discharge reductions in the percentile concentration at the 200 m SW, the 200 m E site and the Titahi Beach sites are more than 99%. Percentile concentrations at the Ti Korohiwa Rocks site decrease by between 96 and 97%. Percentile concentrations at the Mount Couper decrease by between 61 and 93%. Concentrations at the Mount Couper site are higher during the first tidal cycle compared to the existing discharge – this again relates to the travel time for the treated wastewater plume (Figure I-3, Figure I-4, Appendix I).

Figures 5-28 to 5-35 show the spatial plots of the predicted 95th percentile estimates for each of the discharge options. These plots indicate the area impacted by each of the discharges and in particular the significant reduction in concentrations achieved by the outfall options.

Table 17. Percentile estimates of Enterococci concentration (Ent/100 mL) at the monitoring sites, future PWWF for onshore winds and spring tide. Highlighted cells indicate percentile values that are higher than for the existing shoreline discharge.

Discharge Point	Percentile	200 m SW	200 m E	Titahi Beach South	Titahi Beach	Ti Korohiwa	Mount Couper
Existing Shoreline	90	129.6	56.1	73.7	14.1	4.1	0.3
	95	308.7	178.7	102.6	32.2	14.6	1.2
	99	604.7	290.7	139.6	55.5	19.8	3.8
New Shoreline	90	45.8	6.0	4.4	0.4	96.2	0.0
	95	70.4	16.4	7.3	0.9	396.0	0.1
	99	98.2	37.0	13.9	2.7	556.9	0.6
10 m Outfall	90	1.4	3.4	4.4	0.9	2.2	0.2
	95	4.6	5.6	8.9	2.4	4.2	1.0
	99	6.4	13.4	10.2	6.5	7.2	3.3
15 m outfall	90	0.1	0.1	0.1	0.0	0.1	0.0
	95	0.3	0.4	0.1	0.0	0.4	0.4
	99	0.5	0.7	0.7	0.1	0.8	1.5

Table 18 Percentile estimates of Virus concentration (Virus/100 mL) at the monitoring sites, future PWWF for onshore winds and spring tide. Highlighted cells indicate percentile values that are higher than for the existing shoreline discharge.

Discharge Point	Percentile	200 m SW	200 m E	Titahi Beach South	Titahi Beach	Ti Korohiwa	Mount Couper
Existing Shoreline	90	138.4	61.2	81.5	23.5	8.8	0.6
	95	372.5	190.1	109.3	42.0	16.9	2.5
	99	629.2	304.9	151.2	64.4	22.2	4.5
New Shoreline	90	58.1	9.2	6.4	0.9	97.9	0.1
	95	84.0	20.8	11.1	2.3	425.3	0.3
	99	111.7	39.2	15.9	4.2	557.8	0.8
10 m Outfall	90	2.6	3.6	5.3	1.8	2.9	0.3
	95	4.8	5.9	9.2	3.9	4.2	1.1
	99	6.4	13.6	10.6	6.9	7.4	3.3
15 m outfall	90	0.2	0.2	0.1	0.0	0.2	0.0
	95	0.4	0.4	0.2	0.1	0.5	0.4
	99	0.5	0.8	0.7	0.1	0.8	1.6

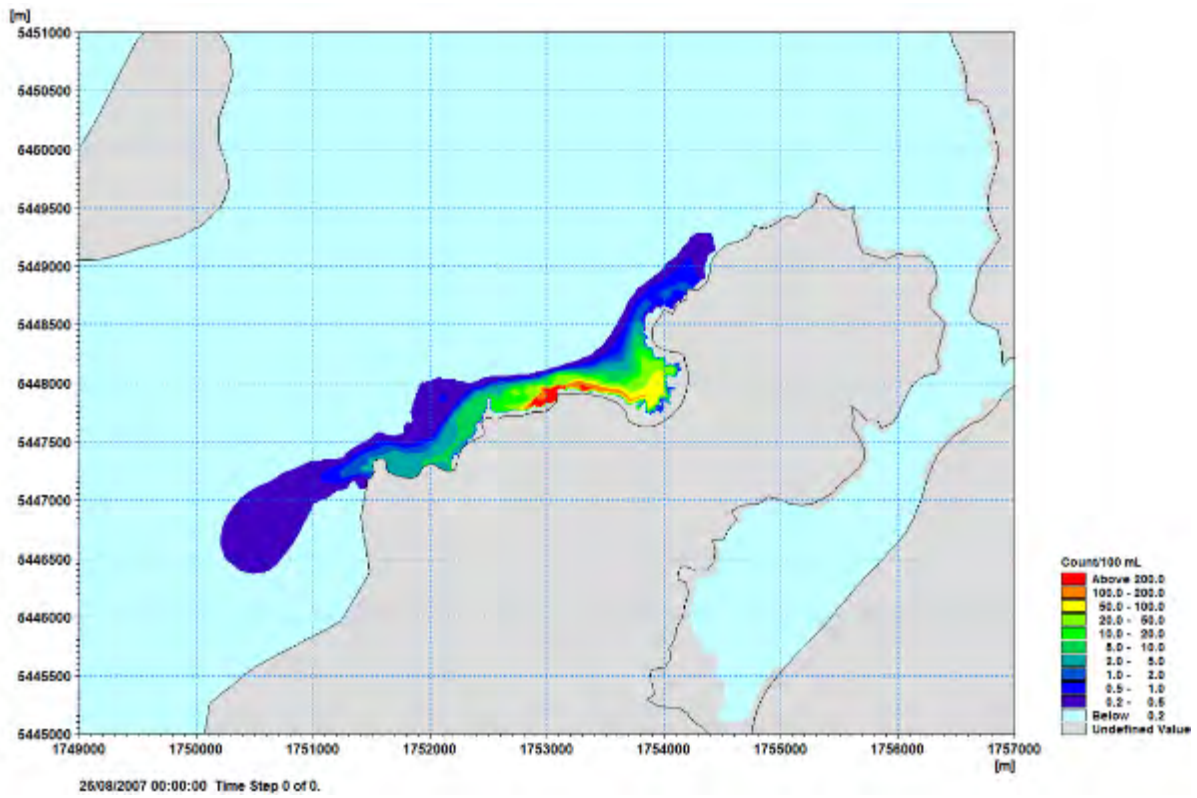


Figure 5-28. Predicted 95th percentile Enterococci concentration (Ent/100 mL), for the existing shoreline discharge for onshore winds and spring tide for the future PWWF flow rate of 1500 L/s.

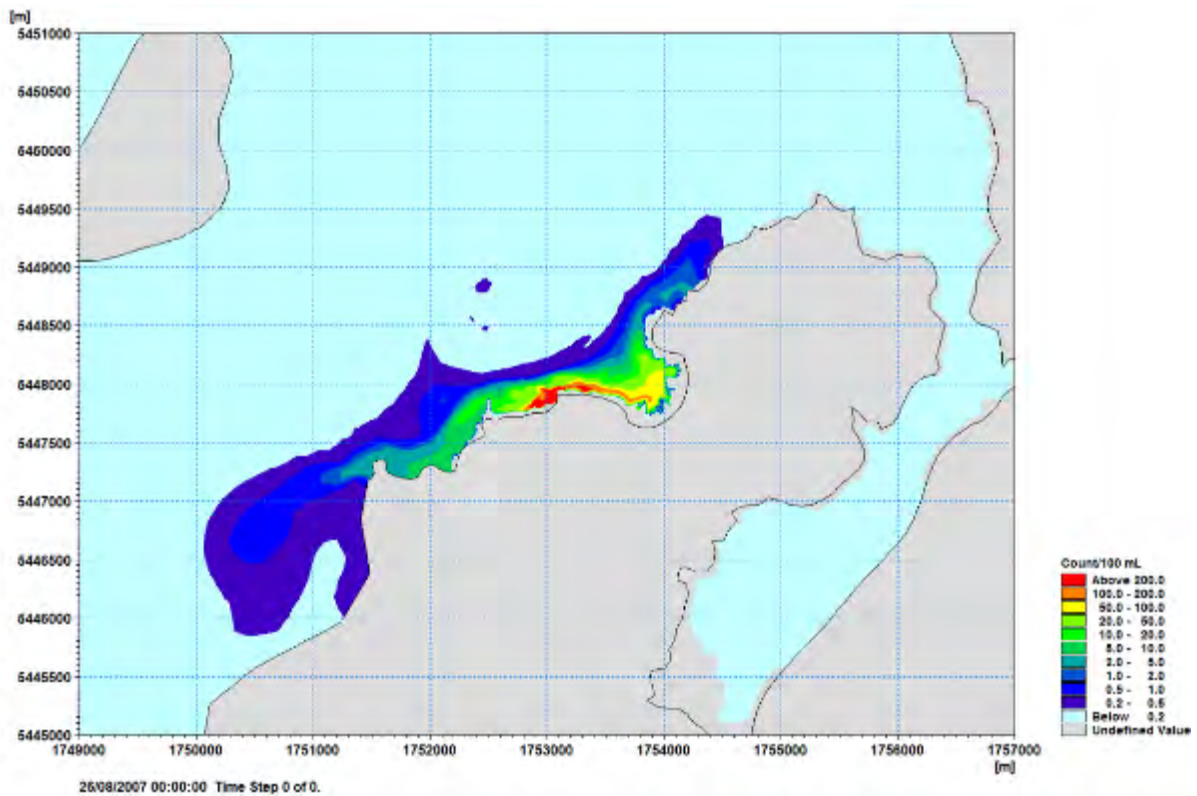


Figure 5-29. Predicted 95th percentile Virus concentration (Virus/100 mL), for the existing shoreline discharge for onshore winds and spring tide for the future PWWF flow rate of 1500 L/s.

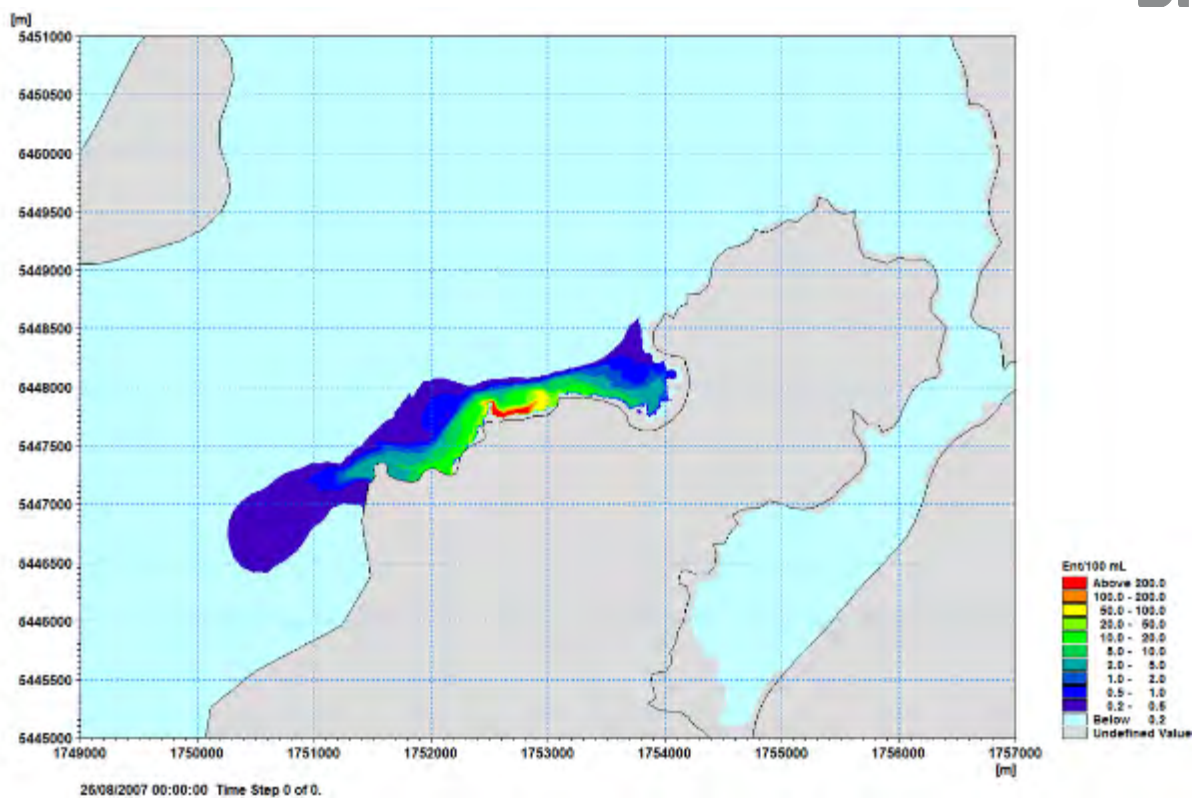


Figure 5-30. Predicted 95th percentile Enterococci concentration (Ent/100 mL), for the new shoreline discharge for onshore winds and spring tide for the future PWWF flow rate of 1500 L/s.

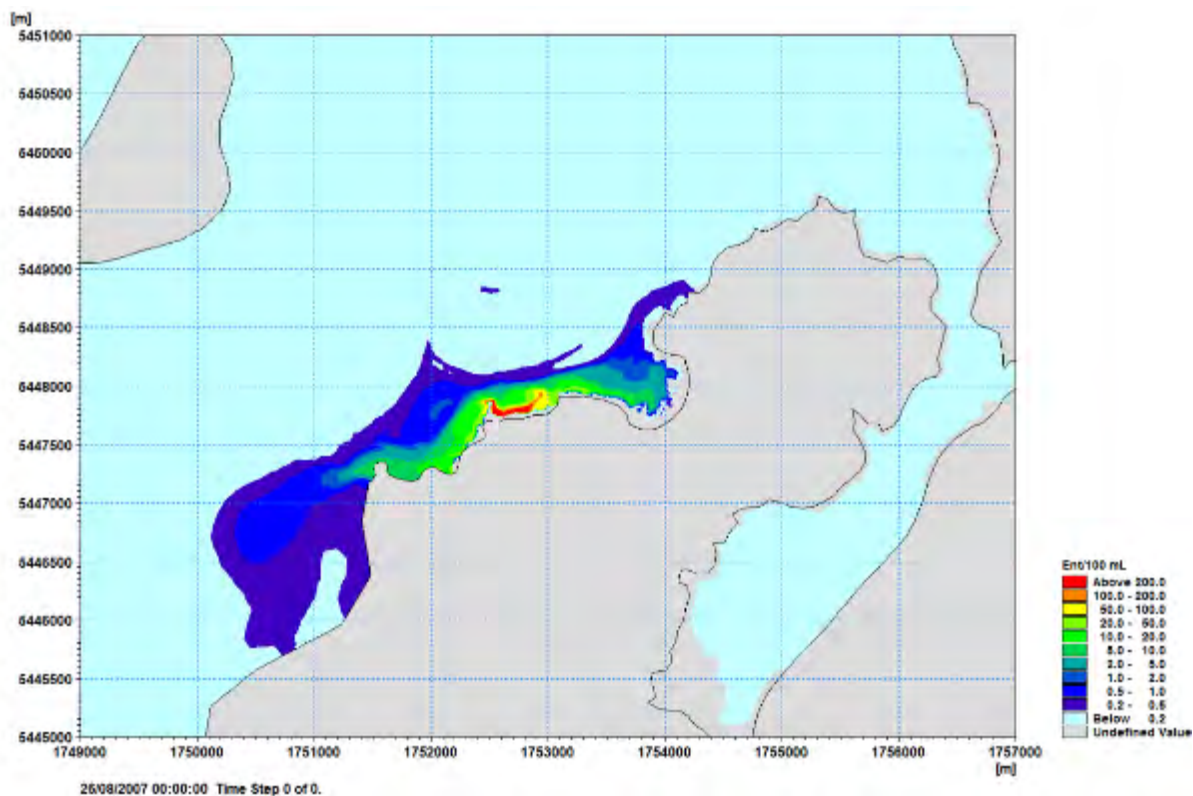


Figure 5-31. Predicted 95th percentile Virus concentration (Virus/100 mL), for the new shoreline discharge for onshore winds and spring tide for the future PWWF flow rate of 1500 L/s.

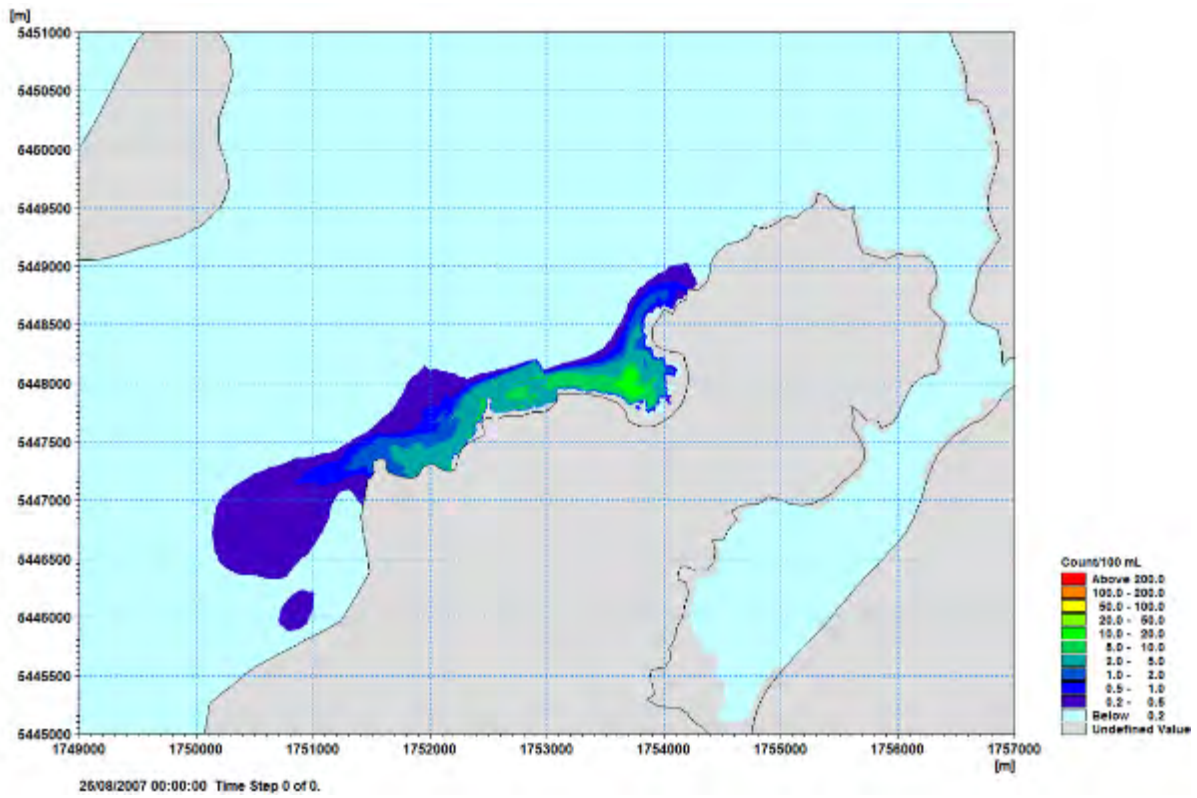


Figure 5-32. Predicted 95th percentile Enterococci concentration (Ent/100 mL), for the 10 m outfall option for onshore winds and spring tide for the future PWWF flow rate of 1500 L/s.

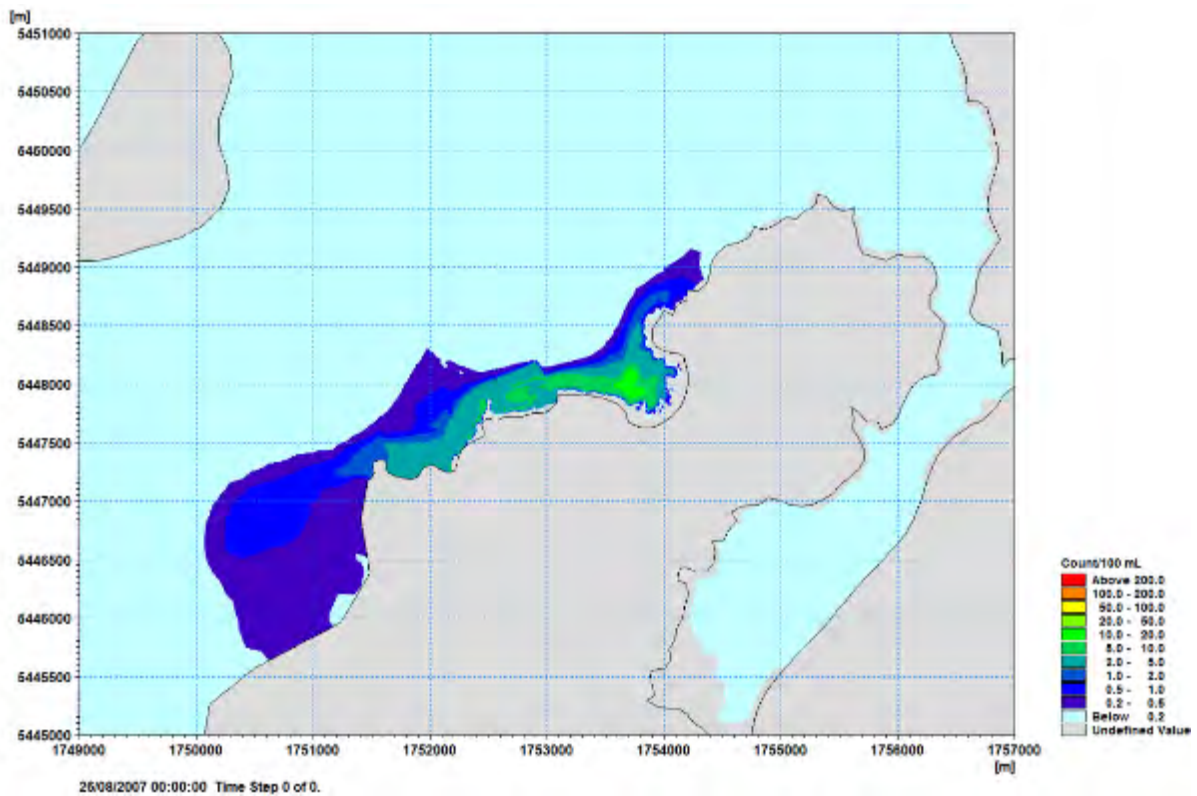


Figure 5-33. Predicted 95th percentile Virus concentration (Virus/100 mL), for the 10 m outfall option for onshore winds and spring tide for the future PWWF flow rate of 1500 L/s.

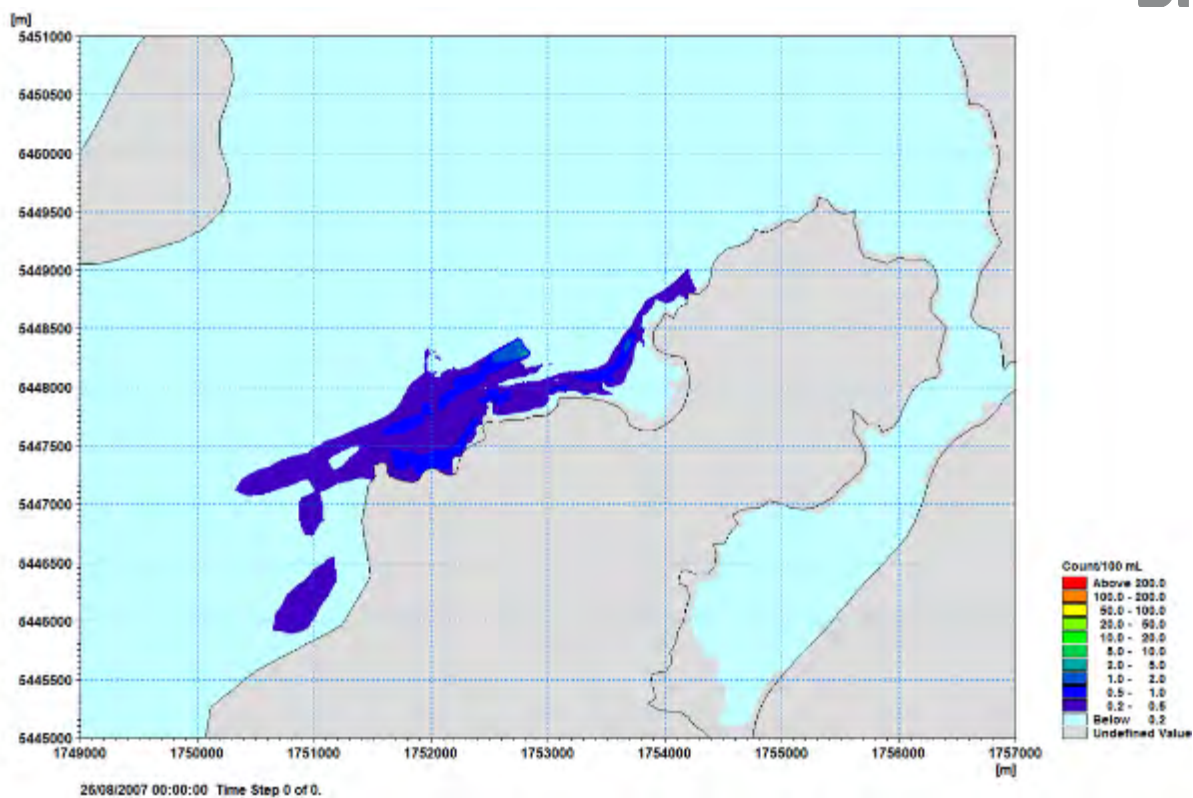


Figure 5-34. Predicted 95th percentile Enterococci concentration (Ent/100 mL), for the 15 m outfall option for onshore winds and spring tide for the future PWWF flow rate of 1500 L/s.

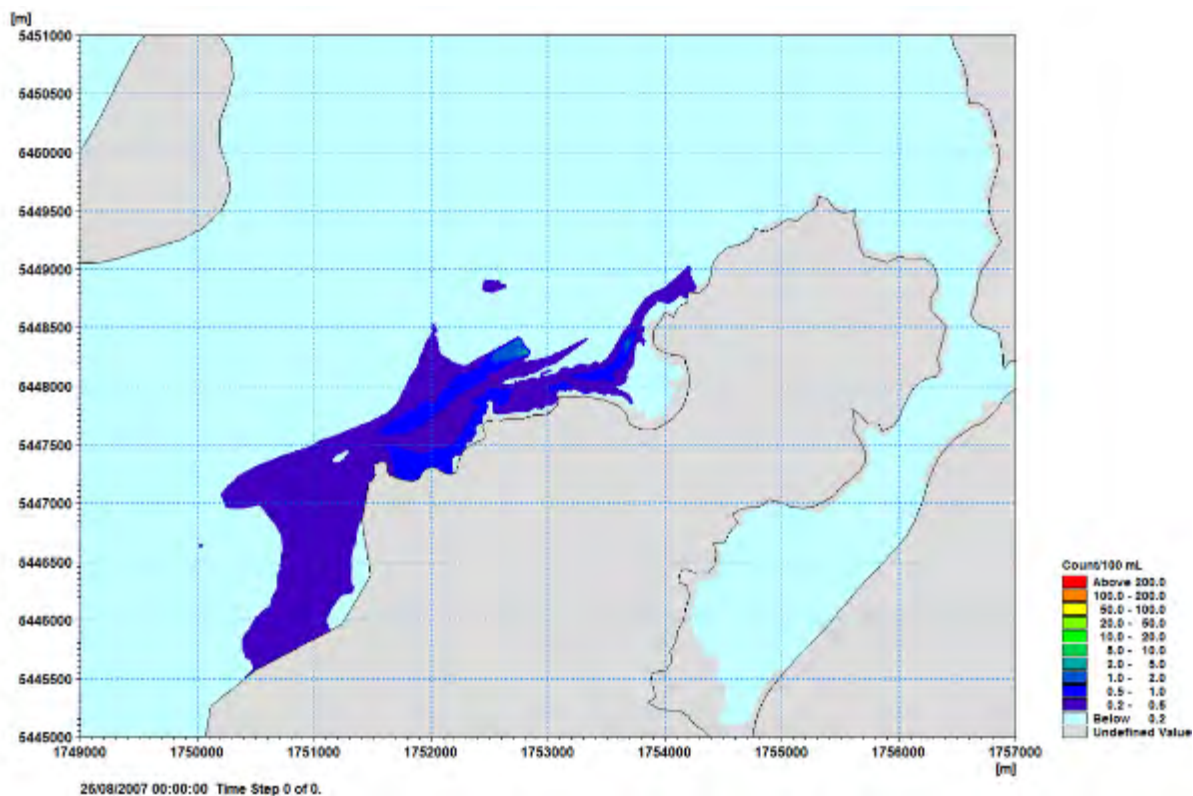


Figure 5-35. Predicted 95th percentile Virus concentration (Virus/100 mL), for the 15 m outfall option for onshore winds and spring tide for the future PWWF flow rate of 1500 L/s.

5.2.3 Typical Winds and Neap Tide - 1500 L/s PWWF

Table 19 and Table 20 provide percentile values for Enterococci and Virus for the existing shoreline discharge and the discharge options for the future PWWF (1500 L/s) for typical winds and neap tides. Appendices D-I contain figures of the predicted time-series of data the monitoring sites.

For the **existing shoreline** discharge the 99th percentile concentration ranges from 312 to 567 count/100 mL at the sites near the existing discharge

At the Titahi Beach sites the 99th percentile concentration ranges from 129 to 204 count/100 mL.

At the Te Korohiwa Rocks and Mount Couper monitoring sites the 99th percentile concentration ranges from 11 to 22 count/100 mL.

For the **new shoreline** discharge reduction in percentile concentrations at the 200 m SW site of between 13 and 71% are achieved. At the 200 m E site percentile concentrations are reduced by between 75 and 85%. At the Titahi Beach sites the percentile concentrations are reduced by between 86 and 95%. At the Ti Korohiwa Rocks site percentile concentrations are increased by a factor of 24 to 54 resulting in 99th percentile value of between 530 and 540 count/100 mL. At the Mount Couper site percentile concentrations are reduced by between 75 and 87%.

For the **10m outfall** discharge reduction in percentile concentrations at the 200 m SW are greater than 95%, while at the 200 m E monitoring site and the Titahi Beach sites reductions in the percentile concentrations range from 86 to 94%. At the Ti Korohiwa Rocks site the 90th and 99th percentile concentrations increase by between 2 and 17% but are still less than 15 count/100 mL (highlighted cells in Table 19 and Table 20) but the 95th percentile reduces from 8.1 count/100 mL to 7.6 count/100 mL. This again relates to the travel time for the treated wastewater plume and the timing of the peak concentration at the site. Figure 5-36 shows that for this particular combination on tides and winds the peak concentration at the at the Ti Korohiwa Rocks site is higher for the 10 m outfall option during the first part of the peak wet weather flow. At the Mount Couper site percentile concentrations are reduced by between 52% and 74%. Concentrations at the Mount Couper site are higher during the first tidal cycle compared to the existing discharge – this again relates to the travel time for the treated wastewater plume (Figure I-5, Figure I-6, Appendix I).

For the **15m outfall** discharge reductions in the percentile concentration at the 200 m SW, the 200 m E site and the Titahi Beach sites are more than 99%. Percentile concentrations at the Ti Korohiwa Rocks site decrease by between 82 and 87%. Percentile concentrations at the Mount Couper decrease by between 69 and 87%. Concentrations at the Mount Couper site are higher during the first tidal cycle compared to the existing discharge – this again relates to the travel time for the treated wastewater plume.

Figures 5-37 to 5-44 show the spatial plots of the predicted 95th percentile estimates for each of the discharge options. These plots indicate the area impacted by each of the discharges and in particular the significant reduction in concentrations achieved by the outfall options.

Table 19. Percentile estimates of Enterococci concentration (Ent/100 mL) at the monitoring sites, future PWWF for typical winds and neap tide. Highlighted cells indicate percentile values that are higher than for the existing shoreline discharge.

Discharge Point	Percentile	200 m SW	200 m E	Titahi Beach South	Titahi Beach	Ti Korohiwa	Mount Couper
Existing Shoreline	90	71.5	60.2	76.7	54.1	3.8	2.9
	95	373.9	234.3	126.0	107.1	8.1	6.3
	99	548.1	312.0	202.3	129.2	10.7	21.6
New Shoreline	90	61.9	13.4	6.7	3.6	104.3	0.6
	95	112.2	35.9	17.6	5.8	438.4	1.5
	99	195.9	77.1	21.6	9.2	535.7	2.8
10 m Outfall	90	3.7	6.7	8.6	6.3	4.5	1.4
	95	7.7	8.1	9.5	9.6	7.6	1.9
	99	9.5	11.8	12.8	11.9	13.0	5.7
15 m outfall	90	0.3	0.3	0.2	0.2	0.5	0.5
	95	0.9	0.8	0.2	0.2	1.5	1.3
	99	1.4	1.4	0.4	0.2	1.9	6.6

Table 20. Percentile estimates of Virus concentration (Virus/100 mL) at the monitoring sites, future PWWF for typical winds and neap tide. Highlighted cells indicate percentile values that are higher than for the existing shoreline discharge.

Discharge Point	Percentile	200 m SW	200 m E	Titahi Beach South	Titahi Beach	Ti Korohiwa	Mount Couper
Existing Shoreline	90	73.5	61.8	76.9	59.8	4.4	4.6
	95	384.1	238.3	130.6	107.5	8.4	9.1
	99	567.3	316.3	204.0	130.8	11.3	22.1
New Shoreline	90	63.0	14.7	9.0	5.1	104.9	0.9
	95	112.8	36.2	18.0	6.7	445.0	2.3
	99	196.6	77.7	22.2	9.6	541.6	3.1
10 m Outfall	90	3.9	6.9	8.8	7.9	4.5	1.7
	95	7.7	8.3	9.8	9.8	7.7	2.5
	99	9.6	12.2	13.4	12.2	13.2	5.8
15 m outfall	90	0.5	0.5	0.4	0.3	0.6	0.6
	95	0.9	0.9	0.4	0.4	1.5	1.3
	99	1.4	1.5	0.5	0.4	1.9	6.9

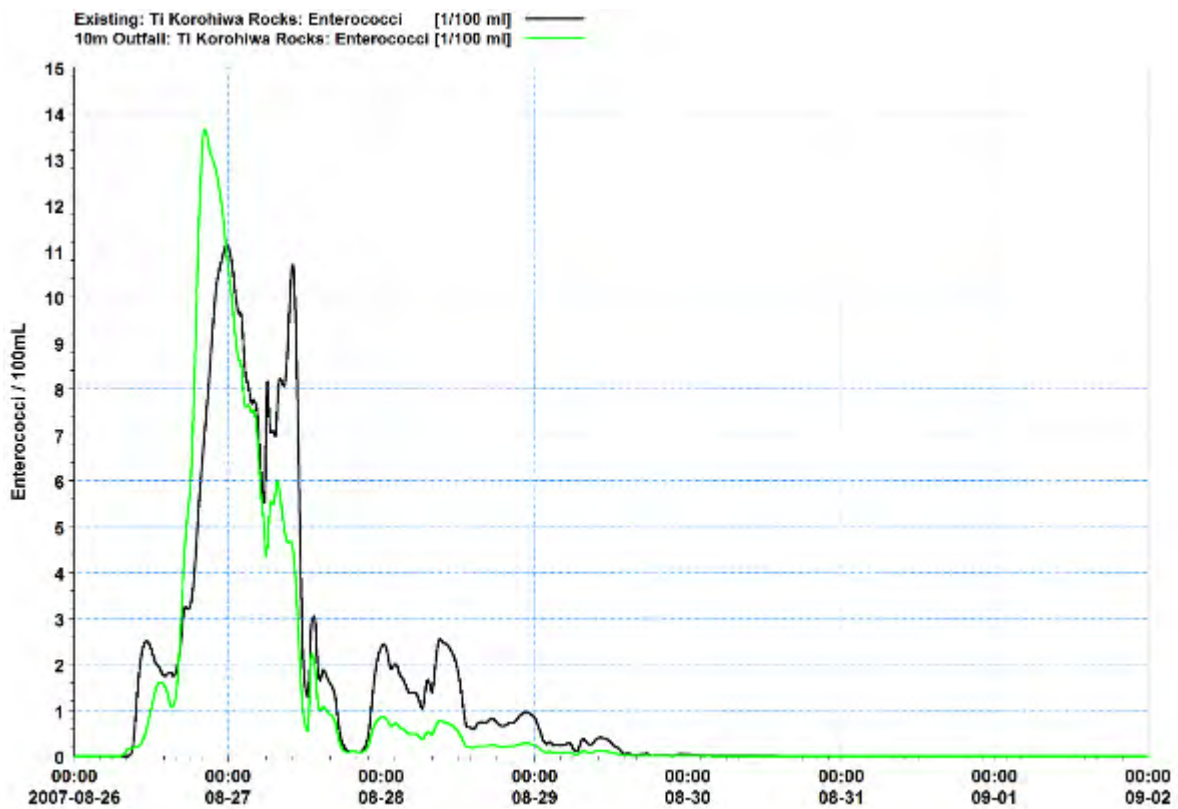


Figure 5-36. Predicted Enterococci concentration (Ent/100 mL) for the existing shoreline discharge and the 10 m outfall option for typical winds and neap tidal conditions.

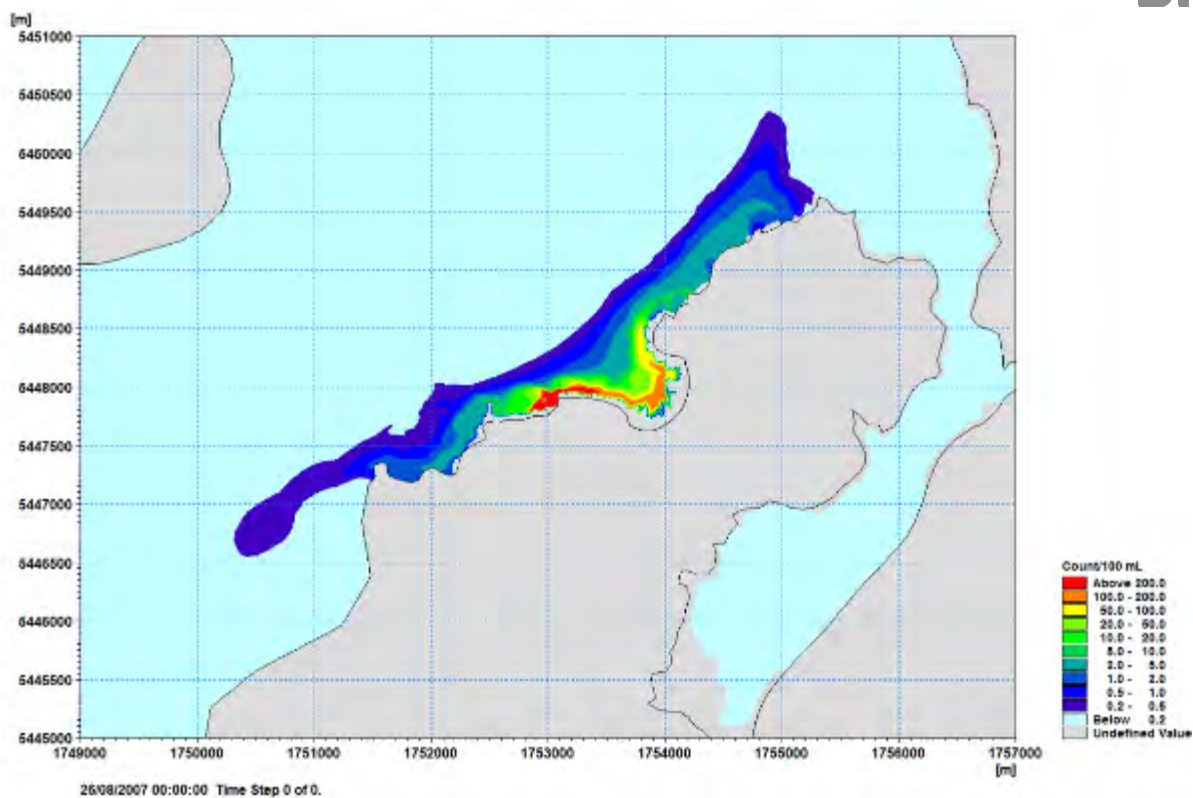


Figure 5-37. Predicted 95th percentile Enterococci concentration (Ent/100 mL), for the existing shoreline discharge for typical winds and neap tide for the future PWWF flow rate of 1500 L/s.

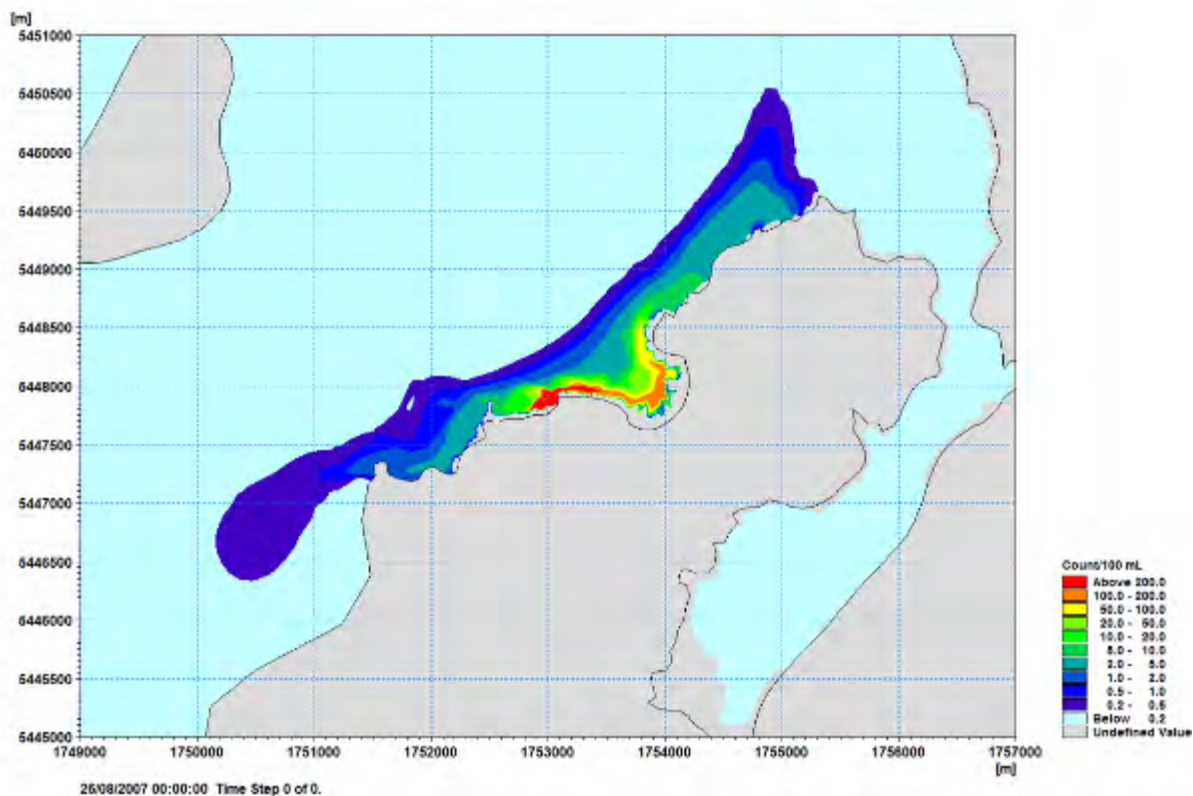


Figure 5-38. Predicted 95th percentile Virus concentration (Virus/100 mL), for the existing shoreline discharge for typical winds and neap tide for the future PWWF flow rate of 1500 L/s.

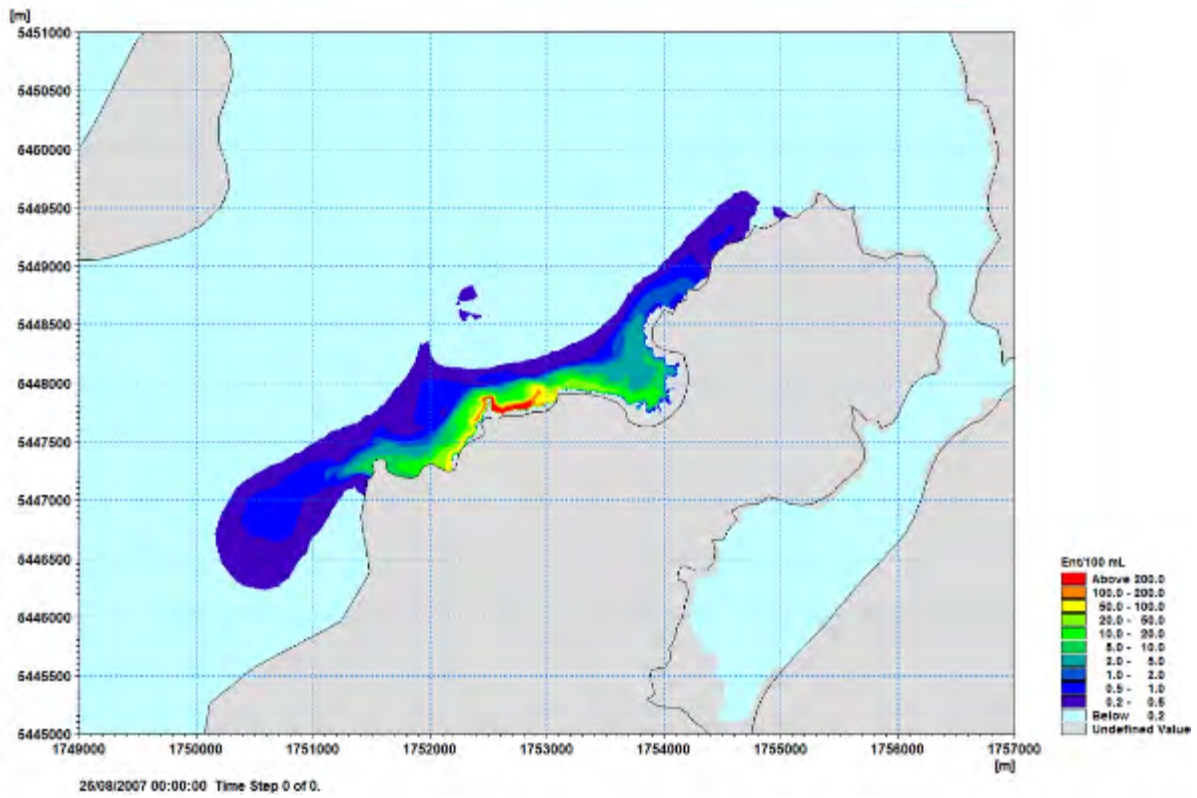


Figure 5-39. Predicted 95th percentile Enterococci concentration (Ent/100 mL), for the new shoreline discharge for typical winds and neap tide for the future PWWF flow rate of 1500 L/s.

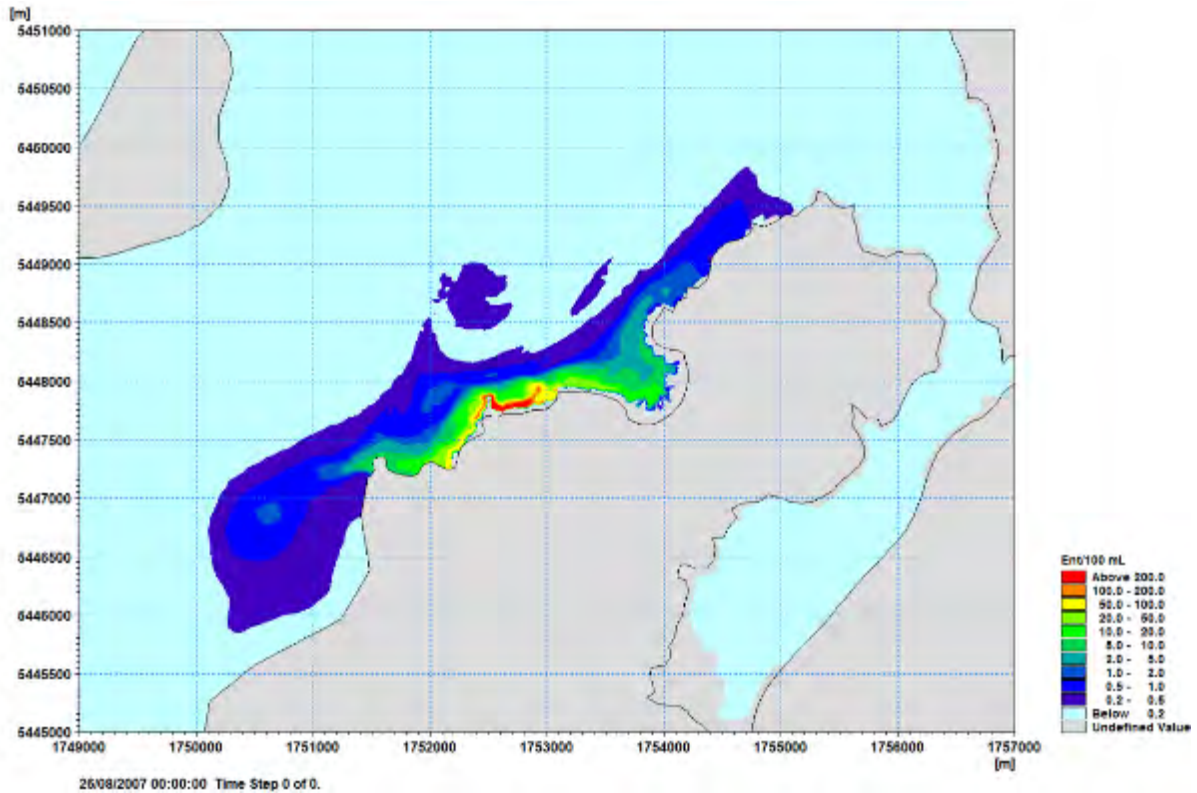


Figure 5-40. Predicted 95th percentile Virus concentration (Virus/100 mL), for the new shoreline discharge for typical winds and neap tide for the future PWWF flow rate of 1500 L/s.

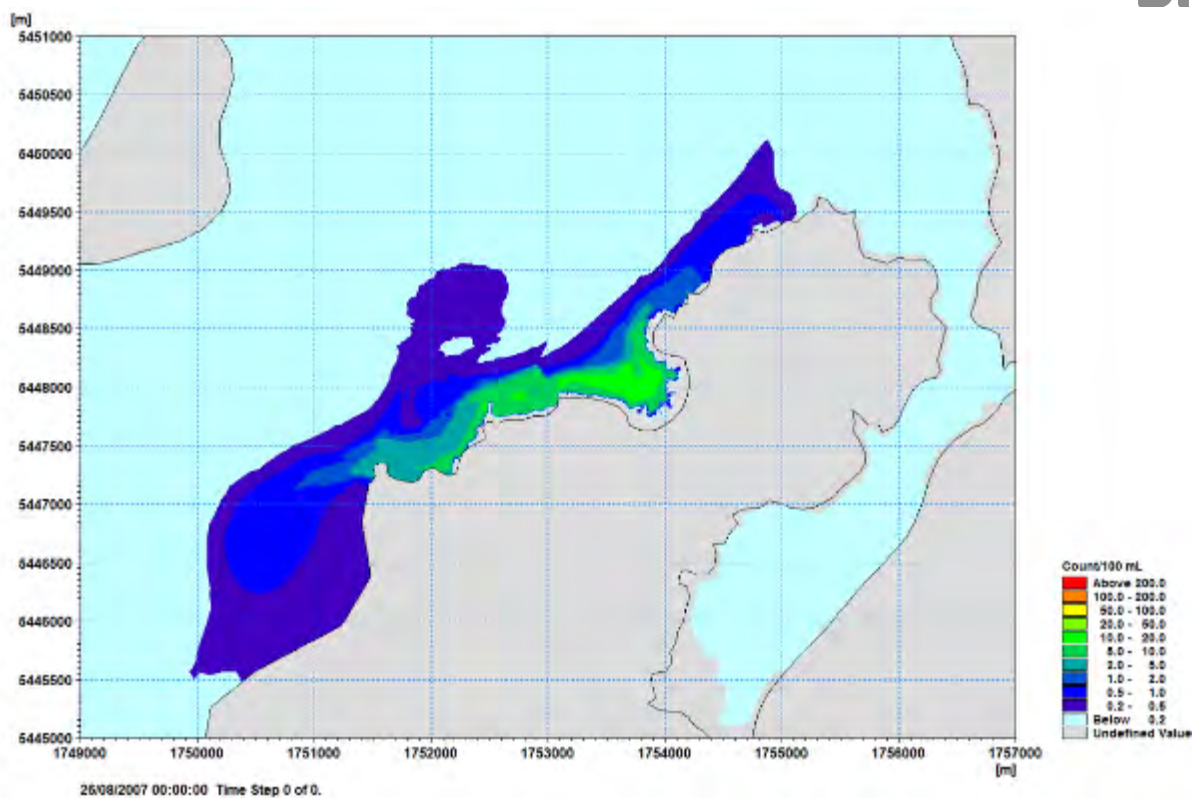


Figure 5-41. Predicted 95th percentile Enterococci concentration (Ent/100 mL), for the 10 m outfall option for typical winds and neap tide for the future PWWF flow rate of 1500 L/s.

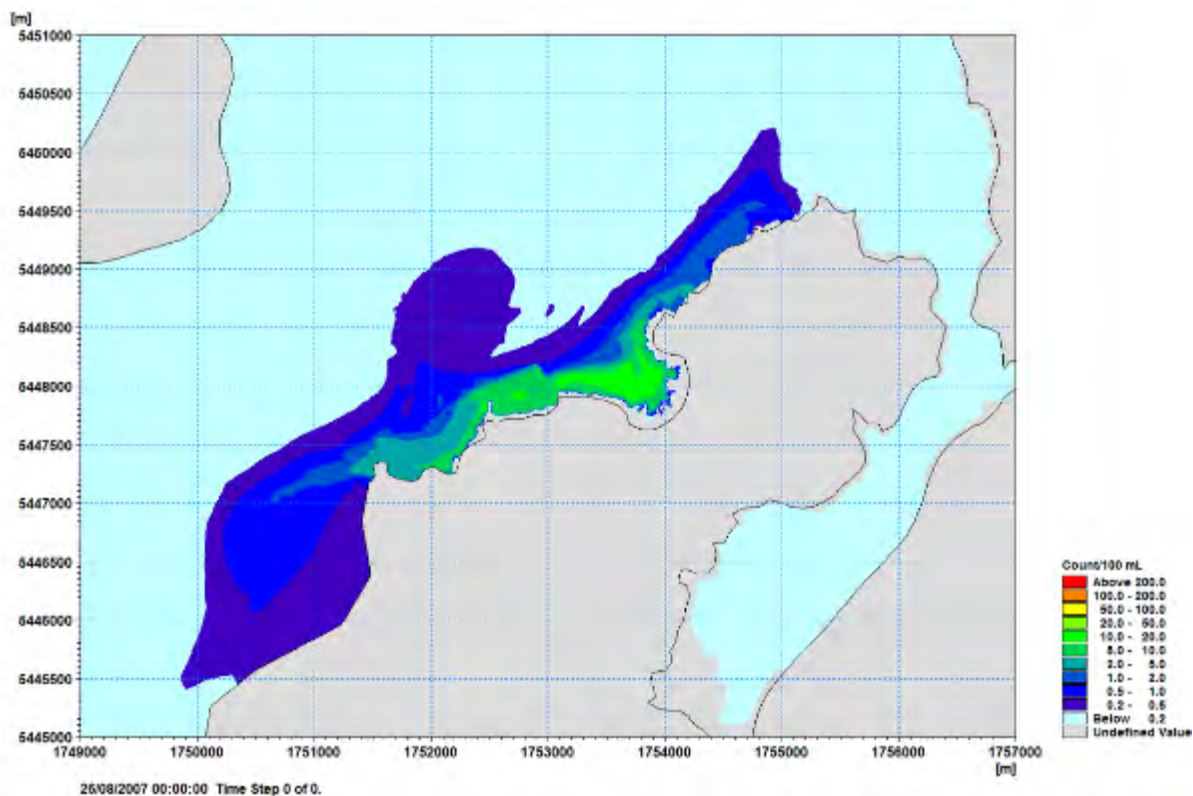


Figure 5-42. Predicted 95th percentile Virus concentration (Virus/100 mL), for the 10 m outfall option for typical winds and neap tide for the future PWWF flow rate of 1500 L/s.

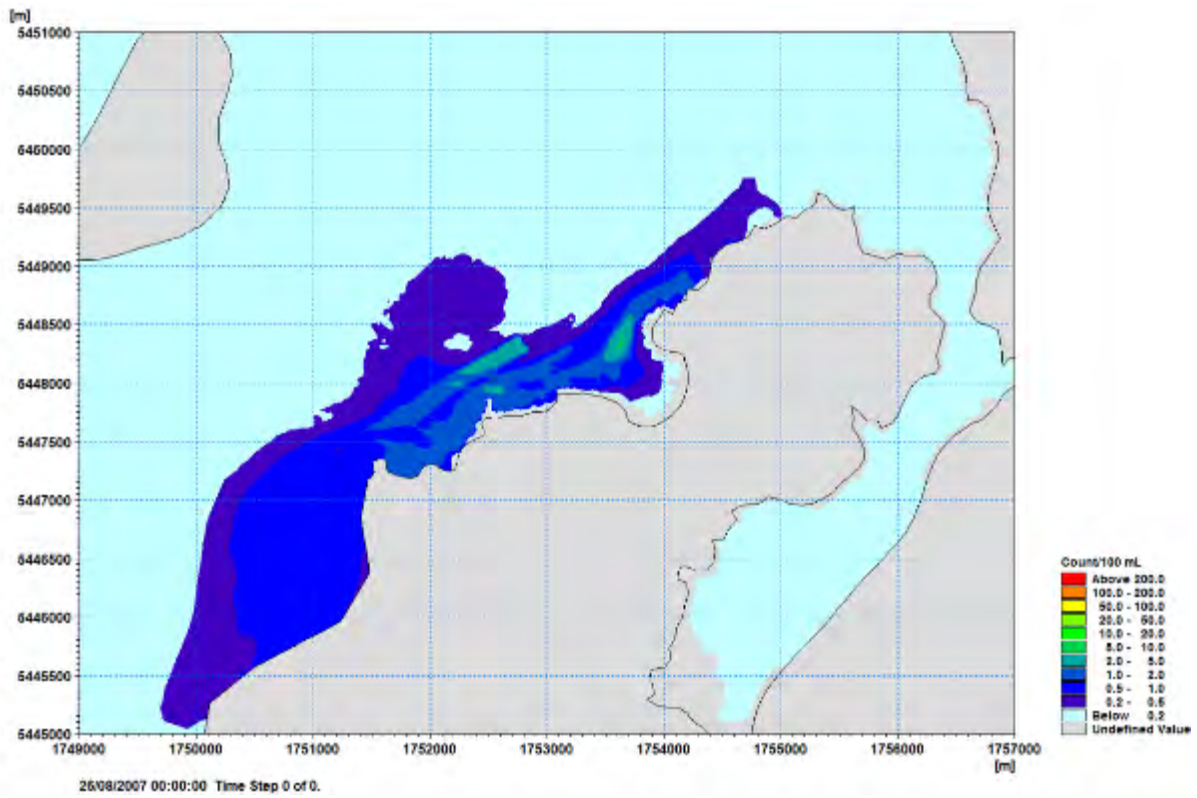


Figure 5-43. Predicted 95th percentile Enterococci concentration (Ent/100 mL), for the 15 m outfall option for typical winds and neap tide for the future PWWF flow rate of 1500 L/s.

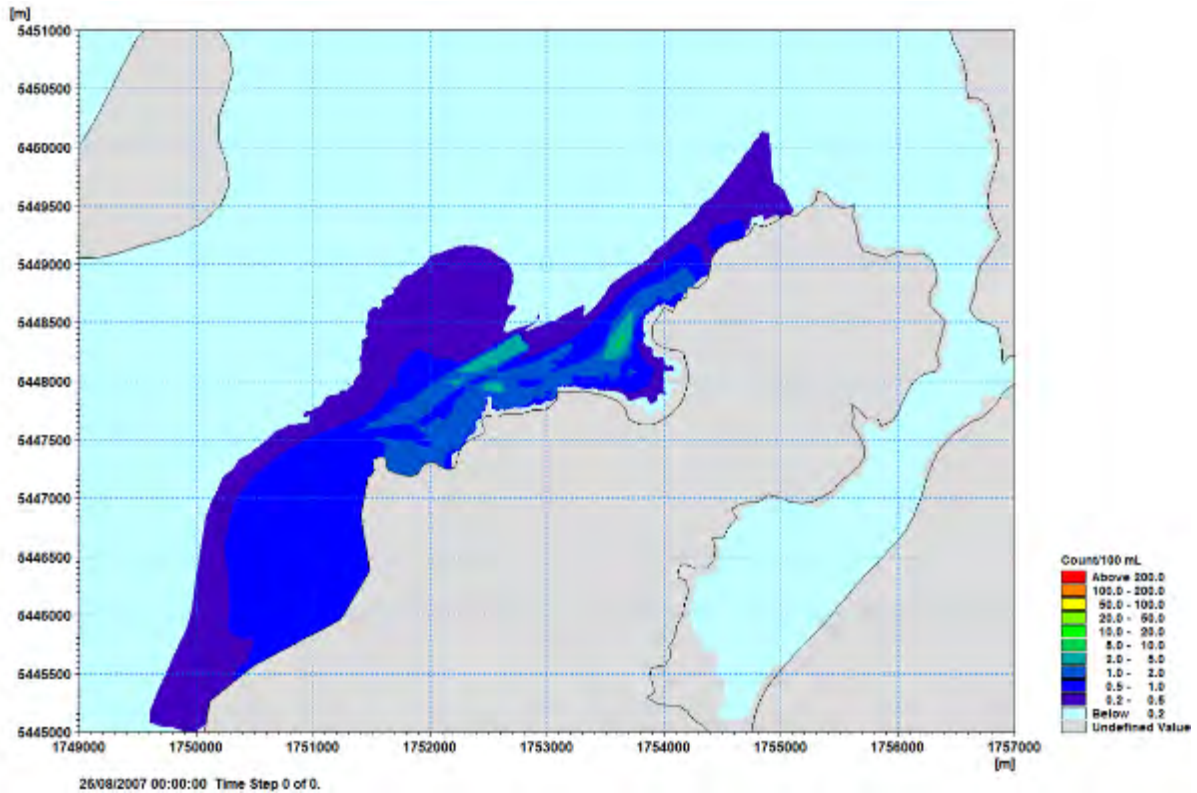


Figure 5-44. Predicted 95th percentile Virus concentration (Virus/100 mL), for the 15 m outfall option for typical winds and neap tide for the future PWWF flow rate of 1500 L/s. Onshore Neap 1500 L/s PWWF

5.2.4 Onshore Winds and Neap Tide - 1500 L/s PWWF

Table 21 and Table 22 provide percentile values for Enterococci and Virus for the existing shoreline discharge and the discharge options for the future PWWF (1500 L/s) for onshore winds and neap tides. Appendices D-I contain figures of the predicted time-series of data the monitoring sites.

For the **existing shoreline** discharge the 99th percentile concentration ranges from 303 to 553 count/100 mL at the sites near the existing discharge

At the Titahi Beach sites the 99th percentile concentration ranges from 95 to 183 count/100 mL.

At the Te Korohiwa Rocks and Mount Couper monitoring sites the 99th percentile concentration is around 15 count/100 mL.

For the **new shoreline** discharge reduction in percentile concentrations at the 200 m SW monitoring site of between 31 and 74% are achieved. At the 200 m E site percentile concentrations are reduced by between 83 and 93%. At the Titahi Beach monitoring sites the reductions in the percentile concentrations range from 93 to 96%. Increased percentile concentrations at the Ti Korohiwa Rocks site range from a factor of 16 to 43 resulting in 99th percentile value of around 530 count/100 mL. At the Mount Couper site percentile concentrations are reduced by between 89% and 92%.

For the **10m outfall** discharge reductions in percentile concentrations at the 200 m SW site are greater than 96% while at the 200 m E site reductions percentile concentrations of at least 91% are achieved. At the Titahi Beach sites reductions in the percentile concentrations of between 87 and 94% occur. At the Ti Korohiwa Rocks site reductions in the percentile concentrations of between 22% and 45% occur. Percentile concentrations at the Mount Couper site are reduced by between 47 and 66%. Concentrations at the Mount Couper site are higher during the first tidal cycle compared to the existing discharge – this again relates to the travel time for the treated wastewater plume.

For the **15m outfall** discharge reductions in percentile concentrations at the 200 m SW, 200 m E and Titahi Beach sites are greater than 99%. At the Ti Korohiwa Rocks site reductions in the percentile concentrations of between 87% and 90% occur. Percentile concentrations at the Mount Couper site are reduced by between 57 and 81%. Concentrations at the Mount Couper site are higher during the first tidal cycle compared to the existing discharge – this again relates to the travel time for the treated wastewater plume (Figure I-7, Figure I-8, Appendix I). At all other site's percentile concentrations are reduced by between 87 and 90%.

Figures 5-45 to 5-52 show the spatial plots of the predicted 95th percentile estimates for each of the discharge options. These plots indicate the area impacted by each of the discharges and in particular the significant reduction in concentrations achieved by the outfall options.

Table 21. Percentile estimates of Enterococci concentration (Ent/100 mL) at the monitoring sites, future PWWF for onshore winds and neap tide. Highlighted cells indicate percentile values that are higher than for the existing shoreline discharge.

Discharge Point	Percentile	200 m SW	200 m E	Titahi Beach South	Titahi Beach	Ti Korohiwa	Mount Couper
Existing Shoreline	90	94.5	84.6	93.3	60.4	5.7	1.9
	95	363.1	242.4	150.6	78.8	10.0	4.1
	99	533.9	303.8	182.0	94.7	15.2	15.1
New Shoreline	90	65.0	10.7	6.8	2.2	124.5	0.2
	95	94.5	17.0	9.0	3.9	431.2	0.4
	99	150.0	53.6	13.7	5.1	527.2	1.2
10 m Outfall	90	3.1	7.4	9.1	5.1	4.2	1.0
	95	7.5	8.8	9.6	10.0	7.8	2.1
	99	9.2	11.3	12.6	11.1	11.9	5.3
15 m outfall	90	0.4	0.4	0.1	0.1	0.6	0.4
	95	0.8	0.7	0.2	0.2	1.3	1.8
	99	1.2	1.1	0.3	0.4	1.9	6.1

Table 22. Percentile estimates of Virus concentration (Virus/100 mL) at the monitoring sites, future PWWF for onshore winds and neap tide. Highlighted cells indicate percentile values that are higher than for the existing shoreline discharge.

Discharge Point	Percentile	200 m SW	200 m E	Titahi Beach South	Titahi Beach	Ti Korohiwa	Mount Couper
Existing Shoreline	90	96.5	85.9	92.9	62.9	7.6	3.0
	95	378.0	246.0	155.0	80.3	10.6	6.4
	99	553.4	306.6	183.2	99.0	15.7	15.7
New Shoreline	90	67.0	12.3	7.2	3.0	125.0	0.2
	95	96.8	17.7	9.5	4.1	438.0	0.7
	99	152.7	54.5	14.1	5.4	532.3	1.2
10 m Outfall	90	4.0	7.6	9.4	6.6	4.2	1.4
	95	7.5	9.1	9.8	10.2	7.9	2.3
	99	9.3	11.7	13.1	11.4	12.1	5.4
15 m outfall	90	0.7	0.6	0.2	0.1	0.8	0.6
	95	0.9	0.8	0.4	0.4	1.4	1.8
	99	1.3	1.1	0.5	0.6	2.0	6.4

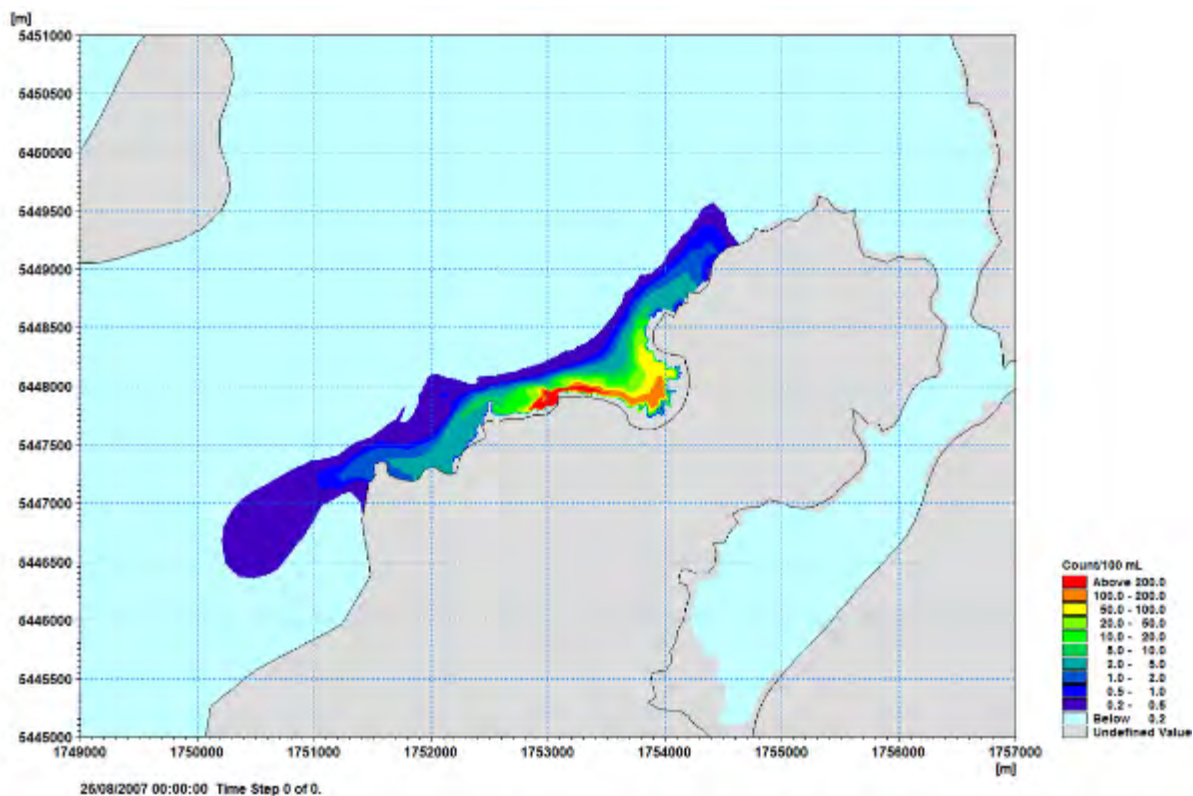


Figure 5-45. Predicted 95th percentile Enterococci concentration (Ent/100 mL), for the existing shoreline discharge for onshore winds and neap tide for the future PWWF flow rate of 1500 L/s.

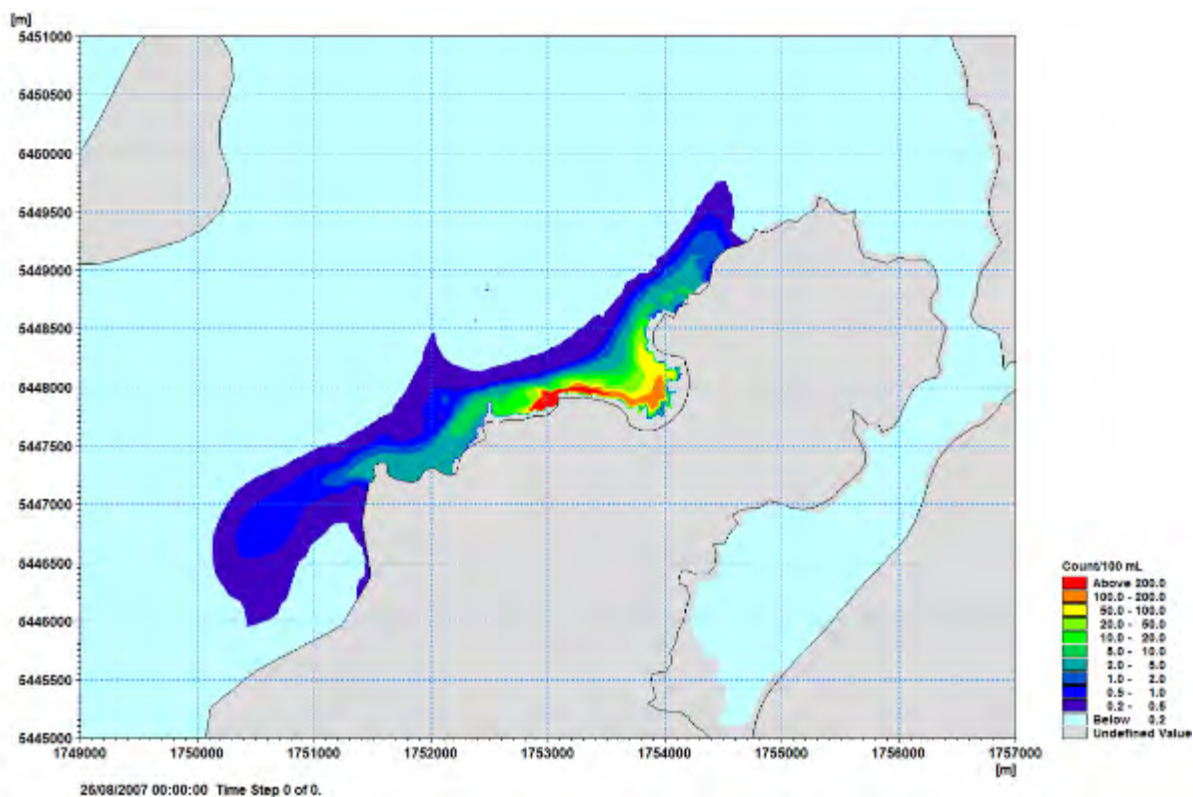


Figure 5-46. Predicted 95th percentile Virus concentration (Virus/100 mL), for the existing shoreline discharge for onshore winds and neap tide for the future PWWF flow rate of 1500 L/s.

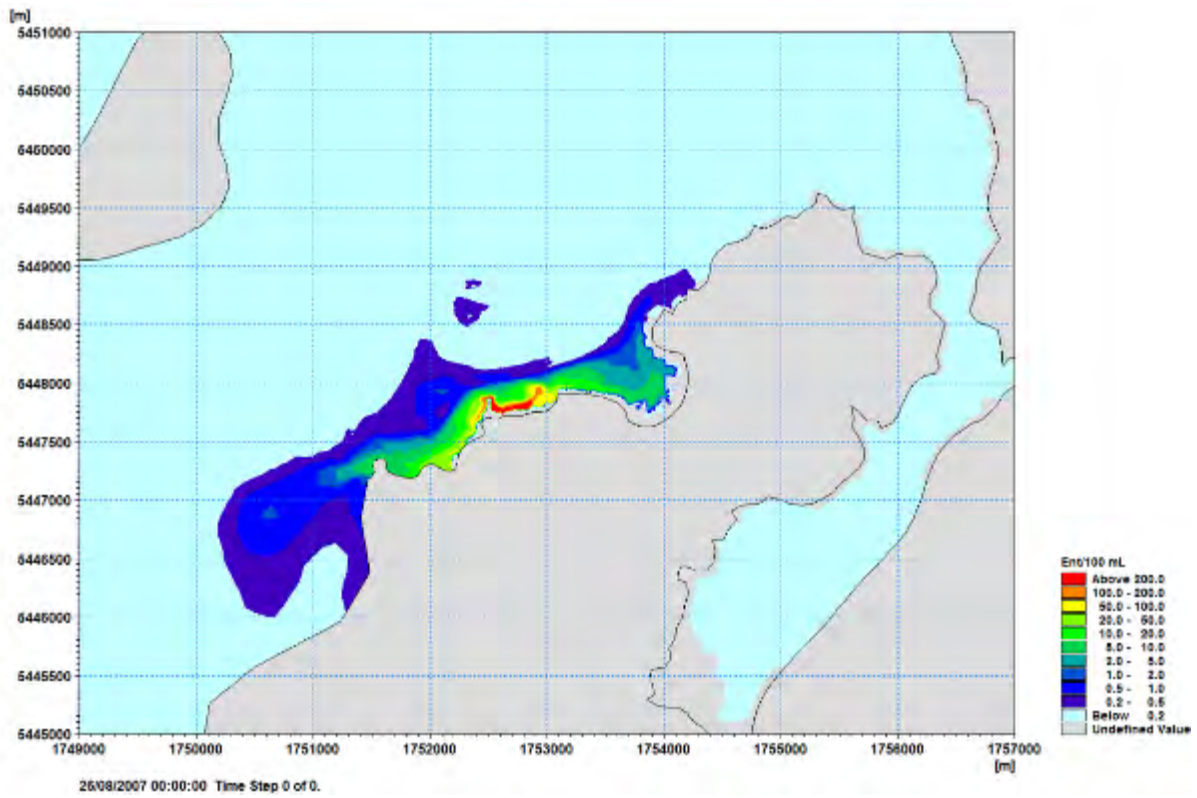


Figure 5-47. Predicted 95th percentile Enterococci concentration (Ent/100 mL), for the new shoreline discharge for onshore winds and neap tide for the future PWWF flow rate of 1500 L/s.

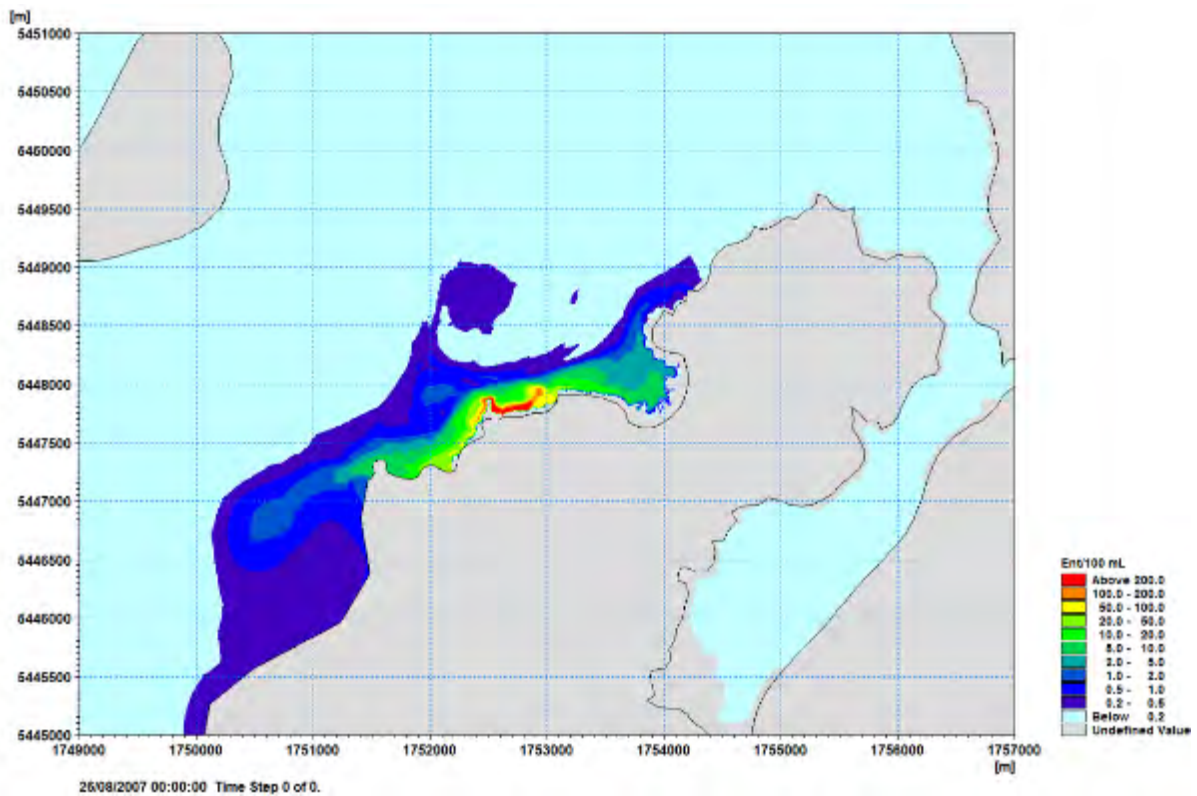


Figure 5-48. Predicted 95th percentile Virus concentration (Virus/100 mL), for the new shoreline discharge for onshore winds and neap tide for the future PWWF flow rate of 1500 L/s.

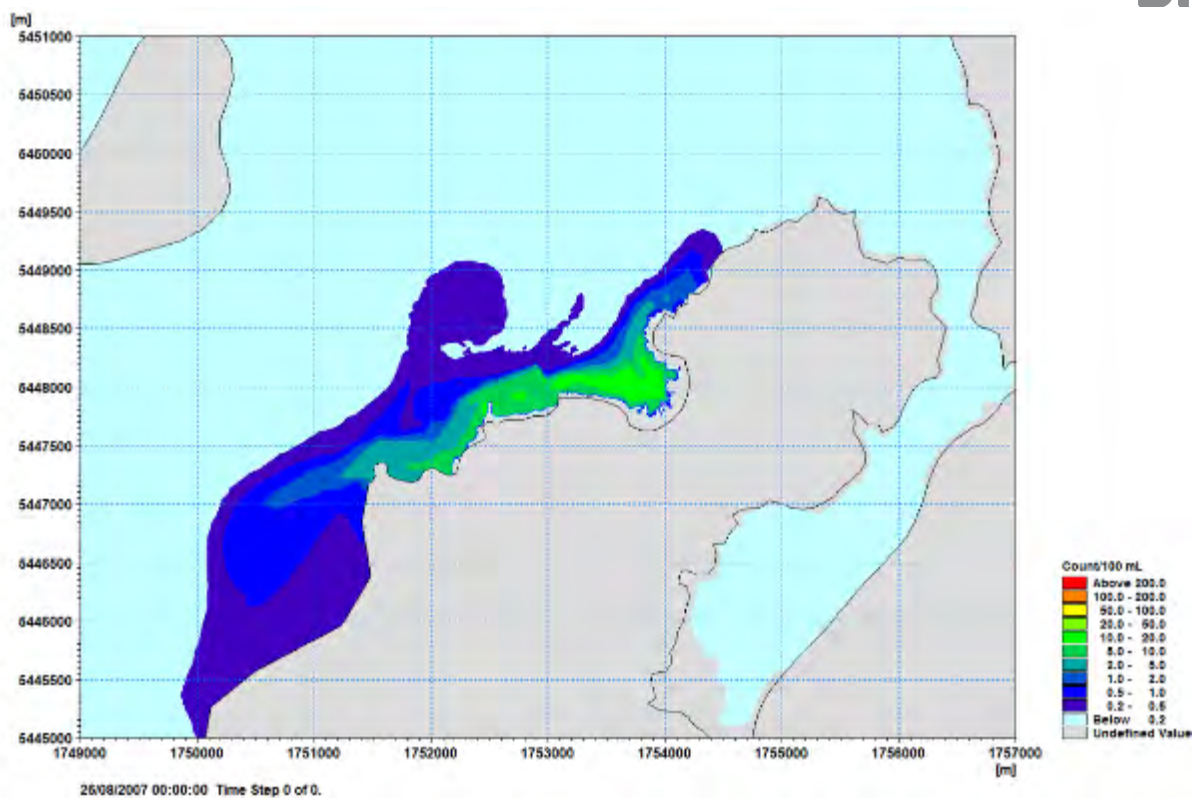


Figure 5-49. Predicted 95th percentile Enterococci concentration (Ent/100 mL), for the 10 m outfall option for onshore winds and neap tide for the future PWWF flow rate of 1500 L/s.

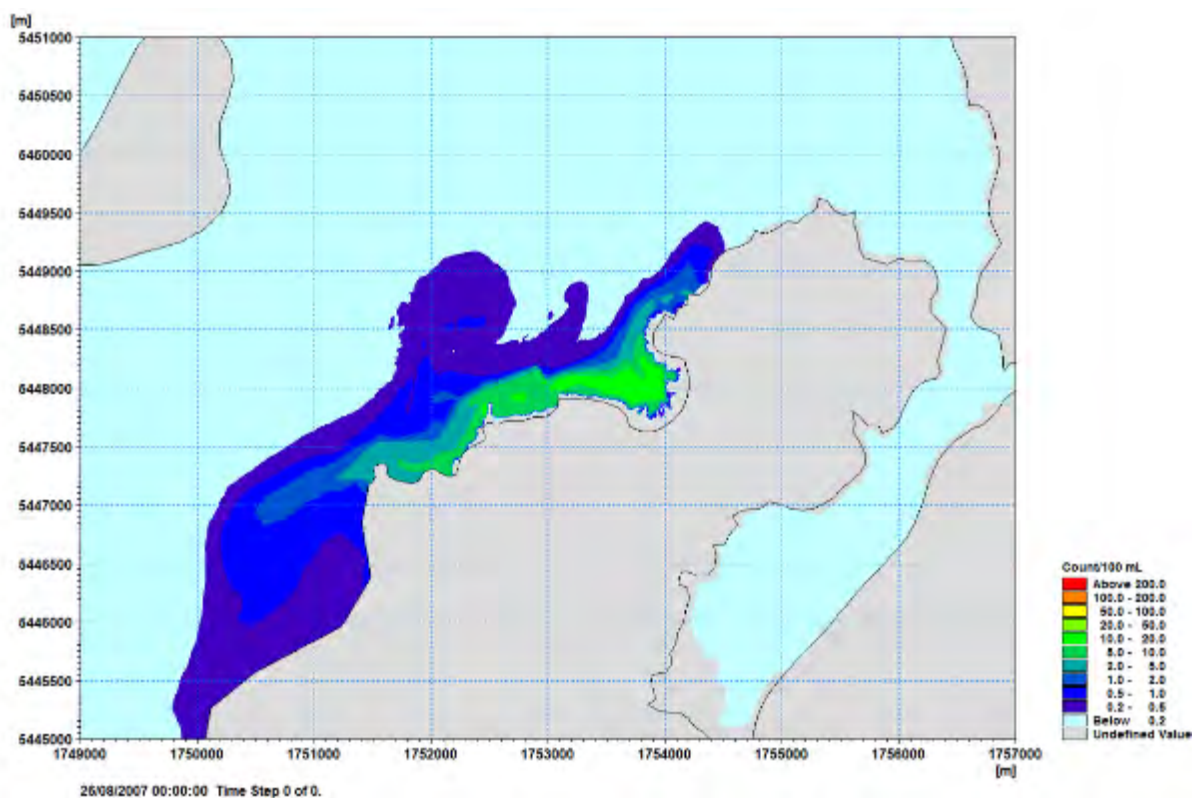


Figure 5-50. Predicted 95th percentile Virus concentration (Virus/100 mL), for the 10 m outfall option for onshore winds and neap tide for the future PWWF flow rate of 1500 L/s.

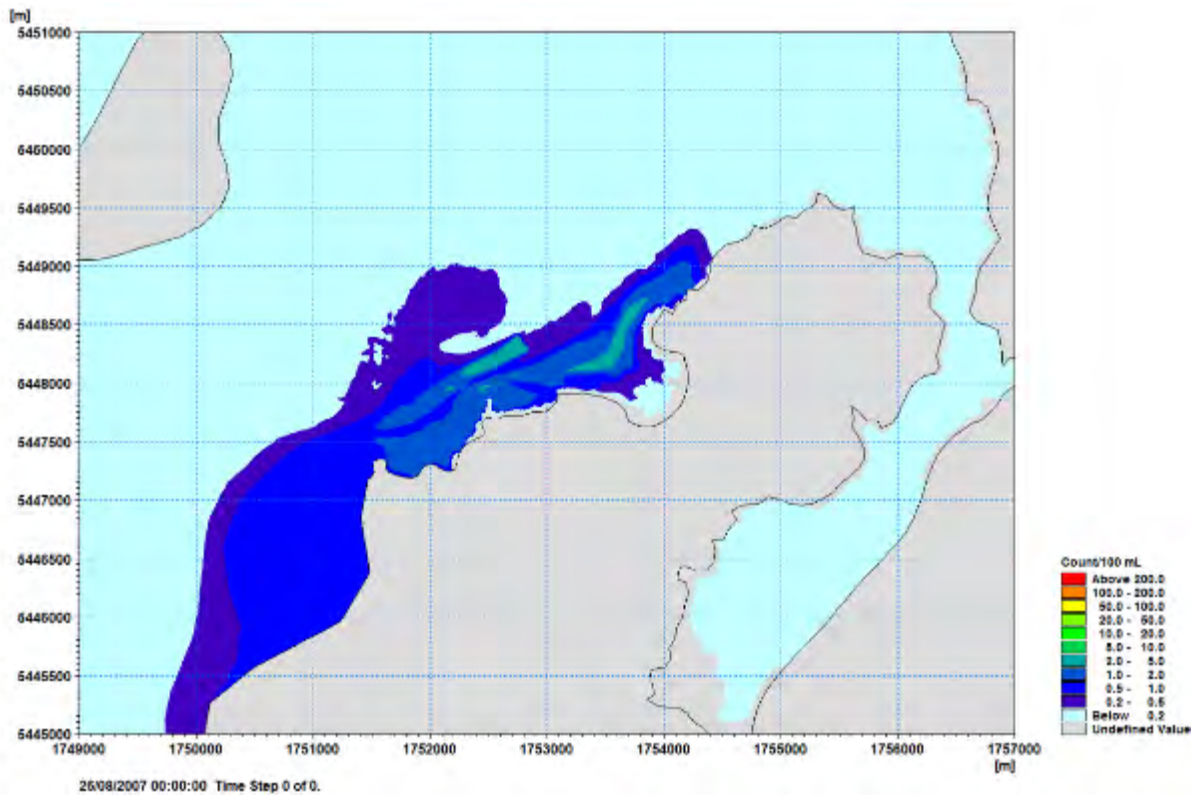


Figure 5-51. Predicted 95th percentile Enterococci concentration (Ent/100 mL), for the 15 m outfall option for onshore winds and neap tide for the future PWWF flow rate of 1500 L/s.

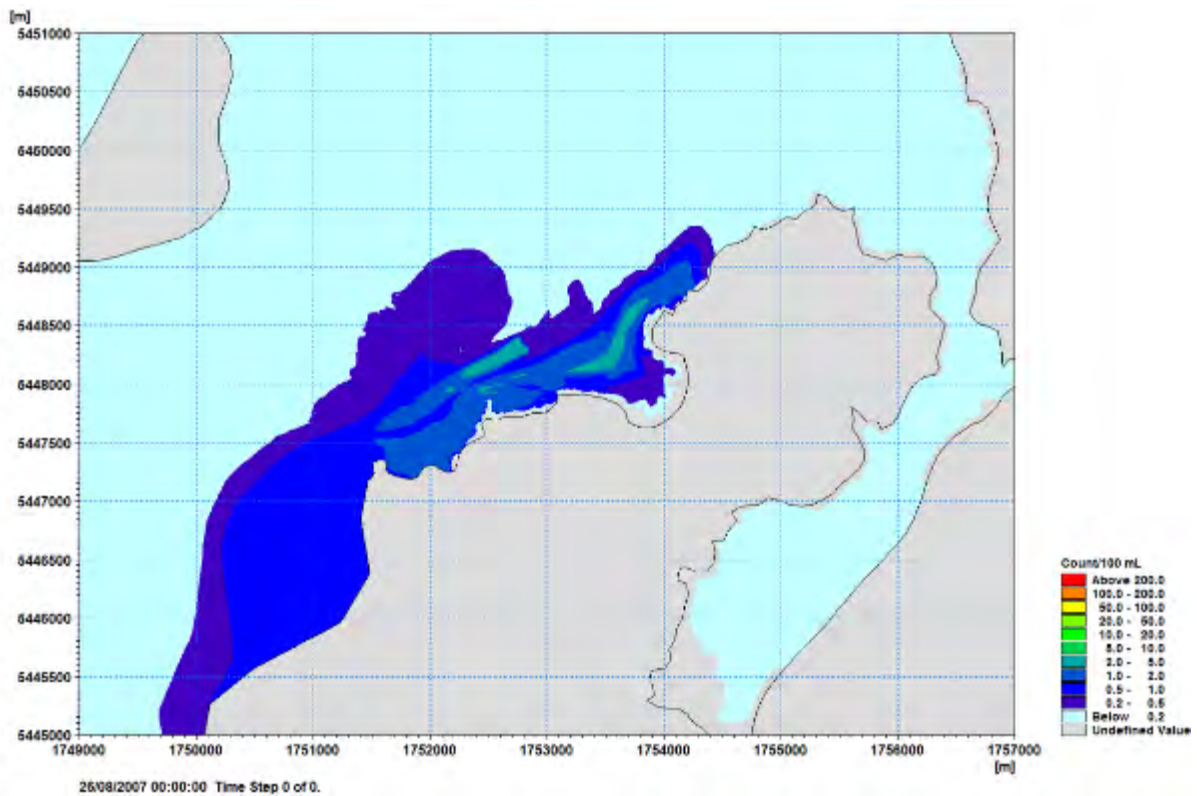


Figure 5-52. Predicted 95th percentile Virus concentration (Virus/100 mL), for the 15 m outfall option for onshore winds and neap tide for the future PWWF flow rate of 1500 L/s.

5.3 Future Overflow Scenarios

In this section of the report, overflow scenarios are considered as shown in Table 23. Four different receiving environment conditions are considered – onshore winds, typical winds for either neap or spring tides.

Unlike the ADF and PWWF scenarios, the overflow scenarios consider a time varying hydrograph (Figure 5-53). The peak flow is split 58% of total flow through the plant and remaining 42% via the overflow.

The peak of the hydrograph (2597 L/s combined flow) coincides with low water to provide a worst-case scenario of minimum initial dilution at the peak flow. The combined discharge exceeds the future ADF flow rate of 390 L/s for a total of 36 hours.

Table 23. Overflow discharge scenarios.

Overflow Scenarios				
	Scenario 9	Scenario 10	Scenario 11	Scenario 12
WWTP Flow and Overflow	Time varying with 36 hours above future ADF rate			
Discharge location	Existing Shoreline Rukutane Point	Existing Shoreline Rukutane Point	New Ocean Outfall Round Point	New Ocean Outfall Round Point
Outfall location	Existing Shoreline Rukutane Point	New Shoreline Round Point	New 10 m Ocean Outfall Round Point	New 15 m Ocean Outfall Round Point

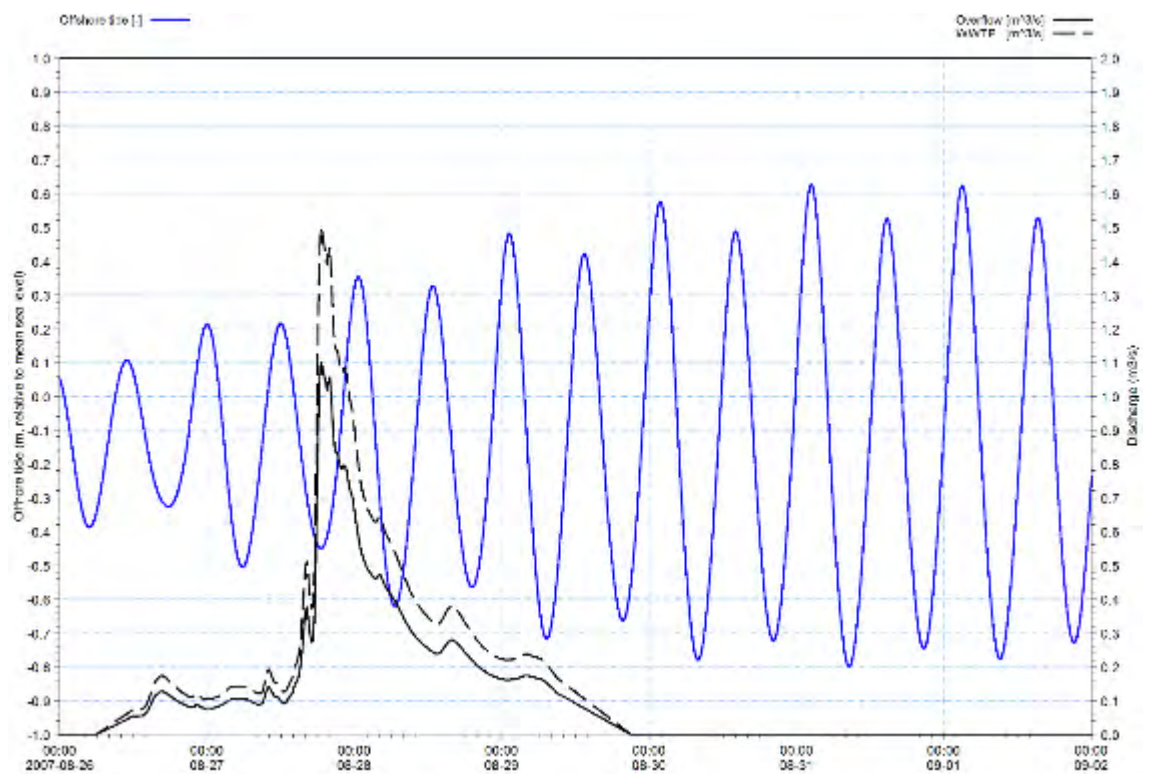
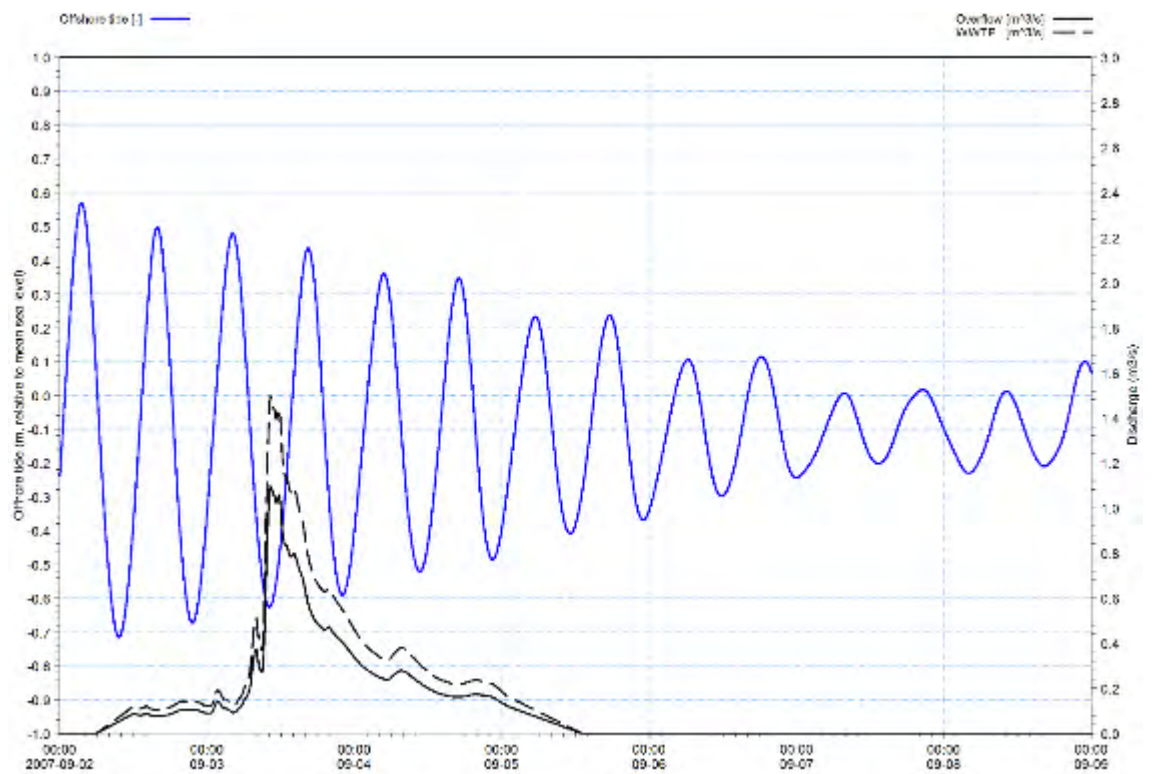


Figure 5-53. Time varying overflows for the spring tide (top panel) and neap tide (bottom panel). The plot shows the discharge via the WWTP and the discharge via the overflow. In both cases the peak of the hydrograph coincides with low tide to provide a worst-case scenario.

5.3.1 Typical Winds and Spring Tide – Overflow Scenarios

Table 24 and Table 25 provide percentile values for Enterococci and Virus for the overflow scenarios for typical winds and spring tides.

Appendices D-I contain figures of the predicted time-series of data the monitoring sites.

For **Scenario 9**, the 99th percentile concentration at the monitoring 200 m SW monitoring site range from 610-680 count/100 mL and reduces to around 340-380 count/100 mL at the site 200 m E monitoring site. At the Titahi Beach sites the 99th percentile concentrations range from 111-225 count/100 mL while at the Ti Korohiwa Rocks and Mount Couper sites 99th percentile concentrations of less than 25 count/100 mL occur.

For **Scenario 10** the 90th percentile concentration at the monitoring site 200 m SW monitoring site increases by between 7 and 13% (highlighted in Table 24 and Table 25) while the other percentile concentrations decrease by between 3 and 38%. At the 200 m E monitoring site percentile concentrations decrease by between 30 and 39%. At the Titahi Beach sites the percentile concentrations are reduced by between 32 and 41%. The percentile concentrations at the Ti Korohiwa Rocks (adjacent to the Round Point overflow point) increase by a factor of between 23 and 33 resulting in 99th percentile value of between 610-660 count/100 mL. At the Mount Couper monitoring site, the percentile concentrations are reduced by between 26 and 38%.

For **Scenario 11** the percentile concentrations are reduced by between 86 and 99% at 200 m SW, 200 m E and Titahi Beach sites. At the Ti Korohiwa Rocks site percentile concentrations are reduced by between 66 and 73% while at the Mount Couper site reductions in the percentile concentrations of between 45 and 60% are achieved. As noted for the Future PWWF scenarios, there are times when the concentration at the Mount Couper site is higher under this scenario compared to the other overflow scenarios (Figure 5-54).

For **Scenario 12** the percentile concentrations are reduced by at least 96% at the 200 m SW, 200 m E, Titahi Beach sites and at the Te Korohiwa Rocks site. At the Mount Couper site percentile concentrations are reduced by between 85 and 90%.

Figures 5-55 to 5-62 show the spatial plots of the predicted 95th percentile estimates for each of the discharge options. These plots indicate the area impacted by each of the discharges and in particular illustrate the significant reduction in concentrations achieved by the two outfall options being considered.

Table 24. Percentile estimates of Enterococci concentration (Ent/100 mL) at the monitoring sites for the overflow scenarios for typical winds and spring tide. Highlighted cells indicate percentile values that are higher than for the existing shoreline discharge.

Discharge Point	Percentile	200 m SW	200 m E	Titahi Beach South	Titahi Beach	Ti Korohiwa	Mount Couper
Scenario 9	90	171.8	201.1	82.2	31.6	11.8	2.9
	95	262.1	255.2	118.3	45.0	14.1	4.6
	99	608.4	344.2	187.7	111.9	18.5	10.9
Scenario 10	90	183.7	122.7	52.5	20.3	322.8	2.1
	95	239.3	161.2	75.6	29.9	443.1	3.2
	99	379.0	226.5	114.1	66.3	610.5	6.9
Scenario 11	90	3.6	4.1	3.8	4.3	3.8	1.6
	95	3.9	5.3	6.5	5.1	4.7	2.4
	99	4.6	7.3	7.7	6.0	5.5	6.0
Scenario 12	90	0.3	0.5	0.2	0.1	0.4	0.4
	95	0.3	0.5	0.4	0.2	0.5	0.7
	99	0.4	0.7	0.5	0.2	0.7	1.5

Table 25. Percentile estimates of Virus concentration (Virus/100 mL) at the monitoring sites for the overflow scenarios for typical winds and spring tide. Highlighted cells indicate percentile values that are higher than for the existing shoreline discharge.

Discharge Point	Percentile	200 m SW	200 m E	Titahi Beach South	Titahi Beach	Ti Korohiwa	Mount Couper
Scenario 9	90	200.8	219.3	96.6	41.2	14.2	4.6
	95	311.0	262.1	133.6	56.8	16.8	6.7
	99	684.0	379.8	225.4	144.1	21.3	15.3
Scenario 10	90	227.3	137.6	64.9	28.2	331.6	3.4
	95	300.2	173.3	87.5	37.8	471.1	4.9
	99	428.3	266.4	140.3	86.6	663.5	9.6
Scenario 11	90	4.3	4.6	4.8	5.5	4.2	1.9
	95	4.8	5.9	7.1	6.2	5.2	2.7
	99	5.1	8.5	8.2	6.5	5.9	6.3
Scenario 12	90	0.4	0.6	0.3	0.2	0.5	0.5
	95	0.4	0.6	0.4	0.3	0.6	0.7
	99	0.4	0.7	0.5	0.3	0.7	1.5

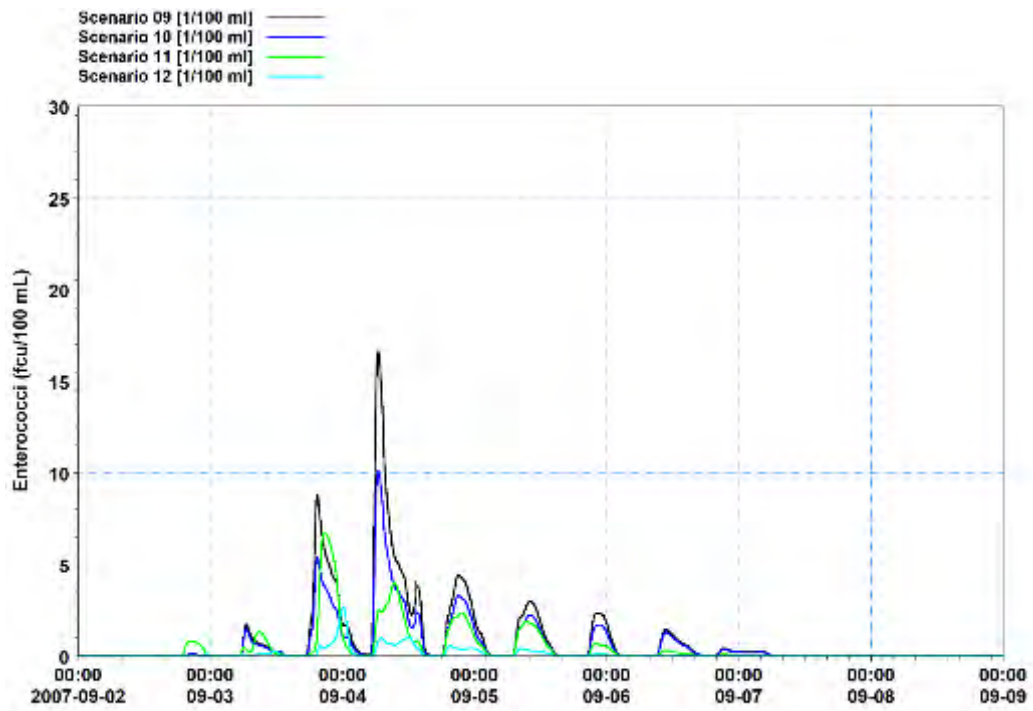


Figure 5-54. Predicted Enterococci (Ent/100 ml) at the Mount Couper monitoring site for the overflow scenarios for typical winds and a spring tide.

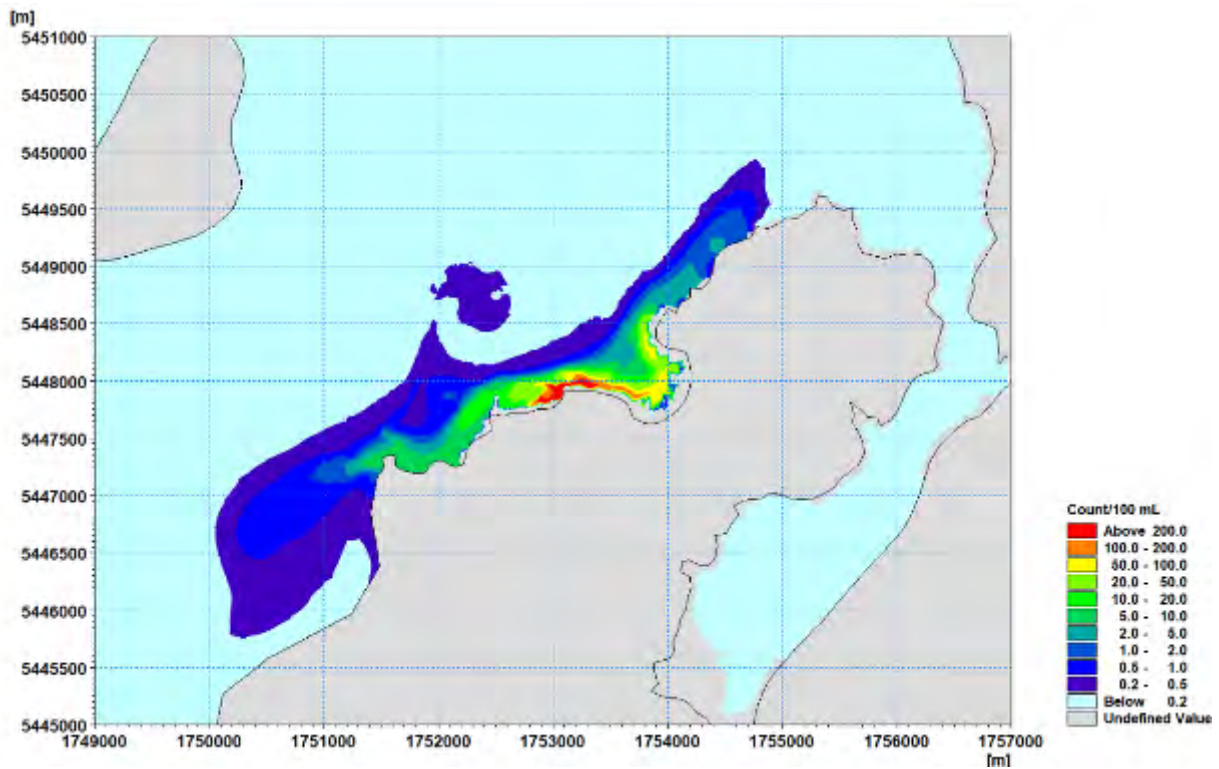


Figure 5-55. Predicted 95th percentile Enterococci concentration (Ent/100 mL), for the Scenario 9 future overflow for typical winds and spring tide.

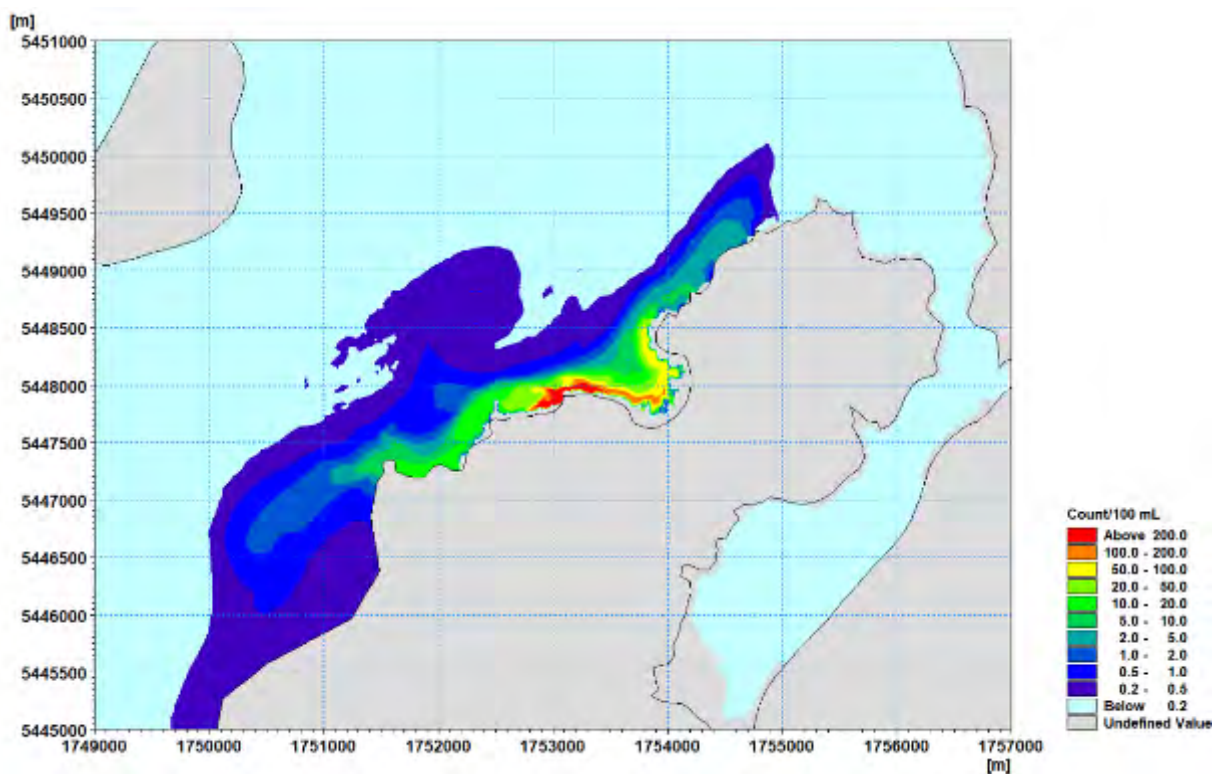


Figure 5-56. Predicted 95th percentile Virus concentration (Virus/100 mL), for the Scenario 9 future overflow for typical winds and spring tide.

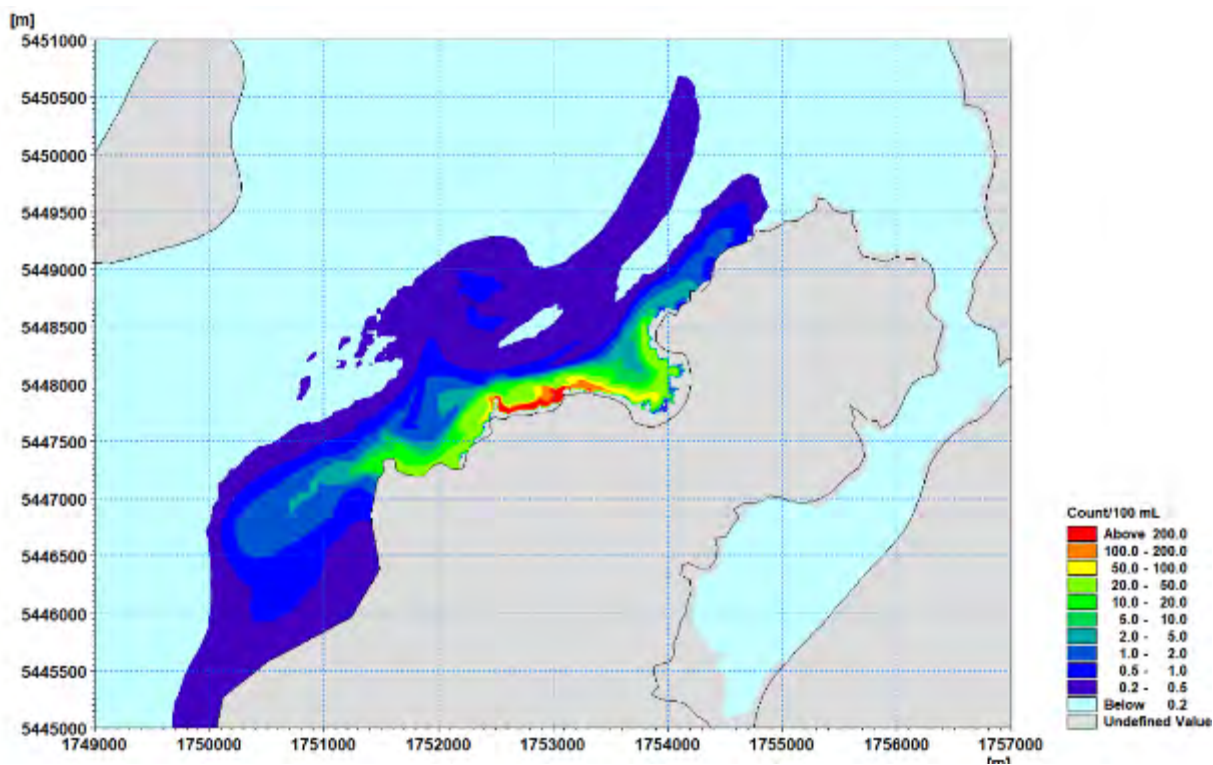


Figure 5-57. Predicted 95th percentile Enterococci concentration (Ent/100 mL), for Scenario 10 future overflow for typical winds and spring tide.

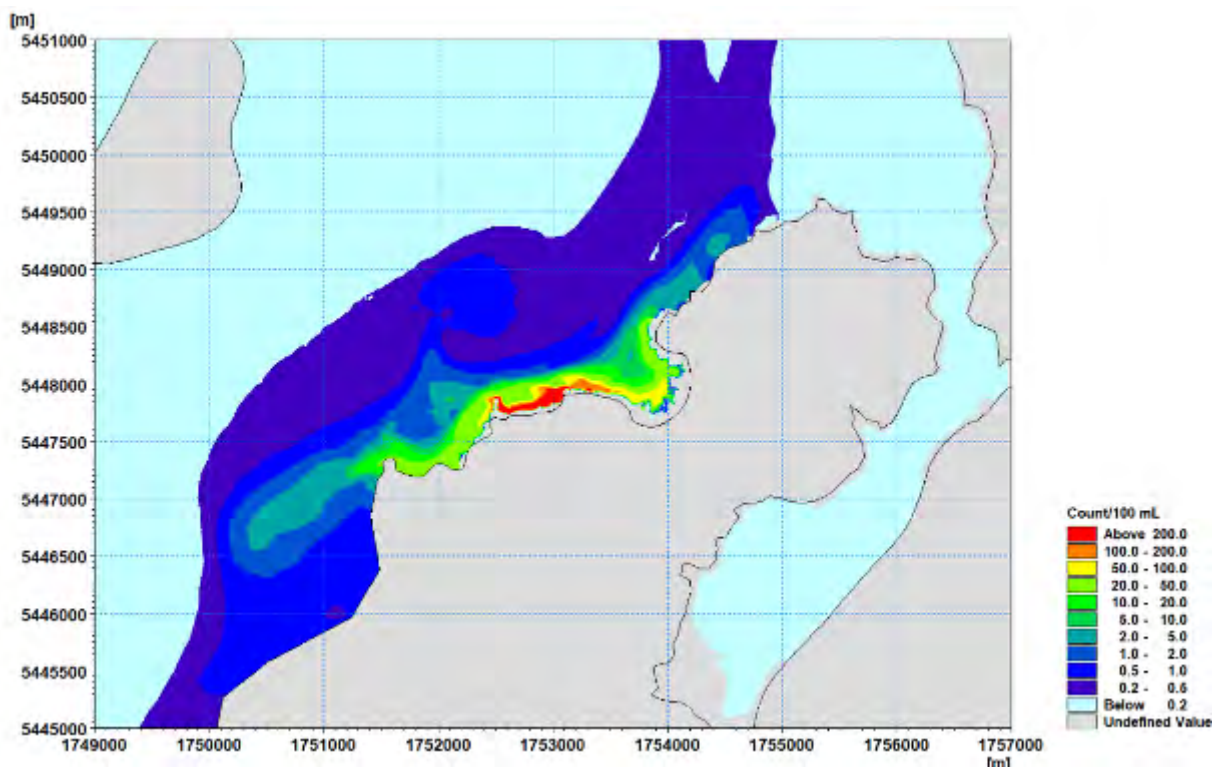


Figure 5-58. Predicted 95th percentile Virus concentration (Virus/100 mL), for Scenario 10 future overflow for typical winds and spring tide.

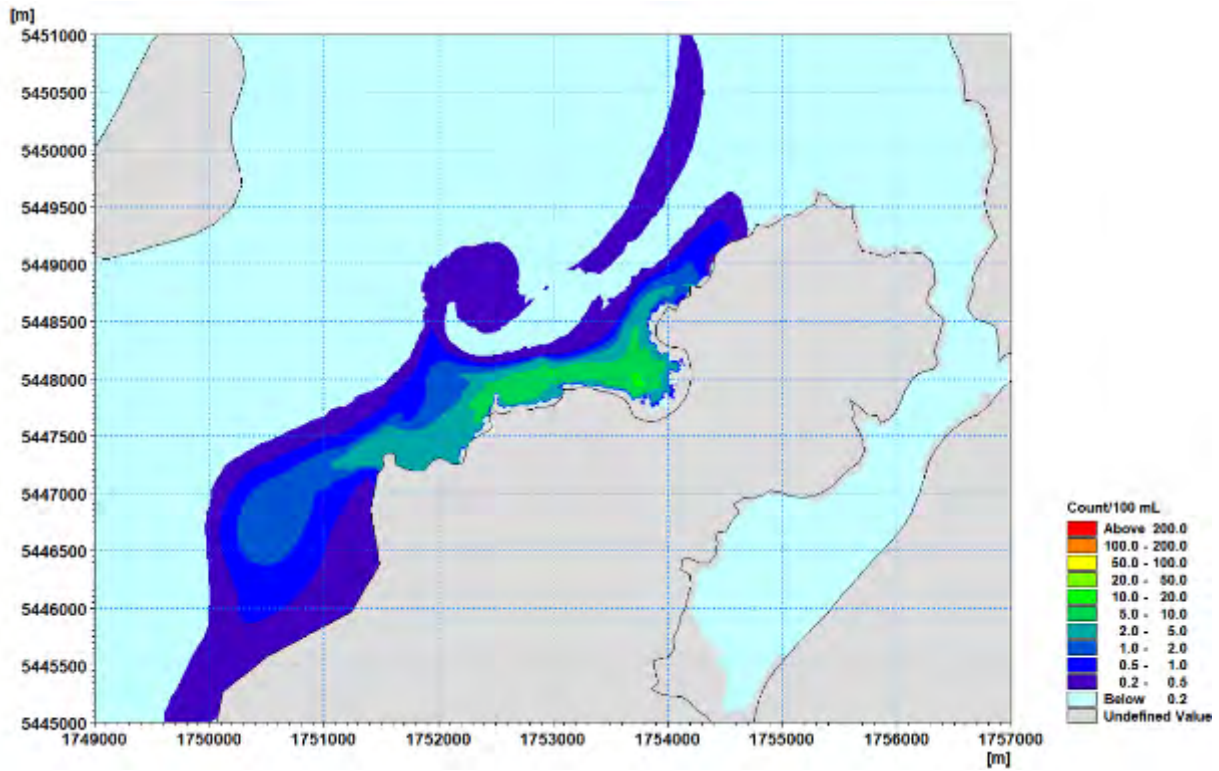


Figure 5-59. Predicted 95th percentile Enterococci concentration (Ent/100 mL), for Scenario 11 future overflow for typical winds and spring tide.

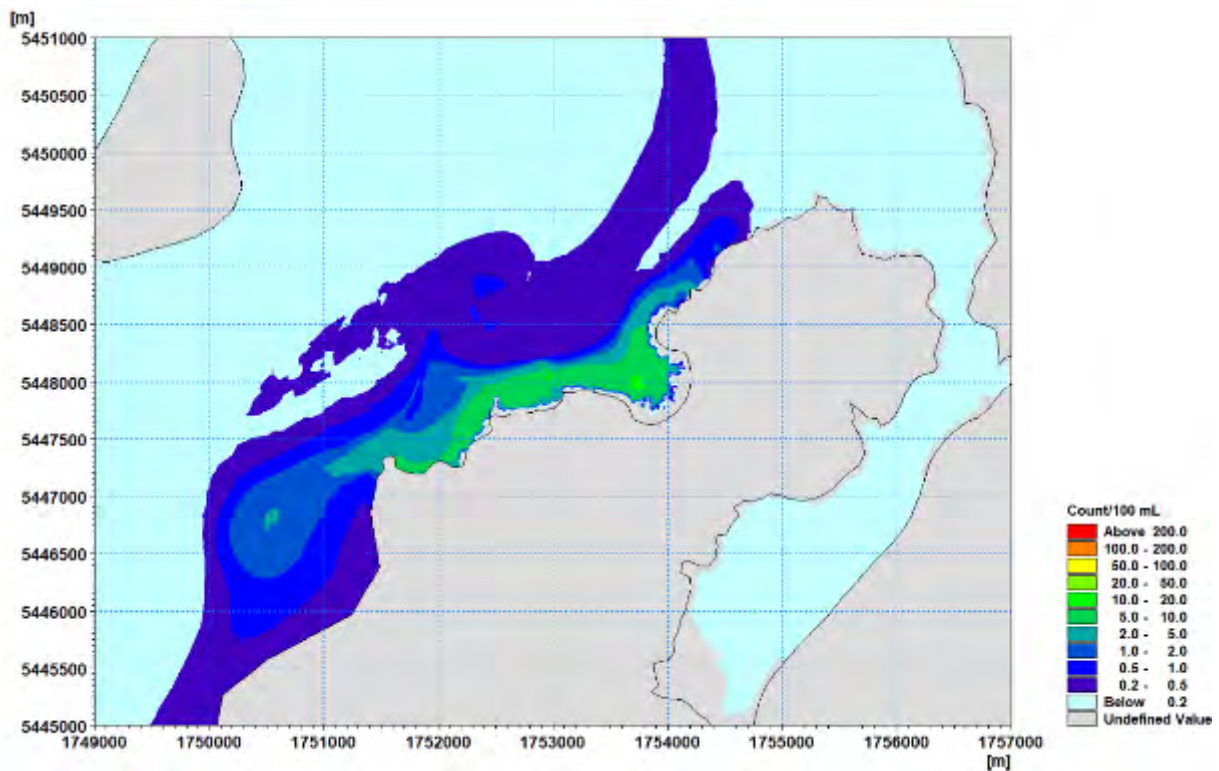


Figure 5-60. Predicted 95th percentile Virus concentration (Virus/100 mL), for Scenario 11 future overflow for typical winds and spring tide.

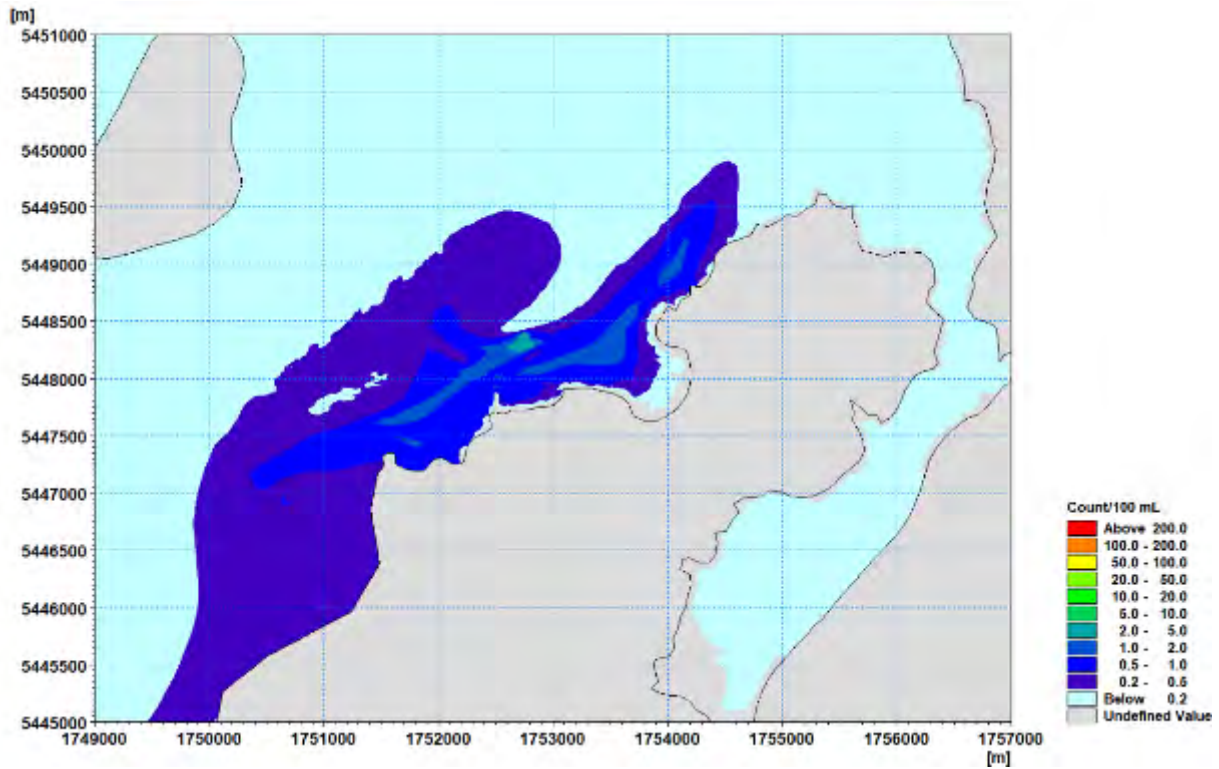


Figure 5-61. Predicted 95th percentile Enterococci concentration (Ent/100 mL), for Scenario 12 future overflow for typical winds and spring tide.

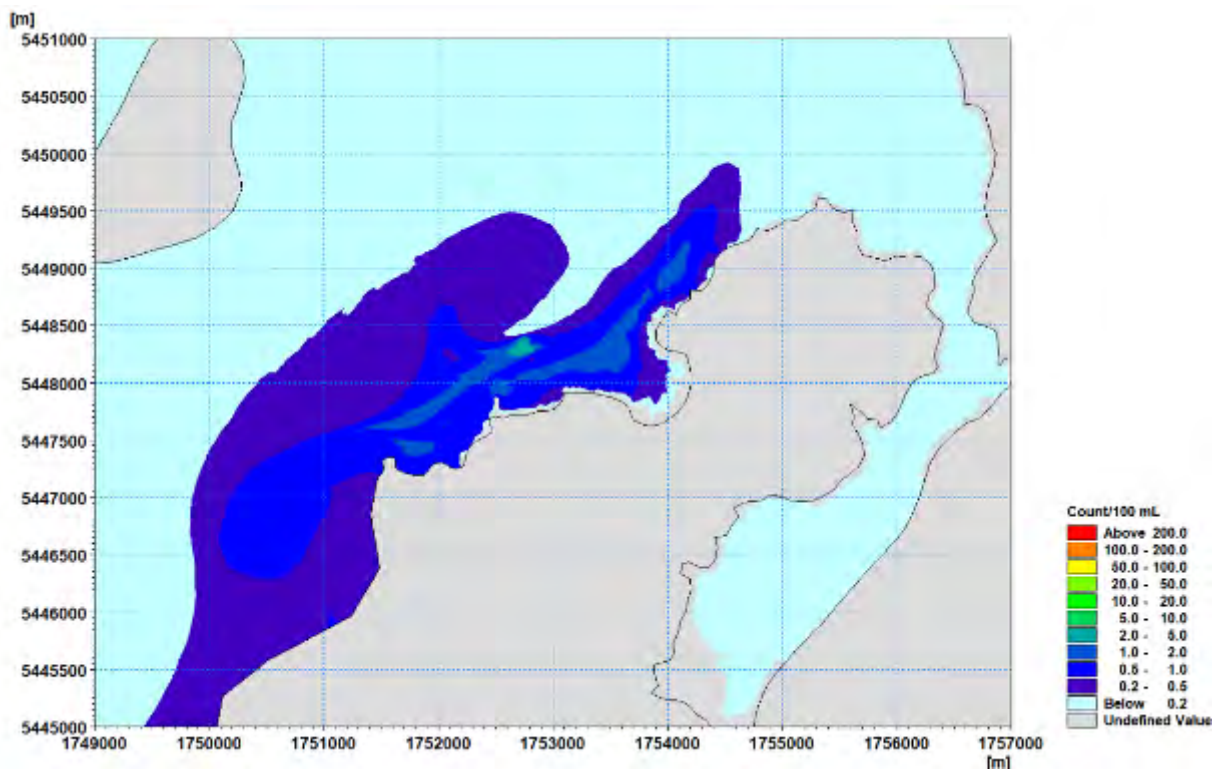


Figure 5-62. Predicted 95th percentile Virus concentration (Virus/100 mL), for Scenario 12 future overflow for typical winds and spring tide.

5.3.2 Onshore Winds and Spring Tide - Overflow Scenarios

Table 26 and Table 27 provide percentile values for Enterococci and Virus for the overflow scenarios for typical winds and spring tides.

Appendices D-I contain figures of the predicted time-series of data the monitoring sites.

For **Scenario 9**, the 99th percentile concentration at the monitoring site 200 m SW range from 640-730 count/100 mL and reduces to between 275-300 count/100 mL at the site 200 m east of the existing outfall. At the Titahi Beach sites the 99th percentile concentrations range from 74-230 count/100 mL while at the Ti Korohiwa Rocks and Mount Couper sites 99th percentile concentrations of less than 25 count/100 mL occur.

For **Scenario 10** the percentile concentrations are reduced by between 26 and 39% are achieved at the 200 m SW and 200 m E monitoring sites and the Titahi Beach sites. Percentile concentrations at the Ti Korohiwa Rocks (adjacent to the Round Point overflow point) increased by a factor of between 27 and 50 resulting in 99th percentile concentrations of between 600 and 657 count/100 mL. At the Mount Couper site percentile concentrations are reduced by between 20 and 30%.

For **Scenario 11** the percentile concentrations are reduced by between 93 and 99.9% at the 200 m SW, 200 m E and the Titahi Beach sites. At the Ti Korohiwa Rocks site percentile concentrations are reduced by between 51 and 64% while at the Mount Couper site reductions in the percentile concentrations of between 63 to 78% are achieved although, as noted above, there are times when the concentration at the Mount Couper site is higher under this scenario compared to the other overflow scenarios (Figure 5-63).

For **Scenario 12** the percentile concentrations are reduced by at least 95% at all monitoring sites.

Figures 5-64 to 5-71 to show the spatial plots of the predicted 95th percentile estimates for each of the discharge options. These plots indicate the area impacted by each of the discharges and in particular illustrate the significant reduction in concentrations achieved by the two outfall options being considered.

Table 26. Percentile estimates of Enterococci concentration (Ent/100 mL) at the monitoring sites, future overflow scenarios for onshore winds and spring tide. Highlighted cells indicate percentile values that are higher than for the existing shoreline discharge.

Discharge Point	Percentile	200 m SW	200 m E	Titahi Beach South	Titahi Beach	Ti Korohiwa	Mount Couper
Scenario 9	90	220.2	146.2	106.5	47.5	7.6	5.3
	95	368.9	177.5	131.4	61.4	9.3	9.0
	99	644.7	274.6	199.5	73.7	11.9	16.9
Scenario 10	90	228.4	98.4	74.3	34.2	279.4	3.7
	95	279.5	118.7	88.3	41.6	426.3	7.2
	99	392.5	171.6	135.0	50.2	600.8	11.9
Scenario 11	90	2.9	4.3	3.6	3.3	3.7	1.4
	95	3.3	5.9	4.8	4.1	4.2	3.0
	99	4.6	8.2	6.3	5.6	5.3	6.3
Scenario 12	90	0.2	0.3	0.2	0.2	0.3	0.1
	95	0.2	0.4	0.3	0.2	0.3	0.2
	99	0.2	0.6	0.5	0.3	0.6	0.4

Table 27. Percentile estimates of Virus concentration (Virus/100 mL) at the monitoring sites, future overflow scenarios for onshore winds and spring tide. Highlighted cells indicate percentile values that are higher than for the existing shoreline discharge.

Discharge Point	Percentile	200 m SW	200 m E	Titahi Beach South	Titahi Beach	Ti Korohiwa	Mount Couper
Scenario 9	90	262.5	150.4	116.8	60.7	10.7	7.7
	95	446.5	197.2	145.8	71.2	12.4	11.7
	99	726.2	306.3	229.4	84.7	15.0	21.0
Scenario 10	90	262.6	108.8	85.7	45.0	290.7	5.9
	95	341.3	134.7	103.2	51.2	436.9	9.4
	99	439.9	199.1	155.2	61.0	657.3	15.3
Scenario 11	90	3.5	4.7	4.3	3.8	3.9	1.7
	95	3.8	6.1	5.0	4.4	4.5	3.3
	99	4.8	8.8	6.9	6.0	5.5	6.3
Scenario 12	90	0.2	0.3	0.2	0.2	0.3	0.2
	95	0.3	0.4	0.3	0.2	0.3	0.3
	99	0.3	0.6	0.5	0.3	0.6	0.4

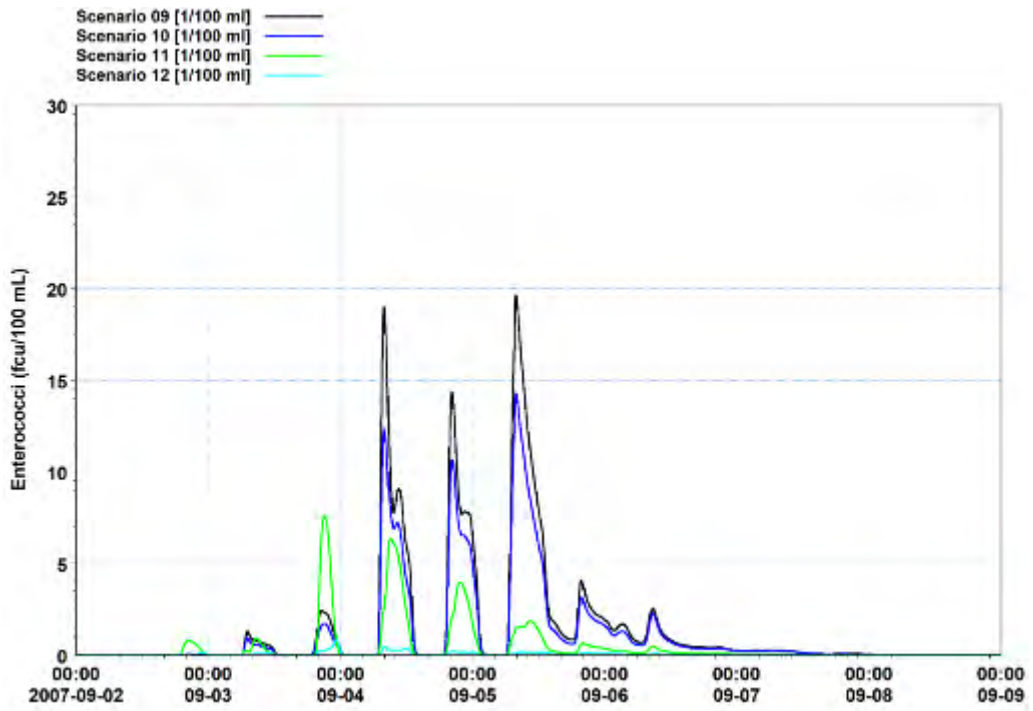


Figure 5-63. Predicted Enterococci (Ent/100 ml) at the Mount Couper monitoring site for the overflow scenarios for onshore winds and a spring tide.

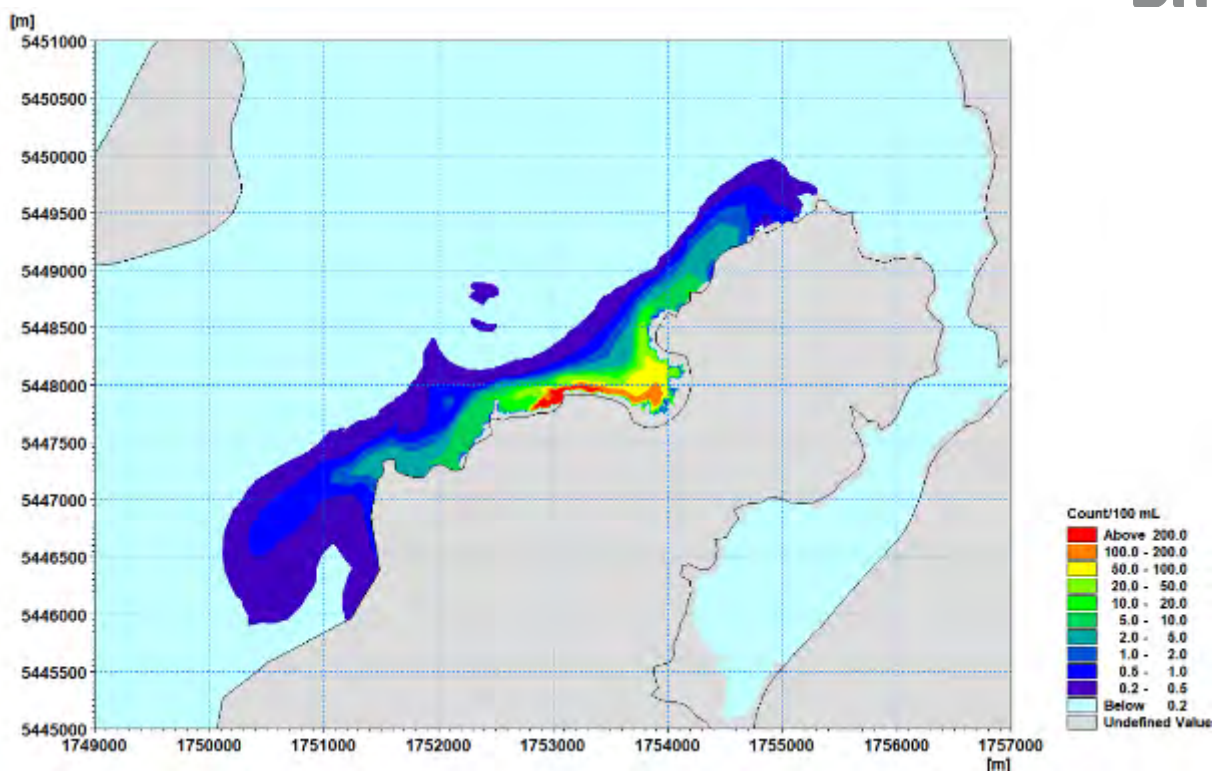


Figure 5-64. Predicted 95th percentile Enterococci concentration (Ent/100 mL), for the Scenario 9 future overflow for onshore winds and spring tide.

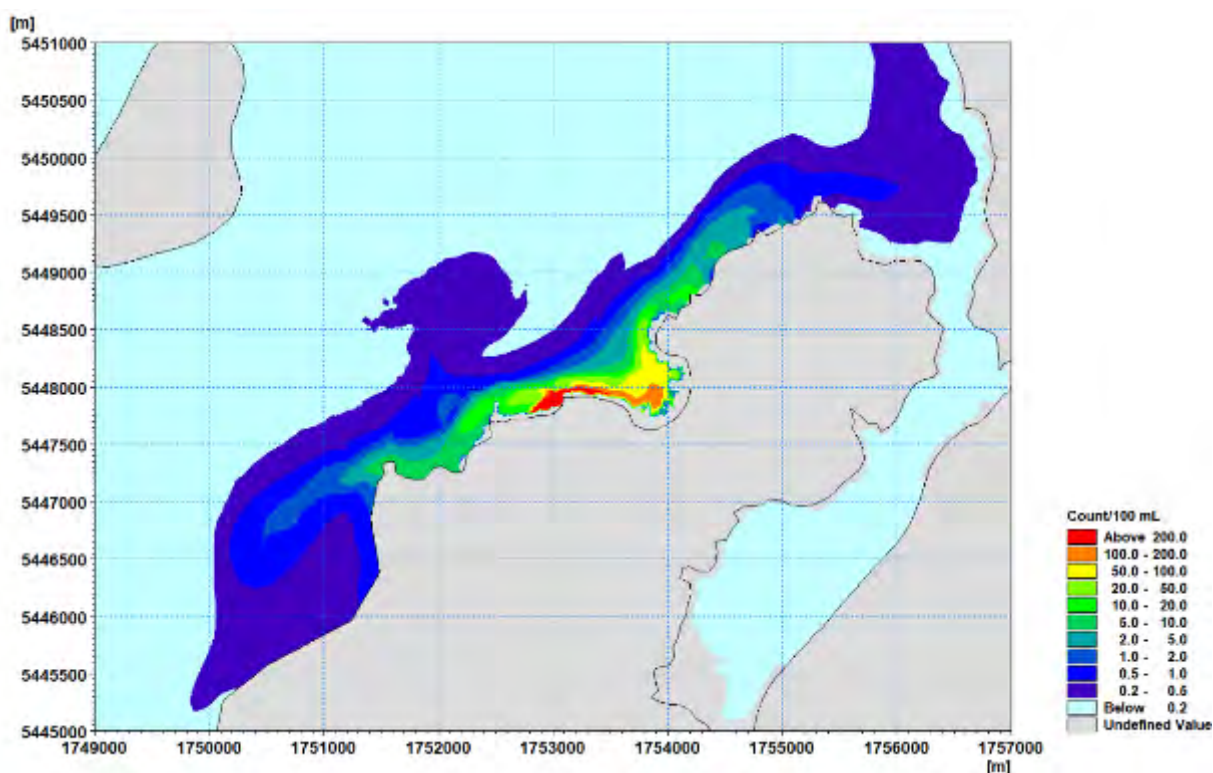


Figure 5-65. Predicted 95th percentile Virus concentration (Virus/100 mL), for the Scenario 9 future overflow for onshore winds and spring tide.

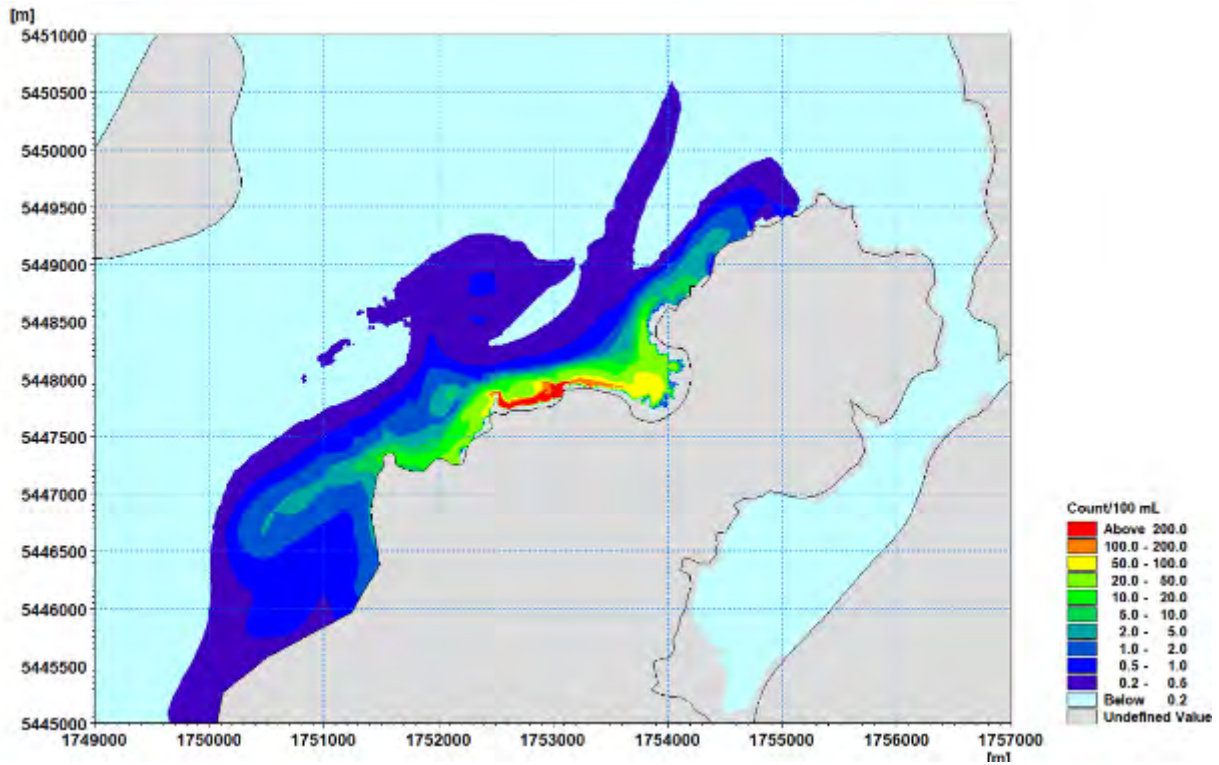


Figure 5-66. Predicted 95th percentile Enterococci concentration (Ent/100 mL), for the Scenario 10 future overflow for onshore winds and spring tide.

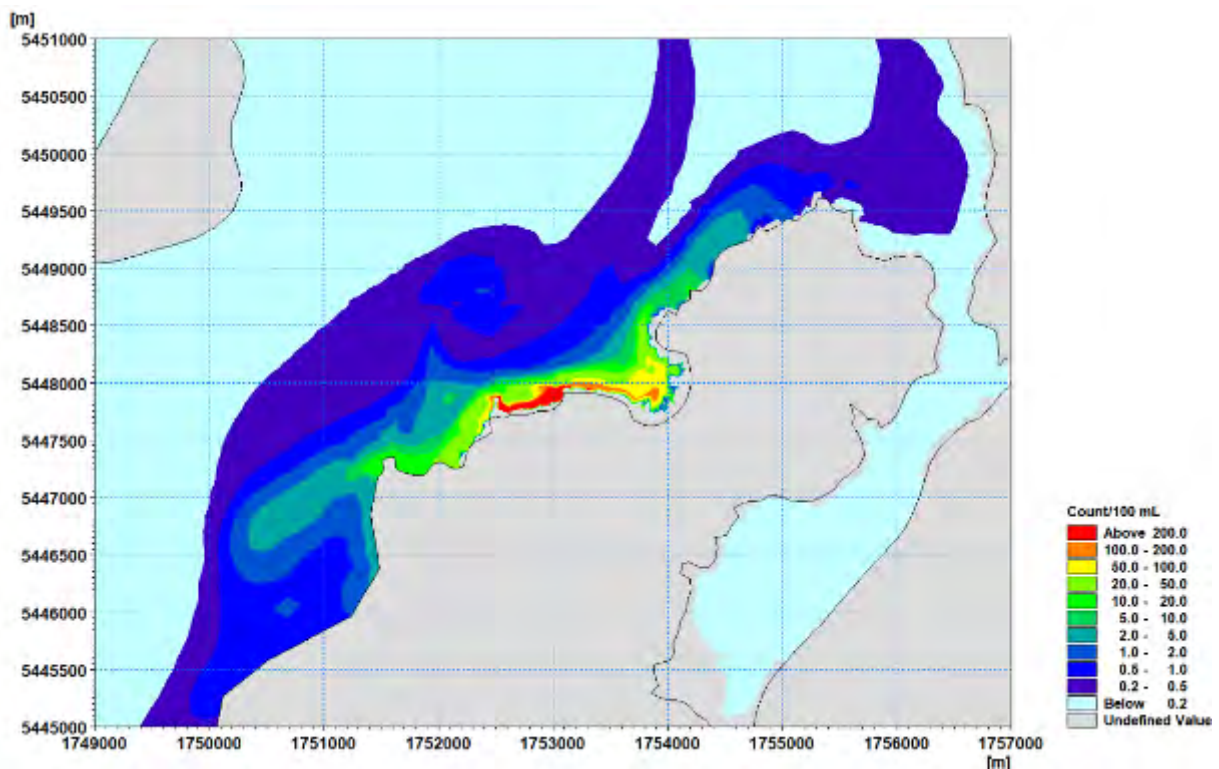


Figure 5-67. Predicted 95th percentile Virus concentration (Virus/100 mL), for the Scenario 10 future overflow for onshore winds and spring tide.

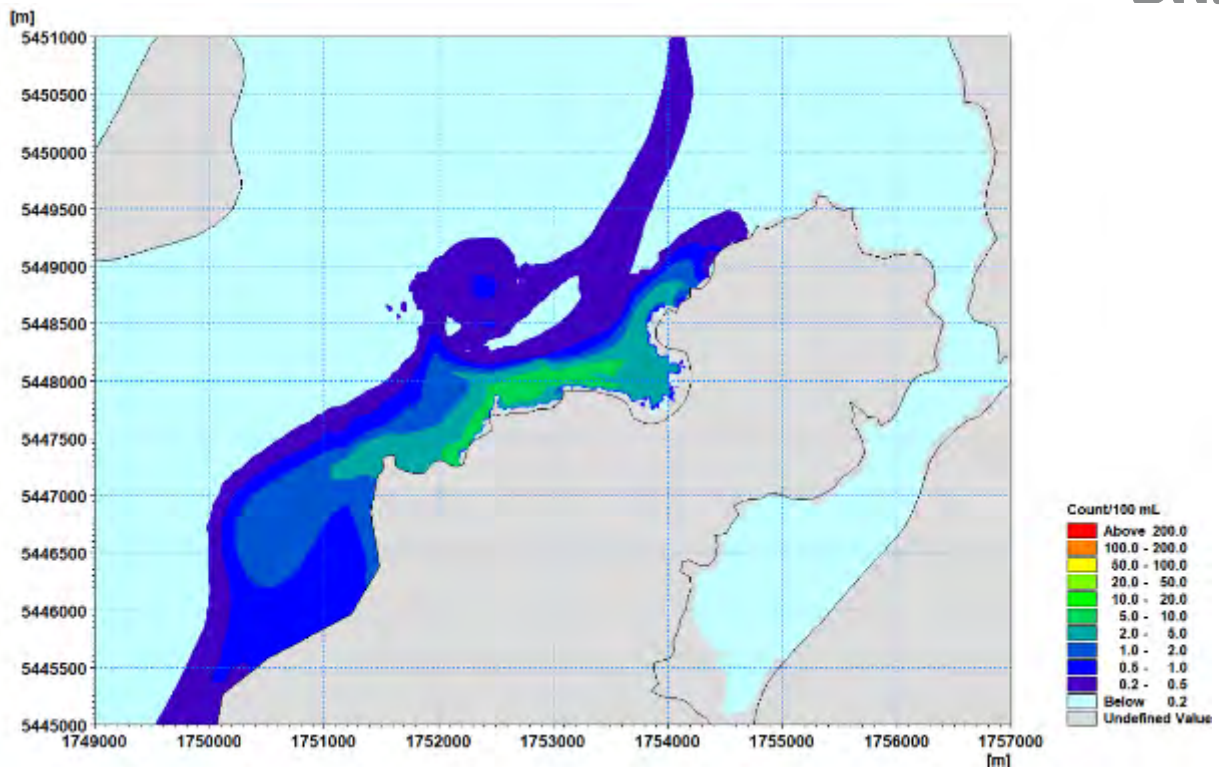


Figure 5-68. Predicted 95th percentile Enterococci concentration (Ent/100 mL), for Scenario 11 future overflow for onshore winds and spring tide.

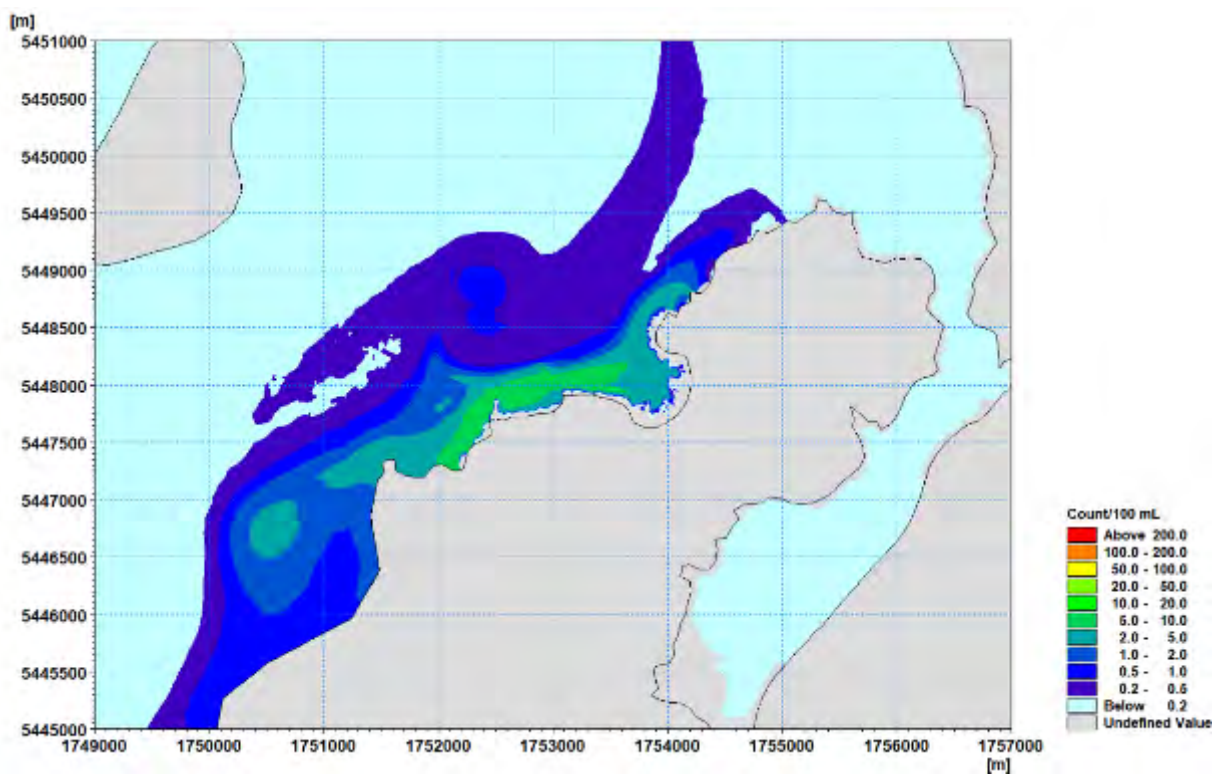


Figure 5-69. Predicted 95th percentile Virus concentration (Virus/100 mL), for Scenario 11 future overflow for onshore winds and spring tide.

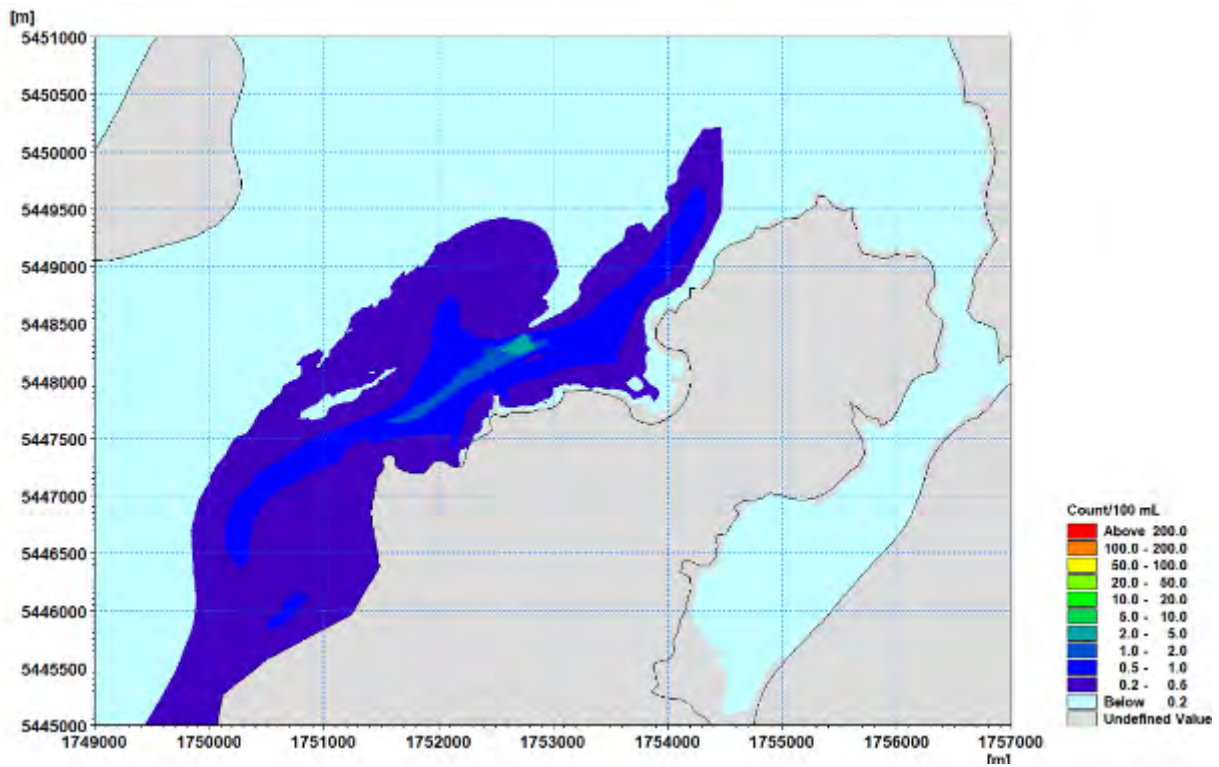


Figure 5-70. Predicted 95th percentile Enterococci concentration (Ent/100 mL), for Scenario 12 future overflow for onshore winds and spring tide.

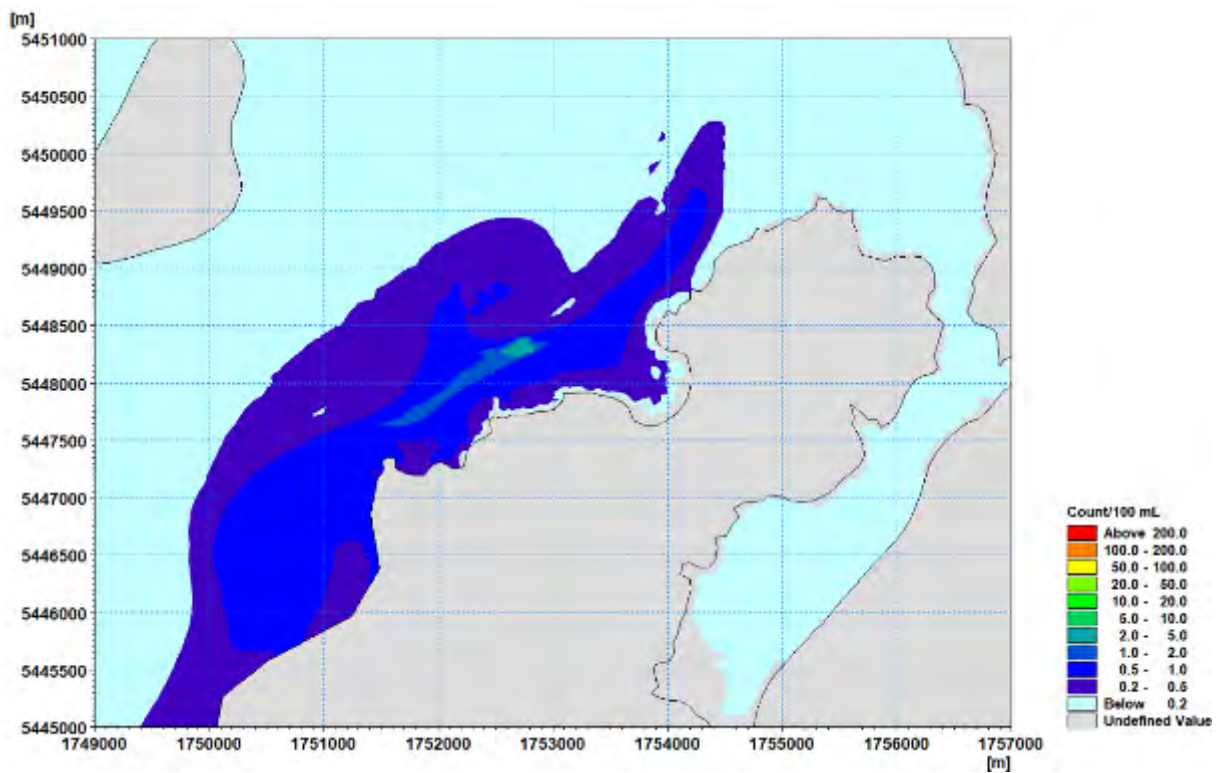


Figure 5-71. Predicted 95th percentile Virus concentration (Virus/100 mL), for Scenario 12 future overflow for onshore winds and spring tide.

5.3.3 Typical Winds and Neap Tide - Overflow Scenarios

Table 28 and Table 29 provide percentile values for Enterococci and Virus for the overflow scenarios for typical winds and spring tides.

Appendices D-I contain figures of the predicted time-series of data the monitoring sites.

For **Scenario 9**, the 99th percentile concentration at the monitoring site 200 m south-west range from 670 count/100 mL and reduces to around 430 count/100 mL at the site 200 m east of the existing outfall. At the Titahi Beach sites the 99th percentile concentrations range from 127-218 count/100 mL while at the Ti Korohiwa Rocks and Mount Couper sites 99th percentile concentrations of less than 25 count/100 mL occur.

For **Scenario 10** the percentile concentrations are reduced by between 9 and 35% at the monitoring site 200 m SW of the existing discharge. While at the 200 m E site and the Titahi Beach sites the percentile concentrations are reduced by between 33 and 41%. Percentile concentrations at the Ti Korohiwa Rocks (adjacent to the Round Point overflow point) increase by a factor of between 27 and 37 resulting in 99th percentile values of 670 count/100 mL. At the Mount Couper site percentile concentrations are reduced by between 13 and 34%.

For **Scenario 11** the percentile concentrations are reduced by at least 89% at the 200 m SW, 200 m E the Titahi Beach sites. At the Ti Korohiwa Rocks site percentile concentrations are reduced by between 69 and 75% while at the Mount Couper site reductions in the percentile concentrations of between 46 and 61% are achieved. As noted for the Future PWWF scenarios, there are times when the concentration at the Mount Couper site is higher under this scenario compared to the other overflow scenarios (Figure 5-72).

For **Scenario 12** the percentile concentrations are reduced by at least 97% at the sites adjacent to the existing discharge, the Titahi Beach sites and the Ti Korohiwa Rocks site. At the Mount Couper sites reductions in the percentile concentrations of between 77 and 92% are achieved.

Figures 5-73 to 5-80 to show the spatial plots of the predicted 95th percentile estimates for each of the discharge options. These plots indicate the area impacted by each of the discharges and in particular illustrate the significant reduction in concentrations achieved by the two outfall options being considered.

Table 28. Percentile estimates of Enterococci concentration (Ent/100 mL) at the monitoring sites, future overflow scenarios for typical winds and neap tide. Highlighted cells indicate percentile values that are higher than for the existing shoreline discharge.

Discharge Point	Percentile	200 m SW	200 m E	Titahi Beach South	Titahi Beach	Ti Korohiwa	Mount Couper
Scenario 9	90	232.5	194.5	90.4	29.4	10.0	2.7
	95	402.3	276.7	124.6	49.9	13.4	4.6
	99	672.0	428.3	218.7	127.4	21.5	7.8
Scenario 10	90	211.5	129.7	56.3	18.5	339.5	2.1
	95	321.8	162.8	74.9	29.7	501.0	3.5
	99	434.0	274.7	127.8	74.8	670.9	5.1
Scenario 11	90	2.9	2.9	2.6	2.8	3.0	1.2
	95	3.5	3.8	3.2	2.9	4.1	1.9
	99	4.1	6.8	4.0	3.2	6.1	4.2
Scenario 12	90	0.2	0.3	0.2	0.1	0.3	0.2
	95	0.2	0.4	0.3	0.1	0.4	0.4
	99	0.3	0.5	0.4	0.2	0.5	1.8

Table 29. Percentile estimates of Virus concentration (Virus/100 mL) at the monitoring sites, future overflow scenarios for typical winds and neap tide. Highlighted cells indicate percentile values that are higher than for the existing shoreline discharge.

Discharge Point	Percentile	200 m SW	200 m E	Titahi Beach South	Titahi Beach	Ti Korohiwa	Mount Couper
Scenario 9	90	257.4	212.4	108.5	43.1	12.5	4.0
	95	402.2	276.4	133.9	52.9	17.4	6.9
	99	674.3	427.1	217.3	126.8	24.6	11.0
Scenario 10	90	228.5	138.2	68.9	29.0	348.6	3.5
	95	323.1	173.0	83.4	31.9	499.9	5.5
	99	438.1	274.3	127.6	75.4	670.5	7.4
Scenario 11	90	3.9	4.1	3.7	4.4	3.9	1.7
	95	4.6	5.1	4.2	4.7	4.9	2.7
	99	5.0	7.1	5.4	5.1	6.2	4.3
Scenario 12	90	0.3	0.5	0.3	0.2	0.4	0.3
	95	0.4	0.5	0.5	0.2	0.5	0.6
	99	0.4	0.6	0.6	0.2	0.7	1.8

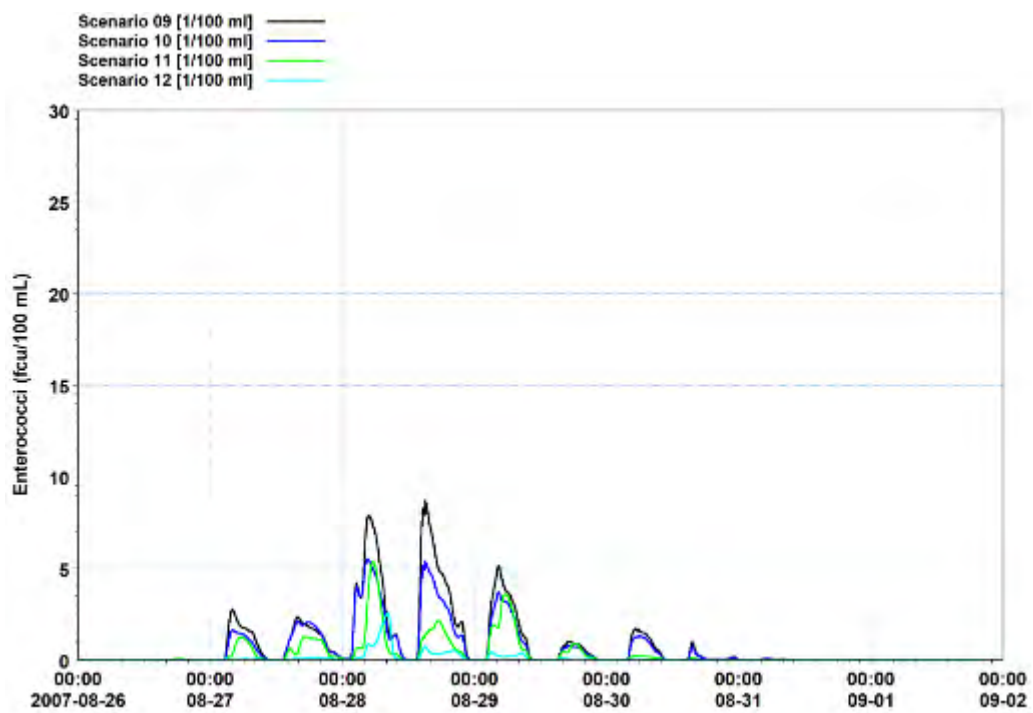


Figure 5-72. Predicted Enterococci (Ent/100 ml) at the Mount Couper monitoring site for the overflow scenarios for typical winds and a neap tide.

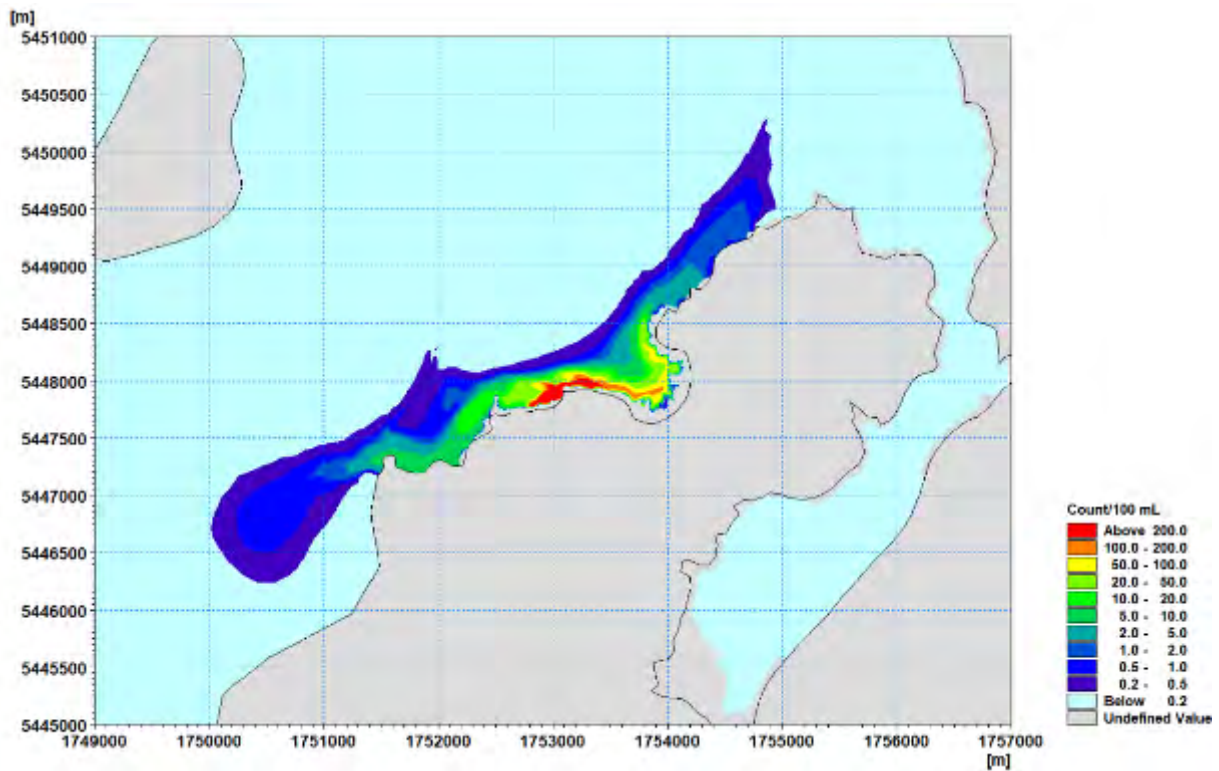


Figure 5-73. Predicted 95th percentile Enterococci concentration (Virus/100 mL), for the Scenario 9 future overflow for typical winds and neap tide.

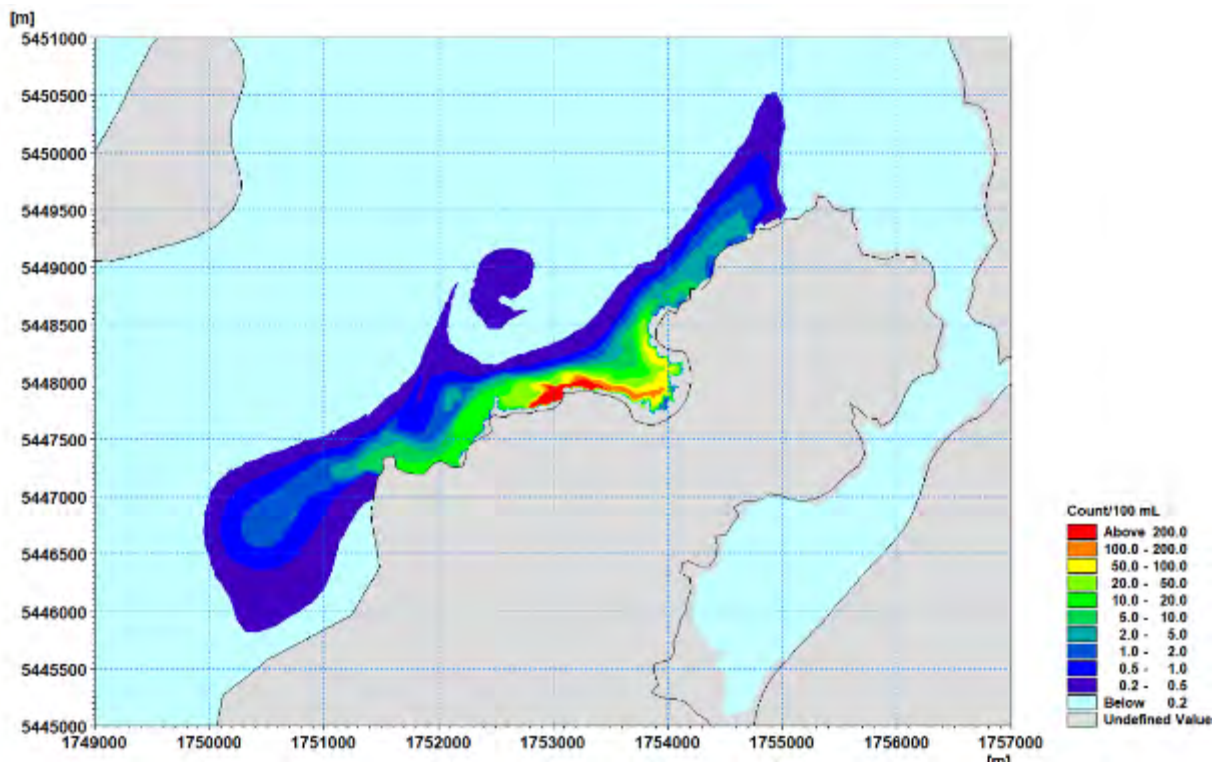


Figure 5-74. Predicted 95th percentile Virus concentration (Virus/100 mL), for the Scenario 9 future overflow for typical winds and neap tide.

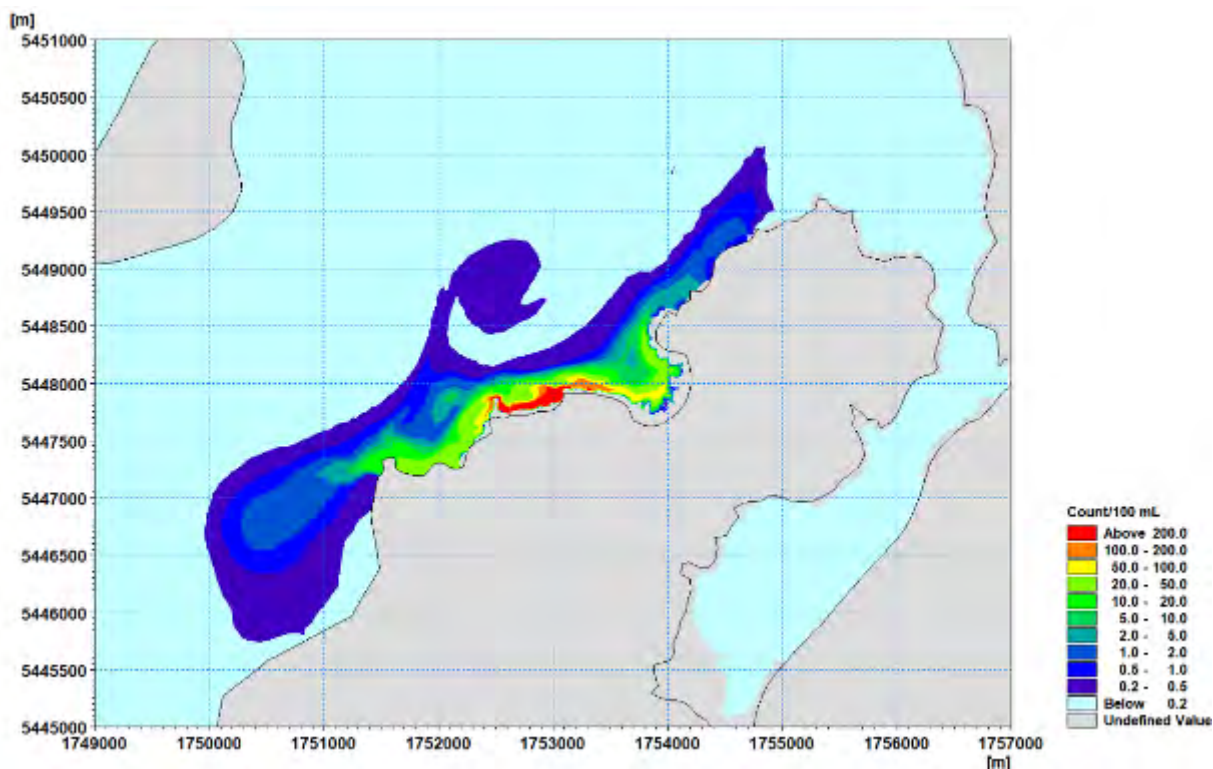


Figure 5-75. Predicted 95th percentile Enterococci concentration (Ent/100 mL), for the Scenario 10 future overflow for typical winds and neap tide.

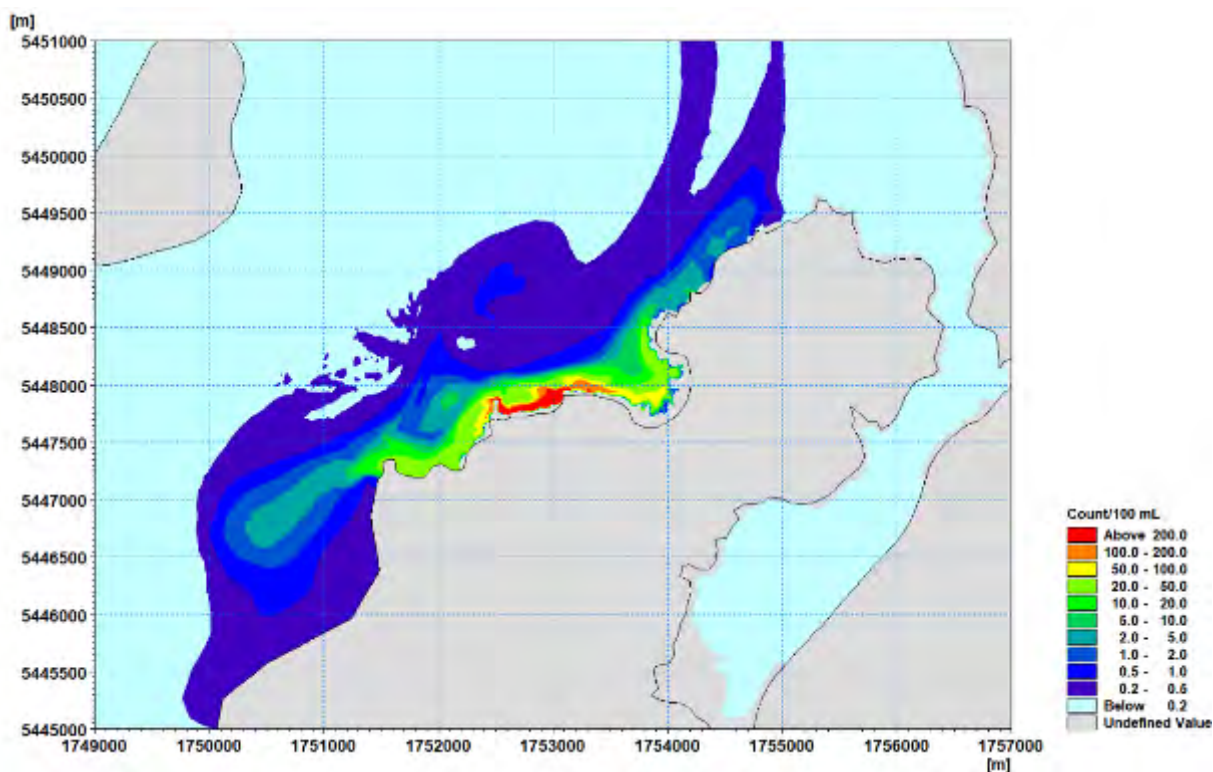


Figure 5-76. Predicted 95th percentile Virus concentration (Virus/100 mL), for the Scenario 10 future overflow for typical winds and neap tide.

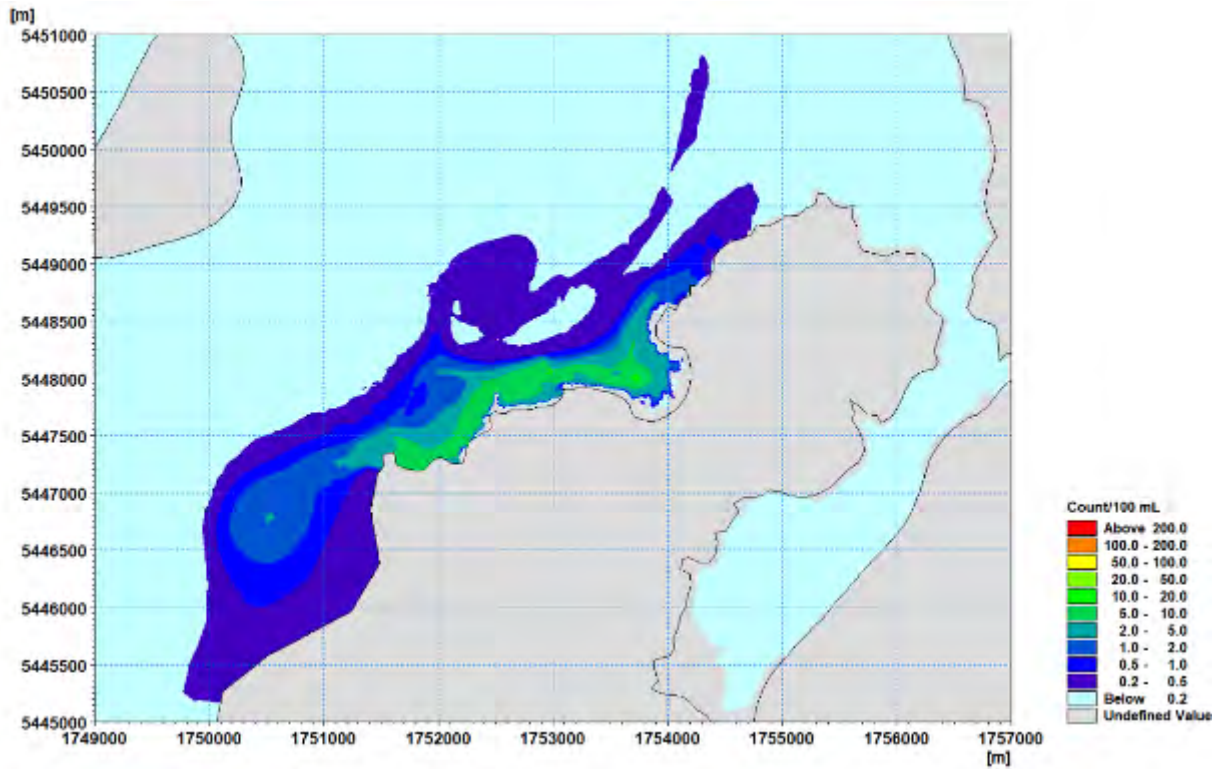


Figure 5-77. Predicted 95th percentile Enterococci concentration (Ent/100 mL), for Scenario 11 future overflow for typical winds and neap tide.

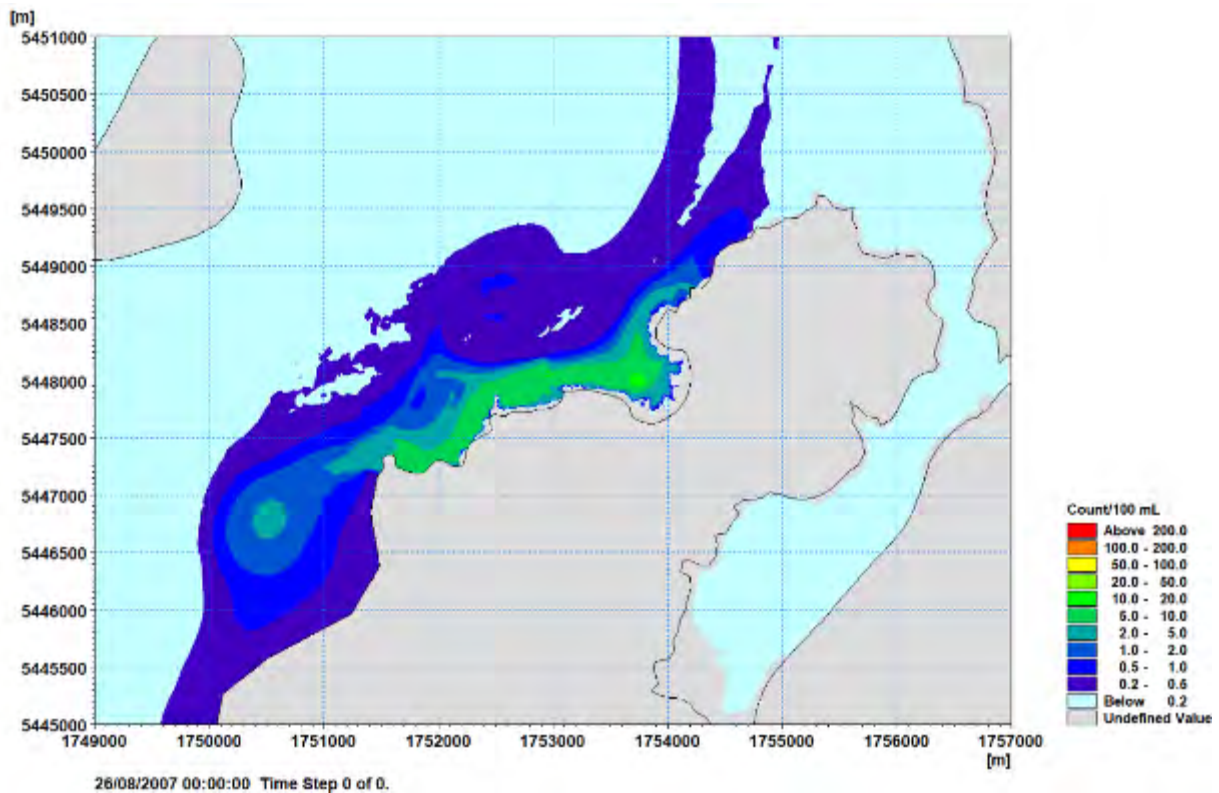


Figure 5-78. Predicted 95th percentile Virus concentration (Virus/100 mL), for Scenario 11 future overflow for typical winds and neap tide.

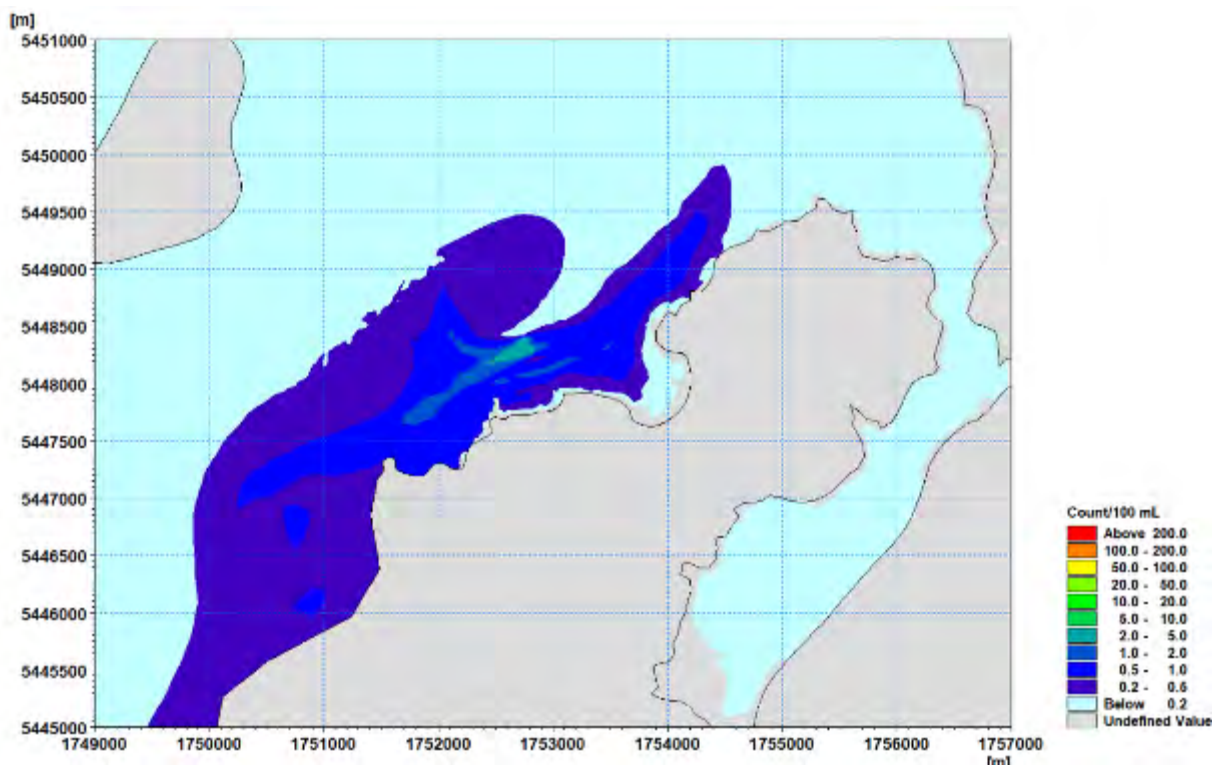


Figure 5-79. Predicted 95th percentile Enterococci concentration (Ent/100 mL), for Scenario 12 future overflow for typical winds and neap tide.

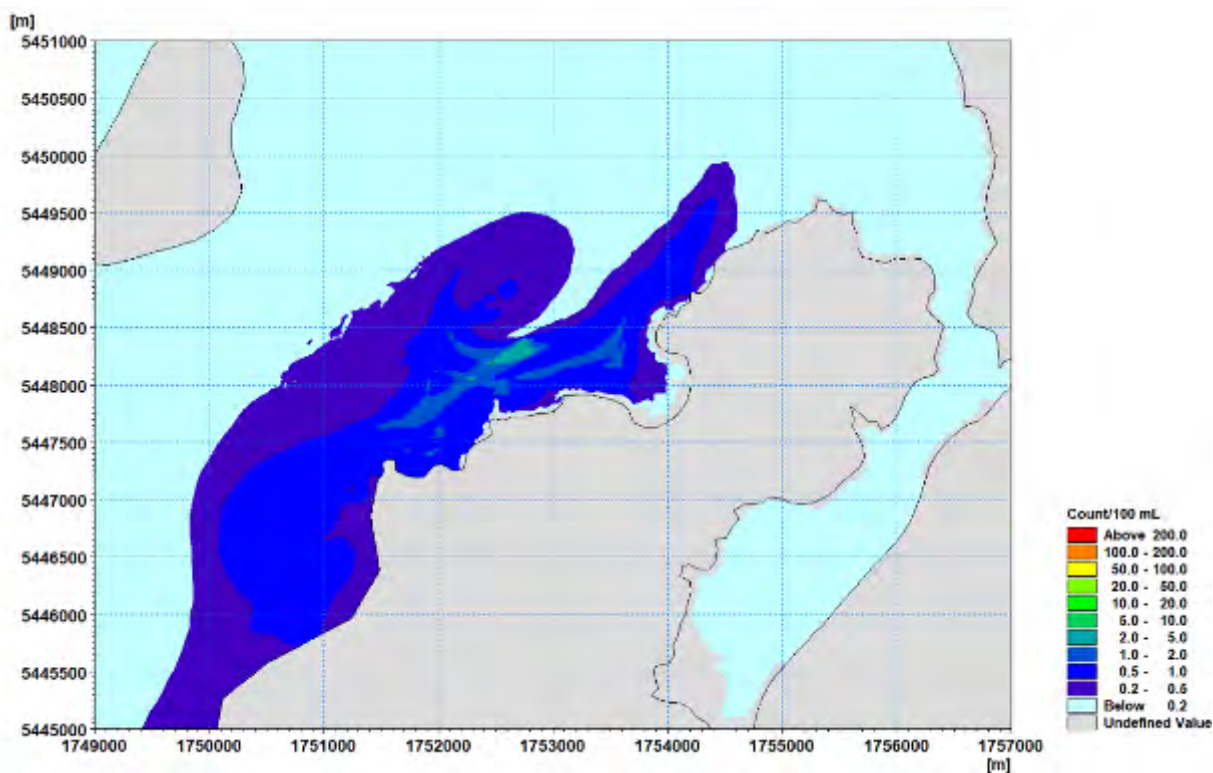


Figure 5-80. Predicted 95th percentile Virus concentration (Virus/100 mL), for Scenario 12 future overflow for typical winds and neap tide.

5.3.4 Onshore Winds and Neap Tide - Overflow Scenarios

Table 30 and Table 31 provide percentile values for Enterococci and Virus for the overflow scenarios for typical winds and spring tides.

Appendices D-I contain figures of the predicted time-series of data the monitoring sites.

For **Scenario 9**, the 99th percentile concentration at the 200 m SW site range from 700-710 count/100 mL and reduces to around 315 count/100 mL at the 200 m E site. At the Titahi Beach sites the 99th percentile concentrations range from 114-247 count/100 mL while at the Ti Korohiwa Rocks and Mount Couper sites 99th percentile concentrations of less than 20 count/100 mL occur.

For **Scenario 10** the 90th percentile concentrations at the monitoring site 200 m SW of the existing discharge increase by between 1 and 5% (highlighted in Table 30 and Table 31) while the other percentile concentrations are reduced by between 17 and 35%. At the 200 m E site percentile concentrations are reduced by between 26 and 37% and at the Titahi Beach sites percentile concentrations are reduced by between 25 and 40%. Percentile concentrations at the Ti Korohiwa Rocks (adjacent to the Round Point overflow point) increase by a factor of between 30 and 52 resulting in 99th percentile concentrations of 614 count/100 mL. At the Mount Couper site percentile concentrations are reduced by between 7 and 27%.

For **Scenario 11** the percentile concentrations are reduced by at least 96% at the 200 m SW, 200 m E and the Titahi Beach sites. At the Ti Korohiwa Rocks site percentile concentrations are reduced by between 46 and 63% while at the Mount Couper site reductions in percentile concentrations of between 27 and 77% are achieved. As noted for the Future PWWF scenarios, there are times when the concentration at the Mount Couper site is higher under this scenario compared to the other overflow scenarios (Figure 5-81).

For **Scenario 12** the percentile concentrations are reduced by at least 96% at all the monitoring sites.

Figures 5-82 to 5-89 to show the spatial plots of the predicted 95th percentile estimates for each of the discharge options. These plots indicate the area impacted by each of the discharges and in particular illustrate the significant reduction in concentrations achieved by the two outfall options being considered.

Table 30. Percentile estimates of Enterococci concentration (Ent/100 mL) at the monitoring sites, future overflow scenarios for onshore winds and neap tide. Highlighted cells indicate percentile values that are higher than for the existing shoreline discharge.

Discharge Point	Percentile	200 m SW	200 m E	Titahi Beach South	Titahi Beach	Ti Korohiwa	Mount Couper
Scenario 9	90	245.1	138.1	108.9	51.9	7.2	3.9
	95	455.3	225.9	152.7	69.4	9.6	6.3
	99	701.5	314.2	247.4	114.0	11.9	11.9
Scenario 10	90	257.5	100.7	81.2	35.8	295.6	3.1
	95	376.9	142.2	106.3	46.4	433.2	5.8
	99	458.9	219.7	176.4	69.0	614.4	8.7
Scenario 11	90	2.5	3.4	2.9	1.7	3.0	1.0
	95	3.1	4.9	5.1	2.0	3.8	2.8
	99	4.0	9.6	8.6	2.5	6.4	8.7
Scenario 12	90	0.1	0.2	0.1	0.1	0.2	0.1
	95	0.2	0.2	0.2	0.1	0.3	0.2
	99	0.2	0.3	0.3	0.2	0.4	0.3

Table 31. Percentile estimates of Virus concentration (Virus/100 mL) at the monitoring sites, future overflow scenarios for onshore winds and neap tide. Highlighted cells indicate percentile values that are higher than for the existing shoreline discharge.

Discharge Point	Percentile	200 m SW	200 m E	Titahi Beach South	Titahi Beach	Ti Korohiwa	Mount Couper
Scenario 9	90	275.1	147.0	121.4	70.9	10.0	6.7
	95	457.8	227.4	161.3	80.8	12.8	9.1
	99	709.0	314.5	246.7	114.2	15.8	16.8
Scenario 10	90	278.2	109.0	91.2	49.9	304.5	5.5
	95	377.2	148.4	113.1	57.2	432.0	8.0
	99	463.5	220.4	176.5	70.2	614.4	12.8
Scenario 11	90	3.5	4.8	4.6	2.7	3.9	1.5
	95	4.1	6.3	5.3	3.1	4.7	3.1
	99	5.0	9.7	8.6	3.5	6.5	8.7
Scenario 12	90	0.2	0.3	0.2	0.1	0.3	0.2
	95	0.3	0.4	0.2	0.2	0.4	0.3
	99	0.3	0.4	0.4	0.2	0.5	0.4

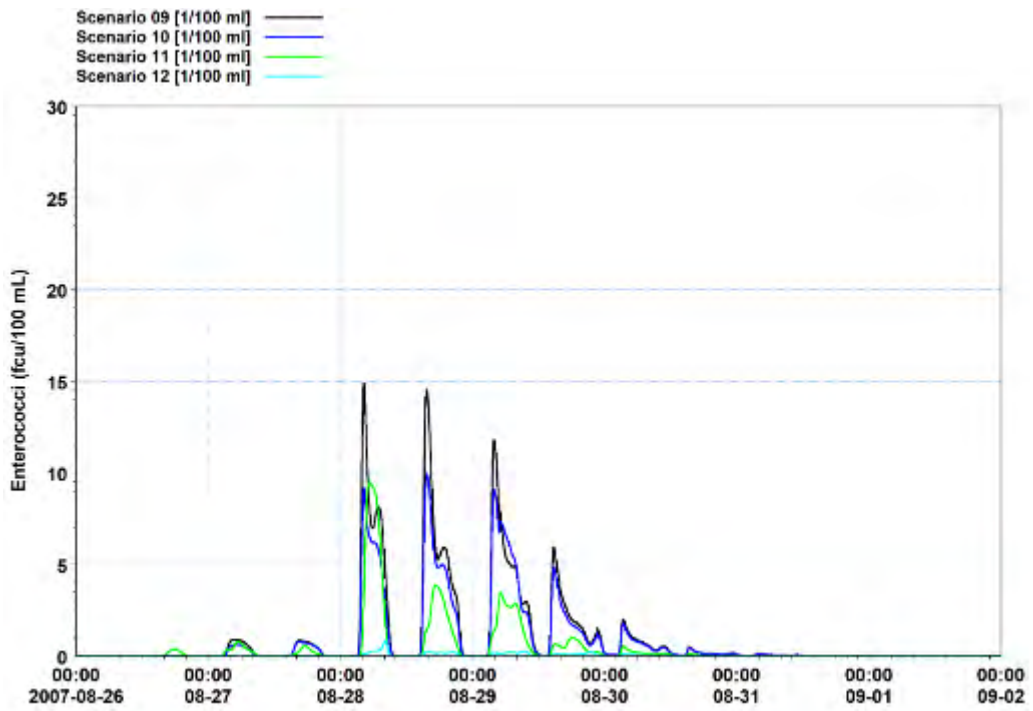


Figure 5-81. Predicted Enterococci (Ent/100 ml) at the Mount Couper monitoring site for the overflow scenarios for onshore winds and a neap tide.

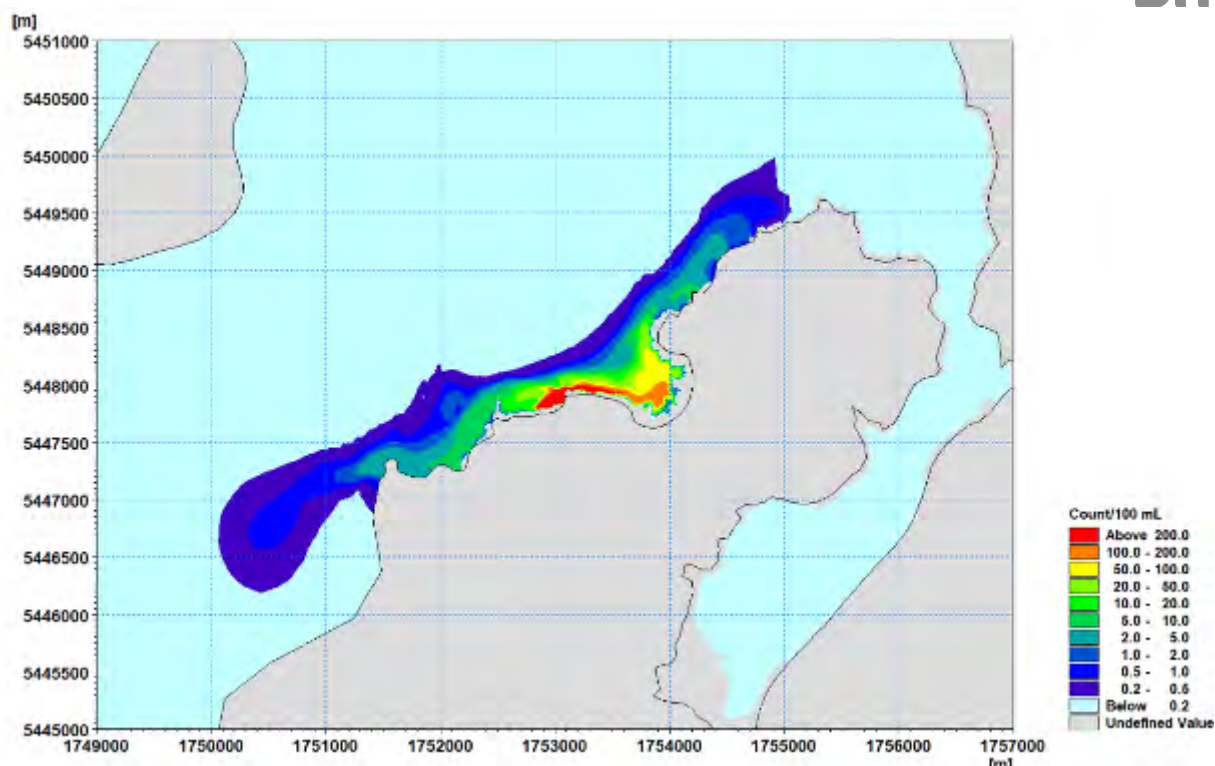


Figure 5-82. Predicted 95th percentile Enterococci concentration (Ent/100 mL), for the Scenario 9 future overflow for onshore winds and neap tide.

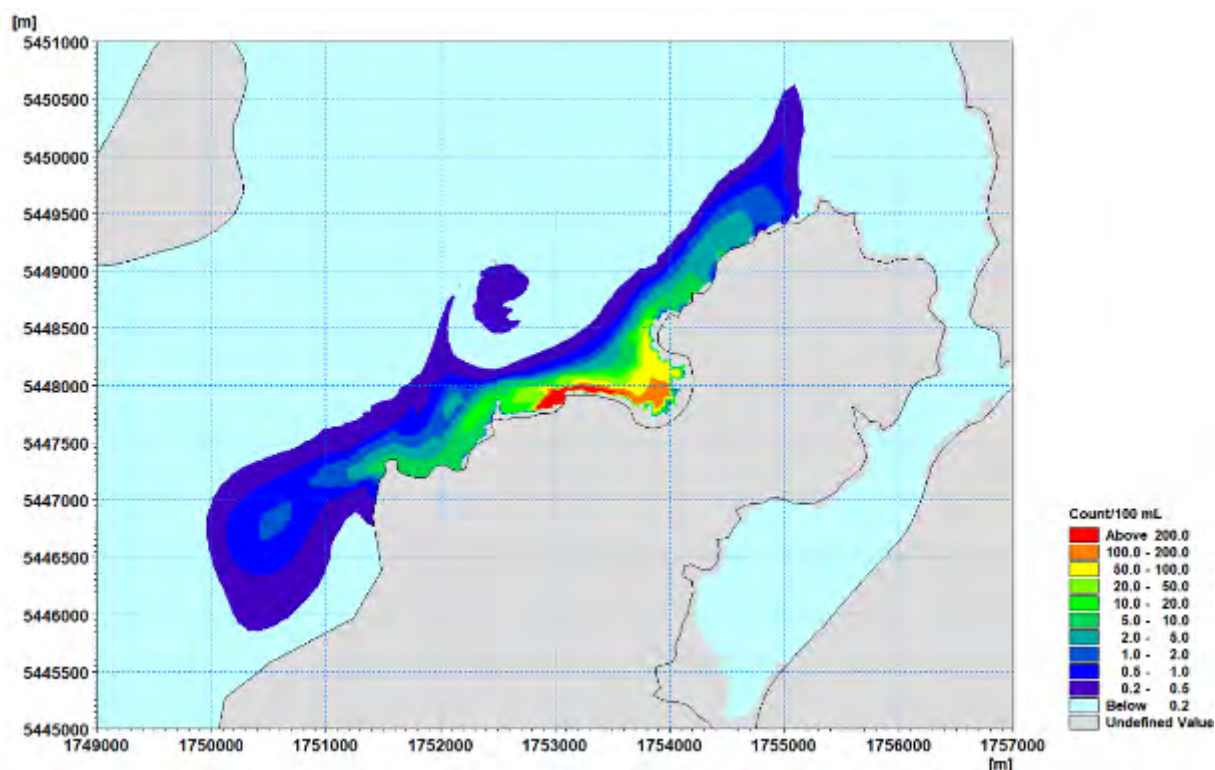


Figure 5-83. Predicted 95th percentile Virus concentration (Virus/100 mL), for the Scenario 9 future overflow for onshore winds and neap tide.

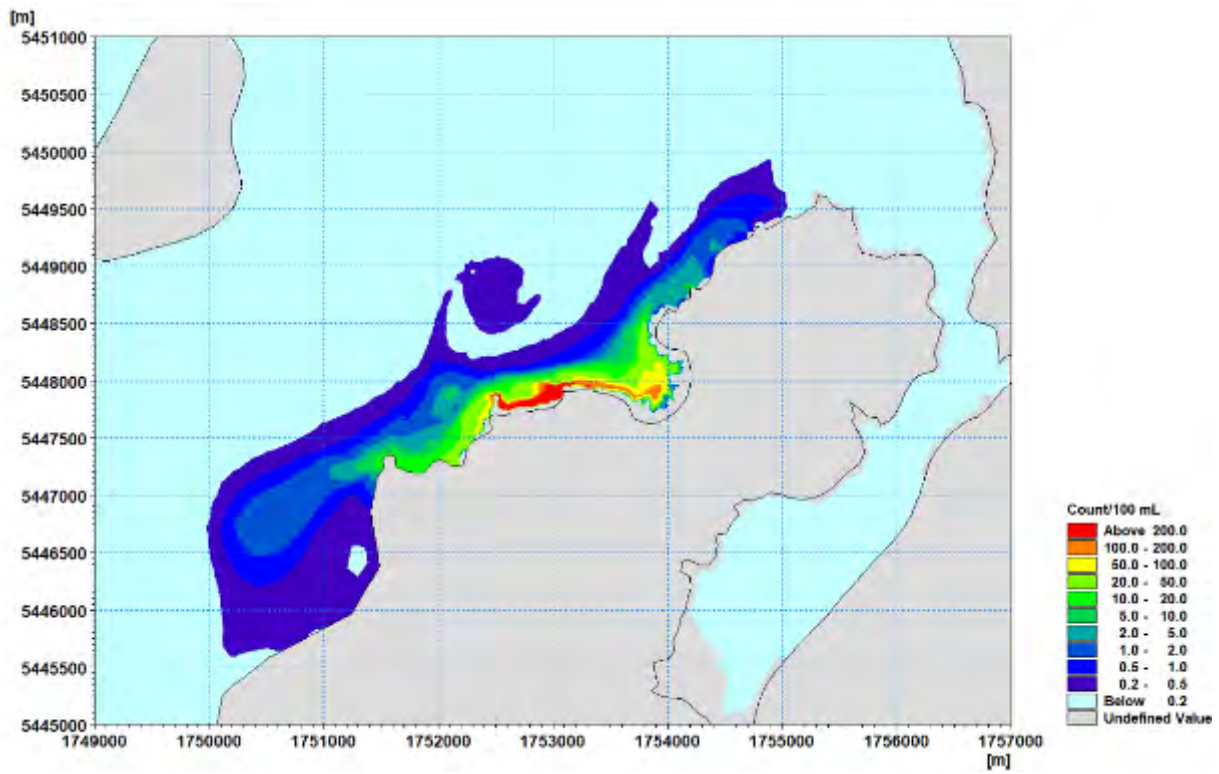


Figure 5-84. Predicted 95th percentile Enterococci concentration (Ent/100 mL), for the Scenario 10 future overflow for onshore winds and neap tide.

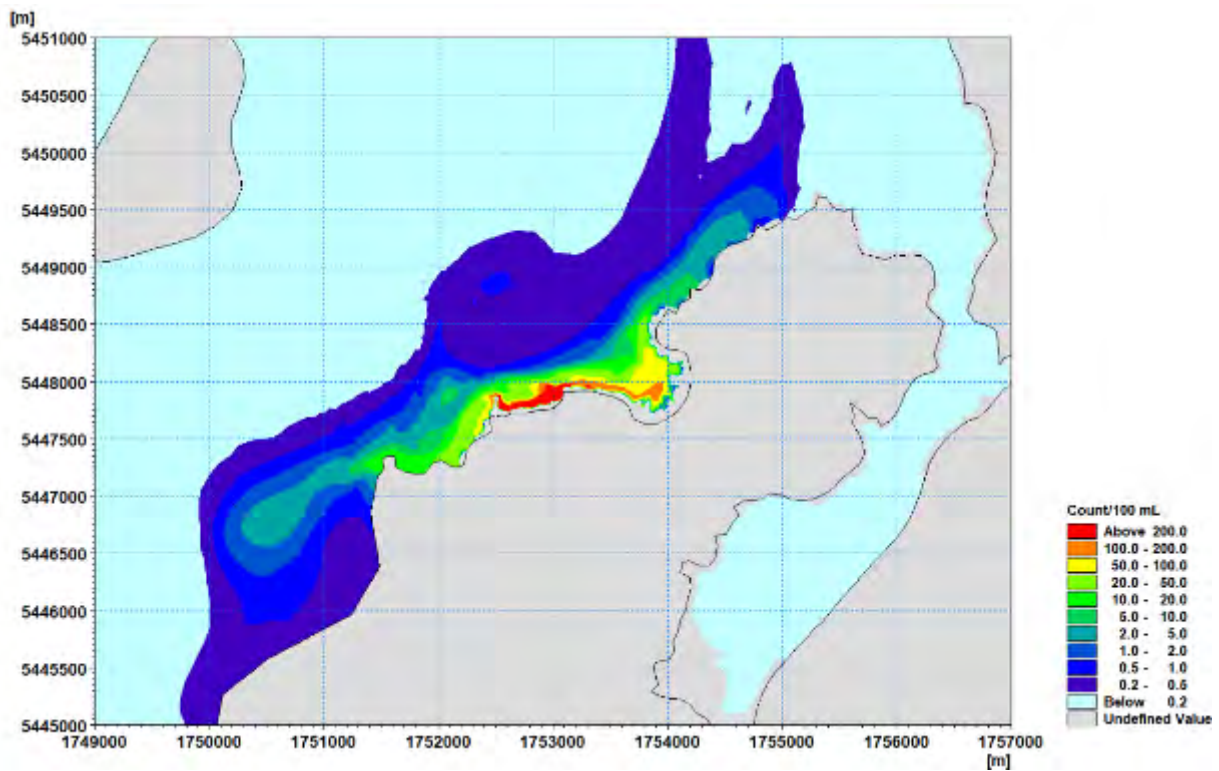


Figure 5-85. Predicted 95th percentile Virus concentration (Virus/100 mL), for the Scenario 10 future overflow for onshore winds and neap tide.

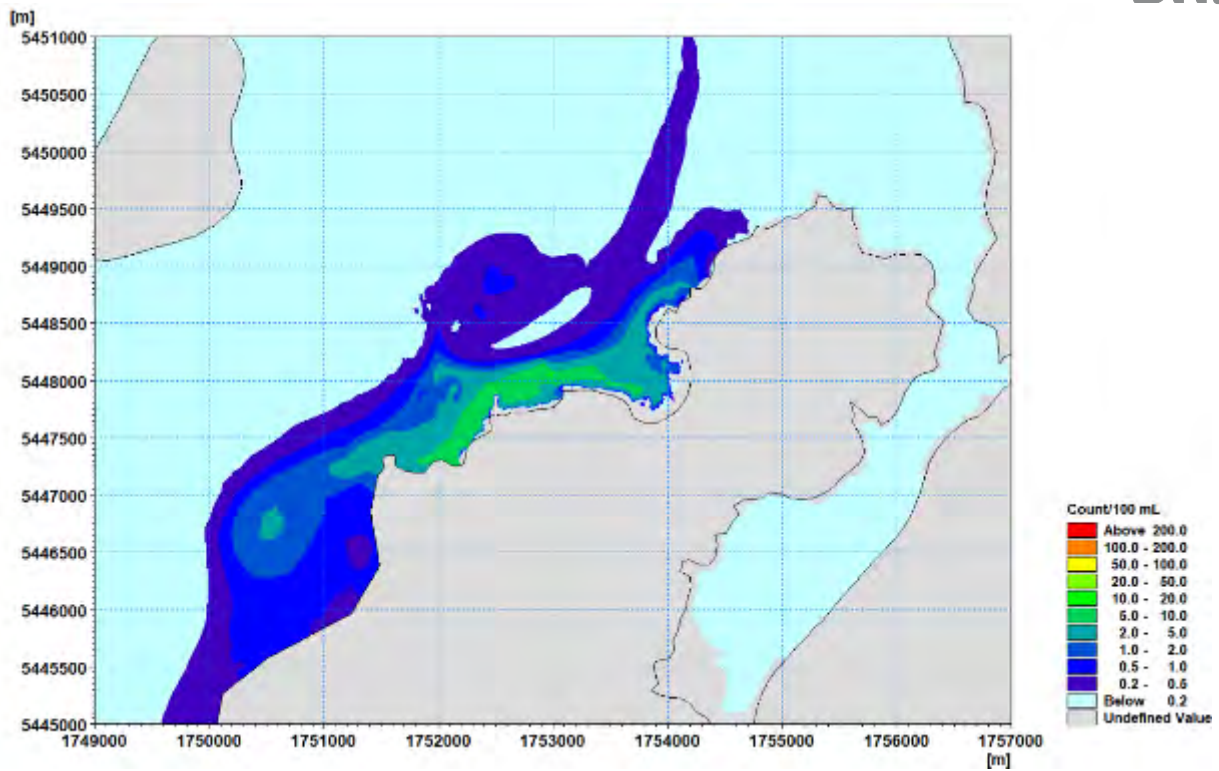


Figure 5-86. Predicted 95th percentile Enterococci concentration (Ent/100 mL), for Scenario 11 future overflow for onshore winds and neap tide.

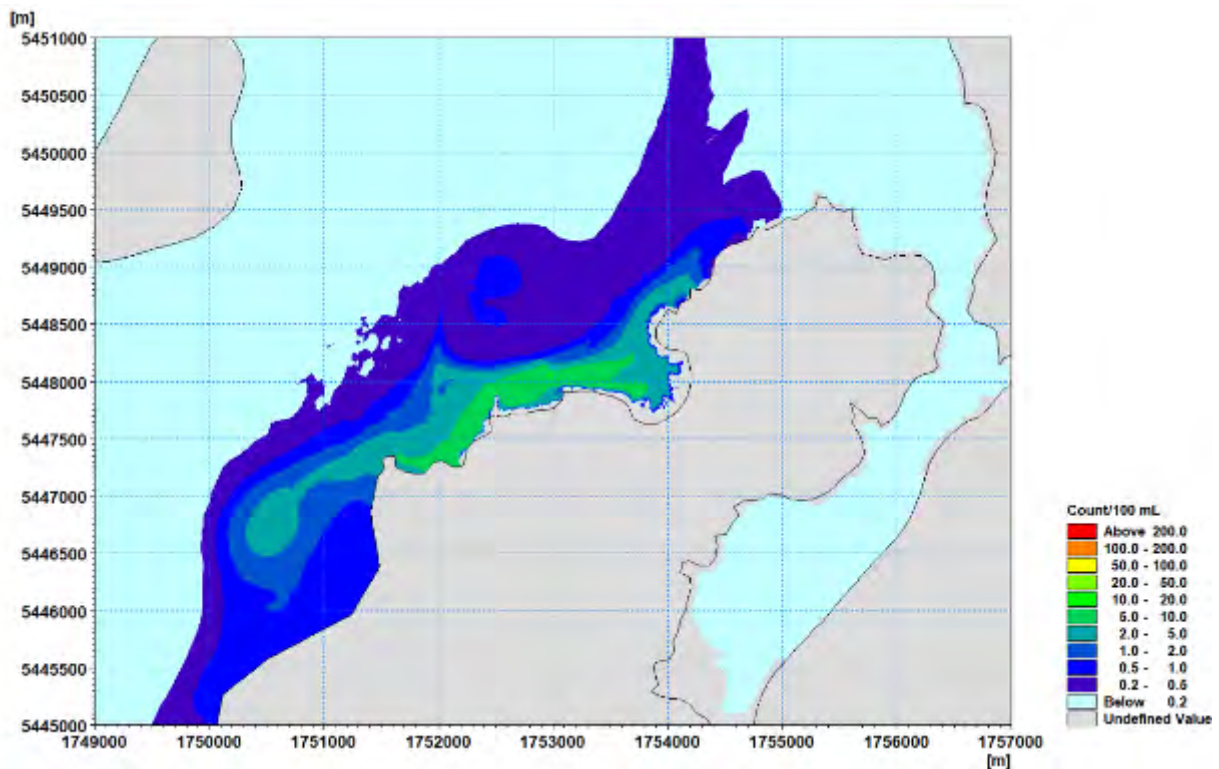


Figure 5-87. Predicted 95th percentile Virus concentration (Virus/100 mL), for Scenario 11 future overflow for onshore winds and neap tide.

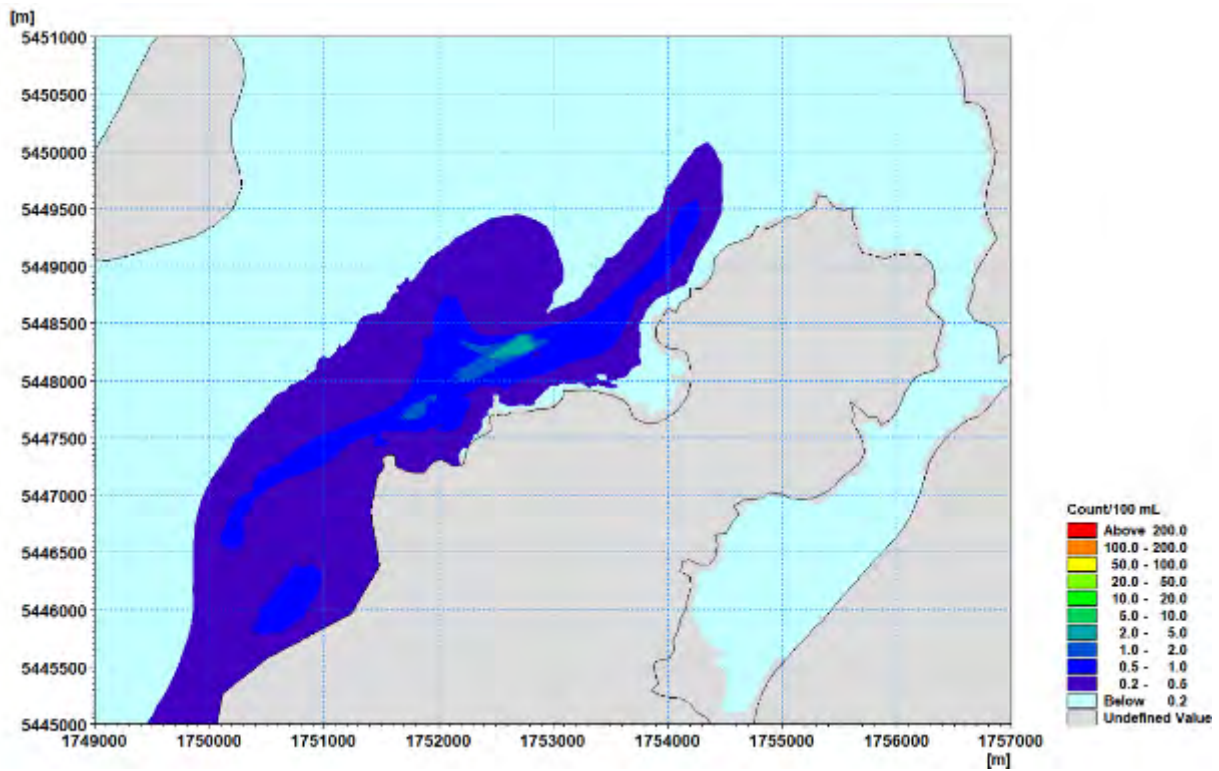


Figure 5-88. Predicted 95th percentile Enterococci concentration (Ent/100 mL), for Scenario 12 future overflow for onshore winds and neap tide.

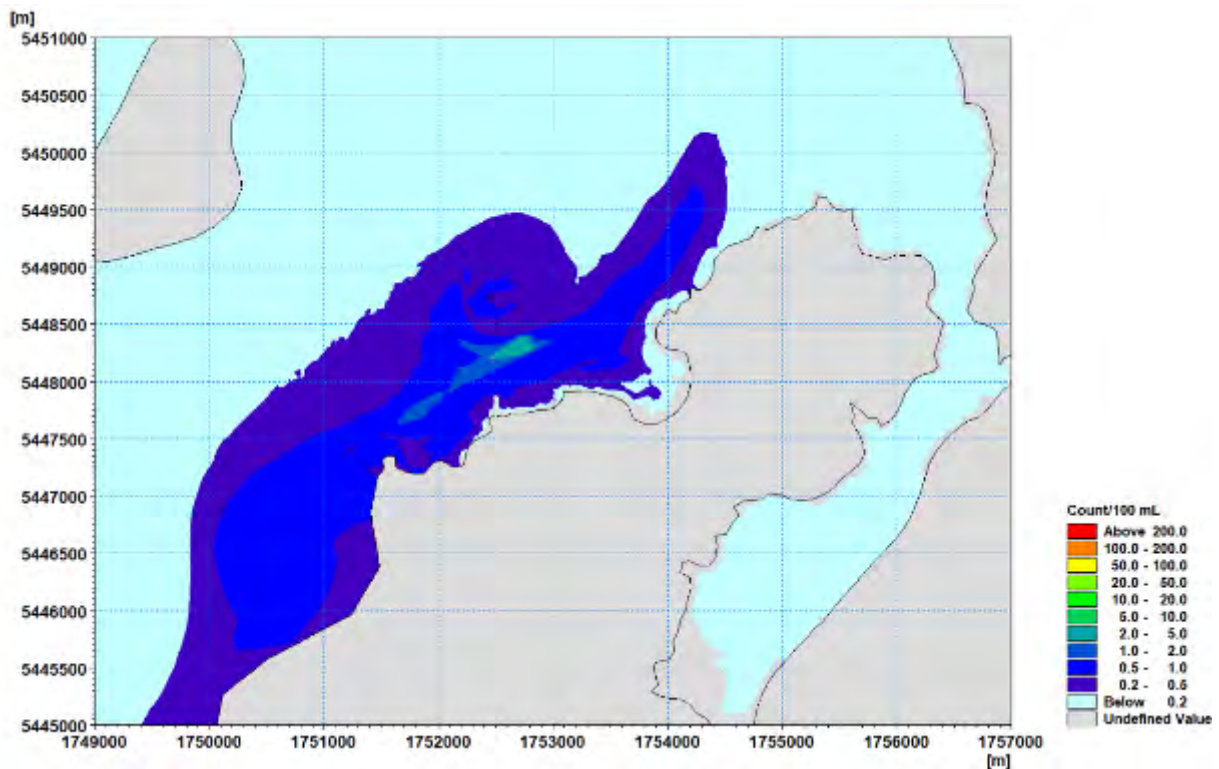


Figure 5-89. Predicted 95th percentile Virus concentration (Virus/100 mL), for Scenario 12 future overflow for onshore winds and neap tide.

References

DHI 2018. Titahi Bay Outfall Modelling. DHI report 44801085 prepared for Wellington Water.

Mott MacDonald 2016. Porirua Wastewater Model Future Populations

Doneker, R.L. and G.H. Jirka, 2007. CORMIX User Manual: A Hydrodynamic Mixing Zone Model and Decision Support System for Pollutant Discharges into Surface Waters", EPA-823-K-07-001.

Jirka, G.H., E.E. Adams, and K.D. Stolzenbach, Buoyant Surface Jets Journ. Hyd. Div., ASCE, Vol. 107, No. HY11, pp. 1467-1487.

Oldman, J.W. and Dada A.C (2019) A Quantitative Microbial Risk Assessment of the Porirua WWTP discharge and receiving environment.

Noble, R.T., Lee, I.M. and Schiff, K.C. 1994. Inactivation of indicator micro-organisms from various sources of faecal contamination in seawater and freshwater. Journal of Applied Microbiology 2004, 96, 464–472

Sinton, L.W., Davies-Colley, R.J., and Bell, R.G. 1994. Inactivation of enterococci and fecal coliforms from sewage and meatworks effluents in seawater chambers. Applied and Environmental Microbiology 2040–2048.

Sinton, L.W., Davies-Colley, R.J., and Bell, R.G. 1994. Inactivation of enterococci and fecal coliforms from sewage and meatworks effluents in seawater chambers. Applied and Environmental Microbiology 2040–2048.

Sinton, L.W., Finaly, R.K., Philippa, A. 1999. Sunlight Inactivation of Fecal Bacteriophages and Bacteria in Sewage-Polluted Seawater. Applied and Environmental Microbiology. 3605-3613. 65(8).

Maraccini P.A., Catharine, M., Mattioli, M., Sassoubre, L.M., Cao, Y., Griffith, J.F., Ervin, J.S., Van De Werfhorst, L.C and Boehm, A.B. 2016. Solar Inactivation of Enterococci and Escherichia coli in Natural Waters: Effects of Water Absorbance and Depth Environ. Sci. Technol. 2016, 50, 5068–5076.

Appendix A – CORMIX Near-field dilution vs Distance

10A.prd Flow Class: MU1H

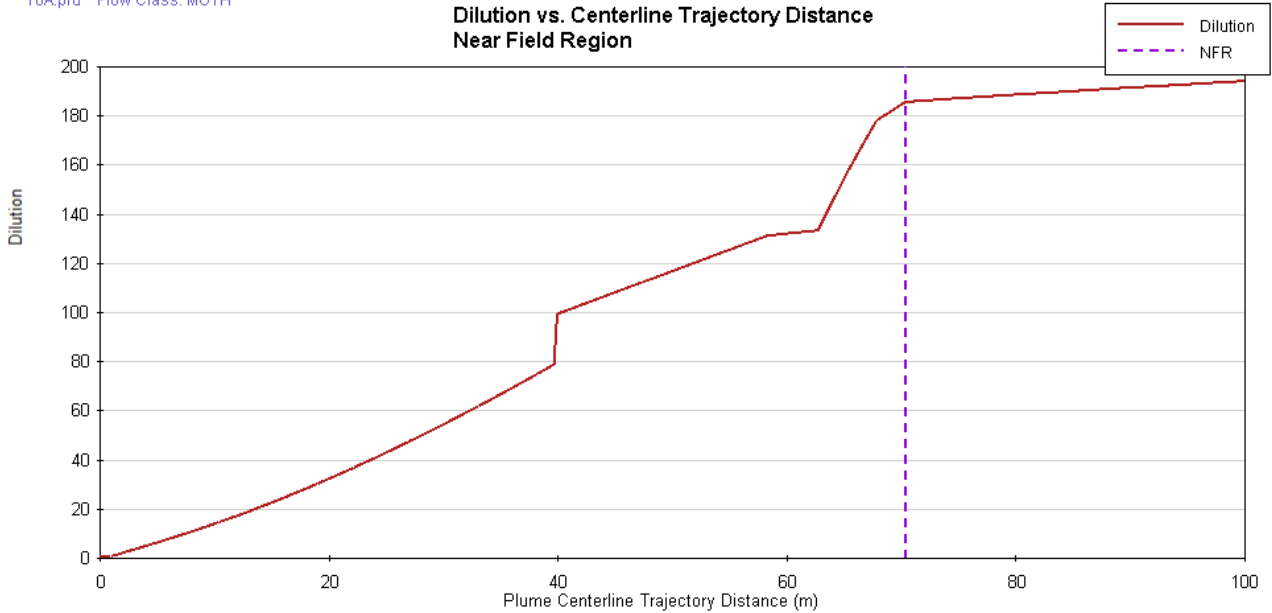


Figure A-1 Predicted dilution versus downstream distance for the 10 m offshore outfall, water depth of 10.1 m and ambient current of 0.08 m/s.

10B.prd Flow Class: MU1H

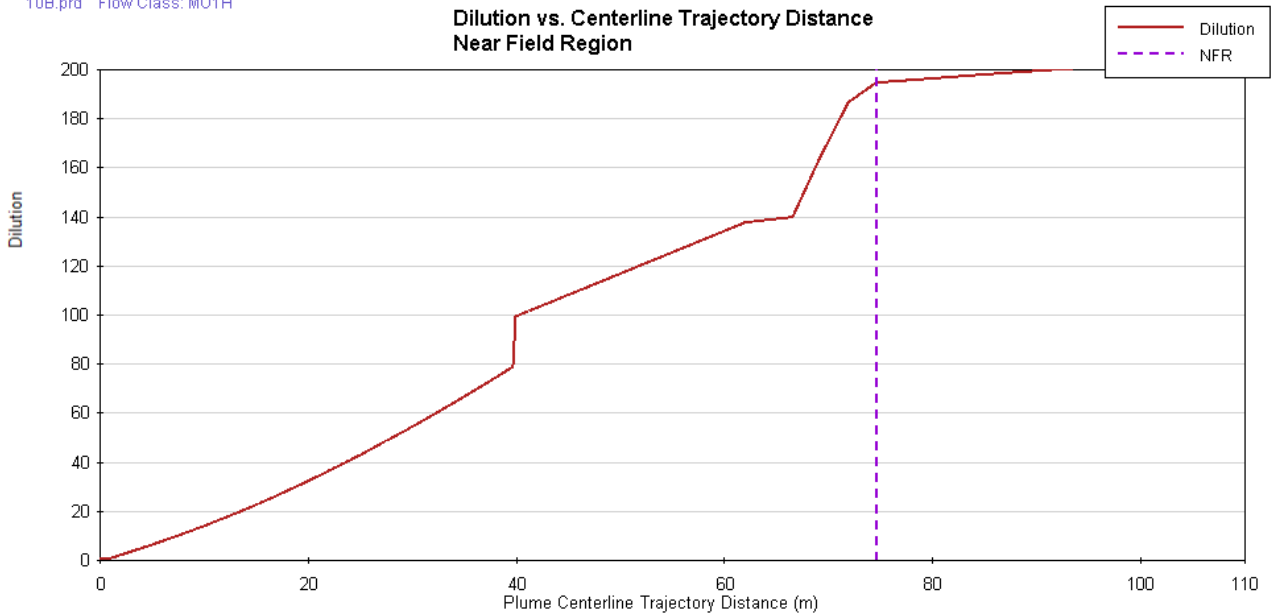


Figure A-2 Predicted dilution versus downstream distance for the 10 m offshore outfall, water depth of 10.5 m and ambient current of 0.08 m/s.

10C.prd Flow Class: MU8

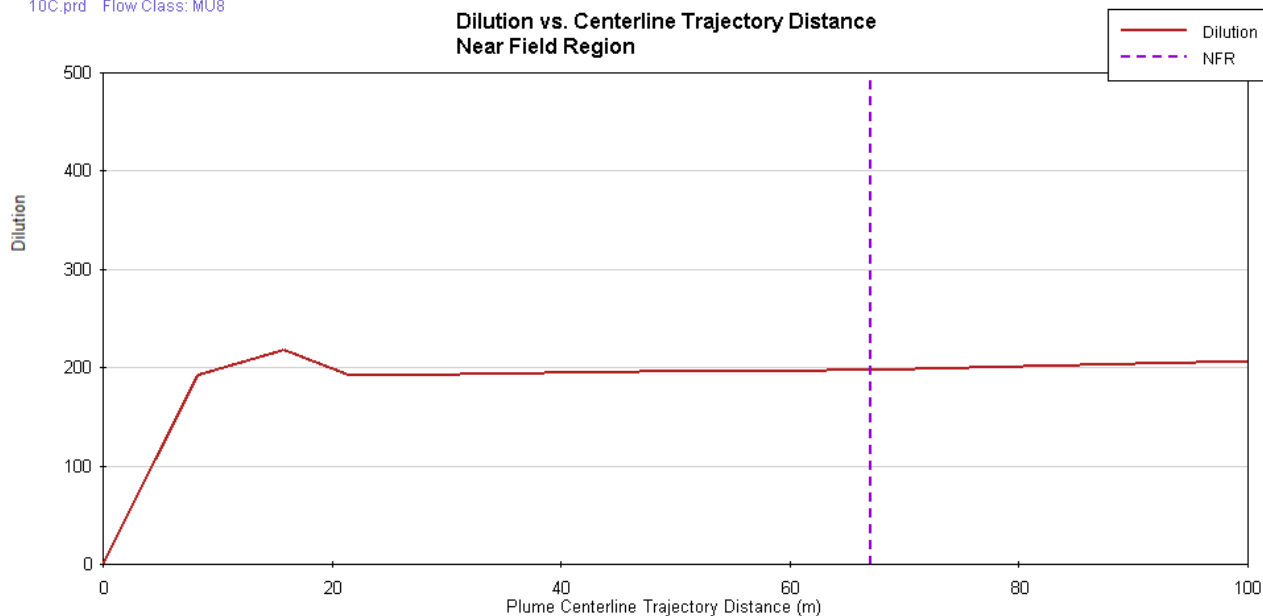


Figure A-3 Predicted dilution versus downstream distance for the 10 m offshore outfall, water depth of 10.9 m and ambient current of 0.16 m/s.

10D.prd Flow Class: MU8

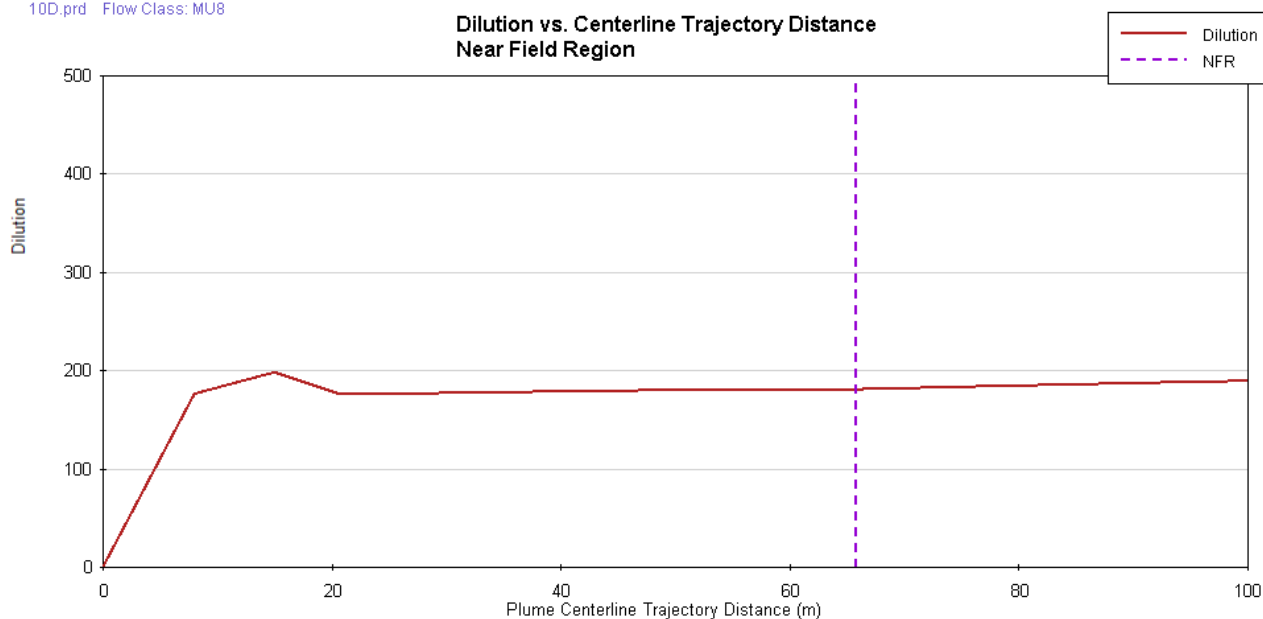


Figure A-4 Predicted dilution versus downstream distance for the 10 m offshore outfall, water depth of 10.0 m and ambient current of 0.16 m/s.

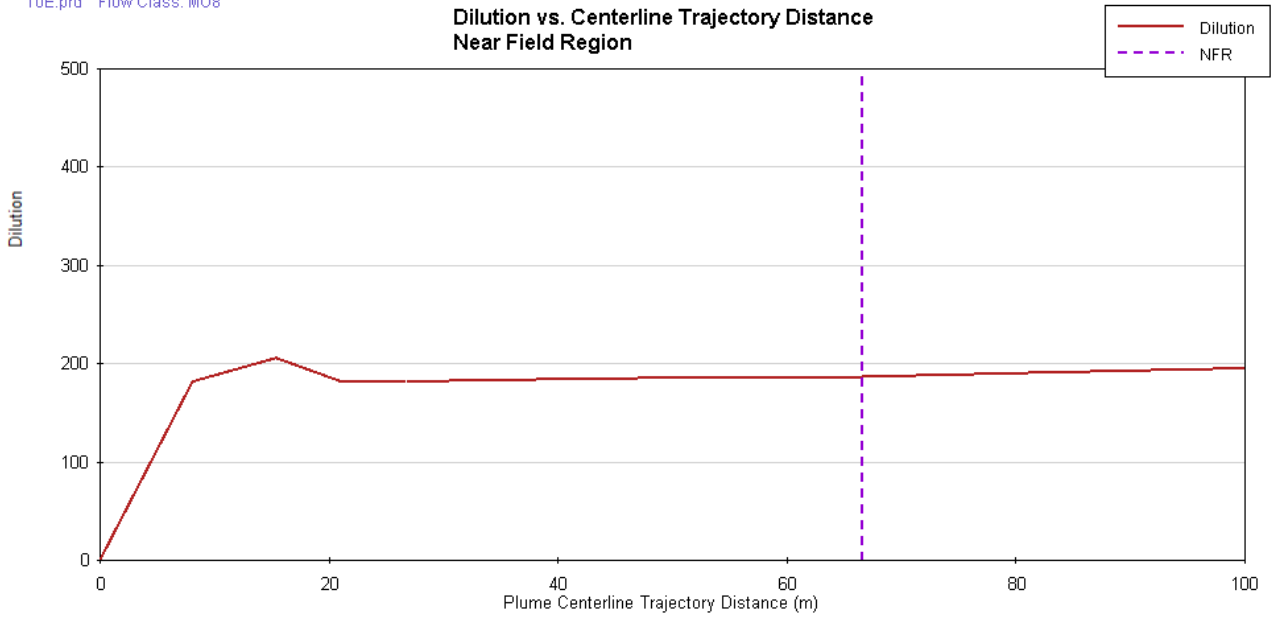


Figure A-5 Predicted dilution versus downstream distance for the 10 m offshore outfall, water depth of 10.3 m and ambient current of 0.16 m/s.

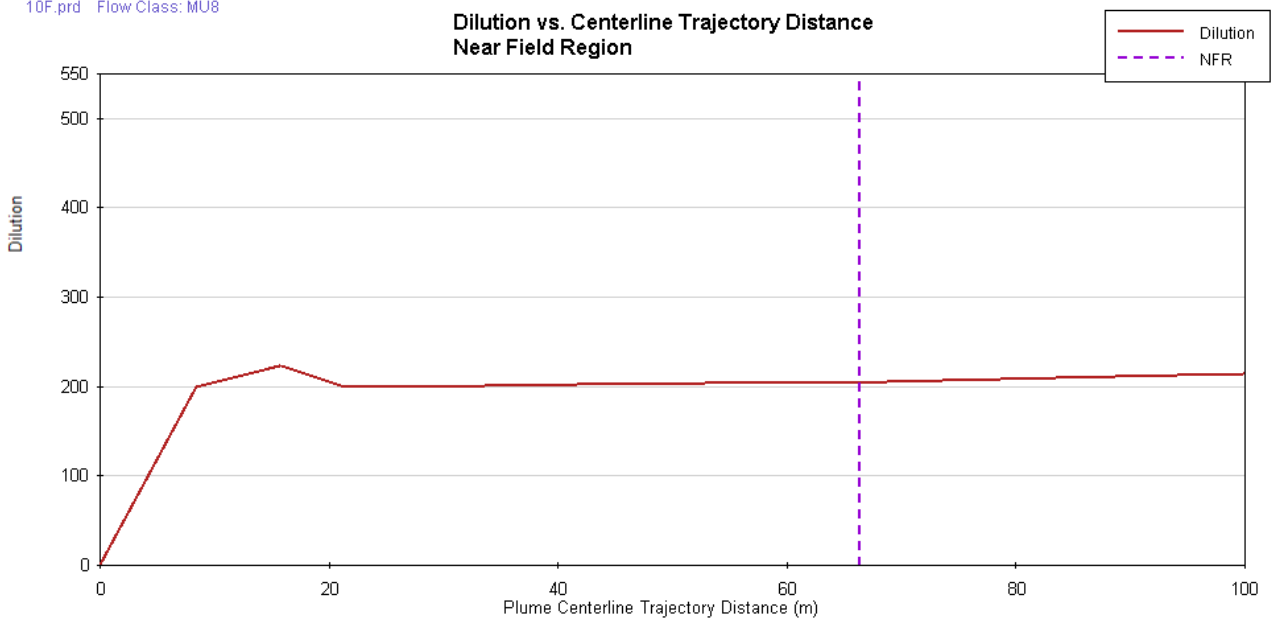


Figure A-6 Predicted dilution versus downstream distance for the 10 m offshore outfall, water depth of 11.3 m and ambient current of 0.16 m/s.

10G.prd Flow Class: MU8

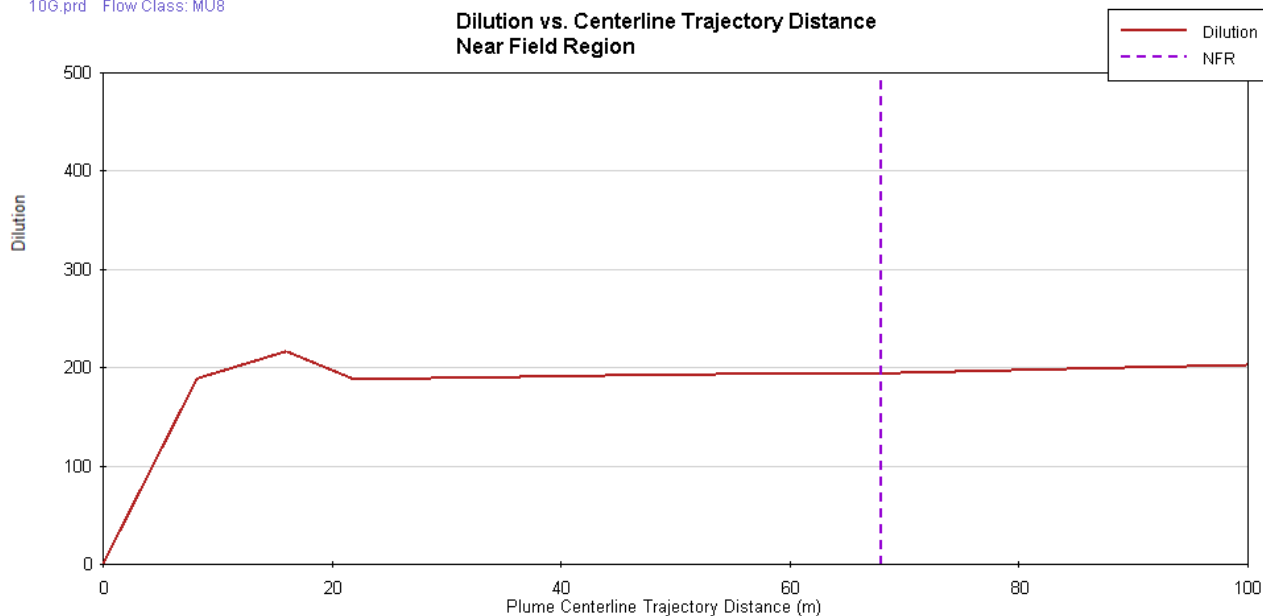


Figure A-7 Predicted dilution versus downstream distance for the 10 m offshore outfall, water depth of 10.7 m and ambient current of 0.16 m/s.

10H.prd Flow Class: MU8

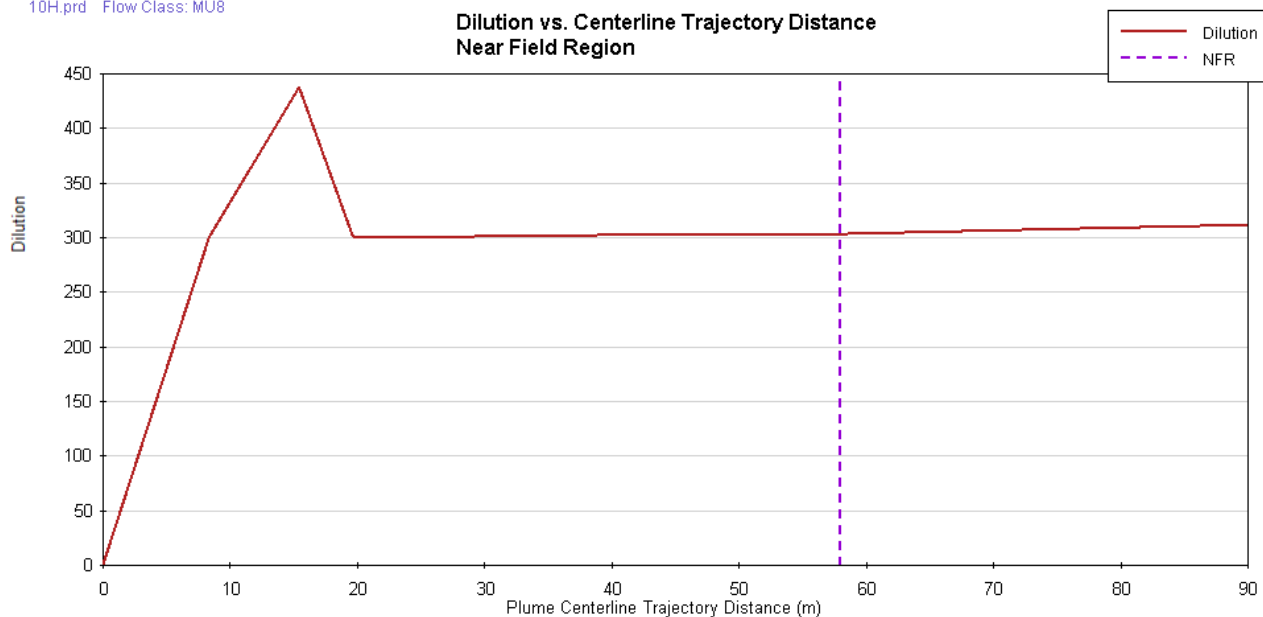


Figure A-8 Predicted dilution versus downstream distance for the 10 m offshore outfall, water depth of 11.1 m and ambient current of 0.26 m/s.

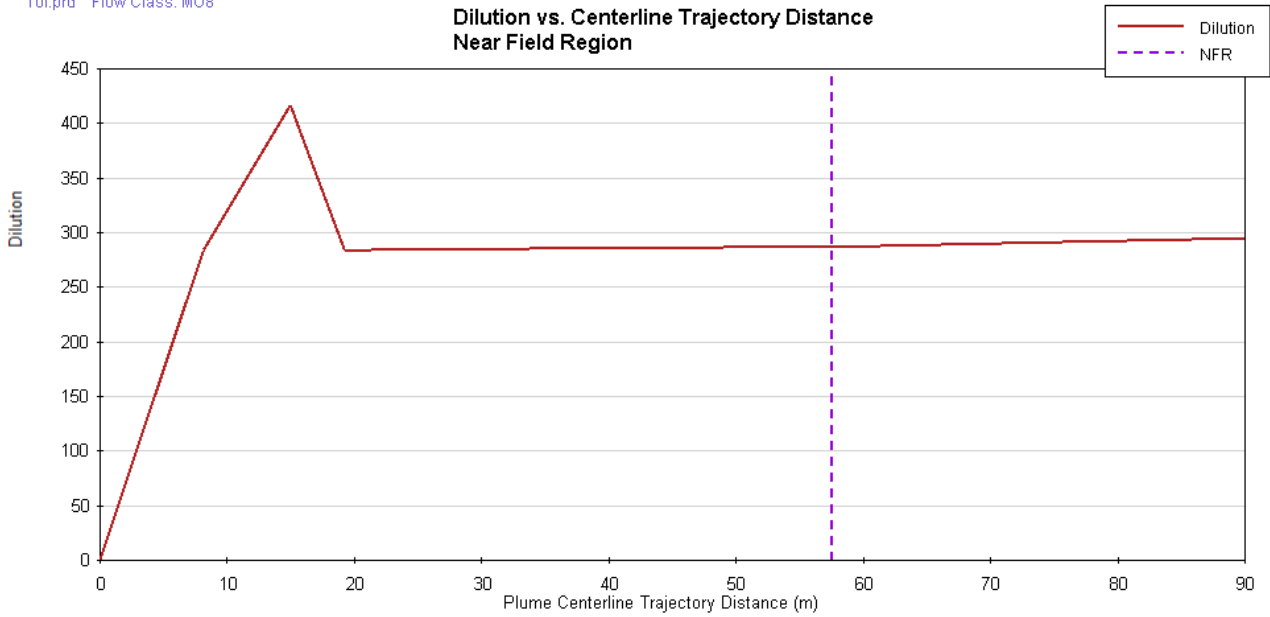


Figure A-9 Predicted dilution versus downstream distance for the 10 m offshore outfall, water depth of 10.5 m and ambient current of 0.26 m/s.

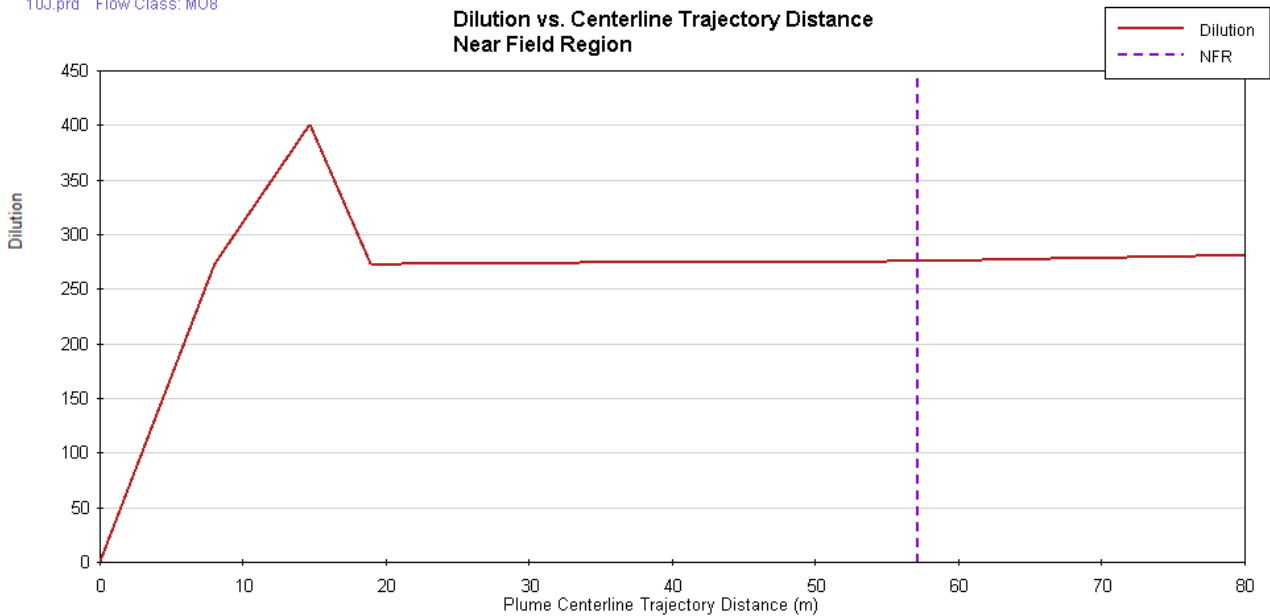


Figure A-10 Predicted dilution versus downstream distance for the 10 m offshore outfall, water depth of 10.1 m and ambient current of 0.26 m/s.

10K.prd Flow Class: MU8

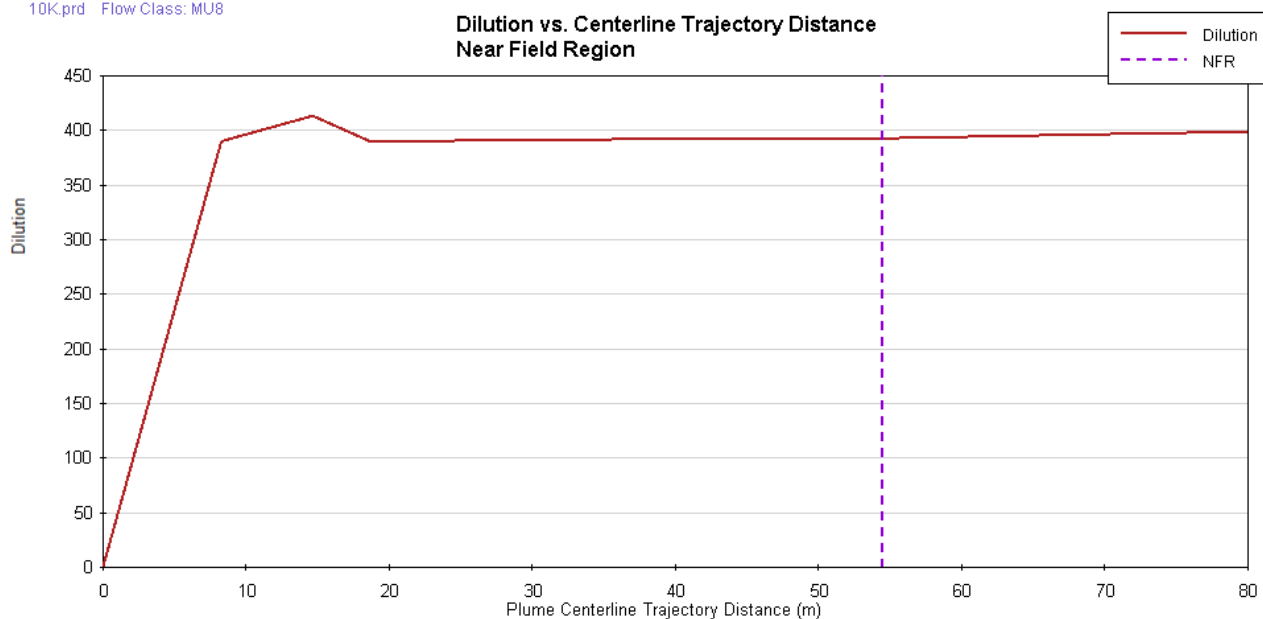


Figure A-11 Predicted dilution versus downstream distance for the 10 m offshore outfall, water depth of 10.9 m and ambient current of 0.35 m/s.

10L.prd Flow Class: MU8

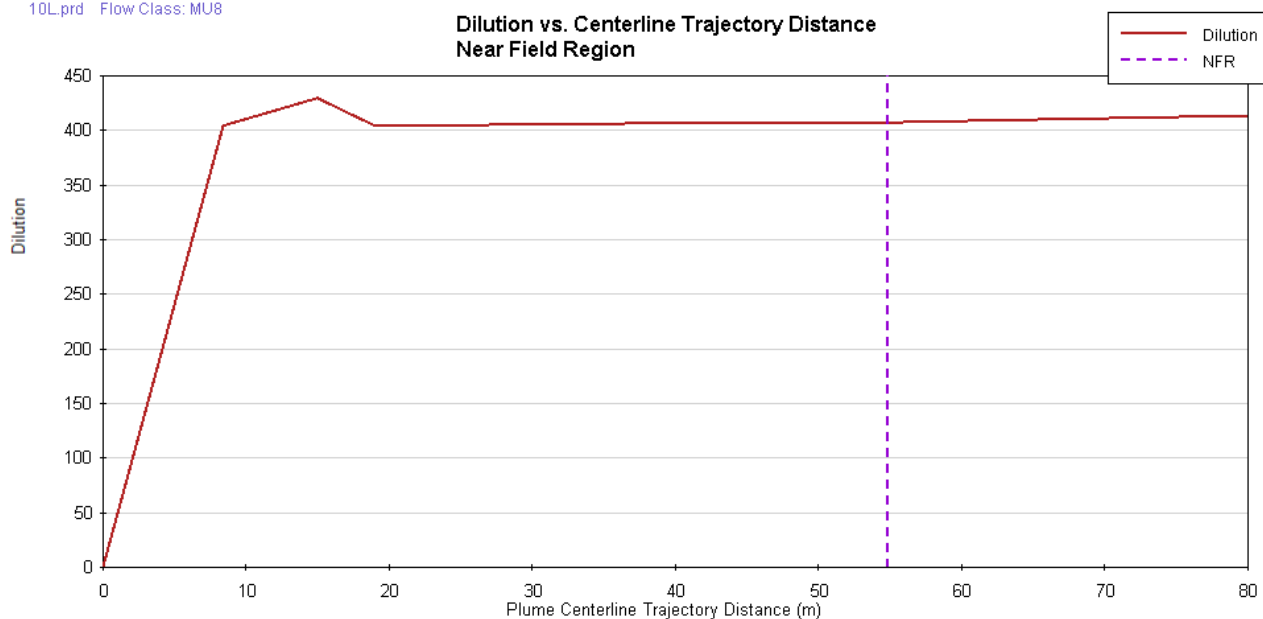


Figure A-12 Predicted dilution versus downstream distance for the 10 m offshore outfall, water depth of 11.3 m and ambient current of 0.35 m/s

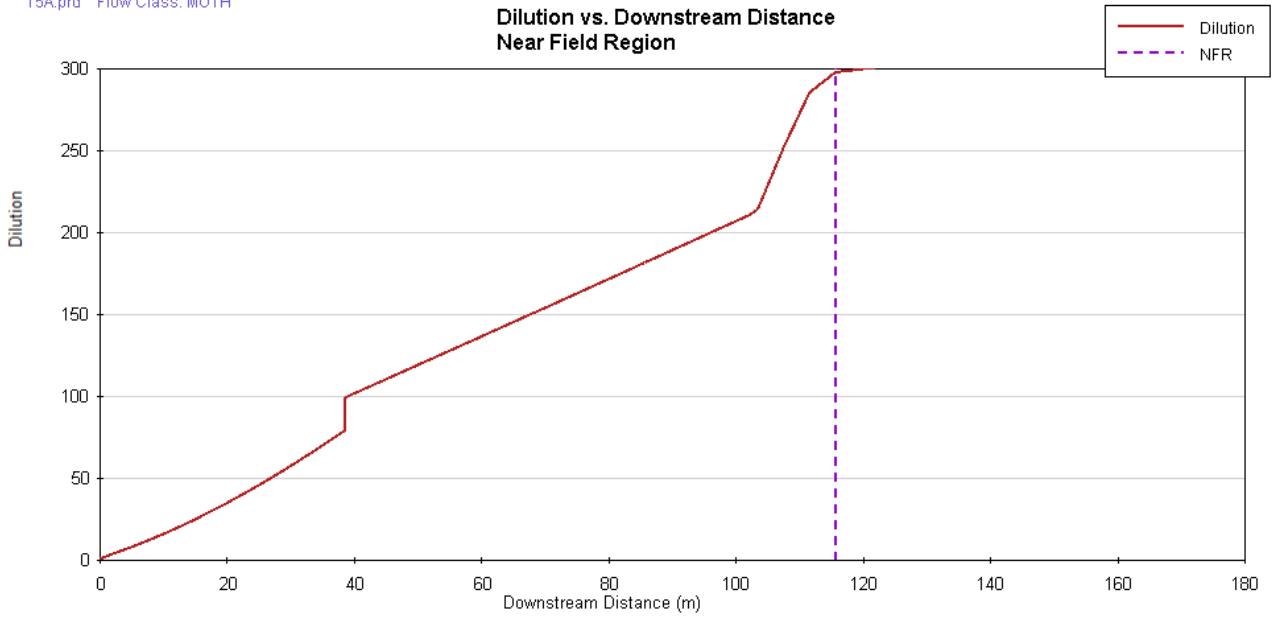


Figure A-13 Predicted dilution versus downstream distance for the 15 m offshore outfall, water depth of 15.1 m and ambient current of 0.08 m/s.

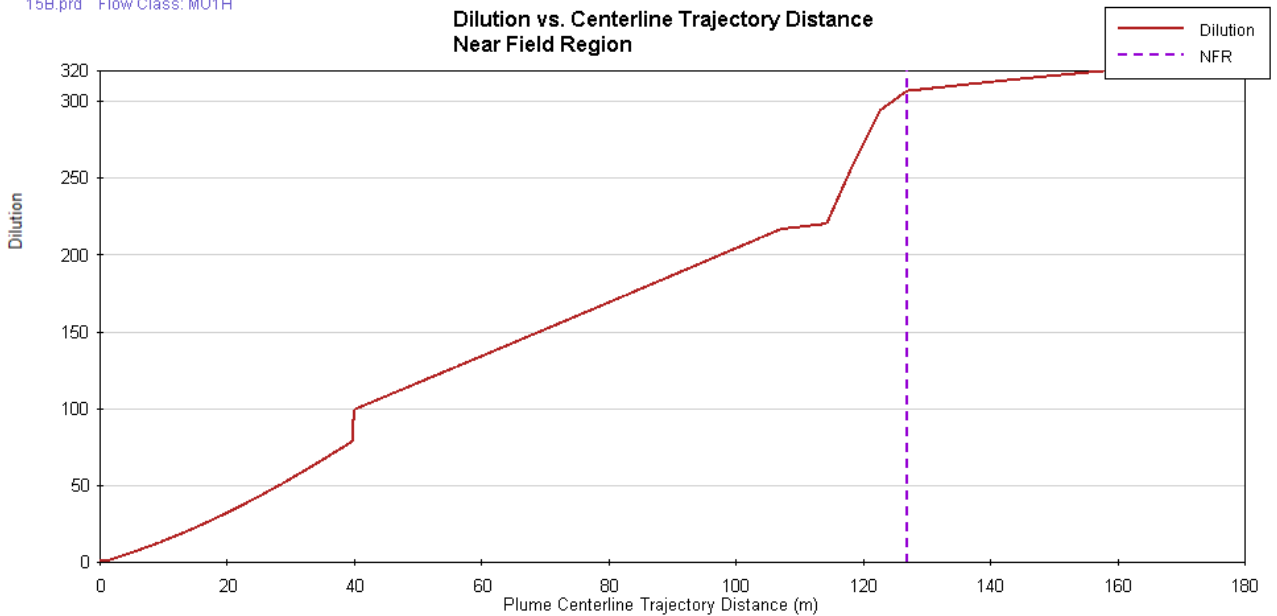


Figure A-14 Predicted dilution versus downstream distance for the 15 m offshore outfall, water depth of 15.5 m and ambient current of 0.08 m/s.

15C.prd Flow Class: MU8

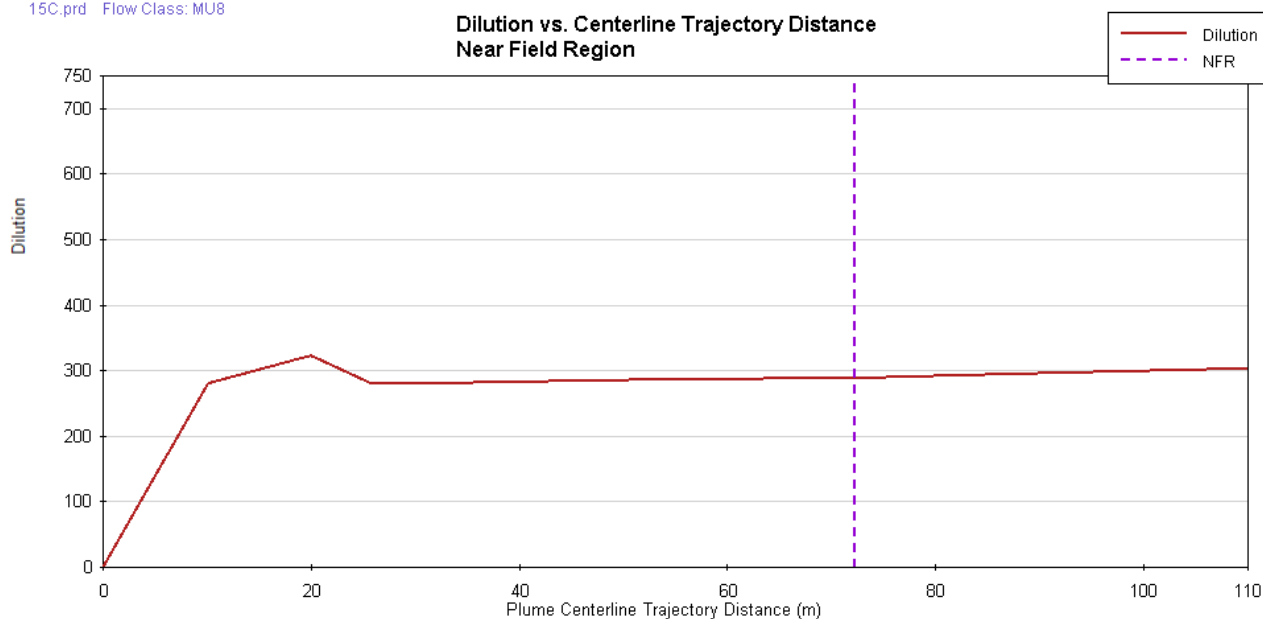


Figure A-15 Predicted dilution versus downstream distance for the 15 m offshore outfall, water depth of 15.9 m and ambient current of 0.16 m/s.

15D.prd Flow Class: MU8

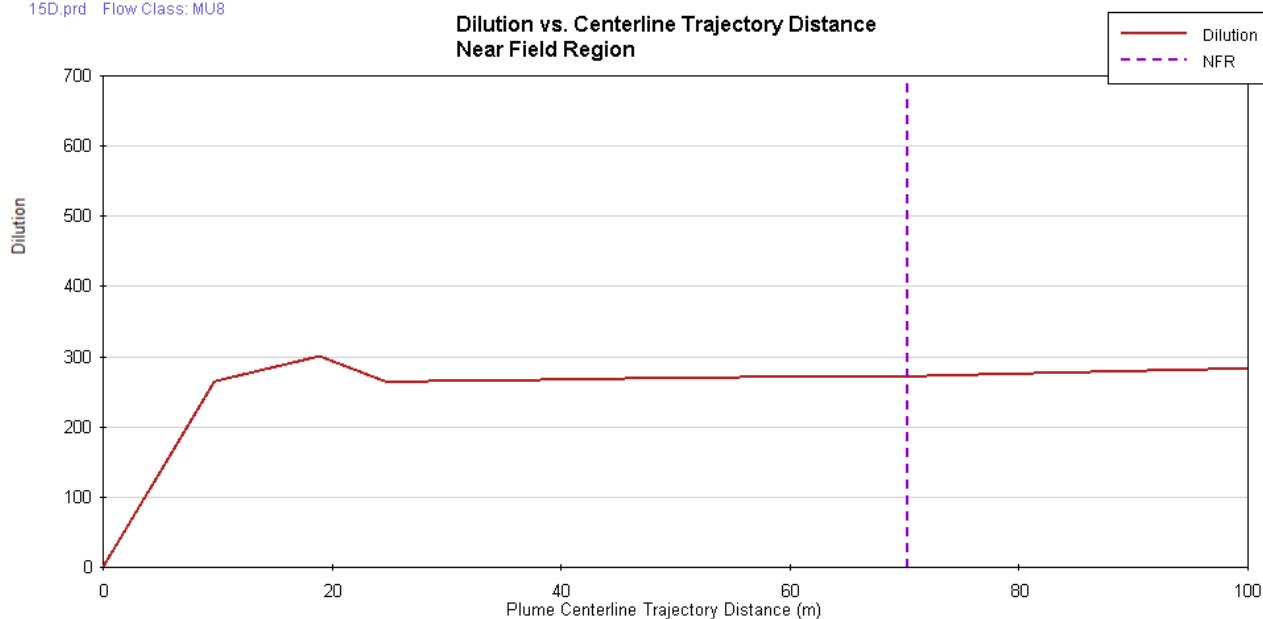


Figure A-16 Predicted dilution versus downstream distance for the 15 m offshore outfall, water depth of 15.0 m and ambient current of 0.16 m/s.

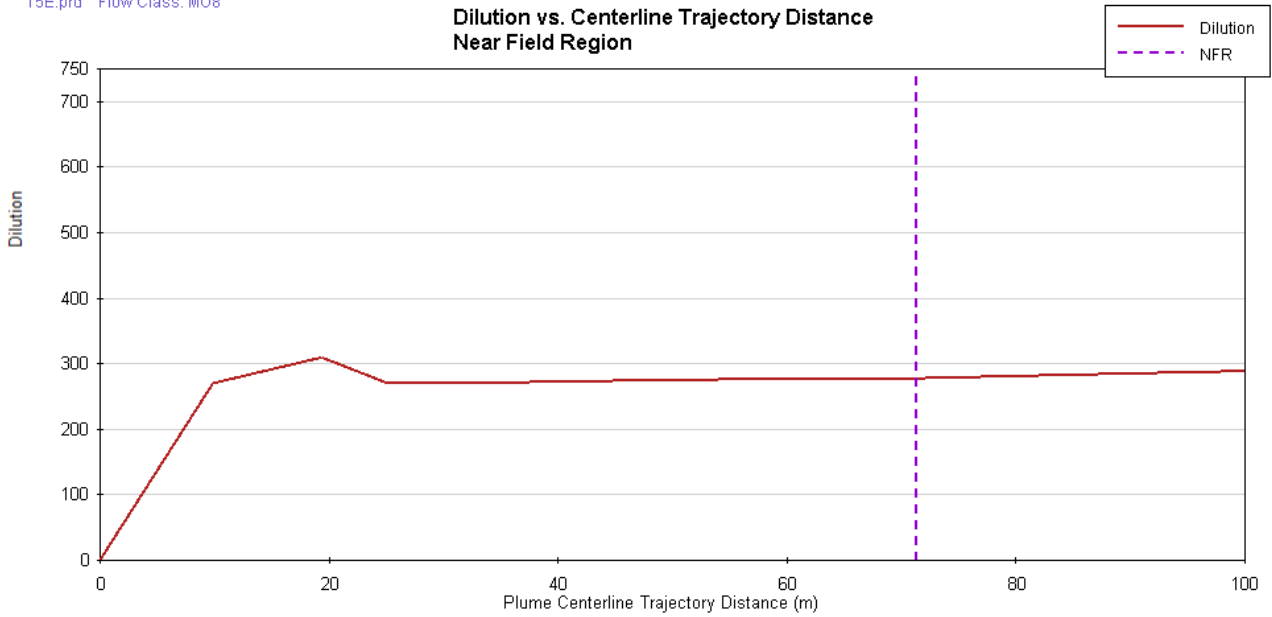


Figure A-17 Predicted dilution versus downstream distance for the 15 m offshore outfall, water depth of 15.3 m and ambient current of 0.16 m/s.

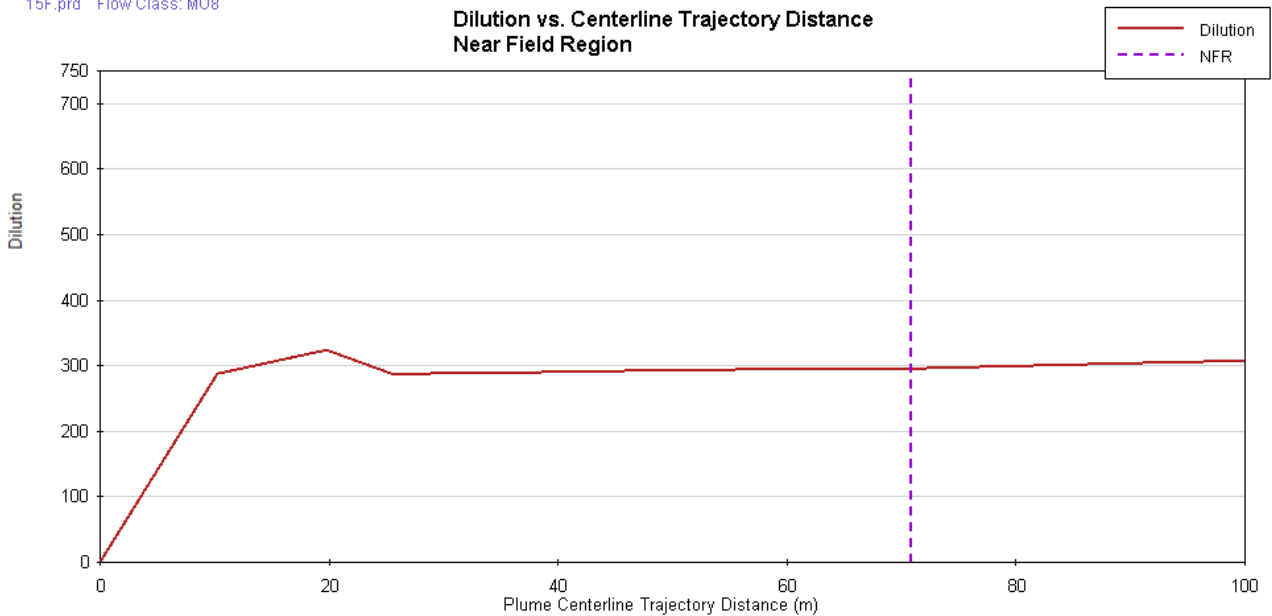


Figure A-18 Predicted dilution versus downstream distance for the 15 m offshore outfall, water depth of 16.3 m and ambient current of 0.16 m/s.

15G.prd Flow Class: MU8

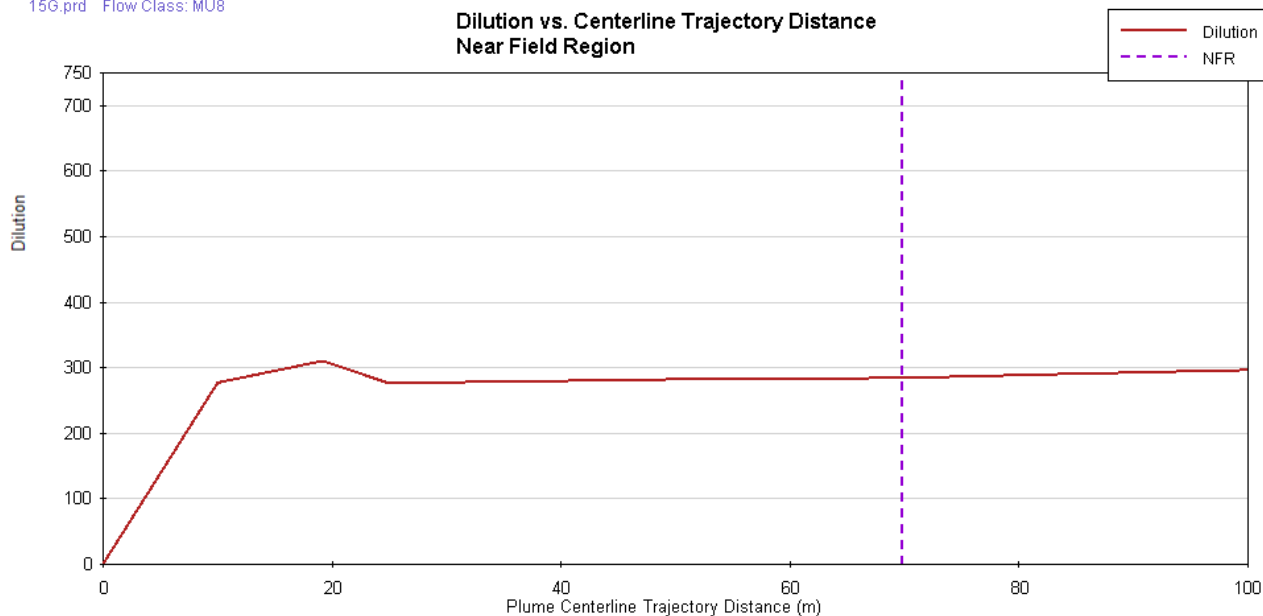


Figure A-19 Predicted dilution versus downstream distance for the 15 m offshore outfall, water depth of 15.7 m and ambient current of 0.16 m/s.

15H.prd Flow Class: MU8

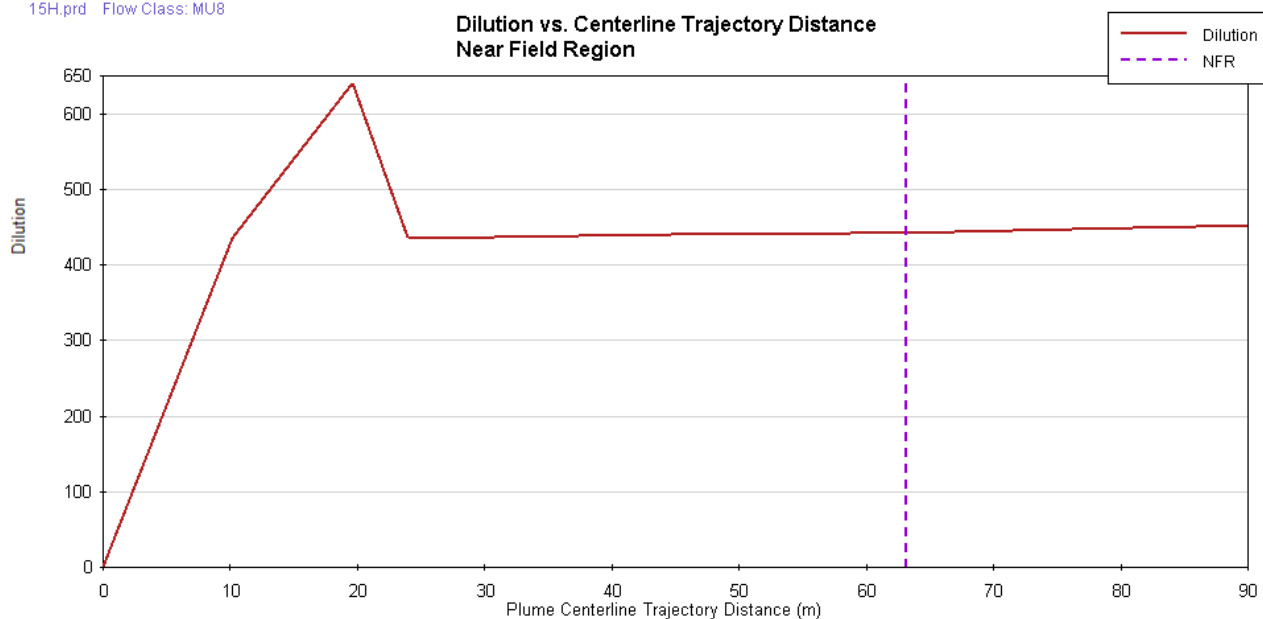


Figure A-20 Predicted dilution versus downstream distance for the 15 m offshore outfall, water depth of 16.1 m and ambient current of 0.26 m/s.

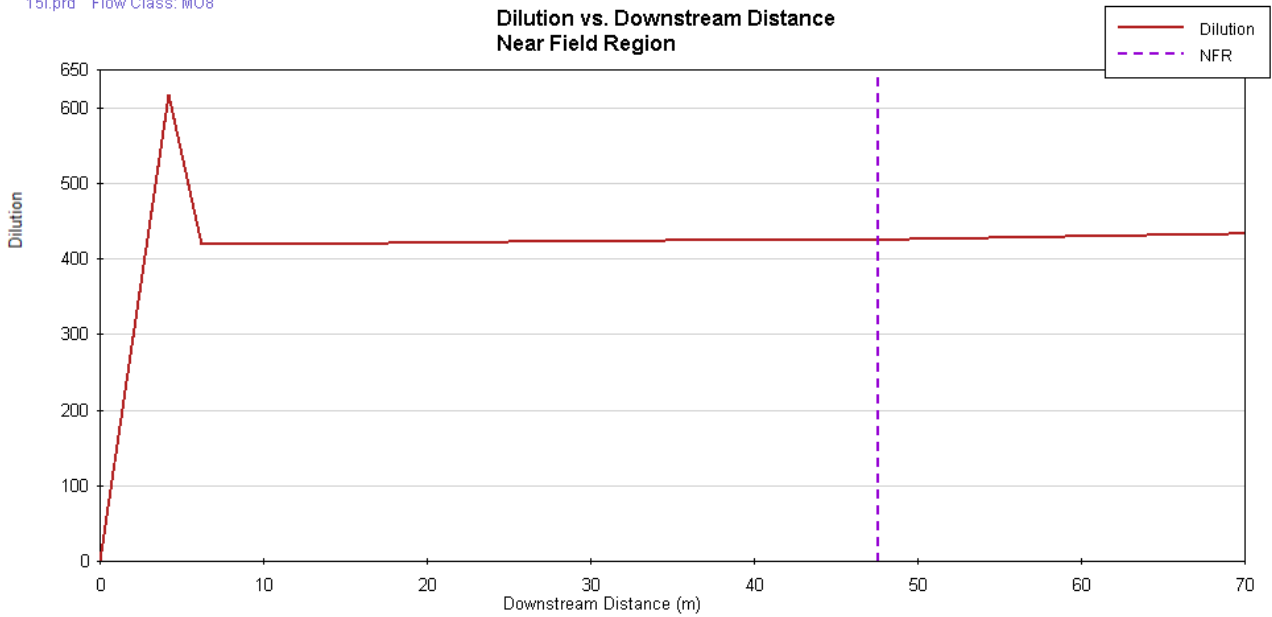


Figure A-21 Predicted dilution versus downstream distance for the 15 m offshore outfall, water depth of 15.5 m and ambient current of 0.26 m/s.

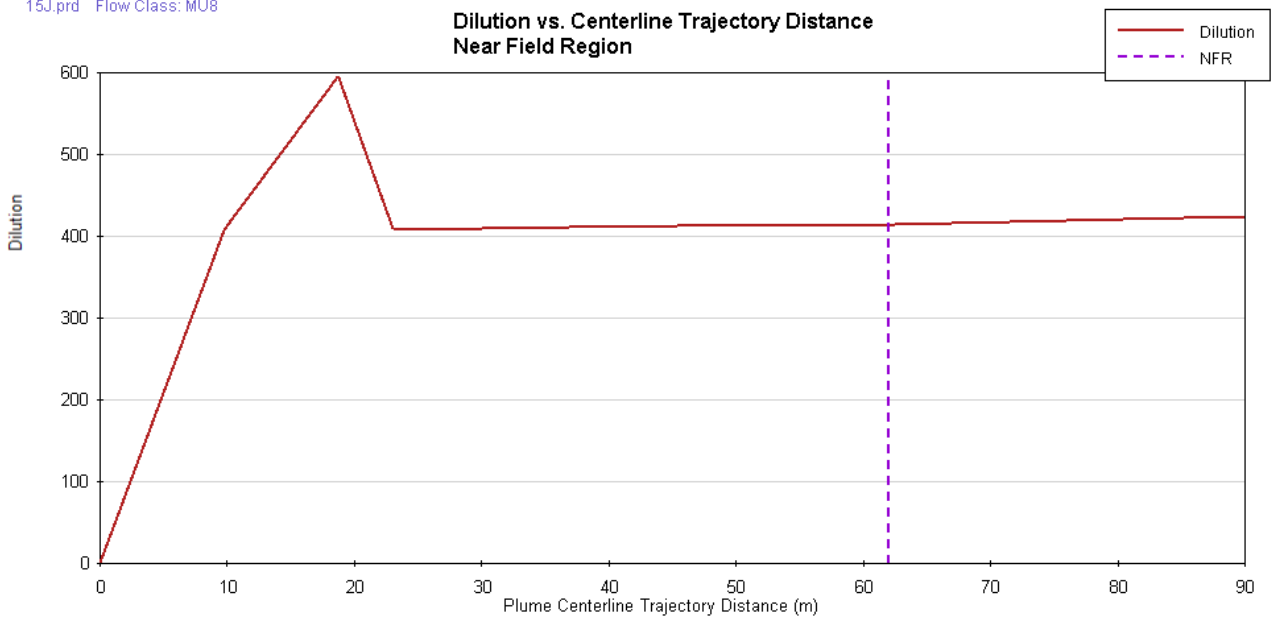


Figure A-22 Predicted dilution versus downstream distance for the 15 m offshore outfall, water depth of 15.1 m and ambient current of 0.26 m/s.

15K.prd Flow Class: MU8

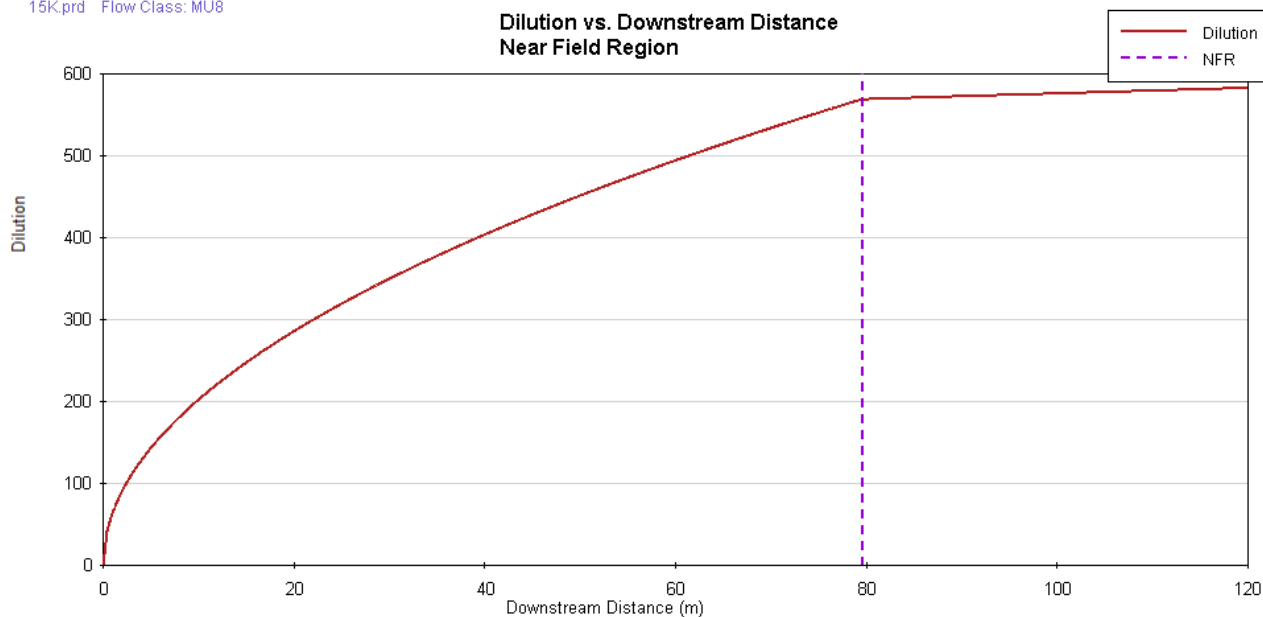


Figure A-23 Predicted dilution versus downstream distance for the 15 m offshore outfall, water depth of 15.9 m and ambient current of 0.35 m/s.

15L.prd Flow Class: MU8

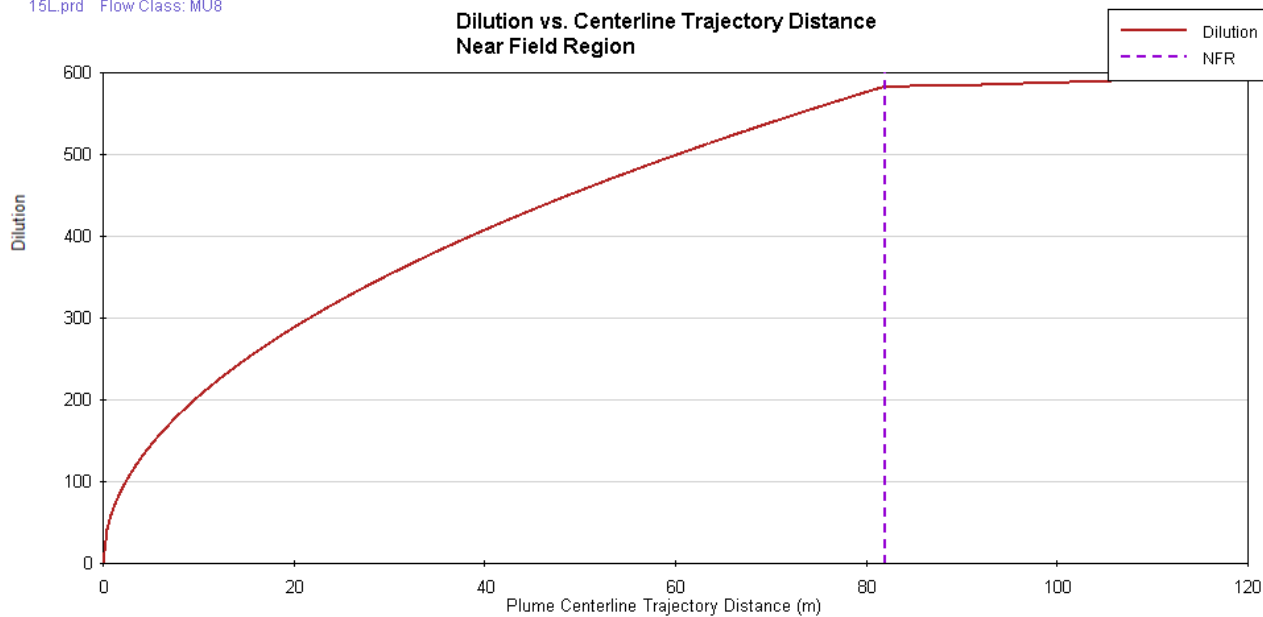


Figure A-24 Predicted dilution versus downstream distance for the 15 m offshore outfall, water depth of 16.3 m and ambient current of 0.35 m/s

Appendix B – Existing ADF time-series results at monitoring sites

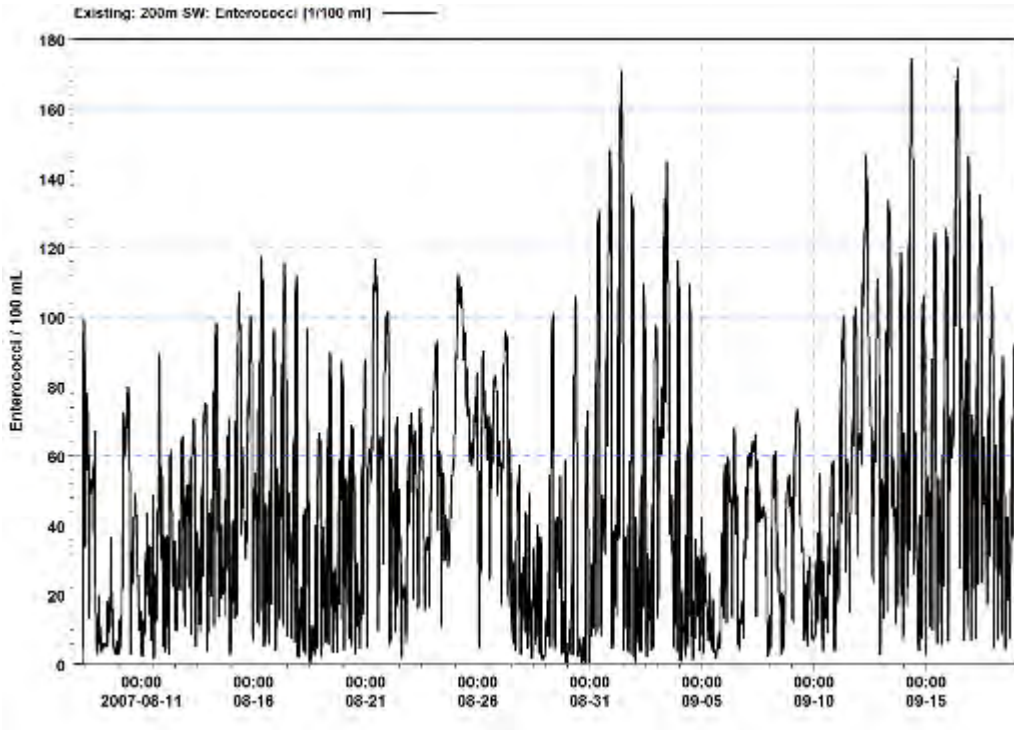


Figure B-1 Predicted Enterococci concentration (Ent/100 mL) at the monitoring site 200 m south-west of the existing shoreline discharge for the existing shoreline discharge for the current ADF flow rate of 300 L/s.

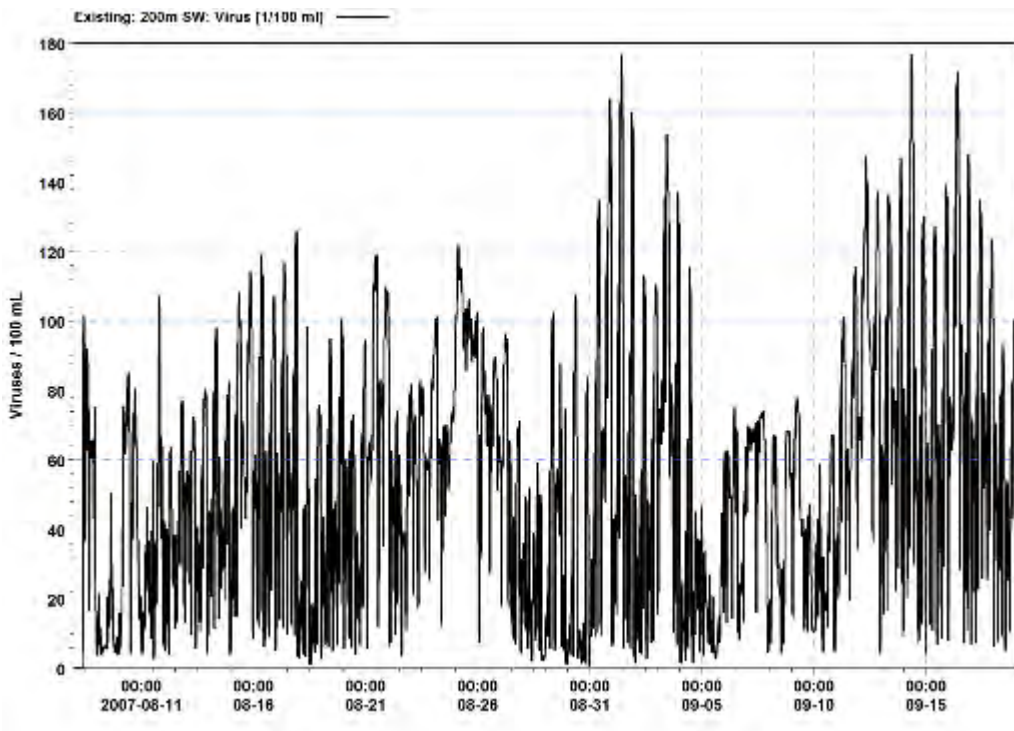


Figure B-2 Predicted Virus concentration (Virus /100 mL) at the monitoring site 200 m south-west of the existing shoreline discharge for the existing shoreline discharge for the current ADF flow rate of 300 L/s.

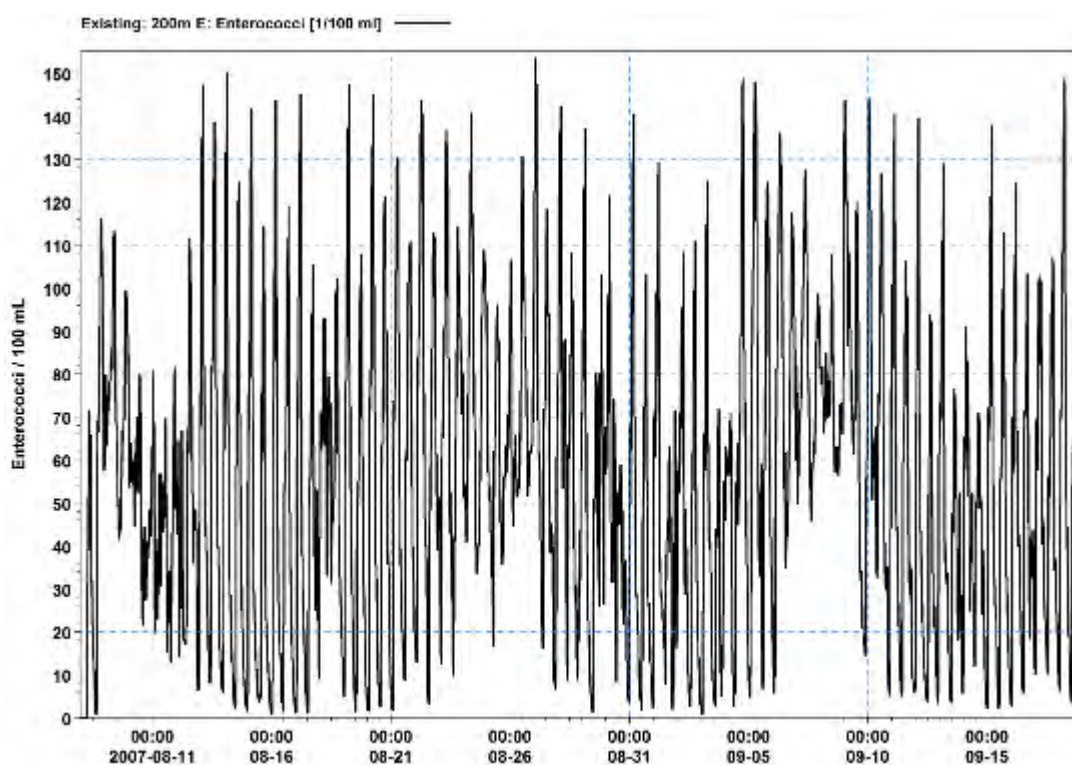


Figure B-3 Predicted Enterococci concentration (Ent/100 mL) at the monitoring site 200 m east of the existing shoreline discharge for the existing shoreline discharge the current ADF flow rate of 300 L/s.

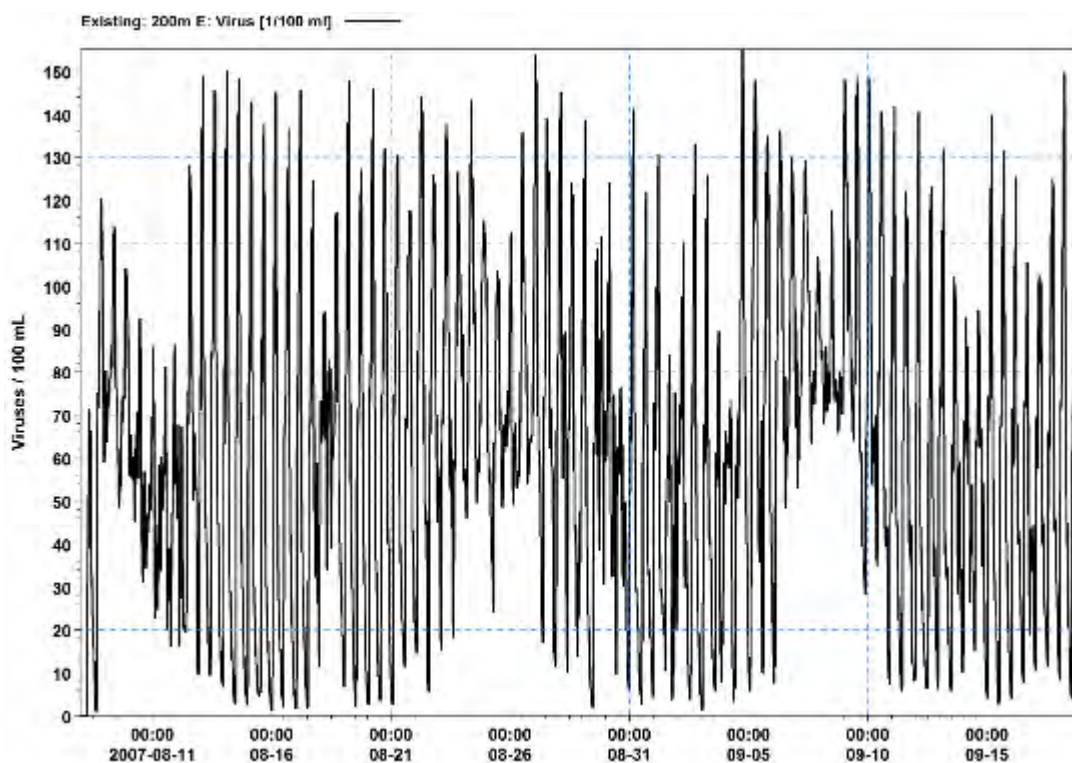


Figure B-4 Predicted Virus concentration (Virus/100 mL) at the monitoring site 200 m east of the existing shoreline discharge for the existing shoreline discharge for the current ADF flow rate of 300 L/s.

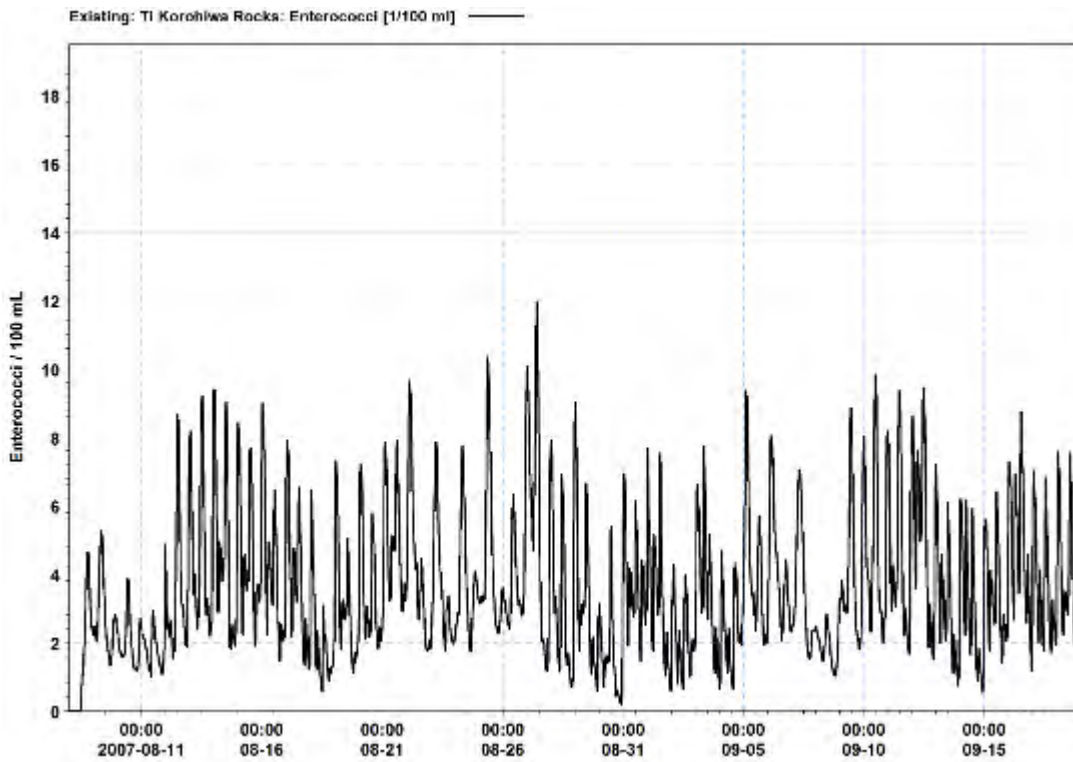


Figure B-5 Predicted Enterococci concentration (Ent/100 mL) at the Ti Korohiwa Rocks monitoring site for the existing shoreline discharge for the current ADF flow rate of 300 L/s.

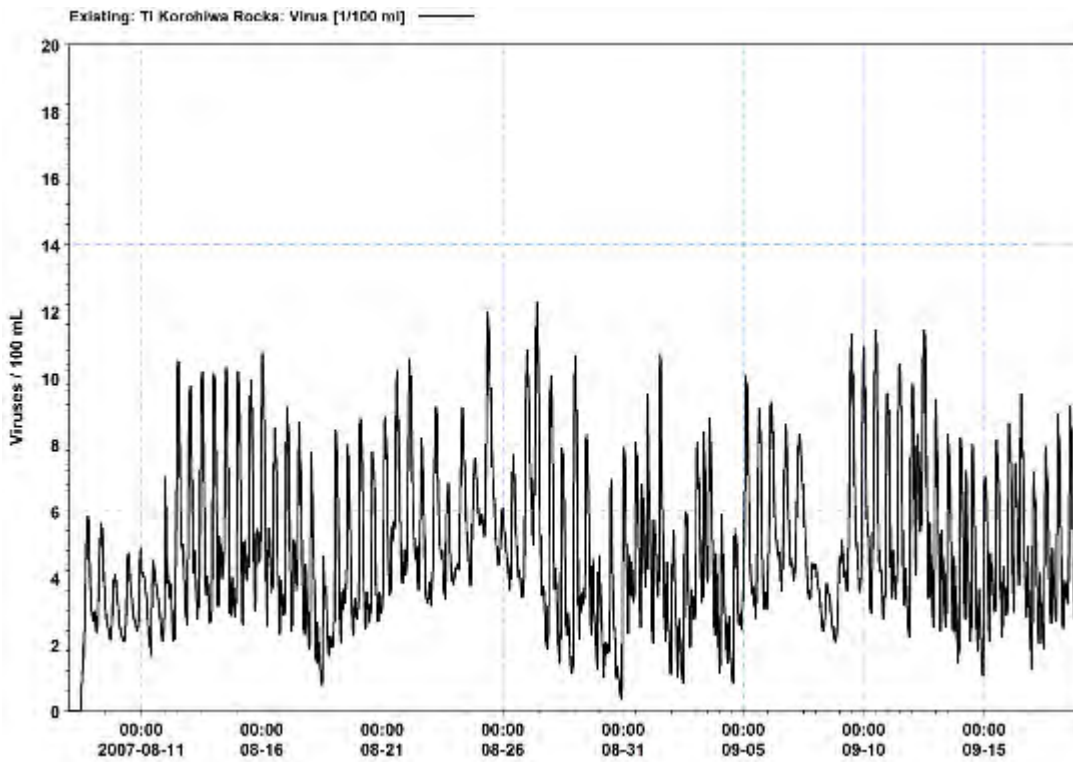


Figure B-6 Predicted Virus concentration (Virus/100 mL) at the Ti Korohiwa Rocks monitoring site for the existing shoreline discharge for the current ADF flow rate of 300 L/s.

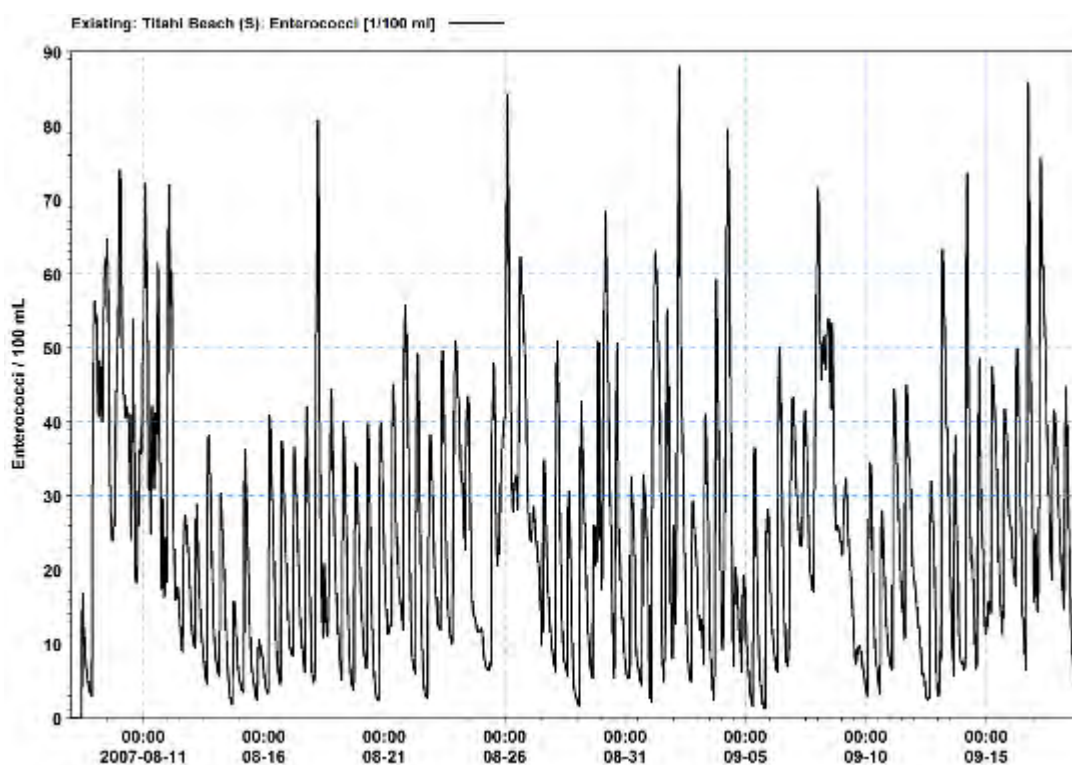


Figure B-7 Predicted Enterococci concentration (Ent/100 mL) at the Titahi Beach South monitoring site for the existing shoreline discharge for the current ADF flow rate of 300 L/s.

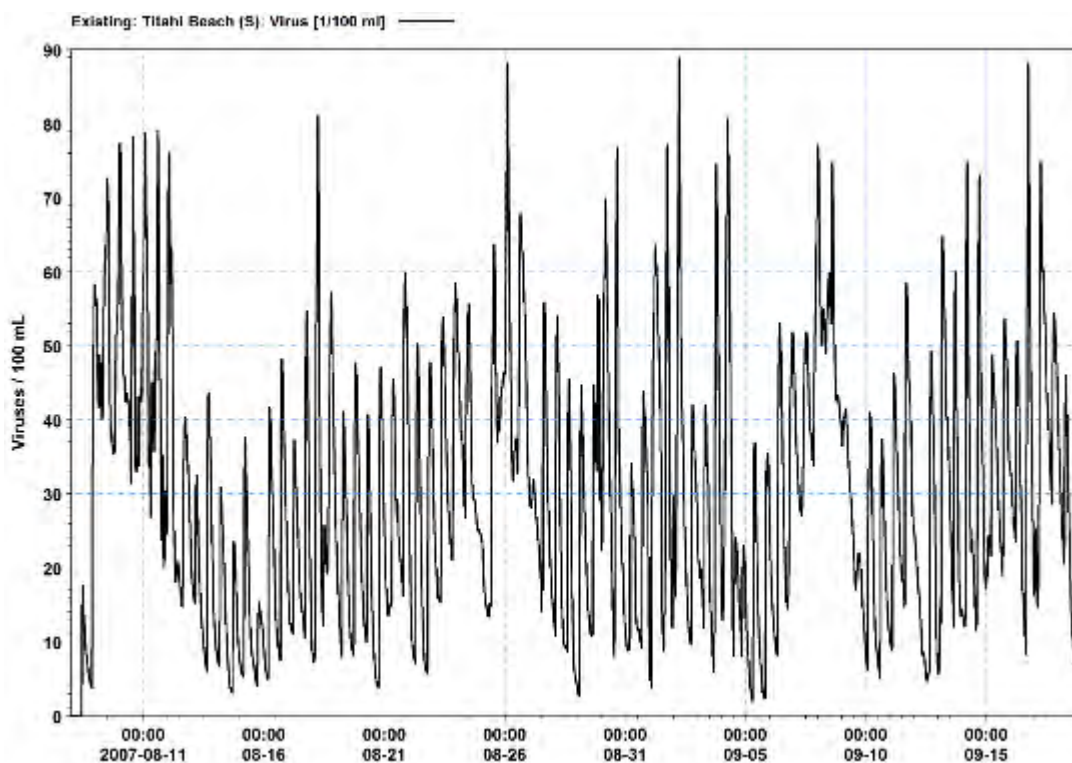


Figure B-8 Predicted Enterococci concentration (Ent/100 mL) at the Titahi Beach South monitoring site for the existing shoreline discharge for the current ADF flow rate of 300 L/s.

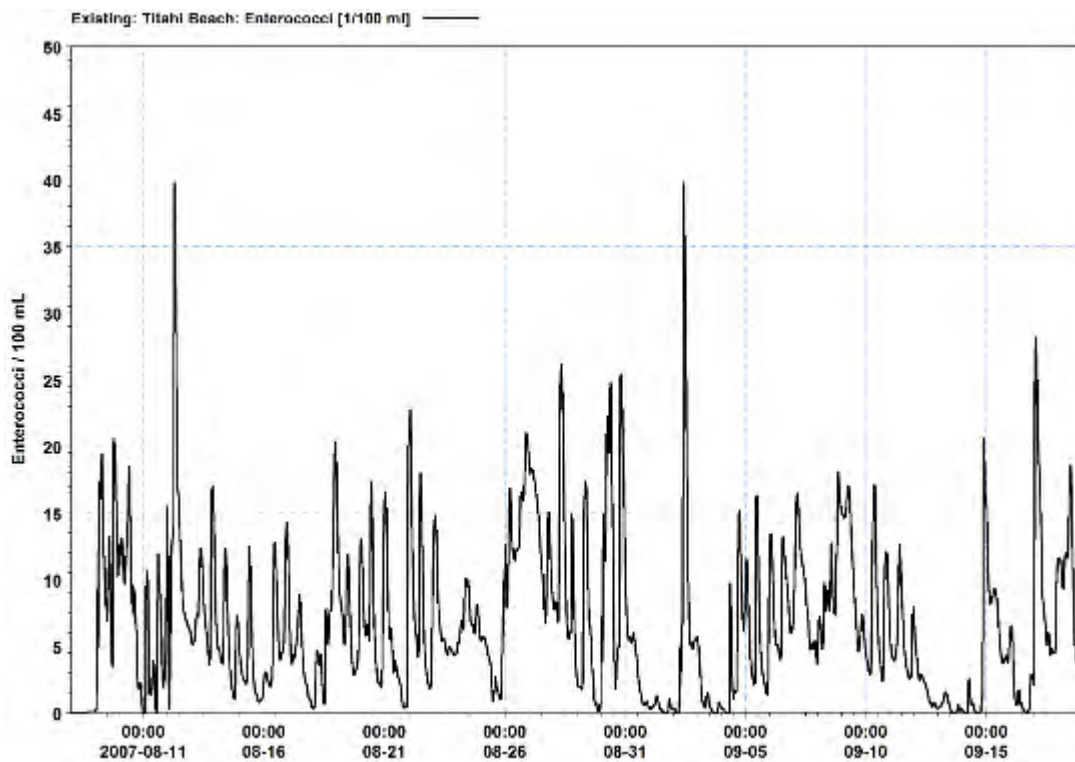


Figure B-9 Predicted Enterococci concentration (Ent/100 mL) at the Titahi Beach monitoring site for the existing shoreline discharge for the current ADF flow rate of 300 L/s.

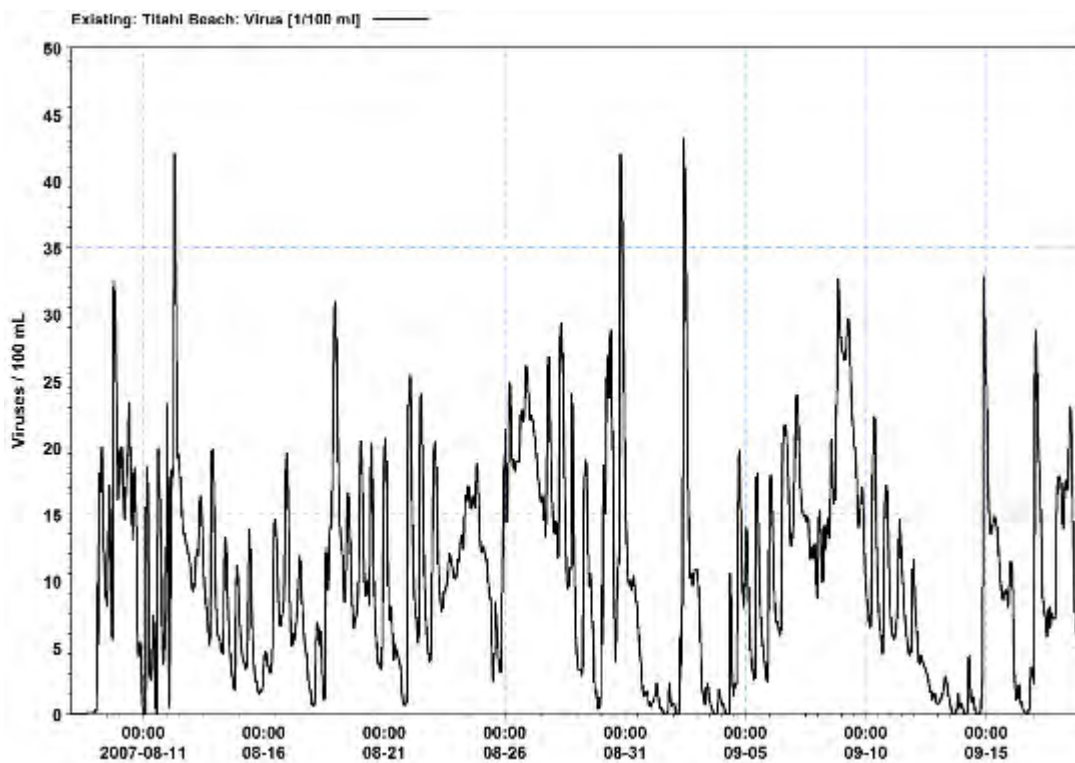


Figure B-10 Predicted Virus concentration (Virus/100 mL) at the Titahi Beach monitoring site for the existing shoreline discharge for the current ADF flow rate of 300 L/s.

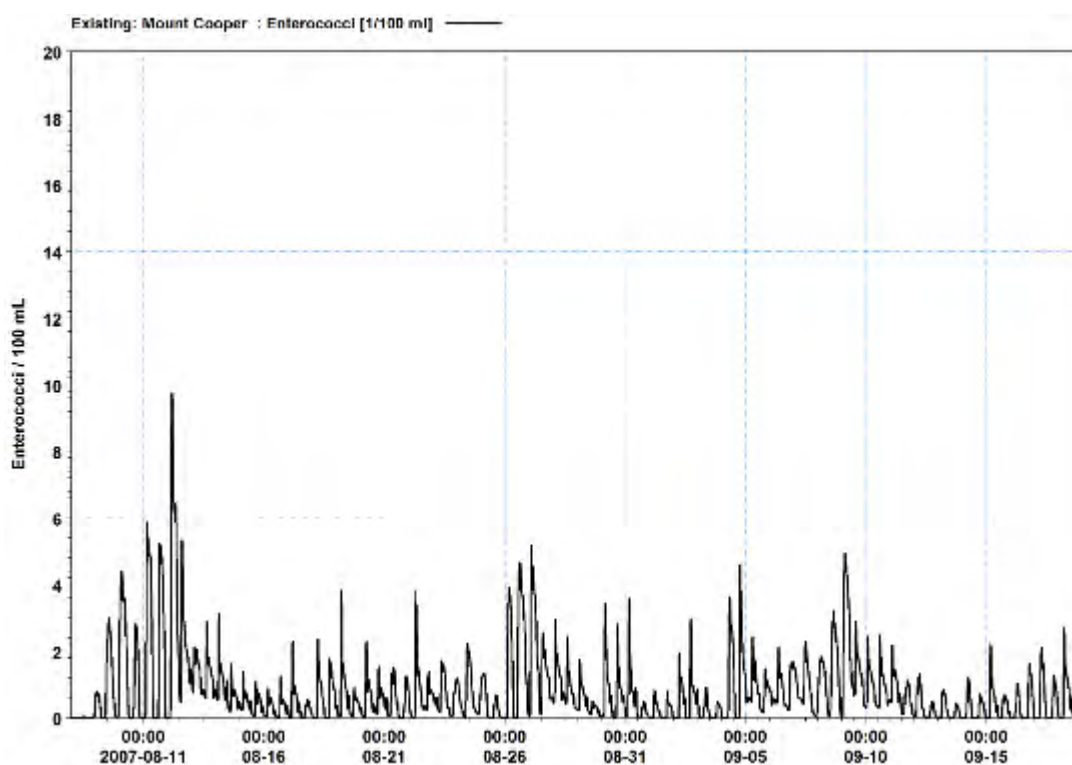


Figure B-11 Predicted Enterococci concentration (Ent/100 mL) at the Mount Couper monitoring site for the existing shoreline discharge for the current ADF flow rate of 300 L/s.

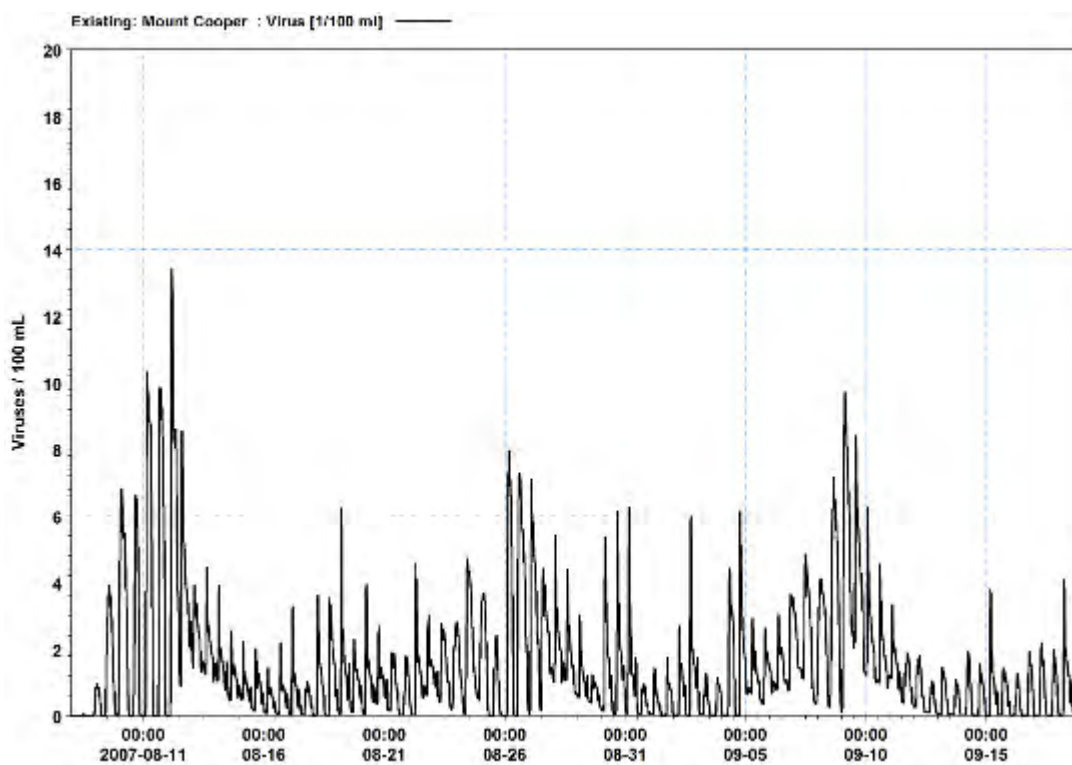


Figure B-12 Predicted Virus concentration (Virus/100 mL) at the Mount Couper monitoring site for the existing shoreline discharge for the current ADF flow rate of 300 L/s.

Appendix C – Time-series results at monitoring sites for a 390 L/s Future ADF

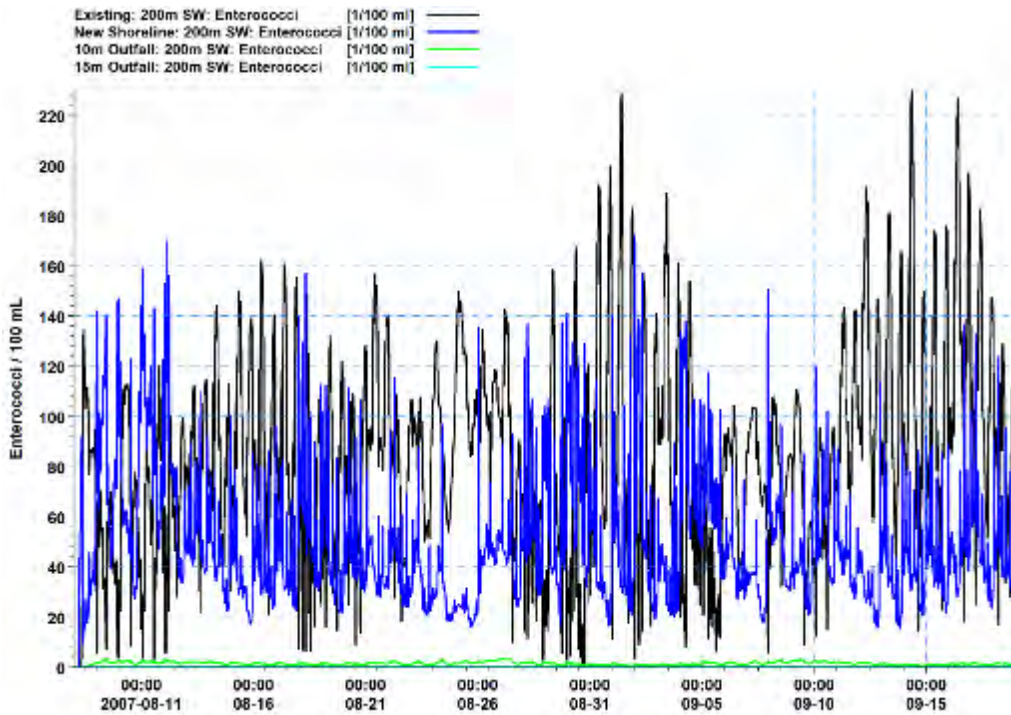


Figure C-1 Predicted Enterococci concentration (Ent/100 ml) at the monitoring site 200 m south-west of the existing shoreline discharge for the future ADF flow rate of 390 L/s.

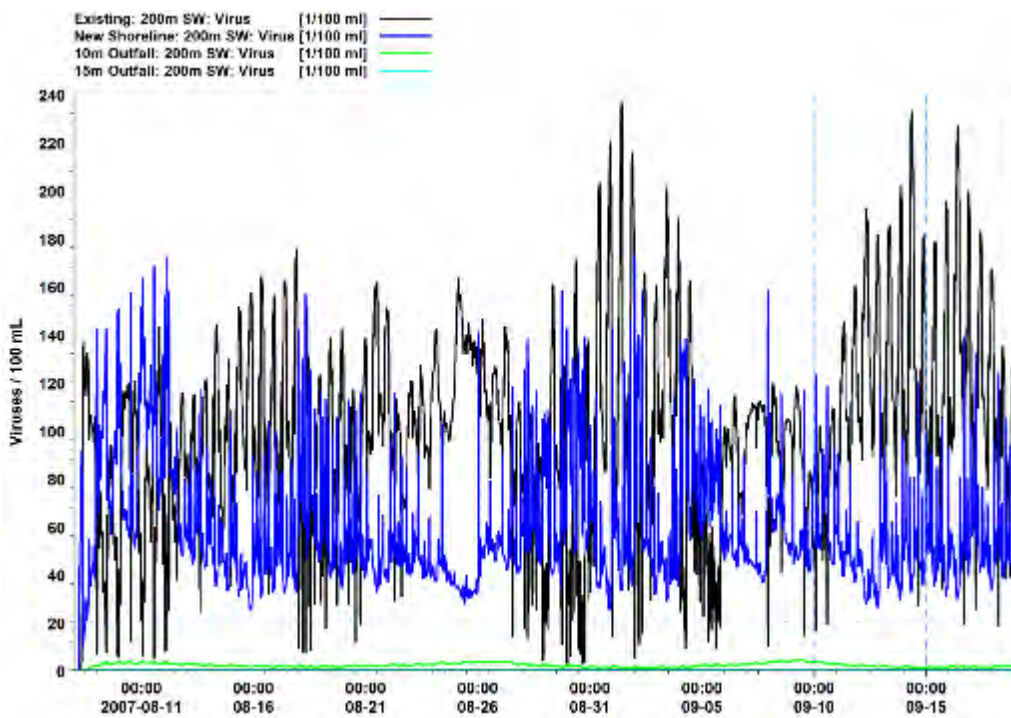


Figure C-2 Predicted Virus concentration (Virus/100 ml) at the monitoring site 200 m south-west of the existing shoreline discharge for the future ADF flow rate of 390 L/s.

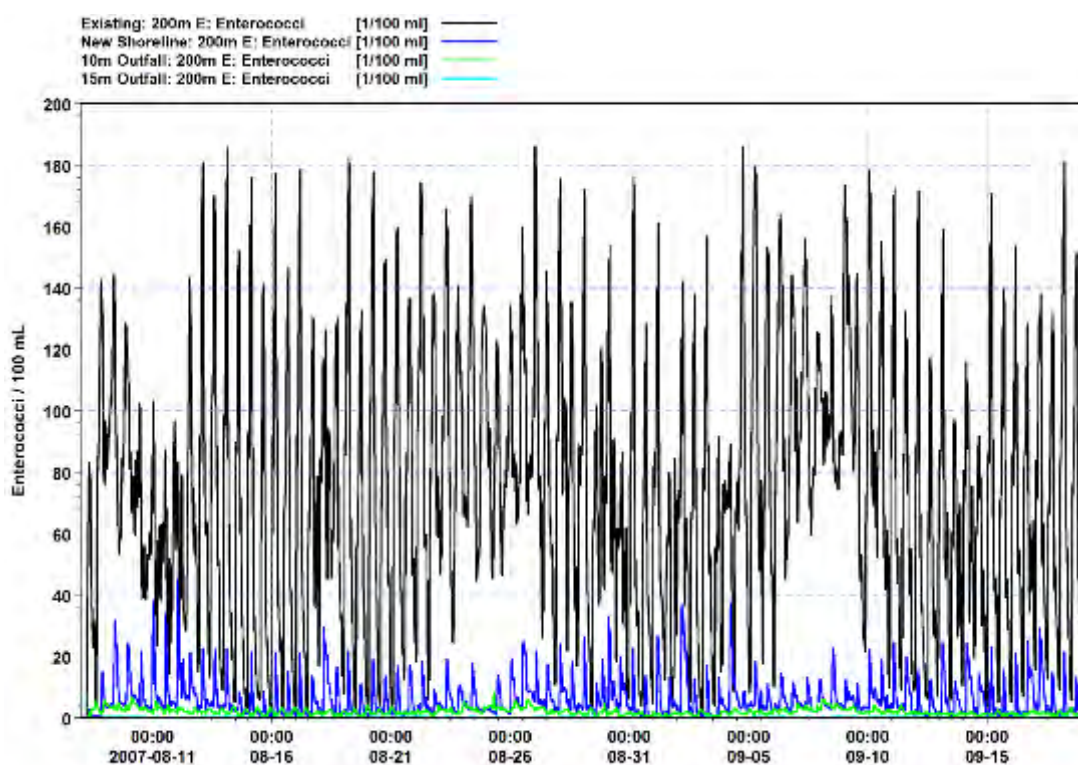


Figure C-3 Predicted Enterococci concentration (Ent/100 ml) at the monitoring site 200 m east of the existing shoreline discharge for the future ADF flow rate of 390 L/s.

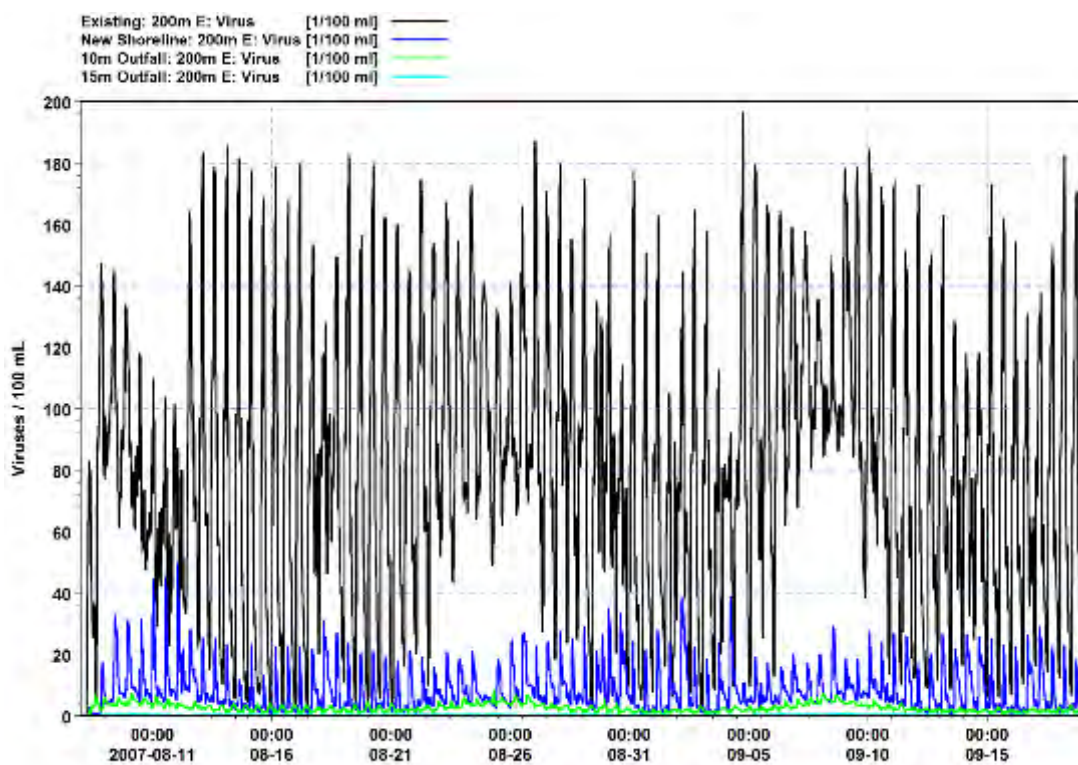


Figure C-4 Predicted Virus concentration (Virus/100 ml) at the monitoring site 200 m east of the existing shoreline discharge for the future ADF flow rate of 390 L/s.

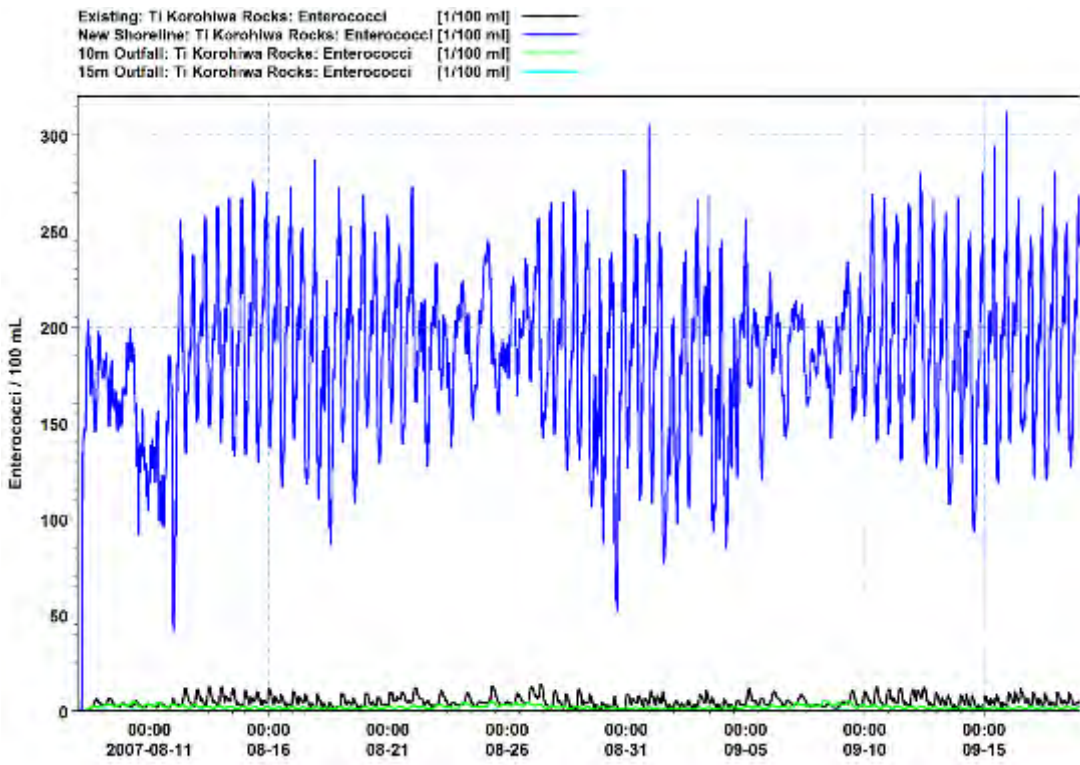


Figure C-5 Predicted Enterococci concentration (Ent/100 ml) at the Ti Korohiwa monitoring site for the discharge options for the future ADF flow rate of 390 L/s.

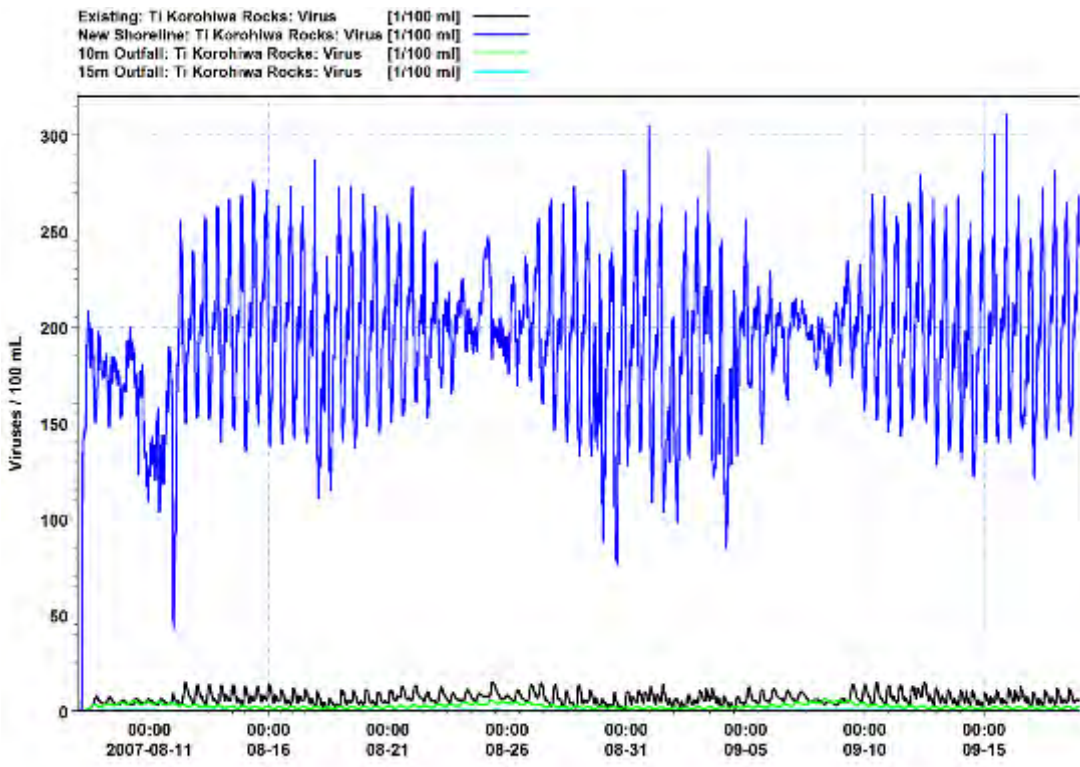


Figure C-6 Predicted Virus concentration (Virus/100 ml) at the Ti Korohiwa monitoring site for the discharge options for the future ADF flow rate of 390 L/s.

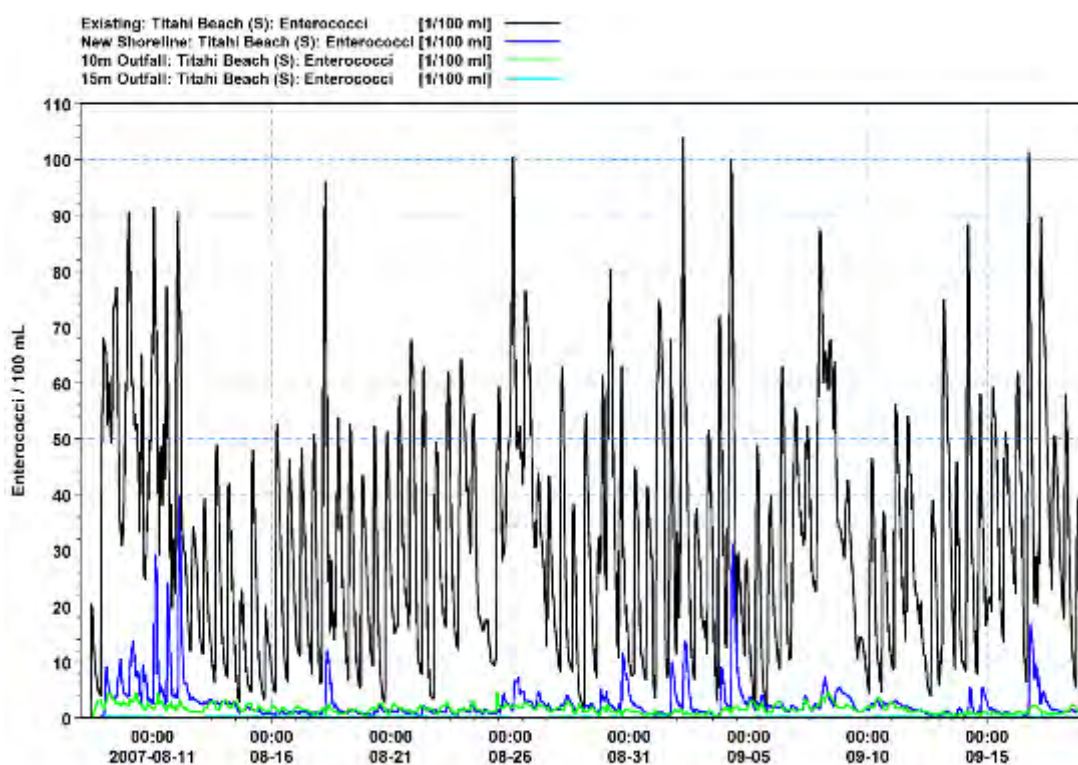


Figure C-7 Predicted Enterococci concentration (Ent/100 ml) at the Titahi Beach South monitoring site for the discharge options for the future ADF flow rate of 390 L/s.

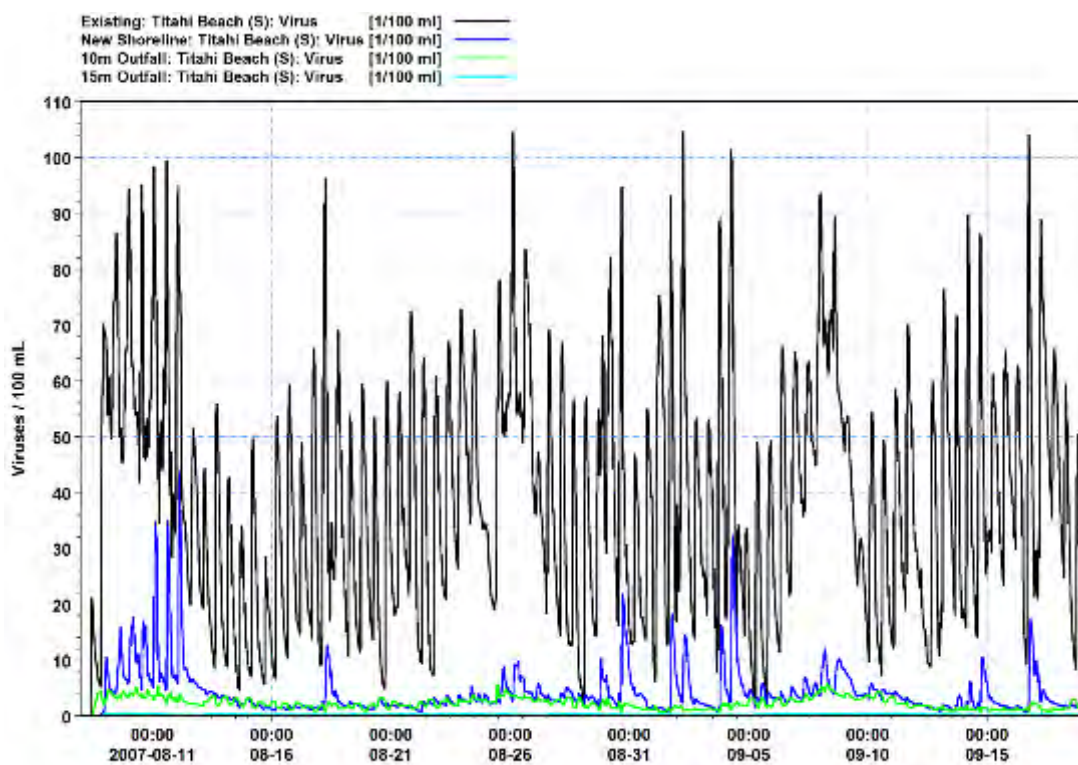


Figure C-8 Predicted Virus concentration (Virus/100 ml) at the Titahi Beach South monitoring site for the discharge options for the future ADF flow rate of 390 L/s.

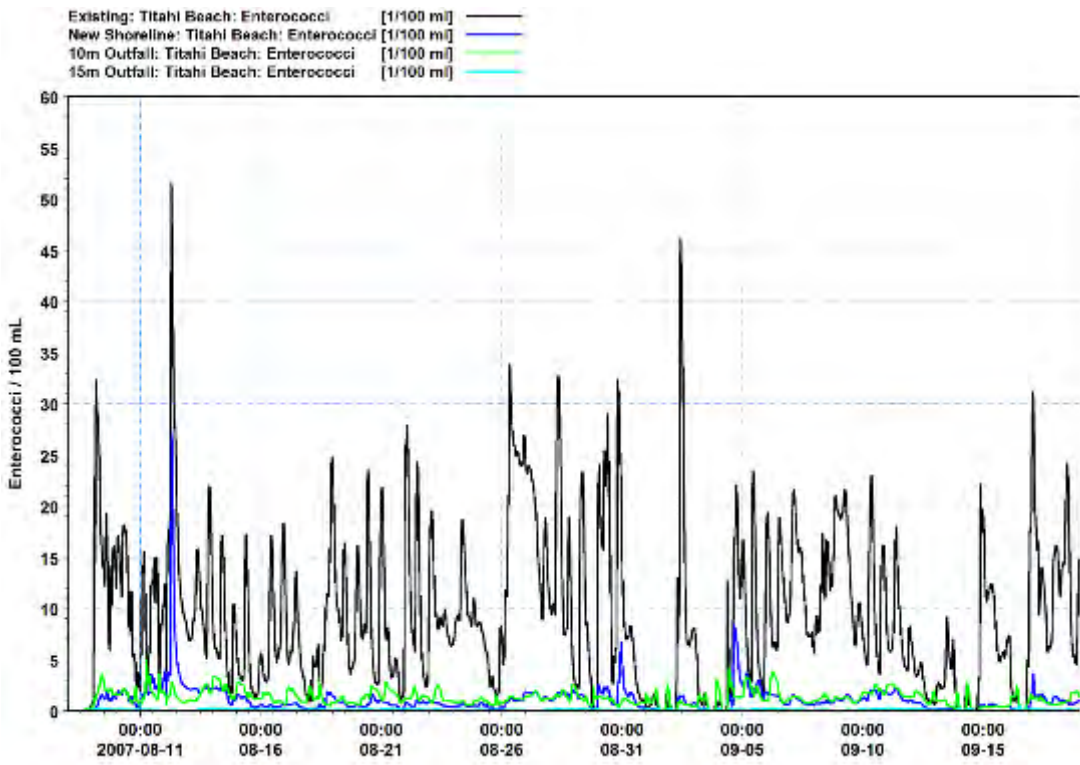


Figure C-9 Predicted Enterococci concentration (Ent/100 ml) at the Titahi Beach monitoring site for the discharge options for the future ADF flow rate of 390 L/s.

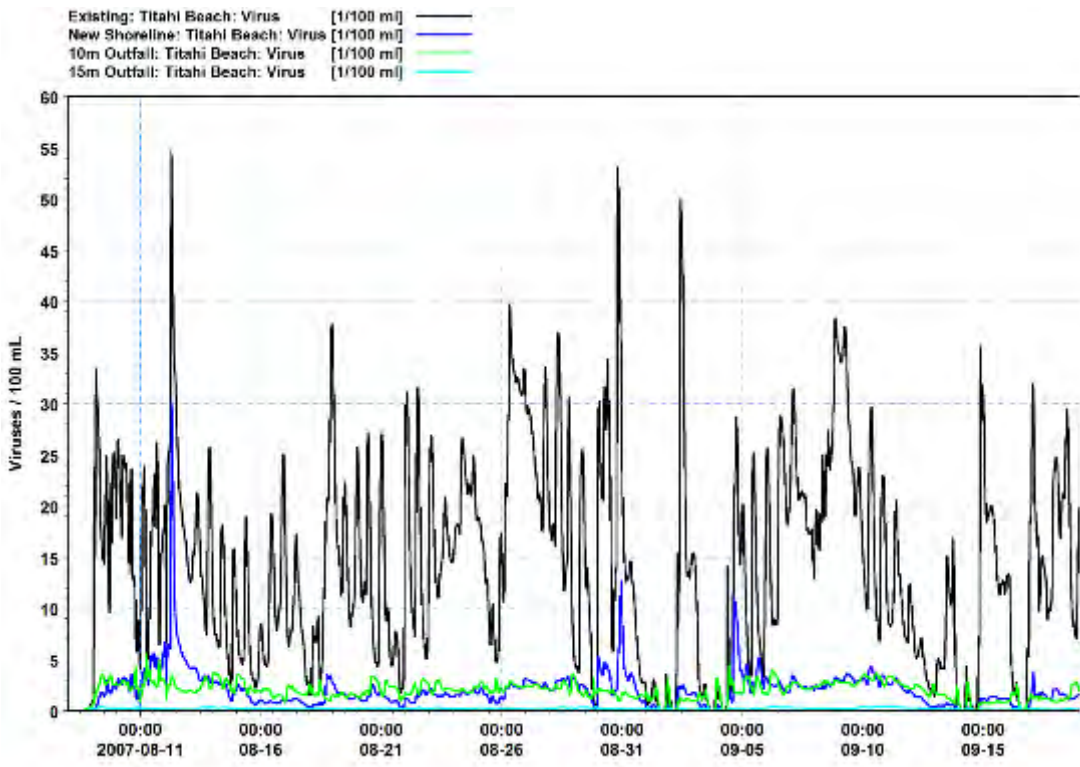


Figure C-10 Predicted Virus concentration (Virus/100 ml) at the Titahi Beach monitoring site for the discharge options for the future ADF flow rate of 390 L/s.

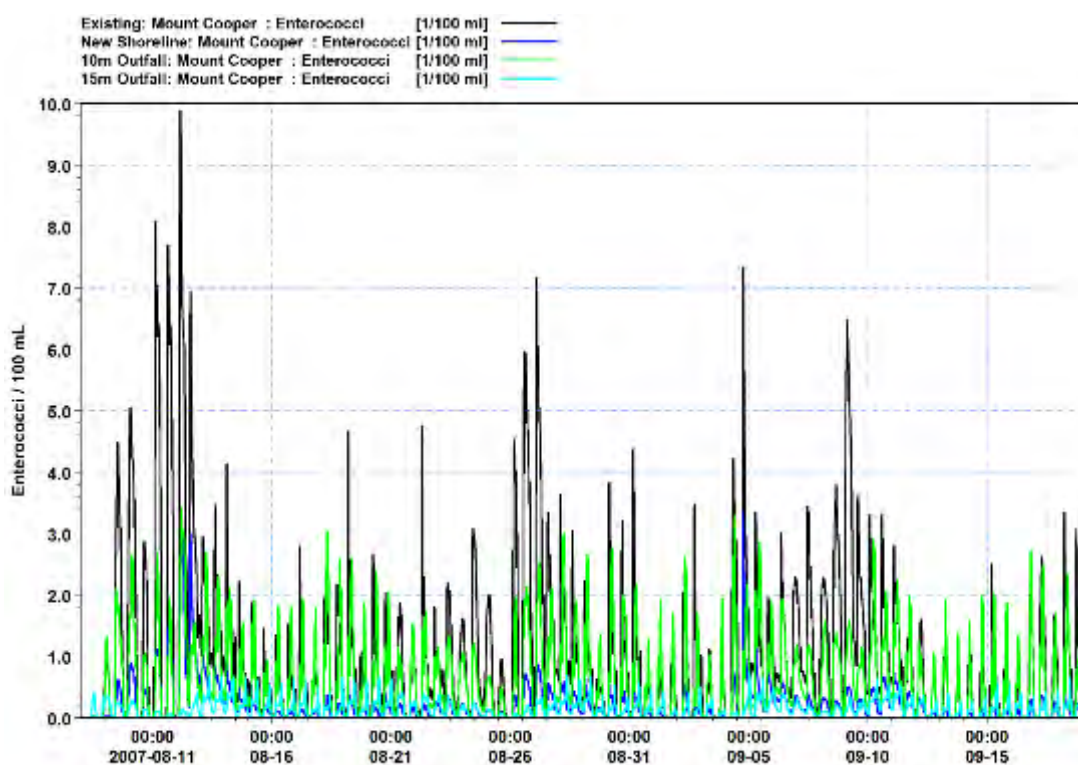


Figure C-11 Predicted Enterococci concentration (Ent/100 ml) at the Mount Couper monitoring site for the discharge options for the future ADF flow rate of 390 L/s.

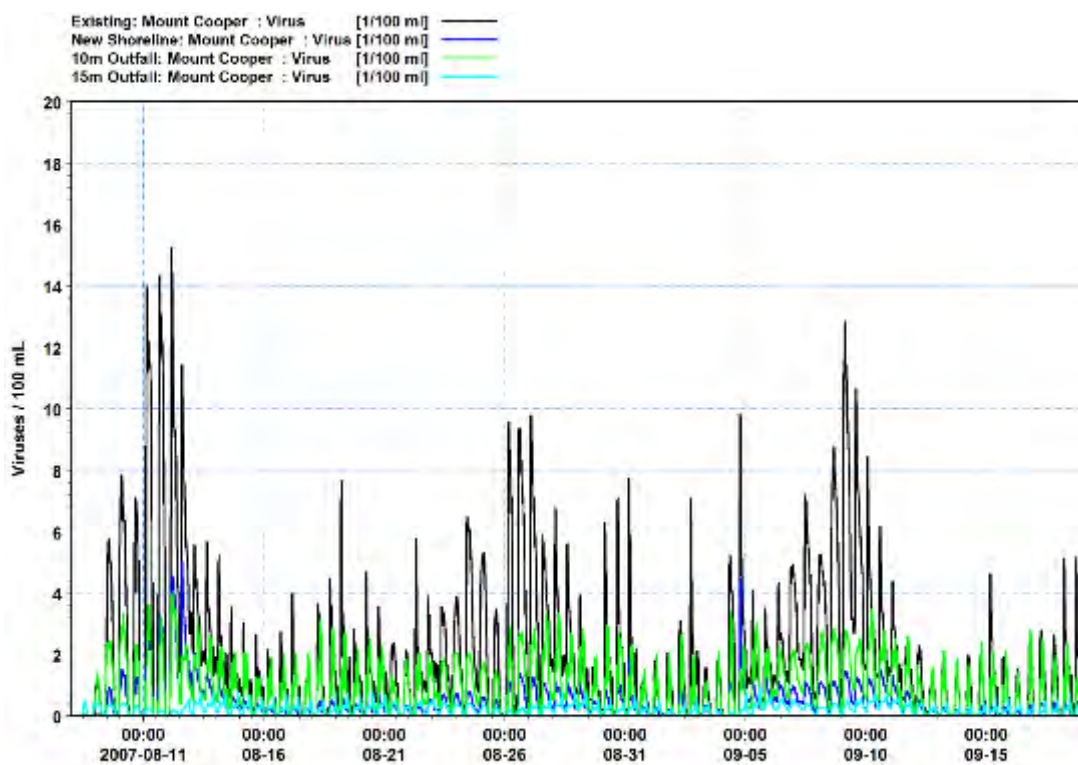


Figure C-12 Predicted Virus concentration (Virus/100 ml) at the Mount Couper monitoring site for the discharge options for the future ADF flow rate of 390 L/s.

Appendix D – Time-series at Monitoring site 200 m SW of existing discharge (PWWF discharge and overflow scenarios)

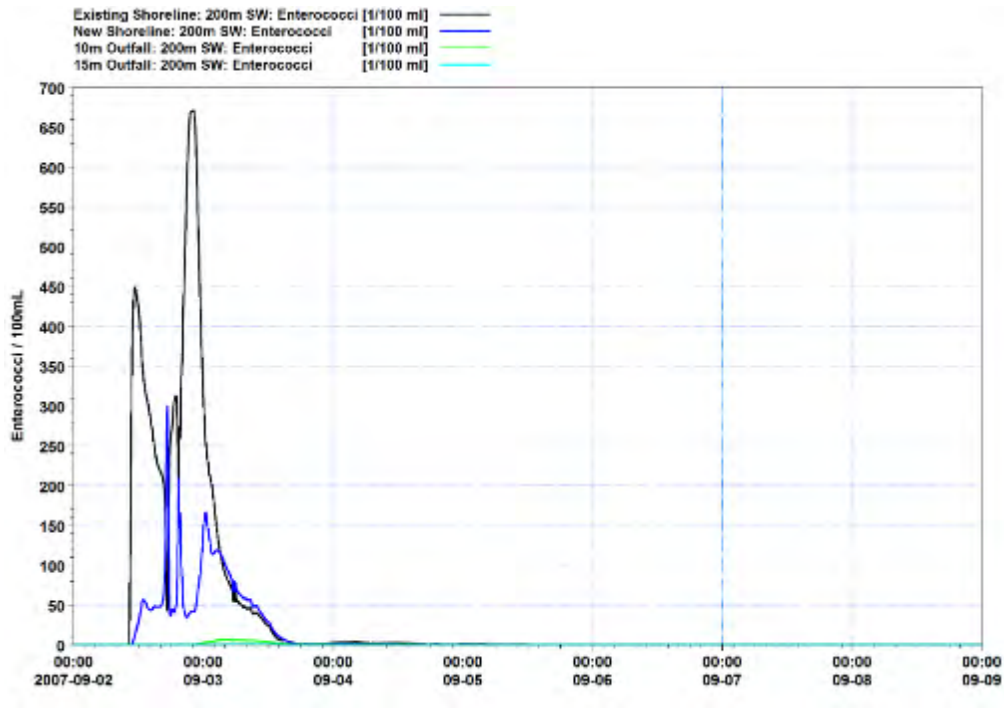


Figure D-1 Predicted Enterococci (Ent/100 ml) at the monitoring site 200 m south-west of the existing shoreline discharge for the future PWWF discharge options for typical winds and a spring tide.

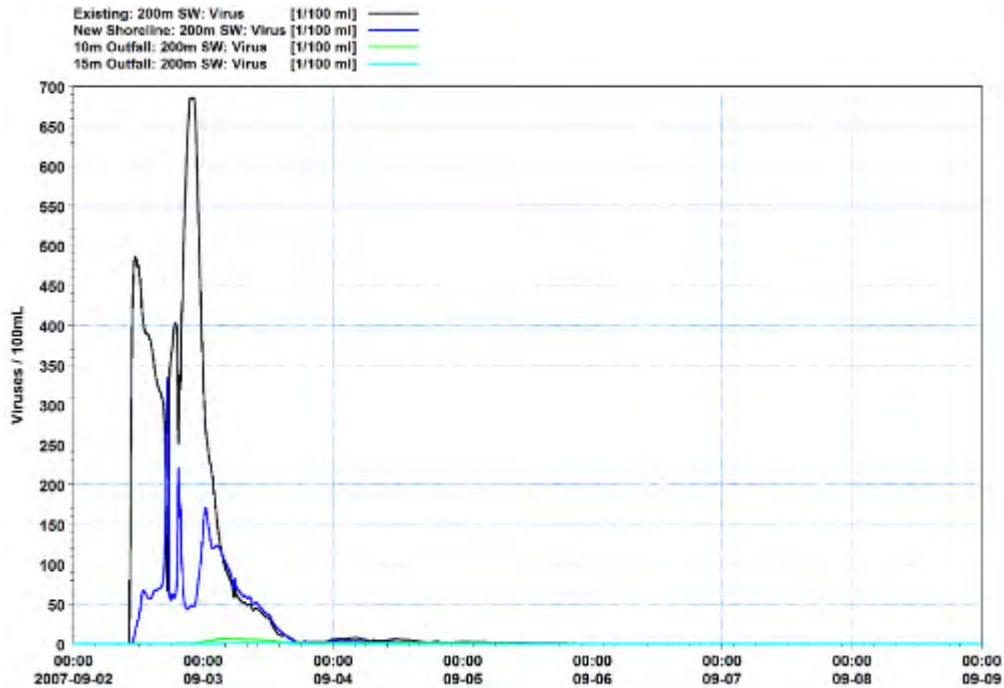


Figure D-2 Predicted Virus (Virus/100 ml) at the monitoring site 200 m south-west of the existing shoreline discharge for the future PWWF discharge options for typical winds and a spring tide.

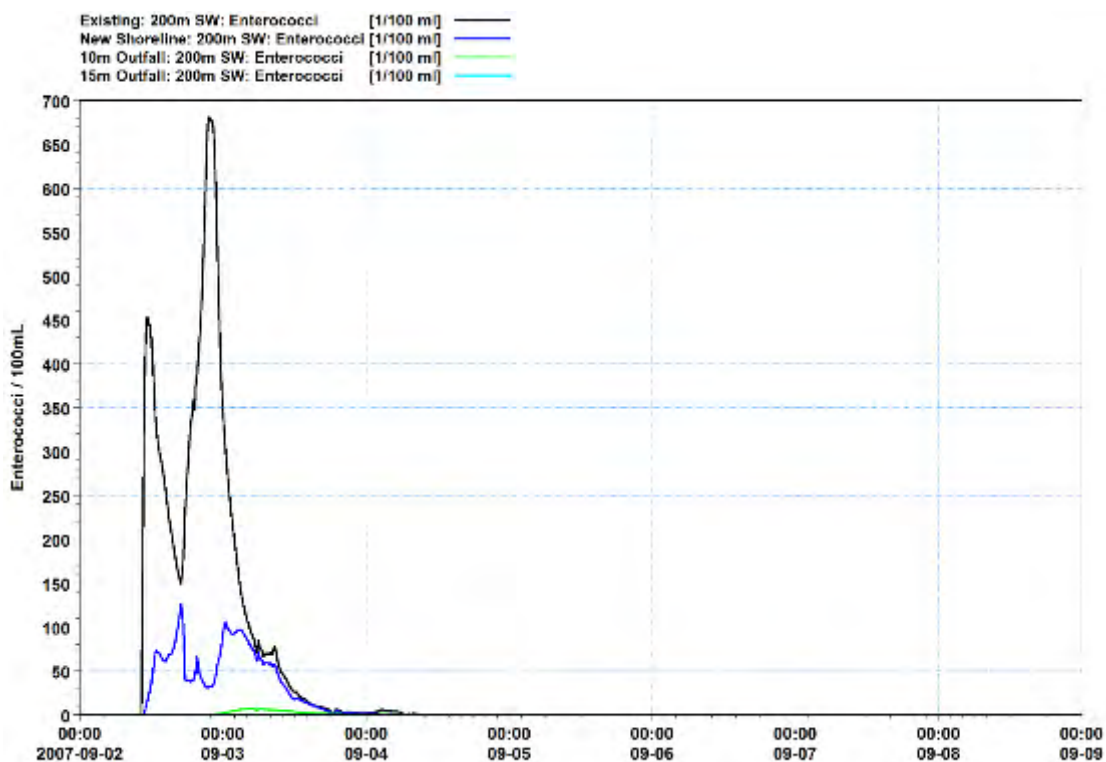


Figure D-3 Predicted Enterococci (Ent/100 ml) at the monitoring site 200 m south-west of the existing shoreline discharge for the future PWWF discharge options for onshore winds and a spring tide.

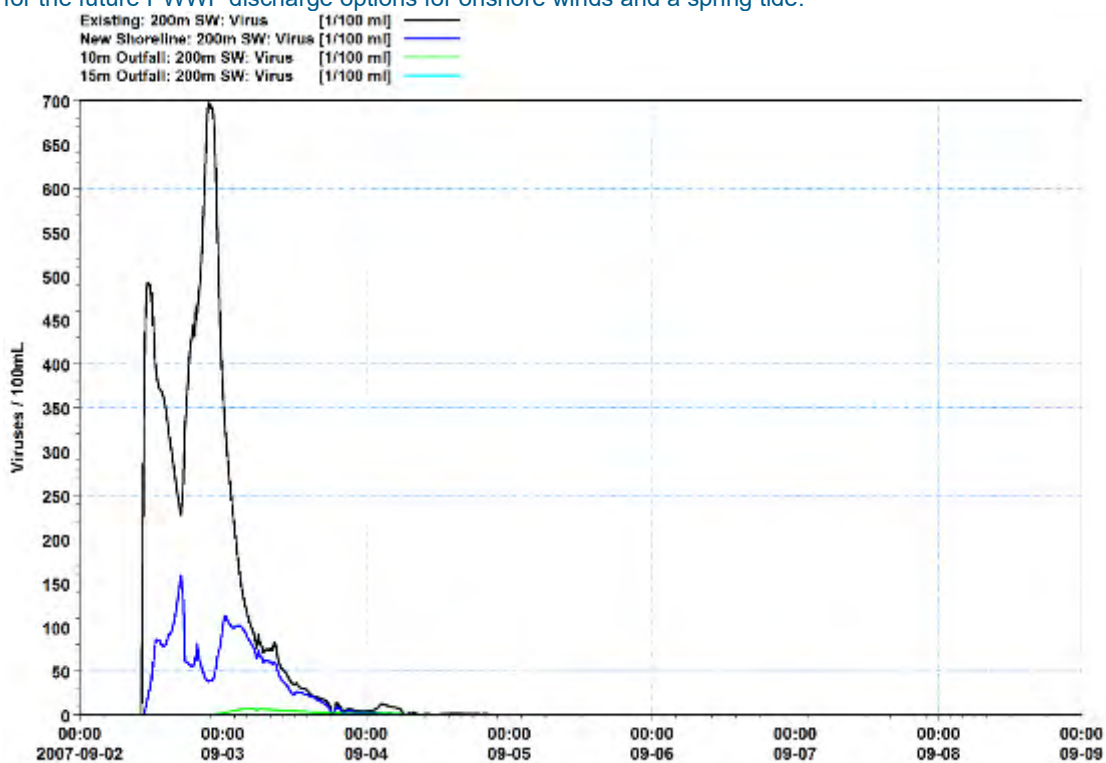


Figure D-4 Predicted Virus (Virus/100 ml) at the monitoring site 200 m south-west of the existing shoreline discharge for the future PWWF discharge options for onshore winds and a spring tide.

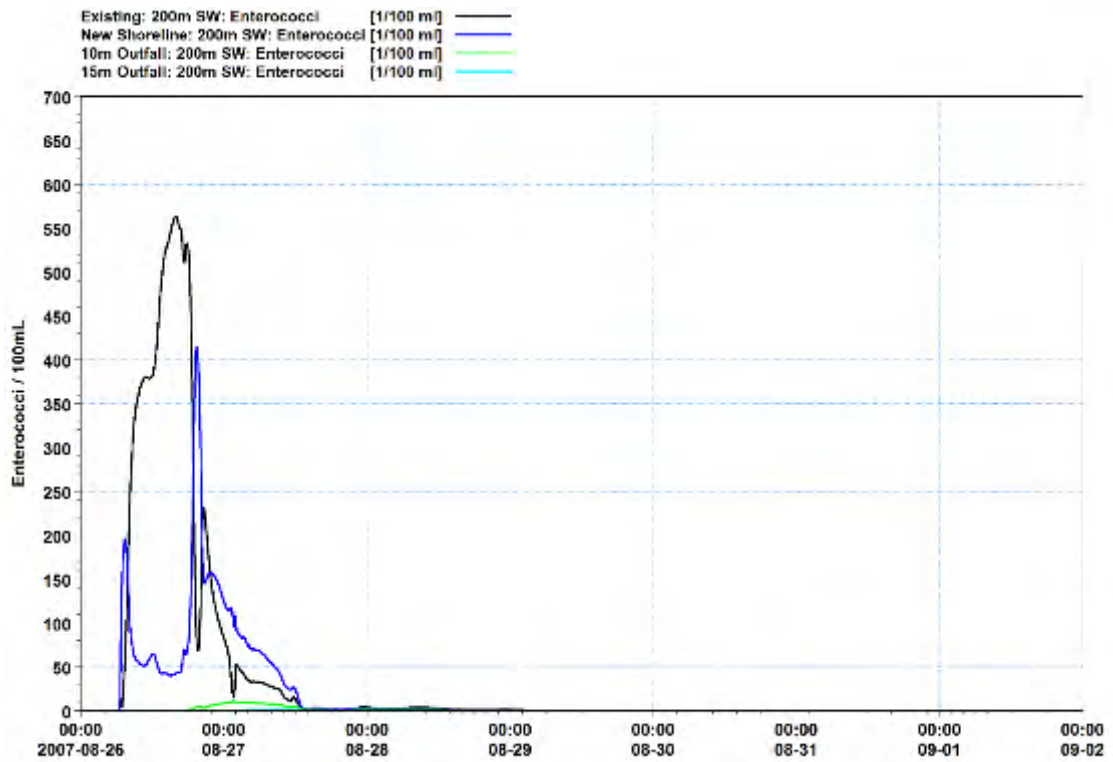


Figure D-5 Predicted Enterococci (Ent/100 ml) at the monitoring site 200 m south-west of the existing shoreline discharge for the future PWWF discharge options for typical winds and a neap tide.

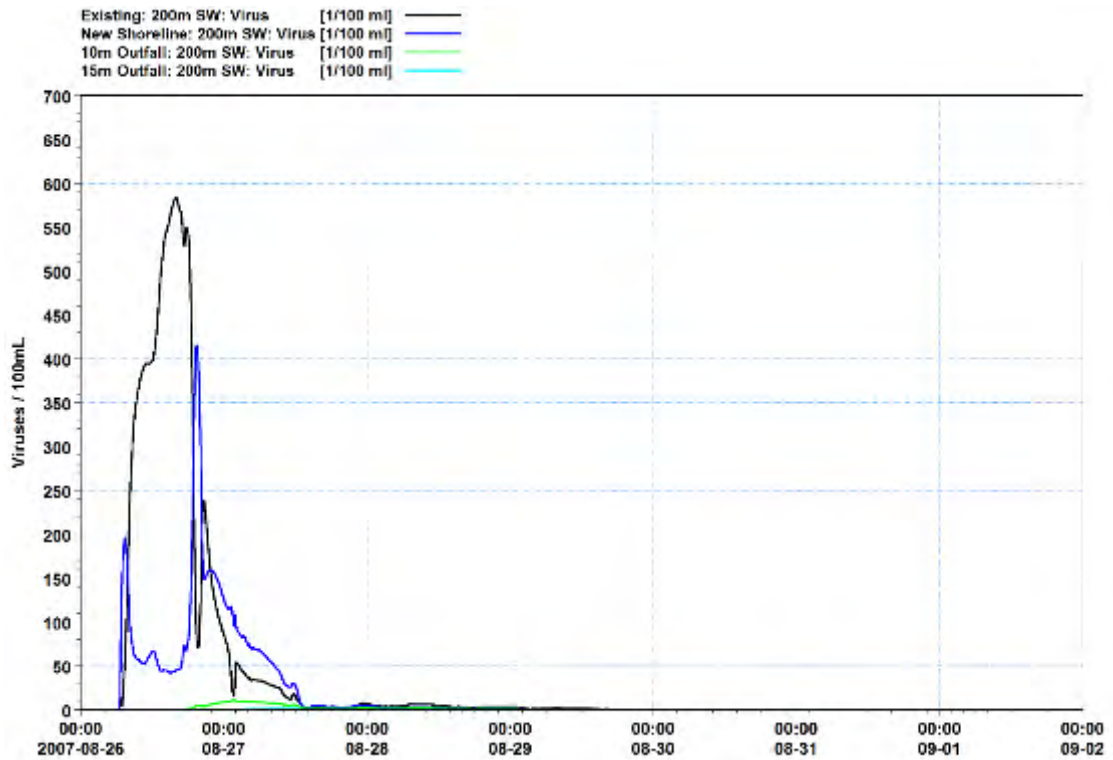


Figure D-6 Predicted Virus (Virus/100 ml) at the monitoring site 200 m south-west of the existing shoreline discharge for the future PWWF discharge options for typical winds and a neap tide.

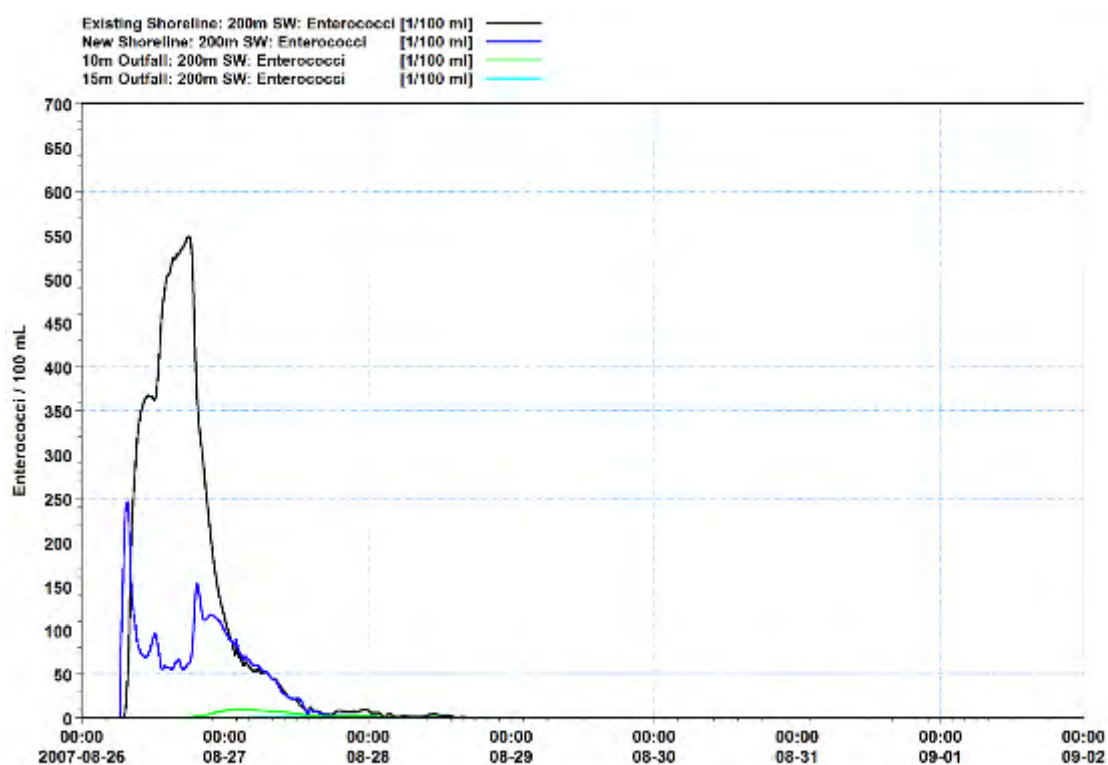


Figure D-7 Predicted Enterococci (Ent/100 ml) at the monitoring site 200 m south-west of the existing shoreline discharge for the future PWWF discharge options for onshore winds and a neap tide.

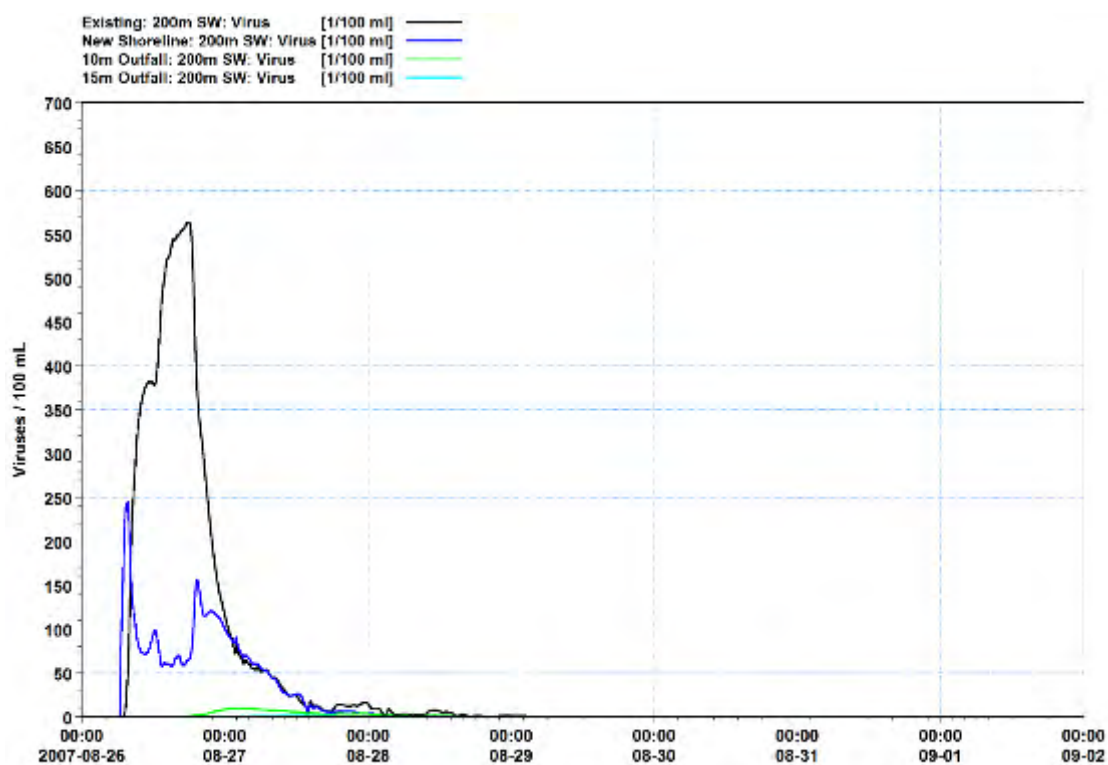


Figure D-8 Predicted Virus (Virus/100 ml) at the monitoring site 200 m south-west of the existing shoreline discharge for the future PWWF discharge options for onshore winds and a neap tide.

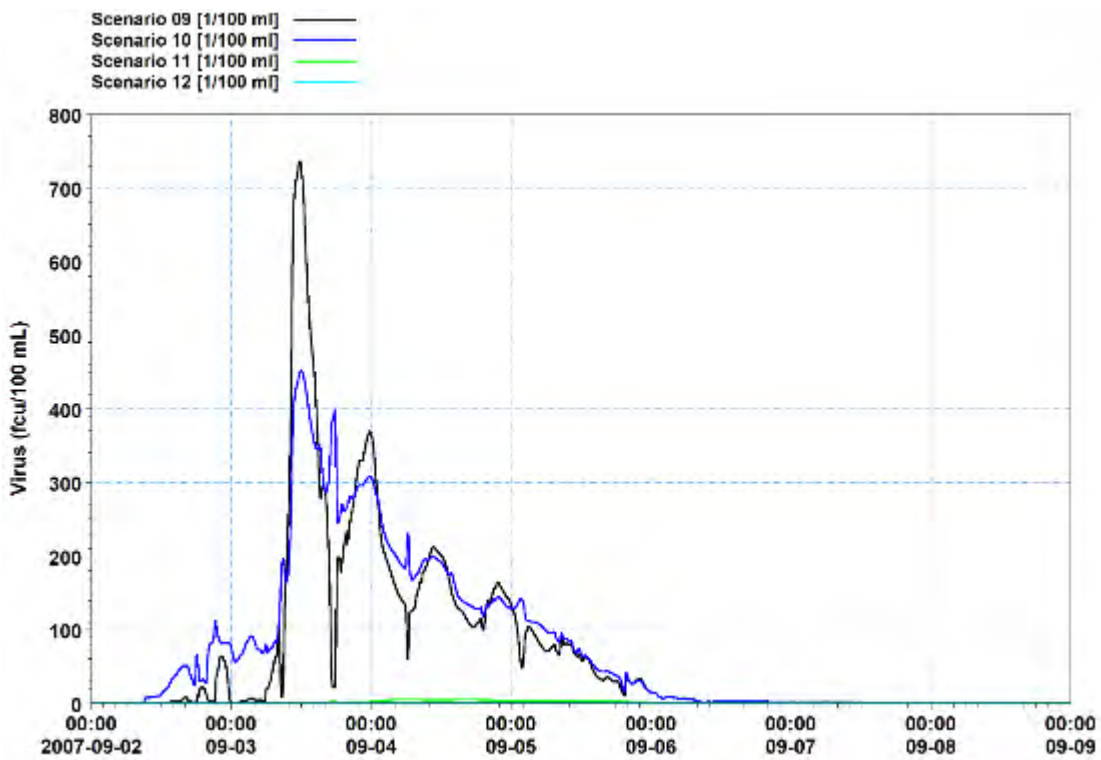


Figure D-9 Predicted Enterococci (Ent/100 ml) at the monitoring site 200 m south-west of the existing shoreline discharge for the overflow scenarios for typical winds and a spring tide.

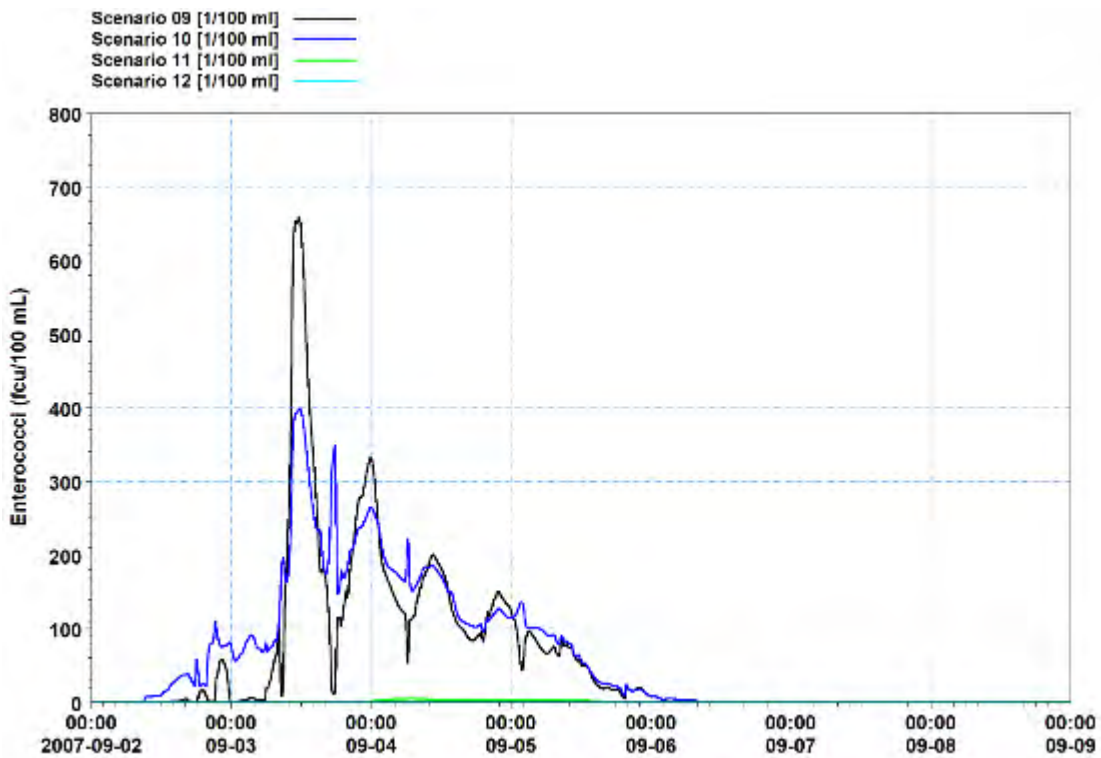


Figure D-10 Predicted Virus (Virus/100 ml) at the monitoring site 200 m south-west of the existing shoreline discharge for the overflow scenarios for typical winds and a spring tide.

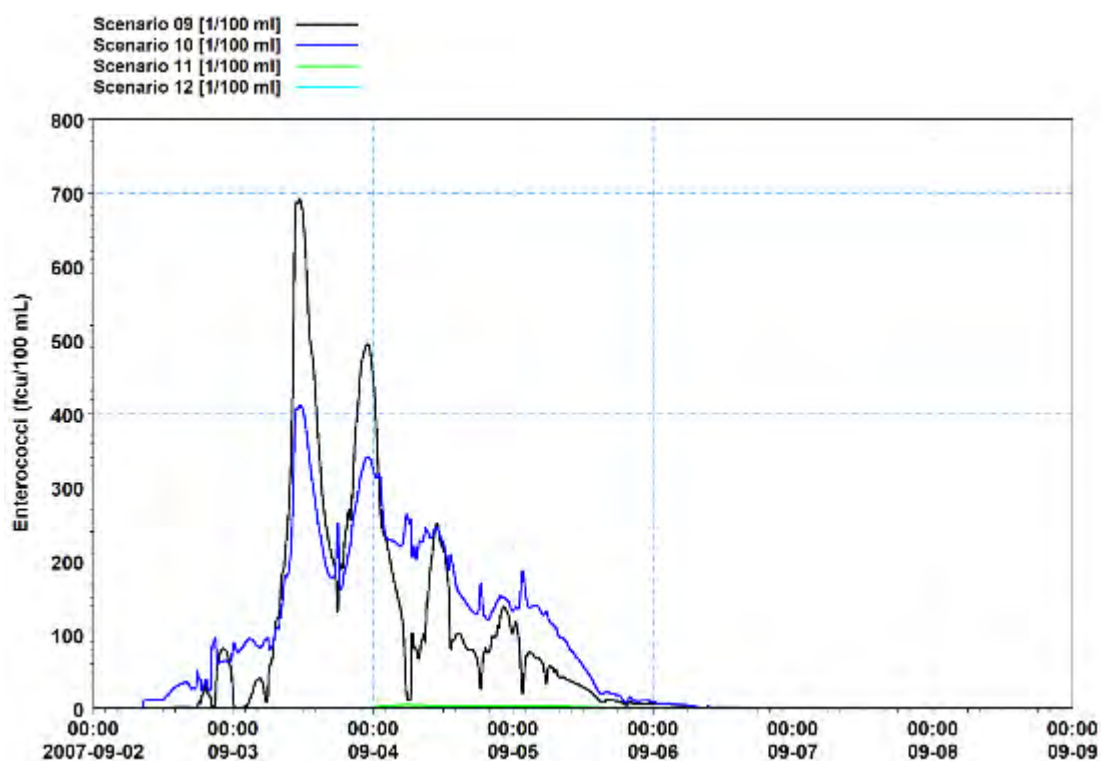


Figure D-11 Predicted Enterococci (Ent/100 ml) at the monitoring site 200 m south-west of the existing shoreline discharge for the overflow scenarios for onshore winds and a spring tide.

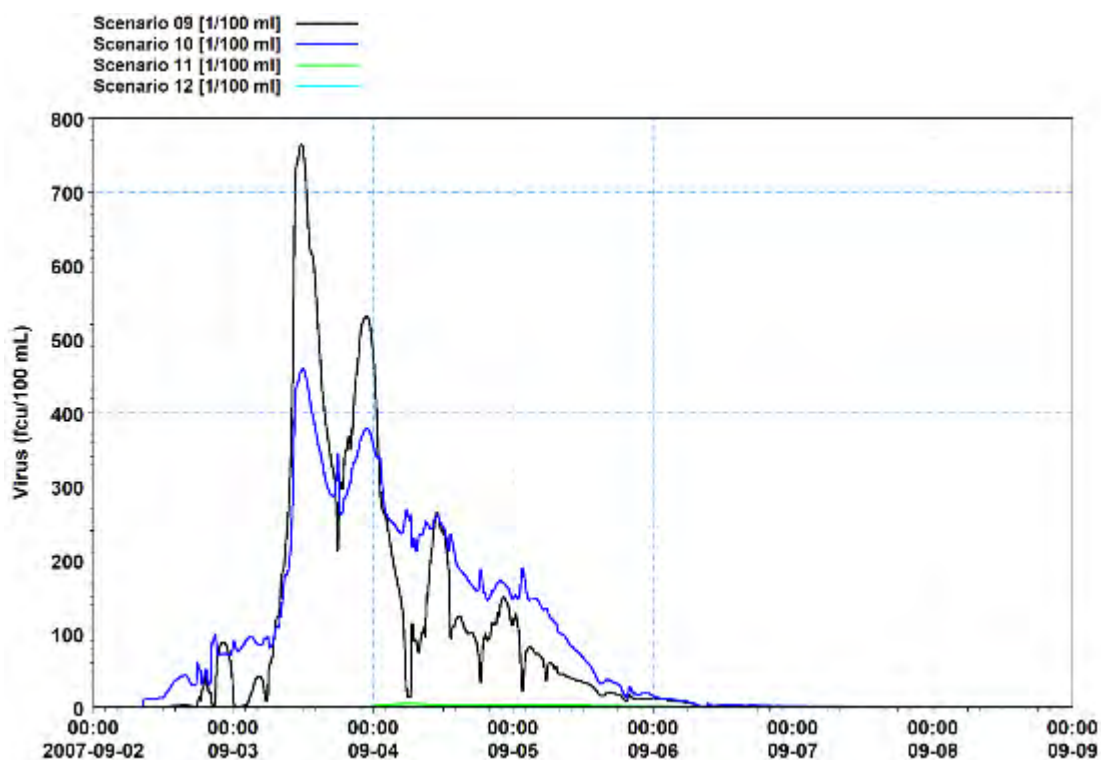


Figure D-12 Predicted Virus (Virus/100 ml) at the monitoring site 200 m south-west of the existing shoreline discharge for the overflow scenarios for onshore winds and a spring tide.

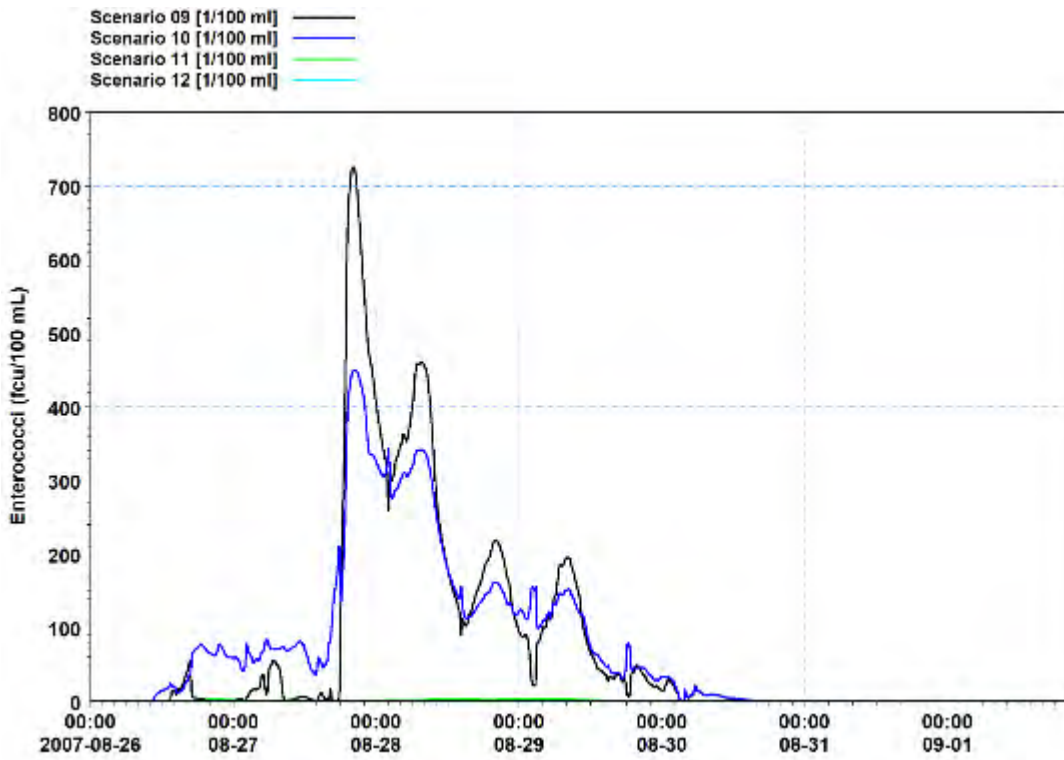


Figure D-13 Predicted Enterococci (Ent/100 ml) at the monitoring site 200 m south-west of the existing shoreline discharge for the overflow scenarios for typical winds and a neap tide.

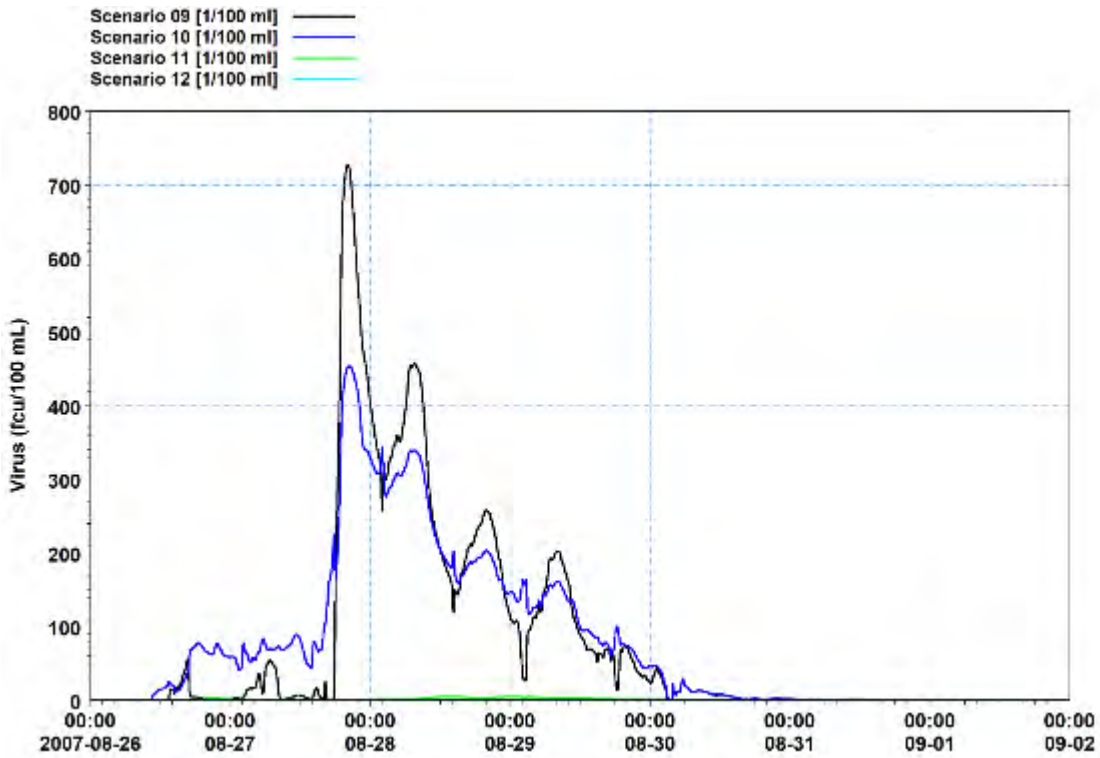


Figure D-14 Predicted Virus (Virus/100 ml) at the monitoring site 200 m south-west of the existing shoreline discharge for the overflow scenarios for typical winds and a neap tide.

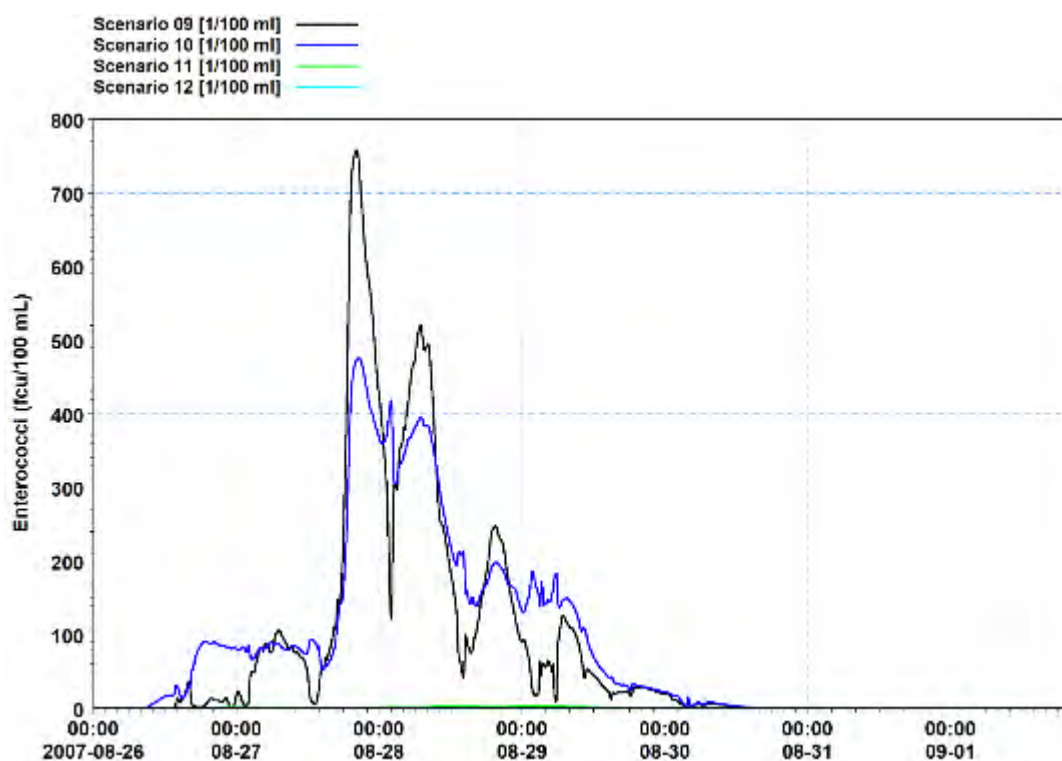


Figure D-15 Predicted Enterococci (Ent/100 ml) at the monitoring site 200 m south-west of the existing shoreline discharge for the overflow scenarios for onshore winds and a neap tide.

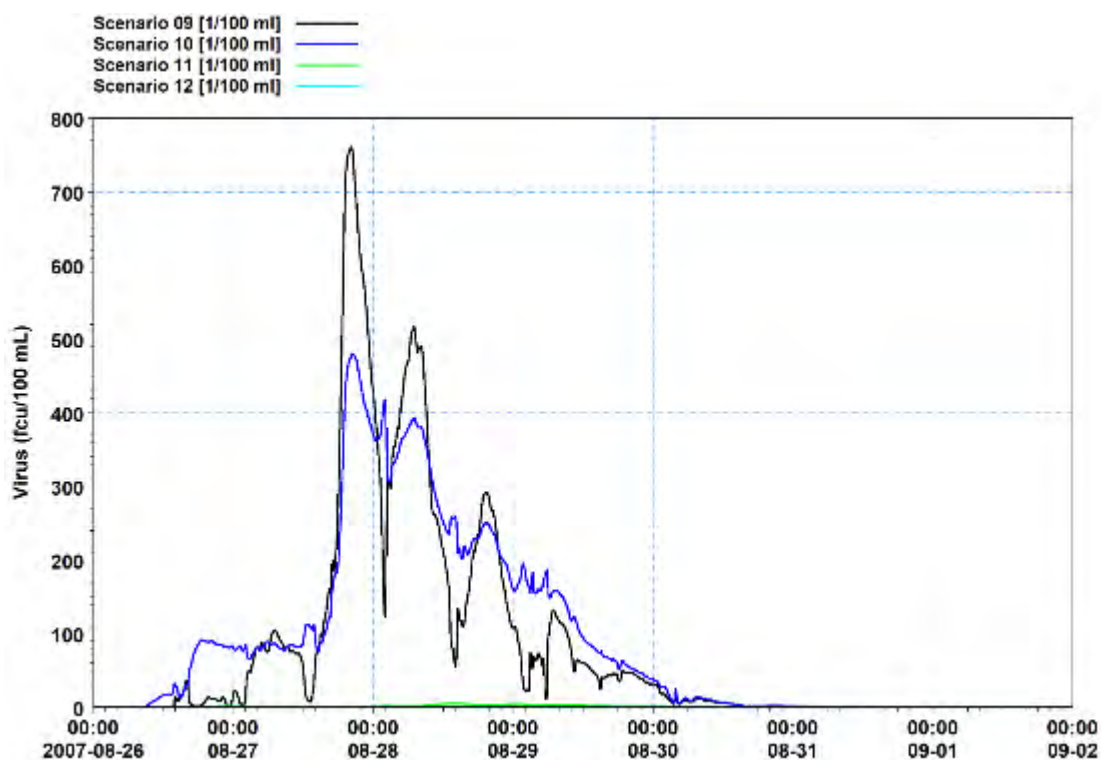


Figure D-16 Predicted Virus (Virus/100 ml) at the monitoring site 200 m south-west of the existing shoreline discharge for the overflow scenarios for onshore winds and a neap tide.

Appendix E – Time-series at Monitoring site 200 m E of existing discharge (PWWF discharge and overflow scenarios)

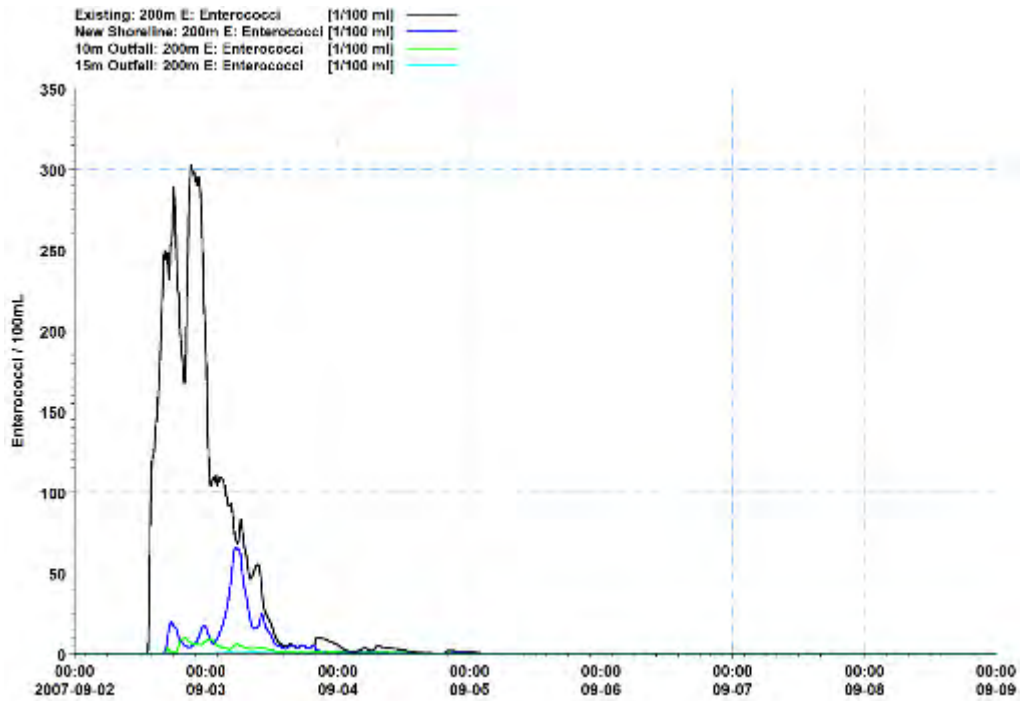


Figure E-1 Predicted Enterococci (Ent/100 ml) at the monitoring site 200 m east of the existing shoreline discharge for the future PWWF discharge options for typical winds and a spring tide.

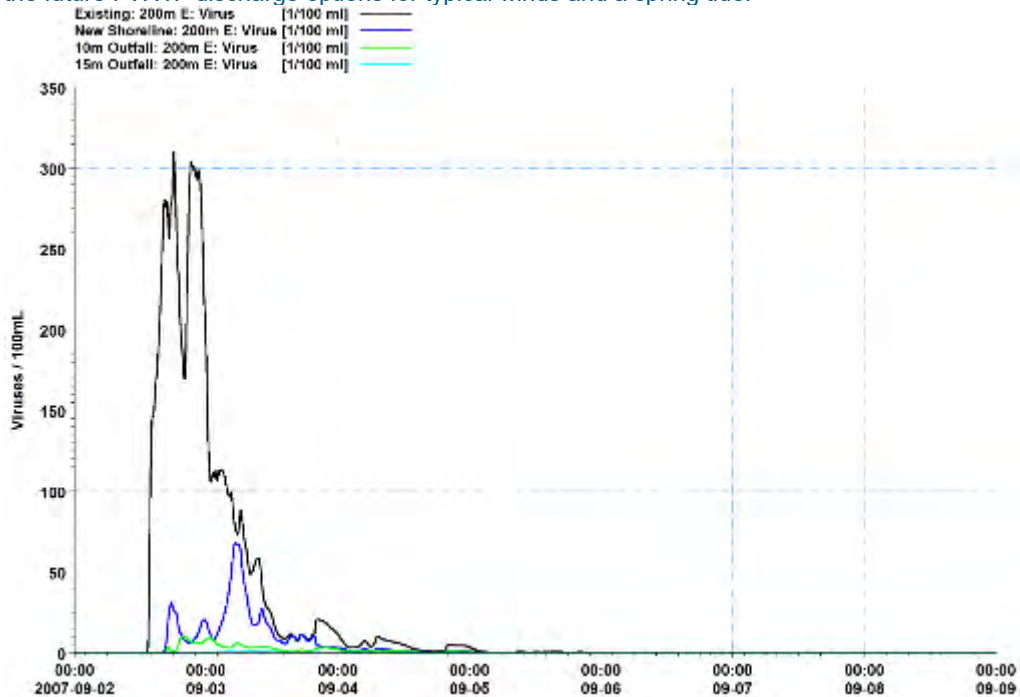


Figure E-2 Predicted Virus (Virus/100 ml) at the monitoring site 200 m east of the existing shoreline discharge for the future PWWF discharge options for typical winds and a spring tide.

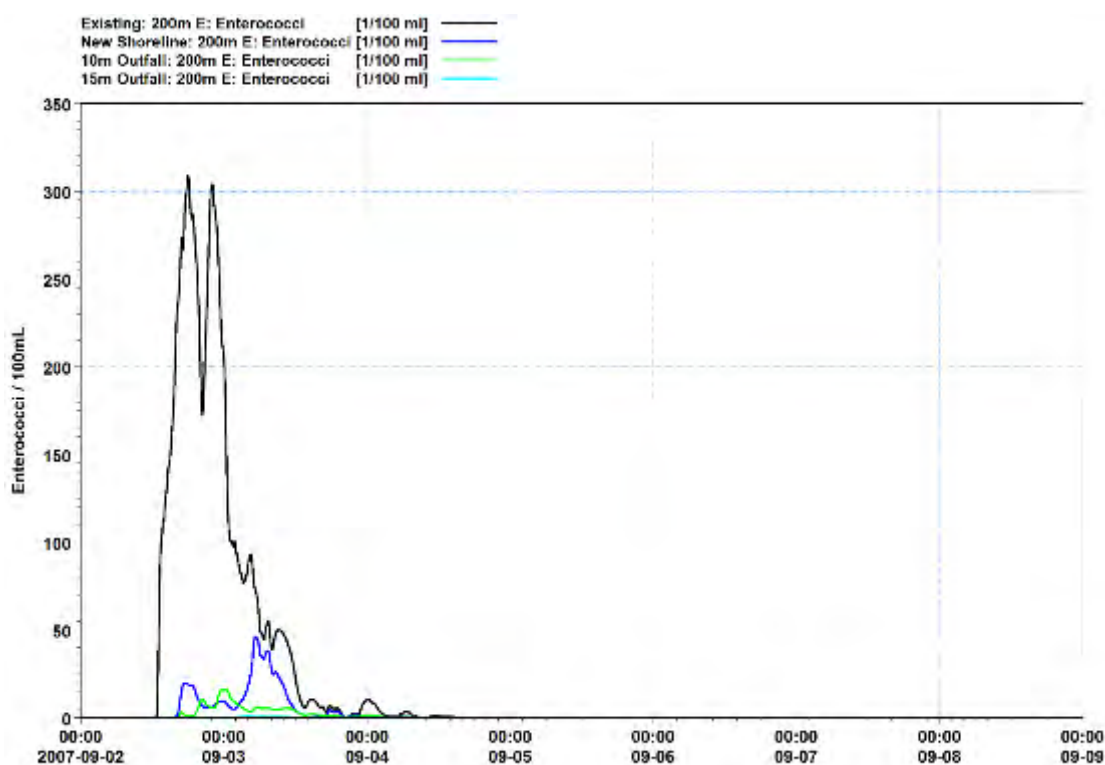


Figure E-3 Predicted Enterococci (Ent/100 ml) at the monitoring site 200 m east of the existing shoreline discharge for the future PWWF discharge options for onshore winds and a spring tide.

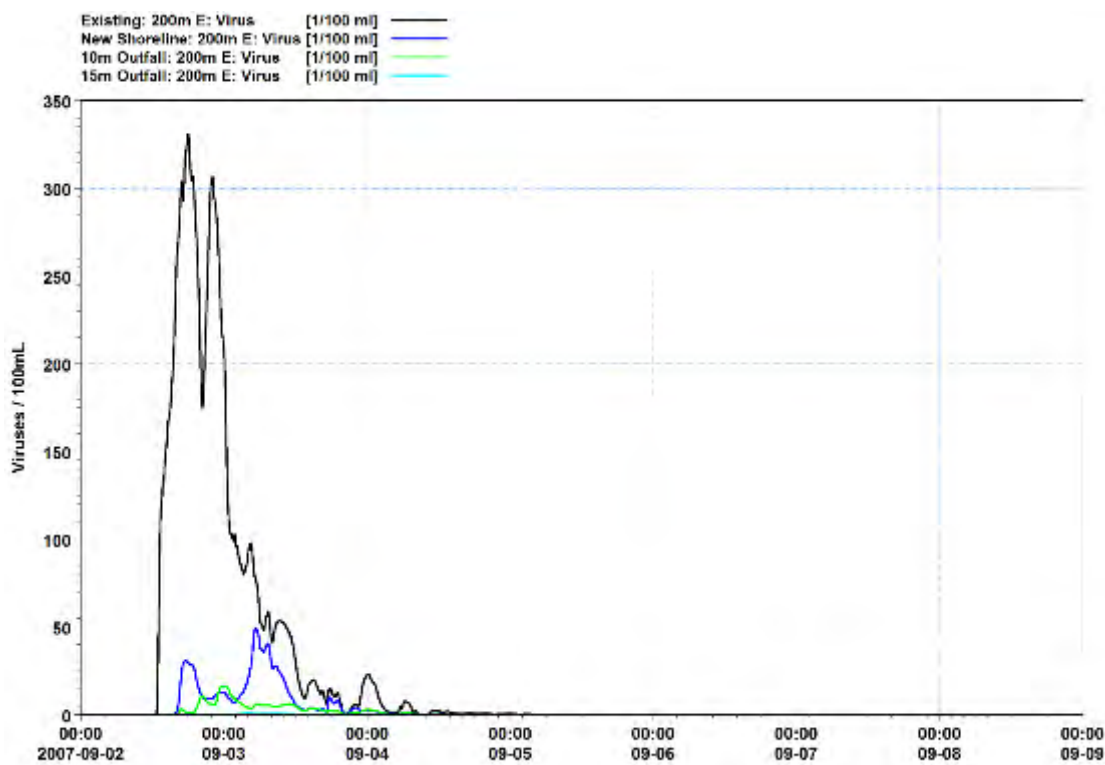


Figure E-4 Predicted Virus (Virus/100 ml) at the monitoring site 200 m east of the existing shoreline discharge for the future PWWF discharge options for onshore winds and a spring tide.

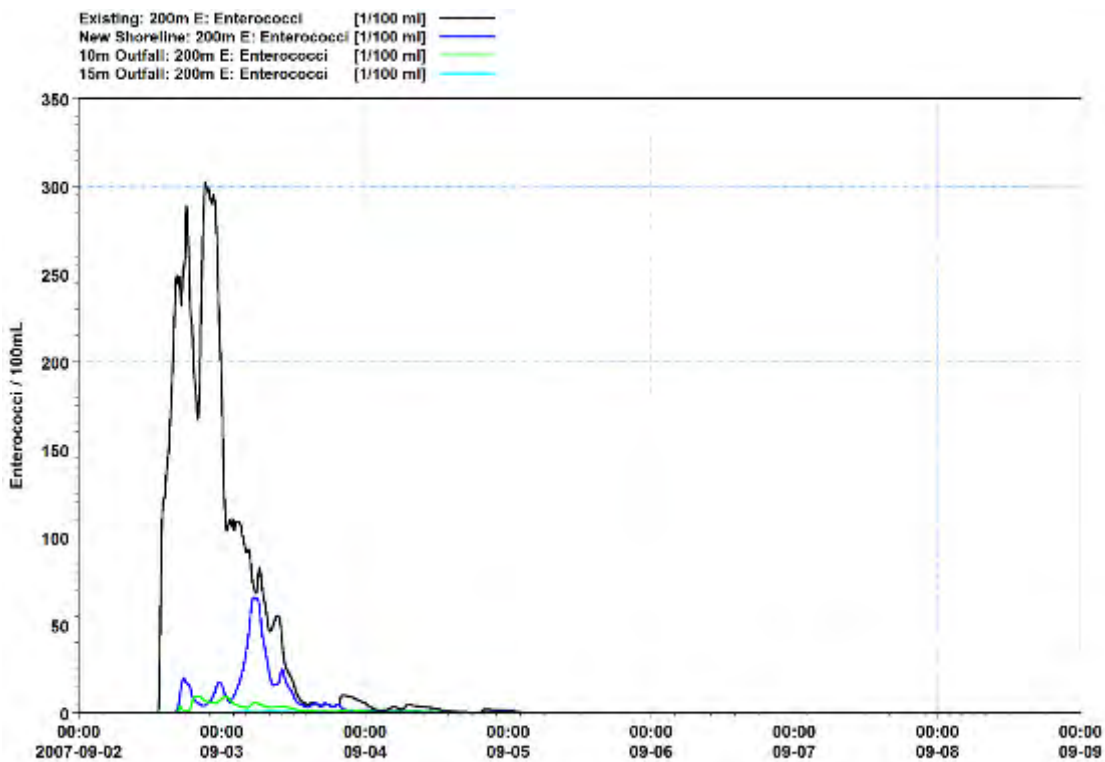


Figure E-5 Predicted Enterococci (Ent/100 ml) at the monitoring site 200 m east of the existing shoreline discharge for the future PWWF discharge options for typical winds and a neap tide.

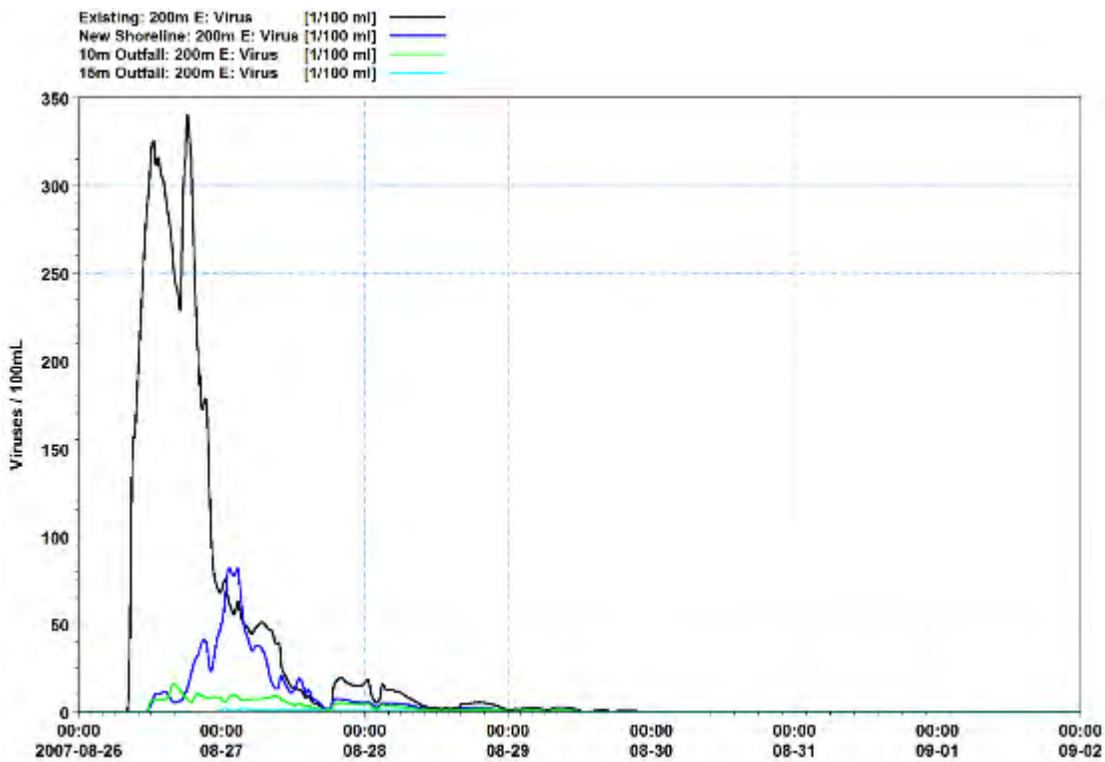


Figure E-6 Predicted Virus (Virus/100 ml) at the monitoring site 200 m east of the existing shoreline discharge for the future PWWF discharge options for typical winds and a neap tide.

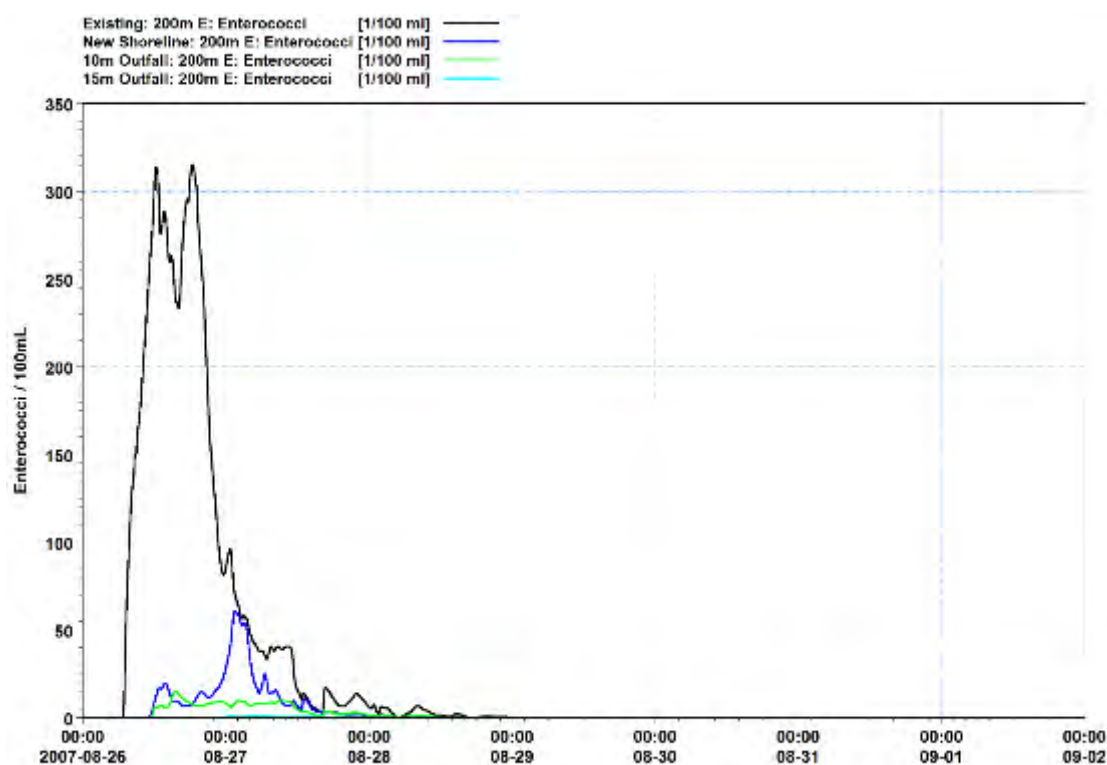


Figure E-7 Predicted Enterococci (Ent/100 ml) at the monitoring site 200 m east of the existing shoreline discharge for the future PWWF discharge options for onshore winds and a neap tide.

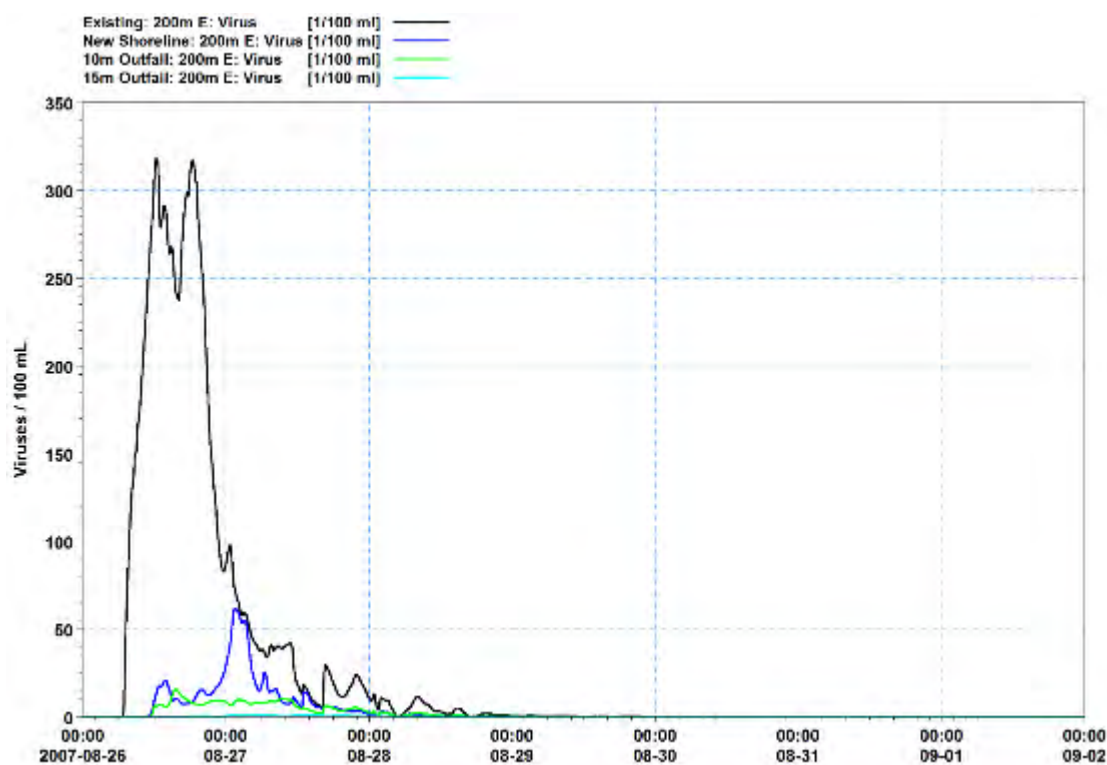


Figure E-8 Predicted Virus (Virus/100 ml) at the monitoring site 200 m east of the existing shoreline discharge for the future PWWF discharge options for onshore winds and a neap tide.

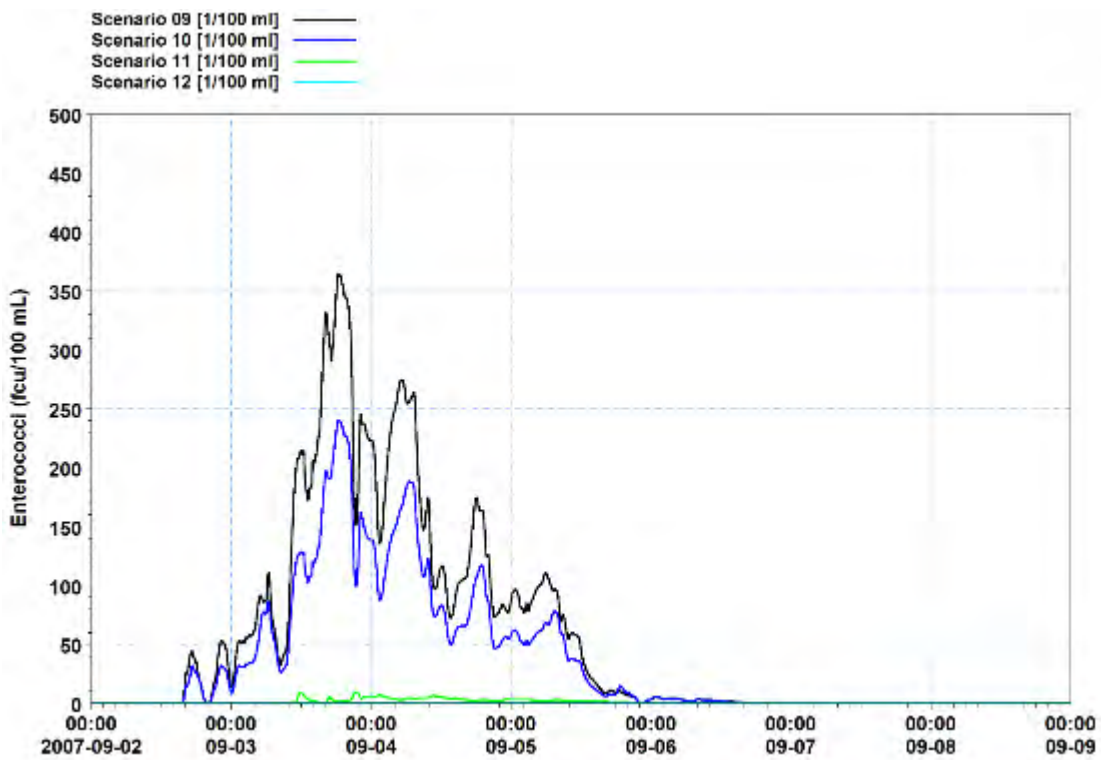


Figure E-9 Predicted Enterococci (Ent/100 ml) at the monitoring site 200 m east of the existing shoreline discharge for the overflow scenarios for typical winds and a spring tide.

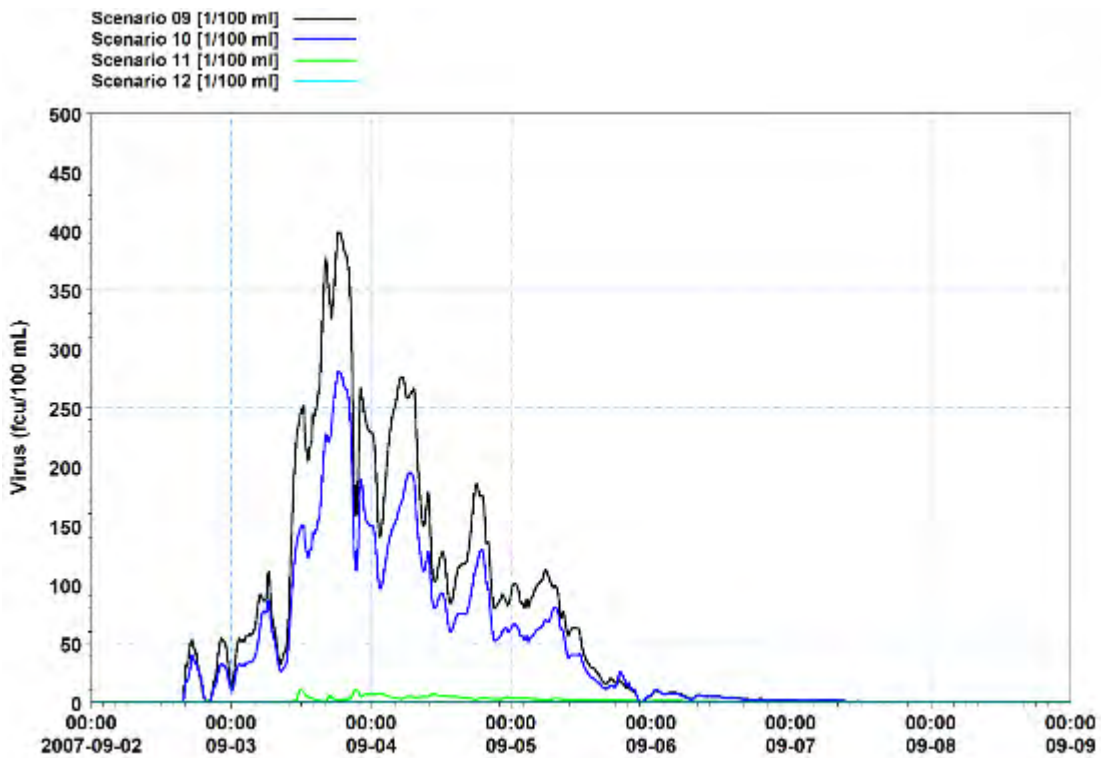


Figure E-10 Predicted Virus (Virus/100 ml) at the monitoring site 200 m east of the existing shoreline discharge for the overflow scenarios for typical winds and a spring tide.

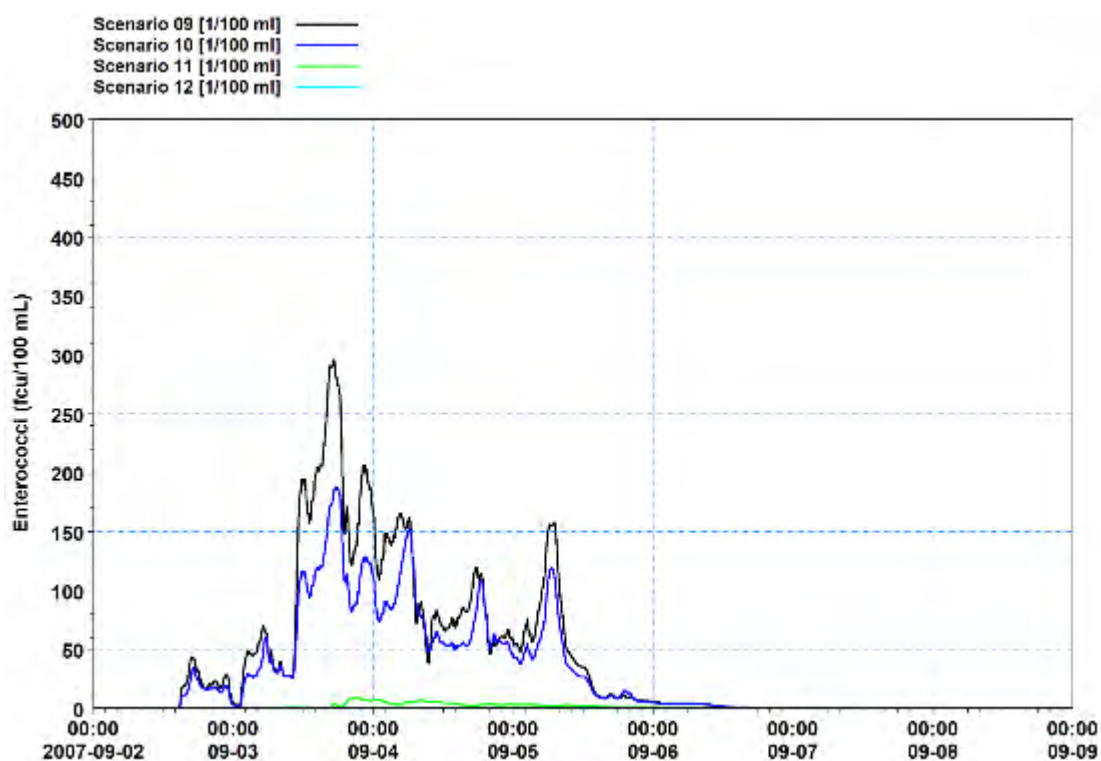


Figure E-11 Predicted Enterococci (Ent/100 ml) at the monitoring site 200 m east of the existing shoreline discharge for the overflow scenarios for onshore winds and a spring tide.

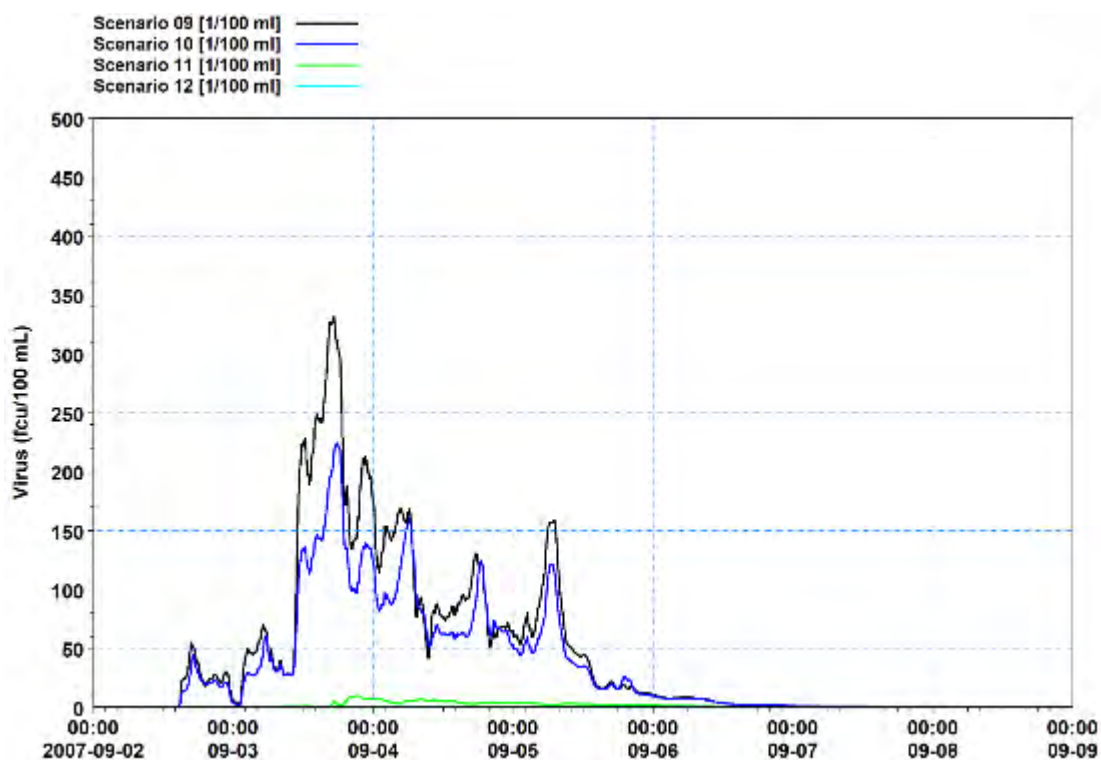


Figure E-12 Predicted Virus (Virus/100 ml) at the monitoring site 200 m east of the existing shoreline discharge for the overflow scenarios for onshore winds and a spring tide.

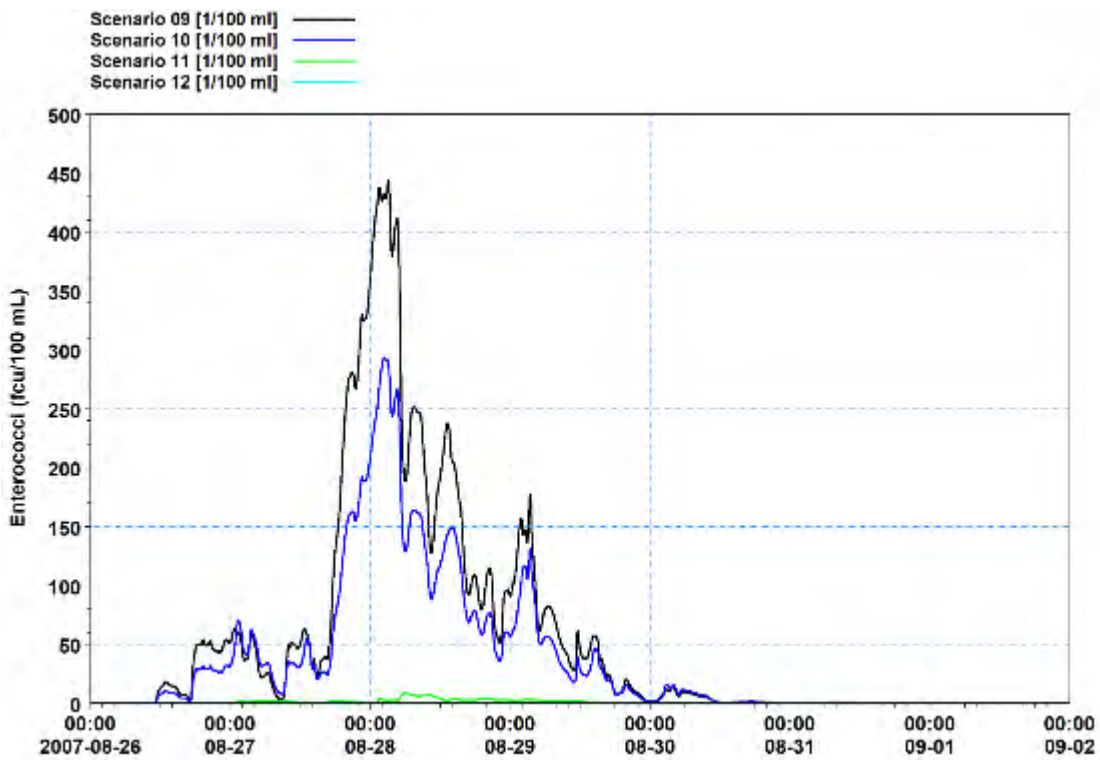


Figure E-13 Predicted Enterococci (Ent/100 ml) at the monitoring site 200 m east of the existing shoreline discharge for the overflow scenarios for typical winds and a neap tide.

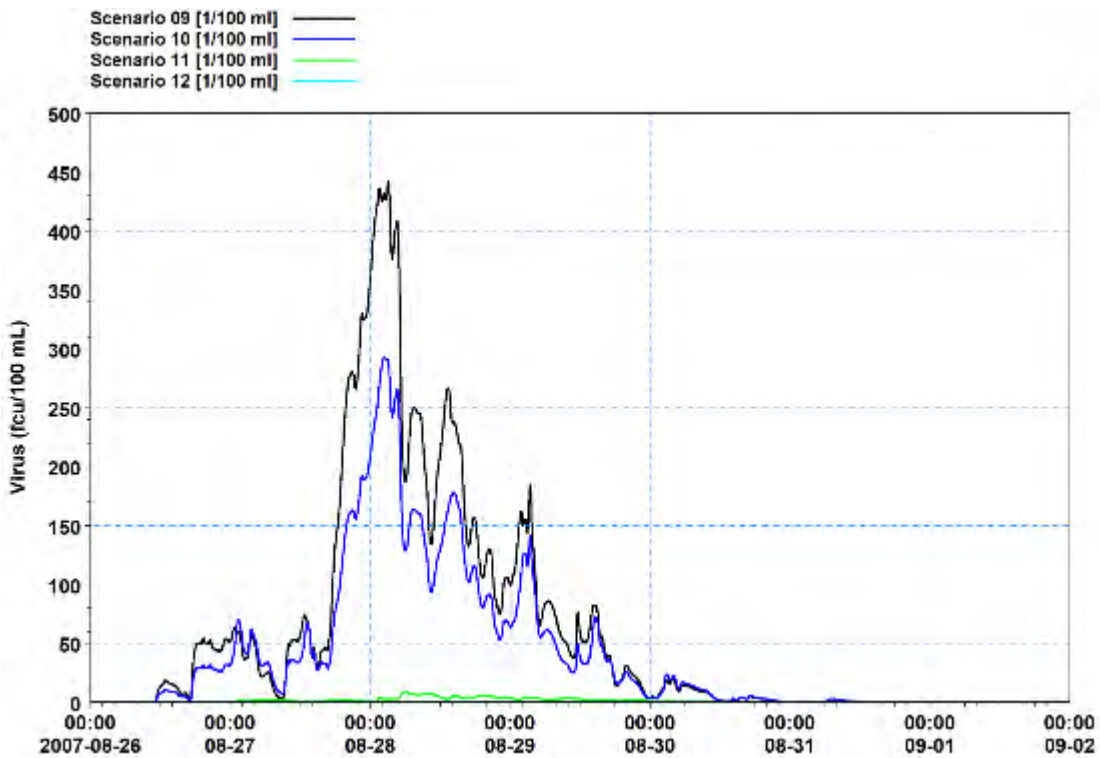


Figure E-14 Predicted Virus (Virus/100 ml) at the monitoring site 200 m east of the existing shoreline discharge for the overflow scenarios for typical winds and a neap tide.

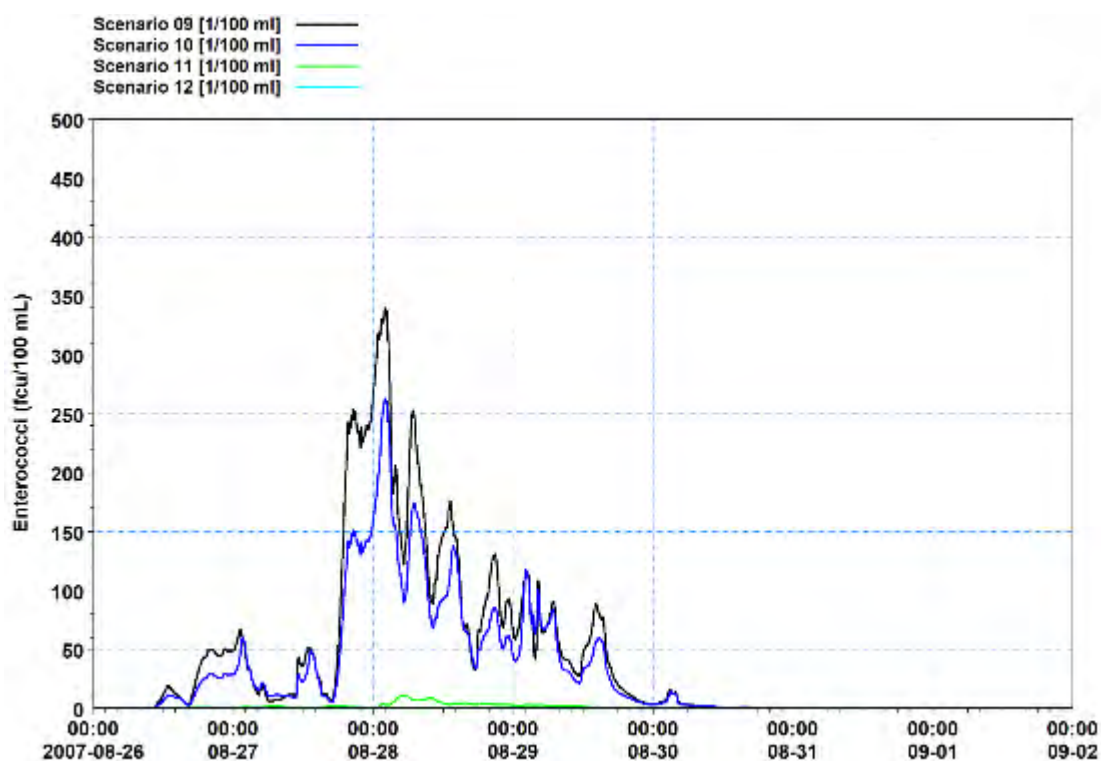


Figure E-15 Predicted Enterococci (Ent/100 ml) at the monitoring site 200 m east of the existing shoreline discharge for the overflow scenarios for onshore winds and a neap tide.

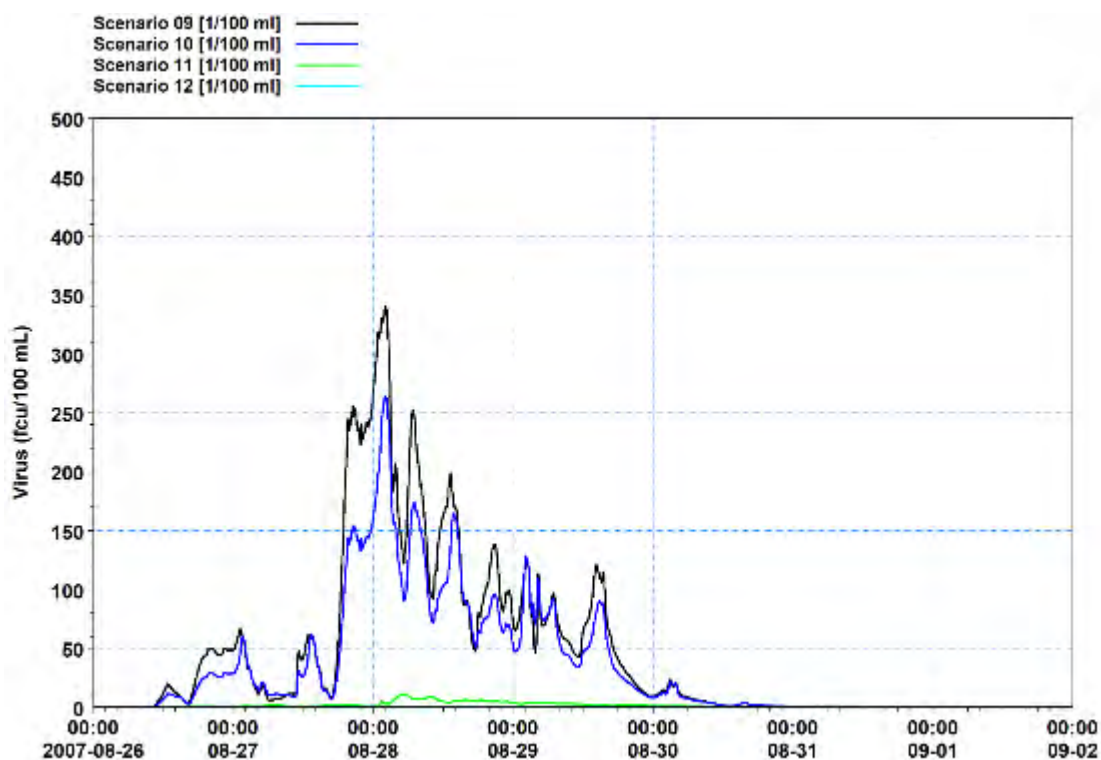


Figure E-16 Predicted Virus (Virus/100 ml) at the monitoring site 200 m east of the existing shoreline discharge for the overflow scenarios for onshore winds and a neap tide.

Appendix F – Time-series at Ti Korohiwa Rocks Monitoring site (PWWF discharge and overflow scenarios)

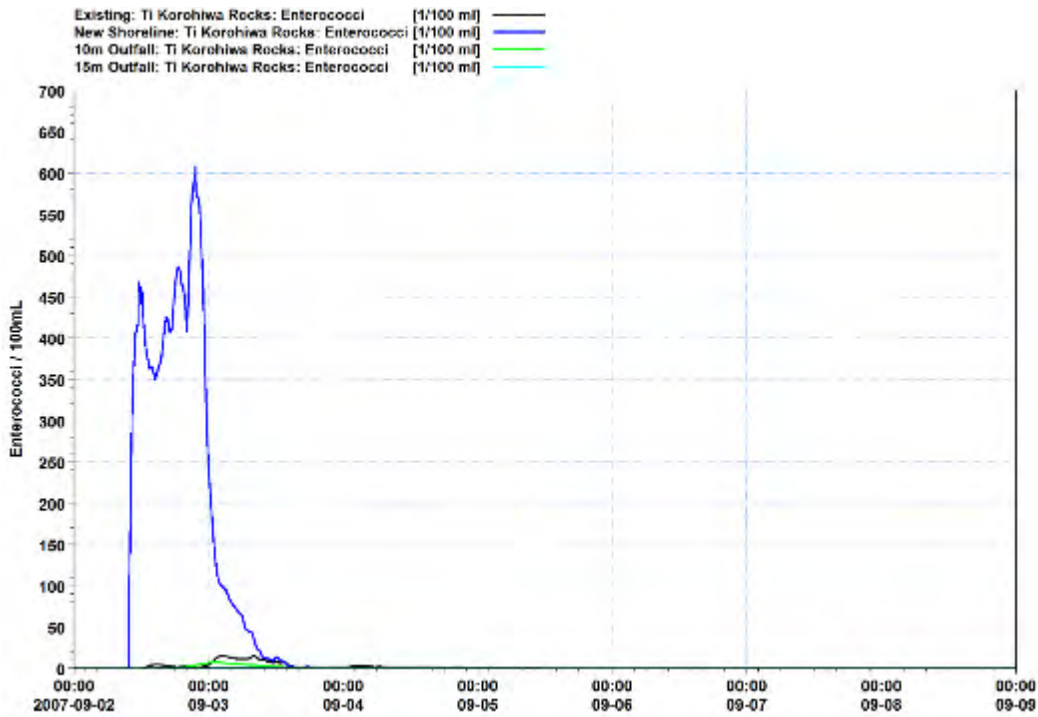


Figure F-1 Predicted Enterococci (Ent/100 ml) at the Ti Korohiwa Rocks for the discharge options for typical winds and a spring tide.

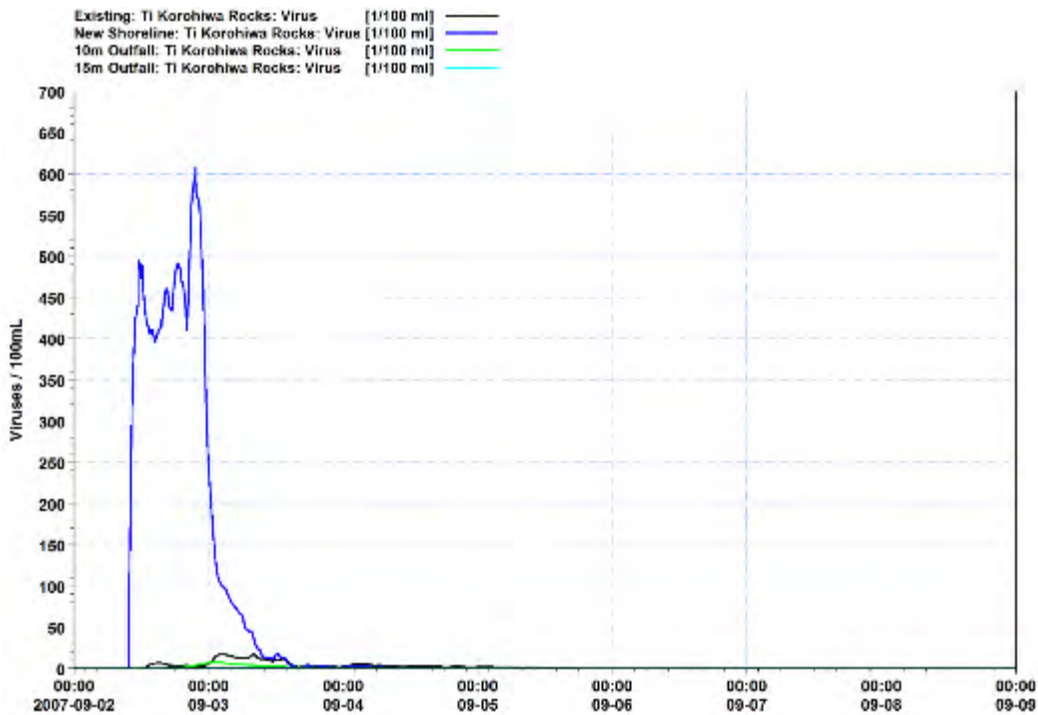


Figure F-2 Predicted Virus (Virus/100 ml) at the Ti Korohiwa Rocks for the discharge options for typical winds and a spring tide.

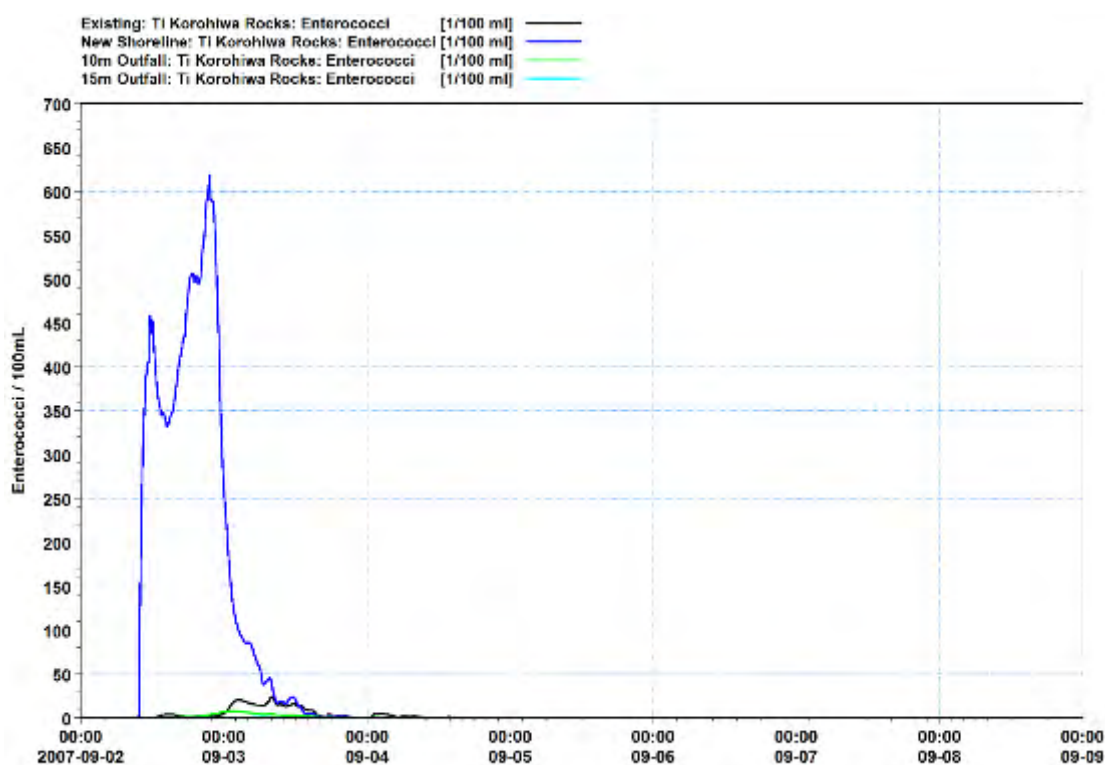


Figure F-3 Predicted Enterococci (Ent/100 ml) at the Ti Korohiwa Rocks for the discharge options for onshore winds and a spring tide.

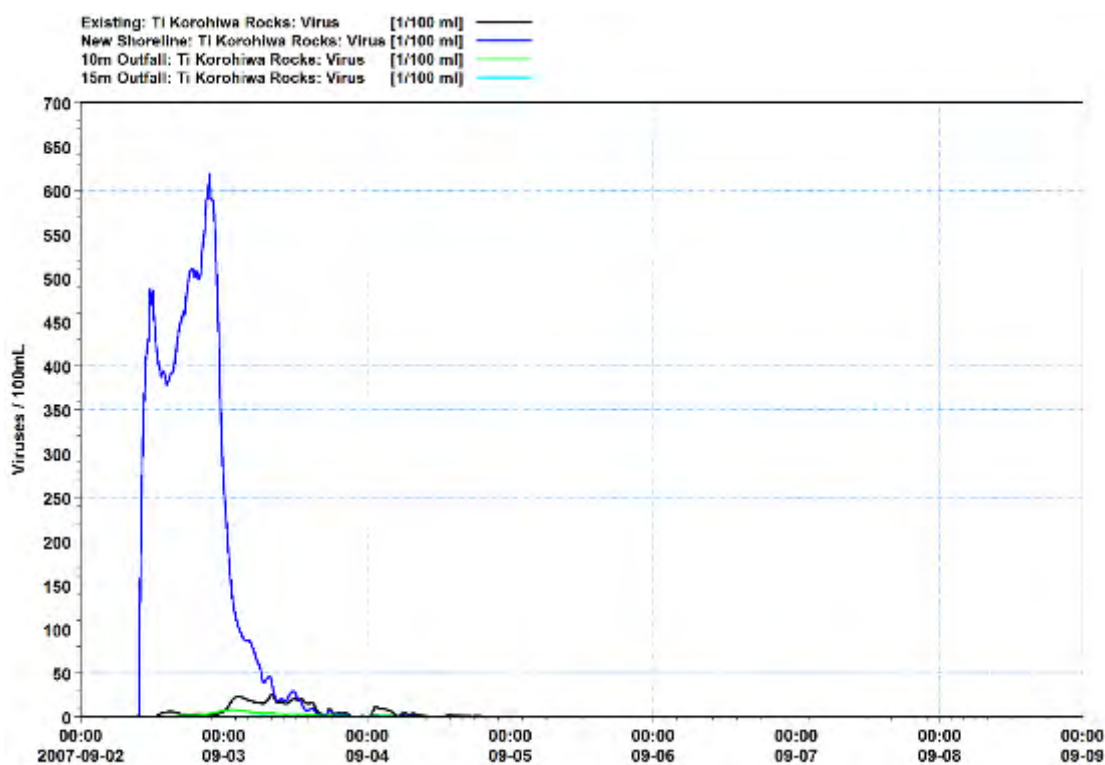


Figure F-4 Predicted Virus (Virus/100 ml) at the Ti Korohiwa Rocks for the discharge options for onshore winds and a spring tide.

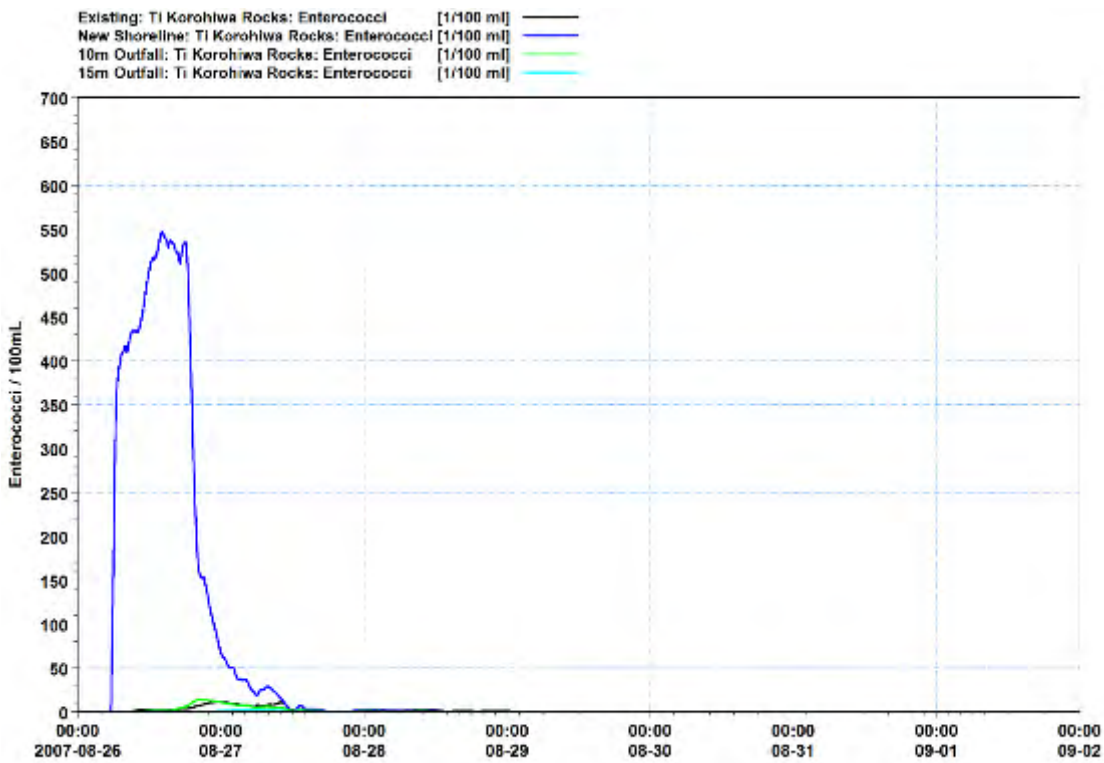


Figure F-5 Predicted Enterococci (Ent/100 ml) at the Ti Korohiwa Rocks for the discharge options for typical winds and a neap tide.

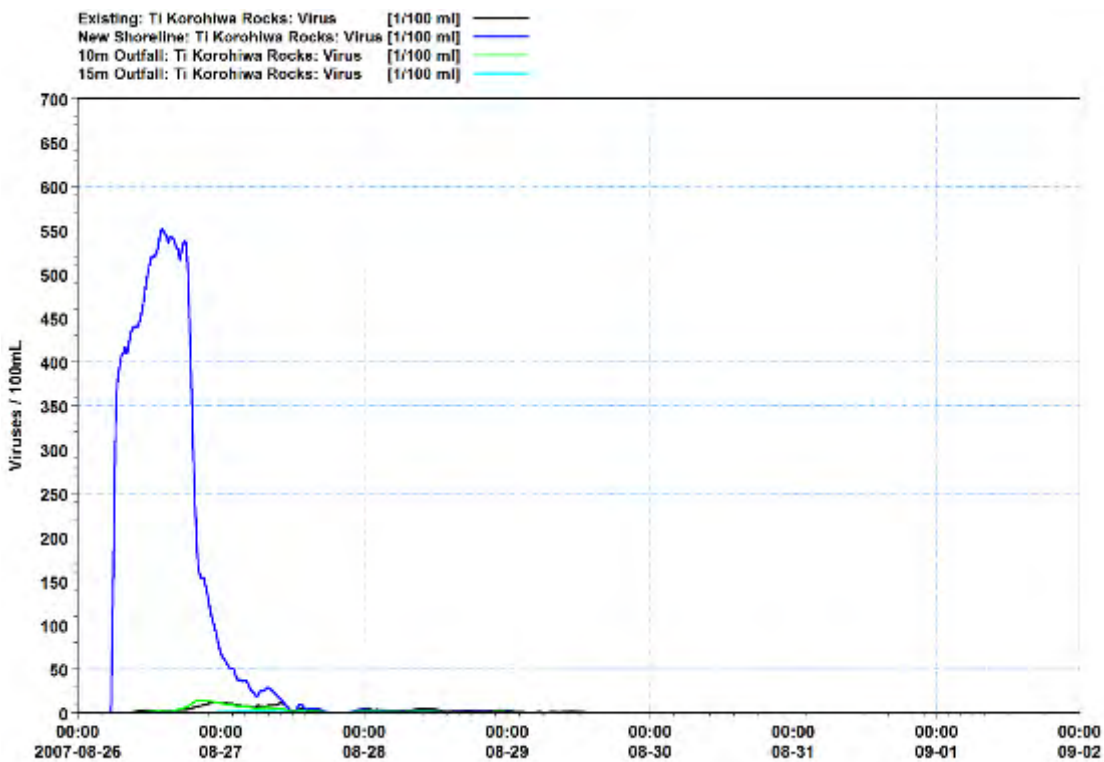


Figure F-6 Predicted Virus (Virus/100 ml) at the Ti Korohiwa Rocks for the discharge options for typical winds and a neap tide.

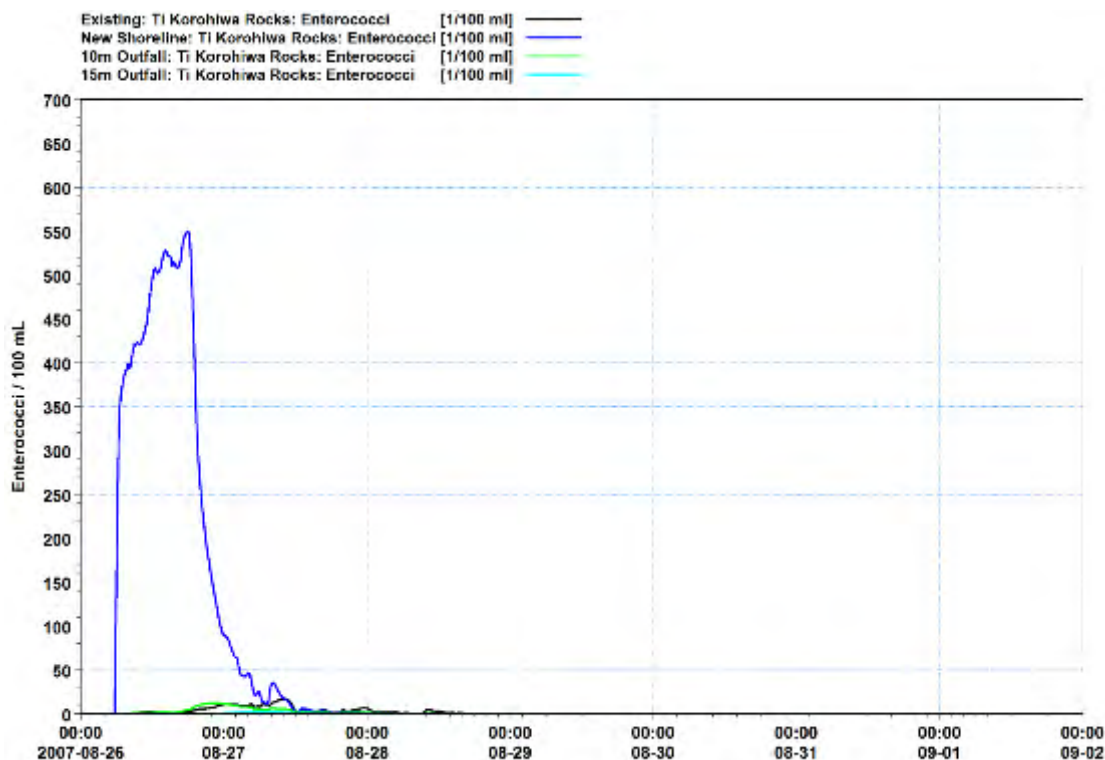


Figure F-7 Predicted Enterococci (Ent/100 ml) at the Ti Korohiwa Rocks for the discharge options for onshore winds and a neap tide.

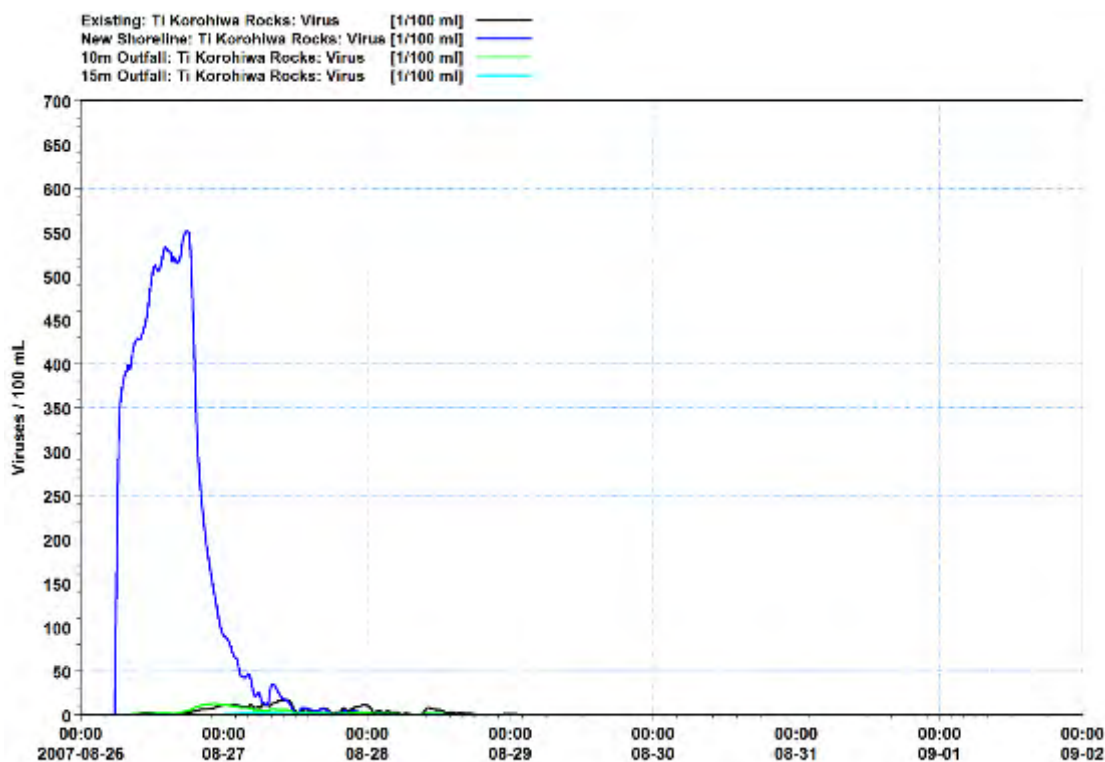


Figure F-8 Predicted Virus (Virus/100 ml) at the Ti Korohiwa Rocks for the discharge options for onshore winds and a neap tide.

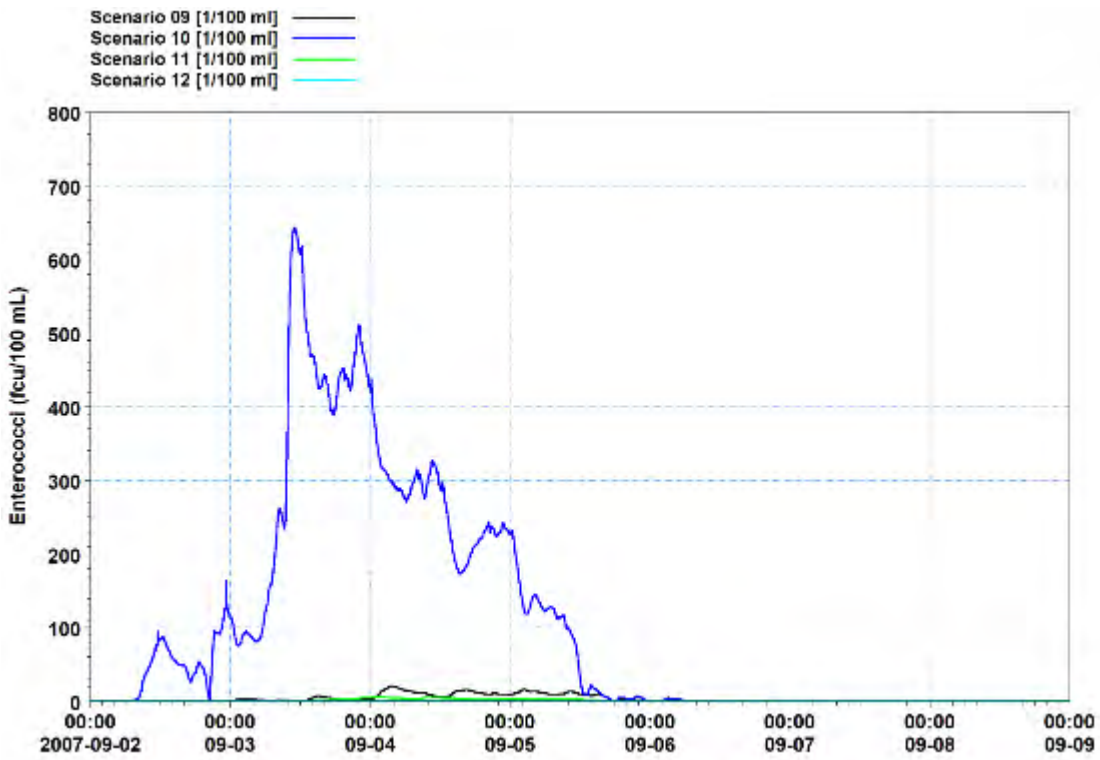


Figure F-9 Predicted Enterococci (Ent/100 ml) at the Ti Korohiwa Rocks monitoring site for the overflow scenarios for typical winds and a spring tide.

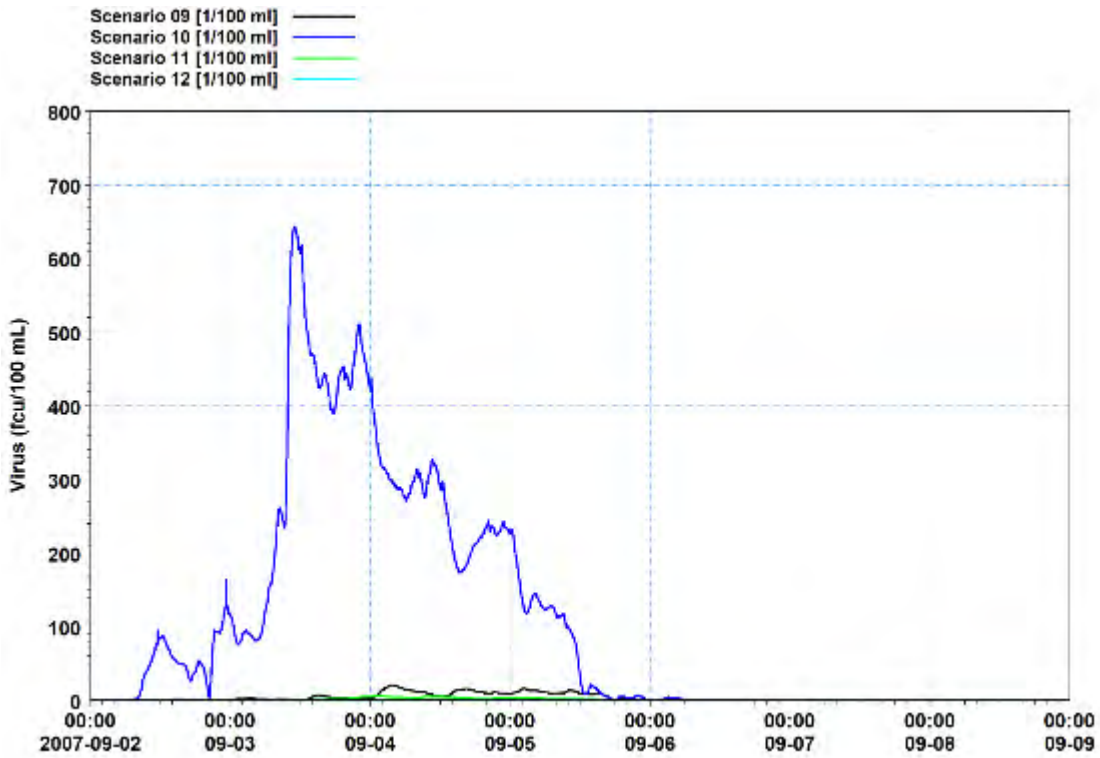


Figure F-10 Predicted Virus (Virus/100 ml) at the Ti Korohiwa Rocks monitoring site for the overflow scenarios for typical winds and a spring tide.

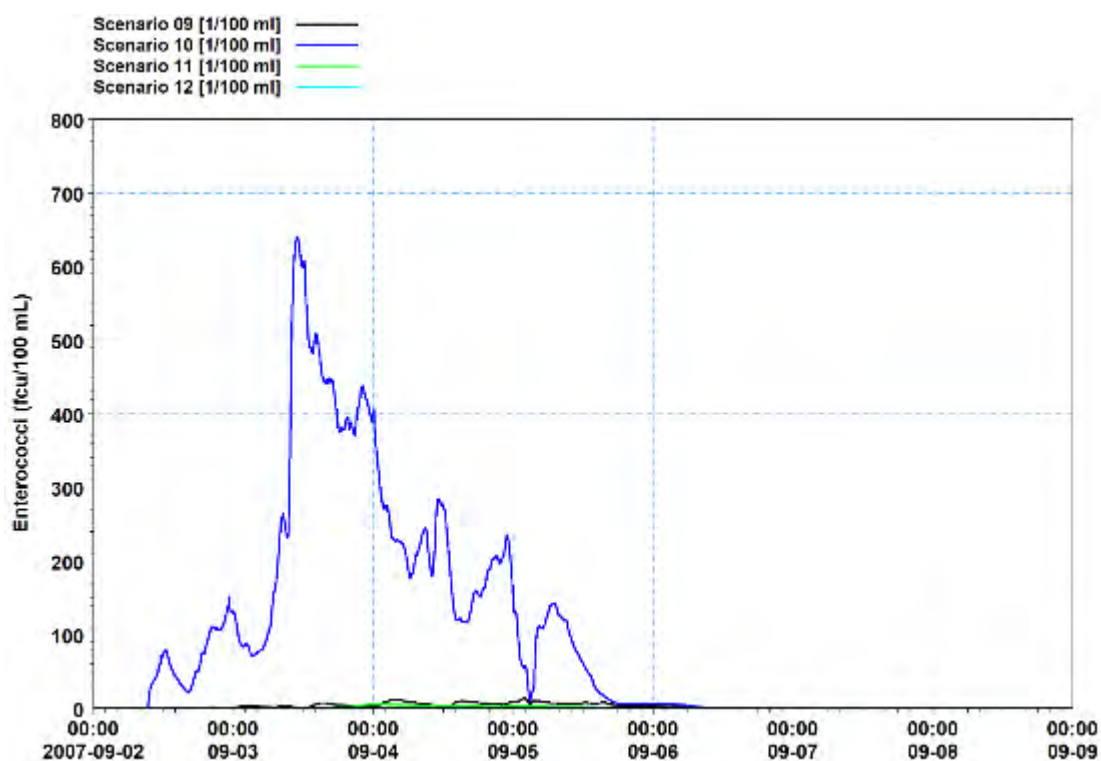


Figure F-11 Predicted Enterococci (Ent/100 ml) at the Ti Korohiwa Rocks monitoring site for the overflow scenarios for onshore winds and a spring tide.

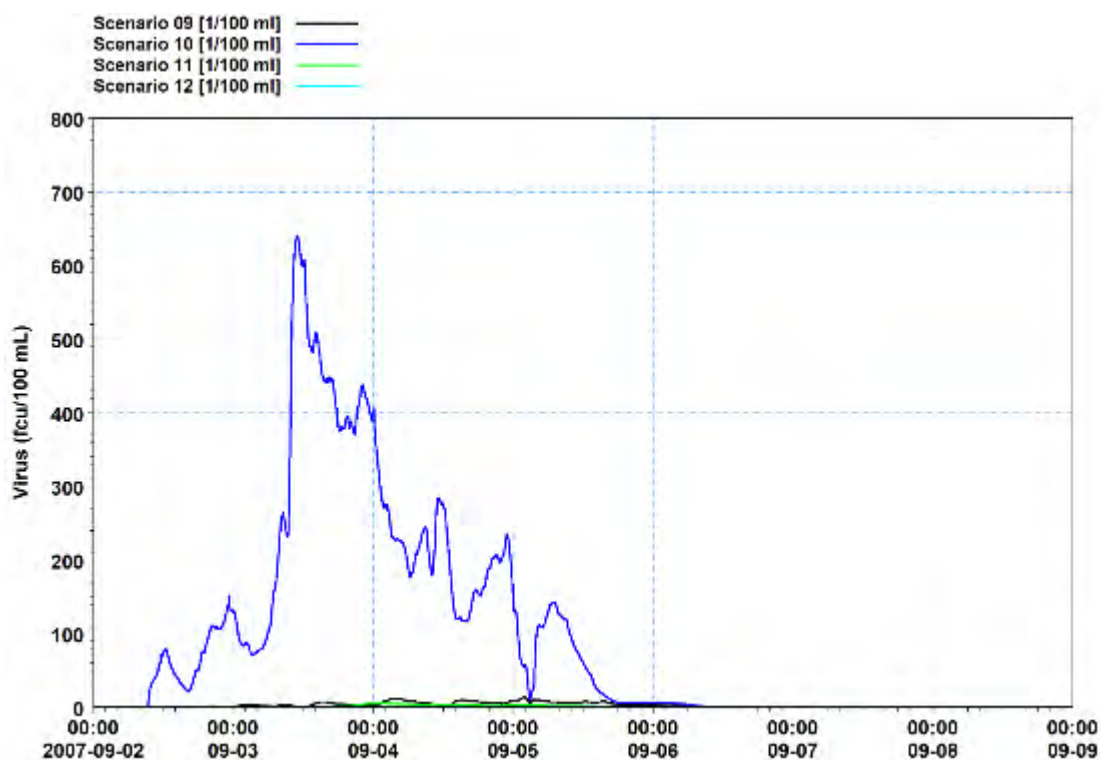


Figure F-12 Predicted Virus (Virus/100 ml) at the Ti Korohiwa Rocks monitoring site for the overflow scenarios for onshore winds and a spring tide.

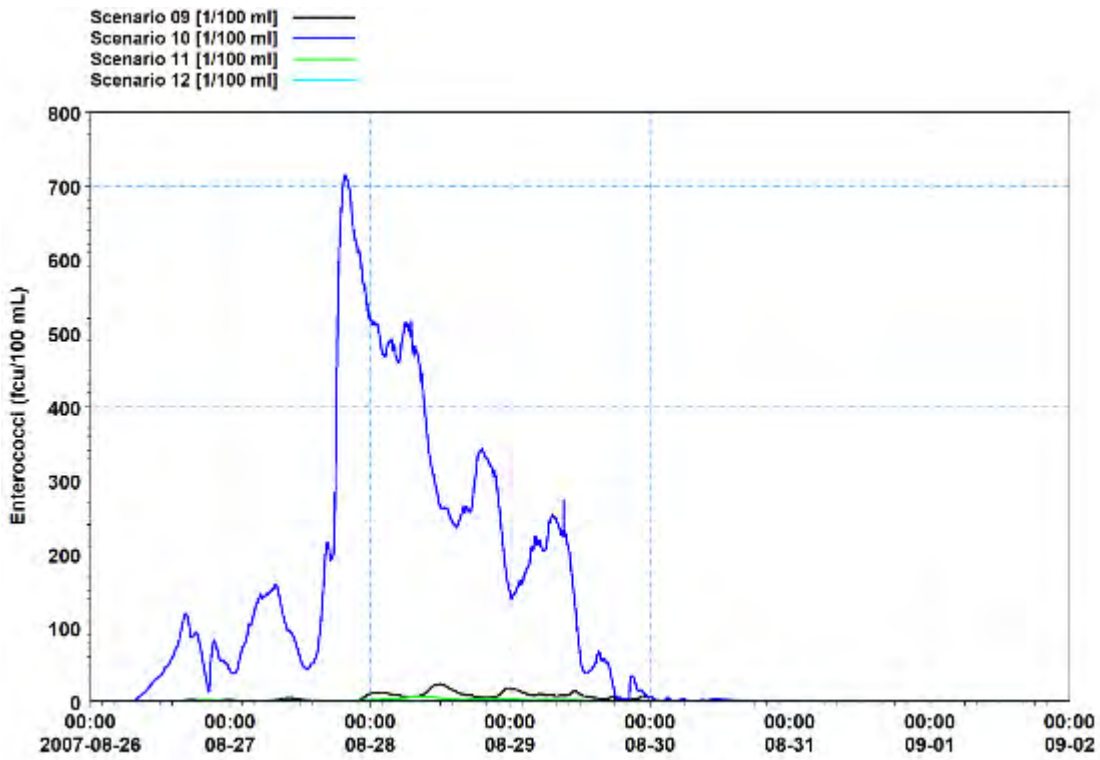


Figure F-13 Predicted Enterococci (Ent/100 ml) at the Ti Korohiwa Rocks monitoring site for the overflow scenarios for typical winds and a neap tide.

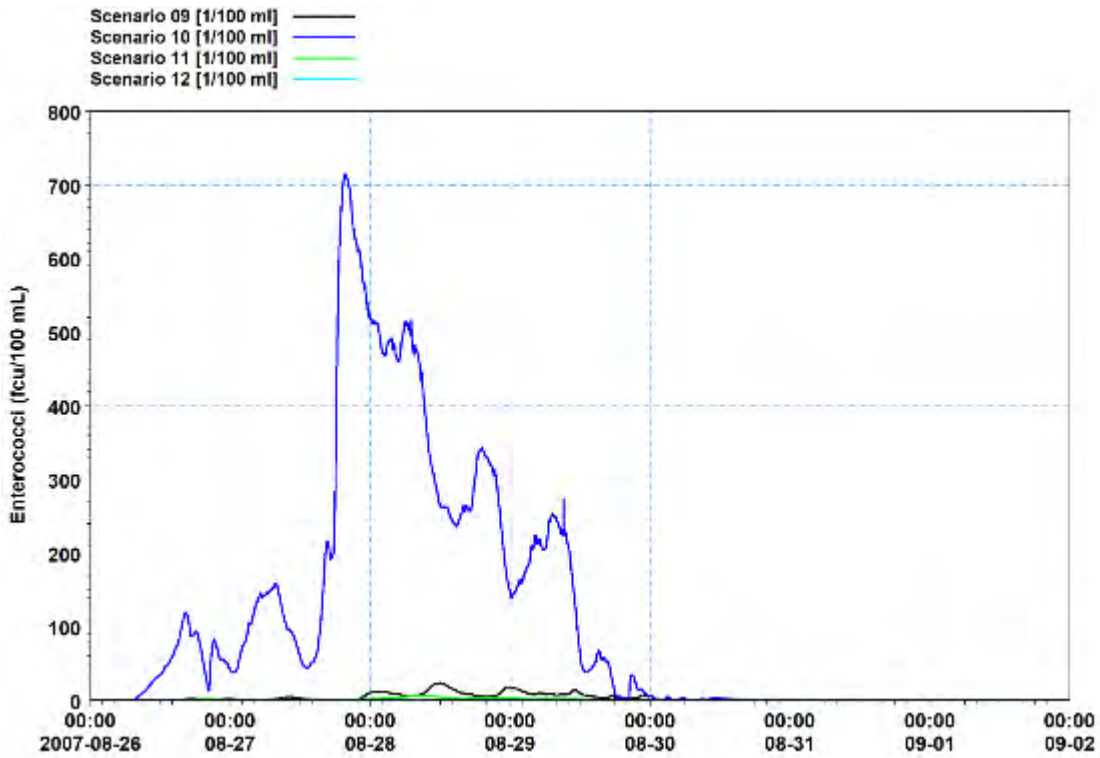


Figure F-14 Predicted Virus (Virus/100 ml) at the Ti Korohiwa Rocks monitoring site for the overflow scenarios for typical winds and a neap tide.

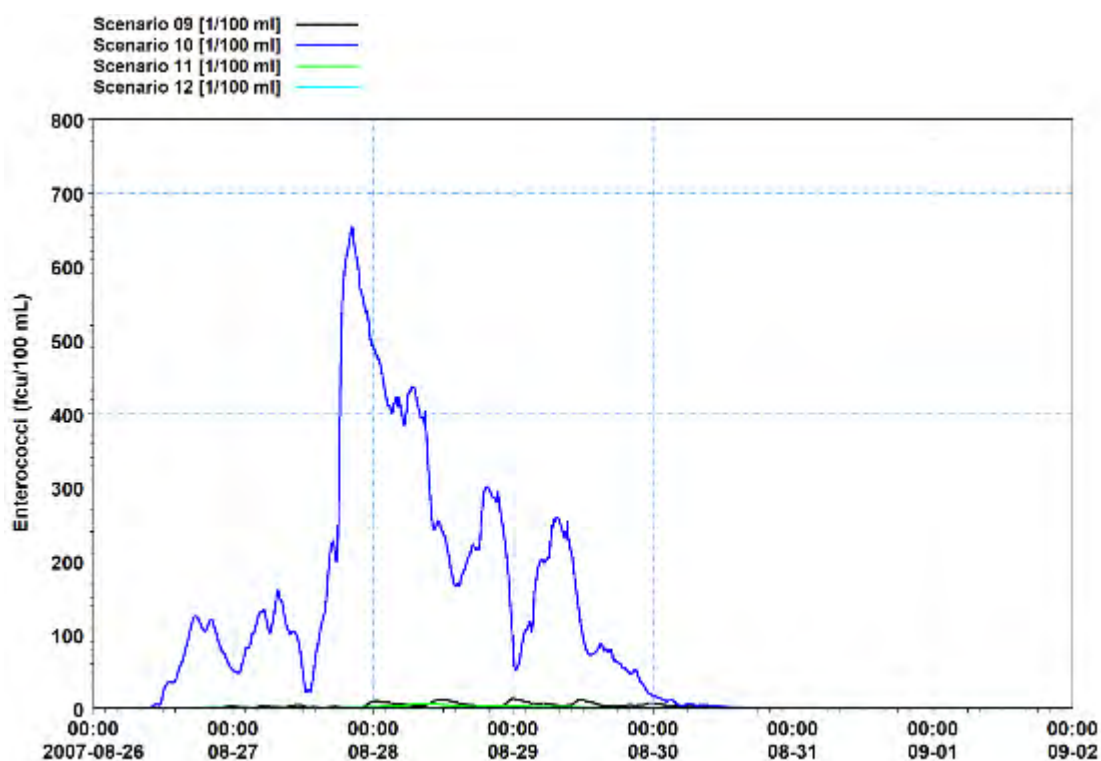


Figure F-15 Predicted Enterococci (Ent/100 ml) at the Ti Korohiwa Rocks monitoring site for the overflow scenarios for onshore winds and a neap tide.

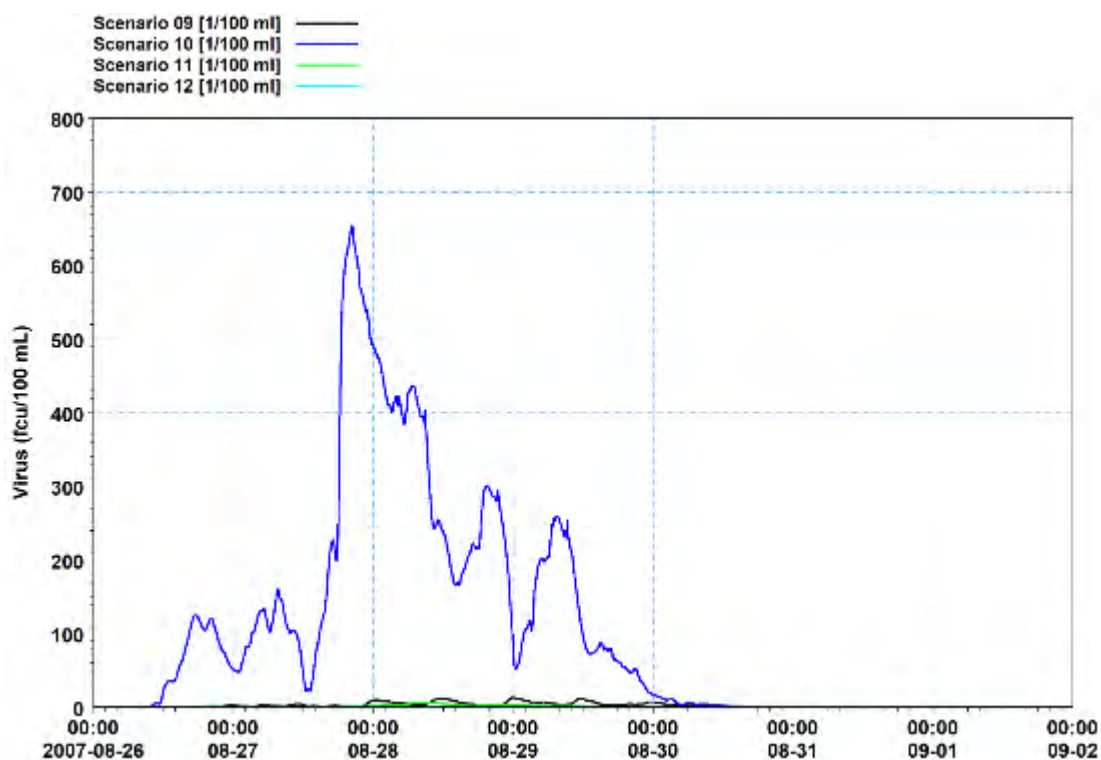


Figure F-16 Predicted Virus (Virus/100 ml) at the Ti Korohiwa Rocks monitoring site for the overflow scenarios for onshore winds and a neap tide.

Appendix G – Time-series at Titahi Beach South Monitoring site (PWWF discharge and overflow scenarios)

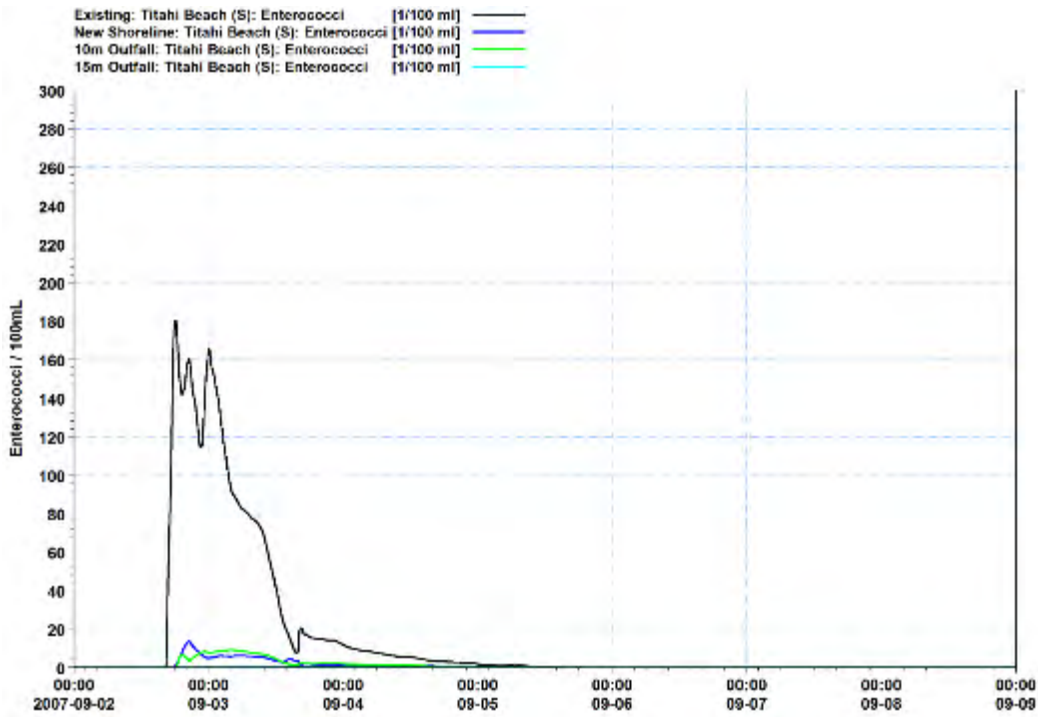


Figure G-1 Predicted Enterococci (Ent/100 ml) at Titahi Beach South for the discharge options for typical winds and a spring tide.

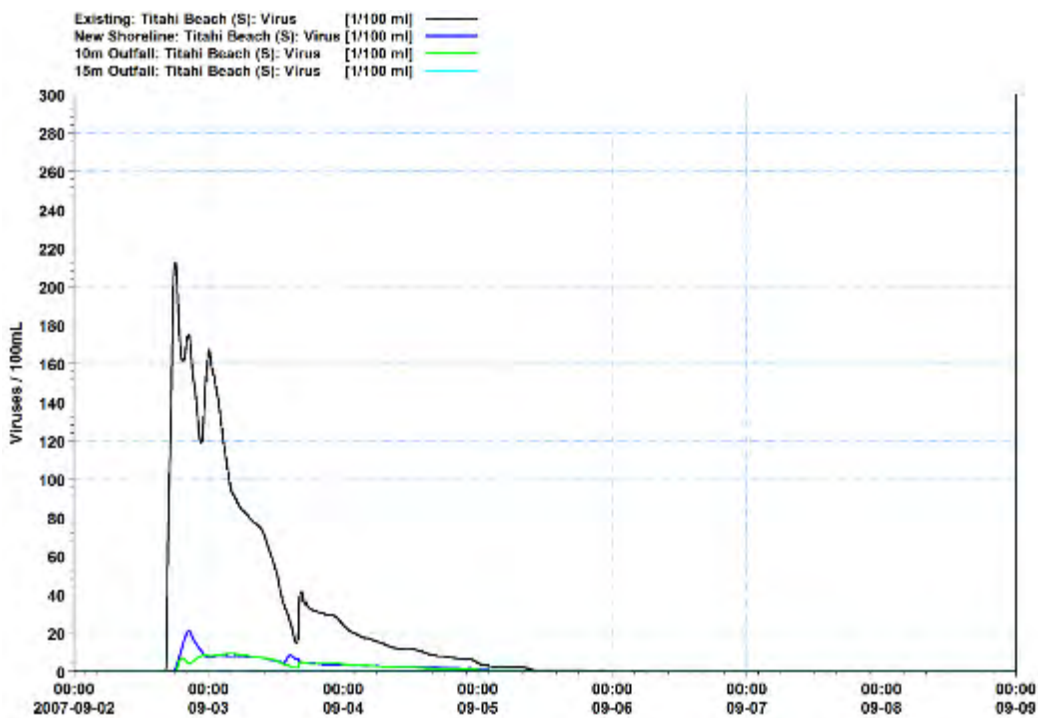


Figure G-2 Predicted Virus (Virus/100 ml) at Titahi Beach South for the discharge options for typical winds and a spring tide.

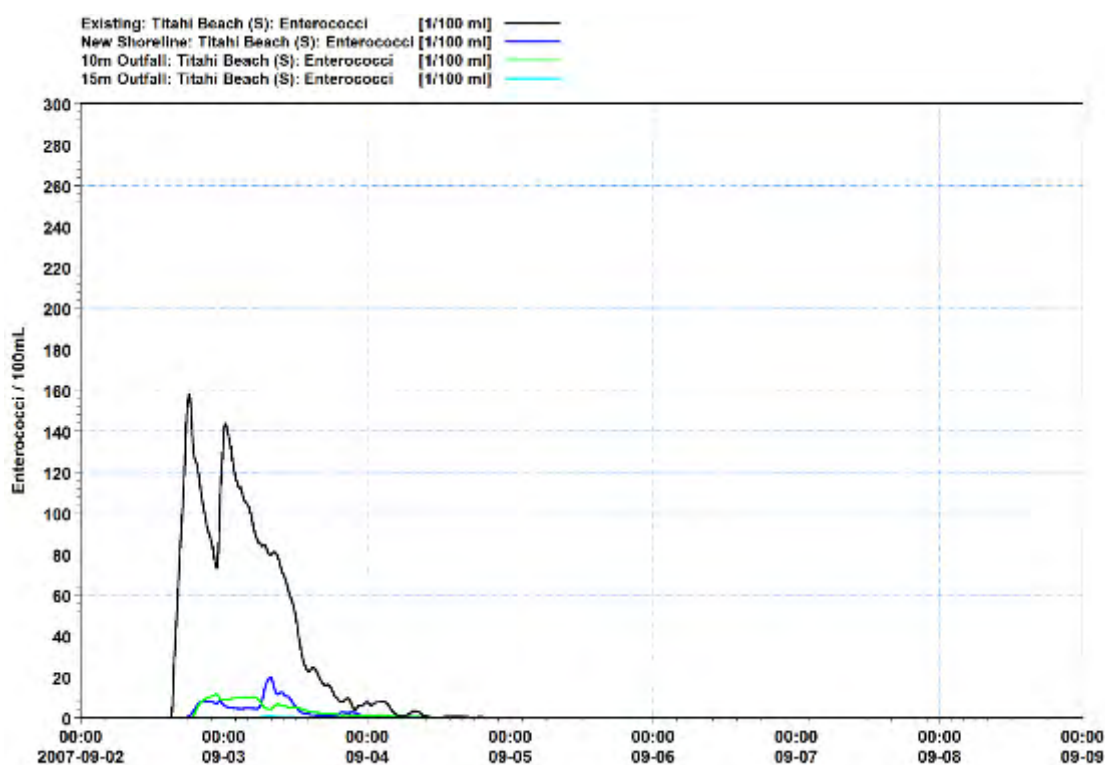


Figure G-3 Predicted Enterococci (Ent/100 ml) at Titahi Beach South for the discharge options for onshore winds and a spring tide.

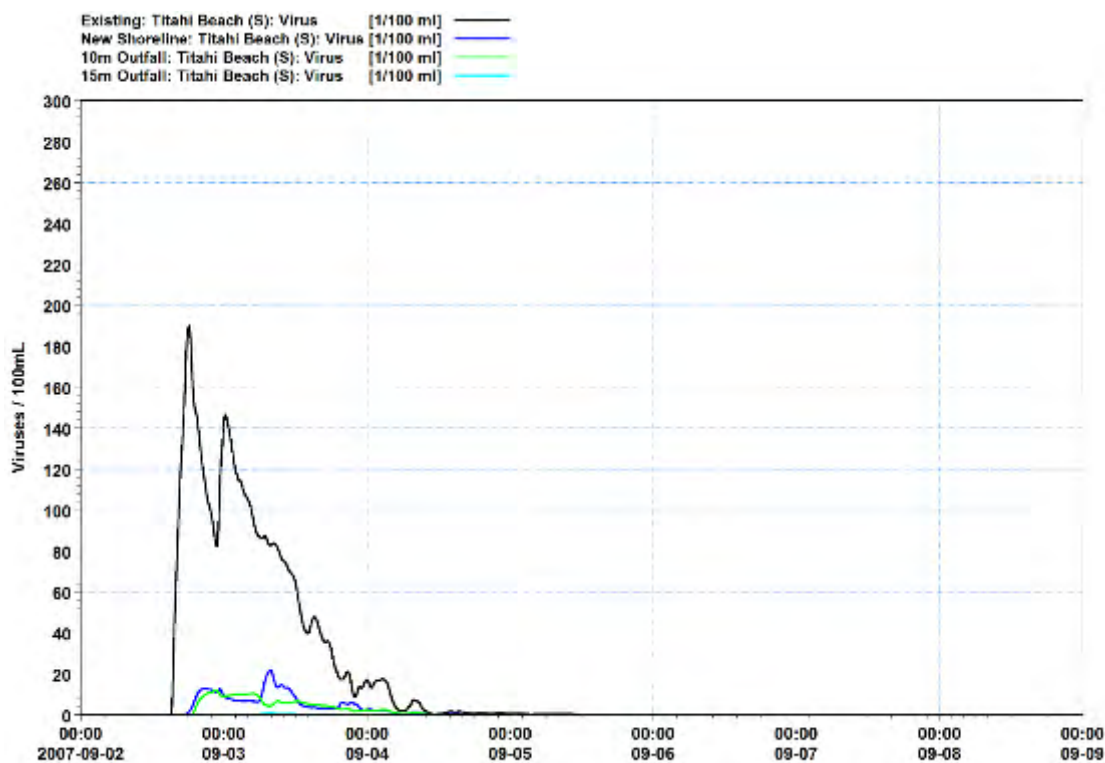


Figure G-4 Predicted Virus (Virus/100 ml) at the Titahi Beach South for the discharge options for onshore winds and a spring tide.

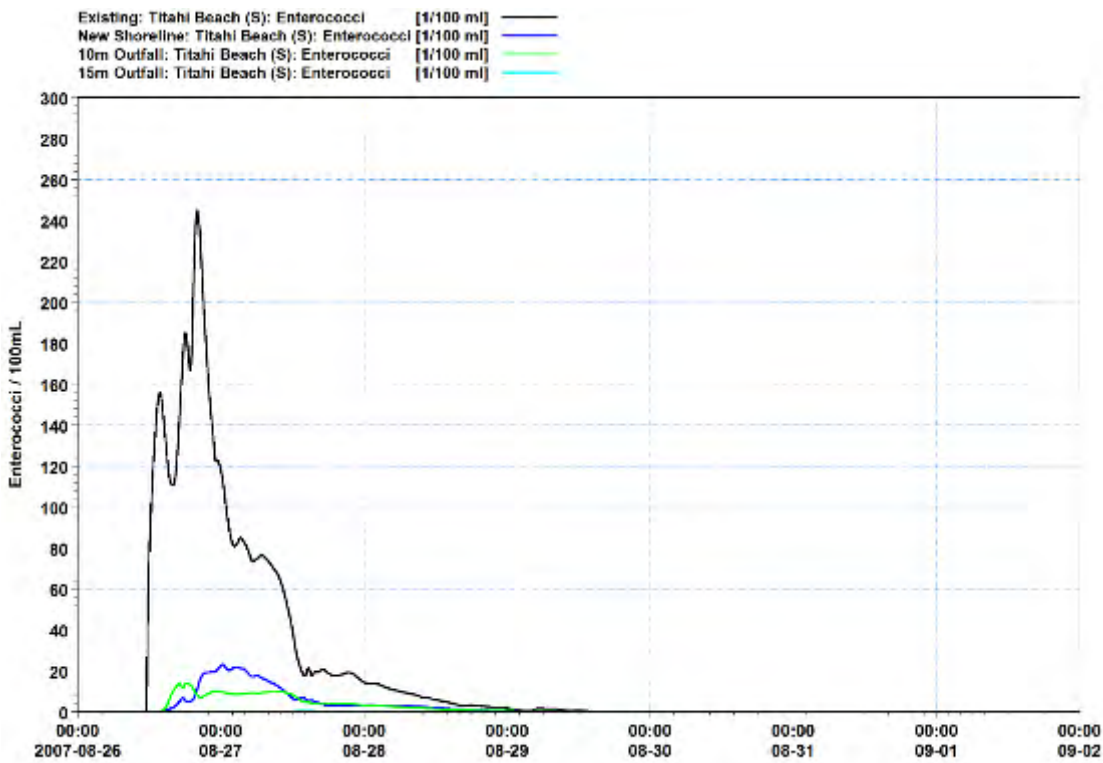


Figure G-5 Predicted Enterococci (Ent/100 ml) at Titahi Beach South for the discharge options for typical winds and a neap tide.

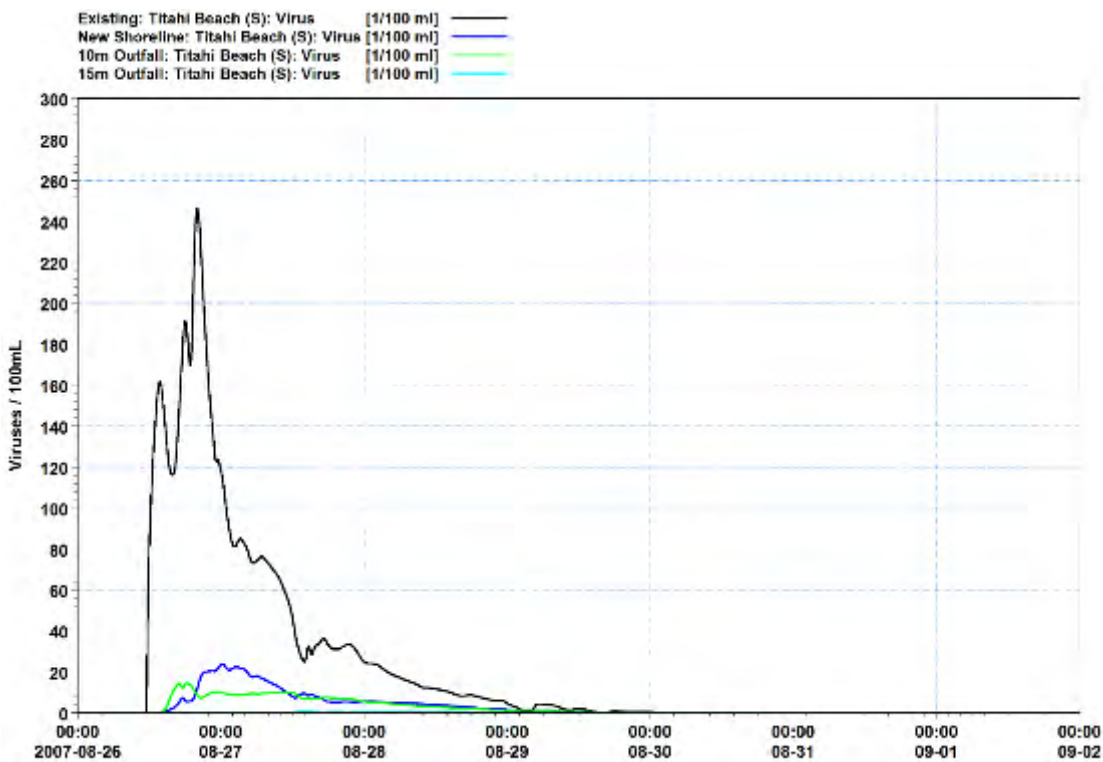


Figure G-6 Predicted Enterococci (Ent/100 ml) at Titahi Beach South for the discharge options for typical winds and a neap tide.

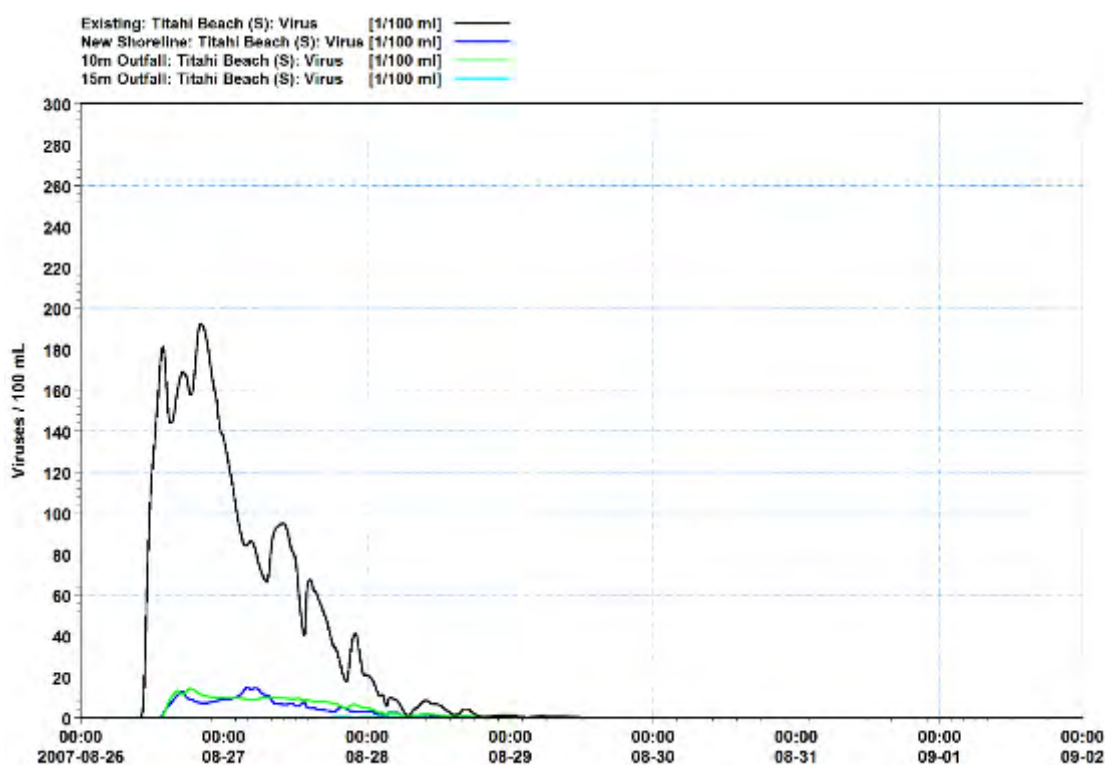


Figure G-7 Predicted Enterococci (Ent/100 ml) at Titahi Beach South for the discharge options for onshore winds and a neap tide.

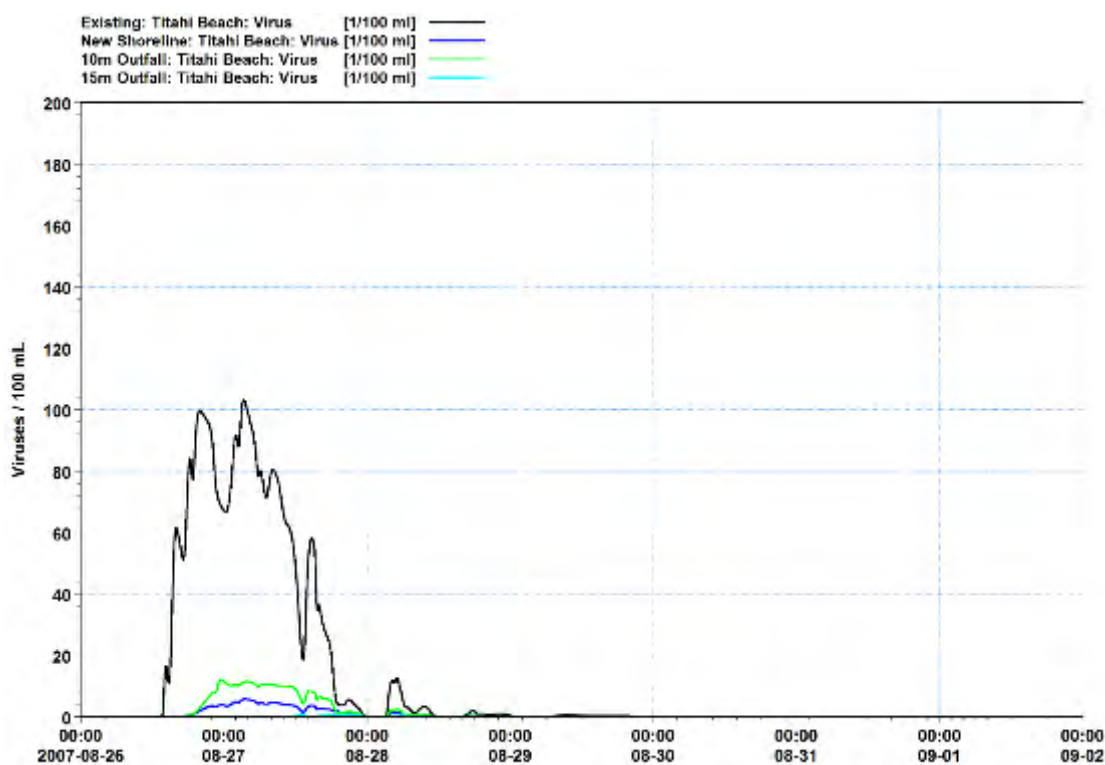


Figure G-8 Predicted Virus (Virus/100 ml) at Titahi Beach South for the discharge options for onshore winds and a neap tide.

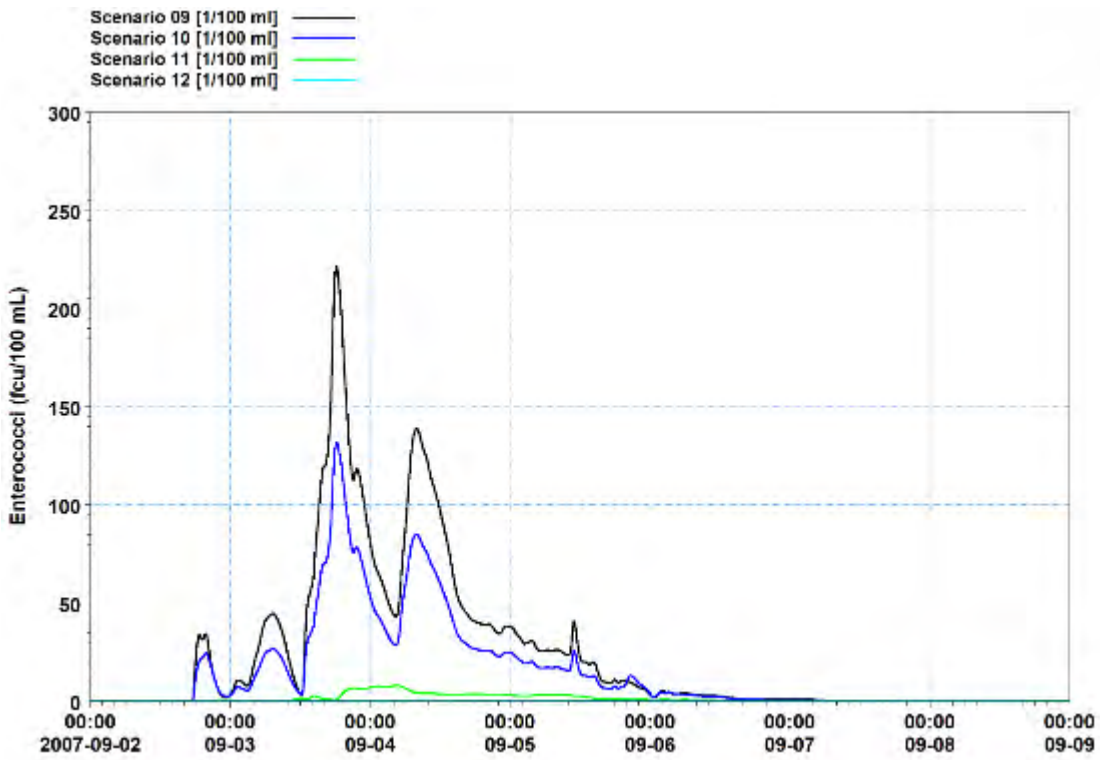


Figure G-9 Predicted Enterococci (Ent/100 ml) at the Titahi Beach South monitoring site for the overflow scenarios for typical winds and a spring tide.

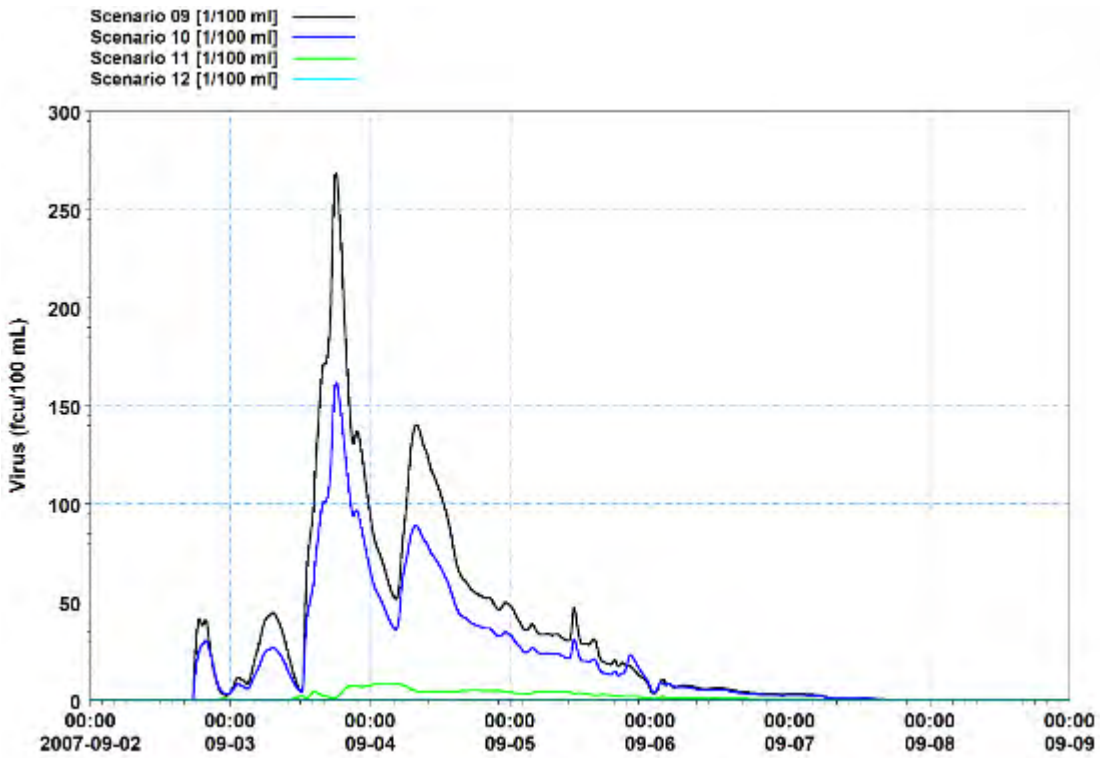


Figure G-10 Predicted Virus (Virus/100 ml) at the Titahi Beach South monitoring site for the overflow scenarios for typical winds and a spring tide.

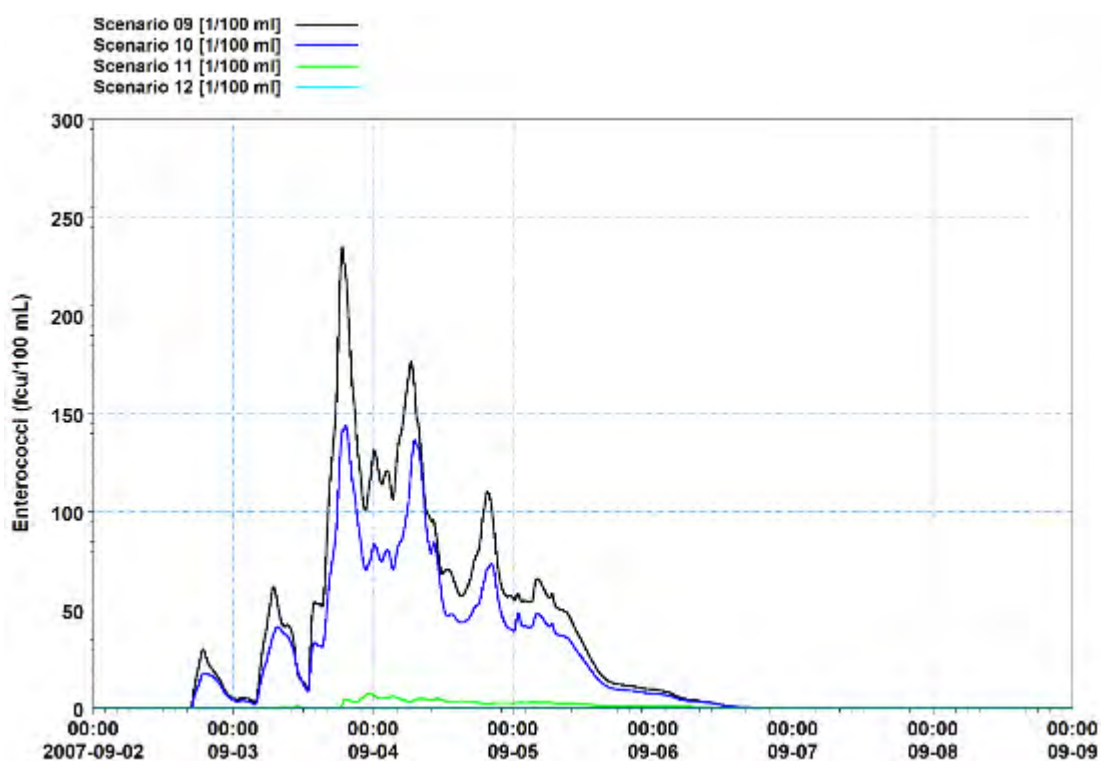


Figure G-11 Predicted Enterococci (Ent/100 ml) at the Titahi Beach South monitoring site for the overflow scenarios for onshore winds and a spring tide.

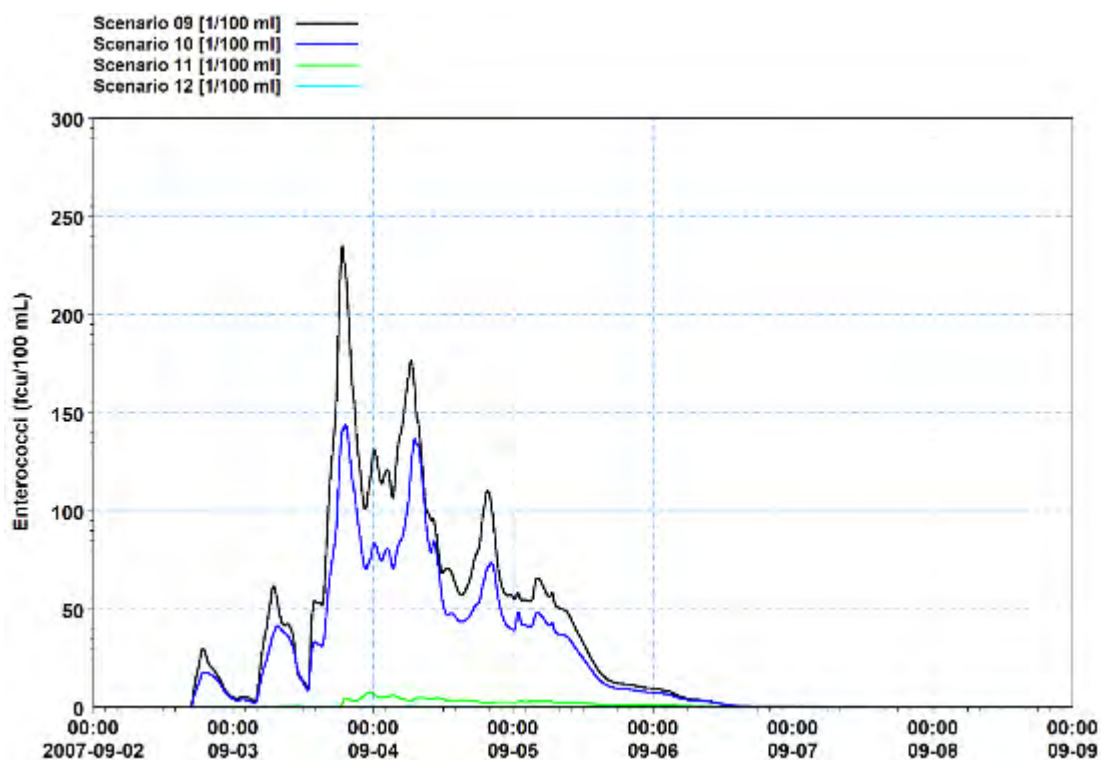


Figure G-12 Predicted Virus (Virus/100 ml) at the Titahi Beach South monitoring site for the overflow scenarios for onshore winds and a spring tide.

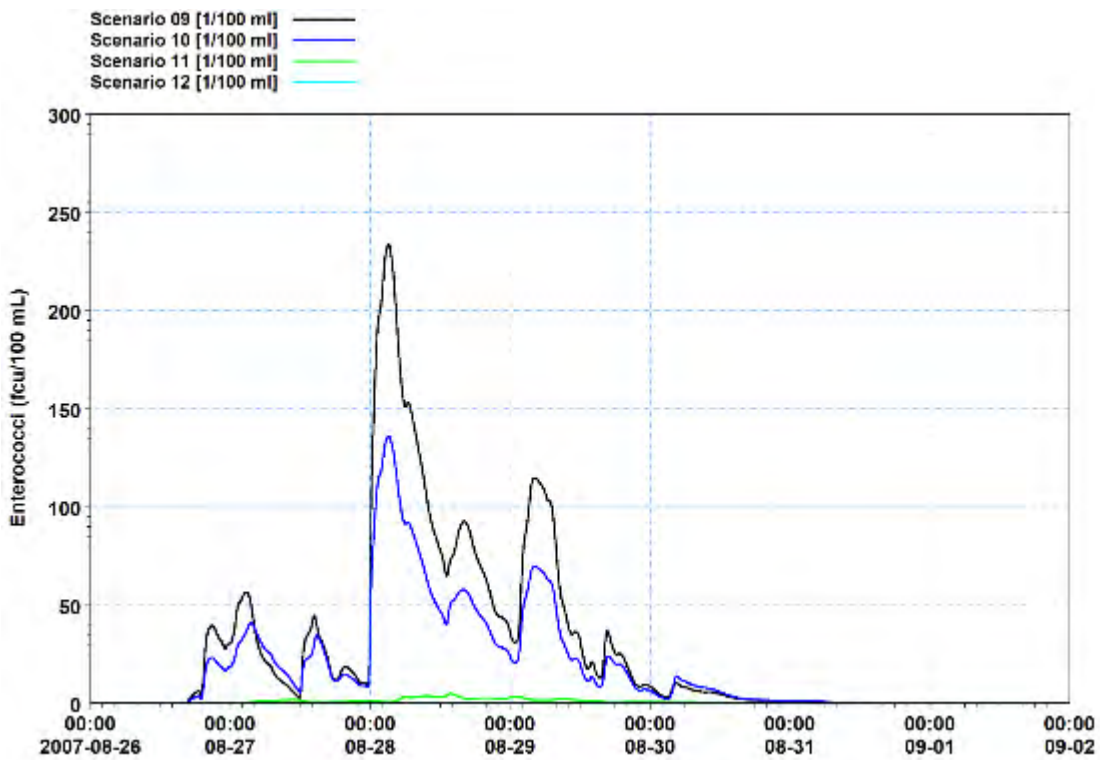


Figure G-13 Predicted Enterococci (Ent/100 ml) at the Titahi Beach South monitoring site for the overflow scenarios for typical winds and a neap tide.

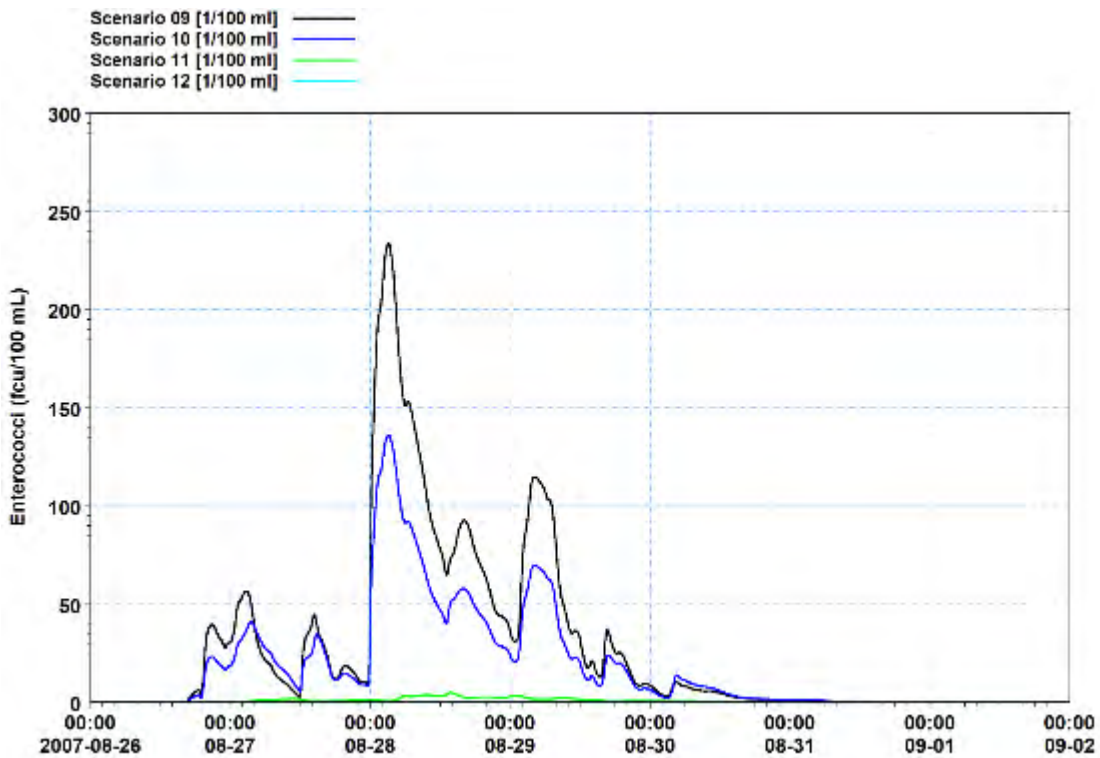


Figure G-14 Predicted Virus (Virus/100 ml) at the Titahi Beach South monitoring site for the overflow scenarios for typical winds and a neap tide.

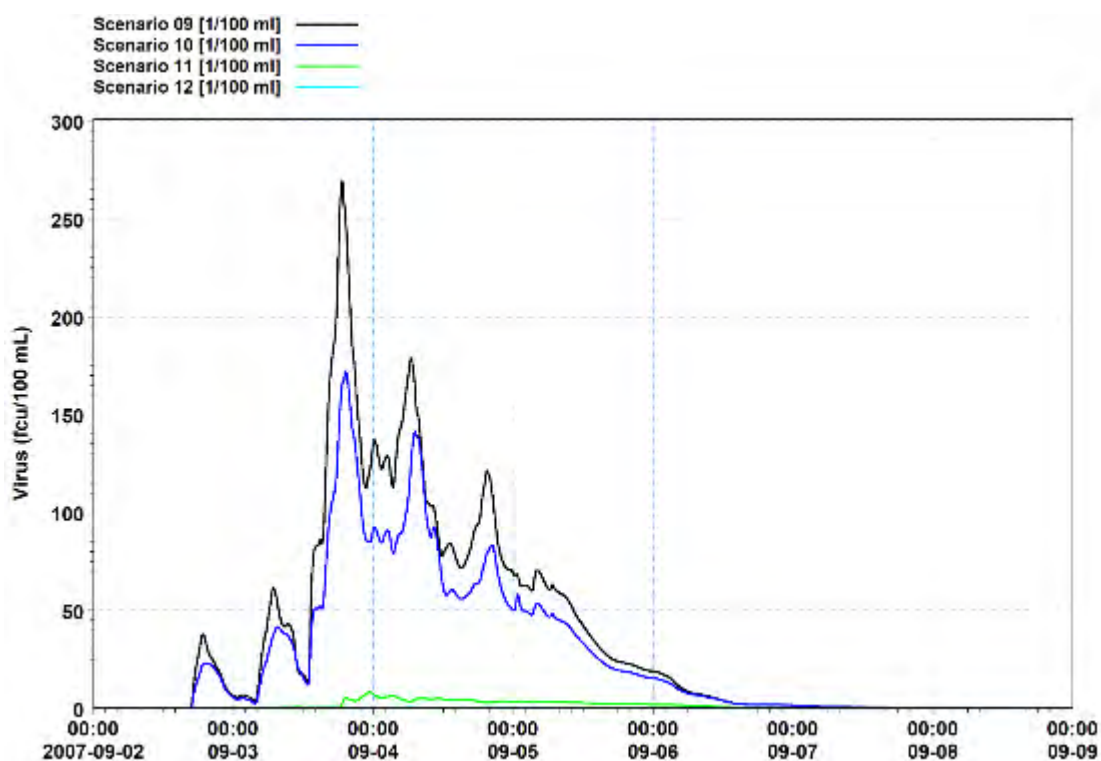


Figure G-15 Predicted Enterococci (Ent/100 ml) at the Titahi Beach South monitoring site for the overflow scenarios for onshore winds and a neap tide.

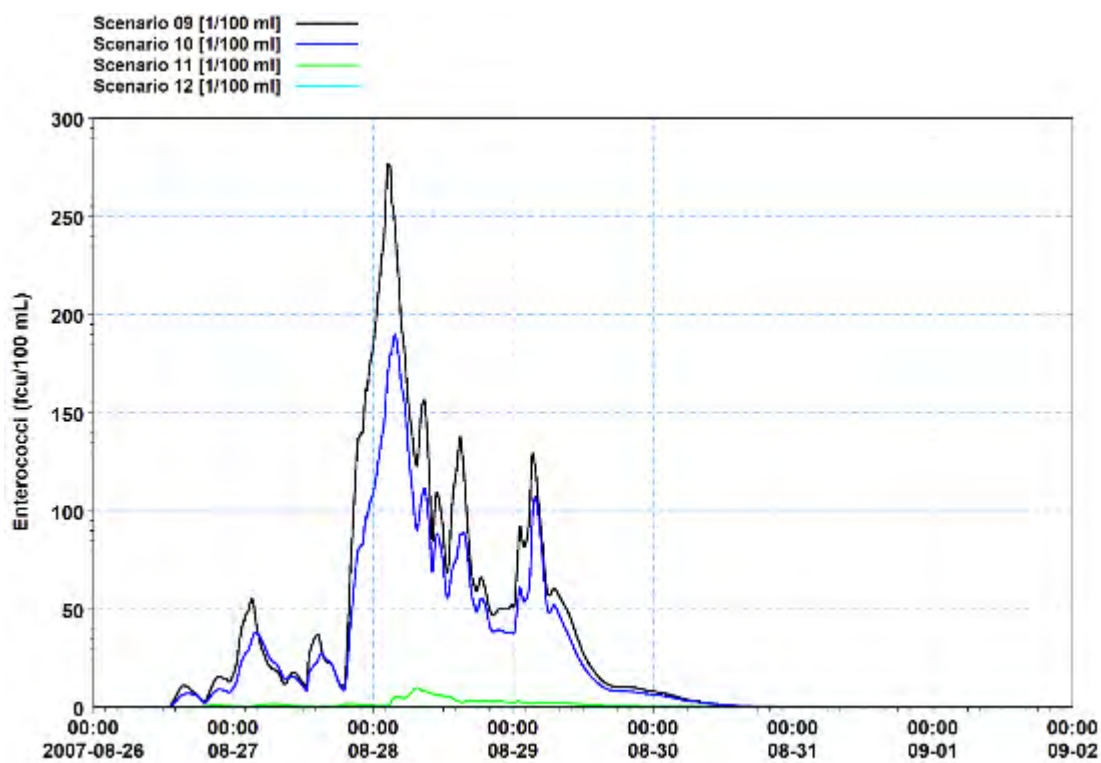


Figure G-16 Predicted Virus (Virus/100 ml) at the Titahi Beach South monitoring site for the overflow scenarios for onshore winds and a neap tide.

Appendix H – Time-series at Titahi Beach Monitoring site (PWWF discharge and overflow scenarios)

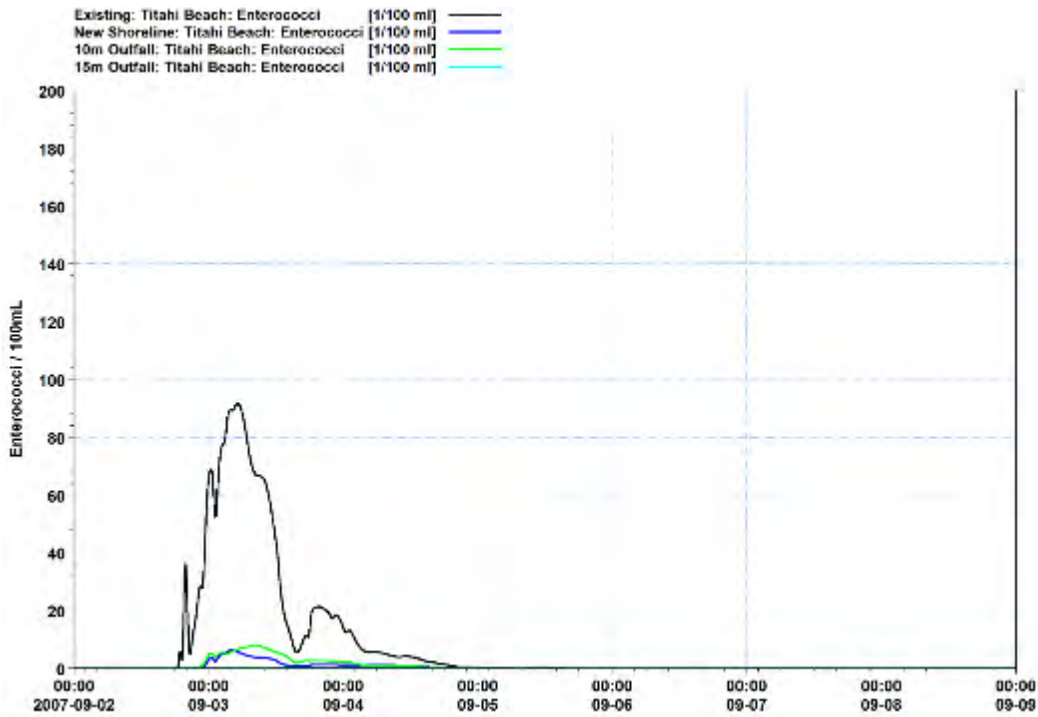


Figure H-1 Predicted Enterococci (Ent/100 ml) at the Titahi Beach for the discharge options for typical winds and a spring tide.

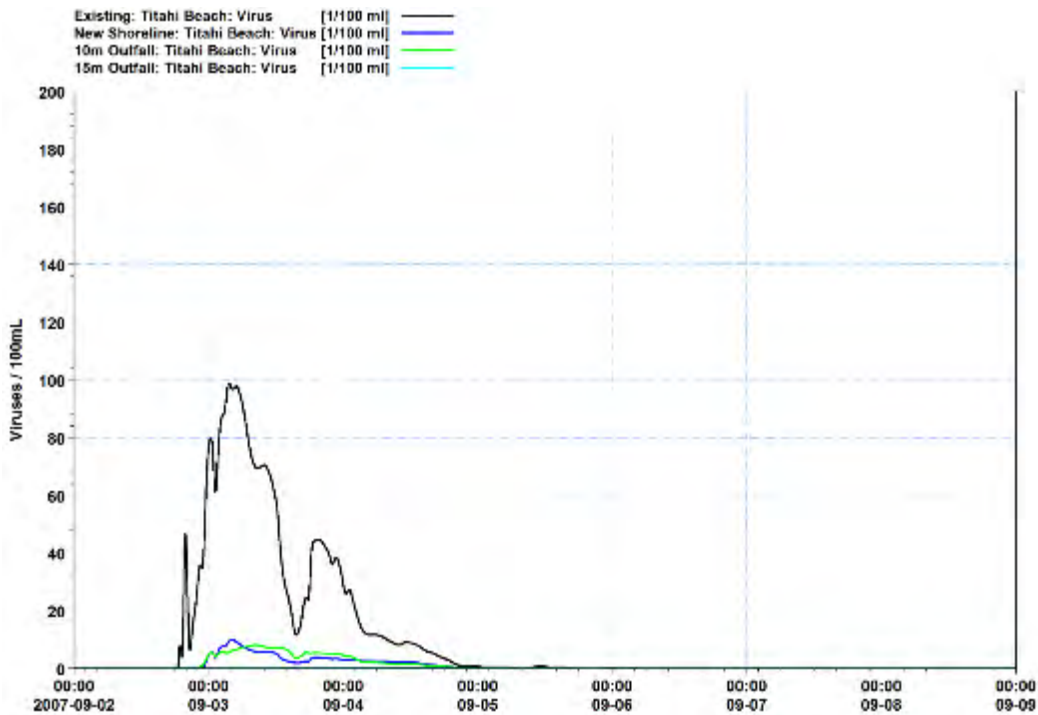


Figure H-2 Predicted Virus (Virus/100 ml) at the Titahi Beach for the discharge options for typical winds and a spring tide.

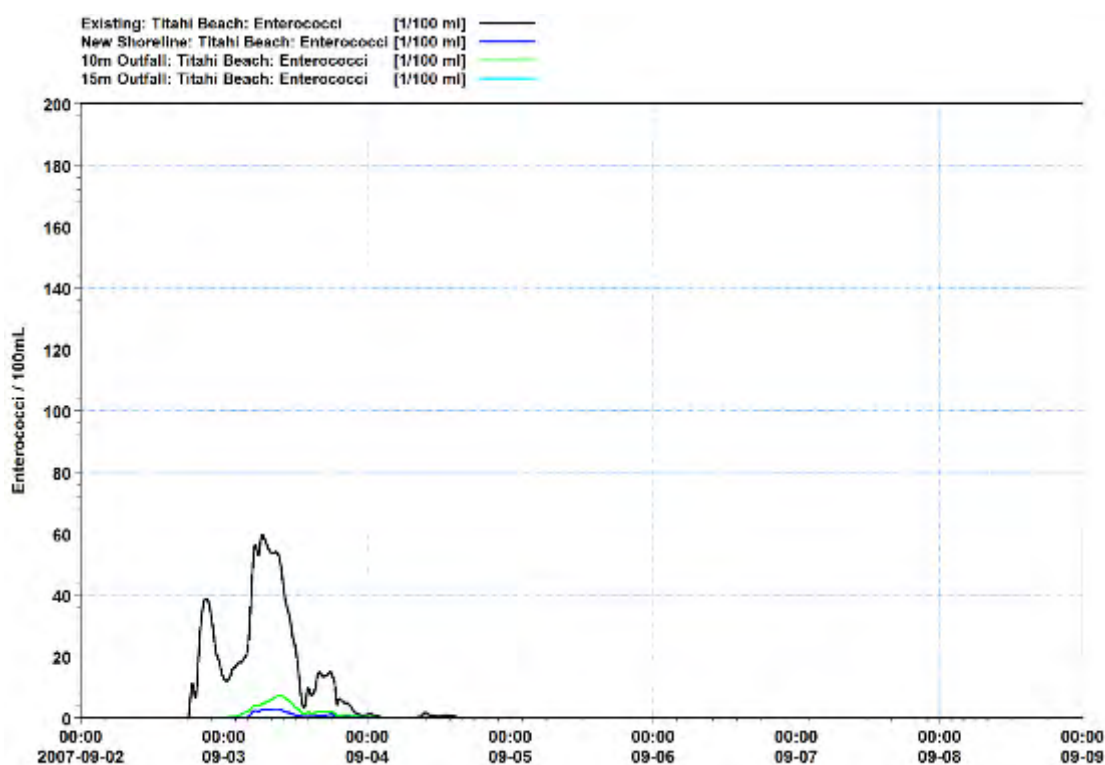


Figure H-3 Predicted Enterococci (Ent/100 ml) at the Titahi Beach for the discharge options for onshore winds and a spring tide.

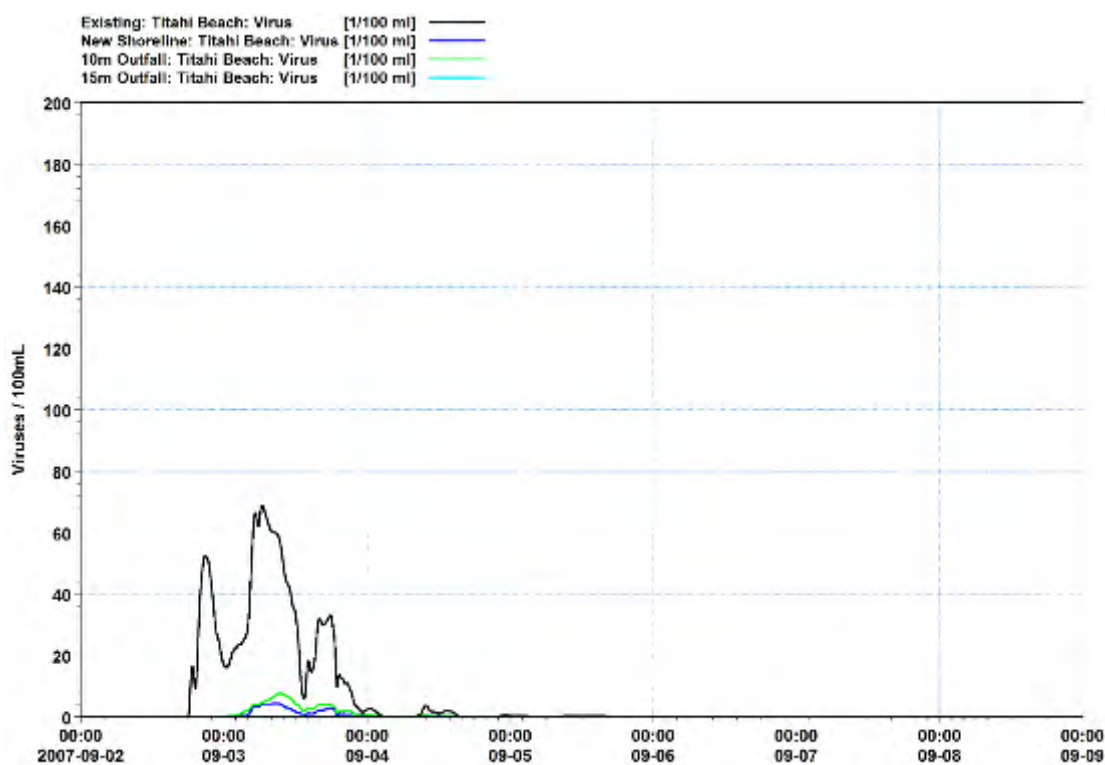


Figure H-4 Predicted Virus (Virus/100 ml) at the Titahi Beach for the discharge options for onshore winds and a spring tide.

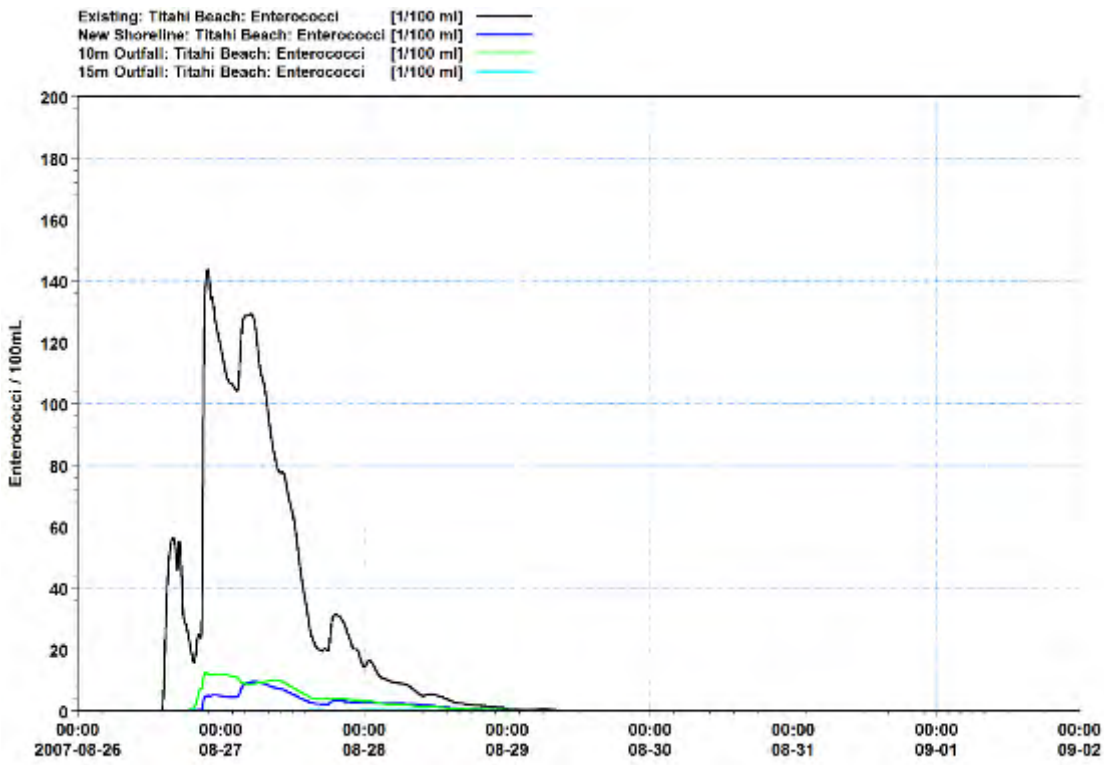


Figure H-5 Predicted Enterococci (Ent/100 ml) at the Titahi Beach for the discharge options for typical winds and a neap tide.

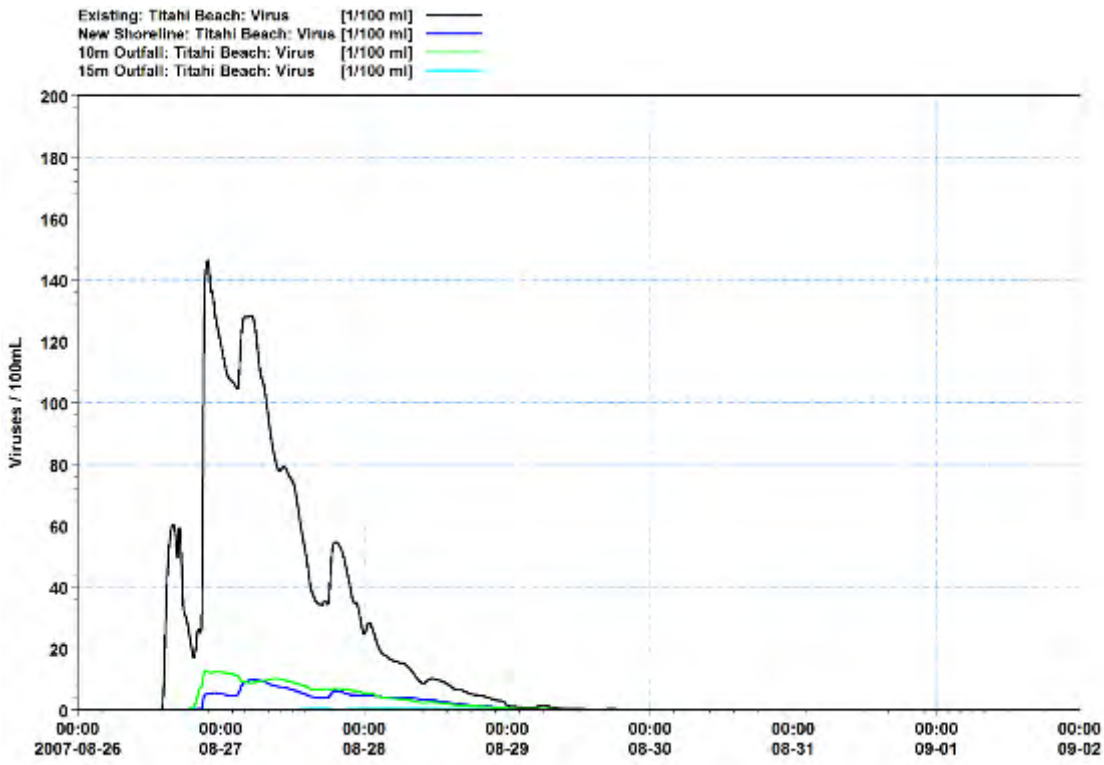


Figure H-6 Predicted Virus (Virus/100 ml) at the Titahi Beach for the discharge options for typical winds and a neap tide.

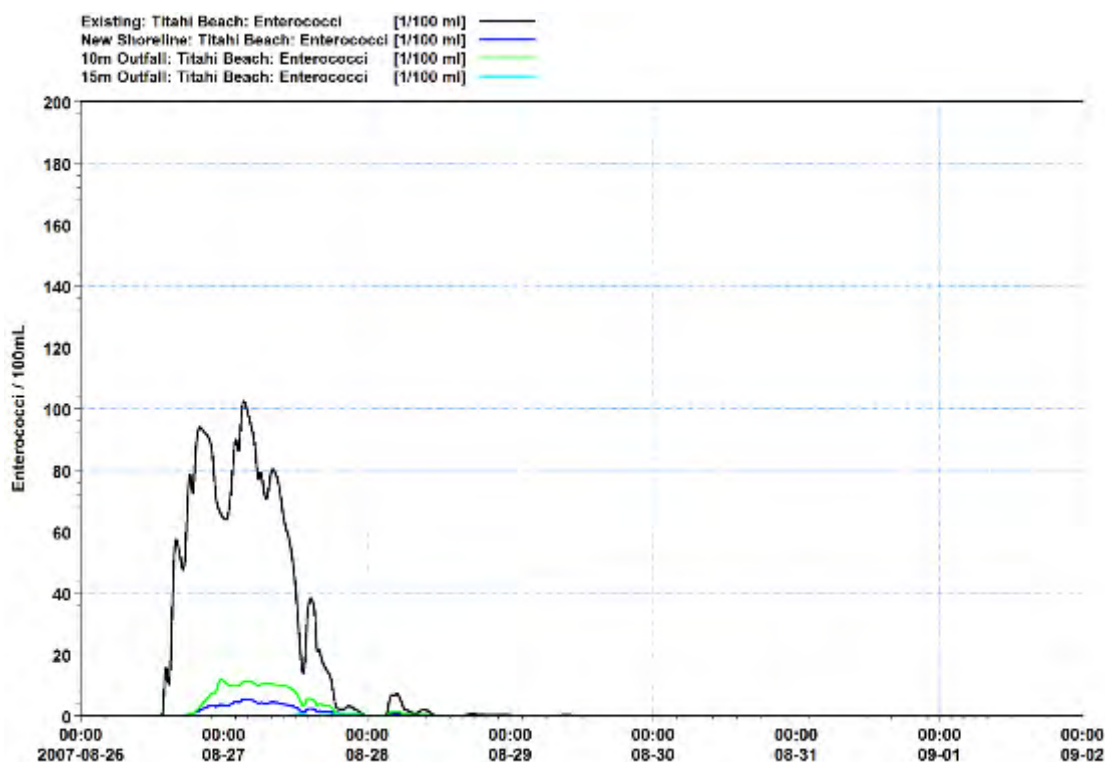


Figure H-7 Predicted Enterococci (Ent/100 ml) at the Titahi Beach for the discharge options for onshore winds and a neap tide.

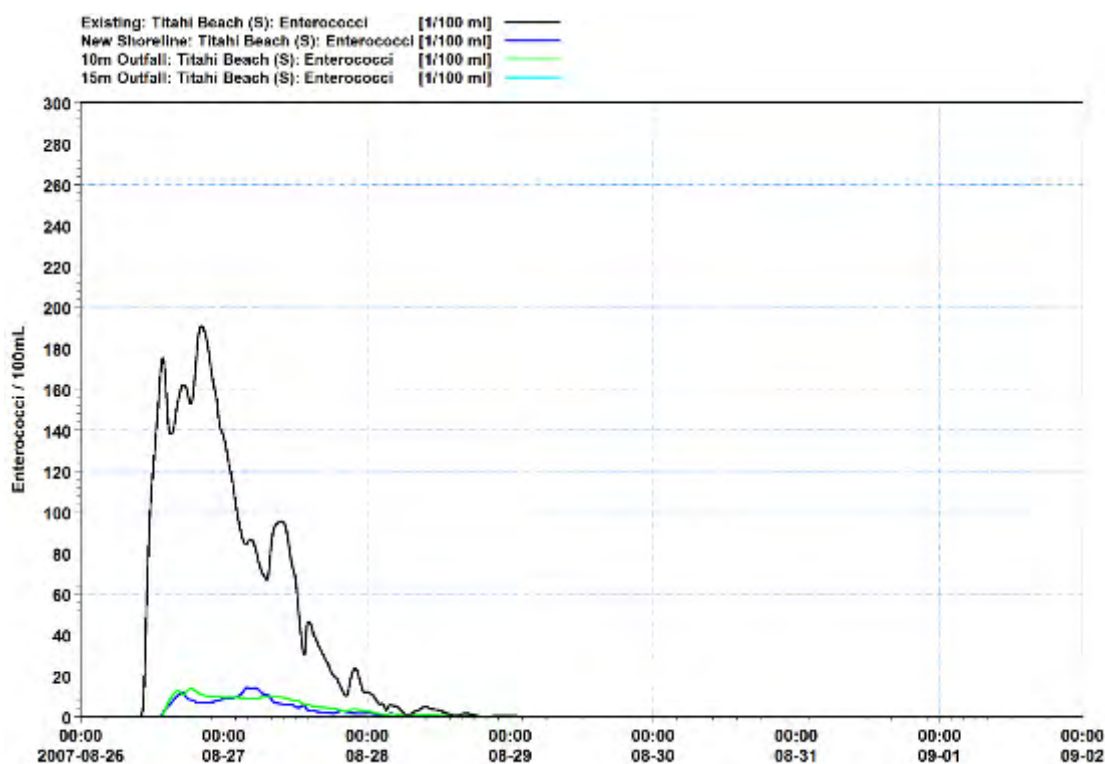


Figure H-8 Predicted Virus (Virus/100 ml) at the Titahi Beach for the discharge options for onshore winds and a neap tide.

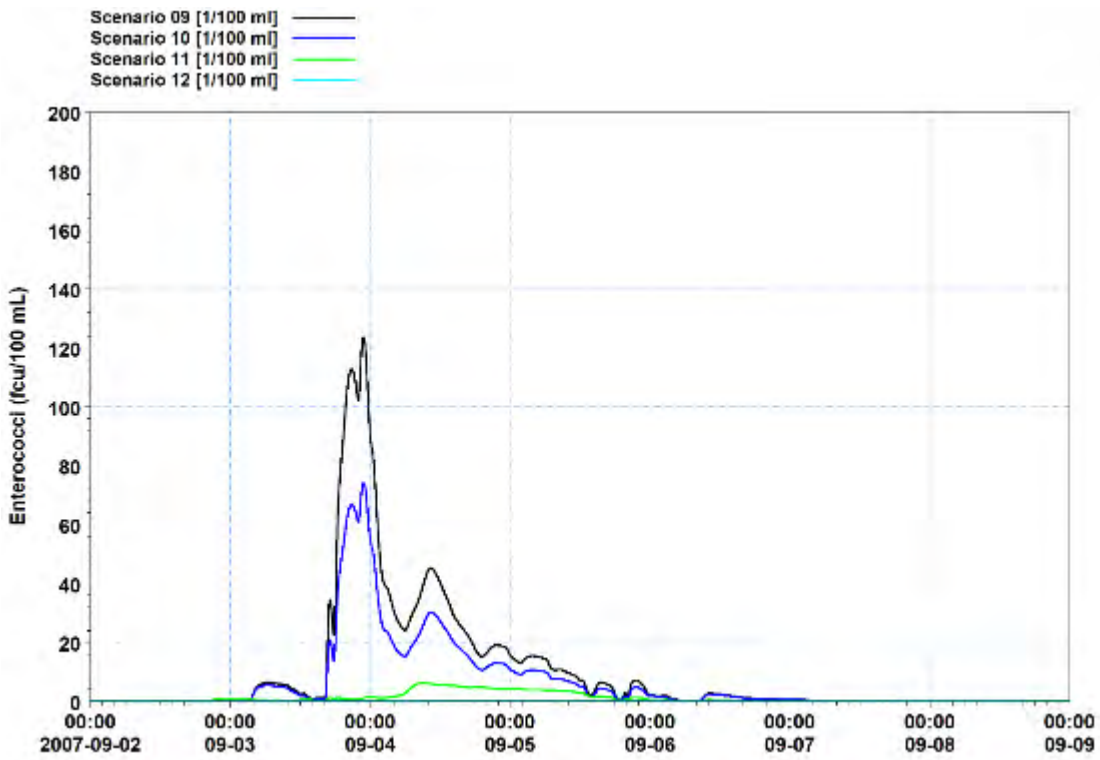


Figure H-9 Predicted Enterococci (Ent/100 ml) at the Titahi Beach monitoring site for the overflow scenarios for typical winds and a spring tide.

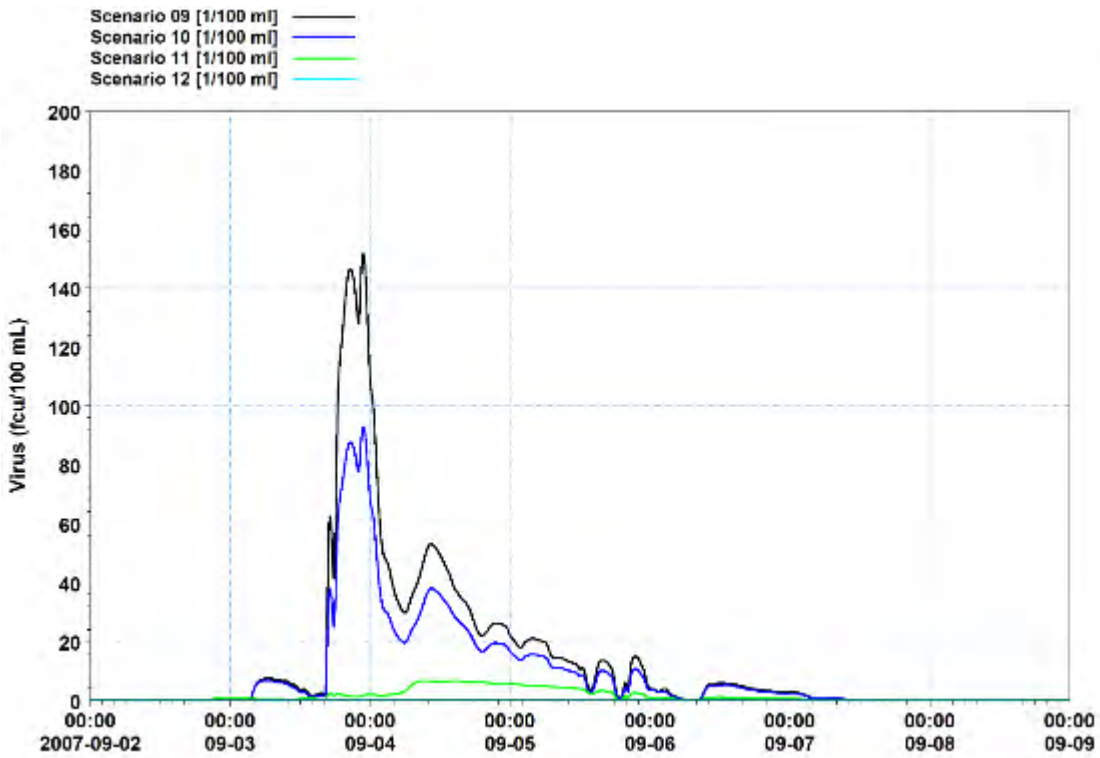


Figure H-10 Predicted Virus (Virus/100 ml) at the Titahi Beach monitoring site for the overflow scenarios for typical winds and a spring tide.

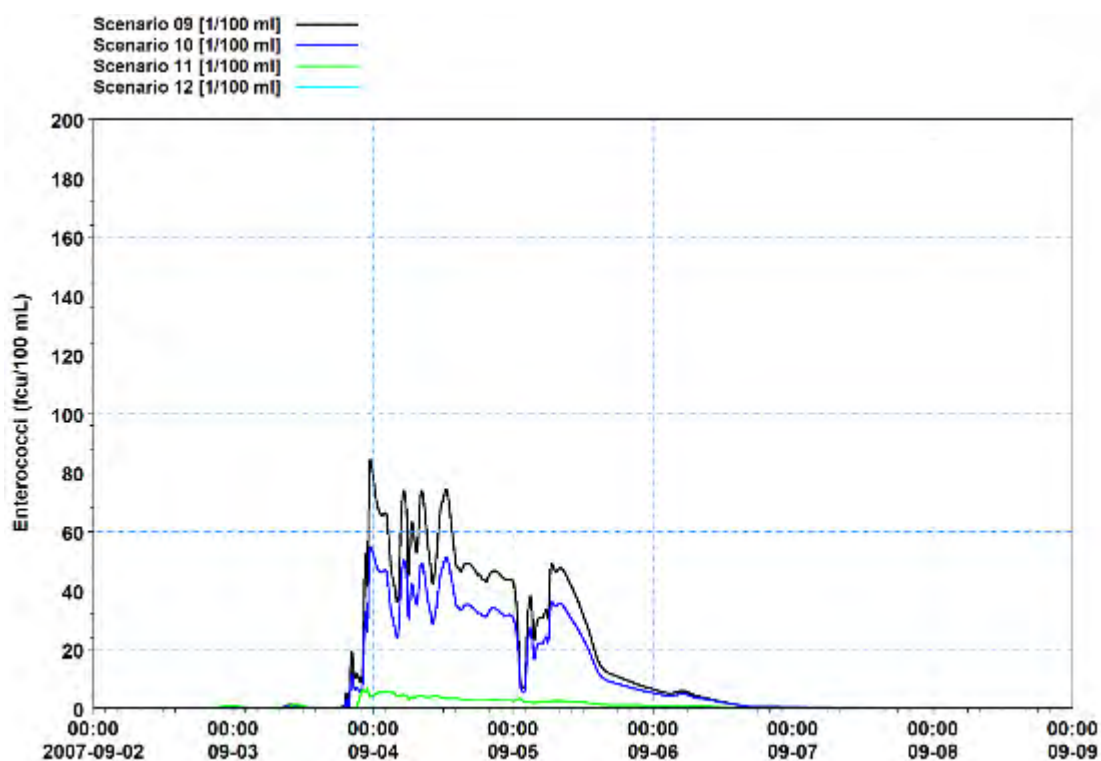


Figure H-11 Predicted Enterococci (Ent/100 ml) at the Titahi Beach monitoring site for the overflow scenarios for onshore winds and a spring tide.

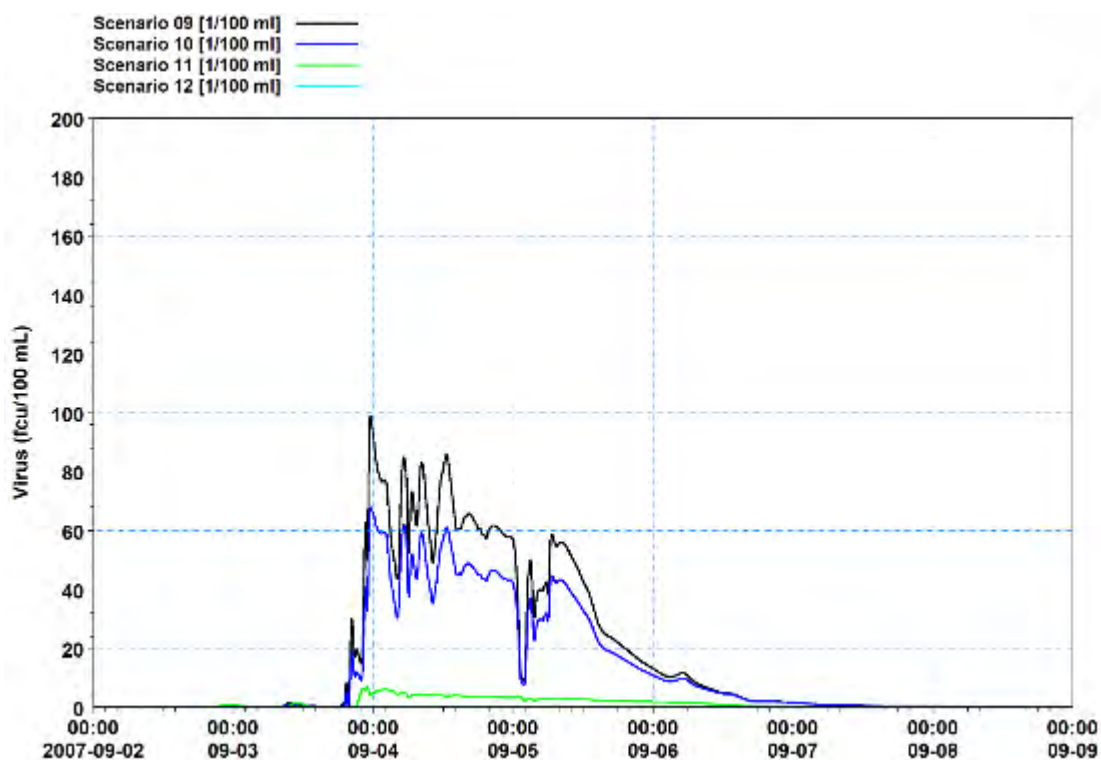


Figure H-12 Predicted Virus (Virus/100 ml) at the Titahi Beach monitoring site for the overflow scenarios for onshore winds and a spring tide.

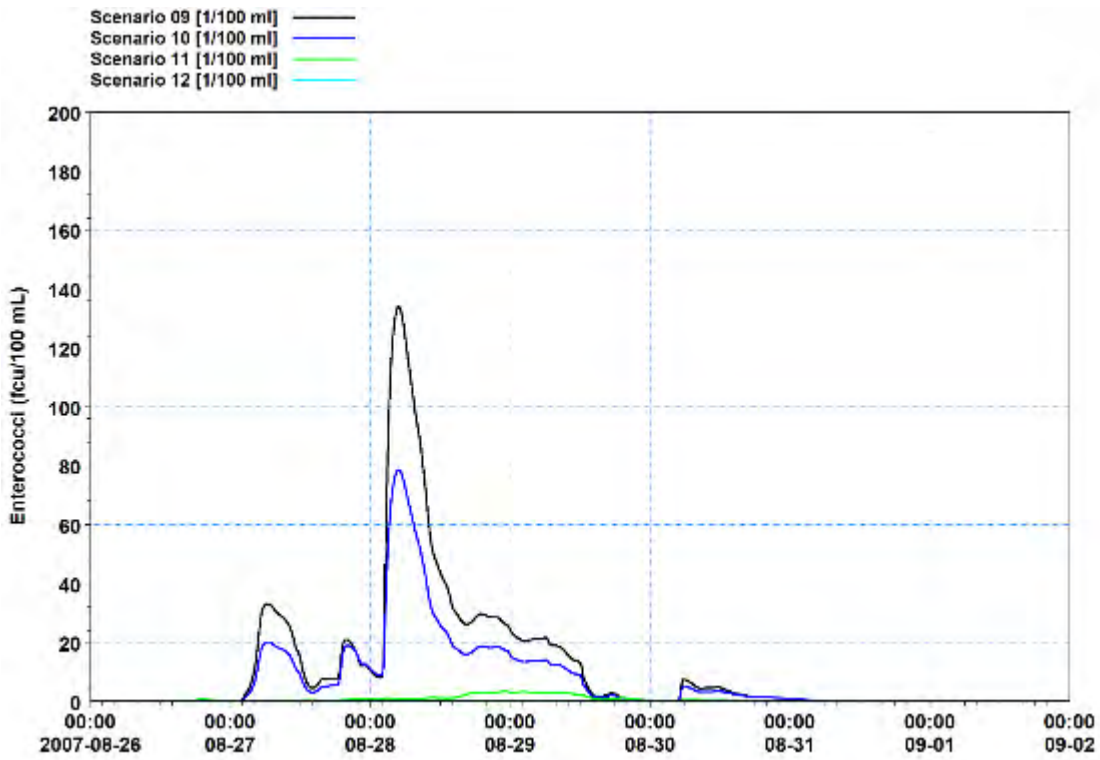


Figure H-13 Predicted Enterococci (Ent/100 ml) at the Titahi Beach monitoring site for the overflow scenarios for typical winds and a neap tide.

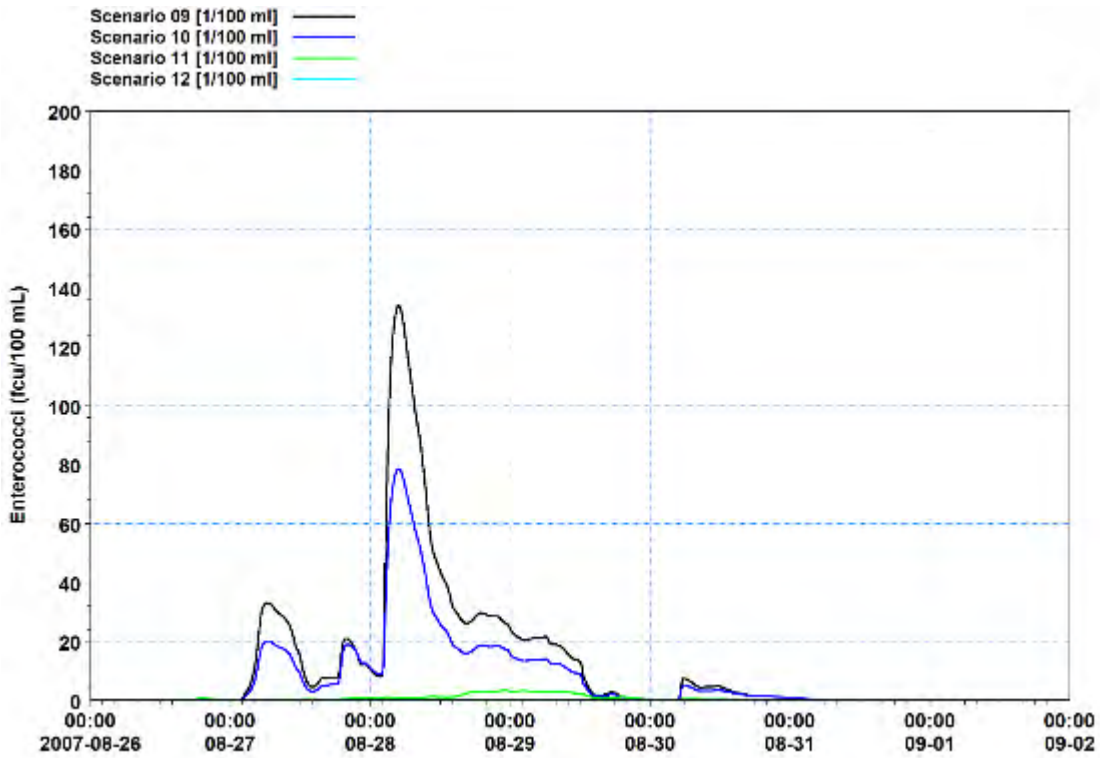


Figure H-14 Predicted Virus (Virus/100 ml) at the Titahi Beach monitoring site for the overflow scenarios for typical winds and a neap tide.

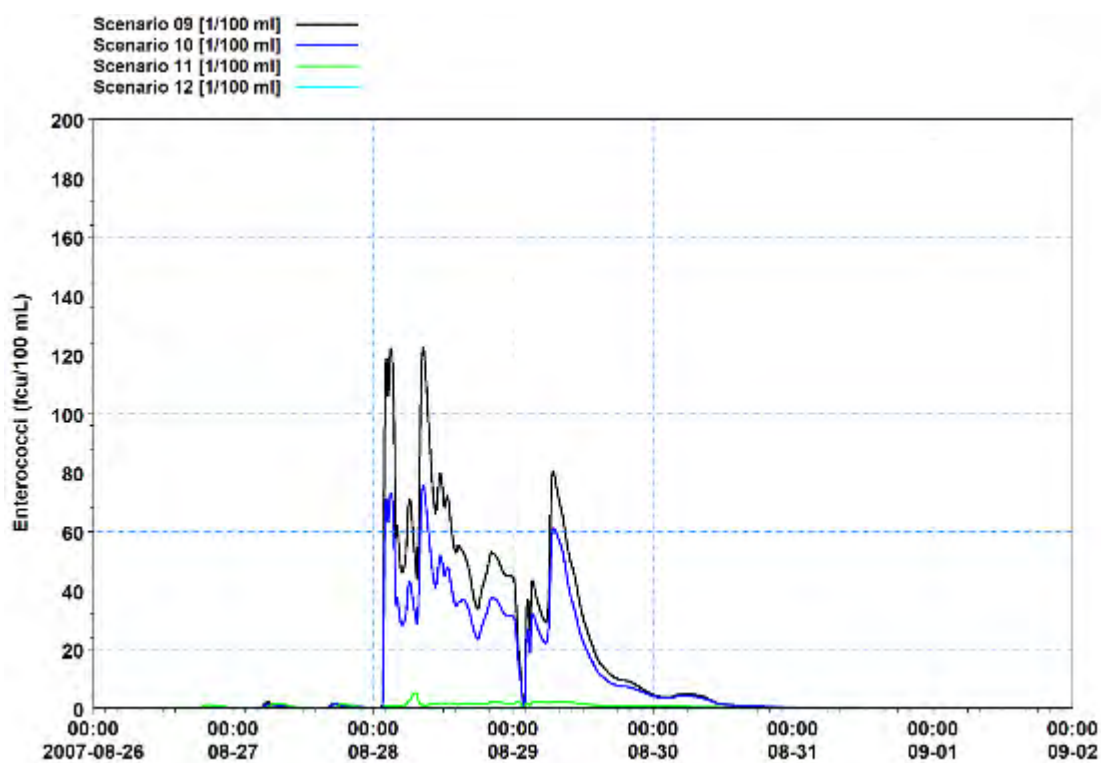


Figure H-15 Predicted Enterococci (Ent/100 ml) at the Titahi Beach monitoring site for the overflow scenarios for onshore winds and a neap tide.

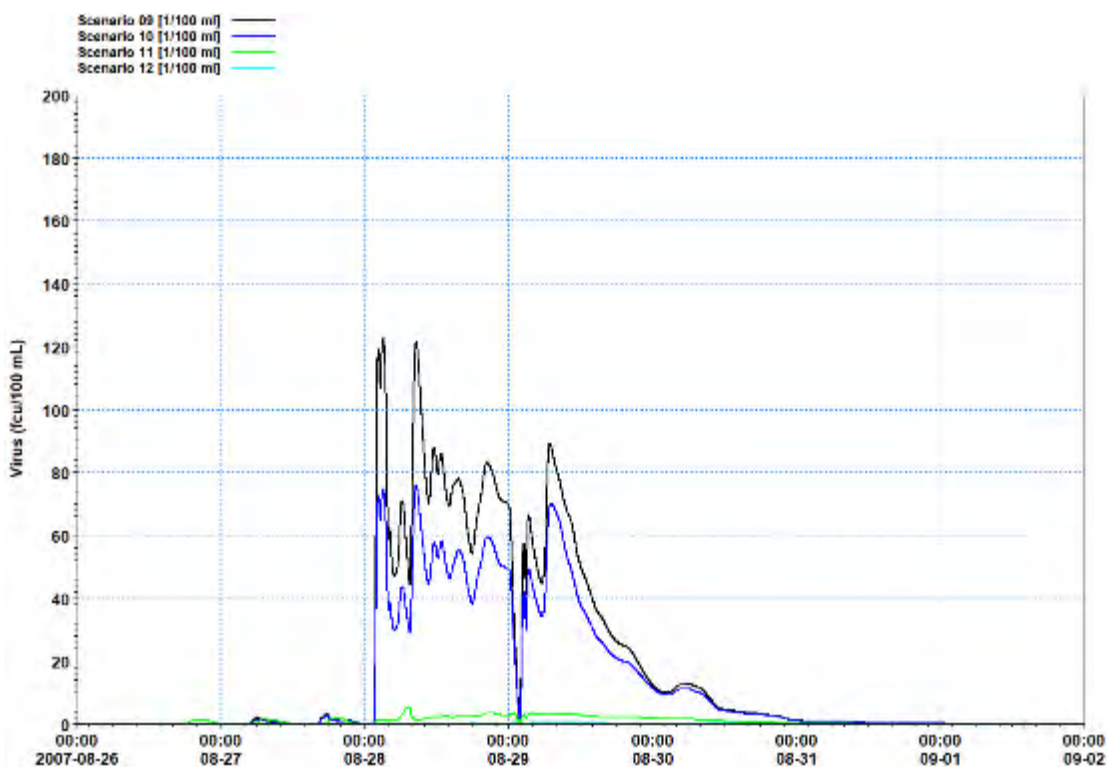


Figure H-16 Predicted Virus (Virus/100 ml) at the Titahi Beach monitoring site for the overflow scenarios for onshore winds and a neap tide.

Appendix I – Time-series at Mt Couper Monitoring site (PWWF discharge and overflow scenarios)

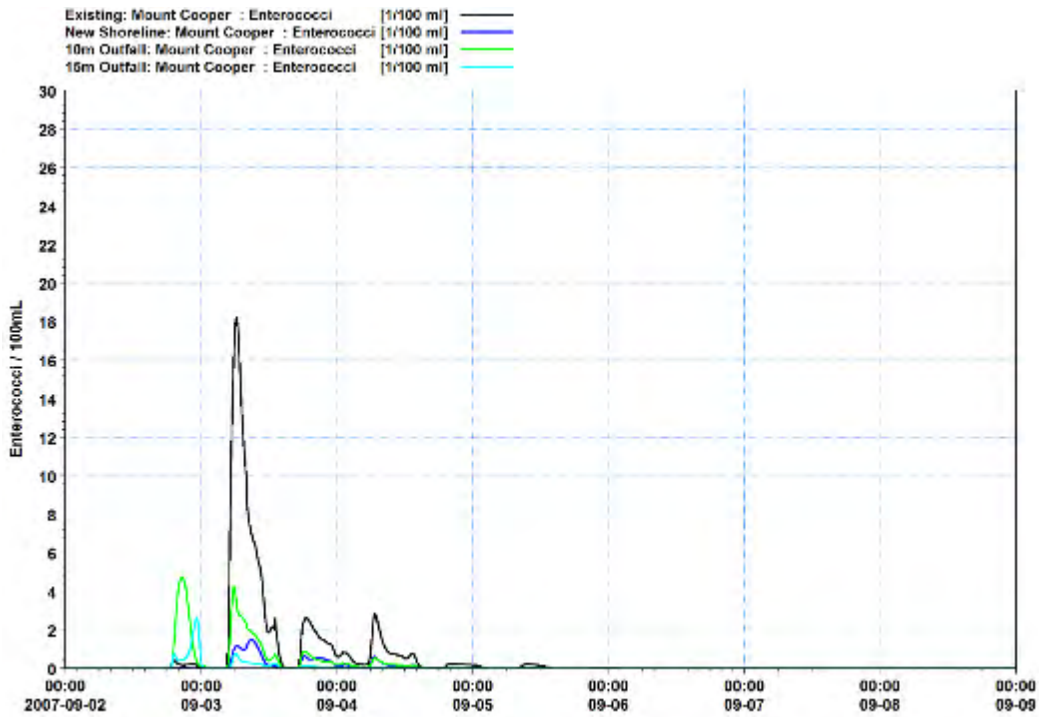


Figure I-1 Predicted Enterococci (Ent/100 ml) at Mount Couper for the discharge options for typical winds and a spring tide.

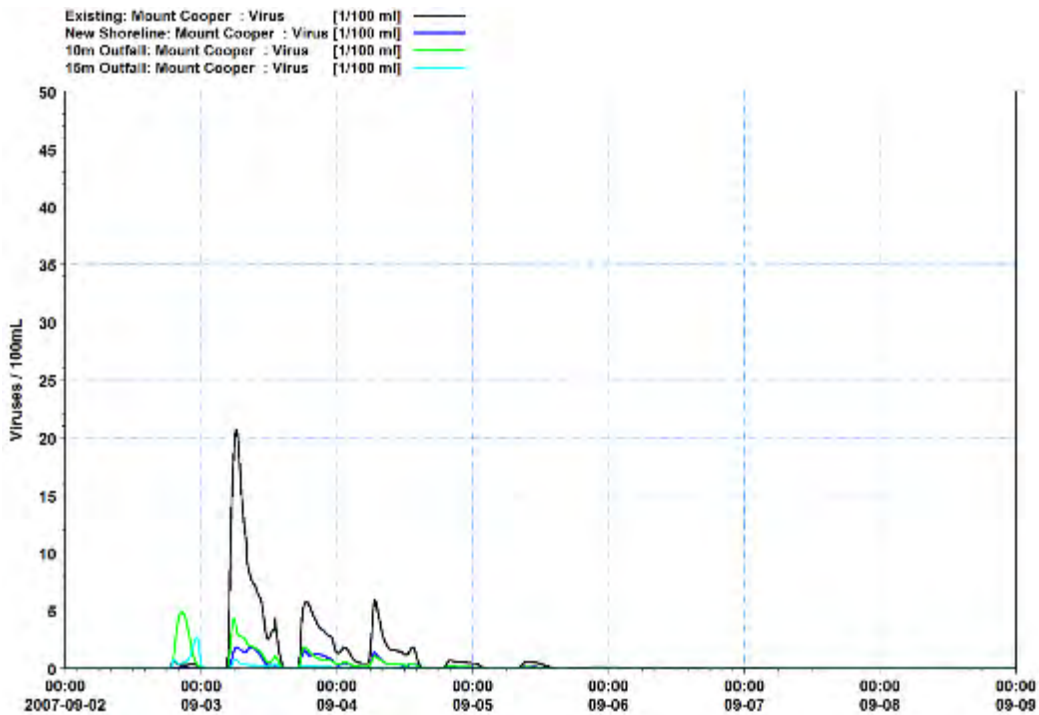


Figure I-2 Predicted Virus (Virus/100 ml) at Mount Couper for the discharge options for typical winds and a spring tide.

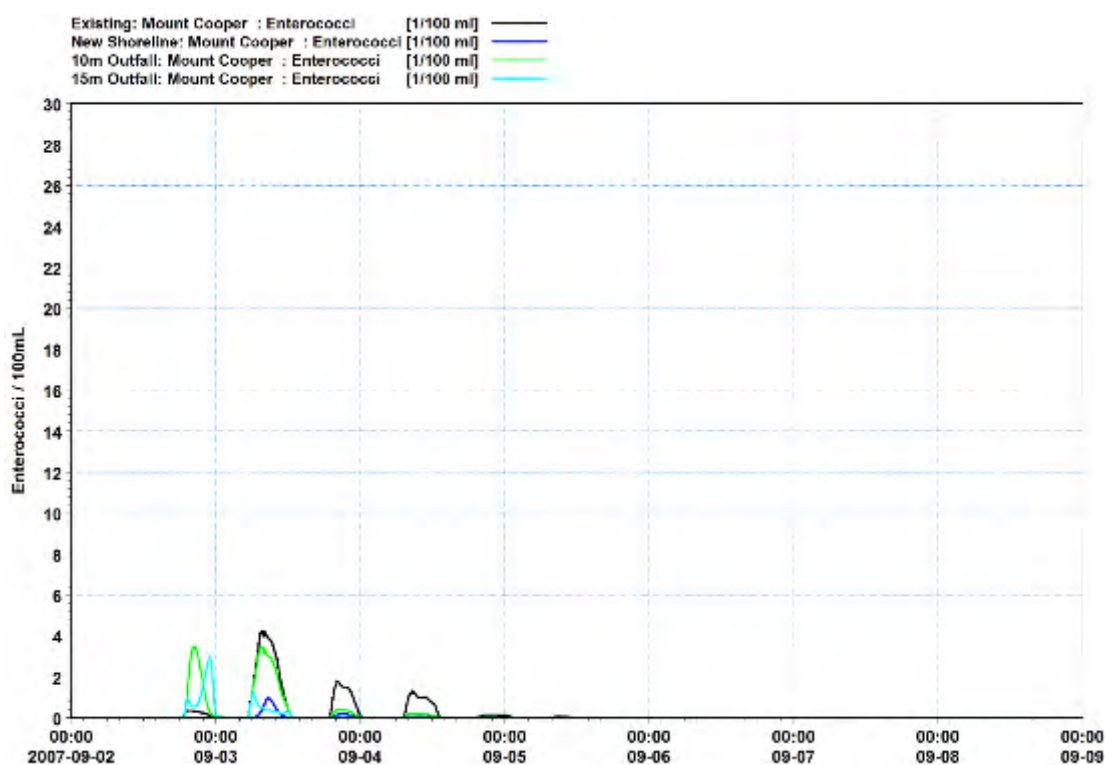


Figure I-3 Predicted Enterococci (Ent/100 ml) at Mount Couper for the discharge options for onshore winds and a spring tide.

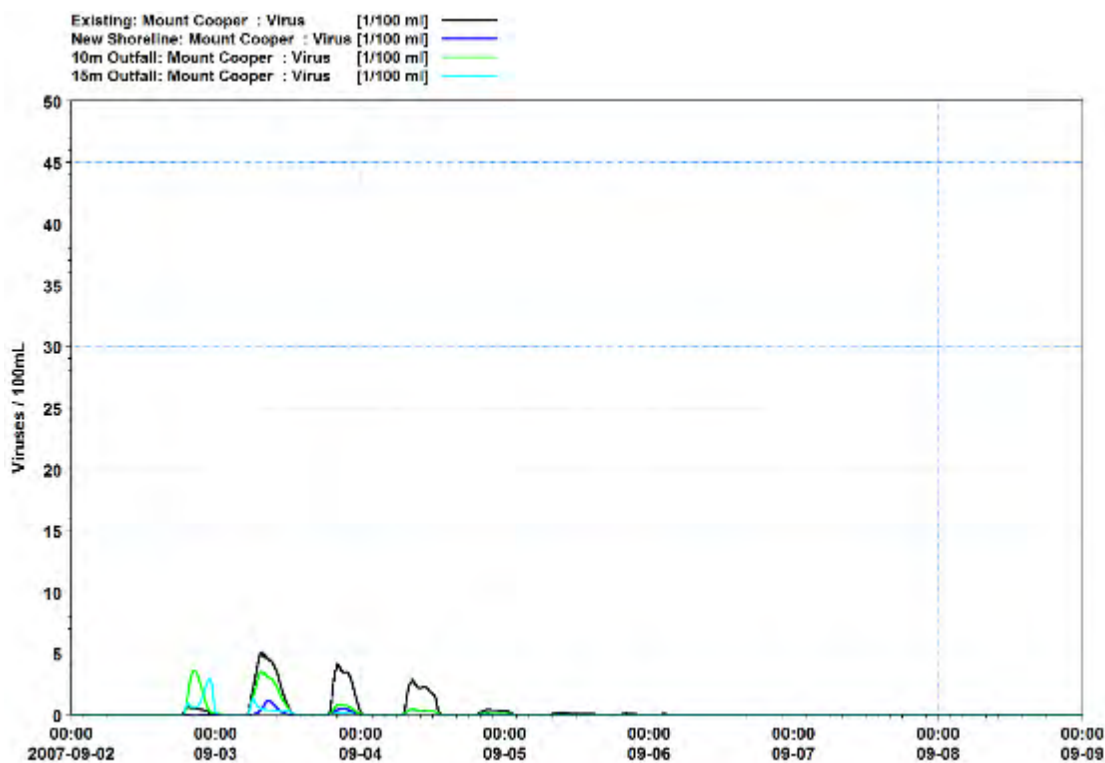


Figure I-4 Predicted Virus (Virus/100 ml) at Mount Couper for the discharge options for onshore winds and a spring tide.

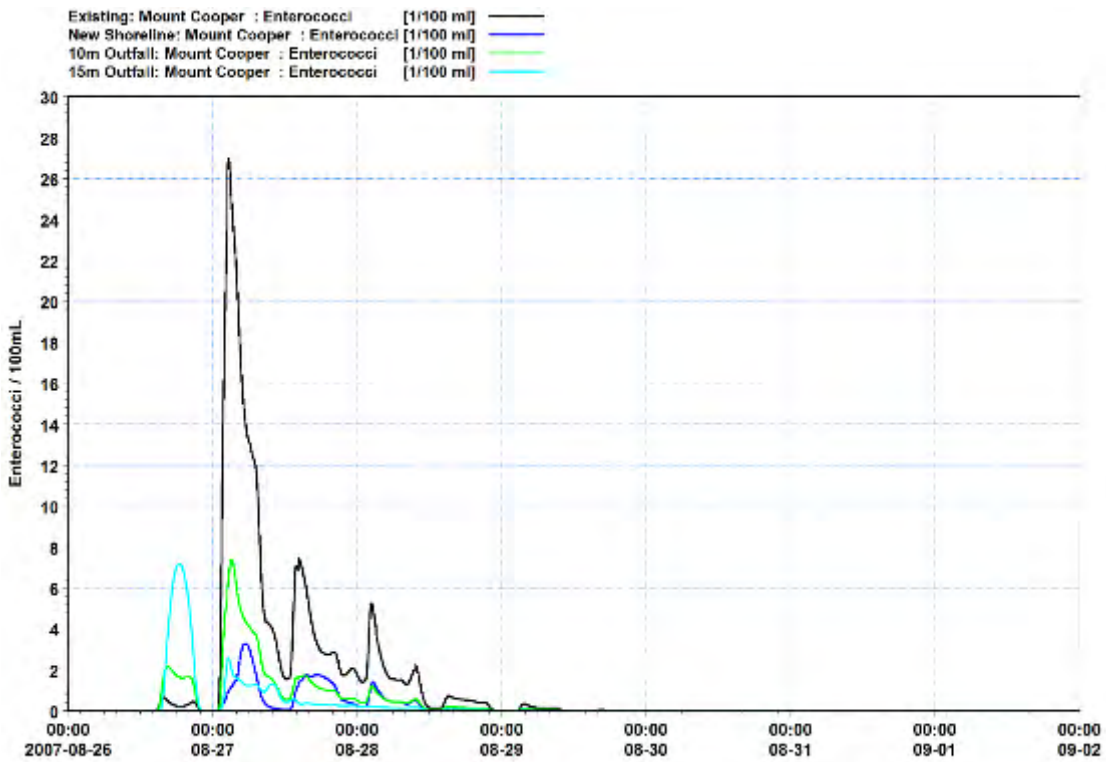


Figure I-5 Predicted Enterococci (Ent/100 ml) at Mount Cooper for the discharge options for typical winds and a neap tide.

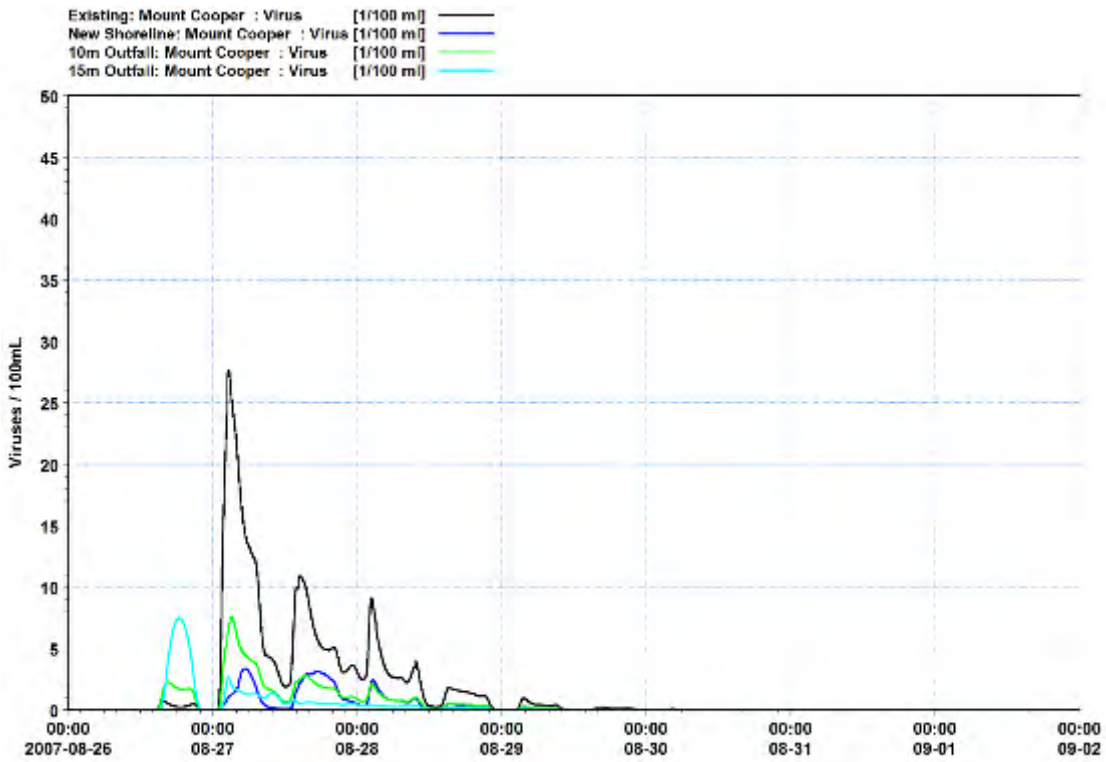


Figure I-6 Predicted Virus (Virus/100 ml) at Mount Cooper for the discharge options for typical winds and a neap tide.

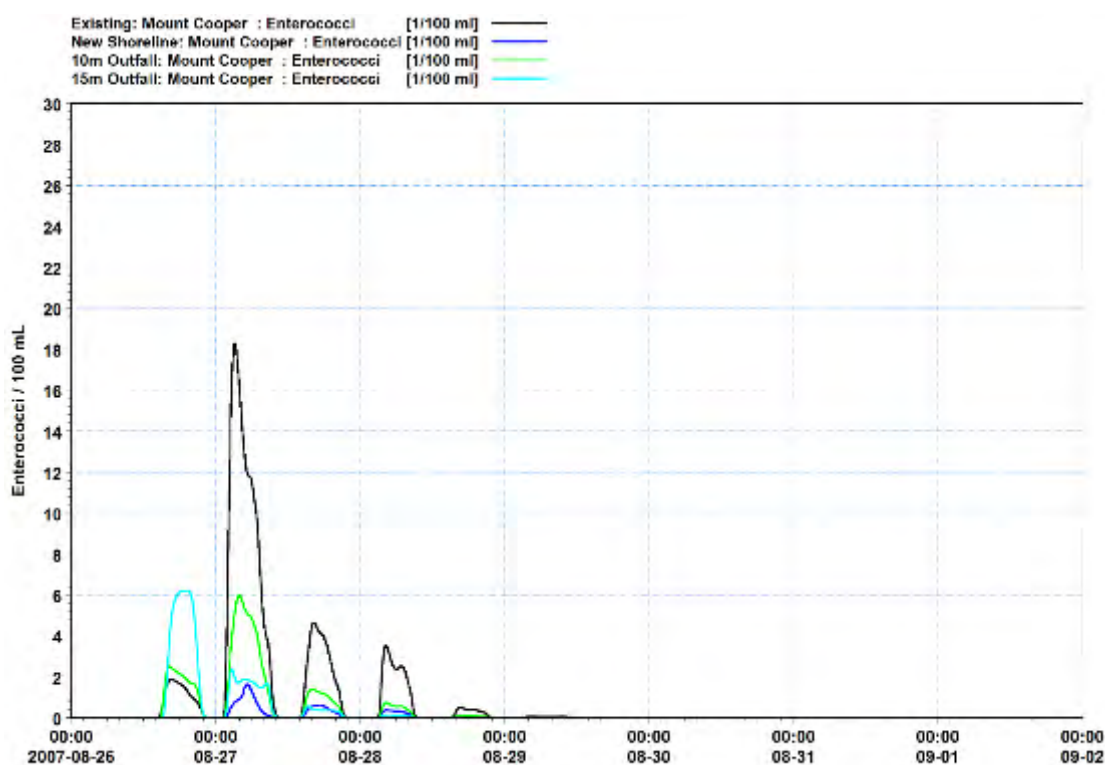


Figure I-7 Predicted Enterococci (Ent/100 ml) at Mount Couper for the discharge options for onshore winds and a neap tide.

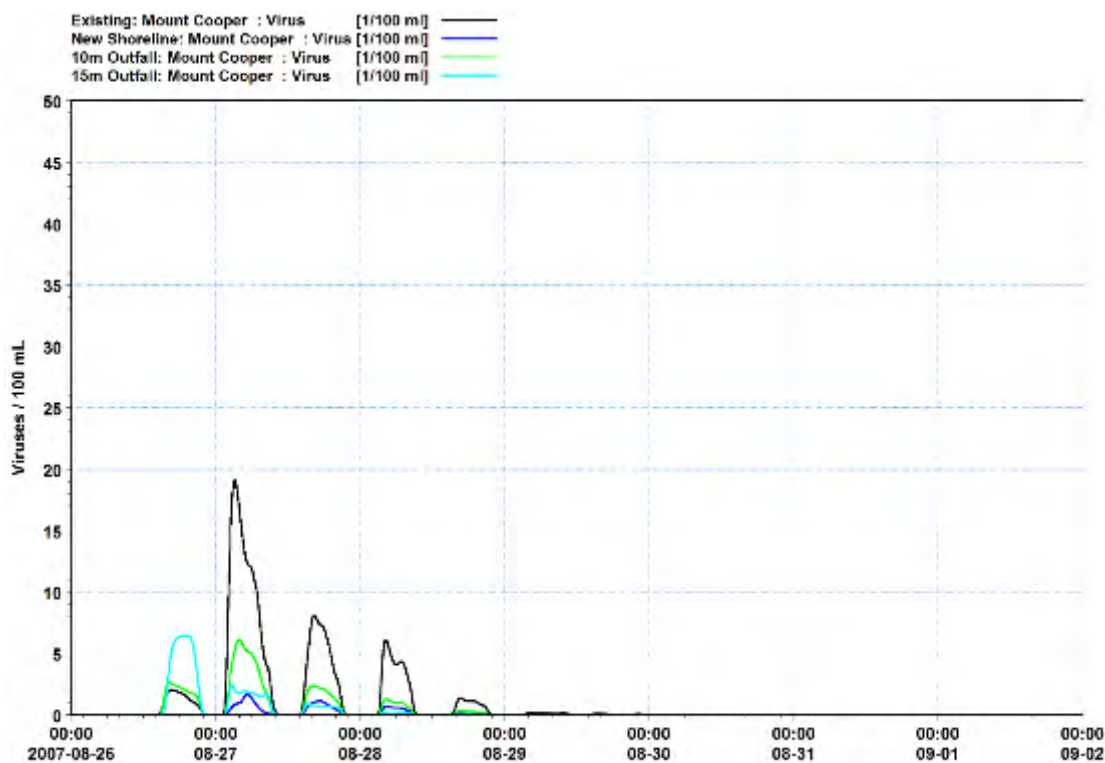


Figure I-8 Predicted Virus (Virus/100 ml) at Mount Couper for the discharge options for onshore winds and a neap tide.

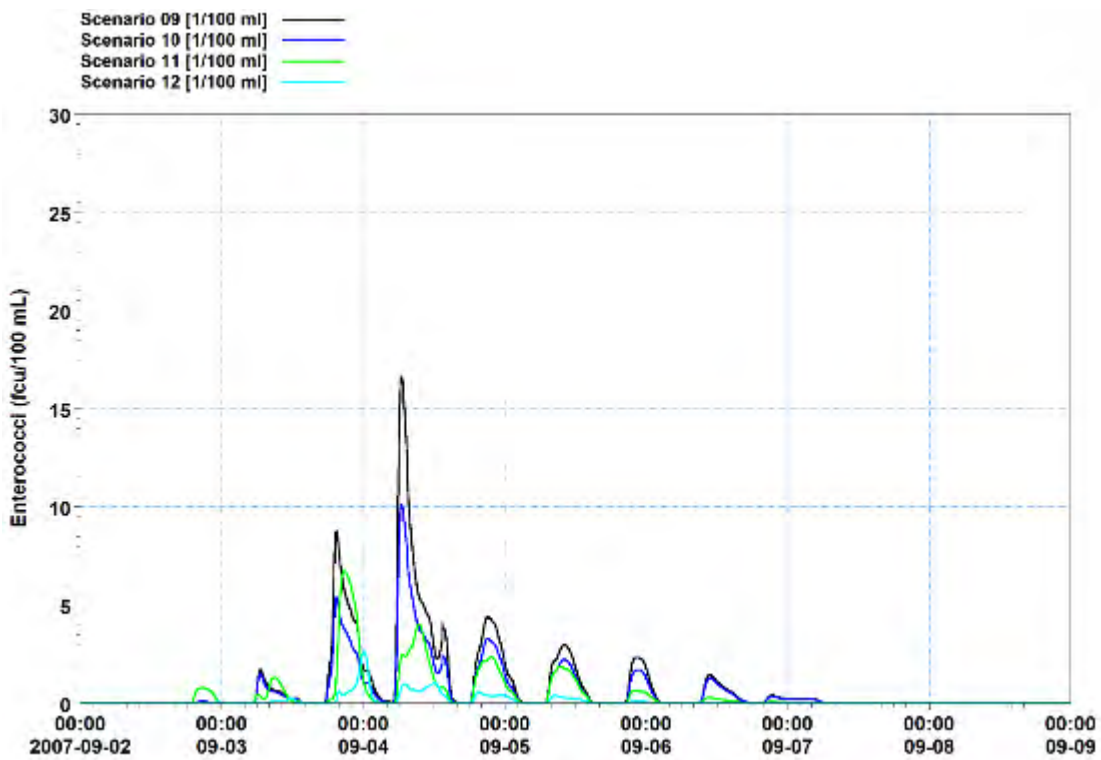


Figure I-9 Predicted Enterococci (Ent/100 ml) at the Mount Couper monitoring site for the overflow scenarios for typical winds and a spring tide.

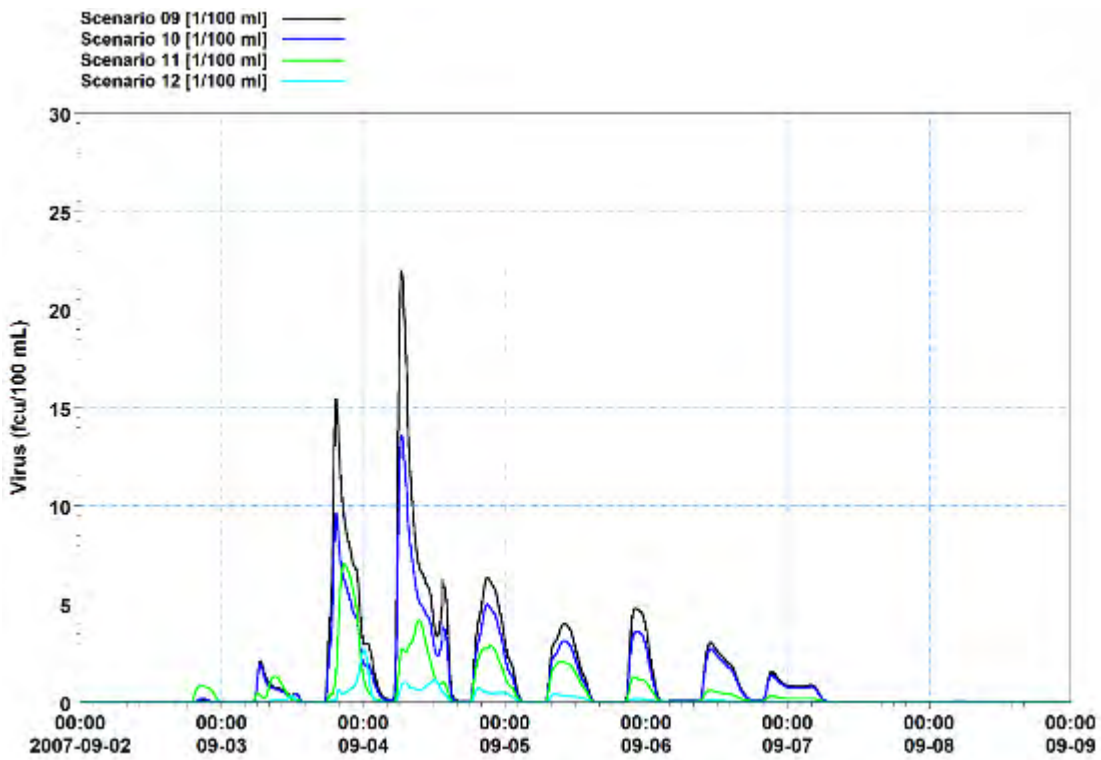


Figure I-10 Predicted Virus (Virus/100 ml) at the Mount Couper monitoring site for the overflow scenarios for typical winds and a spring tide.

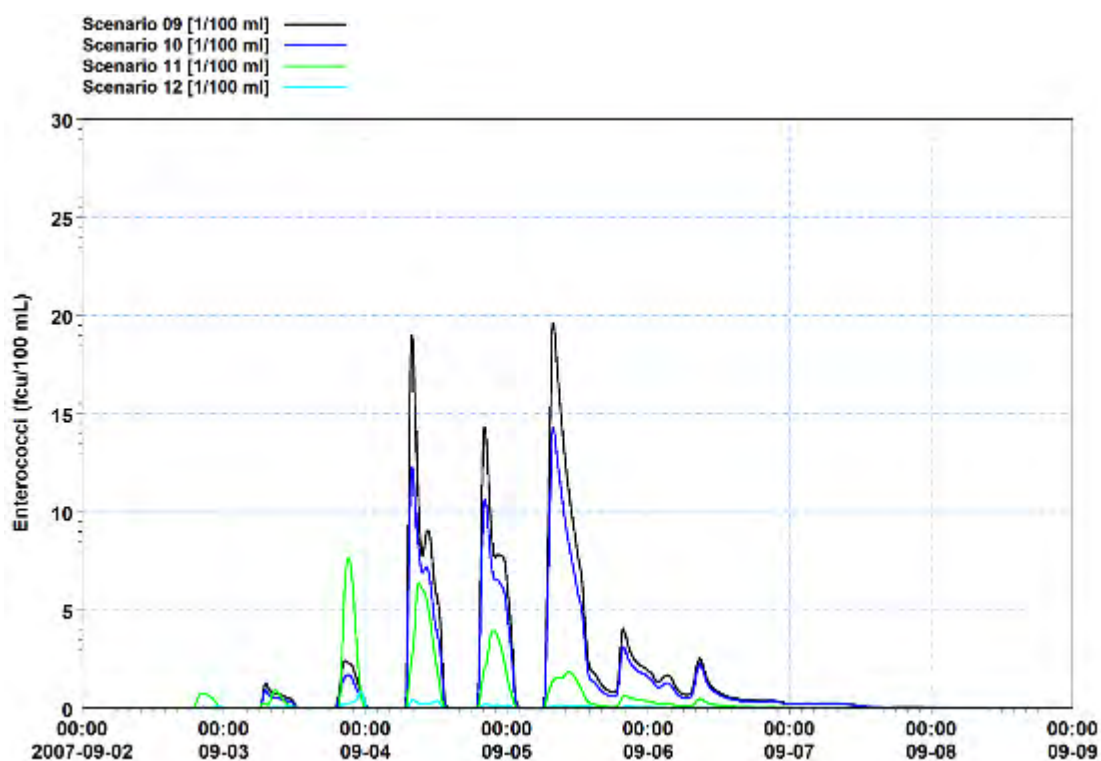


Figure I-11 Predicted Enterococci (Ent/100 ml) at the Mount Couper monitoring site for the overflow scenarios for onshore winds and a spring tide.

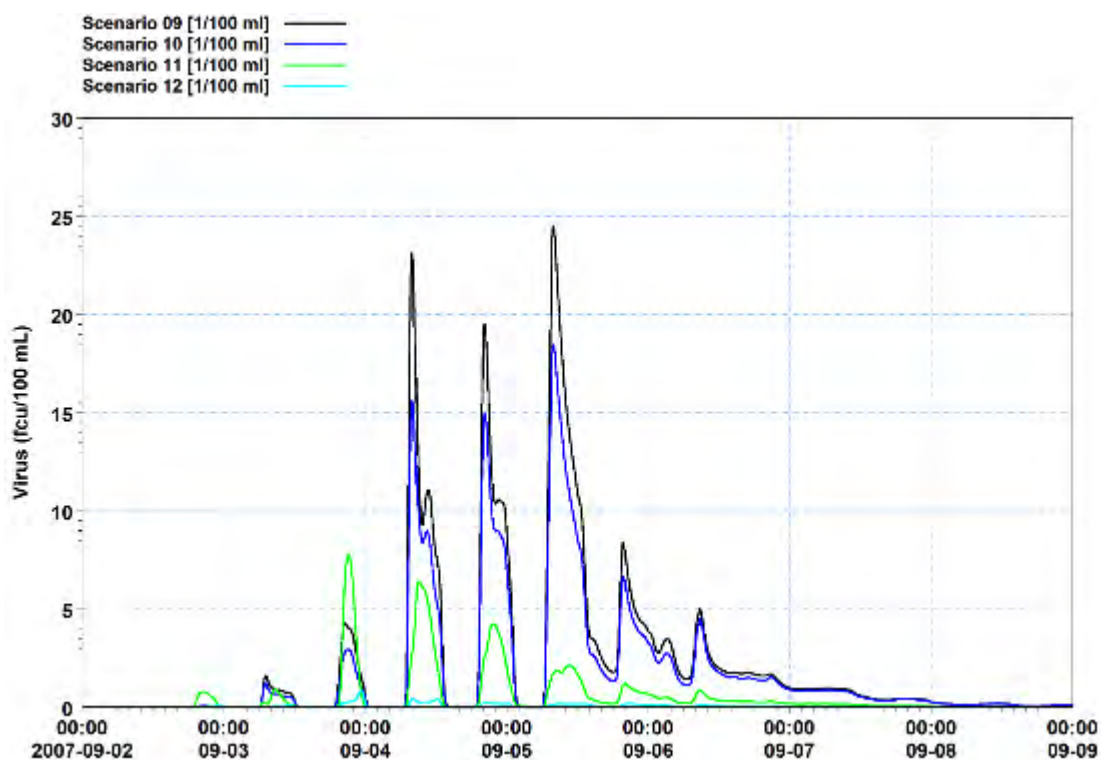


Figure I-12 Predicted Virus (Virus/100 ml) at the Mount Couper monitoring site for the overflow scenarios for onshore winds and a spring tide

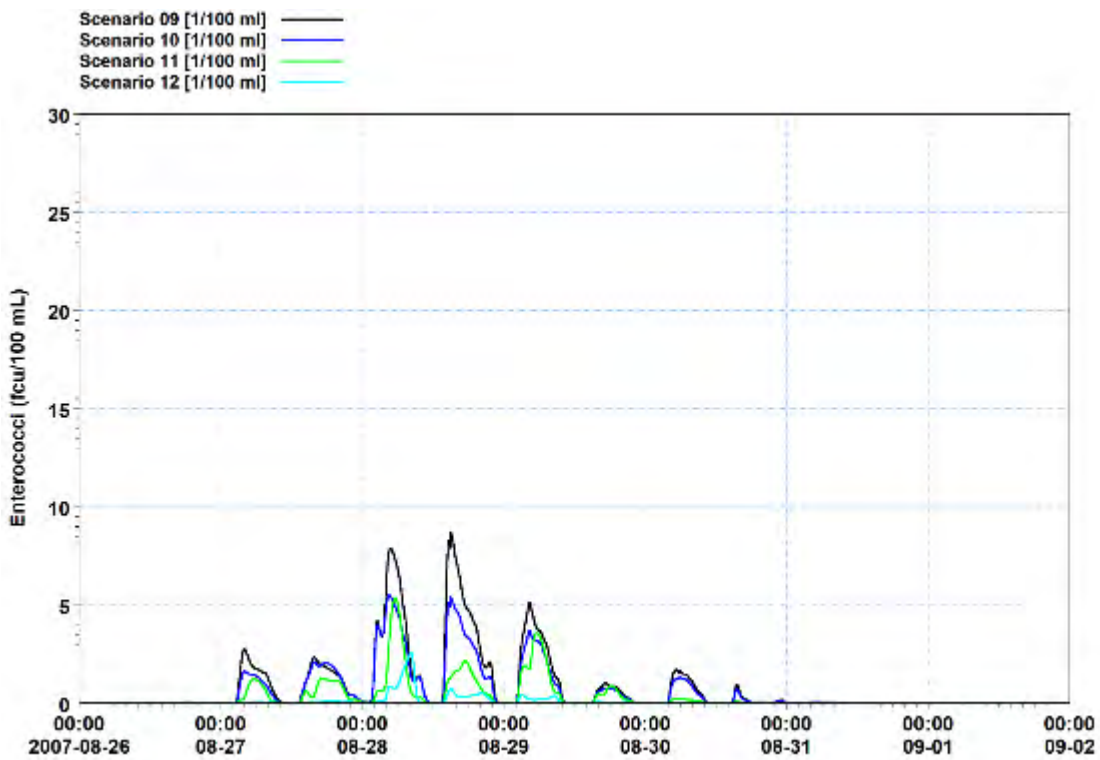


Figure I-13 Predicted Enterococci (Ent/100 ml) at the Mount Couper monitoring site for the overflow scenarios for typical winds and a neap tide.

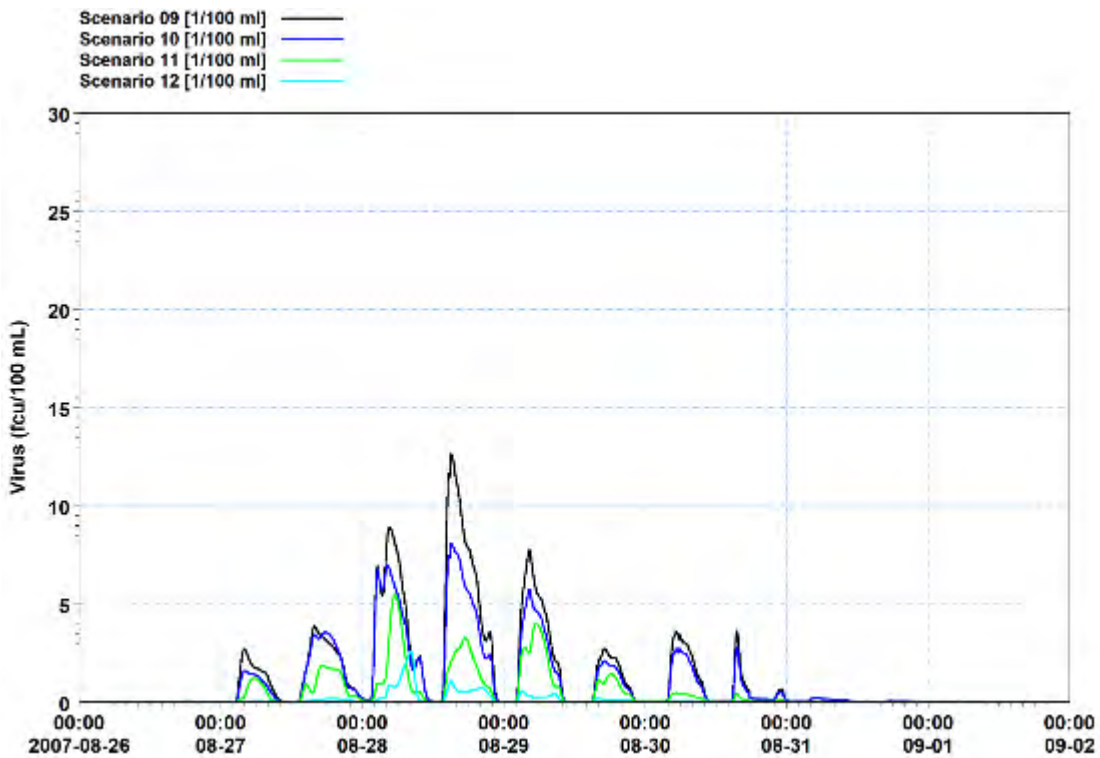


Figure I-14 Predicted Virus (Virus/100 ml) at the Mount Couper monitoring site for the overflow scenarios for typical winds and a neap tide.

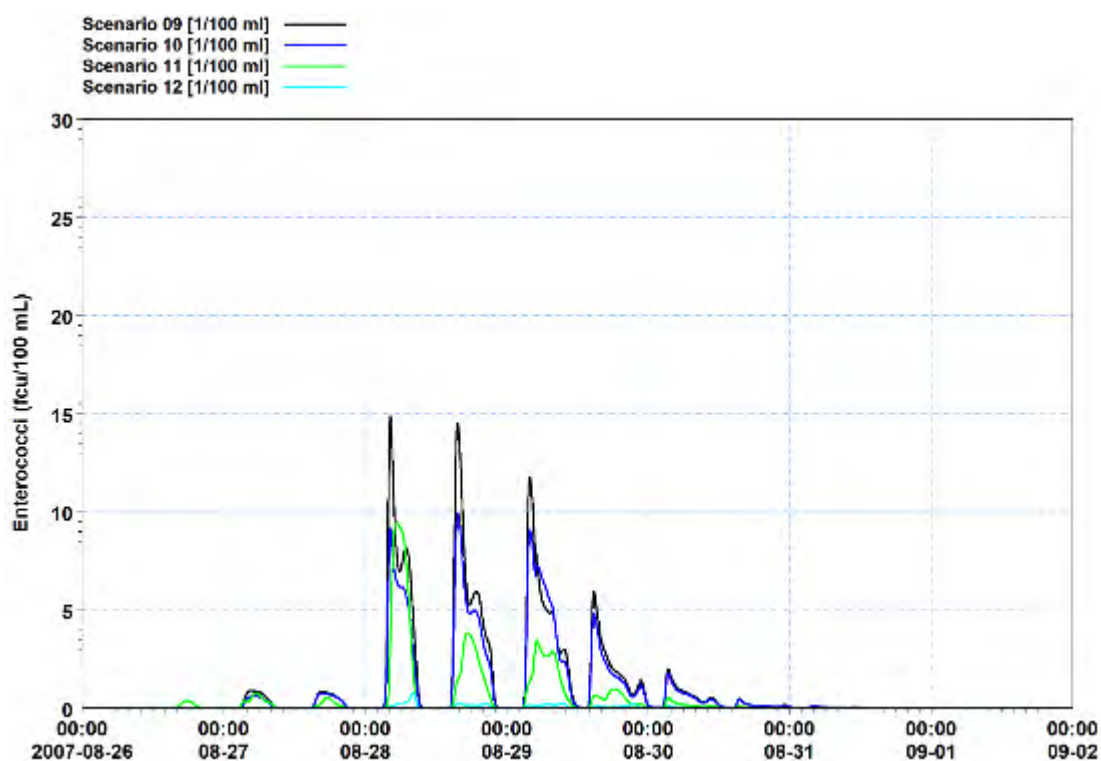


Figure I-15 Predicted Enterococci (Ent/100 ml) at the Mount Couper monitoring site for the overflow scenarios for onshore winds and a neap tide.

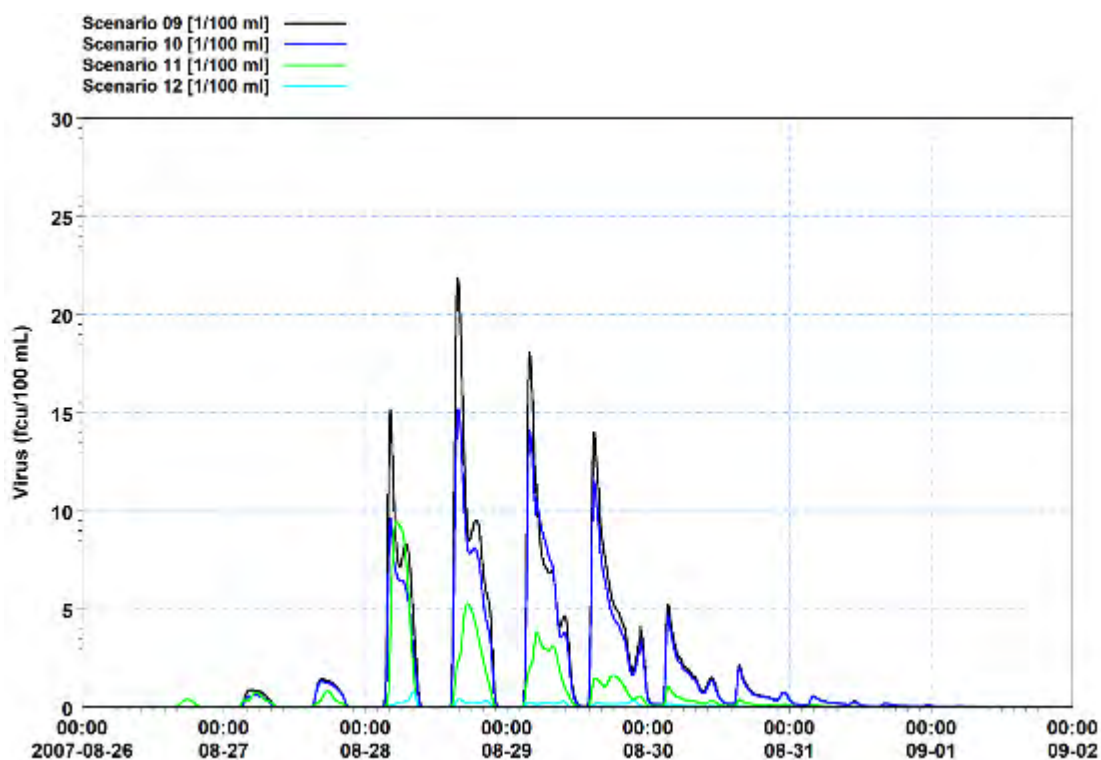


Figure I-16 Predicted Virus (Virus/100 ml) at the Mount Couper monitoring site for the overflow scenarios for onshore winds and a neap tide.

